

UNIVERSIDADE FEDERAL DO PARANA

ASAD ULLAH

**PREPARATION OF DERIVATIVES OF STEVIOL AND ISOSTEVIOL AND
EVALUATION OF SOME BIOLOGICAL ACTIVITIES**

Thesis submitted to the Post-graduation program of the Federal University of Parana in partial fulfillment of the requirements for the degree of Doctor of Philosophy in Chemistry.

Area: Organic Chemistry

Research Supervisor: Prof. Brás Heleno de Oliveira

CURITIBA

2015

Ullah, Asad

Preparation of derivatives of steviol and isosteviol and evaluation of some biological activities / Asad Ullah. – Curitiba, 2015.
364 f. : il.; graf., tab.

Thesis (Doctor) – Universidade Federal do Paraná, Setor de Ciências Exatas, Programa de Pós-Graduação em Química.
Orientador: Brás Heleno de Oliveira

1. Plasmodium falciparum. I. Oliveira, Brás Heleno de. II. Título.

CDD 616.9362

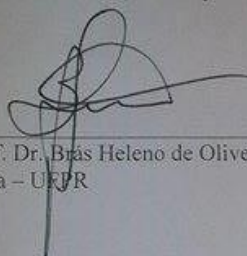
TERMO DE APROVAÇÃO

PREPARATION OF DERIVATIVES OF STEVIOL AND ISOSTEVIOL AND EVALUATION
OF BIOLOGICAL ACTIVITIES

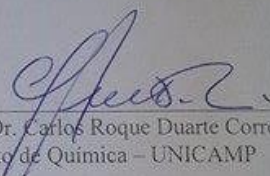
por

ASAD ULLAH

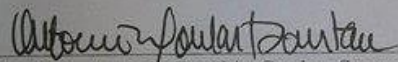
Tese aprovada como requisito parcial para obtenção do grau de Doutor no Programa de Pós-Graduação em Química, pela Comissão Examinadora composta por:



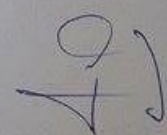
Orientador: Prof. Dr. Brás Heleno de Oliveira
Dep. de Química – UFPR



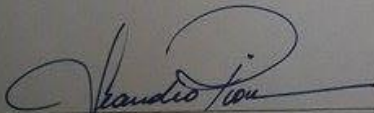
Prof. Dr. Carlos Roque Duarte Correia
Instituto de Química – UNICAMP



Prof. Dr. Antônio Euzébio Goulart Santana
Instituto de Química e Biotecnologia – UFAL



Prof. Dr. Francisco de Assis Marques
Dep. de Química – UFPR



Prof. Dr. Leandro Piovan
Dep. de Química – UFPR

Curitiba, 17 de abril de 2015.

I dedicate this work in loving memory of my father and cousin

ACKNOWLEDGEMENTS

"In the name of God, most gracious, most compassionate"

I would like to express my greatest gratitude and heartfelt thanks to my research advisor and mentor Prof. Dr. Bras Heleno de Oliveira for all his supervision during this work. With my very limited research experience, he took me as his graduate student and with his integrity, patience and guidance encouraged me throughout the years. Besides providing chemicals and instruments, he was always available and accessible all the time to provide suggestions, ideas and helps in every way to make things work.

I am grateful to Federal University of Parana and Department of chemistry for studentship and also i am very indebted to the members of the defense and qualification board Prof. Dr.Francisco de Assis Marques, Prof. Dr. Carlos Roque Duarte correia, Prof. Dr. Antonio Euzebio Goulart Santana Prof. Dr. Leandro Piovan and Prof.Dr.Beatriz Helena Lameiro Noronha Sales Maia for their precious contribution in improving this thesis.

It is beyond the words to express my gratitude to my laboratory fellows Karina B. de Oliveira, Keylla L. Mischiatti, Kelly C. Garcia, Leopoldo and friends from the other laboratories for all kind of support and keeping a very friendly and caring environment in the laboratory which make working enjoyable. All the moments spent together whether, waiting in queue of the university restaurant, social gatherings and barbecue parties. I wish best of luck to all in academic and scientific endeavors and hope the friendship established in Brazil will last in years to come.

I am thankful to Prof. Anderson for free access to the NMR, and also for technician Grazielli da Rocha for IR excess and specially Thiago for assistance in mass spectrum experiments. I am also thankful to Prof. Dr Jaísa Fernandes Soares, Prof. Dr. Ronilson Vasconcelos Barbosa of the Chemistry department, the technical staff for the analysis and to Grace Post-Graduation office for their cooperation and special thanks to Marcelino Camara secretario do PPGQ/UFPR.

I am also thankful to the Conselho Nacional de Desenvolvimento Científico e Tecnológico (CNPq) and the Academy of Sciences for the Developing world (TWAS), Islamia College Peshawar University Pakistan (ICP) for financial support.

I am grateful to all my friends in Brazil, in other parts of the world and my friends and relatives back in Pakistan for their care and moral support. I am extremely indebted to my parents and other family members, for their love, understanding, and support. It was not easy being so far away from you all, but knowing deep and down, you are very proud of me.

ASAD ULLAH

RESUMO

Em relação à contínua necessidade de procurar novas moléculas bioativas e do crescente interesse pelas atividades biológicas de diterpenos tetracíclicos, o principal objetivo deste trabalho foi sintetizar novos derivados de esteviol, isoesteviol e avaliar suas *in vitro* bioatividades contra alvos biológicos selecionados. Os novos derivados foram 2, 4-dinitrofenil-hidrazina (2, 4-DNPH), 4-nitro-fenil-hidrazona (4-NPH), e também mais simples hidrazona, hidrazona isopropílico. Uma série de éster de benzilo e éster de fenacilo p-metoxi também foram preparados. Estes derivados foram avaliados quanto à sua *in vitro* anti-tumoral, anti-maláricos, anti-Trypanosoma cruzi, anti-Corynebacterium diphtheriae e anti-leishmaniose atividades. Os antitumorais bioensaios foram avaliados contra três células tumorais: Carcinoma do pulmão (A549), glioma do cérebro humano (T98MG), glioblastoma humano-astrocitoma (U8MG). Os resultados mostraram que os análogos de isoesteviol possuindo fragmentos de hidrazona e oxima em C16 são citotóxicos. Os ensaios anti-maláricos mostraram que os derivado isoesteviol com 2, 4-dinitro-fenil-hidrazona e 4-nitro-fenil hidrazona moiety eram moderadamente activo contra *plasmodium falciparum* W2 (cloroquine-resistente). Os ensaios de anti-Trypanosoma cruzi mostrou que a modificação em C16 de isoesteviol tem um impacto positivo sobre a actividade de T. cruzi. O derivado de oxima mostrou atividade moderada contra as duas formas de T. cruzi, enquanto os outros derivados eram inativos Os resultados *in vitro* demonstraram que os derivados de hidrazona eram inactivos contra T. cruzi. Uma analyse de *in silico docking* para prever a afinidade de ligação de alguns derivados de C. diphtheriae sortase proteínas também foi realizado, com oito derivados isoesteviol (1e, 2g, 3g, 4g, 5g, 5m, 5i, 5j). Preliminares resultados *in vitro* mostraram que os compostos 3g mostrou melhor inibição em comparação com outros derivados.

ABSTRACT

Regarding the continuous need to search for new bioactive molecules and the increasing interest for the biological activities of tetracyclic diterpenes, the main goal of this work was to synthesize known and new derivatives of steviol and isosteviol and evaluate for their *in vitro* bioactivities against selected biological targets. The new derivatives were 2, 4-dinitro phenyl hydrazone (**2**, **4-DNPH**), 4-nitro phenyl hydrazone (**4-NPH**), and also simpler hydrazone, isopropyl hydrazone. A series of benzyl ester and *p*-methoxy phenacyl ester were also prepared. These derivatives were evaluated for their *in vitro* anti-tumor, anti-malarial, anti-*Trypanosoma cruzi*, anti-Leishmaniasis and anti-*Corynebacterium diphtheriae* activities. The antitumor bioassays were evaluated against three human cancer cell lines: lung carcinoma (A549), human brain glioma (T98MG), human glioblastoma-astrocytoma (U8MG). The results showed that isosteviol analogues having hydrazone and oxime fragments at C16 are cytotoxic. The antimalarial assays showed that isosteviol derivative with 2, 4-dinitro phenyl hydrazone and 4-nitro phenyl hydrazone derivatives were moderately active against *Plasmodium falciparum* W2 (chloroquine-resistant). The anti-*Trypanosoma cruzi* assays showed that the modification at C16 of isosteviol has positive impact on the *T. cruzi* activity. The oxime derivative showed moderate activity against both forms of *T. cruzi* while the other derivatives were inactive. The *in vitro* results showed that hydrazone derivatives were inactive against *T. cruzi*.

An *in silico* docking analysis to predict the binding affinity of some derivatives to *C. diphtheriae* sortase proteins was also carried out, with eight isosteviol derivatives (**1e**, **2g**, **3g**, **4g**, **5g**, **5m**, **5i**, **5j**). Preliminary *in vitro* results showed that compounds **3g** showed good inhibition then other derivatives.

Keywords: Isosteviol, cytotoxicity, *Plasmodium falciparum*, tetracyclic diterpenes.

List of Figures

Figure 1: Chemical structure of <i>E</i> -eleganonal (1) eleganoic acid (2).....	4
Figure 2: Chemical structure of infuscatrienol (3) Jaspaquinol (4).....	4
Figure 3: Chemical structure of <i>Z</i> -abienol (5) labdene diol (6).....	5
Figure 4: Chemical structure of Pimarane (7), Abietanes (8).....	5
Figure 5: Chemical structure of Beyerane (9), Kaurane (10).....	6
Figure 6: Chemical structure of Tasumatrols (11), Echinoic acid (12).....	6
Figure 7: Chemical structures of kaurene (13), <i>ent</i> -kaurene (14).....	8
Figure 8: Chemical structure of beyerane (15), <i>ent</i> -beyerane (16).....	9
Figure 9: Chemical structure of isosteviol (17), steviol (18).....	11
Figure 10: Chemical structure of pyrazole (19), pyrazoline (20), and derivatives of isosteviol.	12
Figure 11: Chemical structure of steviol ester (21), isosteviol ester (22).....	15
Figure 12: Chemical structure of Isosteviol derivatives (23).....	17
Figure 13: Chemical structure of ethyl ester of Isosteviol (24).....	18
Figure 14: Chemical structure of MOM ester (25), carbamate ester of.....	19
Figure 15: Chemical structure of steviol (27), isosteviol derivatives (28).....	20
Figure 16: Chemical structure of dimeric amide of steviol (29).....	22
Figure 17: Chemical structure of 15 α -hydroxy methylene isosteviol (30), and isosteviol (31).....	25
Figure 18: Chemical structures of isosteviol lactone (32), isosteviol lactam (33), and isosteviol indole (34).....	26
Figure 19: Chemical structure of stevioside, steviol and isosteviol dimeric Amides (35).....	27
Figure 20: Chemical structure of bis-quaternized isosteviol (36).....	28
Figure 21: Chemical structure of ethyl ester of isosteviol (37).....	29
Figure 22: Chemical structure of hydrazone hydrazide (38), hydrazone (39), dimeric hydrazone (40), hydrazone and dimeric hydrazide of isosteviol (41). 33	
Figure 23: Chemical structure of steviol (42), dimeric per acid anhydride (43) steviol dimeric anhydride (44).	34

Figure 24: Chemical structure of 15-oxo-thiosemicarbazone (45), 15-oxo 16-oxime derivatives of isosteviol (46).....	35
Figure 25: Chemical structure of alkylated ureide of isosteviol (47).	36
Figure 26: Wagner-Meerwein rearrangement of Kaurene.	82
Figure 27: Baeyer-villager oxidation of isosteviol	87
Figure 28: General mechanism for hydrazone formation includes nucleophilic addition-elimination reaction.....	103
Figure 29: <i>In vitro</i> antitumor activities of isosteviol derivatives in human glioblastoma-astrocytoma, epithelial-like cell line (U87MG).	121
Figure 30: <i>In vitro</i> antitumor activities of isosteviol derivatives human brain glioma cell lines (T98MG).	121
Figure 31: <i>In vitro</i> antitumor activities of isosteviol derivatives human lung carcinoma (A549).	122
Figure 32: 3D cartoon representation of the docking analyses of compound 3g with <i>C. diphtheriae</i> sortase proteins where figure A): sortase (Srt) proteins B, while figure B) represent sortase (Srt) proteins A.....	128
Figure 33: Evaluation of anti <i>Corynebacterium diphtheriae</i> activity of isosteviol derivatives by disk diffusion test. 1) Disk A: correspond to compound 4g, 2) Disk B: correspond to compound 5m, 3) Disk C: correspond to 5j, 4) Disk D: correspond to 3g, 5) Disk E correspond to 5g, 6) Disk F correspond 5i, 7) Disk G, correspond to 1e, 8) Disk H correspond to 2g (1e, 2g, 3g, 4g, 5g, 5m, 5i, 5j) the disk I, correspond to the antibiotic used as positive controle.....	129
Figure 34: IR spectrum of compound 1a.	164
Figure 35: ¹ H-NMR (200 MHz, CDCl ₃) spectrum of compound 1a.	165
Figure 36: ¹³ C { ¹ H} NMR (50 MHz, CDCl ₃) spectrum of compound 1a.....	166
Figure 37: ¹³ C { ¹ H} DEPT NMR (50 MHz, CDCl ₃) spectrum of compound 1a. ...	167
Figure 38: IR spectrum of compound 1b.	168
Figure 39: ¹ H-NMR (200 MHz, CDCl ₃) spectrum of compound 1b.	169
Figure 40 ¹³ C { ¹ H} NMR (50 MHz, CDCl ₃) spectrum of compound 1b.....	170
Figure 41: ¹³ C { ¹ H} DEPT NMR (50 MHz, CDCl ₃) spectrum of compound 1b. ...	171
Figure 42: IR spectrum of compound 1c.	172

Figure 43: ^1H -NMR (200 MHz, CDCl_3) spectrum of compound 1c.	173
Figure 44: ^{13}C $\{^1\text{H}\}$ NMR (50 MHz, CDCl_3) spectrum of compound 1c.	174
Figure 45: ^{13}C $\{^1\text{H}\}$ DEPT NMR (50 MHz, CDCl_3) spectrum of compound 1c. ...	175
Figure 46: ESI-MS spectrum of compound 1d.	176
Figure 47: IR spectrum of compound 1d.	177
Figure 48: ^1H -NMR (200 MHz, CDCl_3) spectrum of compound 1d.	178
Figure 49: ^{13}C $\{^1\text{H}\}$ NMR (50 MHz, CDCl_3) spectrum of compound 1d.	179
Figure 50: ^{13}C $\{^1\text{H}\}$ DEPT NMR (50 MHz, CDCl_3) spectrum of compound 1d. ...	180
Figure 51: ESI-MS spectrum of compound 1e.	181
Figure 52: IR spectrum of compound 1e.	182
Figure 53: ^1H -NMR (200 MHz, CDCl_3) spectrum of compound 1e.	183
Figure 54: ^{13}C $\{^1\text{H}\}$ NMR (50 MHz, CDCl_3) spectrum of compound 1e.	184
Figure 55: ^{13}C $\{^1\text{H}\}$ DEPT NMR (50 MHz, CDCl_3) spectrum of compound 1e. ...	185
Figure 56: ESI-MS spectrum of compound 1f.	186
Figure 57: IR spectrum of compound 1f.	187
Figure 58: ^1H -NMR (200 MHz, CDCl_3) spectrum of compound 1f.	188
Figure 59: ^{13}C $\{^1\text{H}\}$ NMR (50 MHz, CDCl_3) spectrum of compound 1f.	189
Figure 60: ^{13}C $\{^1\text{H}\}$ DEPT NMR (50 MHz, CDCl_3) spectrum of compound 1f.	190
Figure 61: IR spectrum of compound 1h.	191
Figure 62: ^1H -NMR (200 MHz, CDCl_3) spectrum of compound 1h.	192
Figure 63: ^{13}C $\{^1\text{H}\}$ NMR (50 MHz, CDCl_3) spectrum of compound 1h	193
Figure 64: ^{13}C $\{^1\text{H}\}$ DEPT NMR (50 MHz, CDCl_3) spectrum of compound 1h. ...	194
Figure 65: IR spectrum of compound 2h.	195
Figure 66: ^1H -NMR (200 MHz, CDCl_3) spectrum of compound 2h.	196
Figure 67: ^{13}C $\{^1\text{H}\}$ NMR (50 MHz, CDCl_3) spectrum of compound 2h.	197
Figure 68: ^{13}C $\{^1\text{H}\}$ DEPT NMR (50 MHz, CDCl_3) spectrum of compound 2h. ...	198
Figure 69: IR spectrum of compound 4h.	199
Figure 70: ^1H -NMR (200 MHz, CDCl_3) spectrum of compound 4h.	200
Figure 71: ^{13}C $\{^1\text{H}\}$ NMR (50 MHz, CDCl_3) spectrum of compound 4h.	201
Figure 72: ^{13}C $\{^1\text{H}\}$ DEPT NMR (50 MHz, CDCl_3) spectrum of compound 4h. ...	202
Figure 73: IR spectrum of compound 5i.	203

Figure 74: ^1H -NMR (200 MHz, CDCl_3) spectrum of compound 5i.	204
Figure 75: ^{13}C $\{^1\text{H}\}$ NMR (50 MHz, CDCl_3) spectrum of compound 5i.	205
Figure 76: ^{13}C $\{^1\text{H}\}$ DEPT NMR (50 MHz, CDCl_3) spectrum of compound 5i.	206
Figure 77: ESI-MS spectrum of compound 5n.	207
Figure 78: IR spectrum of compound 5n.	208
Figure 79: ^1H -NMR (200 MHz, CD_3OD) spectrum of compound 5n.	209
Figure 80: ^{13}C $\{^1\text{H}\}$ NMR (50 MHz, CD_3OD) spectrum of compound 5n.	210
Figure 81: ^{13}C $\{^1\text{H}\}$ DEPT-NMR (50 MHz, CD_3OD) spectrum of compound 5n. .	211
Figure 82: IR spectrum of compound 5j.	212
Figure 83: ^1H -NMR (200 MHz, Acetone- d_6) spectrum of compound 5j.	213
Figure 84: ^{13}C $\{^1\text{H}\}$ NMR (50 MHz, Acetone- d_6) spectrum of compound 5j.	214
Figure 85: ^{13}C $\{^1\text{H}\}$ DEPT-NMR (50 MHz, Acetone- d_6) spectrum of compound 5j.	215
Figure 86: ESI-MS spectrum of compound 5k.	216
Figure 87: IR spectrum of compound 5k.	217
Figure 88: ^1H -NMR (200 MHz, Methanol- d_4) spectrum of compound 5k.	218
Figure 89: ^{13}C $\{^1\text{H}\}$ NMR (50 MHz, Methanol- d_4) spectrum of compound 5k.	219
Figure 90: ^{13}C $\{^1\text{H}\}$ DEPT-NMR (50 MHz, Methanol- d_4) spectrum of compound 5k.	220
Figure 91: ESI-MS spectrum of compound 2f.	221
Figure 92: IR spectrum of compound 2f.	222
Figure 93: ^1H -NMR (200 MHz, CDCl_3) spectrum of compound 2f.	223
Figure 94: ^{13}C $\{^1\text{H}\}$ NMR (50 MHz, CDCl_3) spectrum of compound 2f.	224
Figure 95: ^{13}C $\{^1\text{H}\}$ DEPT NMR (50 MHz, CDCl_3) spectrum of compound 2f.	225
Figure 96: ESI-MS spectrum of compound 2a.	226
Figure 97: IR spectrum of compound 2a.	227
Figure 98: ^1H NMR (200 MHz, CDCl_3) spectrum of compound 2a.	228
Figure 99: ^{13}C $\{^1\text{H}\}$ NMR (50 MHz, CDCl_3) spectrum of compound 2a.	229
Figure 100: ESI-MS spectrum of compound 2b.	230
Figure 101: IR spectrum of compound 2b.	231
Figure 102: ^1H -NMR (200 MHz, CDCl_3) spectrum of compound 2b.	232

Figure 103: $^{13}\text{C} \{^1\text{H}\}$ NMR (50 MHz, CDCl_3) spectrum of compound 2b.....	233
Figure 104: $^{13}\text{C} \{^1\text{H}\}$ DEPT-NMR (50 MHz, CDCl_3) spectrum of compound 2b.	234
Figure 105: ESI-MS spectrum of compound 2c.....	235
Figure 106: IR spectrum of compound 2c.	236
Figure 107: ^1H -NMR (200 MHz, CDCl_3) spectrum of compound 2c.	237
Figure 108: $^{13}\text{C} \{^1\text{H}\}$ NMR (50 MHz, CDCl_3) spectrum of compound 2c.....	238
Figure 109: $^{13}\text{C} \{^1\text{H}\}$ DEPT-NMR (50 MHz, CDCl_3) spectrum of compound 2c. .	239
Figure 110: ESI-MS spectrum of compound 2d.....	240
Figure 111: IR spectrum of compound 2d.	241
Figure 112: ^1H -NMR (200 MHz, CDCl_3) spectrum of compound 2d.	242
Figure 113: $^{13}\text{C} \{^1\text{H}\}$ NMR (50 MHz, CDCl_3) spectrum of compound 2d.....	243
Figure 114: $^{13}\text{C} \{^1\text{H}\}$ DEPT-NMR (50 MHz, CDCl_3) spectrum of compound 2d. .	244
Figure 115: ESI-MS spectrum of compound 3f.....	245
Figure 116: IR spectrum of compound 3f.	246
Figure 117: ^1H -NMR (200 MHz, CDCl_3) spectrum of compound 3f.	247
Figure 118: $^{13}\text{C} \{^1\text{H}\}$ NMR (50 MHz, CDCl_3) spectrum of compound 3f.....	248
Figure 119: $^{13}\text{C} \{^1\text{H}\}$ DEPT-NMR (50 MHz, CDCl_3) spectrum of compound 3f...	249
Figure 120: ESI-MS spectrum of compound 5l.....	250
Figure 121: IR spectrum of compound 5l.	251
Figure 122: ^1H -NMR (200 MHz, CDCl_3) spectrum of compound 5l.	252
Figure 123: $^{13}\text{C}\{^1\text{H}\}$ NMR (50 MHz, CDCl_3) spectrum of compound 5l.....	253
Figure 124: $^{13}\text{C} \{^1\text{H}\}$ DEPT-NMR (50 MHz, CDCl_3) spectrum of compound 5l. .	254
Figure 125: ESI MS spectrum of compound 6i.	255
Figure 126: IR spectrum of compound 6i.	256
Figure 127: ^1H -NMR (200 MHz, CDCl_3) spectrum of compound 6i.	257
Figure 128: $^{13}\text{C} \{^1\text{H}\}$ -NMR (50 MHz, CDCl_3) spectrum of compound 6i.....	258
Figure 129: $^{13}\text{C} \{^1\text{H}\}$ DEPT-NMR (50 MHz, CDCl_3) spectrum of compound 6i. ...	259
Figure 130: ESI-MS spectrum of compound 6j.....	260
Figure 131: IR spectrum of compound 6j.	261
Figure 132: ^1H -NMR (200 MHz, CDCl_3) spectrum of compound 6j.	262
Figure 133: $^{13}\text{C} \{^1\text{H}\}$ NMR (50 MHz, CDCl_3) spectrum of compound 6j.....	263

Figure 134: ^{13}C $\{^1\text{H}\}$ DEPT-NMR (50 MHz, CDCl_3) spectrum of compound 6j. . .	264
Figure 135: ESI-MS spectrum of compound 3a.....	265
Figure 136: IR spectrum of compound 3a.	266
Figure 137: ^1H -NMR (200 MHz, CDCl_3) spectrum of compound 3a.	267
Figure 138: ^{13}C $\{^1\text{H}\}$ NMR (50 MHz, CDCl_3) spectrum of compound 3a.....	268
Figure 139: ^{13}C $\{^1\text{H}\}$ DEPT-NMR (50 MHz, CDCl_3) spectrum of compound 3a. .	269
Figure 140: ESI-MS spectrum of compound 3b.....	270
Figure 141: IR spectrum of compound 3b.	271
Figure 142: ^1H -NMR (200 MHz, CDCl_3) spectrum of compound 3b.	272
Figure 143: ^{13}C $\{^1\text{H}\}$ NMR (50 MHz, CDCl_3) spectrum of compound 3b.....	273
Figure 144: ^{13}C $\{^1\text{H}\}$ DEPT-NMR (50 MHz, CDCl_3) spectrum of compound 3b. .	274
Figure 145: ESI-MS spectrum of compound 3c.....	275
Figure 146: IR spectrum of compound 3c.	276
Figure 147: ^1H -NMR (200 MHz, CDCl_3) spectrum of compound 3c.	277
Figure 148: ^{13}C $\{^1\text{H}\}$ NMR (50 MHz, CDCl_3) spectrum of compound 3c.....	278
Figure 149: ^{13}C $\{^1\text{H}\}$ DEPT-NMR (50 MHz, CDCl_3) spectrum of compound 3c. .	279
Figure 150: ESI-MS spectrum of compound 3h.....	280
Figure 151: IR spectrum of compound 3h.	281
Figure 152: ^1H -NMR (200 MHz, CDCl_3) spectrum of compound 3h.	282
Figure 153: ^{13}C $\{^1\text{H}\}$ NMR (50 MHz, CDCl_3) spectrum of compound 3h.....	283
Figure 154: ^{13}C $\{^1\text{H}\}$ DEPT-NMR (50 MHz, CDCl_3) spectrum of compound 3h. .	284
Figure 155: ESI-MS spectrum of compound 6k.....	285
Figure 156: IR spectrum of compound 6k.	286
Figure 157: ^1H -NMR (200 MHz, CDCl_3) spectrum of compound 6k.	287
Figure 158: ^{13}C $\{^1\text{H}\}$ NMR (50 MHz, CDCl_3) spectrum of compound 6k.....	288
Figure 159: ^{13}C $\{^1\text{H}\}$ DEPT-NMR (50 MHz, CDCl_3) spectrum of compound 6k. .	289
Figure 160: ESI-MS spectrum of compound 4f.....	290
Figure 161: IR spectrum of compound 4f.	291
Figure 162: ^1H -NMR (200 MHz, CDCl_3) spectrum of compound 4f.	292
Figure 163: ^{13}C $\{^1\text{H}\}$ NMR (50 MHz, CDCl_3) spectrum of compound 4f.....	293
Figure 164: ^{13}C $\{^1\text{H}\}$ DEPT-NMR (50 MHz, CDCl_3) spectrum of compound 4f. . .	294

Figure 165: ESI-MS spectrum of compound 7k.....	295
Figure 166: IR spectrum of compound 7k.	296
Figure 167: ^1H -NMR (200 MHz, CDCl_3) spectrum of compound 7k.	297
Figure 168: ^{13}C $\{^1\text{H}\}$ NMR (50 MHz, CDCl_3) spectrum of compound 7k.....	298
Figure 169: ^{13}C $\{^1\text{H}\}$ DEPT-NMR (50 MHz, CDCl_3) spectrum of compound 7k. .	299
Figure 170: ESI-MS spectrum of compound 2g.....	300
Figure 171: IR spectrum of compound 2g.	301
Figure 172: ^1H -NMR (200 MHz, CDCl_3) spectrum of compound 2g.	302
Figure 173: ^{13}C $\{^1\text{H}\}$ NMR (50 MHz, CDCl_3) spectrum of compound 2g.....	303
Figure 174: ^{13}C $\{^1\text{H}\}$ DEPT-NMR (50 MHz, CDCl_3) spectrum of compound 2g. .	304
Figure 175: ESI-MS spectrum of compound 3g.....	305
Figure 176: IR spectrum of compound 3g.	306
Figure 177: ^1H -NMR (200 MHz, CDCl_3) spectrum of compound 3g.	307
Figure 178: ^{13}C $\{^1\text{H}\}$ NMR (50 MHz, CDCl_3) spectrum of compound 3g.....	308
Figure 179: ^{13}C $\{^1\text{H}\}$ DEPT-NMR (50 MHz, CDCl_3) spectrum of compound 3g. .	309
Figure 180: ESI-MS spectrum of compound 4g.....	310
Figure 181: IR spectrum of compound 4g.	311
Figure 182: ^{13}C $\{^1\text{H}\}$ DEPT-NMR (200 MHz, CDCl_3) spectrum of compound 4g.	312
Figure 183: ^{13}C $\{^1\text{H}\}$ NMR (50 MHz, CDCl_3) spectrum of compound 4g.....	313
Figure 184: ^{13}C $\{^1\text{H}\}$ DEPT-NMR (50 MHz, CDCl_3) spectrum of compound 4g. .	314
Figure 185: ESI-MS spectrum of compound 5g.....	315
Figure 186: IR spectrum of compound 5g.	316
Figure 187: ^1H -NMR (200 MHz, CDCl_3) spectrum of compound 5g.	317
Figure 188: ^{13}C $\{^1\text{H}\}$ NMR (50 MHz, CDCl_3) spectrum of compound 5g.....	318
Figure 189: ^{13}C $\{^1\text{H}\}$ DEPT-NMR (50 MHz, CDCl_3) spectrum of compound 5g. .	319
Figure 190: ESI-MS spectrum of compound 5m.....	320
Figure 191: IR spectrum of compound 5m.	321
Figure 192: ^1H -NMR (200 MHz, CDCl_3) spectrum of compound 5m.	322
Figure 193: ^{13}C $\{^1\text{H}\}$ NMR (50 MHz, CDCl_3) spectrum of compound 5m.....	323
Figure 194: ^{13}C $\{^1\text{H}\}$ DEPT-NMR (50 MHz, CDCl_3) spectrum of compound 5m.	324
Figure 195: ESI-MS spectrum of compound 7m.....	325

Figure 196: IR spectrum of compound 7m.	326
Figure 197: ^1H -NMR (200 MHz, CDCl_3) spectrum of compound 7m.	327
Figure 198: ^{13}C $\{^1\text{H}\}$ NMR (50 MHz, CDCl_3) spectrum of compound 7m.....	328
Figure 199: ^{13}C $\{^1\text{H}\}$ DEPT-NMR (50 MHz, CDCl_3) spectrum of compound 7m.	329
Figure 200: ESI-MS spectrum of compound 6m.....	330
Figure 201: IR spectrum of compound 6m.	331
Figure 202: ^1H -NMR (200 MHz, Acetone- d_6) spectrum of compound 6m.....	332
Figure 203: ^{13}C $\{^1\text{H}\}$ NMR (50 MHz, Acetone- d_6) spectrum of compound 6m.	333
Figure 204: ^{13}C $\{^1\text{H}\}$ DEPT-NMR (50 MHz, Acetone- d_6) spectrum of compound 6m.	334
Figure 205: ESI-MS spectrum of compound 8m.....	335
Figure 206: IR spectrum of compound 8m.	336
Figure 207: ^1H -NMR (200 MHz, CDCl_3) spectrum of compound 8m.	337
Figure 208: ^{13}C $\{^1\text{H}\}$ NMR (50 MHz, CDCl_3) spectrum of compound 8m.	338
Figure 209: ^{13}C $\{^1\text{H}\}$ DEPT-NMR (50 MHz, CDCl_3) spectrum of compound 8m.	339

List of Tables

Table 1: Biological activities of stevioside.	3
Table 2: Diverse types of biological activities of diterpenes.	7
Table 3: Biological activities of Kaurene, <i>ent</i> -kaurene, beyerane, <i>ent</i> -beyerane....	9
Table 4: Cytotoxicity results of pyrazole and pyrazoline derivatives of isosteviol (IC_{50} , $\mu\text{g/mL}$).	13
Table 5: Cytotoxicity of ester derivatives of steviol (21) and isosteviol (22) (IC_{50} , $\mu\text{g/mL}$).	15
Table 6: Cytotoxicity of isosteviol derivatives (IC_{50} , $\mu\text{g/mL}$).	17
Table 7: Cytotoxicity results of isosteviol derivative (24) and (IC_{50} , $\mu\text{g/mL}$).	18
Table 8: Cytotoxicity of isosteviol derivative against cancer cells line (IC_{50} , $\mu\text{g/mL}$)	19
Table 9: Cytotoxicity of steviol, isosteviol derivative and their (IC_{50} , $\mu\text{g/mL}$).	21
Table 10: Cytotoxicity of stevioside, steviol and isosteviol dimeric amide (IC_{50} , $\mu\text{g/mL}$).	22
Table 11: Inhibition activities of isosteviol derivatives against α -glycosidase (IC_{50} , μM).	25
Table 12: Antimicrobial activities of stevioside analogs (IC_{50} , $\mu\text{g/mL}$).	27
Table 13: Antimicrobial activities of isosteviol derivatives (IC_{50} , $\mu\text{g/mL}$).	29
Table 14: MIC 50 $\mu\text{g/mL}$ value of different derivative of steviol and isosteviol.	32
Table 15: Anti-viral activities of isosteviol analogues (IC_{50} , $\mu\text{g/mL}$).	37
Table 16: Anti-malarial activity of the tested samples (IC_{50} , $\mu\text{g/mL}$, mean \pm SD).	119
Table 17: <i>In vitro</i> biological activity of isosteviol derivatives on <i>T. cruzi</i>	123
Table 18: <i>In vitro</i> activity of isosteviol and 17-hydroxy isosteviol derivatives in <i>Leishmaniasis</i> species (IC_{50} , $\mu\text{g/mL}$).	124
Table 19: Docking results of isosteviol derivatives with sortase (Srt) proteins of the <i>C. diphtheria</i>	127
Table 20: ^1H NMR chemical shifts (δ , ppm), for compounds 1a-1d : multiplicity and coupling constants (Hz).....	150

Table 21: ¹ H NMR chemical shifts (δ, ppm), for compounds 1e–2h : multiplicity and coupling constants (Hz).....	151
Table 22: ¹ H NMR chemical shifts (δ, ppm), for compounds 4h–5j : multiplicity and coupling constants (Hz).....	152
Table 23: ¹ H NMR chemical shifts (δ, ppm), for compounds 5k–2b : multiplicity and coupling constants (Hz).....	153
Table 24: ¹ H NMR chemical shifts (δ, ppm), for compounds 2c-3f : multiplicity and coupling constants (Hz).....	154
Table 25: ¹ H NMR chemical shifts (δ, ppm), for compounds 6j-6i : multiplicity and coupling constants (Hz).....	155
Table 26: ¹ H NMR chemical shifts (δ, ppm), for compounds 2g-6m : multiplicity and coupling constants (Hz).....	156
Table 27: ¹ H NMR chemical shifts (δ, ppm), for compounds 7k-6k : multiplicity and coupling constants (Hz).....	157
Table 28: ¹ H NMR chemical shifts (δ, ppm), for compounds 3a-3h : multiplicity and coupling constants (Hz).....	158
Table 29: ¹ H NMR chemical shifts (δ, ppm), for compounds 4g-8m : multiplicity and coupling constants (Hz).....	159
Table 30: ¹³ C NMR chemical shifts (δ, ppm) for compounds 1a—5n	160
Table 31: ¹³ C NMR chemical shifts (δ, ppm) for compounds 5j—6j	161
Table 32: ¹³ C NMR chemical shifts (δ, ppm) for compounds 5l—4f	162
Table 33: ¹³ C NMR chemical shifts (δ, ppm) for compounds 3a—8m	163

List of schemes

Scheme 1: Semi synthesis of compound 1a, 1b, 1c, 2a, 2b, 2c, 3a, 3b, 3c.....	144
Scheme 2: Semi synthesis of compound, 1d, 1e, 1f, 2d, 2f, 2g, 3g,.....	145
Scheme 3: Semi synthesis of compound, 3f, 4f, 4g, 5g.....	146
Scheme 4: Semi synthesis of compound 1h, 2h, 3h, 4h	147
Scheme 5: Semi synthesis of compound, 5i, 5j, 5k, 5l, 5n, 6i, 6j, 6k, 7k.....	148
Scheme 6: Semi synthesis of compound 5m, 6m, 7m, 8m	149

List of abbreviations and acronyms

δ : Chemical shift

$\lambda_{\text{m\acute{a}x}}$: wavelength (nm) of maximum absorption

TLC: thin layer chromatography

CCDC: Centrifugal thin-layer chromatography

HPLC: high performance liquid chromatography

HPLC: RP: reverse phase high performance liquid chromatography

d: doublet

DEPT: Distortionless Enhancement by Polarization Transfer

D-gal: D-galactose

D-glc: D-glucose

MS: mass spectrometry

EI-MS : mass spectrometry electron impact.

Hz: hertz

m: multiplet

ppm : part per million

q : quartet

Rf : Retention Factor

^{13}C NMR: Nuclear Magnetic Resonance Carbon-13

^1H NMR: nuclear magnetic resonance proton

s: singlet

t: triplet

SUMMARY

<u>LIST OF SCHEMES</u>	XVII
------------------------------	------

<u>LIST OF ABBREVIATIONS AND ACRONYMS</u>	XVIII
---	-------

<u>1 INTRODUCTION</u>	1
-----------------------------	---

1.1 NATURAL PRODUCTS IN DRUG DISCOVERY	1
--	---

1.2 STEVIOSIDE.....	3
---------------------	---

1.3 DITERPENES	3
----------------------	---

1.3.1 TETRACYCLIC TERPENOIDS	7
------------------------------------	---

1.3.2 ISOSTEVIOL AND STEVIOL	10
------------------------------------	----

1.3.2.1 BIOLOGICAL ACTIVITY OF STEVIOL, ISOSTEVIOL, AND THEIR DERIVATIVES.....	10
---	----

<u>2 OBJECTIVES</u>	38
---------------------------	----

2.1 GENERAL OBJECTIVES.....	38
-----------------------------	----

2.2 SPECIFIC OBJECTIVES.....	38
------------------------------	----

2.2.1 PREPARATION OF STEVIOL AND ISOSTEVIOL SEMI SYNTHETIC DERIVATIVES BY CHEMICAL METHOD TARGETING, AT C15, C16 AND C19.	38
---	----

2.2.2 EVALUATION OF ANTITUMOR ACTIVITIES AGAINST SELECTED HUMAN CANCER CELL LINE SUCH AS LUNG CARCINOMA (A549), HUMAN BRAIN GLIOMA CELL LINES (T98MG), HUMAN GLIOBLASTOMA-ASTROCYTOMA, EPITHELIAL-LIKE CELL LINE (U8MG).	38
--	----

2.2.3 EVALUATION OF ANTI-MALARIAL ACTIVITY OF ANALOGUES BY THE METHODS OF 3 [H] -HIPOXANTINA AND LACTATE DEHYDROGENASE (LDH).	38
---	----

2.2.4 EVALUATION OF ANTI-TRYPANOSOMAL ACTIVITY OF DERIVATIVES BY MTT [3-(4, 5-DIMETHYLTHIAZOL-2-YL)-2,5-DIPHENYLTETRAZOLIUM BROMIDE].	38
---	----

2.2.5 EVALUATION OF ANTI-LEISHMANICIDAL ACTIVITY OF DERIVATIVES BY MTT [3-(4, 5-DIMETHYLTHIAZOL-2-YL)-2, 5-DIPHENYLTETRAZOLIUM BROMIDE].....	38
---	----

2.2.6 EVALUATION OF ANTI- <i>CORYNEBACTERIUM DIPHTHERIAE</i> ACTIVITY.	38
---	----

3	EXPERIMENTAL	39
3.1	INSTRUMENTATION.....	39
3.1.1	CHROMATOGRAPHY	39
3.1.2	SOLVENTS.....	39
3.2	SEMI SYNTHESIS OF THE STEVIOSIDE DERIVATIVES.....	40
3.2.1	PREPARATION OF ISOSTEVIOL (1A)	40
3.2.1	GENERAL PROCEDURE FOR PREPARATION OF 16-HYDROXY DERIVATIVES OF ISOSTEVIOL AND 17-HYDROXY ISOSTEVIOL.....	41
3.2.1.1	16-HYDROXY ISOSTEVIOL (1b).....	41
3.2.1.2	17, 16-DIHYDROXY ISOSTEVIOL (5i)	42
3.2.2	GENERAL PROCEDURE FOR THE PREPARATION OF 16-OXIME OF ISOSTEVIOL AND 17-HYDROXY ISOSTEVIOL.....	42
3.2.2.1	ISOSTEVIOL 16-OXIME (1c).....	43
3.2.2.2	17-HYDROXY, 16-OXIME OF ISOSTEVIOL (5j)	44
3.2.2.3	ISOSTEVIOL LACTONE (1d).....	44
3.2.3	GENERAL PROCEDURE FOR THE PREPARATION OF 15A-HYDROXY METHYL, 16B-HYDROXY OF ISOSTEVIOL AND 17-HYDROXY ISOSTEVIOL ..	45
3.2.3.1	15 α -HYDROXY METHYL, 16 β -HYDROXY OF ISOSTEVIOL (1e)	46
3.2.3.2	15 α -HYDROXY METHYL, 16 β -HYDROXY OF 17-HYDROXY ISOSTEVIOL (5n).....	46
3.2.4	STEVIOL (1H).....	47
3.2.5	STEVIOL EPOXIDE (2H).....	48
3.2.6	17-HYDROXY ISOSTEVIOL (4H).....	49
3.2.7	GENERAL PROCEDURE FOR THE PREPARATION OF BENZYL ESTER OF ISOSTEVIOL AND ITS DERIVATIVES	50
3.2.7.1	BENZYL ESTER OF ISOSTEVIOL (2a).....	50
3.2.7.2	BENZYL ESTER OF 16-HYDROXY ISOSTEVIOL (2b).....	51
3.2.7.3	BENZYL ESTER OF 16-OXIME ISOSTEVIOL (2c)	51
3.2.7.4	BENZYL ESTER OF ISOSTEVIOL LACTONE (2d)	52
3.2.7.5	BENZYL ESTER OF 17-HYDROXY ISOSTEVIOL (5l)	53

3.2.7.6	BENZYL ESTER OF 17, 16-DIHYDROXY ISOSTEVIOL (6i)	53
3.2.7.7	BENZYL ESTER OF 17-HYDROXY, 16-OXIME ISOSTEVIOL (6j)	54
3.3	GENERAL PROCEDURE FOR THE PREPARATION OF <i>p</i> -METHOXY PHENACYL ESTER	55
3.3.1	<i>p</i> -METHOXY PHENACYL ESTER OF ISOSTEVIOL (3A).....	55
3.3.2	<i>p</i> -METHOXY PHENACYL ESTER OF 16-HYDROXYL ISOSTEVIOL (3B)..	56
3.3.3	<i>p</i> -METHOXY PHENACYL ESTER OF 16-OXIME ISOSTEVIOL (3c).....	57
3.3.4	<i>p</i> -METHOXY PHENACYL ESTER OF STEVIOL (3H).....	58
3.4	GENERAL PROCEDURE FOR THE PREPARATION OF 16-HYDRAZONE..	58
3.4.1	16-HYDRAZONE OF ISOSTEVIOL (1F).....	59
3.4.2	16-HYDRAZONE OF 17-HYDROXY, ISOSTEVIOL (5k).....	59
3.4.3	16-HYDRAZONE BENZYL ESTER OF ISOSTEVIOL (3F)	60
3.4.4	16-HYDRAZONE BENZYL ESTER OF 17-HYDROXY, ISOSTEVIOL (6k)	61
3.5	GENERAL PROCEDURE FOR THE PREPARATION OF ISOPROPYL HYDRAZONE.....	61
3.5.1	ISOPROPYL HYDRAZONE OF ISOSTEVIOL (2F)	62
3.5.2	ISOPROPYL HYDRAZONE BENZYL ESTER OF ISOSTEVIOL (4F)	62
3.5.3	16-ISOPROYL HYDRAZONE BENZYL ESTER OF 17-HYDROXY ISOSTEVIOL (7k)	63
3.6	PROCEDURE FOR THE PREPARATION OF 2, 4 DINITRO PHENYL AND 4-NITRO PENYL HYDRAZONE OF ISOSTEVIOL AND ITS DERIVATIVES	64
3.6.1	2, 4-DINITRO PHENYL HYDRAZONE OF ISOSTEVIOL (2G).....	64
3.6.2	4-NITRO PHENYL HYDRAZONE OF ISOSTEVIOL, (3G)	65
3.6.3	2, 4-DINITRO PHENYL HYDRAZONE BENZYL ESTER OF ISOSTEVIOL (4G)	66
3.6.4	4-NITRO PHENYL HYDRAZONE BENZYL ESTER OF ISOSTEVIOL (5G).	67

3.6.5	2, 4-DINITRO PHENYL HYDRAZONE OF 17-HYDROXY ISOSTEVIOL (5M)	68
3.6.6	2, 4-DINITRO PHENYL HYDRAZONE BENZYL ESTER OF 17-HYDROXY ISOSTEVIOL (7M)	69
3.6.7	4-NITROPHENYL HYDRAZONE OF 17-HYDROXYISOSTEVIOL (6M)..	70
3.6.8	4-NITRO PHENYL HYDRAZONE BENZYL ESTER OF 17-HYDROXY ISOSTEVIOL (8M)	71
3.7	BIOLOGICAL ACTIVITIES	72
3.7.1	ANTI-MALARIAL ACTIVITIES.....	72
3.7.2	ANTI-TUMOR ACTIVITIES	73
3.7.2.1	MATERIAL METHOD.....	73
3.7.2.2	SOLUTIONS, CULTURE MEDIA AND MATERIALS	74
3.7.2.3	CULTURE MEDIA, CELL LINES AND CULTURE CONDITIONS.....	74
3.7.2.4	EVALUATION OF CELL VIABILITY MTT METHOD	75
3.7.3	ANTI- <i>TRYPANOSOMA CRUZI</i> ACTIVITIES.....	75
3.7.3.1	VERO CELLS AND PARASITES	76
3.7.3.2	BIOLOGICAL ASSAYS	77
3.7.3.3	CYTOTOXICITY ASSAYS	77
3.7.4	ANTI-LEISHMANIASIS ACTIVITIES.....	77
3.7.4.1	STRAIN OF PARASITE AND CELL CULTURE	78
3.7.4.2	ASSAY SUSCEPTIBILITY OF PROMASTIGOTE FORMS.....	78
3.7.4.3	TREATMENT <i>IN VITRO</i>	78
3.7.4.4	VIABILITY ASSAY	79
3.7.4.5	STATISTICAL ANALYSIS	79
3.7.5	ANTI- <i>CORYNEBACTERIUM DIPHTHERIAE</i> ACTIVITIES	80
4	<u>RESULTS AND DISCUSSION.....</u>	82
4.1	ISOSTEVIOL (1A).....	82
4.2	16-HYDROXY ISOSTEVIOL (1B)	83
4.3	17, 16-DIHYDROXY ISOSTEVIOL (5i).....	84

4.4	16-OXIME OF ISOSTEVIOL (1c)	84
4.5	17-HYDROXY, 16-OXIME OF ISOSTEVIOL (5J)	85
4.6	ISOSTEVIOL LACTONE (1D).....	86
4.7	15A-HYDROXY METHYL-16B-HYDROXY ISOSTEVIOL (1E)	87
4.8	15A-HYDROXYMETHYL, 17, 16B-DIHYDROXY ISOSTEVIOL (5N).....	88
4.9	STEVIOL (1H).....	89
4.10	STEVIOL EPOXIDE (2H)	90
4.11	17-HYDROXY ISOSTEVIOL (4H).....	91
4.12	BENZYL ESTER OF ISOSTEVIOL (2A).....	91
4.13	BENZYL ESTER OF 16-HYDROXY ISOSTEVIOL (2B)	92
4.14	BENZYL ESTER OF 16-OXIME ISOSTEVIOL (2c)	93
4.15	BENZYL ESTER OF ISOSTEVIOL LACTONE (2D).....	94
4.16	BENZYL ESTER OF 17-HYDROXY ISOSTEVIOL (5L)	95
4.17	BENZYL ESTER OF 17, 16-DIHYDROXY ISOSTEVIOL (6i)	96
4.18	BENZYL ESTER OF 17-HYDOXY, 16-OXIME ISOSTEVIOL (6J).....	97
4.19	<i>P</i> -METHOXYPHENACYL ESTER OF ISOSTEVIOL (3A)	98
4.20	<i>P</i> -METHOXY PHENACYL ESTER OF 16-HYDROXY ISOSTEVIOL (3B) ...	99
4.21	<i>P</i> -METHOXY PHENACYL ESTER OF 16-OXIME ISOSTEVIOL (3c)	100
4.22	<i>P</i> -METHOXY PHENACYL ESTER OF STEVIOL (3H).....	101
4.23	16-HYDRAZONE OF ISOSTEVIOL (1F).....	102
4.24	17-HYDROXY, 16-HYDRAZONE OF ISOSTEVIOL (5k)	103
4.25	BENZYL ESTER 16-HYDRAZONE OF ISOSTEVIOL (3F)	104
4.26	BENZYL ESTER 16-HYDRAZONE 17-HYDROXY ISOSTEVIOL (6k)	105
4.27	16-ISOPROPYL HYDRAZONE OF ISOSTEVIOL (2F)	106
4.28	16-ISOPROPYL HYDRAZONE BENZYL ESTER OF ISOSTEVIOL (4F)..	107
4.29	16-ISOPROYL HYDRAZONE BENZYL OF 17-HYDROXY ISOSTEVIOL- ESTER (7K).....	108
4.30	2, 4-DINITRO PHENYL HYDRAZONE OF ISOSTEVIOL (2G).....	109
4.31	4-NITRO PHENYL HYDRAZONE OF ISOSTEVIOL (3G)	110
4.32	2, 4-DINITRO PHENYL HYDRAZONE BENZYL ESTER ISOSTEVIOL (4G)	111

4.33	4-NITRO PHENYL HYDRAZONE BENZYL ESTER ISOSTEVIOL (5G)....	112
4.34	2, 4-DINITRO PHENYL HYDRAZONE 17-HYDROXY ISOSTEVIOL (5M)	113
4.35	2, 4-DINITRO PHENYL HYDRAZONE BENZYL ESTER 17-HYDROXY ISOSTEVIOL (7M)	114
4.36	4-NITRO PHENYL HYDRAZONE 17-HYDROXY OF ISOSTEVIOL (6M)..	115
4.37	4-NITRO PHENYL HYDRAZONE BENZYL ESTER 17-HYDROXY ISOSTEVIOL (8M)	116
4.38	BIOASSAYS.....	118
4.38.1	ANTIMALARIAL ACTIVITY	118
4.38.2	ANTI-TUMOR ACTIVITY.....	120
4.38.3	ANTI- <i>TRYPANOSOMA CRUZI</i> ACTIVITY	123
4.38.4	ANTI- <i>LEISHMANIASIS</i> ACTIVITY	124
4.38.5	DOCKING ANALYSIS WITH <i>CORYNEBACTERIUM DIPHTHERIAE</i> SORTASES PROTEINS	125
<u>5</u>	<u>CONCLUSION.....</u>	<u>130</u>
<u>6</u>	<u>REFERENCES.....</u>	<u>131</u>
<u>7</u>	<u>ANNEXES.....</u>	<u>144</u>
7.1	SCHEMES	144
7.2	¹ H NMR TABLE	150
7.3	¹³ C NMR TABLE.....	160
7.4	SPECTRA	164

1 INTRODUCTION

1.1 NATURAL PRODUCTS IN DRUG DISCOVERY

Drug discovery and development has a long history and dates back to the early days of human civilization. In those ancient times, drugs were not just used for physical remedies but were also associated with religious and spiritual healing.

Even today, after more than 100 years of research in pharmaceutical industries, there is still a great need for innovative drugs. Only one third of all diseases can be treated efficiently (Müller *et al.*, 2000). Analysis of the number and sources of anti-cancer and anti-infective agents, reported mainly in the Annual Reports of Medicinal Chemistry from 1984 to 1995. It was observed that over 60% of the approved drugs and pre-NDA (New Drug Applications), candidates (for the period 1989-1995), excluding biologics (vaccines, monoclonal antibody, etc. derived from mammalian sources), developed in these disease areas are of natural origin (Cragg *et al.*, 1997).

Nature itself has constantly supplied mankind with a broad and structurally diverse array of pharmacologically active compounds that continue to be utilized as highly effective drugs to combat a multitude of deadly diseases or as lead structures for the development of novel synthetically derived drugs that mirror their models from nature (Proksch *et al.*, 2002). The ancient medical literature reports that when surgery was performed the physicians also recommended the use of some natural, and especially plant products, which represent an interesting point of comparison with current knowledge. Natural products play a key role in the discovery of leads for the development of drugs for the treatment of human disease. The world of plants, and indeed all natural source represents a virtually untapped reservoir of novel drugs (Newman & Cragg, 2007). Natural products play a significant role in cancer therapy today with substantial numbers

of anti-cancer agents used in the clinic being either natural or derived from natural products from various sources such as plants, animals and microorganisms. Large-scale anticancer drug discovery and screening programs such as those promoted by the National Cancer Institute (NCI) have played an important role in the development of anticancer natural compounds (Stefania *et al.*, 2009).

In this background a proposed multidisciplinary approach is important for drug discovery involving a new generation of molecular diversity from natural origin, along with total combinatorial synthesis and optimizing their biosynthetic pathways (Newman *et al.*, 2003). On the basic skeleton of natural products it's feasible to design and facilitates combinatorial libraries with new modified structure and remedial potential and once a biologically active compound is obtained, from natural ancestor and its structure is establish. The basic skeleton of the molecule show the pharmacophore of the molecule and suggest modifications to additional groups attached to it. Most of the natural products compounds have different functional groups such as hydroxyl, group's double bonds, and carbonyl groups etc, which are likely to be modified by simple reaction. With these modifications we can obtain information about the importance of modified activity group in the molecule and also the importance of some effects as changes in hydrophobicity, elimination of donor group hydrogen bonds, changing the electron density of certain groups,(Filho, 2000, Nielsen, 2002).

Developing a new drug from original idea to the launch of a finished product is a complex procedure which can take long time from the discovery to the stage of development. During this long procedure some factors must be considered, such as process: structural simplicity, with possible modifications in order to optimize their pharmacotherapeutic profile, and has good pharmacokinetic properties such as absorption, distribution, metabolism, excretion and toxicity (Lima, 2007).

1.2 STEVIOSIDE

Stevioside is a natural glycoside of steviol found in the leaves of *Stevia rebaudiana* Bertoni. It is used as a low-calorie sugar alternative in foods (Hanson & De oliveira., 1993). Stevia is an herb that belongs to the *Asteraceae* family. Besides its edulcorant properties stevioside also has diverse biological activities described in literature, some of them are outlined in Table 1.

Table 1: Biological activities of stevioside.

Biological activities	Reference
anti-hyperglycemic	Gregersen et al., 2004 ; Cekic et al., 2011 ,
anti-hypertensive effect	Hsu et al., 2002
anti-inflammatory & immunomodulatory	Boonkaewwan et al., 2006
anti-amnesic	(Sharma et al., 2010)
anti-viral	(Takahashi et al., 2001)
anti-cancer	(Nakamura et al., 1995 ; Paul et al., 2012)
anti-tuberculosis	(Sharipova et al., 2011)
anti-bacterial	(Tomita et al., 1997)
anti-atherosclerosis	(Geeraert et al., 2010)

1.3 DITERPENES

Diterpenoids constitute an immense class of isoprenoid natural products, biosynthesized from four unit of mevalonic acid through 2E, 6E, 10E-geranylgeranyl pyrophosphate (GGPP). They are secondary metabolite and widely distributed in plants and fungi. They are classified as

- 1) Acyclic diterpenoids such as *E*-eleanonal (1) eleanoic acid (2).

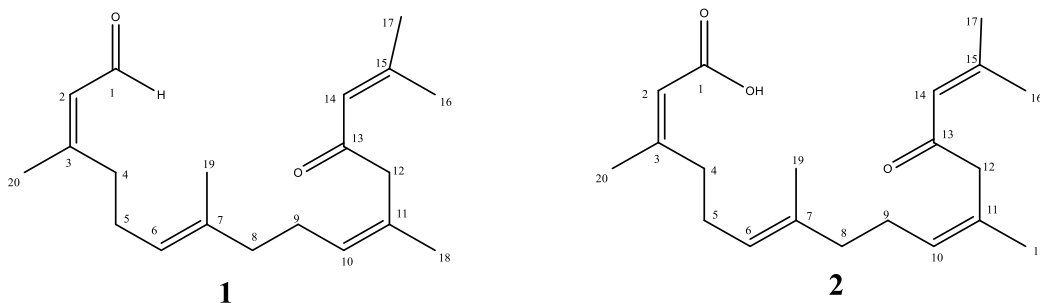


Figure 1: Chemical structure of *E*-eleanonal (1) eleanoic acid (2).

- 2) Monocyclic diterpenoids such as infuscatrienol (3), jaspaquinol (4).

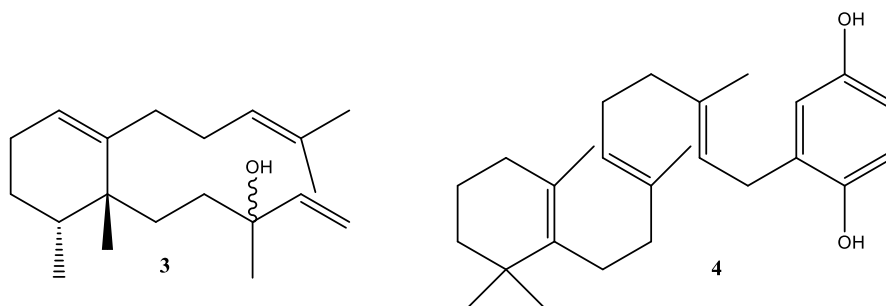


Figure 2: Chemical structure of infuscatrienol (3) Jaspaquinol (4).

- 3) Bicyclic diterpenoids such as Z-abienol (5) labdene diol (6).

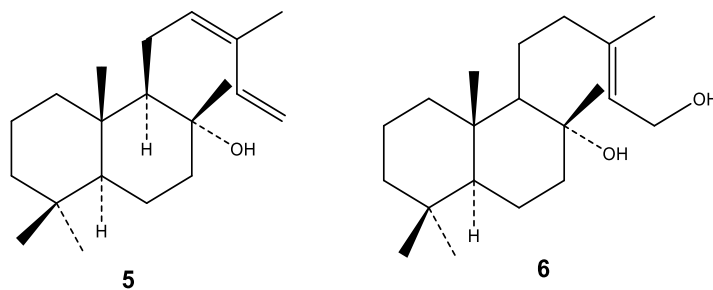


Figure 3: Chemical structure of Z-abienol (5) labdene diol (6).

- 4) Tricyclic diterpenoids such as pimaranes (7) and abietanes (8)

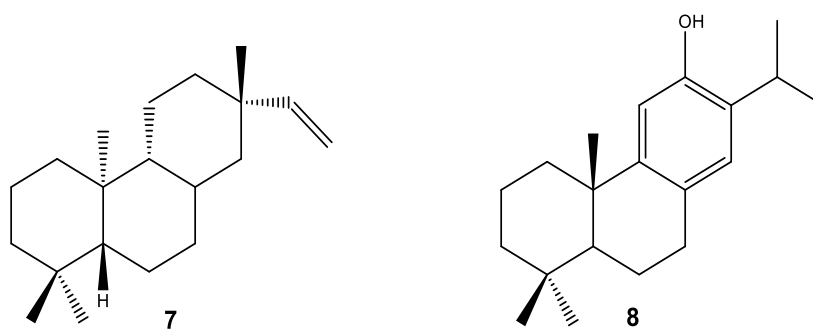


Figure 4: Chemical structure of Pimarane (7), Abietanes (8).

- 5) Tetracyclic diterpenoid are Beyerane (9), Kaurane (10).

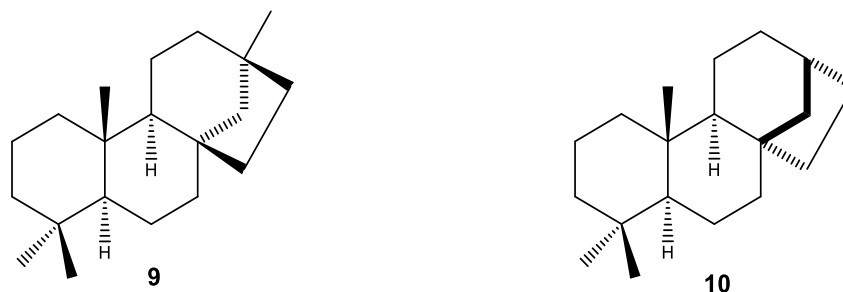


Figure 5: Chemical structure of Beyerane (9), Kaurane (10).

- 6) Macro cyclic diterpenes Tasumatrols (11), Echinoic acid (12).

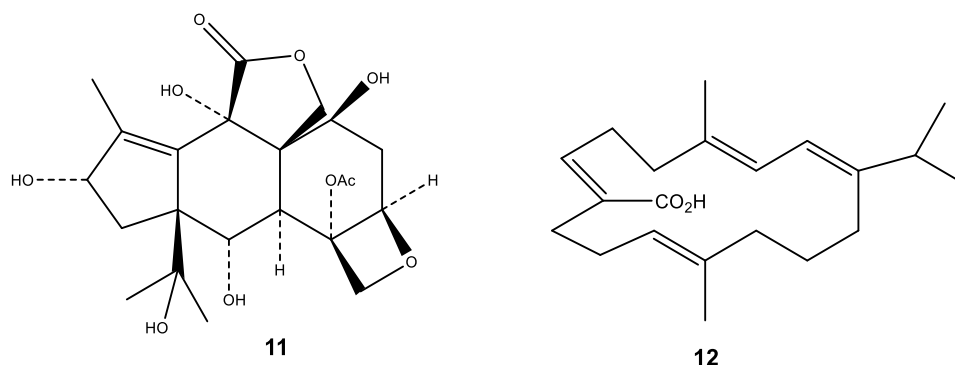


Figure 6: Chemical structure of Tasumatrols (11), Echinoic acid (12).

Diterpenes have drawn increasing attention because of their provoking biological activities and for being is a rich reservoir of compounds for drug discovery and their derivatives possess interesting biological activities. Although thousands of diterpenes compounds have been described in literature from terrestrial and marine organism, only few of them are clinically effective. Some of their biological activities described in literature are listed in Table 2, page 7.

Table 2: Diverse types of biological activities of diterpenes.

Biological activities	Reference
anti-inflammatory	(Chen et al., 2010 ; Chatter et al., 2011 ; Kim et al., 2013 ; Liu et al., 2014)
hepatoprotective	(Jain et al., 2000)
analgesic	(HernandezPerez et al., 1995 ; Wang et al., 2009)
anti-microbial	(Rodriguezlinde et al., 1994 ; Mendoza et al., 1997 ; Murthy et al., 2005 ; Tatsimo et al., 2005 ; Mothana et al., 2009)
anti-mycotic	(Cotoras et al., 2001 ; Yang et al., 2003),
immunomodulatory	(Ayatollahi et al., 2010 ; Aachoui & Ghosh, 2011 ; Lin et al., 2013)
anti-hepatitis	(Yang et al., 2011)
anti-malarial	(Lane et al., 2009 ; Stout et al., 2010)
anti-HIV	(Gustafson et al., 1991 ; de Souza Pereira et al., 2005 ; Bodiwala et al., 2009 ; Vidal et al., 2012 ; Asada et al., 2013)
anti-protozoal	(Mothana et al., 2014),
anti-spasmodic	(Tirapelli et al., 2008)
molluscicidal	(Tringali et al., 1986)
cytostatic and cytotoxic effects	(Kubanek et al., 2005 ; Chen et al., 2011 ; Tai et al., 2013)

1.3.1 TETRACYCLIC TERPENOIDS

The kauranes and beyeranes are important tetracyclic naturally occurring molecules with high biological potential, low water solubility having a rigid tetracyclic skeleton with a per-hydrophenanthrene moiety (rings A, B and C),

fused with a cyclopentane ring (D), at C8 and C13. The nomenclature, stereochemistry and numbering style for skeleton of kaurene (13), *ent*-kaurene (14), beyerane (15), *ent*-beyerane (16), have already been assigned by the IUPAC (García *et al.*, 2007)

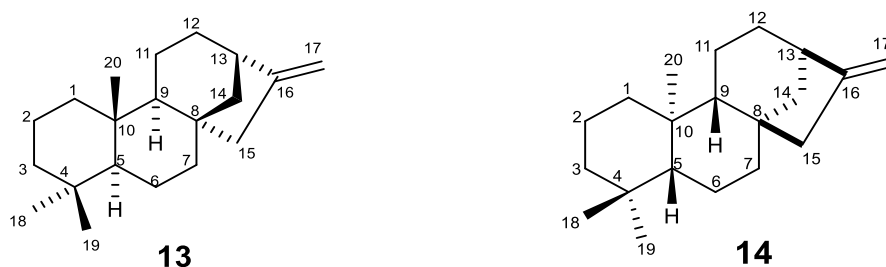


Figure 7: Chemical structures of kaurene (13), *ent*-kaurene (14).

Kaurane diterpenes are commonly found in several species of plants belonging to numerous families such as *Asteraceae* (Le Quesne *et al.*, 1985; Kos *et al.*, 2006), *Annonaceae* (Quijano *et al.*, 1982; Chang *et al.*, 1998), *Euphorbiaceae* (Jia *et al.*, 1994; Jahan *et al.*, 2004), *Celastraceae* (Duan *et al.*, 1999), *Apiaceae* (Somova *et al.*, 2001), *Velloziaceae* (Somova, Shode, Moodley & Govender, 2001), *Lamiaceae* (Ghoumari *et al.*, 2005; LiLiLi *et al.*, 2006), *Fabaceae* (Cunha *et al.*, 2003), *Chrysobalanaceae* (Braca *et al.*, 2005), *Jungermanniaceae* (Kondoh *et al.*, 2005), *Rhizophoraceae* (Han *et al.*, 2004; Han *et al.*, 2005), (*Bruguiera* spp.). Sun *et al.* described about 518 diterpenoids isolated specially with oxygenated and non oxygenated *ent kaurene* skeleton from isodon species (Sun *et al.*, 2006).

Kaurene and *ent*-kaurene, its chemically semi-synthetic and biotransformed product have attracted increasing attention because of their remarkably broad spectrum of biological activities. Some of their derivatives are found to possess interesting *in vitro* biological activities; some of them are described in Table 3.

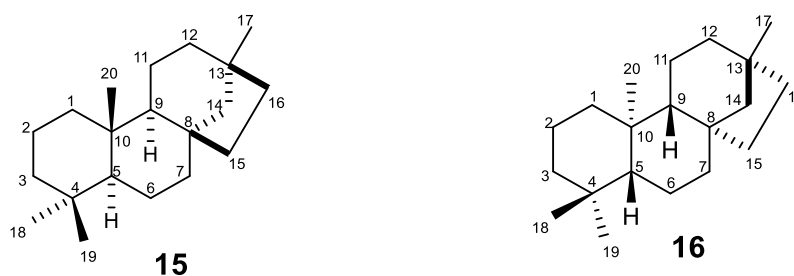


Figure 8: Chemical structure of beyerane (15), *ent*-beyerane (16).

Table 3: Biological activities of Kaurene, *ent*-kaurene, beyerane, *ent*-beyerane.

Biological activities	Reference
Anti-spasmodic	(Aguiar et al., 2012)
Anti-allergic	(Cheenpracha et al., 2006)
Anti-proliferative	(Fatope et al., 1996 ; Gui et al., 2004 ; Li et al., 2006 ; Ding et al., 2010 ; Ding et al., 2011 ; Lizarte Neto et al., 2013),
Anti-bacterial	(Velikova et al., 2000 ; Kubo et al., 2004)
Anti-acetyl cholinesterase	(Thirugnanasampandan et al., 2008)
Immunosuppressive	(Zhao et al., 2004),
Anti-microbial	(Rezende et al., 2000),
Anti-HIV	(Chang, Yang, Lin, Lee & Wu, 1998)
Plant growth regulating, anti-malarial	(Boampong et al., 2013)
Anti-trypomastigote	(Vieira et al., 2002 ; Harauchi et al., 2011)
Insect anti-feedant	(Bondi et al., 2000),
Hypotensive and anti-inflammatory	(Paiva et al., 2002)
Anti-cariogenic	(de Andrade et al., 2011)
Anti-convulsant	(Okoye et al., 2013)

1.3.2 ISOSTEVIOL AND STEVIOL

Isosteviol also known as *ent*-16-ketobeyeran-19-oic acid, is a tetracyclic beyerane diterpenoid synthesized via acid catalyzed Wagner-Meerwein rearrangement of steviol (AVENT *et al.*, 1989). While the steviol is the base catalyzed or enzymatic hydrolytic product of stevioside (OGAWA *et al.*, 1980, SHIBATA *et al.*, 1991). In the literature steviol, isosteviol and their derivatives show an impactful number of pharmacological effects, including anti-inflammatory, anti-hyperglycemic, anti-hypertensive, anti-inflammatory, anti-diarrheal, diuretic, and immunomodulatory actions (Chatsudthipong & Muanprasat, 2009), some synthetic novel derivatives of isosteviol showing anti-bacterial activity (Wu *et al.*, 2010), the hydrazide, hydrazone and phosphate groups show inhibition of *Mycobacterium tuberculosis* (H37Rv, *in vitro*) (Garifullin *et al.*, 2012).

1.3.2.1 BIOLOGICAL ACTIVITY OF STEVIOL, ISOSTEVIOL, AND THEIR DERIVATIVES

The interesting structural feature of steviol (17), isosteviol (18), and its broad spectrum of bioactivities attract researchers to make new modifications in the parent skeleton of these molecules. Positions C15, C16 of isosteviol and C19 have been the main target for chemical modification.

The carboxylic acid carbon (C19) of both compounds has been transformed into esters, amides, azides and reduced to alcohol.

The ketonic carbon (C16) of isosteviol has also been reduced to alcohol, and also converted into hydrazone, oxime, imine, amine etc. The methylene group of steviol has been hydrogenated and halogenated. The C15 of isosteviol has been halogenated, hydroxylated and also used for aldol type condensation etc, the same position of steviol has been hydroxylated (SeO₂).

The bioactivity of some derivatives of both compounds is described in the following section.

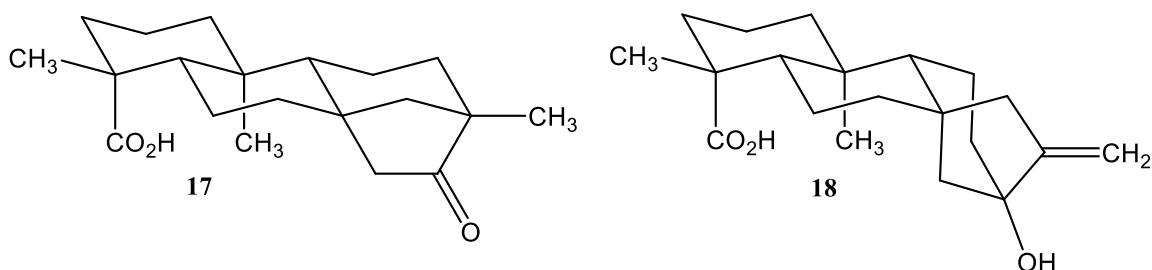


Figure 9: Chemical structure of isosteviol (17), steviol (18).

1.3.2.1.1 ANTI-TUMOR ACTIVITY

There are several reports in the literature describing the antitumor effects of isosteviol and steviol derivatives. Mizushina *et al.*, prepared biotransformed derivatives of isosteviol and studied their inhibitory properties towards both mammalian DNA polymerases (pols), and human DNA topoisomerase (topoII), the *in vitro* results shows that isosteviol with free carboxylic acid was found to inhibit the DNA polymerases (pols), (IC₅₀ 64.0 μ M) and human DNA topoisomerase (topoII) (IC₅₀ 190 μ M). The results were in assessment with other derivative shows that ketone and carboxylic acid is important for the inhibitory effect in mammalian DNA polymerases (pols) (Mizushina *et al.*, 2005).

S.-L. Zhu *et al.* synthesized a set of novel derivatives of isosteviol (Figure 10, page 12), with pyrazole (**19a-19o**, page 12), and pyrazoline (20, page 12), heterocyclic ring and *in vitro* bioassays of these derivatives were evaluated against four human cancer cells line such as Human Gastric cell line (SGC7901), adenocarcinoma human alveolar basal epithelial cells (A549), human Burkitt lymphoma cells (Raji), and Human Negroid cervix epitheloid carcinoma (Hela). The results are summarized in Table 4, page 13.

Mono halogenated pyrazole derivatives such as **19a_19f** (Table 4, page 13), showed slight changes in cytotoxicity value, when the position of halogen is changed from *ortho*, to *para* position while the *meta* halogenated such as **19c** and **19e** derivatives show potent cytotoxicity in Raji cell line. Mono methylated substituted pyrazole derivatives **19g_19i**. The compound **19h** was found inactive in four cell lines, while compound **19g** show moderate cytotoxicity in Raji and was inactive in other three cells line, derivative **19i** show moderate cytotoxicity in three cancer cells line but show potent cytotoxicity in (Raji), with IC_{50} 3.9 μ M.

Dihalogenated pyrazole derivatives **19j**, was found to be moderate cytotoxic in Raji while inactive in other cell line. Compound **19k** showed moderate cytotoxicity in A549 and Raji with 20.2 μ M and 27.6 μ M IC_{50} value and was found inactive in rest of two cell lines. Dimethylated pyrazole derivative such **19n** show moderate cytotoxicity in Raji with IC_{50} 11.1 μ M, while inactive in rest. Compound **19o** showed moderate cytotoxicity in Raji and Hela with IC_{50} 12.6 μ M and IC_{50} 30.3 μ M, was found inactive in other cell lines.

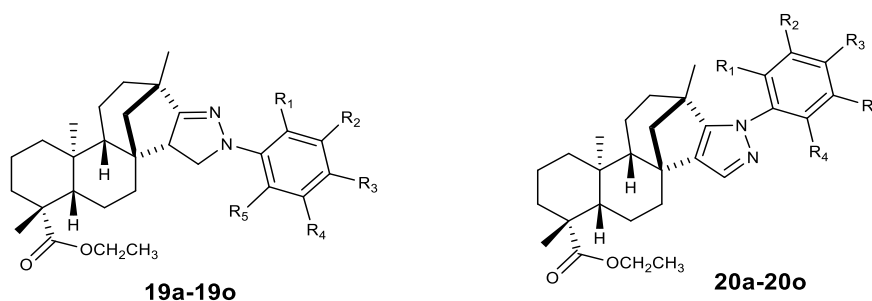


Figure 10: Chemical structure of pyrazole (19), pyrazoline (20), and derivatives of isosteviol.

Another set of halogenated and methylated pyrazoline derivatives of isosteviol (**20a-20o**) were synthesized and the results of cytotoxicity are listed in Table 4, page 13. The compound **20a**, **20b** and **20c** showed potent cytotoxicity while display moderate cytotoxicity in SGC7901 and A549 cell line and in Hela cell line.

Table 4: Cytotoxicity results of pyrazole and pyrazoline derivatives of isosteviol (IC_{50} , $\mu\text{g/mL}$).

	R1	R2	R3	R4	SGC7901	A549	Raji	Hela
19a	F	H	H	H	34.6	32.6	17.2	50
19b	H	F	H	H	50	50	29.1	50
19c	H	H	F	H	50	50	4.5	50
19d	Cl	H	H	H	50	50	50	50
19e	H	Cl	H	H	50	50	4.5	50
19f	H	H	Cl	H	50	50	50	50
19g	CH ₃	H	H	H	50	50	19.8	50
19h	H	CH ₃	H	H	50	50	50	50
19i	H	H	CH ₃	H	29.3	13.6	3.9	29
19j	F	H	F	H	50	50	13.5	50
19k	F	H	H	F	50	20.2	27.6	50
19l	Cl	H	Cl	H	50	50	22.4	50
19m	Cl	H	H	Cl	50	50	25.6	50
19n	CH ₃	H	CH ₃	H	50	50	11.1	50
19o	CH ₃	H	H	CH ₃	50	50	12.6	30.3
20a	F	H	H	H	35.6	26.9	4.1	50
20b	H	F	H	H	35.8	19.1	3.4	50
20c	H	H	F	H	25.5	22.3	7.0	50
20d	Cl	H	H	H	25.4	21.5	10.1	34.5
20e	H	Cl	H	H	26.3	28.2	9.5	50
20f	H	H	Cl	H	8.4	35.3	13.8	50
20g	CH ₃	H	H	H	35.3	19.0	7.7	15.1
20h	H	CH ₃	H	H	13.5	12.3	4.8	50
20i	H	H	CH ₃	H	34.9	18.8	8.6	50
20j	F	H	F	H	28.4	20.11	9.9	50
20k	F	H	H	F	50	50	7.1	50
20l	Cl	H	Cl	H	2.7	3.18	1.0	50
20m	Cl	H	H	Cl	50	50	11.7	50
20n	CH ₃	H	H	H	18.7	16.5	6.6	43.3
20o	CH ₃	H	H	CH ₃	32.9	17.0	7.9	34.3

The compounds **20e** and **20f** were found inactive in HeLa cell line and was moderate cytotoxic in SGC7901, A549 and Raji cell line. The compound **20d** showed moderate inhibitory effect in all four cell line. Methylated derivatives such as **20g**, **20h**, and **20i** showed better cytotoxicity in Raji cell line while **20g** was found moderate cytotoxic in rest of cell line. The compound **20h** and **20i** were found inactive in hela and moderate cytotoxic in rest of two cell lines. The compounds **20j** and **20k** show potent cytotoxicity in Raji, while **20j** showed moderate in rest of two cell lines SGC7901, A549, and were found inactive in HeLa cell line. The **20k** was found inactive in rest of three cell lines. Comparing the results of **20l** and **20m**, the analogue **20l** showed potent cytotoxicity in three cell lines SGC7901, A549 and Raji cell and was found inactive in hela. The compound **20m** showed moderate inhibition in Raji and was inactive in rest of three cell lines. The compound **20n** showed potent cytotoxicity in Raji and were moderate cytotoxic in rest of three cell line.

Comparatively the results in Table 4, page 13, showed that alkylated and halogenated pyrazole derivatives displayed much better cytotoxicity then pyrazoline derivatives of isosteviol (Zhu *et al.*, 2013)

Recently another research group Ukiya *et al.* synthesized a set of new acylated derivatives of steviol and isosteviol (Figure 11, page 15), at 19-o (carboxylic acid) site and these derivatives were *in vitro* screen for cytotoxicity in four human cancer line such as leukemia (hl60), lung (A549), stomach (AZ521), and breast (Sk-Br-3), cancer cell line. The results are listed in (Table 5, page 15). Steviol (**21a-21e**, page15), derivative **21a** and **21c** display potent inhibitory effect in selected cancer cell lines with IC_{50} value 5.3 μ M (HI60), 7.2 μ M (A549), 3.1 μ M (AZ521), 1.7 μ M (Sk-Br-3), for compound **21a**, while for **21c** the IC_{50} values 8.8 μ M (HI60), 2.9 μ M (A549), 1.1 μ M (AZ521), 2.2 μ M (Sk- Br-3). The compound **21b** and **21e** showed beneficial inhibitory effect in three lines, and moderately cytotoxic in HL60. The compound **21d** displayed moderate cytotoxicity in HI60, A549 and Az521, and was found beneficial cytotoxic in SK-Br-3. Isosteviol (**22a-22c**), the compound **22a** showed potent cytotoxicity in three

cell line with IC_{50} value 8.2 μM (A549), 1.2 μM (Az521), 2.4 μM (Sk-Br-3), while moderate cytotoxic in (HL60), cell line with IC_{50} value 24.0 μM .

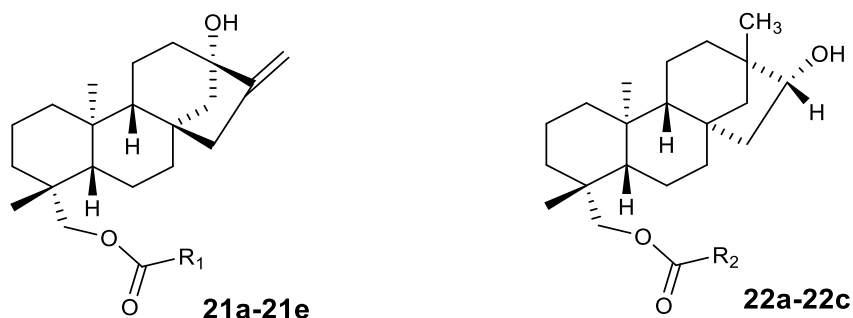


Figure 11: Chemical structure of steviol ester (21), isosteviol ester (22).

Table 5: Cytotoxicity of ester derivatives of steviol (21) and isosteviol (22) (IC_{50} , $\mu\text{g/mL}$).

	R_1/R_2	HL60	A549	AZ521	SKBR-3
21a	2-Me-C ₆ H ₄ CH=CH-	5.3	7.2	3.1	1.7
21b	3-Me-C ₆ H ₄ CH=CH-	15.9	6.0	2.9	4.7
21c	4-Me-C ₆ H ₄ CH=CH-	8.8	2.9	1.1	2.2
21d	Ph-CH ₂ CH ₂ -	56.2	17.0	29.0	9.4
21e	Ph-	41.3	4.3	2.5	2.2
22a	2MeC ₆ H ₄ CH=CH-	24	8.2	1.2	2.4
22b	3MeC ₆ H ₄ CH=CH-	64.4	>100	9.0	25.0
22c	4MeC ₆ H ₄ CH=CH-	20.3	>100	19.8	2.2

The compound **22b** was found to be inactive in A549 with IC_{50} greater than 100 μM and displayed moderate cytotoxicity in two cell line HL60 and SKBR-3 with IC_{50} value 64.4 μM and 25.0 μM , and was found potent cytotoxic in Az521 cell line (IC_{50} 9.0 μM). The **22c** analogue display potent inhibitory effect in

SkBr-3 with IC_{50} value 2.2 μM , while moderate cytotoxic in HL60 and Az521, and was found inactive in A549 cell line. The above results suggest 19-O acylated derivatives of steviol and isosteviol exhibited cytotoxicities, and it was found that *ortho* methylated aromatic derivatives of isosteviol and steviol display potent inhibition in the selected cancer cell line (Ukiya *et al.*, 2013).

T. Zhang *et al.*, synthesized a set of novel semi-synthetic polyhydroxy, oxime and amine, derivatives of isosteviol (Figure 12, page 17), and these analogues were *in vitro* evaluated in four human cancer cells line, such as esophageal carcinoma cell line (ec9706), human esophageal squamous, carcinoma (Eca-109), human-prostate lines (PC-3), and human colon cancer cells (HCT116). These modifications were made at C15 (R2) and C16 (X), (**23a-23h**, page 17). The results of cytotoxicity are listed in (Table 6, page 17). The compound **23h** display much higher cytotoxicity in selected four cancer cells lines with IC_{50} value 4.01 μM in (EC9706), 5.02 μM (Eca109), 15.31 μM (PC-3), 12.25 μM (HCT-116), while **23e** derivative showed moderate inhibitory effect with IC_{50} value 19.33 μM (EC9706), 41.32 μM (Eca109), 25.38 μM (PC-3), and 20.13 μM (HCT-116). These results demonstrate that the presence of NH_2 group either at C15 or C16 enhances the cytotoxicity of the precursor isosteviol. The compound **23b** was found moderately active in two cancer cells line with IC_{50} value 24.42 μM (EC9706), 26.52 μM while found inactive in (Eca109), >100 μM (PC-3), >100 μM (HCT-116), when the position of oxime and the hydroxyl group were exchanged between the C15 and C16 such as in compound **23c** the decrease of cytotoxicity was observed in EC9706 line (IC_{50} 56.64 μM), while increases in Eca109 (IC_{50} 17.87 μM), line and was found inactive in PC-3 (IC_{50} >100 μM), and HCT-116 line (IC_{50} >100 μM). The cytotoxicity of **23f** derivative display low IC_{50} 60.67 μM (EC9706), 69.55 μM (Eca109), and was found inactive in other two cells line. The thio amide derivative such as **23g** show low inhibitory effect with IC_{50} value 72.28 μM (Eca109), and was found inactive in three cell lines (Zhang *et al.*, 2012).

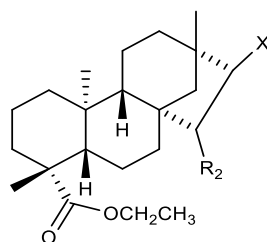
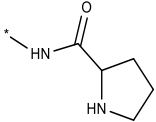
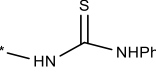
**23a-23h**

Figure 12: Chemical structure of Isosteviol derivatives (23).

Table 6: Cytotoxicity of isosteviol derivatives (IC_{50} , $\mu\text{g/mL}$).

	R2	X	EC9706	Eca109	PC-3	HCT116
23a	OH	-OH	52.08	90.6	87.56	>100
23b	CHO	=NOH	24.42	26.52	>100	>100
23c	=NOH	OH	56.64	17.87	>100	>100
23d	O=	CH=NOH	>100	>100	>100	>100
23e	OH	-NH ₂	19.33	41.32	25.38	20.13
23f	OH		60.67	69.55	>100	>100
23g	-CHO		>100	72.28	>100	>100
23h	-CH ₂ NH ₂	-OH	4.01	5.02	15.31	12.25

Another research group Y. Wu *et al.* synthesized novel derivatives of isosteviol mainly focusing C16, C15 and evaluated cytotoxicity of these derivatives against B16-F10 melanoma cells IC_{50} values for some active derivative are shown in (Table 7, page 18), the modification were made at C15 (R2), and C16 (X). Isoetviol derivative **24a** show moderate cytotoxicity having IC_{50} value 58 μM while derivative **24b** display 68 μM IC_{50} . The analogues **24c**

and **24d** show enhance cytotoxicity with IC_{50} value (25 μ M), and (22 μ M), respectively. The results shown in Table 7, suggest that the introduction of hydroxy methylene, at C15 decrease cytotoxicity while the pyridine carbonyl at C15 and C16 increase cytotoxicity of isosteviol in B16-F10 cell line (Wu *et al.*, 2009).

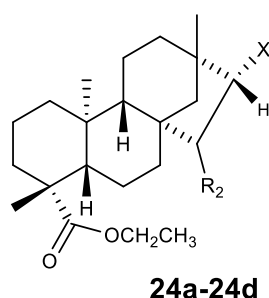
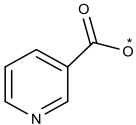
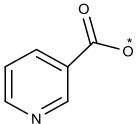
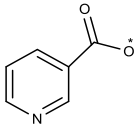


Figure 13: Chemical structure of ethyl ester of Isosteviol (24).

Table 7: Cytotoxicity results of isosteviol derivative (24) and (IC_{50} . μ g/mL)

	R2	X	B16-F10
24a	H	OH	58
24b	-CH ₂ OH	OH	68
24c		-OH	25
24d			22

Methoxy methyl ether (MOM) and carbamate derivatives of isosteviol (Figure 14, page 19) were synthesized by Malki *et al.* and the cytotoxicity of these derivatives were *in vitro* evaluated in human lungs cancer cells line (H1299). MOM ester derivative of isosteviol (**25a-25d**, page 19), such as

compound **25a** demonstrate potent cytotoxicity with IC_{50} 8 μ M, while compound **25b**, and **25d** display moderate cytotoxicity with IC_{50} value 13 μ M, and 20 μ M.

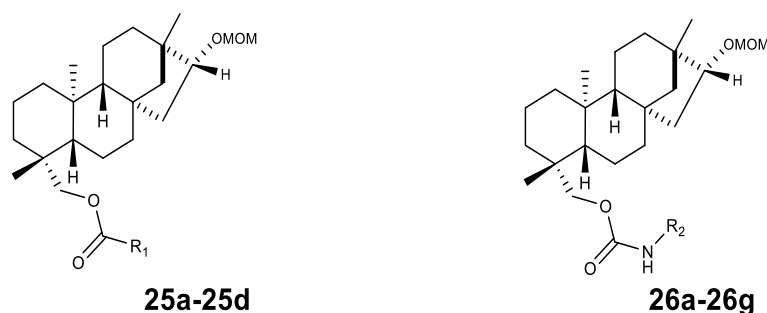


Figure 14: Chemical structure of MOM ester (25), carbamate ester of isosteviol (26).

Table 8: Cytotoxicity of isosteviol derivative against cancer cells line (IC_{50} , μ g/mL)

	R1/R2	Growth inhibition (%)
25a	Ph-	8
25b	CH ₃ -	13
25c	n-C ₇ H ₁₅ -	95
25d	i-Pro	20
26a	Ph-	65
26b	4-(MeCO)-C ₆ H ₄	60
26c	n-C ₃ H ₇	20
26d	4-(MeO)-C ₆ H ₄ CH	89
26e	-CH ₂ Ph	50
26g	n-C ₇ H ₁₅	48

The MOM carbamate ester of isosteviol (**26a-26g**, page 19), derivatives such **26c** show moderate cytotoxicity the result shown in Table 8, while the other carbamate are low cytotoxic. These results demonstrate that isosteviol having

MOM ester at C16 and aromatic nucleus at 19-O carbamate moiety showed potent inhibition then straight chain or branched chain analogues. While in case of MOM carbamate the straight chain derivative display better inhibition then derivative with branched and aromatic nucleus. The results demonstrate that MOM ester analogues display beneficial cytotoxicity then MOM carbamate ester of isosteviol (Malki *et al.*, 2014).

A set of isosteviol and steviol derivatives (Figure 15) were synthesized by Li *et al.* and evaluated for their *in vitro* cytotoxicity in three human cancer cell lines such as breast carcinoma (MDA-MB-231), hepatocellular carcinoma (Hep-G2), and gastric carcinoma (MGC-803). The results are shown in Table 9 page 21.

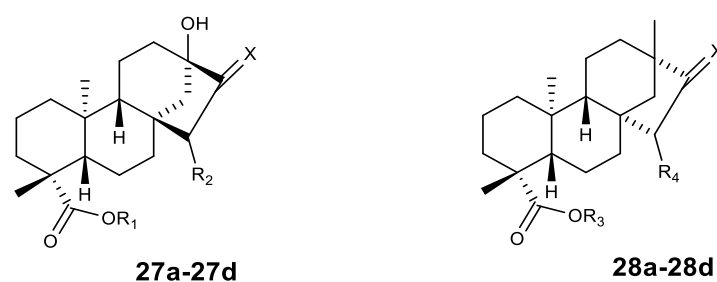


Figure 15: Chemical structure of steviol (27), isosteviol derivatives (28).

The analogue **27a** was found inactive in cancer cell line MDA-MB-231 while showed potent inhibition in Hep-G2 and MGC-803 (IC_{50} 3.69 μ M, 3.38 μ M), respectively the **27b** derivative display potent cytotoxicity in cancer cell lines having IC_{50} 2.51 μ M (MDA-MB-231), 2.7 μ M (Hep-G2), 2.8 μ M (MGC-803), these results indicate that benzyl esterification at 19-O carboxylic site enhance the cytotoxicity of the steviol in cancer cells line. The compound **27d** also display potent inhibition in selected human carcinoma while the **27c** was found inactive in selected cell lines. The results shown in Table 9, page 21 demonstrate that benzyl esterification at 19-O of carboxylic site enhances the cytotoxicity of

compounds, in selected cancer cells lines with IC_{50} 1.24 μ M (MDA-MB-231), 0.95 μ M (Hep-G2), 2.41 μ M (MGC-803).

Table 9: Cytotoxicity of steviol, isosteviol derivative and their (IC_{50} , μ g/mL).

	R1	R2	X	MDA-MB-231	Hep-G2	MGC-803
27a	H	O=	CH ₂	ND	3.69	3.38
27b	Bn	O=	CH ₂	2.51	2.70	1.80
27c	H	CH ₂ =	O=	ND	ND	ND
27d	Bn	CH ₂ =	O=	1.24	0.95	2.41
	R3	R4	X			
28a	H	CH ₂ =	O=	ND	ND	ND
28b	Bn	CH ₂ =	O=	1.58	ND	2.22
28c	H	O=	CH ₂ =	ND	ND	ND
28d	Bn	O=	CH ₂ =	ND	ND	ND

Isosteviol (**28a-28d**, page 20), analogue **28a** don't show inhibition in selected three cancer cells lines while its benzyl derivative **28b** show potent inhibition in two cancer cells lines IC_{50} 1.58 μ M (MDA-MB-231), and 2.22 μ M (MGC-803), compound **28c** and **28d** with free carboxylic and benzyl ester at 19-O (Carboxylic acid), don't show inhibition in selected cancer cells lines. The results shown in Table 9 indicate that the benzyl esterification at 19-O (Carboxylic acid) enhances the cytotoxicity of steviol and isosteviol while exchanging the position of oxymethylene and exocyclic oxygen in isosteviol at C15 and C16 also change the cytotoxicity results (Li *et al.*, 2011).

Another research group Lin *et al.*, synthesized dimeric amides of stevioside, steviol and isosteviol (Figure 16, page 22), and were *in vitro* bio assayed in human cancer cells lines, the results are presented in Table 10, page 22. Stevioside dimeric amide compound **29a** display low cytotoxicity in two cancer cells line the IC_{50} value 90.9 μ M in caucasian promyelocytic leukemia (HL60), and 99.4 μ M in human fetal lung fibroblast cell line (MRC-5). The

analogue **29a** was found inactive with IC_{50} value greater than 100 μM in human liver hepatocellular carcinoma cell line (Hep G2), and in human lungs cancer cell line (H460), while compound **29b** display increase inhibition with IC_{50} value 31.1 μM in (HL60), 31.9 μM (H460). The compound **29c** show low cytotoxicity in the selected cancer cells line. The steviol dimer **29d** demonstrate potent inhibition with IC_{50} value 4.3 μM in (HL60), while moderate cytotoxic in rest of three cells lines with IC_{50} 17.2 μM (HepG2), 10.7 μM (H460), 17.7 μM (MRC-5),

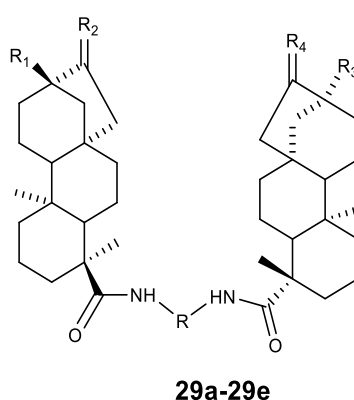


Figure 16: Chemical structure of dimeric amide of steviol (29).

Table 10: Cytotoxicity of stevioside, steviol and isosteviol dimeric amide (IC_{50} , $\mu\text{g/mL}$).

	R	R1	R2	R3	R4	HL60	HepG2	H460	MRC-5
29a	(CH ₂) ₂	O-Glu-Glu	=CH ₂	O-Glu-Glu	=CH ₂	90.9	>100	>100	99.4
29b	(CH ₂) ₄	O-Glu-Glu	=CH ₂	O-Glu-Glu	=CH ₂	>100	31.1	32.9	>100
29c	(CH ₂) ₅	O-Glu-Glu	=CH ₂	O-Glu-Glu	=CH ₂	56.8	60.2	84.7	90.9
29d	CH ₂ CH ₂	OH	=CH ₂	OH	=CH ₂	4.3	17.2	10.7	17.0
29e	CH ₂ CH ₂	CH ₃	=O	CH ₃	=O	4.8	17.4	14.0	22.6

while isosteviol dimeric amide such as compound **29e** also display potent inhibition with IC_{50} value 4.8 μM in (HL60), and found moderate cytotoxic with IC_{50} 17.4 μM (HepG2), 14.0 μM (H460), 22.6 μM (MRC-5). These results specify that dimeric amide of stevioside, steviol and isosteviol at C19 are cytotoxic and their cytotoxicity are dependent on the number of methylene carbon unit the results shown in Table 10, page 22 that increase of number methylene carbon unit in between the nitrogen atoms the cytotoxicity also increase (Lin *et al.*, 2004).

1.3.2.1.2 ANTI-HYPERGLYCEMIC ACTIVITY

Isosteviol is a new addition to anti-diabetic drugs list and is used to lower the glucose level in blood during the treatment of type 2 diabetes. Chen *et al.* explored the potential role of isosteviol on α -cell function and its effects on expression of specific genes following long-term exposure to palmitate. The experimental results indicate that isosteviol decreases palmitate-induced hyperglucagonemia in both cell line of mouse such as pancreatic α -cell line, aTC1–6 cells, and in isolated mice islets (Chen *et al.*, 2012).

Isosteviol is a sole novel chemical entity with proven anti-diabetic capabilities in both man and rodent. Nordentoft *et al.* scrutinizes beneficial effects of isosteviol on the metabolism and gene expression in the diabetic KKAY-mouse. This study demonstrates that Isosteviol may be used as a new insulin sensitizer in the treatment of type 2 diabetes (Nordentoft *et al.*, 2008).

J. Ma *et al.* studied the effect of Isosteviol on blood glucose and insulin level during intravenous glucose tolerance test (IVGTT), in Zucker diabetic fatty (ZDF), rats. The experimental results demonstrated that isosteviol lower the glucose level significantly in the area under the curve (AUC), of glucose during the IVGTT. The glucose-lowering effect of isosteviol may be due to changes in the sensitivity of peripheral tissues to insulin (Ma *et al.*, 2007).

A set of isosteviol derivatives were synthesized and were evaluated *in vitro* by intravenous glucose tolerance test (IVGTT), assays. The results showed that the diesterification at 19-O (Carboxylic acid) exhibited the most effective anti-hyperglycemic effects compared to the positive drug rosiglitazone maleate. The other synthesized derivatives having the lactam, mono ester, hydroxyl group at 19-O (Carboxylic acid) and C16, don't show significant anti-hyperglycemic activities (Chen *et al.*, 2010).

The α -glycosidase plays a key role in digestion of complex carbohydrate, in treating glycoproteins and glycolipids. Alpha-glycosidase inhibitors (AGIs) are drugs that prevent the absorption of carbohydrates from the gut and may be used in the treatment of patients with type 2 diabetes or impaired glucose tolerance. Y.Wu *et al.* prepared and studied the structure–activity correlation of novel isosteviol derivatives (Figure 17). The results (Table 11, page 25) showed that α -glycosidase inhibition was dependent on the nature of the ester moiety, and it was found that ester at 19-O (Carboxylic acid) having more number of carbons show better inhibition. While in comparison of straight chain ester with branched chain, the branched chain ester show low inhibitory effect. The introduction of double bond and aromatic ring in ester chain also show low inhibitory activity against α -glycosidase. The compound **30a** (IC_{50} , 95.5 μ M) display low inhibitory effect then compound **30b** with (IC_{50} , 85.4 μ M). The compound **30c** and **30d** shows slight deference of inhibitory effect against α -glycosidase. The oxime and amine fragments in isosteviol structure also shows inhibitory effect both in ester and free carboxylic form. The results demonstrate that oxo, oxime and amine are low α -glycosidase inhibitor both in ester form while found inactive with free carboxylic acid.

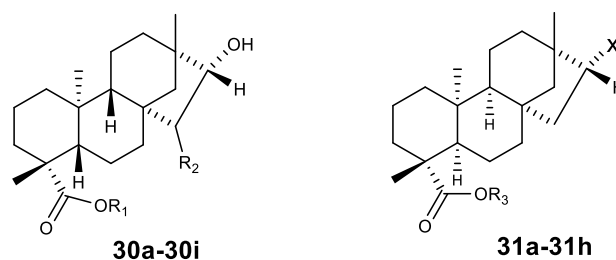


Figure 17: Chemical structure of 15 α -hydroxy methylene isosteviol (30), and isosteviol (31).

Table 11: Inhibition activities of isosteviol derivatives against α -glycosidase (IC_{50} , μ M).

	R1	R2	$IC_{50}(\mu$ M)		R3	x	$IC_{50}(\mu$ M)
30a	-CH ₃	-CH ₂ OH	95.5	31a	H	=O	>200
30b	-CH ₂ CH ₂ CH ₃	-CH ₂ OH	85.4	31b	-CH ₂ CH ₃	=O	>200
30c	-CH(CH ₃) ₂	-CH ₂ OH	97.2	31c	H	=NOH	92.1
30d	-CH ₂ CH(CH ₃) ₂	-CH ₂ OH	102	31d	CH ₂ CH ₃	=NOH	88.9
30e	-C(CH ₃) ₃	-CH ₂ OH	113.8	31e	H	-NH ₂	>200
30f	-CH ₂ CH=CH ₂	-CH ₂ OH	143.2	31f	-CH ₂ CH ₃	-NH ₂	91.2
30g	-CH ₂ -C ₆ H ₅	-CH ₂ OH	132.5	31g	H	-OH	156.3
30h	-CH ₂ CH ₃	-OCOCH ₃	132.5	31h	-CH ₂ CH ₃	-OH	132.1
30i	-CH ₂ CH ₃	OCOC ₆ H ₅	112.4				

The conversion of isosteviol to lactone (**32**), lactam (**33**), and indole (**34**), derivatives display higher inhibition activities especially for lactam and indole. The compound **32** and **33** display IC_{50} 81.6 μ M, IC_{50} 83.2 μ M with free carboxylic acid while ester derivative showed IC_{50} 72.4 μ M and IC_{50} 68.2 μ M. The compound **34** showed 138.6 μ M IC_{50} with free carboxylic acid and display 118.4

$\mu\text{M } IC_{50}$ with ester moiety the result demonstrate that esterification at 19-O (Carboxylic acid) enhances the α -glycosidase inhibition (Wu *et al.*, 2009).

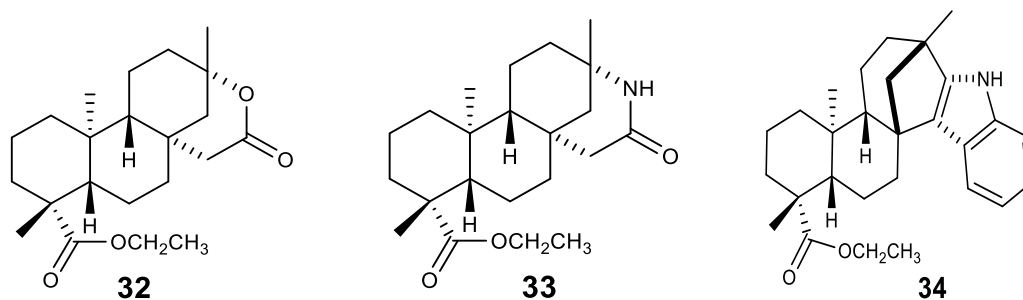


Figure 18: Chemical structures of isosteviol lactone (32), isosteviol lactam (33), and isosteviol indole (34).

1.3.2.1.3 ANTI-MICROBIAL ACTIVITY

The anti-microbial activities of stevioside, steviol and isosteviol have also been reported and these compounds were found active against gram-positive gram-negative and anaerobic bacteria. In this connection anti-microbial activities were investigated by Lin *et al.* A set of dimeric amide of stevioside, steviol and isosteviol (Figure 19, page 27), were semi-synthesized and these semi-synthetic analogues were *in vitro* tested against the *Bacillus subtilis* (BCRC 10029). The results are shown in Table 12, page 27. The compound **35a**, **35b** and **35c** dimeric amides of stevioside displayed inhibition concentration 22.09 $\mu\text{g/mL}$, 45.04 $\mu\text{g/mL}$, 97.81 $\mu\text{g/mL}$ in *Bacillus subtilis* (BCRC 10029), while compound **35d** and **35e** were found inactive against *Bacillus subtilis* (BCRC 10029). The results from the Table 12, page 27 specify that the inhibition against *Bacillus subtilis* increased with the increase of methylene carbons unit in between the nitrogens atoms of the dimeric amides (Lin, Lee, Sheu & Lin., 2004).

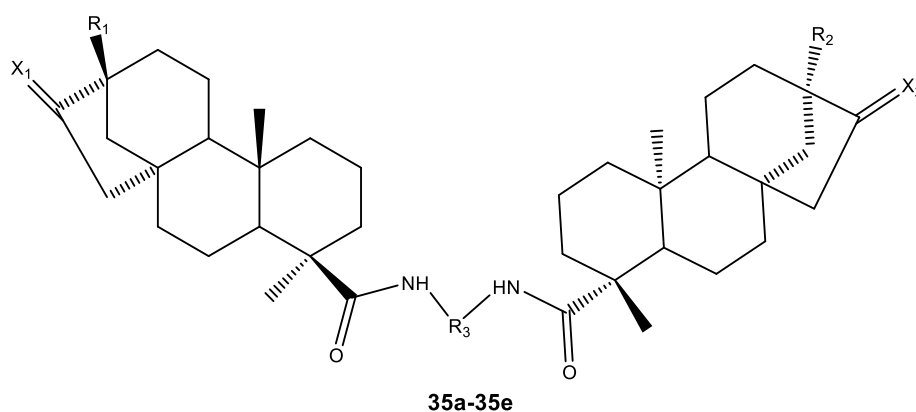


Figure 19: Chemical structure of stevioside, steviol and isosteviol dimeric Amides (35).

Table 12: Antimicrobial activities of stevioside analogs (IC_{50} , $\mu\text{g/mL}$).

	R1	R2	R3	X^1	X^2	$\mu\text{g/mL}$	MIC μM
35a	-O Glu-Glu	-O Glu- Glu	$(\text{CH}_2)_{12}$	=CH2	=CH2	32	22.09
35b	-O Glu- Glu	-O Glu- Glu	$(\text{CH}_2)_{10}$	=CH2	=CH2	64	45.04
35c	-O Glu- Glu	-O Glu- Glu	$(\text{CH}_2)_2$	=CH2	=CH2	128	97.81
35d	OH	OH	$(\text{CH}_2)_2$	=CH2	=CH2	>256	--
35e	CH3	CH3	$(\text{CH}_2)_2$	=O	=O	>256	--

Isosteviol and its bis-quaternized derivative (Figure 20, page 28) were prepared and were *in vitro* tested for bacteriostatic and bactericidal, activities it was found that bacteriostatic and bactericidal activity ($0.5 \mu\text{g/mL}$), of bis-quaternized isosteviol derivatives were correspondent to the antibacterial drug ciprofloxacin ($0.25 \mu\text{g/mL}$). The results for compound (**36**, page 28), where **R1** $(\text{CH}_2)_n$, stand for variable number of methylene carbon unit between two nitrogen

atom in dimer, ($n = 5$, $n = 9$, $n = 12$). These three dimeric analogues with different alkyl chain between two nitrogen display more inhibition towards *Staphylococcus aureus* with 3.0 $\mu\text{g/mL}$, 0.78 $\mu\text{g/mL}$, and 0.5 $\mu\text{g/mL}$ inhibition concentrations respectively. When these three dimers were tested against other bacterial strain, such as *Bacillus cereus* the inhibition concentration values were found 31.1 $\mu\text{g/mL}$, 3.9 $\mu\text{g/mL}$, and 1.5 $\mu\text{g/mL}$, respectively. These results indicate that the increase of the methylene carbon unit chain between two nitrogen of bis-quaternized isosteviol, the percentage of inhibition increases in both strain of bacteria (Korochkina *et al.*, 2012).

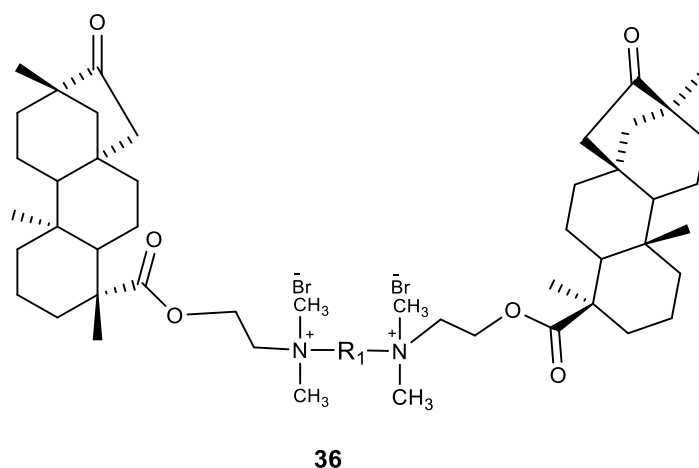


Figure 20: Chemical structure of bis-quaternized isosteviol (36).

Wu *et al.* synthesized a set of isosteviol derivatives and tested *in vitro* for anti-bacterial activities in two strains of bacteria *Bacillus subtilis* and *Staphylococcus aureus* the results are shown in Table 13, page 29. The compound **37a** was found inactive in both strains of bacteria, while **37b**, **37c** and **37d** show significant inhibition with 12.5 $\mu\text{g/mL}$ minimum inhibitory concentrations in *Bacillus subtilis* and was found inactive in *Staphylococcus aureus*.

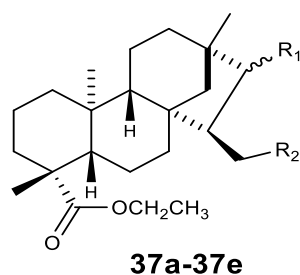
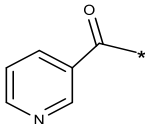
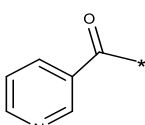
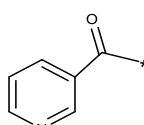


Figure 21: Chemical structure of ethyl ester of isosteviol (37).

The highest inhibition was observed for compound **37e** with 3.12 µg/mL minimum inhibitory concentrations in *Bacillus subtilis* strain and was found inactive in *Staphylococcus aureus* strain. The pyridine carbonyl substitution increases the inhibition in *Bacillus subtilis* strain while the presence of 2NO₂ at both position also show moderate inhibition in *Bacillus subtilis* strain and was found inactive in *Staphylococcus aureus* (Wu *et al.*, 2010).

Table 13: Antimicrobial activities of isosteviol derivatives (*IC*₅₀, µg/mL).

	R ₁	R ₂	<i>Bacillus subtilis</i>	<i>Staphylococcus aureus</i>
37a	-OH	-OH	200	>100
37b	=O	-OH	12.5	>100
37c	-ONO ₂	-ONO ₂	12.5	>100
37d		-OH	12.5	>100
37e			3.12	>100

1.3.2.1.4 ANTI-INFLAMMATORY AND IMMUNOMODULATORY ACTIVITY

Immunomodulation is a procedure, which adjusts the immune system of an organism by interfering with its functions. This interference results in either immunostimulation or immunosuppression. An immunomodulator is any substance that helps to regulate the immune system. This "regulation" is a normalization process, so that an immunomodulator helps to optimize immune response. Boonkaewwan *et al.* investigated the anti-inflammatory and immunomodulatory assays of stevioside and its derivative, steviol using an *in vitro* model lipopolysaccharide (LPS), stimulated human monocytic THP-1 cells and study the production of inflammatory cytokines, tumor necrosis factor α (TNF- α), interleukin 1 β (IL-1 β), and nitric oxide. The intracellular signaling pathway was deliberated by analysis of Inhibitor of nuclear factor kappa-B kinase subunit beta (IKK β), and NF- κ B stimulation, and the direct effect of stevioside on TNF- α secretion mediated by TLR4 was scrutinized. When THP-1 cell was treated with stevioside (1 mm), after 6h the results show significant release of TNF- α (before treatment 20.6 \pm 15 pg/mL after treatment 1135 \pm 193 pg/mL), and IL-1 β (before treatment 0 pg/mL and after treatment 140 \pm 21 pg/mL). While LPS show significant stimulation with (1 μ g/mL), after 6h and release pro-inflammatory cytokines such as TNF- α (2986 \pm 165 pg/mL), and IL-1 β (312 \pm 35 pg/mL). The results on inhibition show that nitric oxide (before treatment 6 \pm 0.4 μ m and after treatment 4.7 \pm 0.5 μ m), production was suppressed when THP-1 was stimulated with LPS (1 μ g/mL), along with stevioside (1 mm), concentration (BOONKAEWWAN *et al.*, 2006).

Recently in another work Boonkaewwan *et al.* study the effect of stevioside and steviol on human colon carcinoma Caco-2 cells along with anti-inflammatory and immunomodulatory factor. Significant decrease in tumor necrosis factor (TNF- α), were observed when Caco-2 cells are treated with LPS and steviol. Stevioside and steviol decreases cytokines production up to 60% in LPS stimulating group during the release of interleukin 1 β (IL-1 β), and also inhibit

IL-6 production in LPS group. The experimental result show partial suppression of stevioside and steviol on the, nuclear factor kappa-B kinase (NF- κ B), in Caco-2 cell line (Boonkaewwan & Burodom, 2013).

In another research work Boonkaewwan *et al.* demonstrate potent biological effect of steviol on increases Cl⁻ secretion in human colonic adenocarcinoma cell line (T84 cells), and decrease of tumor necrosis factor receptor (TNF-R), and Interleukin 8 (IL-8), release was observed in human colonic cell lines T84, Caco-2, and HT29. While the precursor stevioside slightly raises Cl⁻ secretion, at concentrations which not affect cell viability, and hence stevioside does not change TNF-R function. The stevioside did not show any effect on IL-8 release even it high concentration but in Caco-2 and HT29 cells they release significantly IL-8. The result shows decrease of 80% viability in selected three cells with 2 mm stevioside. Steviol has slightly increases the IL-8 in T84 cell but it fails to show results in Caco-2 and HT29 cells. IL-8 release was inhibited 21.1-35.4% in the presence of steviol and TNF- α in T84 cell, 16.2% in Caco-2 and 17% was observed in HT29 cells. The results show that 2 and 5 mm stevioside reduced cell viability to 76-82 and 33-68%, correspondingly. At lower concentrations, 0.2 and 0.8 mm steviol also decreased cell viability to 80-90% and 7-34%, respectively. It is interesting that steviol, at 0.4 and 0.6 mm, and stevioside, at 2 and 5 mm, are less cytotoxic in HT29 and Caco-2 than in T84 cells (Boonkaewwan *et al.*, 2008).

1.3.2.1.5 ANTI-TUBERCULOSIS ACTIVITY

Tuberculosis (TB) remains a foremost worldwide health problem. It was estimated that more than 8.6 million people were infected and nearly 1.3 million people died from tuberculosis in 2012 (WHO 2012).

In the literature around hundred natural product compounds are reported that inhibits the *Mycobacterium tuberculosis* (H37RV strain), growth. In this

connection a series of macro cyclic isosteviol analogue having azine, hydrazone and hydrazide functionality (Figure 22, page 33), were prepared and was *in vitro* evaluated against *Mycobacterium tuberculosis* (H37RV), the results are shown in Table 14. The compound **38** and **39** having hydrazine hydrazone functionality, show strong inhibition with (MIC 1.7 $\mu\text{g}/\text{mL}$) and (MIC 3.1 $\mu\text{g}/\text{mL}$), while compound **40** and **41**, show good inhibition with hydrazone functionality with MIC value 6.3 $\mu\text{g}/\text{mL}$. Generally it was observed that increase of methylene carbon unit between the macrocyclic hydrazide analogues of isosteviol also improves the inhibition against *Mycobacterium tuberculosis* (H37RV) strain (Garifullin *et al.*, 2011).

Table 14: MIC 50 $\mu\text{g}/\text{mL}$ value of different derivative of steviol and isosteviol.

	H37RV		H37RV
38	3.1	42	20.0
39	1.7	43	5.0
40	6.3	44	20.0
41	6.3		

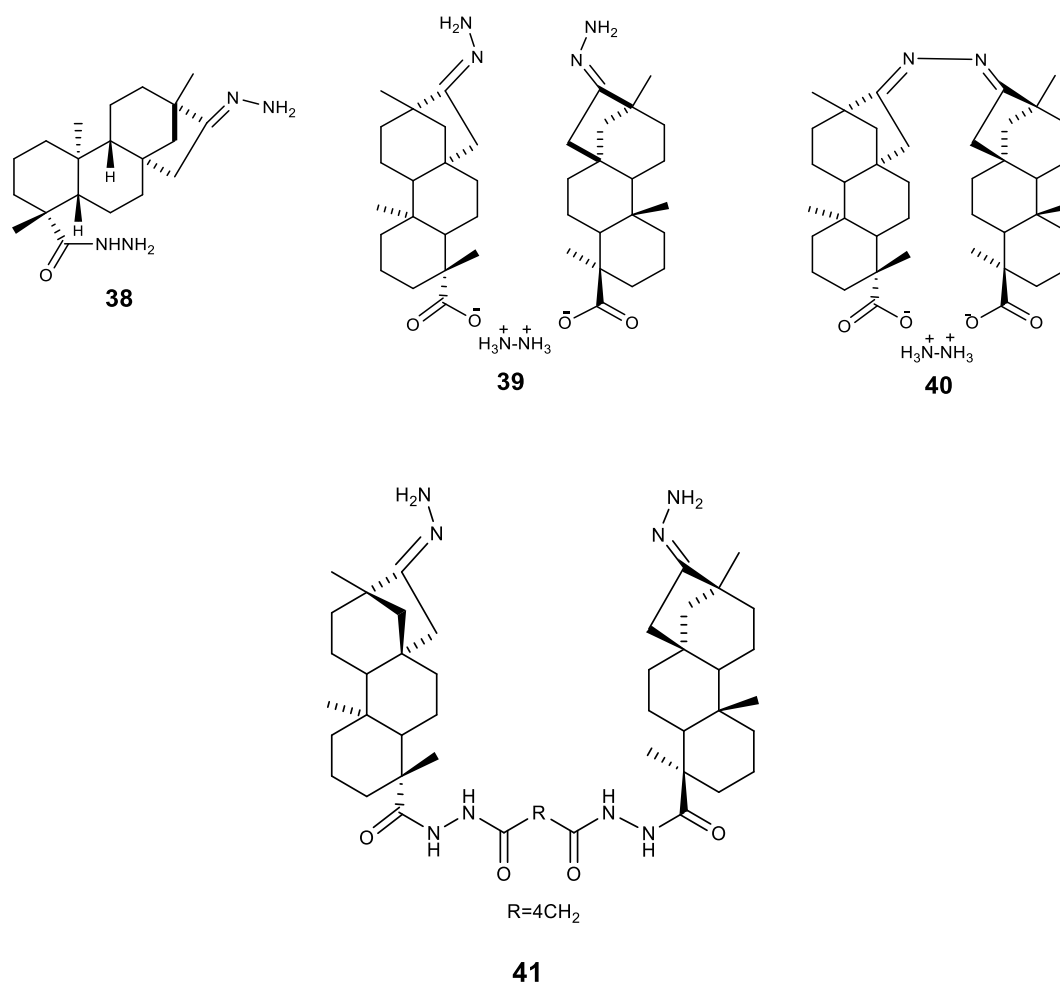


Figure 22: Chemical structure of hydrazone hydrazide (38), hydrazone (39), dimeric hydrazone (40), hydrazone and dimeric hydrazide of isosteviol (41).

Another research group Khaybulline *et al.* prepared saturated steviol **42** and its dimeric compound **44** and **43** these analogues were *in vitro* evaluated against *Mycobacterium tuberculosis* (H37RV) strain, similar inhibitory concentration (MIC 20.0 $\mu\text{g/mL}$) were found for both derivatives, while compound **43**, show potent inhibition (MIC 5.0 $\mu\text{g/mL}$), as shown in Table 14. The inhibitory results showed that per acid and anhydride moiety in dimeric

steviol improves the inhibition in *Mycobacterium tuberculosis* (H37RV strain) (Khaybullin *et al.*, 2012).

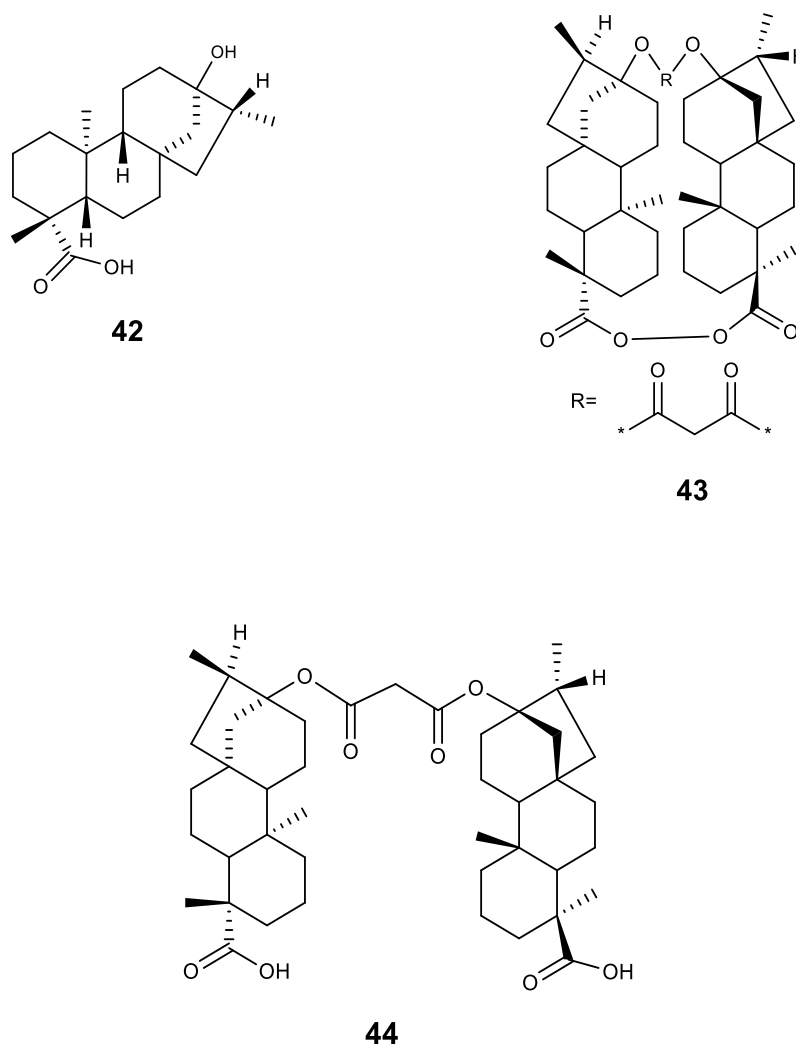


Figure 23: Chemical structure of steviol (42), dimeric per acid anhydride (43) steviol dimeric anhydride (44).

In continuation of the synthesis of biologically active isosteviol derivatives, Sharipova *et al.* synthesized 15-oxo-thiosemicarbazone **45** and 15-oxo-oxime **46**, of isosteviol and these derivatives were *in vitro* evaluated against *Mycobacterium tuberculosis* (H37Rv) strain. The compound **45** showed moderate inhibitory

activity The minimum inhibitory concentration (MIC), of compound 45 (20 µg mL⁻¹), is twofold lower than MIC found for isosteviol.

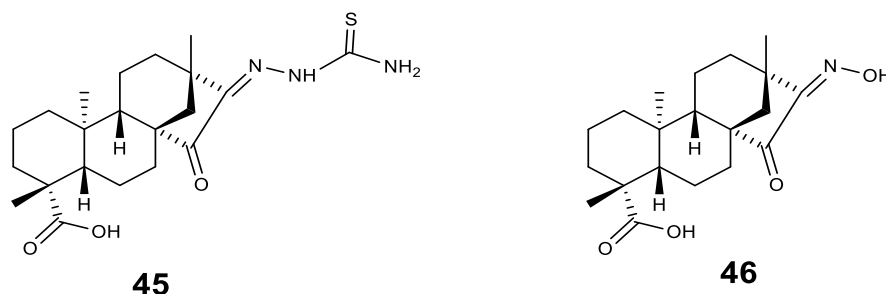


Figure 24: Chemical structure of 15-oxo-thiosemicarbazone (45), 15-oxo 16-oxime derivatives of isosteviol (46).

The higher value of MIC for compound **46** demonstrate that compound with oxo-oxime fragment was found inactive against *Mycobacterium tuberculosis* (H37Rv) strain. It can be assumed that an increase in the activity is associated with the introduction of carbazone fragments in isosteviol skeleton (Sharipova *et al.*, 213).

1.3.2.1.6 ANTI-HEPATITIS B ACTIVITY

Hepatitis B is a viral infection that attacks the liver and can cause both acute and chronic disease, and is a potentially life-threatening disease caused by the hepatitis B virus. It can cause chronic liver disease and chronic infection and puts people at high risk of death from cirrhosis of the liver and liver cancer. Individuals who develop chronic hepatitis may develop significant and potentially fatal disease. In general, the frequency of clinical disease increases with age, whereas the percentage of carriers decreases. Nearly about 1 million global deaths occur each year due to chronic forms of the disease (WHO. 2013).

In the literature several research groups described the effect of natural products and their semi-synthetic analogues against hepatitis B to find novel and potentially bioactive secondary metabolite. In this connection, T-J. Huang *et al.* synthesized a set of alkylated ureide of isosteviol at C19 and these derivatives were *in vitro* evaluated against HBV in HepG2 cells the results are shown in Table 15, page 37. The compound **47a**, (*ent*-16-oxobeyeran-19-N-methylureido), exhibited potent inhibition in HBV surface antigen (HBsAg), strain and moderately active against HBV e antigen (HBeAg) secretion, with IC_{50} 7.89 $\mu\text{g/mL}$ inhibitory concentration and was found moderately active with IC_{50} 24.3 $\mu\text{g/mL}$ in HBsAg secretion. The compound **47c** was moderately active in HBeAg strain while inactive in HBsAg, compound **47b** was inactive in both strains of Hepatitis B. The compound **47d** show potent inhibition against HbeAg strain (IC_{50} 9.36 $\mu\text{g/mL}$), and was found inactive in HBsAg strain. Generally the comparative results demonstrate that the substituted aromatic alkylated ureide nitrogen causes more inhibition, while halogenated ureide nitrogen show moderate inhibition (Huang *et al.*, 2014).

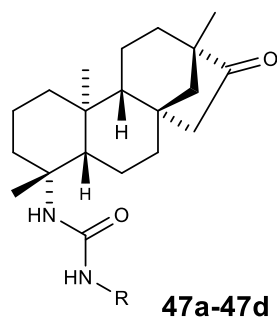


Figure 25: Chemical structure of alkylated ureide of isosteviol (47).

Table 15: Anti-viral activities of isosteviol analogues (IC_{50} , $\mu\text{g/mL}$).

	R	TC_{50}	HBsAg	HBeAg
47a	-CH ₃ (NC-8)	53.52	7.89	24.30
47b	-CH ₂ -C ₆ H ₅	70.30	---	----
47c	<i>p</i> -HOC ₆ H ₄ -	125.86	-----	24.83
47d	3,4(OH)C ₆ H ₃ -	75.18	26.13	9.36

The literature data shown above indicate the potential of kauranes and beyeranes as prototypes for the development of new bioactive compounds. The potency and selectivity profile of steviol and isosteviol along with the semi synthetic derivatives makes it an attractive medicinal chemistry target. Since hydrazone, oxime, polyhydroxy, benzyl ester and *p*-methoxy acetophenone ester usually behaves as a bioactive fragments in various natural products. We planned the semi-synthesis of new derivatives of steviol/isosteviol to shape a new family of bioactive compounds.

2 OBJECTIVES

2.1 GENERAL OBJECTIVES

Derivatization of steviol and isosteviol by chemical methods, and evaluation of some of their biological activities.

2.2 SPECIFIC OBJECTIVES

- 2.2.1** Preparation of steviol and isosteviol semi synthetic derivatives by chemical method targeting, at C15, C16 and C19.
- 2.2.2** Evaluation of anti-tumor activities against selected human cancer cell line such as lung carcinoma (A549), human brain glioma cell lines (T98MG), human glioblastoma-astrocytoma, epithelial-like cell line (U8MG).
- 2.2.3** Evaluation of anti-malarial activity of analogues by the methods of 3 [H] - hipoxantina and lactate dehydrogenase (LDH).
- 2.2.4** Evaluation of anti-*Trypanosomal* activity of derivatives by MTT [3-(4, 5-dimethylthiazol-2-yl)-2,5-diphenyltetrazolium bromide].
- 2.2.5** Evaluation of anti-*Leishmanicidal* activity of derivatives by MTT [3-(4, 5-dimethylthiazol-2-yl)-2, 5-diphenyltetrazolium bromide].
- 2.2.6** Evaluation of Anti-*Corynebacterium diphtheriae* activity.

3 EXPERIMENTAL

3.1 INSTRUMENTATION

The structure identification of compounds was carried out using NMR Bruker DPX-200 (^1H NMR, ^{13}C NMR and DEPT¹³⁵), spectrophotometer TMS as internal standard. IR Spectra: as KBr pellets on a Thermo Nicolet IR200 spectrometer. ESI-MS were carried out using “Thermo Fisher Scientific Inc.LTQ XL Linear Ion Trap Mass Spectrometer” was used at Department of Chemistry of Federal University of Parana.

3.1.1 CHROMATOGRAPHY

All reactions were monitored by thin-layer chromatography, and visualized under UV (254 and 366 nm), or by spraying using methanol/sulphuric acid or vanillin/sulphuric acid reagents, followed by heating. The following chromatographic conditions were used for analysis:

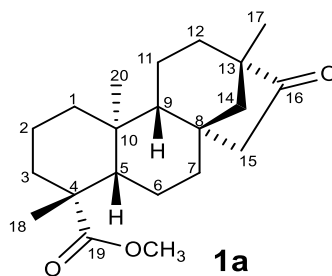
- a) Thin layer chromatographic PF254 pre coated plates with silica gel (0.25mm) (Merck® Germany).
- b) Silica gel 60 (0.04-0.063 mm Merck®, Germany), for column chromatography.
- c) Preparative circular chromatography (Chromatotron, Harrison Research, Palo Alto, CA, USA model 7924T), silica gel, TLC grade 7749, with gypsum binder and fluorescent indicator.

3.1.2 SOLVENTS

All solvents were purchased commercially and were distilled before use. Deuterated (CDCl_3 , CD_3OD , CD_3COCD_3), solvent were used for NMR analysis.

3.2 SEMI SYNTHESIS OF THE STEVIOSIDE DERIVATIVES

3.2.1 PREPARATION OF ISOSTEVIOL (1a)



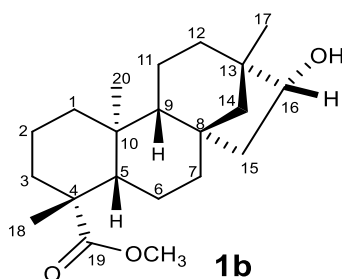
Commercial stevioside (10.00 g, 12.2 mmol) was dissolved in 5% hydrochloric acid solution (200 mL, 12M), and the mixture was heated under reflux for 1 hour. After cooling the reaction mixture was filtered and the filtrate was extracted with ethyl acetate (3 X 100 mL). The organic portion were combined and dried over anhydrous sodium sulphate (Na_2SO_4). The solvent was evaporated in a rotary evaporator providing 4.1 g of a solid residue. The solid obtained was then purified on a silica column (3 x 30 cm), using mixtures of hexane and ethyl acetate of increasing polarity as mobile phase. Similar fractions were combined and the solvent was evaporated. (AVENT, HANSON & OLIVEIRA, 1989).

White crystalline compound **1a** (3.3 g) was obtained, 33% yield after purification using chromatotron. IR; 1734 cm^{-1} , 1692 cm^{-1} , 1269 cm^{-1} . ^1H NMR (200 MHz, CDCl_3), δ 0.68 (3H, s, H20), δ 0.98 (3H, s, H18), δ 1.19 (3H, s, H17), δ 1.55 (1H, dd, $J = 11.30, 2.2\text{ Hz}$, H14), δ 2.62 (1H, dd, $J = 18.62, 3.65\text{ Hz}$, H15), δ 3.64 (3H, s, OCH_3). ^{13}C NMR (50 MHz, CDCl_3), δ 13.2 (C20), δ 18.9 (C2), δ 19.8 (C17), δ 20.3 (C11), δ 21.7 (C6), δ 28.8 (C18), δ 37.3 (C12), δ 37.9 (C3, C10), δ 39.4 (C8), δ 39.8 (C1), δ 41.5 (C7), δ 43.7 (C4), δ 48.4 (C13), δ 48.7 (C15), δ 51.2 (OCH_3), δ 54.3 (14), δ 54.7 (C9), δ 57.1 (C5), δ 177.8 (C19).

3.2.1 GENERAL PROCEDURE FOR PREPARATION OF 16-HYDROXY DERIVATIVES OF ISOSTEVIOL AND 17-HYDROXY ISOSTEVIOL

Sodium borohydride (37.83 mg, 1 mmol), was added portion wise to an ice-cold solution of isosteviol **1a** or 17-hydroxy isosteviol **4h** (318 mg, 0.5 mmol), in dry ethanol (5 mL). The reaction mixture was kept stand for 1h. The progress of reaction was followed by TLC. After complete disappearance of starting material, the reaction mixture was quenched by adding saturated aqueous NH_4Cl (5 mL) solution, along with stirring. The reaction mixture was then brought back to room temperature the ethanol was removed under reduced pressure. The reaction mixture was extracted with ethyl acetate (3 x 30 mL). The organic layer was washed with brine (5 mL), and was dried over anhydrous sodium sulphate (Na_2SO_4). The reaction mixture was filtered and concentrated under reduced pressure.

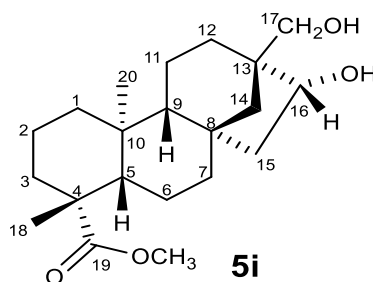
3.2.1.1 16-HYDROXY ISOSTEVIOL (**1b**)



White crystalline solid **1b** (240 mg, 80%). IR; 3468 cm^{-1} , 1723 cm^{-1} , 1454 cm^{-1} , 1141 cm^{-1} . ^1H NMR (200 MHz, CDCl_3), δ 0.72 (3H, s, H20), δ 0.91 (3H, s, H18), δ 1.16 (3H, s, H17), δ 2.15 (1H, d, $J=12.62\text{ Hz}$), δ 3.62 (3H, s, OCH_3), δ 3.85 (1H, dd, $J=10.23, 5.44\text{ Hz}$, H16). ^{13}C NMR (50 MHz, CDCl_3), δ 13.1 (C20), δ 18.9 (C2), δ 20.4 (C11), δ 21.7 (C6), δ 24.9 (C17), δ 28.8 (C18), δ 33.7 (C12), δ 38.0 (C3, C10), δ 39.9 (C1), δ 41.7 (C7), δ 41.9 (C8), δ 42.0 (C13), δ 42.8 (C15), δ

43.7 (C4), δ 51.1 (OCH₃), δ 55.2 (14), δ 55.8 (C9), δ 57.1 (C5), δ 80.5 (C16), δ 178.1 (C19).

3.2.1.2 17, 16-DIHYDROXY ISOSTEVIOL (5i)



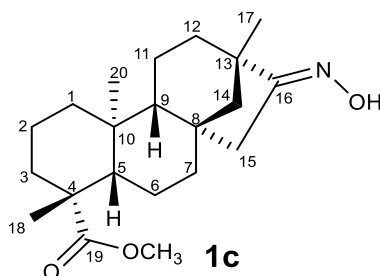
White crystalline solid (218 mg, 73%). IR; 3413 cm⁻¹, 3218 cm⁻¹, 1698 cm⁻¹, 1391 cm⁻¹, 1233 cm⁻¹, 1175 cm⁻¹, 1027 cm⁻¹. ¹H NMR (200 MHz, CDCl₃), δ 0.77 (3H, s, H20), δ 1.20 (3H, s, H17), δ 2.12 (1H, br, d, J = 12.7 Hz, H12), δ 3.45 (1H, d, J = 10.12 Hz, H17), δ 3.5 (1H, d, J = 10.12 Hz, H17), δ 3.66 (3H, s, OCH₃), δ 4.22 (1H, dd, J = 10.3, 5.15 Hz, H16), δ 5.34 (2H, s, H17). ¹³C NMR (50MHz, CDCl₃), δ 13.1 (C20), δ 18.9 (C2), δ 19.9 (C11), δ 21.7 (C6), δ 28.8 (C18), δ 29.3 (C12), δ 38.1 (C3, C10), δ 39.9 (C1), δ 41.6 (C7), δ 42.1 (C15), δ 42.5 (C8), δ 43.7 (C4), δ 46.6 (C13), δ 50.0 (C14), δ 51.1 (OCH₃), δ 56.5 (C9), δ 57.1 (C5), δ 71.2 (C17), δ 78.5 (C16), δ 178.0 (C19).

3.2.2 GENERAL PROCEDURE FOR THE PREPARATION OF 16-OXIME OF ISOSTEVIOL AND 17-HYDROXY ISOSTEVIOL

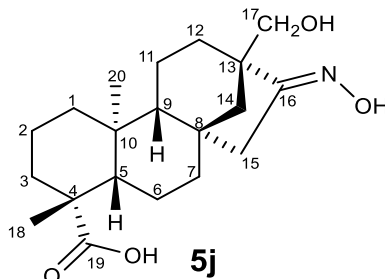
Solution of sodium acetate (164 mg, 2 mmol), and hydroxyl amine chloride (139 mg, 2 mmol), in water (5.3 mL), was added to the solution of isosteviol or 17 hydroxy isosteviol (318 mg, 1 mmol), in ethanol and water (25 mL: 4:1) ratio. The reaction mixture was kept under stirring for 24h at room

temperature. The progress of reaction was monitored by TLC. After complete disappearance of starting material water (50 mL), was added to the reaction mixture which was extracted with ethyl acetate (3x50 mL). The organic layer was dried over anhydrous sodium sulphate. After filtration ethyl acetate was removed under reduced pressure and the product was recrystallized from methanol.

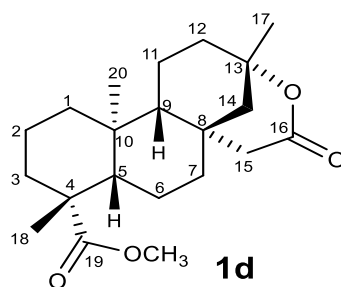
3.2.2.1 ISOSTEVIOL 16-OXIME (1c)



A white crystalline solid (260 mg, 78%). IR; 3446 cm^{-1} , 1720 cm^{-1} , 1694 cm^{-1} , 1601 cm^{-1} , 1262 cm^{-1} , 961 cm^{-1} . ^1H NMR (200 MHz, CDCl_3), δ 0.76 (3H, s, H20), δ 1.12 (3H, s, H17), δ 1.20 (3H, s, H18), δ 1.34 (1H, dd, $J = 17.51, 3.98$ Hz, H14), δ 2.19 (1H, d, $J = 12.65$ Hz), δ 2.98 (1H, dd, $J = 18.30, 2.98$ Hz, H15), δ 3.64 (3H, s, OCH_3). ^{13}C NMR (50 MHz, CDCl_3), δ 13.1 (C20), δ 18.9 (C2), δ 20.4 (C11), δ 21.7 (C6), δ 22.1 (C17), δ 28.7 (C18), δ 36.8 (C12), δ 37.9 (C10), δ 38.0 (C3), δ 39.5 (C15), δ 39.9 (C1), δ 40.6 (C8), δ 40.8 (C7), δ 43.7 (C4, C13), δ 51.1 (OCH_3), δ 54.8 (9), δ 56.2 (C14), δ 57.1 (C5), δ 170.2 (C16), δ 178.0 (C19).

3.2.2.2 17-HYDROXY, 16-OXIME OF ISOSTEVIOL (5j)

White crystalline solid (206 mg: 68%), yield. IR; 3359 cm^{-1} , 1707 cm^{-1} , 1451 cm^{-1} , 1236 cm^{-1} , 1183 cm^{-1} , 925 cm^{-1} , 784 cm^{-1} . ^1H NMR (200 MHz, CDCl_3), δ 0.89 (3H, s, H20), δ 1.21 (3H, s, H17), δ 2.99 (1H, dd, $J = 18.40, 3.0$ Hz, H15), δ 3.55 (1H, dd, $J = 16.70, 10.90$ Hz, H17). ^{13}C NMR (50 MHz, CDCl_3), δ 13.0 (C20), δ 18.9 (C2), δ 19.8 (C11), δ 21.7 (C6), δ 28.5 (C18), δ 34.4 (C12), δ 36.9 (C7), δ 37.8 (C3), δ 38.1 (C10), δ 39.8 (C1), δ 40.7 (C8), δ 40.8 (C15), δ 43.2 (C4), δ 48.9 (C13), δ 51.3 (C14), δ 55.4 (C9), δ 56.8 (C5), δ 66.4 (C17), δ 167.5 (C16), δ 178.7 (C19).

3.2.2.3 ISOSTEVIOL LACTONE (1d)

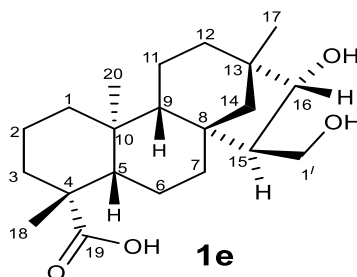
Hydrogen peroxide 30% (1 mL, 9.8 M), was added to a well stirred solution of isosteviol (318 mg, 1 mmol), in acetic acid. The reaction mixture was kept under stirring for 96 hours. The progress of reaction was followed by TLC. The reaction

mixture was added to water and was extracted with chloroform (3x50 mL). The organic layer was dried over anhydrous sodium sulphate. After filtration excess of chloroform was removed under reduced pressure. The reaction mixture was chromatographed on chromatotron using silica rotors (1 mm), and mixture of ethyl acetate and *n*-hexane (2:8) was used as a mobile phase.

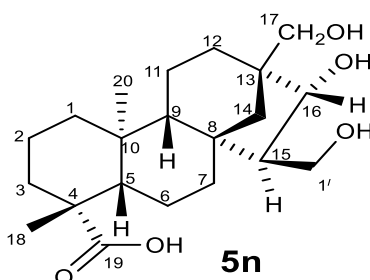
The product recovered was white crystalline solid (130 mg, 39%), yield. The ESI-MS $[M]^+$; 334.25. IR; 1720 cm^{-1} , 1688 cm^{-1} , 1244 cm^{-1} , 1156 cm^{-1} . ^1H NMR (200 MHz, CDCl_3), δ 0.76 (3H, s, H20), δ 1.18 (3H, s, H17), δ 1.35 (3H, s, H18), δ 2.19 (1H, d, $J = 12.97$ Hz), δ 3.09 (1H, dd, $J = 18.67, 2.60$ Hz, H15).), δ 3.64 (3H, s, OCH_3). ^{13}C NMR (50 MHz, CDCl_3), δ 13.4 (C20), δ 18.5 (C11), δ 18.8 (C2), δ 19.5 (C6), δ 28.3 (C17), δ 28.6 (C18), δ 34.9 (C8), δ 37.8 (C10), δ 37.9 (C7), δ 38.4 (C3), δ 38.7 (C12), δ 39.9 (C1), δ 43.6 (C15), δ 43.7 (C4), δ 47.7 (C14), δ 51.1 (OCH_3), δ 55.8 (9), δ 57.2 (C5), δ 80.2 (C13), δ 172.5 (C16), δ 177.5 (C19).

3.2.3 GENERAL PROCEDURE FOR THE PREPARATION OF 15 α -HYDROXY METHYL, 16 β -HYDROXY OF ISOSTEVIOL AND 17-HYDROXY ISOSTEVIOL

Excessive amount of aqueous formaldehyde (37%, 13.3 M, 2 mL), was added drop wise to the solution of isosteviol or 17-hydroxy isosteviol (318 mg, 0.62 mmol), in ethanol (4 mL), and sodium hydroxide (1.6 M), in water (6 mL) the reaction mixture was stirred for 3 hour at 90 $^{\circ}\text{C}$. The progress of reaction was followed by TLC. The reaction mixture was acidified with dilute hydrochloric acid filtered and was chromatographed on chromatotron using silica rotors (1 mm), and mixture of ethyl acetate and *n*-hexane (3:8) was used as a mobile phase.

3.2.3.1 15 α -HYDROXY METHYL, 16 β -HYDROXY OF ISOSTEVIOL (1e)

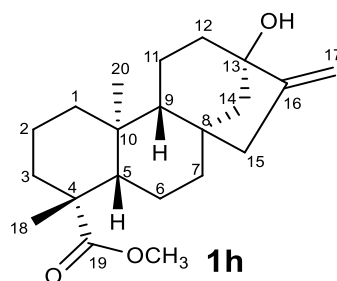
White crystalline solid with (153 mg; 78%), yield. ESI-MS data $[M+Na]^+$; 373.21. IR; 3392 cm^{-1} , 1694 cm^{-1} , 1553 cm^{-1} , 1534 cm^{-1} , 1454 cm^{-1} , 1067 cm^{-1} . ^1H NMR (200 MHz, CDCl_3), δ 0.74 (3H, s, H20), δ 0.93 (3H, s, H18), δ 1.15 (3H, s, H17), δ 2.15 (1H, dd, $J = 13.51$ Hz, H12), δ 3.46 (1H, t, $J = 10.27$ Hz, H1'), δ 3.63 (3H, s, OCH_3). ^{13}C NMR (50 MHz, CDCl_3), δ 13.0 (C20), δ 18.9 (C2), δ 19.5 (C11), δ 22.2 (C6), δ 25.0 (C17), δ 28.9 (C18), δ 33.1 (C12), δ 34.8 (C7), δ 37.9 (C3), δ 38.1 (C10), δ 39.6 (C1), δ 40.9 (C8), δ 42.5 (C13), δ 43.7 (C4), δ 50.3 (C15), δ 51.2 (OCH_3), δ 54.3 (14), δ 57.1 (C9), δ 57.7 (C5), δ 64.9 (C1'), δ 86.7 (C16), δ 177.9 (C19).

3.2.3.2 15 α -HYDROXY METHYL, 16 β -HYDROXY OF 17-HYDROXY ISOSTEVIOL (5n)

White crystalline solid (146 mg, 71%), yield. ESI-MS, $[M-H]^+$ 365.33. IR; 3419 cm^{-1} , 1693 cm^{-1} , 1222 cm^{-1} , 755 cm^{-1} . ^1H NMR (200 MHz, CD_3COCD_3), δ 0.79 (3H, s,

H20), δ 1.17 (3H, s, H18), δ 2.93 (1H, br, d, $J = 4.3$ Hz, H15), δ 3.35 (1H, d, br, $J = 5.84$ Hz, H1'), δ 3.62 (2H, s, H17). ^{13}C NMR (50 MHz, CD_3COCD_3), δ 12.6 (C20), δ 18.8 (C2), δ 19.0 (C11), δ 22.2 (C6), δ 28.2 (C18), δ 34.9 (C12), δ 37.8 (C3, C7), δ 38.1 (C10), δ 39.6 (C1), δ 42.6 (C8), δ 43.4 (C4), δ 45.6 (C13), δ 49.2 (C14), δ 50.2 (C15), δ 50.4 (OCH_3), δ 57.0 (C9), δ 58.5 (C5), δ 63.1 (C1'), δ 68.3 (C17), δ 80.7 (C16), δ 177.1 (C19).

3.2.4 STEVIOL (1h)

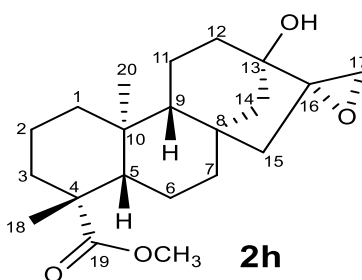


Sodium per iodate (10 g, 46.8 mmol), was added to the solution of commercial stevioside (10g, 12.2 mmol), in water (500 ml), and was kept in dark for 16 hours. Sodium hydroxide (187 mmol) was added to the mixture and was refluxed for 1h. The reaction mixture was cooled immediately by addition of ice. Acetic acid was added to the mixture till the pH 4 of solution was attained. The reaction mixture was immediately extracted with ethyl acetate (100X4 mL). The organic layer was dried over anhydrous sodium sulphate. After filtration ethyl acetate was removed under reduced pressure. The crude product was recrystallized in methanol.

White crystalline solid with (1.3 g: 13%), yield. IR; 3461 cm^{-1} , 1691 cm^{-1} , 1470 cm^{-1} , 1237 cm^{-1} , 1187 cm^{-1} , 1027 cm^{-1} . ^1H NMR (200 MHz, CDCl_3), δ 0.84 (3H, s, H20), δ 1.19 (3H, s, H17), δ 1.29 (1H, dd, $J = 10.82, 2.13$ Hz, H9), δ 1.87 (1H, dd, $J = 10.82, 2.5$ Hz, H14), δ 3.66 (3H, s, OCH_3), δ 4.84 (1H, br, s, H17), δ 5.0 (1H, br, s, H17). ^{13}C NMR (50 MHz, CDCl_3), δ 15.3 (C20), δ 19.1 (C2), δ 20.4

(C11), δ 21.8 (C6), δ 28.7 (C18), δ 38.0 (C3), δ 39.2 (C10, C12), δ 40.8 (C1), δ 41.3 (C7), δ 41.6 (C8), δ 43.7 (C4), δ 46.9 (C15), δ 47.4 (C14), δ 51.1 (OCH₃), δ 53.8 (C9), δ 56.9 (C5), δ 80.2 (C13), δ 102.9 (C17), δ 156.1 (C16), δ 177.9 (C19).

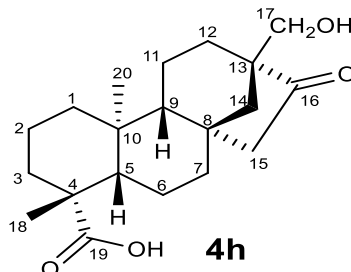
3.2.5 STEVIOL EPOXIDE (2h)



m-chloro per benzoic acid (300 mg: 1.7 mmol), was added into the solution of steviol (318 mg: 1 mmol), in dichloromethane (50mL). The reaction mixture was stirred for 12 hour at room temperature. The progress of reaction was followed by TLC. The reaction mixture was washed with saturated sodium carbonate solution (3x30 mL). The organic layer was dried over anhydrous sodium sulphate (Na₂SO₄). After filtration excess of dichloromethane was removed under reduced pressure. The reaction mixture was chromatographed on chromatotron using ethyl acetate and *n*-hexane (3:7). The product was recovered and recrystallized from ethyl acetate.

White crystalline solid with (196 mg: 60%), yield. IR; 3257 cm⁻¹, 1715 cm⁻¹, 1244 cm⁻¹, 939 cm⁻¹, 794 cm⁻¹. ¹H NMR (200 MHz, CDCl₃), δ 0.86 (3H, s, H20), δ 1.19 (3H, s, H17), δ 2.2 (1H, d, *J* = 11.0 Hz, H12 α), δ 2.79 (1H, d, *J* = 4.34 Hz, H17), δ 2.94 (1H, d, *J* = 4.34 Hz, H17), δ 3.65 (3H, s, OCH₃). ¹³C NMR (50 MHz, CDCl₃), δ 15.5 (C20), δ 19.0 (C2), δ 19.5 (C11), δ 21.8 (C6), δ 28.6 (C18), δ 34.7 (C12), δ 37.9 (C3), δ 39.2 (C10), δ 40.7 (C1), δ 41.2 (C7), δ 41.6 (C8), δ 43.7 (C4), δ 45.7 (C 14), δ 46.5 (C15), δ 48.6 (C17), δ 51.1 (OCH₃), δ 53.8 (C9), δ 56.8 (C5), δ 65.2 (C16), δ 74.7 (C13), δ 177.8 (C19).

3.2.6 17-HYDROXY ISOSTEVIOL (4h)



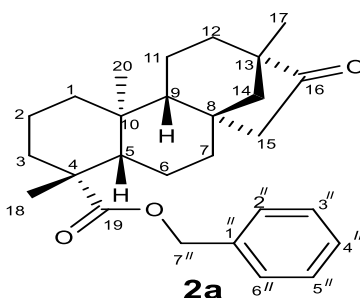
Dilute solution of hydrochloric acid (20 mL: 5%), was added to the solution of steviol epoxide (334 mg: 1 mmol), in acetone (20 mL). The reaction mixture was heated on water bath for 30 minutes at 58 °C. The progress of reaction was followed on TLC. The excess of solvent was removed under reduced pressure and the product was recovered with ethyl acetate (3x50 mL), and dried over anhydrous sodium sulphate. After filtration the reaction mixture was chromatographed over chromatotron using ethyl acetate and n-hexane (3:7). The products were then characterized by spectroscopic methods.

White crystalline product recovered with (215 mg: 64%) yield. IR; 3348 cm^{-1} , 1691 cm^{-1} , 1183 cm^{-1} . ^1H NMR (200 MHz, CDCl_3), δ 0.72 (3H, s, H20), δ 1.21 (3H, s, H17), δ 2.68 (1H, dd, $J = 18.88, 3.74$ Hz, H15), δ 3.52 (1H, d, $J = 10.99$ Hz, H17), δ 3.66 (3H, s, OCH_3). ^{13}C NMR (50 MHz, CDCl_3), δ 13.1 (C20), δ 18.9 (C2), δ 19.8 (C11), δ 21.7 (C6), δ 28.8 (C18), δ 32.1 (C12), δ 37.9 (C3), δ 38.0 (C10), δ 39.6 (C8), δ 39.8 (C1), δ 41.3 (C7), δ 43.7 (C4), δ 48.9 (C15, C14), δ 51.2 (OCH_3), δ 54.1 (C13), δ 55.4 (C9), δ 56.9 (C5), δ 65.1 (C17), δ 177.9 (C19).

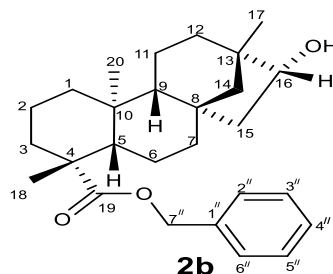
3.2.7 GENERAL PROCEDURE FOR THE PREPARATION OF BENZYL ESTER OF ISOSTEVIOL AND ITS DERIVATIVES

To the solution of isosteviol (**1a**) or 17-hydroxy isosteviol (**4h**) derivatives **1b**, **1c**, **1d**, **5i**, and **5j** (0.5 mmol), in acetone (30 mL), along benzyl chloride (0.7 mL, 0.043 mmol), and K_2CO_3 (1 mmol), were heated under reflux for 2 hour. The progress of reaction was followed by TLC. Excess of acetone and benzyl chloride were removed under vacuum. The reaction mixture was chromatographed on a chromatotron using silica rotors (1 mm), and elution was made with ethyl acetate: *n*-hexane (1:9). The products were then characterized by spectroscopic methods.

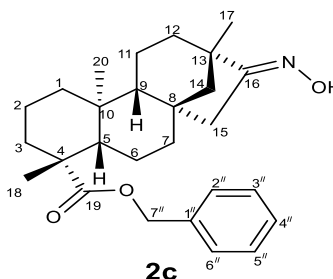
3.2.7.1 BENZYL ESTER OF ISOSTEVIOL (**2a**)



The compound was isolated as a white crystalline solid with (167 mg, 82%), yield. ESI-MS $[M-H]^+$ 407.46. IR; 1738 cm^{-1} , 1720 cm^{-1} , 1453 cm^{-1} , 1147 cm^{-1} , 740 cm^{-1} . ^1H NMR (200 MHz, $CDCl_3$), δ 0.60 (3H, s, H20), δ 0.97 (3H, s, H18), δ 1.21 (3H, s, H17), δ 2.55 (1H, dd, $J = 18.60, 3.6$ Hz, H15), δ 5.1 (1H, dd, $J = 18.16, 12.41$ Hz, H7''), δ 7.35 (5H, s, H2''-H6''). ^{13}C NMR (50 MHz, $CDCl_3$), δ 13.3 (C20), δ 18.9 (C2), δ 19.8 (C17), δ 20.3 (C11), δ 21.7 (C6), δ 28.9 (C18), δ 37.3 (C3), δ 37.9 (C12, C10), δ 39.4 (C8), δ 39.8 (C1), δ 41.5 (C7), δ 43.9 (C4), δ 48.3 (C15), δ 48.7 (C13), δ 54.3 (14), δ 54.7 (C9), δ 57.1 (C5), δ 66.1 (C7''), δ 128.1 (C4''), δ 128.4 (C2'', C6''), δ 128.5 (C3'', C5''), δ 135.9 (C1''), δ 176.9 (C19).

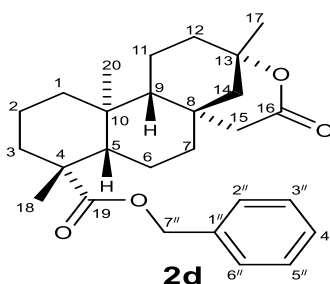
3.2.7.2 BENZYL ESTER OF 16-HYDROXY ISOSTEVIOL (2b)

White crystalline solid, (166 mg, 81%), yield. ESI-MS $[M-H]^+$ 409.39. IR; 3460 cm^{-1} , 1721 cm^{-1} , 1454 cm^{-1} , 1147 cm^{-1} , 696 cm^{-1} . ^1H NMR (200 MHz, CDCl_3), δ 0.71 (3H, s, H20), δ 0.93 (3H, s, H18), δ 1.22 (3H, s, H17), δ 2.22 (1H, br, $J = 12.26\text{ Hz}$, H12), δ 3.87 (1H, dd, $J = 9.61, 5.6\text{ Hz}$, H16), δ 5.0 (1H, d, $J = 12.45\text{ Hz}$, H7''), δ 5.2 (1H, d, $J = 12.45\text{ Hz}$, H7''), δ 7.38 (5H, s, H2''-H6''). ^{13}C NMR (50 MHz, CDCl_3), δ 13.3 (C20), δ 18.9 (C2), δ 20.4 (C11), δ 21.8 (C6), δ 24.9 (C17), δ 29.0 (C18), δ 33.7 (C12), δ 38.0 (C3, C10), δ 39.9 (C1), δ 41.7 (C7), δ 42.0 (C8, C13), δ 42.7 (C15), δ 43.9 (C4), δ 55.2 (14), δ 55.9 (C9), δ 57.3 (C5), δ 65.9 (C7''), δ 80.6 (C16), δ 128.0 (C4''), δ 128.2 (C2'', C6''), δ 128.4 (C3'', C5''), δ 136.1 (C1''), δ 177.3 (C19).

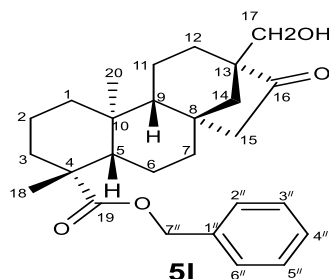
3.2.7.3 BENZYL ESTER OF 16-OXIME ISOSTEVIOL (2c)

White crystalline compound with (172 mg, 81%), yield. ESI-MS $[M-H]^+$ 422.33. IR; 3287 cm^{-1} , 1723 cm^{-1} , 1453 cm^{-1} , 1147 cm^{-1} , 930 cm^{-1} , 696 cm^{-1} . ^1H NMR (200 MHz, CDCl_3), δ 0.73 (3H, s, H20), δ 1.13 (3H, s, H18), δ 1.24 (3H, s, H17), δ 2.95 (1H, dd, $J = 18.62, 3.03\text{ Hz}$, H15), δ 5.00 (1H, d, $J = 12.47\text{ Hz}$, H7''), δ 5.23 (1H, d, $J = 12.47\text{ Hz}$, H7'''), δ 7.4 (5H, s, H2''-H6''). ^{13}C NMR (50 MHz, CDCl_3), δ 13.3 (C20), δ 18.9 (C2), δ 20.4 (C11), δ 21.7 (C6), δ 22.1 (C17), δ 28.9 (C18), δ 36.7 (C12), δ 38.0 (C3, C10), δ 39.5 (C15), δ 39.9 (C1), δ 40.6 (C8), δ 40.9 (C7), δ 43.7 (C4), δ 43.9 (C13), δ 54.8 (C9), δ 56.3 (C14), δ 57.3 (C5), δ 65.9 (C7'''), δ 128.0 (C4''), δ 128.1 (C2''-C6''), δ 128.5 (C3, C5''), δ 136.1 (C1''), δ 170.2 (C16), δ 177.1 (C19).

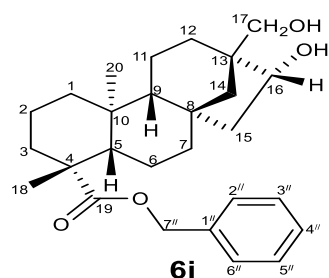
3.2.7.4 BENZYL ESTER OF ISOSTEVIOL LACTONE (2d)



White crystalline solid with (170 mg, 76%), yield. ESI-MS $[M+Na]^+$ ion 447.39. IR; 1713 cm^{-1} , 1453 cm^{-1} , 1237 cm^{-1} , 1146 cm^{-1} , 745 cm^{-1} , 698 cm^{-1} . ^1H NMR (200 MHz, CDCl_3), δ 0.70 (3H, s, H20), δ 1.22 (3H, s, H17), δ 1.36 (3H, s, H18), δ 2.22 (1H, d, $J = 13.70\text{ Hz}$, H12), δ 3.02 (1H, dd, $J = 18.81, 2.37\text{ Hz}$, H15), δ 5.0 (1H, d, $J = 12.34\text{ Hz}$, H7'''), δ 5.1 (1H, d, $J = 12.34\text{ Hz}$, H7''), δ 7.38 (5H, s, H2''-H6''). ^{13}C NMR (50 MHz, CDCl_3), δ 13.5 (C20), δ 18.5 (C11), δ 18.8 (C2), δ 19.5 (C6), δ 28.3 (C17), δ 28.7 (C18), δ 34.8 (C8), δ 37.8 (C10, C3), δ 38.4 (C7), δ 38.5 (C12), δ 39.8 (C1), δ 43.6 (C15), δ 43.7 (C4), δ 47.7 (C14), δ 55.8 (C9), δ 57.3 (C5), δ 66.1 (C7'''), δ 80.2 (C13), δ 128.2 (C4''), δ 128.3 (C2'', C6''), δ 128.5 (C3'', C5''), δ 135.8 (C1''), δ 172.5 (C16), δ 176.7 (C19).

3.2.7.5 BENZYL ESTER OF 17-HYDROXY ISOSTEVIOL (5i)

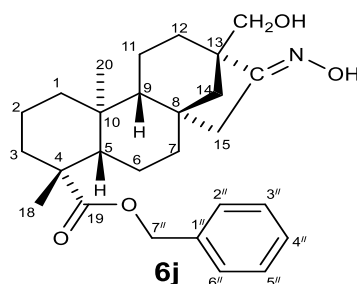
White crystalline solid (147 mg: 69%), yield. ESI-MS data, $[M+H]^+$ 425.33. IR; 3408 cm^{-1} , 1722 cm^{-1} , 1254 cm^{-1} , 1124 cm^{-1} , 772 cm^{-1} , 668 cm^{-1} . ^1H NMR (200 MHz, CDCl_3), δ 0.64 (3H, s, H20), δ 1.24 (3H, s, H17), δ 2.24 (1H, br, d, $J = 13.52$ Hz, H12), δ 2.61 (1H, dd, $J = 18.97, 3.78$ Hz, H15), δ 3.50 (1H, d, $J = 11.37$ Hz, H17), δ 3.6 (1H, d, $J = 11.37$ Hz, H17), δ 5.0 (1H, d, $J = 12.3$ Hz, H7''), δ 5.1 (1H, d, $J = 12.3$ Hz, H7''), δ 7.37 (5H, s, H2''-H6''). ^{13}C NMR (50 MHz, CDCl_3), δ 13.2 (C20), δ 18.9 (C2), δ 19.8 (C11), δ 21.7 (C6), δ 28.9 (C18), δ 32.1 (C12), δ 37.9 (C3), δ 38.1 (C10), δ 39.6 (C8), δ 39.7 (C1), δ 41.3 (C7), δ 43.9 (C4), δ 48.9 (C15, C14), δ 54.1 (C13), δ 55.3 (C9), δ 57.1 (C5), δ 65.1 (C17), δ 66.1 (C7''), δ 128.1 (C4''), δ 128.3 (C2'', C6''), δ 128.5 (C3'', C5''), δ 135.9 (C1''), δ 176.9 (C19).

3.2.7.6 BENZYL ESTER OF 17, 16-DIHYDROXY ISOSTEVIOL (6i)

White crystalline solid with (165 mg: 77%), yield. ESI-MS data, $[M-H]^+$ 425.29. IR; 3391 cm^{-1} , 1720 cm^{-1} , 1453 cm^{-1} , 1147 cm^{-1} , 754 cm^{-1} , 696 cm^{-1} . ^1H

NMR (200 MHz, CD₃COCD₃), δ 0.72 (3H, s, H20), δ 1.18 (3H, s, H18), δ 2.17 (1H, br, J = 12.7 Hz, H12), δ 3.33 (1H, dd, J = 16.93, 10.58 Hz, H17), δ 4.11 (1H, dd, J = 11.28, 4.08 Hz, H16), δ 5.0 (1H, d, J = 12.45 Hz, H7''), δ 5.1 (1H, d, J = 12.45 Hz, H7''), δ 7.39 (5H, s, H2''-H6''). ¹³C NMR (50 MHz, CD₃COCD₃), δ 13.0 (C20), δ 18.8 (C2), δ 19.8 (C11), δ 21.8 (C6), δ 28.2 (C18), δ 29.3 (C12), δ 37.0 (C10), δ 37.9 (C3), δ 39.8 (C1), δ 41.8 (C7), δ 42.0 (C8), δ 42.4 (C15), δ 43.6 (C4), δ 46.9 (C13), δ 50.1 (C14), δ 56.5 (C9), δ 57.1 (C5), δ 65.5 (C7''), δ 68.2 (C17), δ 75.5 (C16), δ 127.9 (C4''), δ 128.2 (C2'', C6''), δ 128.4 (C3', C5''), δ 136.5 (C1''), δ 176.5 (C19).

3.2.7.7 BENZYL ESTER OF 17-HYDROXY, 16-OXIME ISOSTEVIOL (6j)

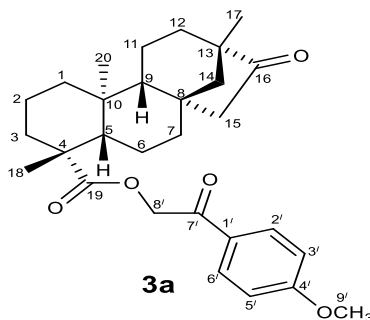


White crystalline solid (147 mg: 66%), yield. ESI-MS data, $[M+H]^+$ 440.4. IR; 1881 cm⁻¹, 1578 cm⁻¹, 1480 cm⁻¹, 1163 cm⁻¹, 999 cm⁻¹, 773 cm⁻¹, 587 cm⁻¹. ¹H NMR (200 MHz, CDCl₃), δ 0.69 (3H, s, H20), δ 1.20 (3H, s, H18), δ 2.20 (1H, br, J = 12.7 Hz, H12), δ 2.92 (1H, br, d, J = 18.30, Hz, H15), δ 3.59 (2H, s, H17), δ 5.01 (1H, d, J = 13.59 Hz, H7''), δ 5.18 (1H, d, J = 12.39 Hz, H7''), δ 7.34 (5H, s, H2''-H6''). ¹³C NMR (50 MHz, CDCl₃), δ 13.3 (C20), δ 18.9 (C2), δ 19.9 (C11), δ 21.7 (C6), δ 28.9 (C18), δ 34.1 (C12), δ 37.0 (C7), δ 37.9 (C3), δ 38.1 (C10), δ 39.8 (C1), δ 40.8 (C15), δ 40.9 (C8), δ 43.9 (C4), δ 49.4 (C13), δ 51.0 (C14), δ 55.6 (C9), δ 57.2 (C5), δ 65.9 (C7''), δ 66.7 (C17), δ 128.1 (C4''), δ 128.2 (C2'', C6''), δ 128.5 (C3', C5''), δ 136.1 (C1''), δ 169.2 (C16), δ 177.1 (C19).

3.3 GENERAL PROCEDURE FOR THE PREPARATION OF *p*-METHOXY PHENACYL ESTER

Steviol (**1h**), isosteviol (**1a**), and derivative such as **1b** and **1c** (0.31 mmol), solution in acetone (10 mL), was treated with a mixture of 2-bromo-4'-methoxy acetophenone (225 mg, 0.983 mmol), and triethylamine (20 mg/mL in acetone), and the reaction mixture was irradiated in a microwave oven for four minutes (Silva & Ferraz, 2006). The reaction progress was followed on TLC. After completion (4 minutes) of reaction, acetic acid (40 μ L), was added and the mixture was irradiated again for 1 minute. The reaction mixture was chromatographed on a chromatotron using silica rotors (1 mm), and elution was made with acetone: *n*-hexane (1:9). The product obtained, was then characterized by spectroscopic methods.

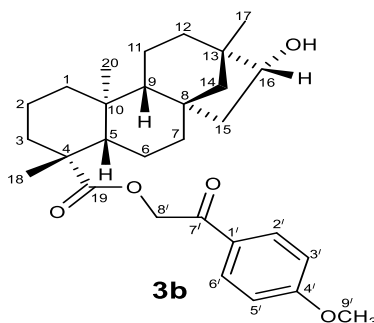
3.3.1 *p*-METHOXY PHENACYL ESTER OF ISOSTEVIOL (**3a**)



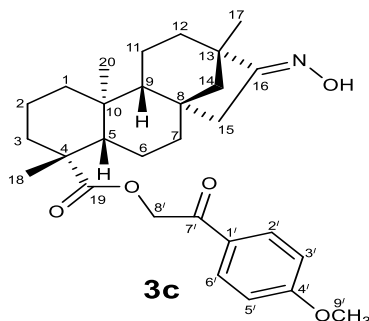
White powder solid with (112 mg: 81%), yield. ESI-MS $[M]^+$ ion 466.63. IR; 1736 cm^{-1} , 1601 cm^{-1} , 1454 cm^{-1} , 1146 cm^{-1} , 966 cm^{-1} , 696 cm^{-1} . ^1H NMR (200 MHz, CDCl_3), δ 0.77 (3H, s, H20), δ 0.98 (3H, s, H18), δ 1.34 (3H, s, H17), δ 2.29 (1H, br, d, $J = 13.2$ Hz, H12), δ 2.65 (1H, dd, $J = 18.69, 3.65$ Hz, H15), δ 3.88 (3H, s, OCH_3), δ 5.2 (1H, d, $J = 16.0$ Hz, H8'), δ 5.3 (1H, d, $J = 16.0$ Hz, H8'), δ 6.95 (2H, d, $J = 9.00$ Hz, H3', H5'), δ 7.90 (2H, d, $J = 8.97$ Hz, H2', H6'). ^{13}C NMR (50

MHz, CDCl₃), δ 13.5 (C20), δ 18.9 (C2), δ 19.8 (C17), δ 20.3 (C11), δ 21.7 (C6), δ 29.1 (C18), δ 37.3 (C3), δ 38.0 (C12), δ 38.1 (C10), δ 39.5 (C8), δ 39.8 (C1), δ 41.5 (C7), δ 44.1 (C4), δ 48.5 (C15), δ 48.7 (C13), δ 54.3 (C14), δ 54.7 (C9), δ 55.5 (OCH₃), δ 57.1 (C5), δ 65.2 (C8'), δ 114.0 (C3', C5'), δ 127.4 (C1'), δ 130.0 (C2', C6'), δ 163.9 (C4'), δ 176.8 (C19), δ 190.9 (C7').

3.3.2 *p*-METHOXY PHENACYL ESTER OF 16-HYDROXYL ISOSTEVIOL (3b)

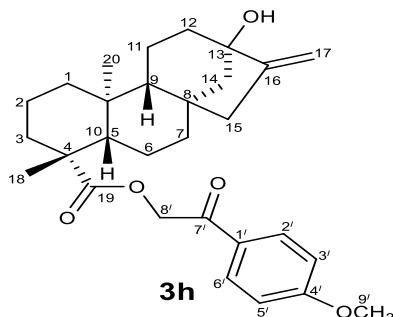


White powder solid with (105 mg: 75%), yield. ESI-MS, [M+Na]⁺ ion 491.35. IR; 3556 cm⁻¹, 1719 cm⁻¹, 1692 cm⁻¹, 1603 cm⁻¹, 1161 cm⁻¹, 966 cm⁻¹, 838 cm⁻¹. ¹H NMR (200 MHz, CDCl₃), δ 0.81 (3H, s, H20), δ 0.92 (3H, s, H18), δ 1.32 (3H, s, H17), δ 2.29 (1H, br, d, *J* = 13.2 Hz, H12), δ 3.88 (3H, s, OCH₃), δ 5.2 (1H, d, *J* = 16.1 Hz H8'), δ 5.3 (1H, d, *J* = 16.1 Hz, H8'), δ 6.95 (2H, d, *J* = 9.0 Hz, H3', H5'), δ 7.90 (2H, d, *J* = 8.97 Hz, H2', H6'). ¹³C NMR (50 MHz, CDCl₃), δ 13.5 (C20), δ 18.9 (C2), δ 20.5 (C11), δ 21.7 (C6), δ 24.9 (C17), δ 29.1 (C18), δ 33.7 (C12), δ 38.1 (C3, C10), δ 39.9 (C1), δ 41.7 (C7), δ 41.9 (C8), δ 42.1 (C13), δ 42.8 (C15), δ 44.0 (C4), δ 55.3 (C14), δ 55.5 (OCH₃), δ 55.8 (C9), δ 57.2 (C5), δ 65.2 (C8'), δ 80.5 (C16), δ 113.9 (C3', C5'), δ 127.5 (C1'), δ 130.0 (C2', C6'), δ 163.9 (C4'), δ 177.0 (C19), δ 191.1 (C7').

3.3.3 *p*-METHOXY PHENACYL ESTER OF 16-OXIME ISOSTEVIOL (3c)

White powder solid with (115 mg: 79%), yield. ESI-MS $[M]^+$ ion 481.39. IR: 3447 cm^{-1} , 1719 cm^{-1} , 1692 cm^{-1} , 1601 cm^{-1} , 1162 cm^{-1} , 963 cm^{-1} . ^1H NMR (200 MHz, CDCl_3), δ 0.86 (3H, s, H20), δ 1.13 (3H, s, H18), δ 1.37 (3H, s, H17), δ 2.2 (2H, s, H12), δ 3.01 (1H, dd, $J = 18.5, 2.6\text{ Hz}$, H15), δ 3.91 (3H, s, OCH_3), δ 5.14 (1H, d, $J = 16.0\text{ Hz}$, H8'), δ 5.42 (1H, d, $J = 16.0\text{ Hz}$, H8'), δ 6.9 (2H, d, $J = 8.9\text{ Hz}$, H3', H5'), δ 7.9 (2H, d, $J = 8.90\text{ Hz}$, H2', H6'). ^{13}C NMR (50 MHz, CDCl_3), δ 13.5 (C20), δ 18.9 (C2), δ 20.4 (C11), δ 21.7 (C6), δ 22.1 (C17), δ 29.0 (C18), δ 36.8 (C12), δ 38.1 (C3, C10), δ 39.5 (C7), δ 39.9 (C1), δ 40.6 (C8), δ 40.9 (C15), δ 43.7 (C4), δ 44.0 (C13), δ 54.9 (C9), δ 55.5 (OCH_3 , 9'), δ 56.3 (C14), δ 57.2 (C5), δ 65.2 (C8'), δ 114.0 (C3', C5'), δ 127.5 (C1'), δ 130.1 (C2', C6'), δ 163.9 (C4'), δ 170.4 (C16), δ 176.9 (C19), δ 191.0 (C7').

3.3.4 *p*-METHOXY PHENACYL ESTER OF STEVIOL (3h)



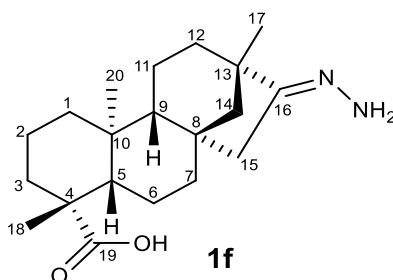
White powder solid, (110 mg: 78 %), yield. ESI-MS $[M+Na]^+$; 489.47. IR; 3488 cm^{-1} , 1728 cm^{-1} , 1692 cm^{-1} , 1602 cm^{-1} , 1263 cm^{-1} , 1149 cm^{-1} , 965 cm^{-1} . ^1H NMR (200 MHz, CDCl_3), δ 0.91 (3H, s, H20), δ 1.32 (3H, s, H18), δ 2.13 (1H, dd, $J = 10.6\text{ Hz}$, H14), δ 3.88 (3H, s, OCH_3), δ 4.8 (1H, br, s, H17), δ 4.9 (1H, br, s, H17), δ 5.2 (1H, d, $J = 16.1\text{ Hz}$, H8'), δ 5.4 (1H, d, $J = 16.1\text{ Hz}$, H8'), δ 6.95 (2H, d, $J = 8.95\text{ Hz}$, H3', H5'), δ 7.91 (2H, d, $J = 8.95\text{ Hz}$, H2', H6'). ^{13}C NMR (50 MHz, CDCl_3): δ 15.7 (C20), δ 19.1 (C2), δ 20.4 (C11), δ 21.8 (C6), δ 29.0 (C18), δ 38.1 (C3), δ 39.2 (C12), δ 39.4 (C10), δ 40.7 (C1), δ 41.3 (C7), δ 41.7 (C8), δ 44.1 (C4), δ 46.9 (C15), δ 47.4 (C14), δ 53.8 (C9), δ 55.5 (C9'), δ 57.0 (C5), δ 65.2 (C8'), δ 80.3 (C13), δ 102.9 (C17), δ 114.0 (C5', C3'), δ 127.4 (C1'), δ 130.1 (C2', C6'), δ 156.2 (C16), δ 163.9 (C4'), δ 176.9 (C19), δ 191.0 (C7').

3.4 GENERAL PROCEDURE FOR THE PREPARATION OF 16-HYDRAZONE

Hydrazine hydrate (3 mL, 10 mm) was added to solution of **1a**, **2a**, **4h** and **5I** (0.314 mm), in methanol (30 mL), the reaction mixture was heated under reflux for 8 hours. The reaction progress was followed by TLC. After reaction completion, the excess of solvent and hydrazine were removed under reduced pressure and the products were re-crystallized from methanol. The products

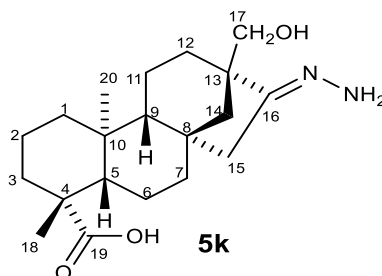
obtained were characterized by spectroscopic methods (Garifullin, Chestnova, Mironov & Kataev., 2012).

3.4.1 16-HYDRAZONE OF ISOSTEVIOL (1f)



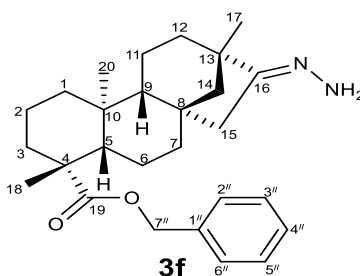
White crystalline solid with (83 mg: 83%), yield, ESI-MS, $[M+H]^+$ 333.31. IR; 3352 cm^{-1} , 1712 cm^{-1} , 1453 cm^{-1} , 1399 cm^{-1} . ^1H NMR (200 MHz, CD_3OD), δ 0.85 (3H, s, H20), δ 1.06 (3H, s, H17), δ 1.24 (3H, s, H18), δ 2.17 (1H, br, d, $J = 13.14$ Hz, H12), δ 2.66 (1H, dd, $J = 17.6, 2.0$ Hz, H15 α). ^{13}C NMR (50 MHz, CD_3OD), δ 13.5 (C20), δ 18.9 (C2), δ 20.5 (C11), δ 21.7 (C6), δ 22.1 (C17), δ 29.1 (C18), δ 36.3 (C12), δ 37.9 (C3), δ 38.2 (C10), δ 39.3 (C7), δ 39.9 (C1), δ 40.8 (C8), δ 41.2 (C15), δ 43.6 (C4), δ 44.1 (C13), δ 54.9 (9), δ 56.3 (C14), δ 57.1 (C5), δ 165.5 (C16), δ 182.4 (C19).

3.4.2 16-HYDRAZONE OF 17-HYDROXY, ISOSTEVIOL (5k)



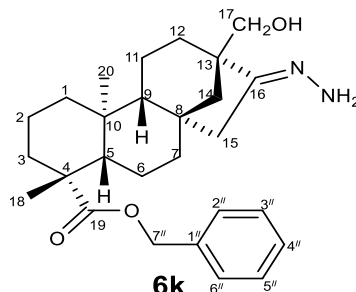
White crystalline solid with (90 mg: 86%), yield. ESI MS, $[M-H]^+$ 347.33. IR; 3412 cm^{-1} , 3221 cm^{-1} , 1698 cm^{-1} , 1234 cm^{-1} , 1175 cm^{-1} , 1027 cm^{-1} . ^1H NMR (200 MHz, CD_3OD), δ 0.96 (3H, s, H20), δ 1.19 (3H, s, H18), δ 2.16 (1H, br, d, $J = 12.9$ Hz, H12), δ 2.89 (1H, br, d, $J = 17.9$ Hz, H15), δ 3.57 (2H, br, s, H17), δ 3.65 (3H, s, OCH_3). ^{13}C NMR (50 MHz, CD_3OD), δ 12.9 (C20), δ 19.2 (C2), δ 19.7 (C11), δ 21.9 (C6), δ 28.8 (C18), δ 34.2 (C12), δ 36.8 (C7), δ 38.0 (C10), δ 38.6 (C3), δ 40.2 (C1), δ 40.8 (C8), δ 41.3 (C15), δ 44.1 (C4), δ 49.1 (C13), δ 51.0 (C14), δ 55.6 (C9), δ 57.4 (C5), δ 66.1 (C17), δ 165.4 (C16), δ 182.9 (C19).

3.4.3 16-HYDRAZONE BENZYL ESTER OF ISOSTEVIOL (3f)



White crystalline solid with (105 mg: 84%), yield, ESI-MS, $[M+2H]^+$ 423.30. IR; 3432 cm^{-1} , 1713 cm^{-1} , 1453 cm^{-1} , 1237 cm^{-1} , 1146 cm^{-1} , 745 cm^{-1} , 698 cm^{-1} . ^1H NMR (200 MHz, CDCl_3), δ 0.66 (3H, s, H20), δ 1.06 (3H, s, H18), δ 1.22 (3H, s, H17), δ 2.22 (1H, br, d, $J = 13.17$ Hz, H12), δ 2.55 (1H, dd, $J = 17.5, 2.8$ Hz, H15), δ 5.1 (1H, d, $J = 12.4$ Hz, H7''), δ 5.2 (1H, d, $J = 12.4$ Hz, H7''), δ 7.36 (5H, s, H2''-H6''). ^{13}C NMR (50 MHz, CDCl_3), δ 13.4 (C20), δ 18.9 (C2), δ 20.5 (C11), δ 21.7 (C6), δ 22.2 (C17), δ 28.9 (C18), δ 35.8 (C12), δ 37.9 (C3), δ 38.0 (C10), δ 39.3 (C7), δ 39.8 (C1), δ 40.7 (C8), δ 41.2 (C15), δ 43.8 (C4), δ 43.9 (C13), δ 54.9 (C9), δ 55.8 (C14), δ 57.3 (C5), δ 66.1 (C7''), δ 128.2 (C4''), δ 128.3 (C2'', C6''), δ 128.5 (C3'', C5''), δ 135.9 (C1''), δ 172.6 (C16), δ 176.7 (C19).

3.4.4 16-HYDRAZONE BENZYL ESTER OF 17-HYDROXY, ISOSTEVIOL (6k)

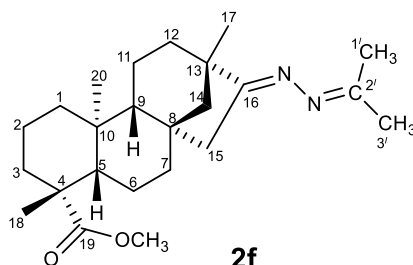


White crystalline solid with (96 mg: 73%), yield, ESI-MS, $[M]^+$ 439.42. IR; 3432 cm^{-1} , 1721 cm^{-1} , 1453 cm^{-1} , 996 cm^{-1} , 752 cm^{-1} , 695 cm^{-1} . $^1\text{H NMR}$ (200 MHz, CDCl_3), δ 0.65 (3H, s, H20), δ 1.20 (3H, s, H18), δ 2.2 (1H, br, d, $J = 12.9$ Hz, H12), δ 2.56 (1H, dd, $J = 17.3, 2.4$ Hz, H15), δ 3.5 (1H, d, $J = 11.0$ Hz, H17), δ 3.6 (1H, d, $J = 11.0$ Hz, H17), δ 5.0 (1H, d, $J = 12.50$ Hz, H7''), δ 5.1 (1H, d, $J = 12.50$ Hz, H7''), δ 7.35 (5H, s, H2''-H6''). $^{13}\text{C NMR}$ (50 MHz, CDCl_3), δ 13.4 (C20), δ 18.9 (C2), δ 20.0 (C11), δ 21.7 (C6), δ 28.9 (C18), δ 33.9 (C12), δ 36.2 (C7), δ 37.9 (C3), δ 38.1 (C10), δ 39.8 (C1), δ 41.1 (C15), δ 41.4 (C8), δ 43.9 (C4), δ 48.8 (C13), δ 51.1 (C14), δ 55.7 (C9), δ 57.2 (C5), δ 65.9 (C17), δ 67.9 (C7''), δ 128.0 (C4''), δ 128.2 (C2'', C6''), δ 128.4 (C3'', C5'), δ 136.1 (C1''), δ 164.8 (C16), δ 177.0 (C19).

3.5 GENERAL PROCEDURE FOR THE PREPARATION OF ISOPROPYL HYDRAZONE

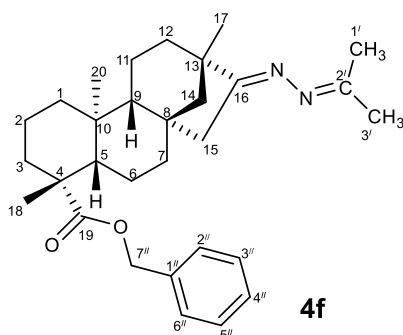
Hydrazone of isosteviol **1f**, **3f** and **6k** (0.3 mmol), were heated under refluxed in acetone (4 mL), for 1h. The progress of reaction was followed by TLC. The excess of acetone was removed and the residue was recrystallized from methanol. The products, **2f**, **4f** and **7k**, were characterized by spectroscopic methods.

3.5.1 ISOPROPYL HYDRAZONE OF ISOSTEVIOL (2f)



Light yellow crystalline solid (98 mg: 84%), yield. ESI-MS $[M]^+$ ion 386.29. IR; 1721 cm^{-1} , 1658 cm^{-1} . ^1H NMR (200 MHz, CDCl_3), δ 0.69 (3H, s, H20), δ 1.12 (3H, s, H17), δ 1.17 (3H, s, H18), δ 1.83 (3H, s, H1'), δ 2.01 (3H, s, H3'), δ 2.68 (1H, dd, $J = 18.5, 3.2\text{ Hz}$, H15), δ 3.63 (3H, s, OCH_3). ^{13}C NMR (50 MHz, CDCl_3), δ 13.2 (C20), δ 17.6 (C3'), δ 18.9 (C2), δ 20.5 (C11), δ 21.7 (C6), δ 22.2 (C1'), δ 24.9 (C17), δ 28.8 (C18), δ 37.9 (C3, 10), δ 39.0 (C12), δ 39.4 (C7), δ 39.9 (C1), δ 40.6 (C8), δ 41.1 (C15), δ 43.8 (C4), δ 44.2 (C13), δ 51.2 (OMe), δ 55.0 (C9), δ 56.0 (C14), δ 57.2 (C5), δ 159.1 (C2'), δ 174.3 (C16), δ 177.9 (C19).

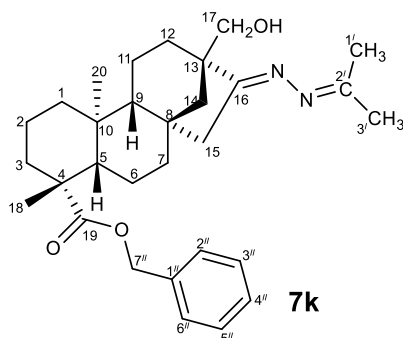
3.5.2 ISOPROPYL HYDRAZONE BENZYL ESTER OF ISOSTEVIOL (4f)



Light yellow crystalline solid (105 mg, 75 %), yield. ESI-MS $[M+H]^+$ 463.39. IR: 1721 cm^{-1} , 1658 cm^{-1} , 1453 cm^{-1} , 1147 cm^{-1} , 753 cm^{-1} , 698 cm^{-1} . ^1H

NMR (200 MHz, CDCl₃), δ 0.63 (3H, s, H20), δ 1.13 (3H, s, H18), δ 1.21 (3H, s, H17), δ 1.83 (3H, s, H3'), δ 2.03 (3H, s, H1'), δ 2.20 (1H, d, J = 14.8 Hz, H12), δ 2.63 (1H, dd, J = 18.5, 3.1 Hz, H15), δ 5.11 (1H, dd, J = 17.7, 12.3 Hz, H7''), δ 7.3 (5H, s, H2''-H6''). ¹³C NMR (50 MHz, CDCl₃), δ 13.4 (C20), δ 17.6 (C1'), δ 18.9 (C2), δ 20.5 (C11), δ 21.7 (C6), δ 22.2 (C3'), δ 24.9 (C17), δ 28.9 (C18), δ 37.9 (C3), δ 38.0 (C10), δ 38.9 (C12), δ 39.3 (C7), δ 39.8 (C1), δ 40.6 (C8), δ 41.1 (C15), δ 43.9 (C4), δ 44.2 (C13), δ 54.9 (C9), δ 55.9 (C14), δ 57.3 (C5), δ 65.9 (C7''), δ 127.9 (C4''), δ 128.2 (C2''-C6''), δ 128.4 (C3'', C5''), δ 136.1 (C1''), δ 158.7 (C2'), δ 174.1 (C16), δ 177.1 (C19).

3.5.3 16-ISOPROYL HYDRAZONE BENZYL ESTER OF 17-HYDROXY ISOSTEVIOL (7k)



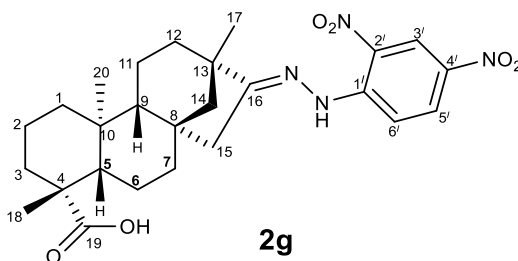
Light yellow crystalline solid (94 mg: 65%), yield. ESI-MS [M+H]⁺ 479.50. IR; 3426 cm⁻¹, 1720 cm⁻¹, 1656 cm⁻¹, 1455 cm⁻¹, 1147 cm⁻¹, 771 cm⁻¹, 694 cm⁻¹. ¹H NMR (200 MHz, CDCl₃), δ 0.66 (3H, s, H20), δ 1.22 (3H, s, H17), δ 1.9 (3H, s, H1'), δ 2.07 (3H, s, H3'), δ 2.19 (2H, s, H12), δ 2.8 (1H, dd, J = 18.8, 3.0 Hz, H15), δ 3.55 (1H, d, J = 10.7 Hz, H17), δ 3.76 (1H, d, J = 10.9 Hz, H17), δ 5.1 (1H, dd, J = 12.45 Hz, H7''), δ 5.2 (1H, dd, J = 12.45 Hz, H7''), δ 7.39 (5H, s, H2''-H6''). ¹³C NMR (50 MHz, CDCl₃), δ 13.4 (C20), δ 18.1 (C1'), δ 18.9 (C2), δ 20.0 (C11), δ 21.7 (C6), δ 25.0 (C3'), δ 28.9 (C18), δ 33.9 (C12), δ 37.9 (C3), δ 38.1 (C10), δ 39.5 (C7), δ 39.8 (C1), δ 40.9 (C15), δ 41.3 (C8), δ 43.9 (C4), δ

48.9 (C13), δ 50.9 (C14), δ 55.7 (C9), δ 57.2 (C5), δ 65.9 (C7"), δ 68.0 (C17), δ 128.0 (C4"), δ 128.2 (C2", C6"), δ 128.4 (C3", C5"), δ 136.1 (C1"), δ 162.2 (C16), δ 177.0 (C2'), δ 177.9 (C19).

3.6 PROCEDURE FOR THE PREPARATION OF 2, 4 DINITRO PHENYL AND 4-NITRO PENYL HYDRAZONE OF ISOSTEVIOL AND ITS DERIVATIVES

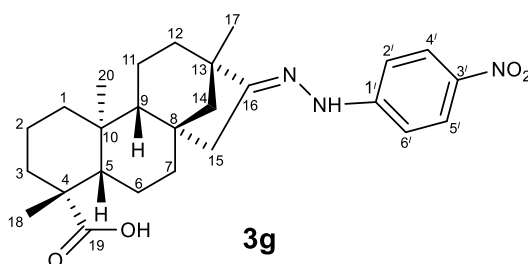
To the solution of isosteviol **1a** or 17-hydroxy isosteviol **4h** and their derivatives **2a** and **5l** (0.3 mm), in ethanol (10 mL), was combined with solution of 2, 4-dinitro phenyl hydrazine, or 4-nitro phenyl hydrazine (2 mmol), in sulphuric acid, water and ethanol (1:1.5:1.5), the reaction mixture was kept stirred for 12 hours, at room temperature. The progress of reaction was followed by TLC. Water (20 mL), was added to the reaction mixture and the product was recovered with ethyl acetate. The organic layer was dried over anhydrous sodium sulphate. After filtration the solvent was removed under reduced pressure. The residue was chromatographed on a chromatotron using silica rotors (1 mm), and elution was made with acetone: n-hexane (1:9). The products, **2g**, **3g**, **4g**, **5g**, **5m**, **6m**, **7m** and **8m** were then characterized by spectroscopic methods.

3.6.1 2, 4-DINITRO PHENYL HYDRAZONE OF ISOSTEVIOL (2g)



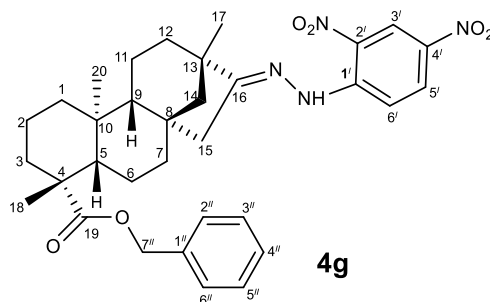
Yellow crystalline solid with (80 mg: 70%), yield. ESI-MS, $[M-H]^+$ ion 497.36. IR; 3315 cm^{-1} , 1692 cm^{-1} , 1618 cm^{-1} , 1517 cm^{-1} , 1337 cm^{-1} . ^1H NMR (200 MHz, CDCl_3), δ 0.93 (3H, s, H20), δ 1.20 (3H, s, H17), δ 1.29 (3H, s, H18), δ 2.65 (1H, dd, $J = 18.69, 3.65\text{ Hz}$, H15), δ 7.8 (1H, d, $J = 9.61\text{ Hz}$, H6'), δ 8.11 (1H, dd, $J = 9.66, 2.5\text{ Hz}$, H5'), δ 8.96 (1H, d, $J = 2.52\text{ Hz}$, H3'), δ 10.6 (1H, s, NH). ^{13}C NMR (50 MHz, CDCl_3), δ 12.8 (C20), δ 18.8 (C2), δ 20.3 (C11), δ 21.5 (C6), δ 22.1 (C17), δ 28.9 (C18), δ 37.4 (C12), δ 37.6 (C3), δ 38.3 (C10), δ 39.5 (C1), δ 39.5 (C15), δ 40.7 (C7), δ 41.4 (C8), δ 43.6 (C4), δ 45.2 (C13), δ 54.8 (C9), δ 55.8 (C14), δ 56.9 (C5), δ 116.2 (C6'), δ 123.4 (C5'), δ 128.4 (C1'), δ 129.5 (C3'), δ 137.2 (C2'), δ 144.9 (C4'), δ 171.7 (C16), δ 184.0 (C19).

3.6.2 4-NITRO PHENYL HYDRAZONE OF ISOSTEVIOL, (3g)

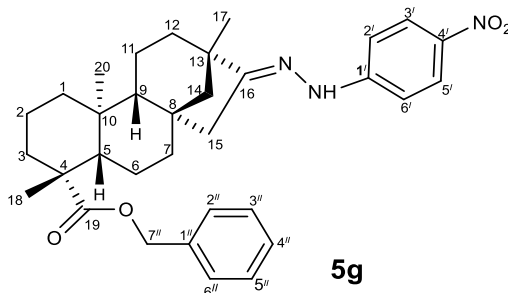


Yellow crystalline solid with (70 mg: 51%), yield. ESI-MS, $[M-H]^+$ ion 452.36. IR; 3319 cm^{-1} , 1693 cm^{-1} , 1595 cm^{-1} , 1322 cm^{-1} , 1109 cm^{-1} , 841 cm^{-1} , 751 cm^{-1} . ^1H NMR (200 MHz, CDCl_3), δ 0.90 (3H, s, H20), δ 1.2 (3H, s, H17), δ 1.3 (3H, s, H18), δ 2.8 (1H, d, $J = 16.9\text{ Hz}$, H15), δ 7.07 (2H, s, H2'-6'), δ 8.15 (2H, s, H3'-5'). ^{13}C NMR (50 MHz, CDCl_3), δ 13.6 (C20), δ 18.9 (C2), δ 20.6 (C11), δ 21.6 (C6), δ 22.2 (C17), δ 29.0 (C18), δ 36.7 (C12), δ 37.7 (C3), δ 38.3 (C10), δ 39.4 (C7), δ 39.8 (C1), δ 41.1 (C15), δ 41.4 (C8), δ 43.8 (C4), δ 44.3 (C13), δ 54.8 (C9), δ 55.9 (C14), δ 56.9 (C5), δ 111.4 (C2', C6'), δ 126.1 (C3', C5'), δ 139.6 (C1'), δ 150.6 (C4'), δ 163.5 (C16), δ 184.0 (C19).

3.6.3 2, 4-DINITRO PHENYL HYDRAZONE BENZYL ESTER OF ISOSTEVIOL (4g)

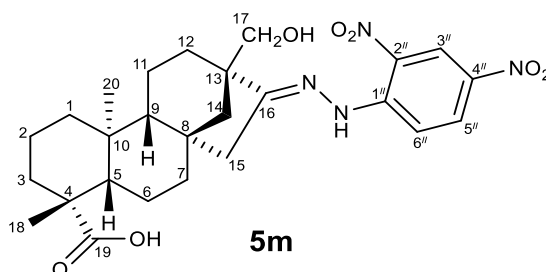


Yellow crystalline solid with (80 mg: 45%), yield. ESI-MS $[M]^+$ 587.46. IR, 3316 cm^{-1} , 1720 cm^{-1} , 1619 cm^{-1} , 1591 cm^{-1} , 1335 cm^{-1} , 1141 cm^{-1} , 755 cm^{-1} , 697 cm^{-1} . $^1\text{H NMR}$ (200 MHz, CDCl_3), δ 0.67 (3H, s, H20), δ 1.19 (3H, s, H17), δ 1.22 (3H, s, H18), δ 2.88 (1H, dd, $J = 17.82, 2.54\text{ Hz}$, H15), δ 5.1 (2H, s, H7'), δ 7.4 (5H, s, H2''-H6''), δ 7.96 (1H, d, $J = 9.65\text{ Hz}$, H6'), δ 8.28 (1H, dd, $J = 9.72, 2.60\text{ Hz}$, H5'), δ 9.13 (1H, $J = 2.5\text{ Hz}$, H3'), δ 10.7 (1H, s, NH). $^{13}\text{C NMR}$ (50 MHz, CDCl_3), δ 13.3 (C20), δ 18.9 (C2), δ 20.5 (C11), δ 21.6 (C6), δ 22.1 (C17), δ 28.9 (C18), δ 37.4 (C12), δ 37.9 (C3), δ 38.1 (C10), δ 39.4 (C7), δ 39.8 (C1), δ 40.9 (C15), δ 41.4 (C8), δ 43.8 (C4), δ 45.2 (C13), δ 54.8 (C9), δ 55.9 (C14), δ 57.1 (C5), δ 66.2 (C7''), δ 116.3 (C6'), δ 123.4 (C5'), δ 128.2 (C4''), δ 128.5 (C2'', C6''), δ 128.6 (C3'', C5''), δ 128.9 (C4'), δ 129.5 (C3'), δ 135.9 (C1''), δ 137.5 (C2'), δ 145.2 (C1'), δ 171.2 (C16), δ 176.9 (C19).

3.6.4 4-NITRO PHENYL HYDRAZONE BENZYL ESTER OF ISOSTEVIOL (5g)

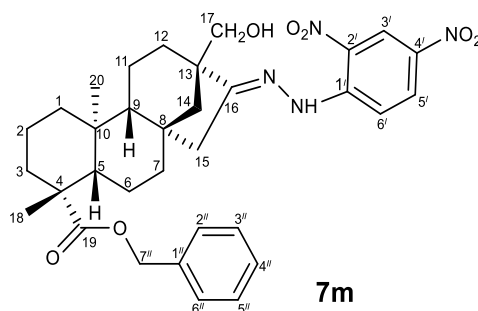
Yellow crystalline solid with (75 mg: 46%), yield. ESI-MS, $[M-H]^+$ 542.69, IR; 3320 cm^{-1} , 1738 cm^{-1} , 1598 cm^{-1} , 1321 cm^{-1} , 1172 cm^{-1} , 752 cm^{-1} , 695 cm^{-1} . ^1H NMR (200 MHz, CDCl_3), δ 0.69 (3H, s, H20), δ 1.16 (3H, s, H17), δ 1.23 (3H, s, H18), δ 2.67 (1H, dd, $J = 17.4, 2.4\text{ Hz}$, H15), δ 5.0 (1H, d, $J = 12.58\text{ Hz}$, H7''), δ 5.1 (1H, d, $J = 12.58\text{ Hz}$, H7''), δ 7.0 (2H, dd, $J = 6.7, 2.0\text{ Hz}$, H2', H6'), δ 7.4 (5H, s, H2''-H6''), δ 8.1 (2H, dd, $J = 6.54, 1.99\text{ Hz}$, H3', H5'). ^{13}C NMR (50 MHz, CDCl_3), δ 13.6 (C20), δ 18.9 (C2), δ 20.6 (C11), δ 21.7 (C6), δ 22.2 (C17), δ 28.9 (C18), δ 36.5 (C12), δ 37.8 (C3), δ 38.1 (C10), δ 39.4 (C7), δ 39.8 (C1), δ 41.1 (C15), δ 41.4 (C8), δ 43.9 (C4), δ 44.7 (C13), δ 54.7 (C9), δ 55.9 (C14), δ 57.2 (C5), δ 65.9 (C7''), δ 111.4 (C2', C6'), δ 126.2 (C3', C5'), δ 128.0 (C2'', C4'', C6''), δ 128.5 (C3'', C5''), δ 136.6 (C1''), δ 139.6 (C1'), δ 150.6 (C4'), δ 163.5 (C16), δ 177.0 (C19).

3.6.5 2, 4-DINITRO PHENYL HYDRAZONE OF 17-HYDROXY ISOSTEVIOL (5m)

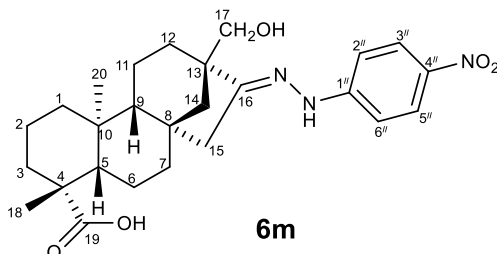


Yellow crystalline solid with (88 mg: 57%), yield. ESI-MS, $[M-H]^+$ 513.29. IR; 3315 cm^{-1} , 1692 cm^{-1} , 1618 cm^{-1} , 1591 cm^{-1} , 1518 cm^{-1} , 1337 cm^{-1} . ^1H NMR (200 MHz, CD_3COCD_3), δ 0.94 (3H, s, H20), δ 1.30 (3H, s, H17), δ 2.98 (1H, br, dd, $J = 18.3, 2.86\text{ Hz}$, H15), δ 3.84 (1H, d, $J = 11.4\text{ Hz}$, H17), δ 3.73 (1H, d, $J = 11.4\text{ Hz}$, H17), δ 7.71 (1H, d, $J = 9.58\text{ Hz}$, H6'), δ 8.20 (1H, dd, $J = 9.58, 2.51\text{ Hz}$, H5'), δ 9.00 (1H, d, $J = 2.53\text{ Hz}$, H3'), δ 10.70 (1H, s, NH). ^{13}C NMR (50 MHz, CD_3COCD_3), δ 12.9 (C20), δ 18.7 (C2), δ 19.8 (C11), δ 21.5 (C6), δ 28.9 (C18), δ 34.3 (C12), δ 37.6 (C7), δ 37.9 (C3), δ 38.3 (C10), δ 39.6 (C1), δ 40.6 (C15), δ 41.5 (C8), δ 43.6 (C4), δ 50.5 (C14), δ 50.6 (C13), δ 55.4 (C9), δ 56.8 (C5), δ 66.4 (C17), δ 115.8 (C6''), δ 123.4 (C5''), δ 128.8 (C1''), δ 129.9 (C3''), δ 137.7 (C2''), δ 144.5 (C4''), δ 170.9 (C16), δ 183.7 (C19).

3.6.6 2, 4-DINITRO PHENYL HYDRAZONE BENZYL ESTER OF 17-HYDROXY ISOSTEVIOL (7m)

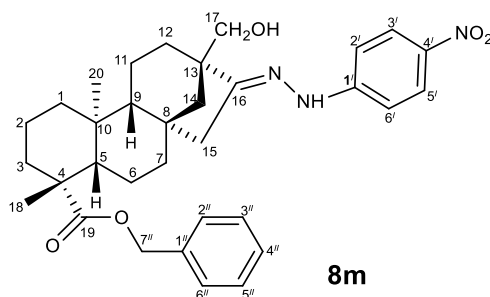


Yellow crystalline solid with (73 mg: 40%), yield. ESI-MS $[M-H]^+$ 603.39. IR; 3315 cm^{-1} , 1718 cm^{-1} , 1618 cm^{-1} , 1517 cm^{-1} , 1134 cm^{-1} , 1143 cm^{-1} , 754 cm^{-1} , 697 cm^{-1} . $^1\text{H NMR}$ (200 MHz, CDCl_3), δ 0.67 (3H, s, H20), δ 1.23 (3H, s, H18), δ 2.86 (1H, dd, $J = 17.80, 2.60\text{ Hz}$, H15), δ 3.73 (1H, dd, $J = 17.9, 11.39\text{ Hz}$, H17), δ 5.1 (2H, s, H7''), δ 7.39 (5H, s, H2'' to H6''), δ 7.76 (1H, d, $J = 9.61\text{ Hz}$, H6'), δ 7.78 (1H, d, $J = 9.70, 2.54\text{ Hz}$, H5'), δ 9.14 (1H, d, $J = 2.54\text{ Hz}$, H3'), δ 10.78 (1H, d, s, NH). $^{13}\text{C NMR}$ (50 MHz, CDCl_3), δ 13.3 (C20), δ 18.9 (C2), δ 19.9 (C11), δ 21.6 (C6), δ 28.9 (C18), δ 34.2 (C12), δ 37.9 (C3, C7), δ 38.1 (C10), δ 39.8 (C1), δ 40.8 (C15), δ 41.5 (C8), δ 43.8 (C4), δ 50.6 (C13, C14), δ 55.4 (C9), δ 57.0 (C5), δ 66.2 (C17), δ 66.5 (C7''), δ 115.9 (C6'), δ 123.5 (C5'), δ 128.2 (C4''), δ 128.5 (C2'', C6''), δ 128.6 (C3'', C5''), δ 129.2 (C4'), δ 130.1 (3'), δ 135.9 (C1''), δ 137.9 (C2'), δ 144.7 (1'), δ 170.6 (C16), δ 176.8 (C19).

3.6.7 4-NITROPHENYL HYDRAZONE OF 17-HYDROXYISOSTEVIOL (6m)

Yellow crystalline solid (69 mg: 49%), yield. ESI-MS, $[M-H]^+$ 468.39. IR, 3527 cm^{-1} , 3341 cm^{-1} , 1696 cm^{-1} , 1600 cm^{-1} , 1322 cm^{-1} , 1109 cm^{-1} , 838 cm^{-1} . ^1H NMR (200 MHz, CD_3COCD_3), δ 0.87 (3H, s, H20), δ 1.22 (3H, s, H17), δ 2.95 (1H, dd, $J = 18.23, 2.86\text{ Hz}$, H15), δ 3.6 (1H, d, $J = 10.9\text{ Hz}$, H17), δ 3.7 (1H, d, $J = 10.9\text{ Hz}$, H17), δ 7.18 (2H, d, $J = 9.33\text{ Hz}$, H2', H6'), 8.12 (2H, d, $J = 9.36\text{ Hz}$, H3', H5'), δ 9.14 (1H, s, NH). ^{13}C NMR (50 MHz, CD_3COCD_3), δ 13.1 (C20), δ 18.9 (C2), δ 19.8 (C11), δ 21.7 (C6), δ 28.5 (C18), δ 34.6 (C12), δ 37.8 (C7), δ 37.9 (C3), δ 38.0 (C10), δ 39.8 (C1), δ 40.9 (C15), δ 41.1 (C8), δ 43.2 (C4), δ 50.0 (C13), δ 50.8 (C14), δ 55.3 (C9), δ 56.7 (C5), δ 65.9 (C17), δ 111.1 (C2', C6'), δ 125.7 (C3', C5'), δ 138.9 (C1'), δ 151.5 (C4'), δ 162.7 (C16), δ 178.1 (C19).

3.6.8 4-NITRO PHENYL HYDRAZONE BENZYL ESTER OF 17-HYDROXY ISOSTEVIOL (8m)



Yellow crystalline solid (87 mg: 51%), yield. ESI-MS, $[M]^+$ 559.29. IR; 3472 cm^{-1} , 1727 cm^{-1} , 1458 cm^{-1} , 1320 cm^{-1} , 1147 cm^{-1} , 753 cm^{-1} , 697 cm^{-1} . ^1H NMR (200 MHz, CDCl_3), δ 0.69 (3H, s, H20), δ 1.23 (3H, s, H18), δ 2.73 (1H, dd, $J = 17.43, 2.35\text{ Hz}$, H15), δ 5.0 (1H, d, $J = 12.61\text{ Hz}$, H17), δ 5.2 (1H, d, $J = 12.64\text{ Hz}$, H7''), δ 6.96 (2H, d, $J = 9.15\text{ Hz}$, H2', H6'), δ 7.39 (5H, s, H2''-H6''), δ 8.14 (2H, d, $J = 9.15\text{ Hz}$, H3', H5'). ^{13}C NMR (50 MHz, CDCl_3), δ 13.6 (C20), δ 18.9 (C2), δ 20.0 (C11), δ 21.7 (C6), δ 28.9 (C18), δ 34.1 (C12), δ 37.0 (C7), δ 37.8 (C3), δ 38.2 (C10), δ 39.7 (C1), δ 40.9 (C15), δ 41.7 (C8), δ 43.9 (C4), δ 49.8 (C13), δ 50.7 (C14), δ 55.4 (C9), δ 57.1 (C5), δ 65.9 (C17), δ 67.2 (C7''), δ 111.5 (C2', C6'), δ 126.2 (C3', C5'), δ 128.0 (C3'', C4'', C5''), δ 128.5 (C2'', C6''), δ 136.2 (C1''), δ 140.1 (C1'), δ 149.8 (C4'), δ 163.6 (C16), δ 176.9 (C19).

3.7 BIOLOGICAL ACTIVITIES

3.7.1 ANTI-MALARIAL ACTIVITIES

The assessment of *in vitro* antimalarial activity of steviol, Isosteviol and its derivatives was performed at the bioassays Laboratory of the Faculty of Pharmacy, Federal University of Minas Gerais (UFMG), as part of the Natural Products Network for Antimalarial Chemotherapy - PRONEX Project CNPq / FAPEMIG under coordination of Prof. Alaíde Braga de Oliveira (UFMG) and Prof. Fernando de Pilla Varotti (UFSJ). The tests were performed using erythrocytes infected with *P. falciparum* clone W2 resistant to chloroquine, by the method of incorporation of [3H] -hipoxantine (DESJARDINS et al., 1979) to AB method and lactate dehydrogenase (LDH) (MAKLER; HINRICHS, 1993) for other derivatives.

The experiments were performed as follows: 1) Incubation 1-parasite drugs: 20 µL of each test compound dilution placed in 96-well microplates in triplicate, which were already 180 µL suspension of infected erythrocytes (1% hematocrit, 2% parasitemia), from a culture kept in the laboratory bioassays. Controls without drugs with infected red blood cells (positive control), or uninfected erythrocytes (negative control), were used. hematocrit, 2% parasitemia), from a culture kept in the laboratory bioassays. Controls without drugs with infected red blood cells (positive control), or uninfected erythrocytes (negative control), were used. Plates were incubated in an atmosphere of 5% CO₂ at 37 °C for 48 hours, with samples and controls. After this period, the microplates were frozen (-20 °C for at least 24h), to promote lysis of erythrocytes. The cell lysate was transferred to 96-well plates to which were added 100 µL Malstat reagent and reagent 25 µL NBT / PES. After 1h incubation, the absorbance of each well of the plates was recorded in a spectrophotometer (540 nm).

The following experiments were conducted: In the first experiment, two concentrations of the samples, 25 and 50 mg / mL, each in triplicate to evaluate

the percentage reduction of parasitemia that was determined by the LDH method were employed. The percentage reductions in the growth of parasites were calculated from the absorbance. Reduction of samples with parasitaemia >50% at the concentrations tested had their IC_{50} determined in three separate experiments in six different concentrations, with triplicates of each concentration. The results were analyzed with Origin 8.0 software to determine the dose-response curves plotted with sigmoidal fit. We determined the inhibitory concentration of 50% growth of the parasites (IC_{50}), compared to controls without drugs. According to the results, the samples were classified as:

VERY ACTIVE - IC_{50} values below 1 mg / mL;

LIVE - IC_{50} values of 1 to 15 μ g / mL;

MODERATELY ACTIVE - IC_{50} values between 15.1 and 25 mg / mL,

LITTLE LIVE - IC_{50} values between 25.1 and 50 mg / mL,

INACTIVE - IC_{50} above 50 g / mL

3.7.2 ANTI-TUMOR ACTIVITIES

The anti-tumor activity *in vitro* of steviol, isosteviol derivatives against three cancer lines were performed at Laboratory of Cell Biology (Biochemistry Department UFPR/ Curitiba, PR), by Otávio Martins Cruzii under the supervision of Prof. Dr. Sheila M. B. Winnischofe. Initially nine compounds were tested for cytotoxicity's in human glioblastoma astrocytoma cell line (U87MG), human lungs carcinoma cell line (A549), and human glioblastoma multiform cell line (T98G).

3.7.2.1 MATERIAL METHOD

All glassware used for materials and procedures for cell cultivation (solutions for vials and culture medium, solution filtration equipment, covers, plastic tips for automatic pipettes and glass pipettes), were sterilized by

autoclaving at 120 °C for 30 minutes under a pressure of 1 atm. After sterilization, the material was dried in an incubator at 50 °C. The handling of cell cultures for experimentation was performed under sterile conditions inside a laminar flow hood.

3.7.2.2 SOLUTIONS, CULTURE MEDIA AND MATERIALS

The phosphate buffered saline (PBS) used for washing the cells in culture was prepared as a concentrated stock solution five times (NaCl 680 mmol/L, KCl 13.4 mmol/L, Na₂HPO₄, 40.5 mmol/L) and diluted for further use. This solution is adjusted to pH 7.4, and sterilized by autoclaving and stored in the above conditions at room temperature. Adherent cells were released from their substrate using trypsin-EDTA solution (NaCl, 137 mmol/L, KCl, 54 mmol/L, glucose, 5 mmol/L, Na₂HPO₄, 0.42 mmol/L, KH₂PO₄, 0.44 mmol/L, NaHCO₃, 2,3 mmol/L, EDTA, 0.53 mmol/L and 50 mg % trypsin, pH 7.4). This solution is sterilized by sterile filtration with a pore 0.22 µm membranes (Millipore) apparatus under pressure Sartorius laminar and stored at -20 °C flow.

3.7.2.3 CULTURE MEDIA, CELL LINES AND CULTURE CONDITIONS

The culture medium used was DMEM High Glucose (Sigma-Aldrich). The medium was supplemented with 10% fetal bovine serum (FBS - Gibco) and 100 µg/mL of gentamicin (Sigma-Aldrich). The studied cell lines (U87MG, T98G and A549), were kindly provided by Dr. Mari Clyde Sogayer (USP). The cells grow as adherent cultures grown in sterile polystyrene bottles (Techno Plastic Products - TPP). These cultures were maintained in an incubator under an atmosphere of 5% CO₂ and 37 °C. The sub-culture was performed according to the confluence of the cells using a trypsin-EDTA solution to detach them from the plastic substrate. The medium changes, when necessary, were made every 48-72 hours by monitoring

the indicator color of pH of the culture medium. For the storage of strains, cells were suspended in culture medium supplemented with 10% DMSO and cryopreserved in liquid nitrogen.

3.7.2.4 EVALUATION OF CELL VIABILITY MTT METHOD

The U87MG, T98G, A549 and inbred lines were plated in 96-well plates in DMEM high glucose supplemented with 10% FBS, totaling $1,5 \times 10^4$ cells / well and 24 hours were allowed to adhere. Cells were treated control using only the vehicle of drugs, DMSO (dimethylsulfoxide), at a concentration corresponding to 10 μ M, 25 and 50 μ M of the compounds examined at 24h. After the treatment period, the medium was removed from culture and added to 900 μ L HBSS solution and 100 μ L of solution of MTT in HBSS at a concentration of 5 mg/mL. The plates were kept in an incubator at 37 °C in an atmosphere of 5% CO₂ for 3 hours protected from light. After the time, the MTT solution was removed and formazan crystals dissolved in 1 mL of DMSO (dimethylsulfoxide). The absorbance was determined in a microplate reader (TECAN Infinite 200) using a 540 nm filter. Results were calculated from the mean absorbance values of the experimental triplicates and expressed as a percentage of crystal formazan formed compared to control (considered as 100%).

3.7.3 ANTI-TRYPANOSOMA CRUZI ACTIVITIES

The *in vitro* anti-*Trypanosoma cruzi* activity of steviol, isosteviol and its derivatives was performed at the Laboratory of Cell Biology, Carlos Chagas Institute/ Fiocruz-PR, Curitiba, PR under coordination of Maurilio Jose Soares and Luz Helena Villamizar is a fellow of the Students Program–Post-Graduation Agreement PEC-PG from CAPES/CNPq-Brazil.

The tests were performed using epimastigotes or trypomastigotes, by cell viability marker MTT [3-(4, 5-dimethylthiazol-2-yl)-2, 5-diphenyltetrazolium bromide], according to standard protocols (Rita & Francis., 1986; Keet al., 1999). The assays were quantified at 550 nm using the ELISA reader BIOTEXEL-800 (Biotek, Winooski, VT, USA).

3.7.3.1 VERO CELLS AND PARASITES

Verocells (ATCC CRL-1586), were maintained at 37°C in a humidified 5% CO₂ atmosphere. The cells were grown in 75 cm² culture flasks with RPMI-1640 medium supplemented with 5% fetal calf serum (FCS), 1% L-glutamine, 1% penicillin and 10 mg/mL streptomycin. For the cytotoxicity bioassays, 4-day-old confluent Vero cells monolayers were washed with phosphate buffered saline (PBS, pH 7.2), and detached from the substrate by treatment with 0.25% trypsin +0.1% EDTA for 5 minutes at 37°C. The cells were then resuspended in the same medium, centrifuged for 2 minutes at 800g and the cell pellet was collected. Culture epimastigote forms of *Trypanosomacruzi* clone Dm28c were maintained in LIT (liver infusion-tryptose), medium at 28°C (Camargo, 1964), with serial passages at every three days (mid-log phase of growth). For the experiments, parasites obtained from 72-hour cultures were inoculated into fresh LIT medium and then added to 96-well plates at a concentration of 5x10⁷ cells/well. To obtain cell-derived trypomastigote forms, Vero cell cultures were infected with trypomastigote forms at a 10:1 parasite: host cell ratio. After four hours of interaction, the host cell monolayers were washed with PBS to remove non-internalized parasites. The cultures were kept for 96 hours at 37°C in RPMI / 2.5% FCS in a 5% CO₂ humidified atmosphere. After that period, trypomastigotes released to the supernatant were collected and washed with PBS by centrifugation at 3000g. The purified trypomastigotes were transferred to RPMI-1640 medium at a concentration of 5x10⁷ cells/mL and then added to 96-well plates at 100 µL/well.

3.7.3.2 BIOLOGICAL ASSAYS

Steviol and Isosteviol derivatives were diluted in dimethyl sulfoxide (DMSO), and added to 96 well plates containing parasites (epimastigotes or trypomastigotes), at final concentrations ranging from 12 to 500 μM . The concentration that inhibited parasite growth in 50% after 24 hours of incubation ($IC_{50}/24\text{h}$), was determined with the cell viability marker MTT [3-(4,5-dimethylthiazol-2-yl)-2,5-diphenyltetrazolium bromide], according to standard protocols (Rita & Francis, 1986; Keet al, 1999). The assays were quantified at 550 nm using the ELISA reader BIOTEXEL-800 (Biotek, Winooski, VT, USA). All experiments were performed in biological and technical triplicate. The CompuSyn software was used to calculate the $IC_{50}/24\text{h}$. Controls were grown in medium containing 0.5% DMSO, without addition of derivatives.

3.7.3.3 CYTOTOXICITY ASSAYS

Vero cells were seeded at a concentration of 2×10^4 cells/well in 96-well plates containing RPMI-1640 medium supplemented with 5% FCS and maintained at 37°C and 5% CO_2 atmosphere. After 24 hours the steviol/isosteviol derivatives were added at different concentrations, ranging from 50 to 1000 μM . The cytotoxic concentration ($CC_{50}/24\text{h}$), was determined after 24h of incubation using the MTT enzymatic assay, as described above.

The Selectivity Index (SI) was determined based on the ratio of the CC_{50} value in the host cell divided by the IC_{50} value of the parasite.

3.7.4 ANTI-LEISHMANIASIS ACTIVITIES

The *in vitro* anti-*Leishmania* bioassays were carried out by Keylla Lençone, at the Laboratory of Hematology (Pharmacy Department, UFPR), under the supervision of Dr. Almeriane Maria Weffort Santos. The viability of the parasites

was assessed by the colorimetric method of death bromide 3 (4, 5-dimethylthiazol-2-yl), -2, 5-diphenyl tetrazolium bromide (MTT).

3.7.4.1 STRAIN OF PARASITE AND CELL CULTURE

Two commercial strains of Leishmaniasis obtained from the Collection of the Oswaldo Cruz Institute, National Reference Laboratory for typing of Leishmania, called L. (L.) amazonensis (IFLA / BR / 1967 / PH8), L. (V.) braziliensis (MHOM / BR, 1975 / M2903), were used in the experiments.

The promastigote forms on blood agar seeded with a low passage number (three or seven), were collected and transferred to culture flasks of 25 cm² containing M199 medium (Gibco-BRL), which was prepared by diluting the powder to medium 199 in distilled water and by adding 40 mM Hepes, pH 7.4, 0.1 mM adenine, 0.005% hemin, supplemented with 20% fetal calf serum heat inactivated (FBS). The medium was sterilized by filtration and maintained sterility in the competition for 24h at 37°C. Cultures were maintained and an incubator at 25 °C.

3.7.4.2 ASSAY SUSCEPTIBILITY OF PROMASTIGOTE FORMS

The promastigotes in logarithmic phase (5 days) were counted in NeubauerLate chamber under light microscopy and the concentration was adjusted to 2x10⁷ cells / mL. Promastigosta forms of leishmania were plated in 96-well plates 50-100 microliters was added to each well (3x10⁶ cells / well) and maintained at 25 °C for 24 hours.

3.7.4.3 TREATMENT *IN VITRO*

Substances **2g**, **3g**, **1f**, **2f**, **5k**, **5m**, and **6m** were dissolved in DMSO at a concentration of 0.1% and then diluted in culture medium to final concentrations of

1, 10, 100 and 1000 mM. The effects of the substance against promastigote forms were evaluated in triplicate from 24 to 48 hours. DMSO dissolved in culture medium was used as control.

3.7.4.4 VIABILITY ASSAY

The viability of the parasites was assessed by the colorimetric method of death bromide 3 (4, 5-dimethylthiazol-2-yl)-2,5-diphenyl tetrazolium bromide (MTT). After each incubation period, 30 μ l of bromide 3 (4,5-dimethylthiazol-2-yl), -2,5-diphenyl tetrazolium bromide (M2128 - Sigma-Aldrich), at a concentration of 5 mg / mL was added and kept for 2h at 24 °C. The reaction was stopped by adding 50 μ L of a solution of sodium dodecyl sulfate, SDS. Each well was homogenized and the absorbance was read at 595 nm using as reference 690 nm in microplate Fluostar Optima (BMG Labtech), reader. The results obtained were compared with the absorbance of a control culture cells, treated in the same manner. The experiments were performed in triplicate and the results expressed as percentage of viable cells compared to control (untreated cells), which was assigned to 100%. Amphotericin B, Triton X-100 and Glucantime were used as positive control death.

3.7.4.5 STATISTICAL ANALYSIS

The biological tests were carried out three times in independent experiments and each concentration was tested in triplicate. All data obtained from biological activity were subjected to statistical analysis. The results of biological activities are presented as mean \pm standard deviation (SD) of several repetitions of the experiments. For statistical analysis, we used the "t" test analysis of variance (ANOVA), with Tukey's test execution and test. The calculations were performed using the GraphPad Prism-5, version 2007, and Microsoft Office Excel 2010 programs. Values of $p \leq 0.05$ were considered statistically significant. IC_{50}

values (concentration required to cause 50% inhibition) were calculated by linear regression analysis from the K_c values for each concentration.

3.7.5 ANTI-CORYNEBACTERIUM DIPHTHERIAE ACTIVITIES

The *in silico* and experimental *in vitro* anti-*Corynebacterium diphtheriae* activity of isosteviol derivatives was performed at Laboratory of Cell Biology (Biochemistry Department UFMG), with help of Dr. Syed Shah Hassan under the supervision of Prof. Dr. Vasco Ariston de Carvalho Azevedo.

We performed Homology modeling. To carry out Homology modeling, we retrieved the FASTA sequences of all sortases proteins of the *Corynebacterium diphtheria*, from the UniProt (<http://www.uniprot.org>). The query sequence was searched for sequence identity using the Basic Local Alignment Search Tool (BLAST) against Protein Database (PDB) for the corresponding template. The computational 3D (three-dimensional) structure of target proteins were generated by comparative homology modeling using the respective template structures obtained from SWISS-MODEL (Arnold K., 2006), that is a fully automated protein structure homology-modeling server, accessible via the ExPASy web server. We used a set 28 synthesized compounds for our docking analysis against these drug resistant proteins via MVD software (Thomsen R., 2006).

Furthermore these docking results were validated. For the validation we followed the protocol mention by Bhar *et al* 2013. The 8 best compounds with more H-bonds & comparatively low MolDock scores were tested for their individual growth inhibition efficacy against *C. diphtheria*. The bacteria were cultured in

Brain-Heart Infusion (BHI) broth (Sigma-Aldrich Co. LLC), at 37 °C for 48 hours to reach the log phase. Then, cells were harvested by centrifugation and 10 CFU mL cells were re-suspended in tubes containing BHI broth and 1, 25, 50, 75 and 100 µg/mL concentrations of the compounds. Treatment with 100 µg/mL of chloramphenicol and Kanamycin was used as control. Cultures were then incubated at 37 °C for 24 hours in a shaker. The number of colony-forming units (CFUs) was counted each 30 min interval by obtaining the CFU/mL from serial 10-fold dilutions prepared in BHI agar (Sigma-Aldrich Co. LLC).

4 RESULTS AND DISCUSSION

4.1 ISOSTEVIOL (1a)

A known derivative compound **1a** (3.3g) was recovered as a white crystalline solid in 33 %, yield (Scheme 1, page 144). IR spectrum (Figure 34, page 164) showed the expected absorption bands (cm^{-1}), at 1734 (ketone), 1692 (ester), 1269 (ester carbon oxygen).

The spectral ^1H NMR (Figure 35, page 165) data is found in Table 20, page 150 revealed the presence of 3CH_3 at δ 0.68, δ 0.97, and δ 1.19, correspond to H20, H18 and H17, respectively. A broad doublet visible at δ 2.17 corresponds to 1H at H12. Multiplet visible at δ 2.63, correspond to 1H at H15.

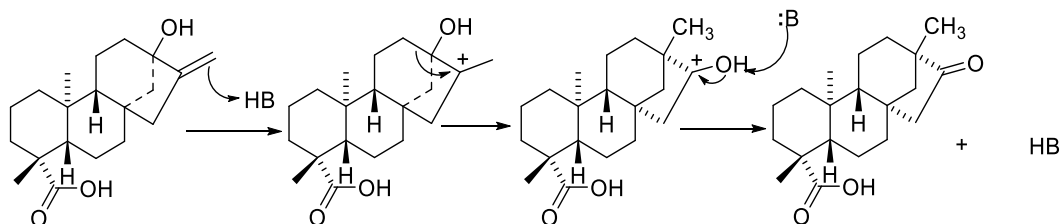


Figure 26: Wagner-Meerwein rearrangement of Kaurene.

Additionally the ^{13}C NMR (Figure 36, page 166) data reported in Table 30 page 160 show twenty carbons signals. The carboxylic resonance observed at δ 177.8 (C19) in low field region. The presence of 2 angular methyl was confirmed at resonance of δ 13.1 (C20), δ 19.8 (C13), and one methyl at δ 28.8 (C18). The experimental DEPT 135 spectrum (Figure 37, page 167) multiplicities indicate four quaternary carbons, two methine carbons, nine methylene carbons, three methyl carbons, one carboxylic carbon, and one oxymethyl carbon, on the basis of

comparison of the spectral data with the literature of the compound **1a**, was identified as a isosteviol (Avent, Hason & Oliveira., 1989).

4.2 16-HYDROXY ISOSTEVIOL (**1b**)

Known compound **1b** (240 mg) was recovered as a white crystalline solid in 80%, yield (Scheme 1, page 144). IR spectrum (Figure 38, page 168) showed the predictable absorption bands (cm^{-1}), at 3468 (alcohol), 1723 (ester), 1454 (alcoholic), 1267 (ester carbon oxygen).

The ^1H NMR spectrum (Figure 39, page 169) revealed several key signals that assisted in determination of its structure. The spectral ^1H NMR data is found in Table 20, page 150. Three methyl signals were visible at δ 0.71, δ 0.90, δ 1.16 corresponds to H20, H18, H17, respectively. Broad doublet at δ 2.17 corresponds to H12. Quaternary ^1H resonance observed at δ 3.85 assigned to H16.

The ^{13}C NMR spectrum (Figure 40, page 170) of 16-hydroxy isosteviol methyl ester show twenty one carbons signals, the spectral data is reported in Table 30 page 160. The resonance at δ 80.5 indicates that ketone carbon is reduced to the secondary alcohol. The signal at δ 178.1 shows the presence of carbomethoxy functionality. Tertiary methyl resonance detected at δ 28.8 (C18), δ 24.9 (C17), and δ 13.1 (C20). The DEPT 135 spectrum (Figure 41, page 171) multiplicities indicate four quaternary carbons, three methine, nine methylene, three methyl one oxymethyl, and an carboxylic carbon on the basis of comparison of the spectral data with the literature of the compound **1b**, was identified as a 16-hydroxy isosteviol (Lin *et al.*, 2007).

4.3 17, 16-DIHYDROXY ISOSTEVIOL (5i)

Known analogue **5i** (218 mg) was recovered as a white crystalline solid in 68 % Yield (Scheme 1, page 148). IR spectrum (Figure 73, page 203) showed the expected absorption peaks (cm^{-1}), at 3413 (primary hydroxyl), 3218 (secondary hydroxyl), 1698 (ester), 1175 (secondary hydroxyl), 1027 (primary hydroxyl).

The spectral ^1H NMR (Figure 74, page 204) data is found in Table 22, page 152 showed the visible signals at δ 0.77, δ 1.20, related to 2CH_3 at H20, H18. A visible doublet at δ 3.51 with coupling constant 10.1 Hz corresponds to 1H at H17. Another doublet at δ 3.45 with J 10.1 Hz is related to 1H at H17. Multiplet at δ 4.2 having J 10.0 and 5.3 Hz correspond to H16.

The ^{13}C NMR spectral (Figure 75, page 205) data reported in Table 30, page 160, shows twenty one carbons signals. The resonance visible at δ 78.5 specifies that ketonic carbon (C16) is reduced to secondary alcoholic moiety. The signal at δ 178.0 is the characteristic region of carbomethoxy functionality. Resonance at δ 71.2 corresponds to methylene unit at C17. Resonance of tertiary methyl groups was appears at δ 28.8 (C18) and δ 13.1 (C20). The experimental DEPT¹³⁵ spectrum (Figure 76, page 206) multiplicities indicate four quaternary carbon, three methine carbons, ten methylene carbons, two methyl carbons, one carboxylic carbon and one oxymethyl carbon the structure of compound **5i** was confirm with reported literature data (Oliveira *et al.*, 2008).

4.4 16-OXIME OF ISOSTEVIOL (1c)

The recovered known derivative **1c** (260 mg) was a white crystalline solid in 78 %, yield (Scheme 1, page 144). The IR spectrum showed (Figure 42, page 172) the expected absorption bands (cm^{-1}), at 3449 (oxime), 1720 (ester), 1694 (carbon nitrogen double bond), 1262 (carbon carbon), 961 (nitrogen oxide).

^1H NMR spectrum (Figure 43, page 173) reported in Table 20, page 150 shows the presence of three tertiary methyl resonance at δ 0.76, δ 1.11, δ 1.19 correspond to H20, H17, H18 respectively. Broad doublet resonance visible at δ 2.19 corresponds to H12. Multiplet observed at δ 2.98 for H15. Singlets at δ 3.62 indicate the presence of oxymethyl.

The ^{13}C NMR spectral (Figure 44, page 174) data reported in Table 30 page 160 of compound **1c** shows twenty one carbons resonance. The resonance at δ 170.21 specifies that keto carbon (C16) is changed to oxime functionality. The resonance at δ 178.0 is the characteristic region of carbomethoxy functionality. Resonance of tertiary methyl groups was observed at δ 28.7 for (C18), δ 22.9 (C17), and δ 13.1 (C20). The experimental DEPT¹³⁵ spectrum (Figure 45, page 175) multiplicities indicate four quaternary carbons, two methine carbons, nine methylene carbons, three methyl carbons, one oxime carbon, one carboxylic carbon and one oxymethyl carbon. The structure of compound **1c** was confirmed with reported literature data (Change *et al.*, 2009)

4.5 17-HYDROXY, 16-OXIME OF ISOSTEVIOL (5j)

Known compound **5j** (206 mg) was recovered as a white crystalline solid in 68% yield (Scheme 5, page 148). IR spectrum (Figure 82, page 212) showed the expected absorption peaks (cm^{-1}), at 3441 (oxime), 1709 (ester), 1262 (carbon carbon).

The ^1H NMR spectral (Figure 83, page 213) data reported in Table 22, page 152, display signals at δ 0.90, δ 1.22 were attributed to two tertiary methyl protons at H20, H18. Broad singlet visible at δ 2.13 corresponds to 2H, at H12. Multiplet at δ 3.54 with coupling constant 16.70 and 10.99 Hz correspond to H17. Another multiplet for a one proton at δ 2.99 with coupling constant 18.40 and 3.0 Hz correspond to H15.

The ^{13}C NMR spectral (Figure 84, page 214) data of 17-Hydroxy-16-oxime isosteviol reported in Table 31, page 161 show twenty carbons signals, oxime functionality resonance at δ 167.5 related to C16. The rest of twenty carbons multiplicities were derived from the DEPT 135 spectrum (Figure 85, page 215) as four quaternary, two methine, ten methylene and two methyl carbons, one hydrazone carbon, one carboxylic carbon, one oxymethyl carbon. The ^{13}C signal at the δ 178.7 and δ 66.4 show the presence of carbomethoxy and primary alcoholic functionalities respectively at C20 and C17. The ^{13}C signals at δ 28.5 and δ 13.0 correspond to two tertiary methyl at C18, and C20 respectively on the basis of comparison of the spectral data with the literature of the compound **5j**, was identified as a 16-hydroxy isosteviol (Oliveira *et al.*, 2008).

4.6 ISOSTEVIOL LACTONE (1d)

The recovered known derivative **1d** (130 mg) was a white crystalline solid in 39% yield (Scheme 2, page 145). The molecular formula $\text{C}_{20}\text{H}_{30}\text{O}_4$ determined on the basis of ESI-MS (Figure 46, page 176) data, which showed the $[\text{M}]^+$ ion; 334.25, corresponding to the calculated mass of the compound. The IR spectrum (Figure 47, page 177) showed the absorption bands (cm^{-1}), at 1720 (lactone carbonyl), 1688 (ester carbonyl), 1244 cm^{-1} (ethereal).

The ^1H NMR (Figure 48, page 178) spectral data reported in Table 20, page 150 displays the presence of three tertiary methyl protons resonance at δ 0.75 (H20), δ 1.17 (H18), δ 1.34 (H17). Multiplet detected at δ 3.89 corresponds to 1H (H15). Broad doublet visible at δ 2.18 corresponds to H12. Singlet visible at δ 3.62 corresponds to oxymethyl.

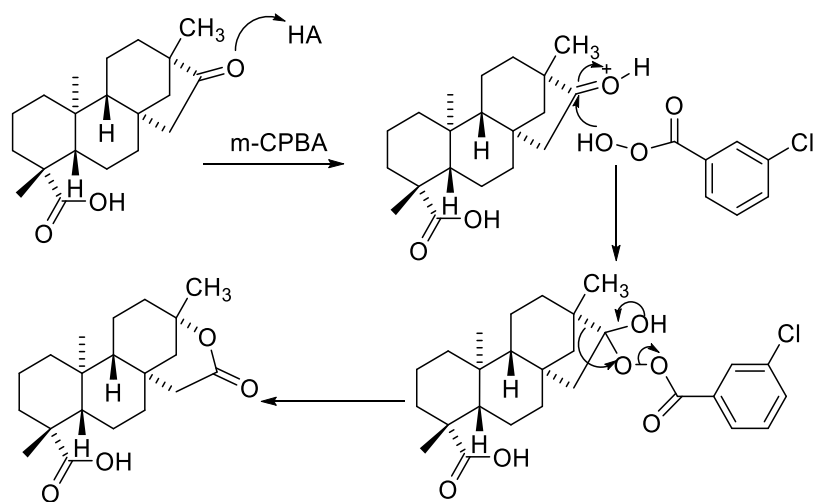


Figure 27: Baeyer-villager oxidation of isosteviol

The ^{13}C NMR (Figure 49, page 179) spectral data reported in Table 30, page 160 revealed twenty one carbons signals. The signal at δ 172.5 represents lactone carbonyl (C16). The signal at δ 177.5 is the characteristic region of carbomethoxy functionality. Resonance of tertiary methyl groups was observed at δ 28.56 (C18), δ 28.25 (C17), and δ 13.9 (C20). The experimental DEPT¹³⁵ spectrum (Figure 50, page 180) multiplicity specifies four quaternary carbons, two methine carbons, nine methylene carbons, three methyl carbons two carboxylic carbons and one oxymethyl carbon the spectral data was corresponding to the literature data of compound **1d** (Change *et al.*, 2009).

4.7 15 α -HYDROXY METHYL-16 β -HYDROXY ISOSTEVIOL (**1e**)

Known compound **1e** (153 mg) was obtained as white crystalline solid in 78% yield (Scheme 2, page 145). The molecular formula $\text{C}_{21}\text{H}_{34}\text{O}_4$ determined on the basis of ESI-MS (Figure 51, page 181) data, which showed the $[\text{M}+\text{Na}]^+$ ion 373.21, which corresponds to the calculated mass of the compound. The IR spectrum (Figure 52, page 182) showed the bands (cm^{-1}), at 3392 (Hydroxyl),

1694 (ester carbonyl), 1553, 1534, 1454 (hydroxyl bending), and at 1067 (carbon oxygen).

^1H NMR spectral (Figure 53, page 183) data reported in Table 21, page 151 showed key resonance information at δ 0.74, δ 0.93, δ 1.15 corresponds to 3CH_3 at H20, H18, and H17 respectively. Triplet visible at δ 3.46 corresponds to 1H, with coupling constant 10.3 Hz (H1'). Singlet at δ 3.62 (OCH_3), attributed to the methyl ester at C19, and quartet at δ 3.99 correspond to (H15).

^{13}C NMR spectral (Figure 54, page 184) data reported in Table 30, page 160, also shows twenty two carbons signals. The resonance at δ 86.7 specifies that ketonic carbon is reduced to secondary alcohol functionality. The carbon resonance at δ 177.9 is the characteristic region of carbomethoxy functionality. Resonance of tertiary methyl groups was observed at δ 28.9 (C18), δ 24.9 (C17), and δ 13.0 (C20). The experimental DEPT 135 spectrum (Figure 55, page 185) multiplicities specify four quaternary carbons, four methine carbons, nine methylene carbons, three methyl carbons, one carboxyl and an oxymethyl carbon. The spectral data was corresponding to the literature data of compound **1e** (Y.wu *et al.*, 2009)

4.8 15α -HYDROXYMETHYL, 17 , 16β -DIHYDROXY ISOSTEVIOL (**5n**)

New derivative **5n** (146 mg) was obtained as a white crystalline solid in 71%, yield (Scheme 5, page 148). The calculated molecular formula $\text{C}_{21}\text{H}_{34}\text{O}_5$ on the basis of ESI-MS (Figure 77, page 207) data, $[\text{M}-\text{H}]^+$ 365.33, which corresponds to the calculated mass of the compound. The IR spectrum (Figure 78, page 208) showed the interested absorption bands (cm^{-1}), at 3419 (broad band Hydroxyl), 1692 (ester carbonyl), 1222 (primary hydroxyl).

The ^1H NMR (Figure 79, page 209) spectral data reported in Table 22, page 152 showed resonance at δ 0.79, δ 1.16; corresponds to 2CH_3 at H20, H18. The resonance appeared at δ 2.9 corresponds to methylenic proton at H15.

Resonance visible at δ 3.34 with broad doublet corresponds to H1'. Resonance of proton at δ 3.6 was assigned to H17.

The ^{13}C NMR (Figure 80, page 210) spectral data is outline in Table 30, page 160 showed twenty two carbons signals. The resonance observed at δ 80.7 specifies that ketonic carbon was reduced to secondary alcohol functionality. The resonance at δ 177.1 is the characteristic region of carbomethoxy functionality. Resonances of tertiary methyl groups at δ 28.1 (C18), and δ 12.6 (C20), and two hydroxy methylene unit at δ 68.3 (C17), and δ 63.1 (C1'), were observed. The experimental DEPT¹³⁵ spectrum (Figure 81, page 211) multiplicities specify four quaternary carbons, four methine carbons, ten methylene carbons, two methyl carbons one oxymethyl and a carboxylic carbon.

4.9 STEVIOL (1h)

Known compound **1h** (1.3 g), was obtained as a white crystalline solid in 13%, yield (Scheme 4, page 147). The IR spectrum (Figure 61, page 191) showed the interested bands (cm^{-1}), at 3274 (hydroxyl), 1691 (carbonyl ester), 1237 (hydroxyl bending), 1087 (carbon oxygen).

The ^1H NMR (Figure 62, page 192) spectral data reported in Table 21 page 151 revealed the resonance at δ 0.84, δ 1.19 corresponds to tertiary methyl protons at H20 and H18. Multiplet observed at δ 1.87 with J 10.82, 2.13 Hz corresponds to 1H at H14. Singlet visible at δ 3.66 corresponds to (OCH₃). Two broad singlet's at δ 4.9 and at δ 4.83 related to two olefinic protons at H17.

The ^{13}C NMR (Figure 63, page 193) data reported in Table 30, page 160 showed twenty one carbon signals, resonance at δ 102.9 and δ 156.1 correspond to olefinic carbons at (C17), and (C16). The rest of twenty carbons multiplicities were derived from the DEPT¹³⁵ spectrum (Figure 64, page194) as four quaternary carbons, two methine carbons, ten methylene carbons and two methyl carbons one carboxylic one exocyclic olefinic carbon and one oxymethyl. The ^{13}C signal at

δ 177.9 (C20), for carbomethoxy, δ 80.2 (C13), for tertiary alcoholic functionalities. Resonance at δ 28.7 and δ 15.3 corresponds to 2CH₃ at C20, and C18 respectively. The spectral data was corresponding to the literature data of compound **1h** (Yang *et al.*, 2007)

4.10 STEVIOL EPOXIDE (2h)

Known compound **2h** (196 mg) was recovered as white crystalline solid in 60% yield (Scheme 4, page 147). The IR spectrum (Figure 65, page 195) showed the absorption bands (cm⁻¹), at 3257 (hydroxyl), 1715 (carbonyl ester), 1244 (hydroxyl bending),

The ¹H NMR (Figure 66, page 196) data reported in Table 21, page 151 showed resonance at δ 0.86, δ 1.19 correspond to tertiary methyl protons at H20 and H18. Doublet at δ 2.20 corresponds to H12. Two doublet at δ 2.79 and δ 2.94 with 4.35 Hz coupling constant correspond to 2H at H17. Singlet at δ 3.65 corresponds to (OCH₃).

The ¹³C NMR spectrum (Figure 67, page 197) showed twenty one carbons signals reported in Table 30, page 160, resonance at δ 65.2 and δ 48.7 corresponds to carbons at (C16), and (C17). The rest of nineteen carbons multiplicities were derived from the DEPT¹³⁵ spectrum (Figure 68, page 198) as five quaternary, two methine, ten methylene carbons, two methyl carbons one carboxylic and one oxymethyl. The ¹³C signal detected at δ 177.8 (C20), for carbomethoxy, and δ 74.7 (C13), for tertiary alcoholic functionalities. Resonance at δ 28.6 and δ 15.5 corresponds to 2CH₃ at C20 and C18 respectively. The spectral data was found to be corresponding to the literature data of compound **2h** (Yang *et al.*, 2007).

4.11 17-HYDROXY ISOSTEVIOL (4h)

Known compound **4h** (215 mg), was obtained as a white crystalline solid, in 64% yield (Scheme 4, page 147). The IR spectrum (Figure 69, page 199) showed the interested absorption bands (cm^{-1}), at 3448 (primary alcohol), 1691 (ester), 1183 (carbon oxygen).

The ^1H NMR (Figure 70, page 200) data mentioned in Table 22, page 152 showed the signals of 2CH_3 at δ 0.70, and δ 1.21 attributed to H20, H18 respectively. Broad doublet observed at δ 2.2 corresponds to H12. Doublet of doublet appear at δ 2.68 with coupling constant 18.88, and 3.74 Hz correspond to 1H at H15. Doublet visible at δ 3.52 with coupling constant 10.99 Hz related to 1H, at H17.

The ^{13}C NMR (Figure 71, page 201) data found in Table 30, page 160 showed 21 carbons signals. The carboxylic carbon was observed at δ 177.7 (C19), and the primary alcoholic moiety at δ 65.1 (C17). The signals at δ 28.8 and δ 13.1 assigned to 2CH_3 at C20 and C18. The carbonyl group at C16 is missing. The carbon multiplicities were derived from DEPT¹³⁵ spectrum (Figure 72, page 202) as four quaternary, two methine, ten methylene and two methyl carbons, one carboxylic carbon and one oxymethyl carbon. The spectral data was corresponding to the literature data of compound **4h** (Oliveira *et al.*, 1999).

4.12 BENZYL ESTER OF ISOSTEVIOL (2a)

A New analogue **2a** (167 mg) was isolated as a white crystalline solid in 82% yield (Scheme 1, page 144). The ESI-MS (Figure 96, page 226) data showed $[\text{M}-\text{H}]^+$ ion at 407.46, which corresponds to the calculated mass of the compound with the formula $\text{C}_{27}\text{H}_{36}\text{O}_3$. IR spectrum (Figure 97, page 227) showed the expected absorption peaks (cm^{-1}), at 1738 (ketone), 1720 (ester carbonyl), 1453, 1147, 740 (aromatic ring).

The spectral data results of ^1H NMR (Figure 98, page 228) mention in Table 23, page 153 showed three methyl singlet's at δ 0.60, δ 0.97 and δ 1.21 corresponding to the H20, H18 and H17, respectively. Broad doublet visible at δ 2.2 was assigned to H12. Quartet at δ 2.55 corresponds to 1H at H15. A doublet at δ 5.08 having J 17.58 and 12.46 Hz corresponds to 1H (H7''). Singlet at δ 7.34 corresponds to aromatic 5H (H2'' to H6''), of the benzoate.

The ^{13}C NMR (Figure 99, page 229) data reported in Table 31, page 161 display 26 carbons signals. The carboxylic carbon signal was observed at δ 176.98 (C19). The evidence of the benzyl group was confirmed by the presence of signals at δ 136.5 (C1''), δ 128.2 (C2'', C6''), δ 128.5 (C3'', C5''), δ 128.1 (C4''), and the methylene carbon at δ 65.8 (C7''). The carbons multiplicities were derived from DEPT¹³⁵ spectrum as five quaternary, seven methine, ten methylene, three methyl carbons, and one carboxylic carbon.

4.13 BENZYL ESTER OF 16-HYDROXY ISOSTEVIOL (2b)

A New compound **2b** (240 mg) was recovered as a white crystalline solid, in 80 %, yield (Scheme 1, page 144). Its molecular formula has been determined as $\text{C}_{27}\text{H}_{38}\text{O}_3$ on the basis of ESI-MS (Figure 100, page 230) data which showed the $[\text{M}-\text{H}]^+$ ion at 409.39, which corresponds to the calculated mass of the compound. The IR spectrum (Figure 101, page 231) showed the absorption bands (cm^{-1}), at 3460 (alcohol), 1721 (ester), 1454, 1147, 740 (aromatic ring).

The ^1H NMR (Figure 102, page 232) data reported in Table 23, page 153 showed the signals of 3 CH_3 at δ 0.70, δ 0.93 and δ 1.21 attributed to H20, H18, and H17 respectively. Doublet visible at δ 2.22, with coupling constant 12.26 Hz corresponds to H12. Doublet of doublet visible at δ 3.86 corresponds to 1H (H16). Multiplet at δ 5.10 corresponds to methylene 1H (H7''). Singlet visible at δ 7.3 corresponds to 5H (2H''-6H'').

The ^{13}C NMR (Figure 103, page 233) data mention in Table 31 page 161 showed 27 carbons signals. The carboxylic carbon was detected at δ 177.3 and the secondary alcoholic moiety at δ 80.5. The benzyl group was evidenced by the presence of the aromatic carbons δ 136.1 (C1''), δ 128.2 (C2'', C6''), δ 128.4 (C3'', C5''), δ 127.9 (C4''), and methylene carbon at δ 65.9 (C7''). The assignment of the observed signals in the ^{13}C NMR spectrum was confirmed by comparison with the DEPT 135 spectrum (Figure 104, page 234) as five quaternary, eight methine, ten methylene, three methyl carbons, and one carboxylic carbon.

4.14 BENZYL ESTER OF 16-OXIME ISOSTEVIOL (2c)

The compound **2c** (172 mg) new derivative was recovered as a white crystalline solid in 81% yield (Scheme 1, page 144). The molecular formula $\text{C}_{27}\text{H}_{37}\text{NO}_3$ was confirmed on the basis of ESI-MS (Figure 105, page 235) data which showed the $[\text{M}-\text{H}]^+$ ion 422.33, corresponds to the calculated mass of the compound. The IR spectrum (Figure 106, page 236) showed the concerned absorption bands (cm^{-1}), at 3294 (oxime), 1721 (carbonyl), 1454 (hydroxyl bending), 1146, 696 (aromatic ring).

The ^1H NMR (Figure 107, page 237) data reported in Table 24, page 154 showed the resonance of 3CH_3 at δ 0.73, δ 1.13 and δ 1.24 assigned to H20, H18 and H17 respectively. Multiplet at δ 2.95 corresponds to H15. Doublet at δ 5.0 corresponds to 1H at H7''. Another doublet visible at δ 5.2 assigned to 1H at H7''. A singlet at δ 7.38 corresponds to aromatic 5H (2H'' to 6H'').

The ^{13}C NMR (Figure 108, page 238) data outlined in Table 31, page 161 showed resonance at δ 128.1 (C2'' and C6''), and δ 128.5 (C3'' and C5''), correspond to two carbons each, totaling 27 carbons. The benzyl group was evidenced by the presence of the aromatic carbons δ 136.5 (C1''), δ 128.2 (C2'', C6''), δ 128.5 (C3'', C5''), δ 128.1 (C4''), and for methylene carbon at δ 65.8 (C7''). The assignments were confirmed by comparison with the DEPT 135 spectrum

(Figure 109, page 239) as five quaternary, seven methine, ten methylene, three methyl carbons, one carboxylic carbon and one oxime carbon.

4.15 BENZYL ESTER OF ISOSTEVIOL LACTONE (2d)

The compound **2d** (170 mg) new derivative was obtained as a white crystalline solid in 76% yield (Scheme 2, page 145) had molecular formula $C_{27}H_{36}O_4$ on the basis of ESI-MS (Figure 110, page 240) data which showed the presence of an $[M+Na]^+$ ion 447.39, which corresponds to the calculated mass of the compound. The IR spectrum (Figure 111, page 241) showed the absorption bands (cm^{-1}), at 1721 (ester carbonyl), 1454 (hydroxyl bending), 1237, 1143 (asymmetric stretch ester), 745, 698 (Aromatic ring).

The 1H NMR (Figure 112, page 242) spectral data outlined in Table 24, page 154 showed resonance at δ 0.70, δ 1.22, and δ 1.35, assigned to three methyl at H20, H18, and H17. Doublet at δ 2.22 was assigned to H12. Multiplet at δ 3.01, represent methylene unit at H15. Two doublets visible at δ 5.0, and δ 5.2, with 12.3 Hz coupling constant was assigned to 2H, at H7". Resonance at δ 7.36, corresponds to the aromatic 5H (H2" to H6"), of the benzoate.

The ^{13}C NMR (Figure 113, page 243) spectral data outlined in Table 31, page 161, showed 25 carbons signal. Resonance at δ 128.3 (C2", C6"), and δ 128.5 (C3", C5"), is equivalent to two carbons, totaling 27 carbons. The benzyl group was evidenced by the presence of the aromatic carbons δ 136.5 (C1"), δ 128.2 (C2", C6"), δ 128.5 (C3", C5"), and δ 128.1 (C4"), and methylene carbon unit at δ 65.8 (C7"). The assignment of the observed signals in the ^{13}C NMR spectrum was confirmed by comparison with the DEPT 135 spectrum (Figure 114, page 244) as five quaternary, seven methine, ten methylene, three methyl carbons, and two carboxylic carbons.

4.16 BENZYL ESTER OF 17-HYDROXY ISOSTEVIOL (5I)

A new compound **5I** (147 mg) was recovered as a white crystalline solid in 69% yield (Scheme 5, page 148). The molecular formula $C_{27}H_{36}O_4$ was derived from the ESI-MS (Figure 120, page 250) data, $[M+H]^+$ 425.23, which corresponds to the calculated mass of the compound. The IR spectrum (Figure 121, page 251) showed the interested absorption bands (cm^{-1}), at 3408 (Hydroxyl), 1722 (carbonyl), 1124 (carbon-oxygen), and at 772, 668 (Aromatic ring).

The 1H NMR (Figure 122, page 252) spectral data reported in Table 25, page 155 showed the signals at δ 0.63, and δ 1.25, was assigned to H20 and H18. The multiplet observed at δ 2.61 ($J = 18.97$ and 3.78 Hz), was attributed to H15. Doublet visible at δ 2.24 corresponds to 1H at H12. Two doublets visible at δ 3.52, and δ 3.66, with coupling constant 11.4 Hz was assigned to 2H at H17. The doublet at δ 5.0 and δ 5.1 corresponds to 2H of methylene carbon unit (H7''). The benzyl group was evidence at δ 7.37, assigned to 5H (H2'' to H6'').

The ^{13}C NMR (Figure 123, page 253) spectral data reported in Table 32, page 162 showed twenty six carbons signals. The multiplicities were derived from the DEPT 135 spectrum (Figure 124, page 254) as five quaternary, seven methine, eleven methylene and two methyl carbons and one carboxylic carbon. The signals at δ 176.9 and δ 65.0 indicate the presence of carbomethoxy and primary alcoholic functionalities at C20, and C17, respectively. The signals at δ 28.9, and δ 12.9, correspond to $2CH_3$ at C20, and C18. The carbonyl group at C16 is missing. The benzyl group was confirmed by the presence of aromatic carbons resonance at δ 135.9 (C1''), δ 128.3 (C2'', C6''), δ 128.5 (C3'', C5''), δ 128.1 (C4''), and methylene carbon (C7''), resonance was observed at δ 66.09.

4.17 BENZYL ESTER OF 17, 16-DIHYDROXY ISOSTEVIOL (6i)

The compound **6i** (165 mg) a new derivative was obtained as a white crystalline solid in 77% yield (Scheme 5, page 148). The molecular formula $C_{27}H_{38}O_4$ was derived from the ESI-MS (Figure 125, page 255) data, $[M+H]^+$ 425.29, which corresponds to the calculated mass of the compound. The IR spectrum (Figure 126, page 256) showed the absorption bands (cm^{-1}), at 3391 (broad band Alcohol), 1720 (ester carbonyl), 1454 (hydroxyl bending), 1147 (carbon oxygen stretch), 754, 696 (Aromatic ring)

The 1H NMR (Figure 127, page 257) spectral data reported in Table 25, page 155 showed signals at δ 0.72, δ 1.21 corresponds to $2CH_3$ at H20, H18. The doublet visible at δ 3.4 ($J = 10.1$ Hz), was assigned to H17 and the multiplet visible at δ 5.1 correspond to the one proton resonance of methylene unit at H7". A singlet was observed at δ 7.4 (H2" to H6") corresponds to the aromatic 5H protons of the benzoate.

The ^{13}C NMR (Figure 128, page 258) spectral data outlined in Table 31, page 161 showed twenty five carbons signals. Resonance visible at δ 128.44 (C3", C5"), δ 128.20 (C2", C6"), corresponds to two carbons each totaling 27 carbons. The carbons multiplicities were derived from DEPT 135 spectrum (Figure 129, page 259) as five quaternary, eight methine, eleven methylene two methyl carbons and one carboxylic carbon. The resonance at δ 177.0, δ 71.0 and δ 78.3, showed the presence of carbomethoxy, primary alcoholic and tertiary alcoholic functionalities at C19, C17 and C16 respectively. The signals at δ 28.9, and δ 13.5, correspond to $2CH_3$ at C20, and C18. The signal relative to the benzyl group were observed at δ 136.1 (C1"), δ 128.2 (C2", C6"), δ 128.4 (C3", C5"), δ 127.9 (C4"), and methylene carbon (C7"), resonance was observed at δ 65.9.

4.18 BENZYL ESTER OF 17-HYDOXY, 16-OXIME ISOSTEVIOL (6j)

A new compound **6j** (147 mg) was obtained as a white crystalline solid in 66% yield (Scheme 5, page 148). The molecular formula $C_{27}H_{37}NO_4$ was derived from the ESI-MS (Figure 130, page 260) data, $[M+H]^+$ 440.39, which corresponds to the calculated mass of the compound. The IR spectrum (Figure 131, page 261) showed the absorption bands (cm^{-1}), at 1881 (ester carbonyl), 1578 (oxime carbon nitrogen), 1480, 1163 (carbon oxygen), 999 (nitrogen oxide), 773, 587 (aromatic ring).

The 1H NMR (Figure 132, page 262) spectral data reported in Table 25, page 155 indicates the signals at δ 0.69 and δ 1.20 corresponds to $2CH_3$ at H20 and H18. Doublet visible at δ 2.20 corresponds to H12. Broad, doublet resonance visible at δ 2.92, having $J = 18.30$ Hz, correspond to H15, singlet at δ 3.59 was assigned to 2H at H17. Resonance of two protons at δ 5.01 and δ 5.18 with 12.39 Hz coupling constant corresponds to 2H at H7". A singlet was observed at δ 7.34 assigned to 5H (H2"-H6") of benzoate.

The ^{13}C NMR (Figure 133, page 263) spectral data outlined in Table 31, page 161 showed twenty five carbons resonance. Signals visible at δ 128.5 (C3", C5"), δ 128.2 (C2", C6"), corresponds to two carbons each totaling 27 carbons. The carbons multiplicities were derived from DEPT¹³⁵ spectrum (Figure 134, page 264) as five quaternary carbons, seven methine carbons, eleven methylene carbons, two methyl carbons one oxime functional and one carboxylic carbon. The resonance at δ 177.0, δ 169.2 and δ 66.7, showed the presence of carbomethoxy, oxime and primary alcoholic functionalities at C19, C16 and C17 respectively. The signal visible at δ 28.9 and δ 13.3 corresponds to $2CH_3$ at C20, and C18. The signals relative to the benzyl group were visible at δ 136.1 (C1"), δ 128.2 (C2", C6"), δ 128.5 (C3", C5"), δ 128.1 (C4"), and methylene carbon (C7"), resonance was observed at δ 65.9.

4.19 *p*-METHOXYPHENACYL ESTER OF ISOSTEVIOL (3a)

The product **3a** (112 mg) a new derivative was obtained as a white powder solid in 82% yield (Scheme 1, page 144), had the molecular formula $C_{29}H_{38}O_5$ determined on the basis of ESI-MS (Figure 135, page 265) data, which showed the $[M]^+$ ion 466.59, corresponds to the calculated mass of the compound. The IR spectrum (Figure 136, page 266) revealed the interested absorption bands (cm^{-1}), at 1736 (carbonyl), 1454 (methylene C-H), 1146, 696 (aromatic ring).

The 1H NMR (Figure 137, page 267) spectral data reported in Table 28, page 158 spectrum showed the resonance at δ 0.77, δ 0.98, and δ 1.34 was assigned to H20, H18 and H17 respectively. Multiplet at δ 2.66 (1H, J 18.69 and 3.65 Hz) was attributed to H15. The singlet at δ 3.88 was assigned to oxymethyl functionality. Two doublets at δ 5.2 and δ 5.3 having 16.1 Hz coupling constant corresponds to 2H was attributed to H8'. Doublet visible at δ 6.95 (2H, J 9.00 Hz), was attributed to H3' and H5'. The signal at δ 7.90 (2H, J 8.97 Hz), was assigned to H2' and H6'.

The ^{13}C NMR (Figure 138, page 268) spectral data outlined in Table 33 page 163 showed 26 carbons resonance. The signals at δ 130.1 (C2', C6'), and δ 114.0 (C3', C5'), is equivalent to two carbons, totaling 28 carbons, ketonic carbon at C16 was not observed. Carboxylic functionality resonance was visible at δ 176.8. The *p*-methoxy acetophenone group was evidenced by the presence of the aromatic carbons, methoxy carbon, carbonyl group and methylene carbon. The carbonyl carbon resonance visible at δ 190.9 (C7'). The aromatic carbon resonance observed at δ 127.4 (C1'), δ 130.1 (C2', C6'), δ 114.0 (C3', C5'), and δ 163.9 (C4'). The methylene carbon resonance appears at δ 65.2 (C8'), and methoxy linked with aromatic ring visible at δ 55.5 (C9'). The assignments were confirmed with the DEPT 135 spectrum (Figure 139, page 269) as six quaternary, six methine, ten methylene carbons, three methyl carbons, one carbonyl functional, one carboxylic carbon and one oxymethyl carbon.

4.20 *p*-METHOXY PHENACYL ESTER OF 16-HYDROXY ISOSTEVIOL (**3b**)

The compound **3b** (105 mg) a new derivative was obtained as a white powder solid in 75% yield (Scheme 1, page 144). The molecular formula $C_{29}H_{40}O_5$ was determined on the basis of ESI-MS (Figure 140, page 270) data, which showed the $[M+Na]^+$ ion 491.35, which corresponds to the calculated mass of the compound. The IR spectrum (Figure 141, page 271) exhibit the absorption bands (cm^{-1}), at 3556 (secondary hydroxyl), 1719 (ester carbonyl), 1603 (aromatic ring stretching), 1161 (aromatic C-H stretch).

The 1H NMR (Figure 142, page 272) spectral data reported in Table 28, page 158 the resonance at δ 0.81, δ 0.92 and δ 1.32 corresponds to $3CH_3$ at H20, H18 and H17. Singlet visible at δ 3.88 corresponds to 3H at (OCH_3) . Two doublets at δ 5.2 and δ 5.3, with coupling constant 16.1 Hz corresponds to 2H at H8'. Another doublet at δ 6.95 with 8.92 Hz coupling constant was assigned to 2H at $(H3', H5')$. Resonance visible at δ 7.9 ($J = 8.9$ Hz) corresponds to 2H at $(H2', H6')$.

The ^{13}C NMR (Figure 143, page 273) spectral data reported in Table 33, page 163 showed 27 carbons resonance. The resonance observed at δ 130.0 ($C2', C6'$), and δ 113.9 ($C3', C5'$), is equivalent to two carbons, totaling 29 carbons. The *p*-acetophenone carbonyl group resonance visible at δ 191.1 ($C7'$). The aromatic carbons resonance are at δ 127.5 ($C1'$), δ 130.0 δ ($C2', C6'$), δ 113.9 ($C3', C5'$), and δ 163.9 ($C4'$). The methylene carbon unit resonance observed at δ 65.2 ($C8'$), and resonance of (OCH_3) , with aromatic ring at δ 55.5 ($C9'$). The assignments were confirmed with the DEPT 135 spectrum (Figure 144, page 274) as six quaternary, seven methine, ten methylene carbons, three methyl carbons one carbonyl functional one carboxylic carbon and one oxymethyl carbon.

4.21 *p*-METHOXY PHENACYL ESTER OF 16-OXIME ISOSTEVIOL (**3c**)

The product **3c** (115 mg) a new derivative was recovered as white powder solid in 79% yield (Scheme 1, page 144). The molecular formula $C_{29}H_{39}NO_5$ was deduced on the basis of ESI-MS (Figure 145, page 275) data, showing $[M]^+$ ion 481.35, which corresponds to the calculated mass of the compound. The IR spectrum (Figure 146, page 276) showed absorption bands (cm^{-1}), at 3447 (oxime), 1719 (ester), 1692 (ketone), 1601, 1162 (aromatic ring), 963 (N-O).

The 1H NMR (Figure 147, page 277) spectral data reported in Table 28 page 158 revealed the signals at δ 0.86, δ 1.13 and δ 1.37 assigned to H20, H18 and H17 respectively. The singlet at δ 3.91 (3H), was assigned to the oxymethyl functionality. Two doublets visible at δ 5.1, and 5.4, with 16.0 Hz coupling constant was attributed to 2H at oxymethylene unit (H8'). The doublet at δ 6.99 (J 8.9 Hz, 2H), was assigned to H3', H5'. Another doublet visible at δ 7.93 (J 8.9 Hz, 2H), was attributed to 2H at H2' and H6'.

The ^{13}C NMR (Figure 148, page 278) spectral data outlined in Table 33, page 163 showed 27 carbons resonance, at δ 130.1 (C2', C6'), and δ 114.0 (C3', C5'), is equivalent to two carbons, totaling 29 carbons. The *p*-methoxy acetophenone group was evidenced by the presence of the aromatic carbons, methoxy carbon, carbonyl group and methylene carbon. The acetophenone carbonyl resonance appears at 191.0 (C7'). The aromatic carbon resonance are at δ 127.5 (C1'), δ 130.1 (C2', C6'), δ 114.0 (C3', C5'), and δ 163.9 (C4'). The methylene carbon unit resonance appears at 65.2 (C8'), and methoxy linked with aromatic ring was observed at δ 55.5 (C9'). The assignments were confirmed with the DEPT 135 spectrum (Figure 149, page 279) as six quaternary, six methine, ten methylene carbons, three methyl carbons one carbonyl functional one carboxylic carbon one oxime carbon and one oxymethyl carbon.

4.22 *p*-METHOXY PHENACYL ESTER OF STEVIOL (3h)

A new analogue **3h** (110 mg) was recovered as a white powder solid in 78% yield (Scheme 4, page 147). The molecular formula $C_{29}H_{38}O_5$ was deduced on the basis of MS-ESI (Figure 150, page 280) data, showing $[M+Na]^+$; 489.46, which corresponds to the calculated mass of the compound. The IR spectrum (Figure 151, page 281) showed characteristic absorption bands (cm^{-1}), at 3493 (tertiary hydroxyl), 1731 (ester), 1692 (ketone), 1603, 1262 (Aromatic).

The 1H NMR (Figure 152, page 282) spectral data outlined in Table 28, page 158 showed signals at δ 0.91, δ 1.32, corresponds to 2H at H20 and H18. Doublet observed at δ 2.28 with, ($J = 12.1$ Hz), corresponds to 1H at H12. Singlet at δ 3.88 corresponds to aromatic methoxy 3H. Two broad singlet's visible at δ 4.81 and δ 4.97 were assigned to H17. Two doublets visible at δ 5.2 and δ 5.4 with coupling constant 16.11 Hz were related to methylene unit at H8'. The doublet at δ 6.95 were assigned to 2H at H3' and H5'. Doublet at δ 7.91 with $J = 8.95$ Hz, related to 2H at H2' and H6'.

The ^{13}C NMR (Figure 153, page 283) spectral data is reported in Table 33, page 163 showed 27 carbons resonance, at δ 130.1 (C2', C6'), and δ 114.0 (C3', C5'), is equivalent to two carbons, totaling 29 carbons. Olefinic carbon resonance at δ 102.9 (C17). Tertiary alcoholic functionality resonance observes at δ 80.3 (C13). The *p*-methoxy acetophenone group was evidenced by the presence of the aromatic carbons, methoxy carbon, carbonyl group and methylene carbon. The acetophenone carbonyl resonance appears at δ 191.0 (C7'). The aromatic carbons resonance were observed at δ 127.5 (C1'), δ 130.1 (C2', C6'), δ 114.0 (C3', C5'), and δ 163.90 (C4'). The methylene carbon unit resonance appears at δ 65.2 (C8'), and methoxy linked with aromatic ring was observed at δ 55.5 (C9'). The assignments were confirmed with the DEPT¹³⁵ spectrum (Figure 154, page 284) as six quaternary, six methine, eleven methylene, two methyl carbons one carbonyl, one carboxylic carbon, one olefinic carbon and one oxymethyl carbon.

4.23 16-HYDRAZONE OF ISOSTEVIOL (1f)

A known product **1f** (83 mg) was obtained as white crystalline solid in 83% yield (Scheme 2, page 145). The calculated molecular formula $C_{20}H_{32}N_2O_2$ was derived on the basis of ESI-MS (Figure 56, page 186) data, $[M+H]^+$ 333.3, which corresponds to the calculated mass of the compound. The IR spectrum (Figure 57, page 187) showed characteristic bands (cm^{-1}), at 3352 (hydrazone), 1712 (carboxylic), 1453 (methylene C-H), 1399 (methyl C-H).

The 1H NMR spectrum (Figure 58, page 188) of **1f** revealed several key signals that assisted in the determination of its structure. The 1H NMR spectral data found in Table 21, page 151 showed the resonance at δ 0.85, δ 1.06 and δ 1.24, are the characteristics proton shift region for the basic skeleton of isosteviol. The resonance at δ 2.2 is attributed to 1H at H12. Multiplet at δ 2.66 having coupling constant 17.44 and 1.84 Hz, are assigned to H15. Oxymethyl proton resonance appears at δ 3.64.

The ^{13}C NMR spectrum (Figure 59, page 189) showed twenty carbons signal. ^{13}C NMR spectral data reported in Table 30, page 160. The hydrazone functionality signal was observed at δ 165.5 (C16). The rest of nineteen carbons multiplicities were derived from the DEPT 135 spectrum (Figure 60, page 190) as four quaternary, two methine, nine methylene three methyl one carboxyl and one hydrazone carbons. The three tertiary methyl and carbomethoxy functionality resonance were observed at δ 13.6 (C20), δ 22.1 (C17), δ 29.1 (C18), and δ 182.4 (C19), respectively (Garifullin *et al.*, 2012).

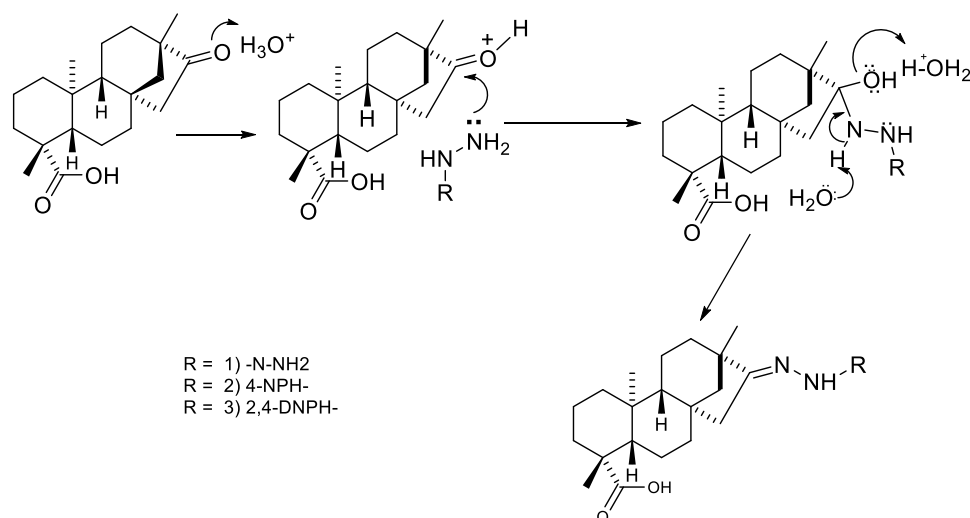


Figure 28: General mechanism for hydrazone formation includes nucleophilic addition-elimination reaction.

4.24 17-HYDROXY, 16-HYDRAZONE OF ISOSTEVIOL (5k)

The product **5k** (90 mg) new derivative was recovered as a white crystalline solid in 86% yield (Scheme 5, page 148). The calculated molecular formula $C_{20}H_{32}N_2O_3$ was derived on the basis of ESI-MS (Figure 86, page 216) data, $[M-H]^+$ 347.33, which corresponds to the calculated mass of the compound. The IR spectrum (Figure 87, page 217) showed characteristic absorption bands (cm^{-1}), at 3412 (primary hydroxyl), 3221 (nitrogen hydrogen), 1698 (ester carbonyl).

The 1H NMR (Figure 88, page 218) spectral data reported in Table 23 page 153 showed the resonance at δ 0.96, δ 1.19, ascribed to $2CH_3$, at H20 and H18, respectively. The broad doublet at δ 2.16 corresponds to 1H at H12. Another broad doublet at δ 2.89 (J 18.20 Hz), corresponds to 1H at H15 and a broad singlet visible at δ 3.57 was assigned to H17.

The ^{13}C NMR (Figure 89, page 219) spectral data are reported in Table 31, page 161, and display the hydrazone functionality resonance at δ 165.4 (C16). The rest of nineteen carbons multiplicities were derived from the DEPT¹³⁵ spectrum (Figure 90, page 220) as four quaternary, two methine, ten methylene two methyl carbons, one carboxylic and one hydrazone carbon. The signals at the δ 182.9 and δ 66.1 were attributed to the carbomethoxy (C20), and primary alcoholic (C17), functionalities, respectively. The signals at δ 28.8 and δ 13.0 correspond to 2CH₃ at C20 and C18 respectively.

4.25 BENZYL ESTER 16-HYDRAZONE OF ISOSTEVIOL (3f)

The compound **3f** (105 mg) a new derivative was obtained as a white crystalline solid in 84% yield (Scheme 3, page 146). The molecular formula C₂₇H₃₈N₂O₂ was based on the ESI-MS (Figure 115, page 245) data [M+H]⁺ 423.40, which corresponds to the calculated mass of the compound. The IR spectrum (Figure 116, page 246) showed characteristic absorption bands (cm⁻¹), at 3391 (hydrazone NH), 1720 (ester carbonyl), 1453 (methylene C-H), 1147 (ether carbon oxygen), 754, 697 (aromatic ring C-H).

The ^1H NMR spectrum (Figure 117, page 247) of **3f** revealed several key signals that helped in the determination of its structure. The ^1H NMR spectral data is found in Table 24, page 154 showed resonance at δ 0.66, δ 1.06 and δ 1.22, assigned to 3CH₃ at H20, H18 and H17 respectively. Multiplet at δ 2.55 (*J* 17.5 and 2.8 Hz, 1H), was attributed to 1H at H15 and the two doublet at δ 5.1 and δ 5.2, with 12.45 coupling constant were assigned to 2H at H7". A singlet observed at δ 7.4 corresponded to 5H at (H2" to H6").

The ^{13}C NMR spectrum (Figure 118, page 248) showed 25 signals. The spectral data outlined in Table 31, page 161. The signals visible at δ 128.2 (C2", C6") and δ 128.4 (C3", C5"), in benzoate ring corresponds to two carbons each totaling 27 carbons. The hydrazone resonance appeared at δ 164.4 (C16). The

carboxylic carbon (C19), resonance appeared at δ 177.0. The benzyl group was evidenced by the presence of the aromatic carbons at δ 136.1 (C1''), δ 128.2 (C2'', C6''), δ 128.4 (C3'', C5''), δ 128.0 (C4''), and methylene carbon unit at δ 65.9 (C7''). The DEPT¹³⁵ spectrum (Figure 119, page 249) show as five quaternary, seven methine, ten methylene, three methyl carbons, one carboxylic and one hydrazone carbon.

4.26 BENZYL ESTER 16-HYDRAZONE 17-HYDROXY ISOSTEVIOL (6k)

The product **6k** (96 mg) new derivative was obtained as a white crystalline solid in 73% yield (Scheme 5, page 148). The calculated molecular formula C₂₇H₃₈N₂O₃ on the basis of ESI-MS (Figure 155, page 285) data which showed the presence of an [M+H]⁺ 439.42, which corresponds to the calculated mass of the compound. The IR spectrum (Figure 156, page 286) revealed characteristic absorption bands (cm⁻¹), at 3426 (broad band hydrazone NH and hydroxyl), 1720 (ester carbonyl), 1656 (hydrazone C=N), 1455 (methylene C-H), 1147 (ether carbon oxygen), 771, 694 (aromatic ring, C-H).

The ¹H NMR (Figure 157, page 287) spectral data is shown in Table 27, page 157 showed the resonance at δ 0.65, and δ 1.20, were assigned to 2CH₃ at H20 and H18, respectively. Multiplet observed at δ 2.56 (*J* 17.26 and 2.45 Hz), corresponds to 1H at H15. Doublet at δ 3.49 (*J* 11.10 Hz), and another doublet at δ 3.64 with coupling constant 11.10 Hz were assigned to 2H, at H17. Multiplet at δ 5.09 (*J* 18.5, 12.6 Hz) corresponds to 1H, at H7''. A singlet was observed at δ 7.35 (H2'' to H6''), corresponds to the aromatic 5H, of the benzoate.

The ¹³C NMR (Figure 158, page 288) spectral data in Table 32, page 162 showed twenty five carbons resonance. Signals visible at δ 128.44 (C3'', C5''), δ 128.20 (C2'', C6''), corresponds to two carbons each totaling 27 carbons. The multiplicity of the 27 carbons were derived from DEPT¹³⁵ spectrum (Figure 159, page 289) as five quaternary, seven methine, eleven methylene two methyl

carbons, one carboxylic and one hydrazone carbon. The resonance at the δ 177.0, and δ 67.9 showed the presence of carbomethoxy and primary alcoholic functionalities at C19 and C17. The resonance visible at δ 164.8 was assigned to (C16). The ^{13}C signals at δ 28.9, and δ 13.4, corresponds to 2CH_3 at C20, and C18. The Benzyl group was confirmed by the presence of aromatic carbon at δ 136.1 (C1''), δ 128.2 (C2'', C6''), δ 128.4 (C3'', C5''), δ 128.0 (C4''), and methylene carbon (C7'') resonance observed at δ 66.1.

4.27 16-ISOPROPYL HYDRAZONE OF ISOSTEVIOL (2f)

A new compound **2f** (98 mg) was obtained as a light yellow powder solid in 84%, yield (Scheme 2, page 145). The molecular formula $\text{C}_{24}\text{H}_{38}\text{N}_2\text{O}_2$ was determined on the basis of ESI-MS (Figure 91, page 221) data showing $[\text{M}]^+$ ion 386.29, which corresponds to the calculated mass of the compound. The IR spectrum (Figure 92, page 222) showed the interested absorption band (cm^{-1}), at 1721 (carbomethoxy), 1658 (C=N), 1452 (methylene C-H), 1235 (carbon nitrogen), 1170 (ether carbon oxygen).

The ^1H NMR (Figure 93, page 223) spectral data outlined in Table 23, page 153. Analysis of the ^1H NMR spectrum revealed the resonance of 5CH_3 at δ 0.69, δ 1.13, δ 1.18, δ 1.84, and δ 2.01, at H20, H18, H17, H1', H3' respectively. The multiplet at δ 2.68 (J 18.47 and 3.20 Hz), corresponds to H15 and the singlet at δ 3.64, was assigned to 3H (OCH_3).

The ^{13}C NMR (Figure 94, page 224) spectral data mentioned in Table 31, page 161 showed 24 signals. The resonance at δ 174.3 and δ 159.1, specifies that ketonic carbon was reduced to hydrazone moiety at (C16), and (C2'), respectively. The resonance at δ 177.9 is characteristic region for the carbomethoxy functionality (C19). The five methyl resonance appears at δ 28.8 (C18), δ 24.9 (C17), δ 22.2 (C1'), δ 17.6 (C3'), and at δ 13.2 (C20). The DEPT 135 spectrum (Figure 95, page 225) showed the expected multiplicity with four quaternary

carbons, two methine carbons, nine methylene carbons, five methyl carbons one carboxylic carbon, and one oxymethyl carbon.

4.28 16-ISOPROPYL HYDRAZONE BENZYL ESTER OF ISOSTEVIOL (4f)

A new product **4f** (105 mg) was obtained as a light yellow crystalline solid in 75% yield (Scheme 3, page 146). The molecular formula $C_{30}H_{42}N_2O_2$ was based on the ESI-MS (Figure 160, page 290) data which showed the $[M+H]^+$ 463.39, which corresponds to the theoretically calculated mass of the compound. The IR spectrum (Figure 161, page 291) showed the interested absorption bands (cm^{-1}), at 1721 (carbomethoxy), 1658 (C=N), 1453 (methylene C-H), 1147 (ether C-O), 753, 698 (aromatic C-H).

The 1H NMR (Figure 162, page 292) spectral data is reported in Table 27, page 157. The resonance observed at δ 0.63, δ 1.13, δ 1.21, δ 1.83, and δ 2.03, corresponding to the $5CH_3$ at H20, H18, H17, H1', H3', respectively. The multiplet at δ 2.63 (J 18.54 and 3.12 Hz, 2H), was assigned to 1H at H15 and another multiplet at δ 5.09 (J 18.98 and 12.38 Hz, 1H), was attributed to 1H at H7''. A singlet appeared at δ 7.35, was assigned to 5H at H2'' to H6''.

The ^{13}C NMR (Figure 163, page 293) spectral data outlined in Table 32, page 162 showed 28 carbons resonance; the signals at δ 128.2 (C2'', C6''), and δ 128.4 (C3'', C5''), for benzoate ring corresponds to two carbons each, totaling of 30 carbons. The hydrazone resonance visible at δ 174.1 and δ 158.7 corresponding to C16 and C2' respectively. There was a slightly upshift of hydrazone at C2' due to absence of ring strain. The carboxylic carbon signal C19 was evident at δ 177.1, and the benzyl group was evidenced by the presence of the aromatic carbons at δ 136.1 (C1''), δ 128.2 (C2'', C6''), δ 128.4 (C3'', C5''), δ 127.9 (C4''), and methylene carbon unit at δ 65.9 (C7''). The two methyl carbon resonance for C1' and C3' were also evident at δ 22.2, and δ 17.6. The DEPT¹³⁵ spectrum (Figure 164, page 294) showed the expected multiplicity with five

quaternary carbons, seven methine carbons, ten methylene carbons, five methyl carbons, one carboxylic carbon, and two hydrazone carbons.

4.29 16-ISOPROYL HYDRAZONE BENZYL OF 17-HYDROXY ISOSTEVIOL-ESTER (7K)

A new compound **7k** (94 mg) was isolated as a light yellow solid in 65% yield (Scheme 5, page 148). The molecular formula $C_{30}H_{42}N_2O_3$ was based on the ESI-MS (Figure 165, page 295) data which showed the $[M+H]^+$ 479.50, which corresponds to the calculated mass of the compound. The IR spectrum (Figure 166, page 296) display the interested absorption bands (cm^{-1}), at 3426 (broad band hydrazone NH, and hydroxyl OH), 1720 (ester carbonyl), 1656 (C=N), 1455 (methylene C-H), 1147 (ether carbon oxygen), 771, 694 (aromatic C-H).

The 1H NMR (Figure 167, page 297) spectral data reported in Table 27, page 157 displayed the basic skeleton resonance at δ 0.66, δ 1.22, corresponding to $2CH_3$ at H20, H18. Two singlet's visible at δ 1.89, and δ 2.06, correspond to $2CH_3$ at H1', H3' of isopropyl hydrazone moiety. The multiplet visible at δ 2.80 (J 18.7 and 3.0 Hz), corresponds to 1H at H15 and another doublet at δ 3.7 (J 10.8 Hz), was assigned to 1H at H17. Multiplet at δ 5.11 (J 18.5, 12.5 Hz) corresponds to 1H at H7''. A singlet was also observed at δ 7.4 (H2'' to H6''), corresponds to the aromatic 5H of the benzoate.

The ^{13}C NMR (Figure 168, page 298) spectral data shown in Table 32, page 162 exhibited twenty eight carbons signals. The resonance at δ 128.44 (C3'', C5''), and δ 128.20 (C2'', C6''), corresponds to two carbons each, totaling 30 carbons. The carbons multiplicity were derived from DEPT 135 spectrum (Figure 169, page 299) show five quaternary, seven methine, eleven methylene and four methyl, two hydrazone carbons and one carboxylic carbon. The signals at δ 177.9, and δ 67.9 were attributed to the carbomethoxy and primary alcoholic functionalities at C19 and C17. Two hydrazone carbons resonance visible at δ

177.0 and δ 162.2 was assigned to C16 and C2' respectively. The signals detected at δ 28.9, and δ 13.5 corresponds to 2CH₃ at C20, and C18 and the resonance at δ 18.0, and δ 25.1 corresponds to 2CH₃ at C1' and C3'. The benzyl group was confirmed by the presence of aromatic carbons at δ 136.1 (C1''), δ 128.4 (C3'', C5''), δ 128.2 (C2'', C6''), δ 128.0 (C4''), and methylene carbon (C7''), resonance observed at δ 65.9.

4.30 2, 4-DINITRO PHENYL HYDRAZONE OF ISOSTEVIOL (2g)

A known product **2g** (80 mg) was isolated as a yellow crystalline solid in 70%, yield (Scheme 2, page 145). The molecular formula C₂₆H₃₄N₄O₆ was determined on the basis of ESI-MS (Figure 170, page 300) data which showed the [M-H]⁺ ion 497.36, related to the calculated mass of the compound. The IR spectrum (Figure 171, page 301) showed characteristic absorption bands (cm⁻¹), at 3315 (hydrazone, N-H), 1692 (ester carbonyl), 1618 (aromatic ring), 1517 (NH).

The ¹H NMR (Figure 172, page 302) spectral data found in Table 26, page 156 showed the characteristic signals of basic isosteviol skeleton. The 3CH₃ signals were observed at δ 0.92, δ 1.19 and δ 1.28 at H20, H18 and H17 respectively, multiplet visible at δ 2.65 (J = 18.69 and 3.65 Hz, 1H), was assigned to 1H at H15. The doublet observed at δ 7.80 (J = 9.61Hz), was assigned to 1H at H6' while the doublet at δ 8.96 (J = 2.52 Hz), was assigned to 1H at H3'. Multiplet visible at δ 8.11 (J = 9.66 and 2.55 Hz), was attributed to 1H at H5'.

The ¹³C NMR (Figure 173, page 303) spectral data shown in Table 32, page 162 showed twenty five carbons signals, where resonance at δ 39.55 (C1, C15), corresponds to two carbons, totaling 26 carbons. The carbons multiplicity were derived from DEPT¹³⁵ spectrum (Figure 174, page 304) show seven quaternary, five methine, nine methylene three methyl carbons, one hydrazone carbon and one carboxylic carbon. The carboxylic resonance appears at δ 184.4 (C19). The formation of the 2, 4-dinitro phenyl hydrazone moiety is evidenced by

the resonance visible at δ 171.7 (C16). The 2, 4-dinitro phenyl hydrazone group was confirmed by the resonance of the carbons of 2, 4-dinitro benzene group at δ 144.9 (C1'), δ 137.3 (C2'), δ 129.5 (C3'), δ 128.4 (C4'), δ 123.4 (C5'), and δ 116.2 (C6').

4.31 4-NITRO PHENYL HYDRAZONE OF ISOSTEVIOL (3g)

The compound **3g** (70 mg) a new derivative was isolated as a yellow crystalline solid in 51% yield (Scheme 2, page 145). The molecular formula, $C_{26}H_{35}N_3O_4$, was deduced from the ESI-MS (Figure 175, page 305) data which showed the presence of an $[M]^+$ ion 452.36 corresponding to the calculated mass of the compound. The IR spectrum (Figure 176, page 306) showed the absorption bands (cm^{-1}), at 3319 (hydrazone, N-H), 1693 (ester carbonyl), 1595 (aromatic C=C), and 1322 (N-O).

The 1H NMR (Figure 177, page 307) spectral data found in Table 26, page 156 revealed the presence of 3CH₃ resonance at δ 0.89, δ 1.19 and δ 1.30, at H20, H18 and H17, respectively. The doublet at δ 7.06 (J 9.12 Hz, 2H), was assigned to 2H at H2', H6'. The doublet at δ 8.15 (J 9.12 Hz, 2H), was attributed to 2H at H3' and H5'.

The ^{13}C NMR (Figure 178, page 308) spectral data shown in Table 32, page 162 exhibited 24 carbons resonance, where the signals at δ 126.13 (C3', C5'), and δ 111.41 (C2', C6'), corresponds to two carbons, totaling 26 carbons. The carboxylic functionality observed at δ 184.0 (C19). The formation of the 4-nitro phenyl hydrazone is evidenced by the presence of a signal at δ 163.5 (C16). The 4-nitro phenyl hydrazone group was evidenced by the presence of the carbons of 4-nitrobenzene group at δ 139.6 (C1'), δ 111.4 (C2'), δ 126.1 (C3'), δ 150.6 (C4'), δ 126.1 (C5'), and δ 111.4 (C6'). The carbons multiplicity were derived from DEPT¹³⁵ spectrum (Figure 179, page 309) show six quaternary, six methine, nine

methylene three methyl carbons, one hydrazone carbon and one carboxylic carbon.

4.32 2, 4-DINITRO PHENYL HYDRAZONE BENZYL ESTER ISOSTEVIOL (4g)

The product **4g** (80 mg) a new derivative was recovered as a yellow crystalline solid in 45% yield (Scheme 3, page 146). The molecular formula $C_{33}H_{40}N_4O_6$ was based on the ESI-MS (Figure 180, page 310) data which showed the presence of an $[M-H]^+$ 587.46 which are in close agreement with the calculated mass of the compound. The IR spectrum (Figure 181, page 311) showed characteristic absorption bands (cm^{-1}), at 3316 (hydrazone N-H), 1719 (ester carbonyl), 1619 (aromatic ring C=C), 1591 (NH), 1335 (nitrogen oxygen N-O), 1141 (ether C-O), 755, 697 (aromatic ring C-H).

The 1H NMR (Figure 182, page 312) spectral data reported in Table 29, page 159 exhibited the resonance of $3CH_3$ at δ 0.70, δ 1.22 and δ 1.25, are the characteristic signals of isosteviol skeleton. Singlet observed at δ 5.15 corresponds to 2H at methylene unit (H7''). Another singlet visible at δ 7.42 corresponds to aromatic 5H at (H2'' to H6''). Broad doublet observed at δ 7.99 (J 9.68 Hz), corresponds to 1H (H6'). Multiplet observed at δ 8.3 (J 9.68 and 2.5 Hz), corresponds to 1H at H5'. Doublet at δ 9.16 with weak coupling constant 2.5 Hz corresponds to 1H (H3'). Singlet detected at δ 10.8, was assigned to (NH).

The ^{13}C NMR (Figure 183, page 313) spectral data found in Table 33, page 163 revealed the resonance of 31 carbons, the signals at δ 128.5 (C2'', C6''), and δ 128.5 (C3'', C5''), in benzoate ring, corresponds to two carbons each total 33 carbons. The formation of the hydrazone bond with C16 was confirmed at δ 171.2. The carboxylic carbon resonance (C19), visible at δ 176.9. The benzyl group was evidenced by the presence of the aromatic carbons at δ 135.9 (C1''), δ 128.5 (C2'', C6''), δ 128.5 (C3'', C5''), and δ 128.2 (C4''), and methylene carbon at δ 66.2 (C7''). The 2, 4-dinitro phenyl hydrazone group was confirmed by the

presence of aromatic carbon at δ 145.2 (C1'), δ 137.5 (C2'), δ 129.8 (C3'), δ 128.9 (C4'), δ 123.5 (C5'), δ 116.4 (C6'). The assignments were further confirmed by DEPT¹³⁵ spectrum (Figure 184, page 314) as eight quaternary, ten methine, ten methylene three methyl carbons, one hydrazone carbon and one carboxylic carbon.

4.33 4-NITRO PHENYL HYDRAZONE BENZYL ESTER ISOSTEVIOL (5g)

The product **5g** (75 mg) a new derivative was obtained as a yellow crystalline solid in 46% yield (Scheme 3, page 146). The molecular formula C₃₃H₄₁N₃O₄ was founded on the ESI-MS (Figure 185, page 315) data, [M-H]⁺ 542.69, which corresponds to the calculated mass of the compound. The IR spectrum (Figure 186, page 316) showed the characteristic absorption bands (cm⁻¹), at 3320 (hydrazone N-H), 1720 (ester carbonyl), 1598 (aromatic ring C=C), 1321 (nitrogen oxygen, N-O), 1172 (ether C-O), 752, 670, 695 (aromatic C-H).

The ¹H NMR (Figure 187, page 317) spectral data found in Table 29, page 159 exhibited the basic resonance of isosteviol skeleton at δ 0.68, δ 1.15 and δ 1.23, corresponds to 3CH₃ at H20, H18 and H17. Doublet at δ 5.0 and δ 5.2 having coupling constant 12.6 Hz represent methylene unit 2H at H7". Singlet visible at δ 7.36 corresponds to aromatic 5H (H2" to H6"). Doublet observed at δ 7.03 (*J* 9.2 Hz), corresponds to 2H (H2', H6'). Another doublet visible at δ 8.13 (*J* 9.3 Hz), corresponds to 2H (H3', H5'). Singlet at δ 9.04 corresponds to (NH).

The ¹³C NMR (Figure 188, page 318) spectral data mention in Table 33, page 163 showed 29 carbons signals, the resonance at δ 128.0 (C2", C6"), and δ 128.5 (C3", C5"), in benzoate ring, and at δ 111.4 (C2', C6'), δ 126.2 (C3', C5'), in *p*-nitro phenyl hydrazone correspond to two carbons each total 33 carbons. The formation of the hydrazone bond at C16 was confirmed at δ 163.5. The carboxylic carbon (C19), resonance visible at δ 177.0 and the benzyl group was evidenced by the presence of the aromatic carbons at δ 136.2 (C1"), δ 128.2 (C2", C6"), δ

128.5 (C3'', C5''), δ 128.0 (C4''), and for the methylene carbon at δ 65.9 (C7''). The *p*-nitro phenyl hydrazone group was confirmed by the presence of aromatic carbon resonance at δ 139.6 (C1'), δ 111.4 (C2', C6'), δ 126.2 (C3', C5'), δ 150.5 (C4'). The assignment of the observed signals in the ^{13}C NMR spectrum was confirmed by comparison with the spectrum DEPT 135 (Figure 189, page 319) as seven quaternary, eleven methine, ten methylene three methyl carbons, one hydrazone and one carboxylic carbon

4.34 2, 4-DINITRO PHENYL HYDRAZONE 17-HYDROXY ISOSTEVIOL (5m)

The product **5m** (88 mg) a new derivative was obtained as a yellow crystalline solid in 57% yield (Scheme 6, page 149). The calculated molecular formula $\text{C}_{26}\text{H}_{34}\text{N}_4\text{O}_7$ was based on ESI-MS (Figure 190, page 320) data, $[\text{M}-\text{H}]^+$ 513.29, corresponding to the calculated mass of the compound. The IR spectrum (Figure 191, page 321) showed characteristic absorption bands (cm^{-1}), at 3432 (prim hydroxyl OH), 3341 (hydrazone N-H), 1692 (carbonyl ester), 1618, 1591 (aromatic ring C=C), 1518, 1337 (nitrogen oxygen N-O).

The ^1H NMR (Figure 192, page 322) spectral data found in Table 26, page 156 showed the resonance at δ 0.94, δ 1.30, corresponds to 2CH_3 at H20 and H18 respectively. Multiplet observed at δ 2.97 (J 18.23 and 2.05 Hz), was attributed to 1H at H15. The doublet of doublets visible at δ 3.78 (J 21.3, 11.50 Hz), was assigned to 1H at H17. The 2, 4-dinitro phenyl hydrazone moiety was characterized by the doublet at δ 7.70 (J 9.58 Hz, H6'). The multiplet δ 8.19 (J 9.63 and 2.54 Hz), corresponds to 1H at H5'. The doublet observed at δ 8.99 (J 2.53 Hz), was assigned to 1H at H3' and the singlet visible at δ 10.7 corresponds to hydrazone proton (-NH).

The ^{13}C NMR (Figure 193, page 323) spectral data outlined in Table 32, page 162 displayed twenty six carbons signals. The hydrazone functionality resonance was observed at δ 170.9 (C16). The rest of twenty four carbons multiplicities were

derived from the DEPT¹³⁵ spectrum (Figure 194, page 324) as seven quaternary, five methine, ten methylene, two methyl carbons, one carboxylic and one hydrazone carbon. The signals at δ 183.7 and δ 66.4 were assigned to the carbomethoxy and primary alcoholic functionalities (C20 and C17), respectively. The signals at δ 28.9 and δ 12.9 correspond to 2CH₃ at C20, and C18, respectively. The 2, 4-dinitro phenyl hydrazone moiety was confirmed by the presence of aromatic carbon resonances at δ 144.5 (C1'), δ 137.7 (C2'), δ 129.9 (C3'), δ 128.8 (C4'), δ 123.4 (C5'), δ 115.8 (C6').

4.35 2, 4-DINITRO PHENYL HYDRAZONE BENZYL ESTER 17-HYDROXY ISOSTEVIOL (7m)

The product **7m** (73 mg) a new derivative was recovered as a yellow crystalline solid in 40% yield (Scheme 6, page 149), the calculated molecular formula C₃₃H₄₀N₄O₇ on the basis of ESI-MS (Figure 195, page 325) data showed the presence of an [M-H]⁺ 603.39, which corresponds to the calculated mass of the compound. The IR spectrum (Figure 196, page 326) showed characteristic absorption bands (cm⁻¹), at 3315 (broad band for hydrazone NH and alcohol, OH), 1720 (ester carbonyl), 1618 (aromatic ring, C=C), 1517 (aromatic-NO₂), 1334 (nitrogen oxygen N-O), 1143 (ether C-O), 754, 697 (aromatic C-H).

The ¹H NMR (Figure 197, page 327) spectral data found in Table 29, page 159 revealed the resonance at δ 0.66, and δ 1.22, corresponds to 2CH₃ at H20, H18. The multiplet at δ 2.1 (*J* 17.20 and 2.76 Hz), was assigned to H15 and the doublet of doublet observed at δ 3.73 (*J* 18.20 and 11.40 Hz), was attributed to H17. The singlet at δ 5.12 corresponds to the methylene 2H at H7'', of benzyl group. A singlet was observed at δ 7.37 (H2'' to H6''), corresponding to the aromatic 5H protons of the benzoate. The signals relative to 2, 4-dinitro phenyl hydrazone moiety were evident at δ 7.78 (d, *J* 9.54 Hz, H6'), at δ 8.31 (*J* 9.68 and

2.51 Hz, H5'), and δ 9.14 (J 2.58 Hz, H3'). The singlet at δ 10.8 is characteristic resonance of hydrazone proton ($-\text{NH}$).

The ^{13}C NMR (Figure 198, page 328) spectral data reported in Table 33, page 163 showed thirty one carbons signals. The signals at δ 128.6 (C2'', C6''), and δ 128.5 (C3'', C5''), corresponds to two carbons each, totaling 33 carbons. The thirty three carbons multiplicities were derived from the DEPT 135 spectrum (Figure 199, page 329) as eight quaternary carbons, ten methine carbons, eleven methylene carbons, two methyl carbons, one hydrazone and one carboxylic carbon. The signal at δ 176.8 and δ 65.5 were attributed to the carbomethoxy and primary alcoholic functionalities at C19 and C17, respectively. The signals at δ 28.9 and δ 12.9 correspond to 2CH₃ at C20, and C18. The benzyl group was confirmed by the presence of aromatic carbon at δ 135.9 (C1'''), δ 128.6 (C2'', C6'''), δ 129.5 (C3'', C5''), δ 128.2 (C4'''), and methylene carbon (C7'''), resonance observed at δ 66.1. The 2, 4-dinitro phenyl hydrazone group was evidenced by the presence of aromatic carbon at δ 144.7 (C1'), δ 137.9 (C2'), δ 130.1 (C3'), δ 129.2 (C4'), δ 123.5 (C5'), δ 115.9 (C6').

4.36 4-NITRO PHENYL HYDRAZONE 17-HYDROXY OF ISOSTEVIOL (6m)

The product **6m** (69 mg) a new derivative was recovered as a yellow crystalline solid in 49% yield (Scheme 6, page 149). The molecular formula C₂₆H₃₅N₃O₅ derived from the ESI-MS (Figure 200, page 330) data, $[\text{M}-\text{H}]^+$ 468.39, which corresponds to the calculated mass of the compound. The IR spectrum (Figure 201, page 331) showed characteristic absorption bands (cm⁻¹), at 3527 (primary hydroxyl), 3341 (hydrazone, N-H), 1696 (carboxylic carbonyl), 1600 (aromatic ring).

The ^1H NMR spectral (Figure 202, page 332) data reported in Table 26, page 156 revealed the resonance at δ 0.87, δ 1.21 is related to 2CH₃ at H20, and H18 respectively. Multiplet at δ 2.97 (J 18.23 and 2.86 Hz), corresponds to 1H at

H15 and the doublet visible at δ 3.66 (J 7.36 Hz), was assigned to 1H at H17. The 4-nitro phenyl hydrazone moiety was characterized by the doublet at δ 7.18 (J 9.29 Hz, 2H), relative to H2' and H6'. Another doublet visible at δ 8.11 (J 9.34 Hz, 2H), was assigned to 2H at H3' and H5'.

The ^{13}C NMR (Figure 203, page 333) spectral data found in Table 32, page 162 showed twenty six signals. The hydrazone functionality resonance was observed at δ 162.7 (C16). The rest of carbons multiplicities were derived from the DEPT 135 spectrum (Figure 204, page 334) as a six quaternary, six methine, ten methylene, two methyl carbons, one hydrazone, and one carboxylic carbon. The signals at δ 178.1 and δ 66.1 show the presence of carbomethoxy and primary alcoholic functionalities at C20 and C17. The resonance at δ 28.8 and δ 12.9 corresponds to 2CH₃ at C20 and C18. The 4-nitro phenyl hydrazone group was confirmed by the presence of aromatic carbons at δ 138.8 (C1'), δ 111.1 (C2', C6'), δ 125.6 (C3', C5'), δ 151.5 (C4').

4.37 4-NITRO PHENYL HYDRAZONE BENZYL ESTER 17-HYDROXY ISOSTEVIOL (8m)

The product **8m** (87 mg) a new derivative was obtained as yellow crystalline solid in 51% yield (Scheme 6, page 149). The molecular formula C₃₃H₄₁N₃O₅ derived from the ESI-MS (Figure 205, page 335) data, [M]⁺ 559.29, which corresponds to the calculated mass of the compound. The IR spectrum (Figure 206, page 336) showed the interested absorption bands (cm⁻¹), at 3472 (broad band for hydroxyl OH, and hydrazone NH), 1727 (ester carbonyl), 1458 (methylene C-H), 1320 (hydroxyl), 1147 (ether C-O), 753, 697 (aromatic ether C-H).

The ^1H NMR (Figure 207, page 337) spectral data outlined in Table 29, page 159 showed the resonance at δ 0.69, δ 1.23 was assigned to 2CH₃ at H20, H18 respectively. Multiplet visible at δ 2.73 (J 17.5 and 2.35 Hz), corresponds to 1H at H15 and singlet at δ 3.69 was assigned to H17. Two doublets visible at δ 5.0

and δ 5.2 (J 12.6 Hz) correspond to 2H at (H7''), of benzyl group. The 4-nitro phenyl hydrazone moiety was characterized by the doublet at δ 6.95 (J 9.1 Hz, 2H), relative to 2H at H2' and H6'. A singlet was observed at δ 7.37 (H2'' to H6''), corresponding to the aromatic 5H protons of the benzoate. Another doublet detected at δ 8.14 (J 9.1 Hz, 2H), was assigned 2H at to H3' and H5'.

The ^{13}C NMR (Figure 208, page 338) spectral data found in Table 33, page 163 showed twenty nine carbons signals. The hydrazone functionality resonance was observed at δ 163.6 (C16). The signals at δ 128.5 (C2'', C6''), and δ 128.0 (C3'', C5''), and δ 111.5 (C2', C6'), δ 126.2 (C3', C5'), corresponds to two carbons each, totaling 33 carbons. The rest of carbons multiplicities were derived from the DEPT 135 spectrum, (Figure 209, page 339) as seven quaternary, eleven methine, eleven methylene two methyl one carboxyl, and one hydrazone carbons. The signals at δ 176.9 and δ 67.2 showed the presence of carbomethoxy and primary alcoholic functionalities at C20 and C17. The signals observed at δ 28.9, and δ 13.6 corresponds to 2CH₃ at C20 and C18. The 4-nitro phenyl hydrazone group was confirmed by the presence of aromatic carbon at δ 140.1 (C1'), δ 111.5 (C2', C6'), δ 126.2 (C3', C5'), δ 149.8 (C4'). The benzyl group was confirmed by the presence of aromatic carbon at δ 136.2 (C1''), δ 128.5 (C2'', C6''), δ 128.0 (C3'', C5''), δ 128.0 (C4''), and methylene carbon (C7''), resonance observed at δ 65.9.

4.38 BIOASSAYS

4.38.1 ANTIMALARIAL ACTIVITY

In an initial screening, steviol and isosteviol along with twenty derivatives were tested against *Plasmodium falciparum* W2 (chloroquine-resistant), at two different concentrations, 25 and 50 $\mu\text{g}/\text{mL}$. The percentage of growth reduction was determined and the IC_{50} values were calculated. Eighteen out of the twenty two samples were found inactive. Compounds **2g** ($IC_{50} = 21.06 \mu\text{g} / \text{mL}$), **3g**, ($IC_{50} = 17.50 \mu\text{g} / \text{mL}$), **5m** ($IC_{50} = 18.80 \mu\text{g} / \text{mL}$), and **6m**, ($IC_{50} = 22.58 \mu\text{g}/\text{mL}$), were considered moderately active. Dose-response curves of samples tested against blood parasites cycle of *P. falciparum* (W2 strain), showing the values of the inhibitory concentration of 50% of growth (IC_{50}). Interestingly, the results shown in Table 16 (page 119), chemical modification made at C16, in primary skeleton of isosteviol and 17-hydroxy isosteviol lead to increase anti-malarial activities. The isosteviol skeleton having one molecule of 2, 4-dinitro phenyl hydrazone or 4-nitro phenyl hydrazone at C16 with free carboxylic acid shows moderate anti-plasmodic activity against *P. falciparum* W2 (chloroquine-resistant). Anti-plasmodial activity seemed to be influenced by the introduction of hydrazone functionality in the parent structure of isosteviol or 17-hydroxy isosteviol. Analogues having hydrazone substituent in the D-ring display better anti-malarial activity, while presence of other functional groups such as hydroxyl, oxime, lactone, at C16, C15 and ester 19-O (carboxylic acid) shows reduced activities having IC_{50} , greater than 50 $\mu\text{g}/\text{mL}$, and hence are consider to be inactive.

Table 16: Anti-malarial activity of the tested samples (IC_{50} , $\mu\text{g/mL}$, mean \pm SD).

S	IC_{50}	Classification	S	IC_{50}	Classification
2g	21.06 \pm 3.15	Moderately active	3c	>50	Inactive
3g	17.50 \pm 4.83	Moderately active	5i	>50	Inactive
5m	18.80 \pm 6.00	Moderately active	1d	>50	Inactive
6m	22.58 \pm 4.92	Moderately active	4h	>50	Inactive
1a	>50	Inactive	5j	>50	Inactive
2h	>50	Inactive	1e	>50	Inactive
1b	>50	Inactive	2a	>50	inactive
3h	>50	Inactive	5h	>50	Inactive
3a	>50	Inactive	2f	>50	Inactive
3b	>50	Inactive	1f	>50	Inactive
1c	>50	Inactive	5l	>50	Inactive
Chloroquine	0,145 \pm0,00	very active			

4.38.2 ANTI-TUMOR ACTIVITY

Compounds **1c**, **1f**, **2g**, **2f**, **3g**, **5m**, **6m**, **5k**, and **5i** were evaluated in three human cell lines; lung carcinoma (A549), human brain glioma cell lines (T98MG), human glioblastoma-astrocytoma, and epithelial-like cell line (U87MG). The cells were exposed to different concentrations of compounds (10–50 $\mu\text{mol.L}^{-1}$), and then cellular viability was determined by MTT. The modifications made at C16 and C19 were designed to evaluate the influence of oxime, hydrazone, functionality and presence of polar or lipophilic groups (such as carboxylic acids, aromatic rings) on activity. The experimental results showed that compounds having oxime, hydrazone, functionality show improved antiproliferative activity than the parent molecule.

It was observed that the presence of hydrazone and oxime fragments at C16 potentiate the antiproliferative activities of the molecules, the compound **1c**, **1f** and **2f** demonstrate much similar inhibition at 10 μM , 25 μM and 50 μM concentration in human cancer cell line glioblastoma-astrocytoma, epithelial (U87MG), while compound **2g**, **3g**, and **5m** display favorable cytotoxicity in (U87MG), cell line. The compound **6m**, **5k** and **5j** show limited cytotoxicity in (U87MG), cell line. These findings suggest that oxime and hydrazone moiety at C16 demonstrate impactful cytotoxicity from their parent molecule (Figure 29, page 121).

Bioscreening results of compound **1c**, **5j**, and **1f**, **2f**, **5m** as shown in (Figure 30, page 121), having oxime and hydrazone fragments respectively demonstrate inhibitory activities against human brain glioma cell lines (T98G). The compounds **2g**, **1f** and **5m** having hydrazone display favorable cytotoxicity at higher concentration than the other analogues. The compounds **6m** and **5k** display weak inhibitory activities in T98G cell line but the results demonstrate that these molecules are much better cytotoxic than the parent molecules.

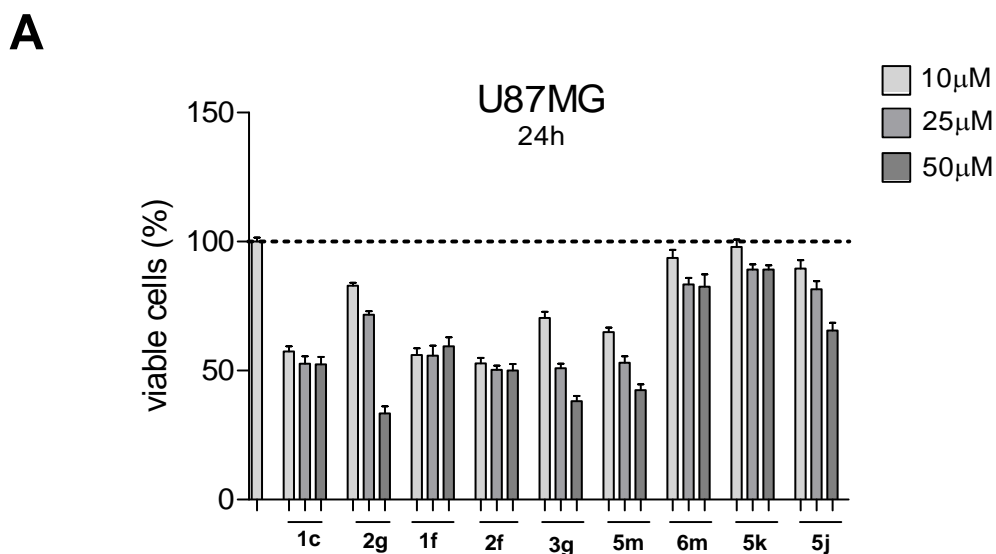


Figure 29: *In vitro* antitumor activities of isosteviol derivatives in human glioblastoma-astrocytoma, epithelial-like cell line (U87MG).

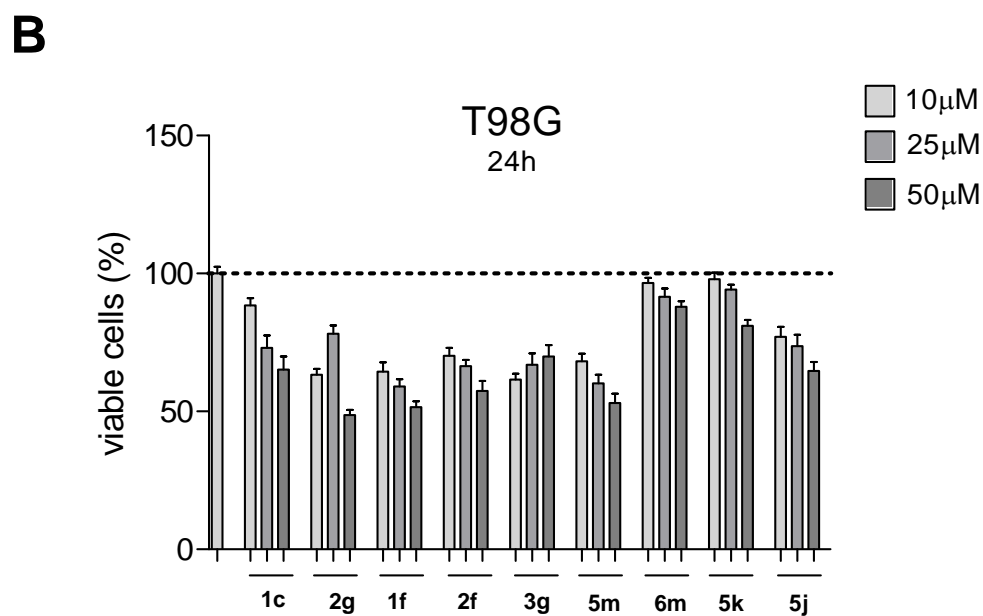


Figure 30: *In vitro* antitumor activities of isosteviol derivatives human brain glioma cell lines (T98MG).

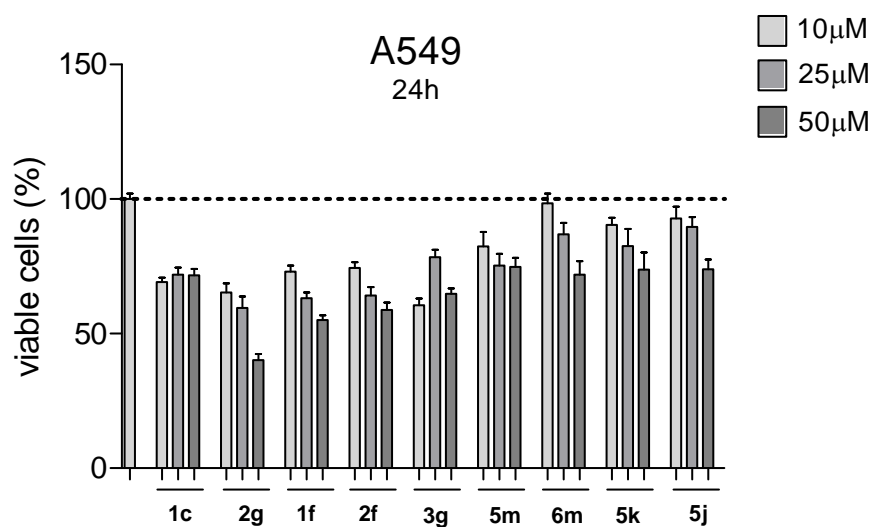
C

Figure 31: *In vitro* antitumor activities of isosteviol derivatives human lung carcinoma (A549).

The *in vitro* bioscreening results of nine derivatives shown in Figure 31. Nearly all derivatives showed higher cytotoxicity than the parent compound isosteviol in human lung carcinoma (A549). The results in the Figure 31 demonstrate that compound **2g**, **1f**, and **2f** display better cytotoxicity at higher concentration in A549 cell line, while compounds **6m**, **5k** and **5j** display nearly same cytotoxicity. The compound **1c**, **3g** and **5m** showed limited cytotoxicity and are consider to be inactive.

4.38.3 ANTI-*TRYPANOSOMA CRUZI* ACTIVITY

The present study report the biological potential of ten (10) semi synthetic derivatives of steviol, isosteviol and is aimed at the evaluation of the anti-*Trypanosoma cruzi*. The results are shown in Table 17. Only compound **1c** showed moderate activity, against the epimastigotes form (IC_{50} 167.9 μ), but the compound **1c** was found highly cytotoxic when evaluated in Vero cells (selectivity index SI = 0.81). The compound was further evaluated against cell-derived trypomastigote forms, but the results in Table 17 shows weak activity of **1c** against the developmental form of the parasite ($IC_{50}/24h$ of 106.08 μ M, SI = 1.27).

Table 17: *In vitro* biological activity of isosteviol derivatives on *T. cruzi*.

	$IC_{50}/24h$		SI
A) Epimastigotes			
1c	167.9	135.32	0.81
2g	>400	NT	
3g	>400	NT	
2f	>500	NT	
1f	>600	NT	
5m	>700	NT	
6m	>700	NT	
5k	>1400	NT	
5j	>2300	NT	
1b	>18,000	NT	
Benznidazole	45	3954.3	87.87
B) Trypomastigotes			
1c	106.08	135.32	1.27
Benznidazole		3954.3	

SI: (selectivity index), NT: (Not tested)

All other derivatives having hydrazone, hydroxyl fragments at C15 and C16 with free carboxylic acid and the ester derivatives at C19 were active at their highest concentration but fail to inhibit of *T. cruzi* at lower concentration. The results show that only isosteviol with oxime moiety at C16 show moderate activity in both form of *T. cruzi*, while other functional groups either at C15, C16, and C19 was inactive.

4.38.4 ANTI-LEISHMANIASIS ACTIVITY

This study considers the biological potential of the steviol and isosteviol derivatives, and is aimed at the evaluation of the anti-Leishmaniasis activity of seven semi synthetic derivatives with hydrazone moiety were assayed *in vitro* against two species such as *L. braziliensis* and *L. amazonensis*.

Table 18: *In vitro* activity of isosteviol and 17-hydroxy isosteviol derivatives in *Leishmaniasis* species (IC₅₀, µg/mL).

	<i>L. amazonensis</i>		<i>L. braziliensis</i>	
	24 hr.	48hr	24 hr.	48 hr.
2g	1824	1044	2979	1861
3g	1151	543	1617	1208
2f	77939	9078	870860	3.46 e+006
1f	9263	4232	19749	2406
5m	602.4	275.8	942.1	354
6m	548	302.2	926	432
5k	938.8	632.0	17838	2539

The results are listed in Table 18, page 124. At highest concentration the compound **5m** and **6m** show inhibition against both strains, The results show that modification made at C16 has positive impact on the Leishmaniasis activity. While the other five compounds don't show inhibition against both strains. These results showed that derivatives having hydrazone functionality at C16 with free carboxylic acid at C19 and its ester derivatives were inactive in both strains of *Leishmaniasis* showing high IC_{50} value.

4.38.5 DOCKING ANALYSIS WITH *Corynebacterium diphtheriae* SORTASES PROTEINS

A recent trend in the search for new drugs is the *in silico* determination of proteins–ligand docking. Computer software may be able to determine which ligand molecules provide the best fit to the active site near proteins surface by adjusting some algorithm's function. The best docking involves lower energy (Ordog & Grolmusz., 2008).

Corynebacterium diphtheriae is the causative agent of pharyngeal diphtheriae. They possess very important transpeptidases; e.g. sortase proteins, which help a majority of the Gram +ve bacteria in decorating the surface with a diverse array of proteins that enable the microbe to effectively interact with its environment (Scott & Zahner., 2006). These enzymes help to polymerize and assemble pili proteins to construct multi-subunit hair-like fibers that extend from the cell surface to promote bacterial adhesion and subsequent colonization. Sortases help in the polymerization of very important virulence factors by deploying them as surface proteins that mediate bacterial adhesion to host tissues, host cell entry, evasion, and suppression of the immune response as well as acquisition of essential nutrients (Spirig et al., 2011). The presence of different types of sortase proteins in the *C. diphtheriae* motivated a search for the treatment

of pharyngeal *diphtheriae* by considering these transpeptidases as potential drug targets.

Twenty eight isosteviol derivatives were used for the docking analysis to check their binding affinity to those proteins. The docking protocol was used in order to find the binding modes of the selected compounds against the sortases proteins. The results showed that eight compounds (**1e**, **2g**, **3g**, **4g**, **5g**, **5m**, **5i**, **5j**), have good *in silico* protein-ligand interaction with all target sortase proteins (Table 19, page 127). They were considered to be used as potential therapeutic candidates for the treatment of pharyngeal *diphtheriae*.

The selected analogues were tested at various concentrations, ranging from 1, 25, 50 and 100 μ M. All the semi-synthetic analogues showed activity to some extent against *C. diphtheriae* at their highest concentration (Figure 33, page 129), while compound **3g** show better inhibition than other derivatives. The results show that isosteviol with hydrazone moiety show inhibition against *C. diphtheriae* while the derivative having hydroxy, oxime and ester fragments at C16, and C19 were found inactive at lower concentration.

Table 19: Docking results of isosteviol derivatives with sortase (Srt) proteins of the *C. diphtheria*.

Compounds	Docking Results: Moldock scores and the number of hydrogen bonds											
	SrtA		SrtB		SrtC		SrtD		SrtE		SrtF	
	MolDock score	H-bonds	MolDock score	H-bonds	MolDock score	H-bonds	MolDock score	H-bonds	MolDock score	H-bonds	MolDock score	H-bonds
1a	-109.644	1	-95.8812	1	-108.296	1	-94.113	X	-108.271	1	-106.213	3
1d	-93.3209	1	-86.14	1	-103.333	3	-85.1104	3	-112.984	1	-93.3558	1
2g	-129.045	5	-139.508	3	-118.333	1	-135.498	2	-158.577	1	-140.176	3
3a	-141.097	2	-136.902	2	-118.325	X	-113.063	X	-151.086	1	-145.005	2
3c	-117.05	1	-118.275	X	-103.65	1	-108.911	1	-112.294	1	-114.087	1
1e	-101.072	4	-92.8812	4	-100.606	4	-82.283	4	-109.978	3	-97.5614	3
1f	-101.819	3	-100.893	1	-97.669	1	-92.5786	1	-99.9926	4	-94.3074	1
2f	-99.9629	2	-115.433	1	-88.0048	1	-101.899	X	-99.6108	3	-111.599	X
3g	-112.242	3	-148.841	3	-130.111	2	-118.547	1	-135.274	4	-126.458	3
5m	-133.706	5	-145.339	1	-122.861	6	-119.362	3	-141.599	3	-143.337	3
6m	-121.698	2	-123.584	4	-98.9196	1	-128.983	X	-126.02	3	-124.036	3
5k	-92.7654	1	-97.0916	7	-94.5068	4	-85.8314	X	-91.3941	3	-122.946	4
4h	-96.1753	4	-91.5551	3	-96.3454	3	-72.373	X	-86.0154	2	-88.2836	5
5i	-90.0133	3	-103.929	2	-75.5317	4	-96.745	4	-104.289	2	-88.9098	1
5j	-91.0568	2	-98.8959	4	-78.3456	2	-88.267	2	-105.816	3	-92.75.37	4
2d	-103.661	1	-111.787	1	-127.241	1	-130.015	X	-125.387	X	-122.086	X
3f	-111.75	1	-120.905	1	-126.79	4	-119.886	1	-131.845	1	-134.108	1
5g	-146.347	3	-147.027	1	-168.48	3	-166.435	2	-151.747	3	-165.615	1
4g	-163.785	4	-161.075	5	-155.417	3	-156.698	3	-157.93	2	-159.385	3

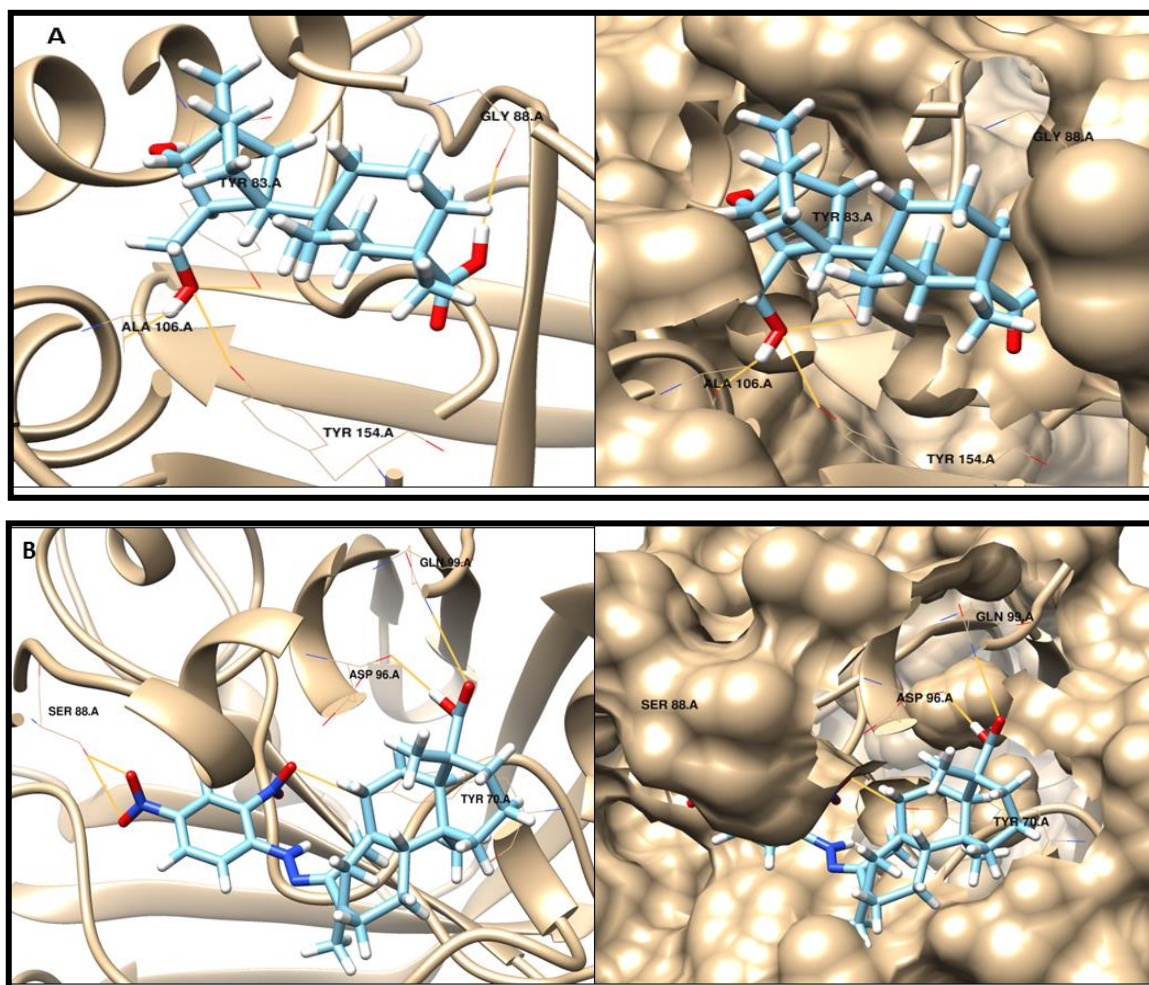


Figure 32: 3D cartoon representation of the docking analyses of compound **3g** with *C. diphtheriae* sortase proteins where figure A): sortase (Srt) proteins B, while figure B) represent sortase (Srt) proteins A.

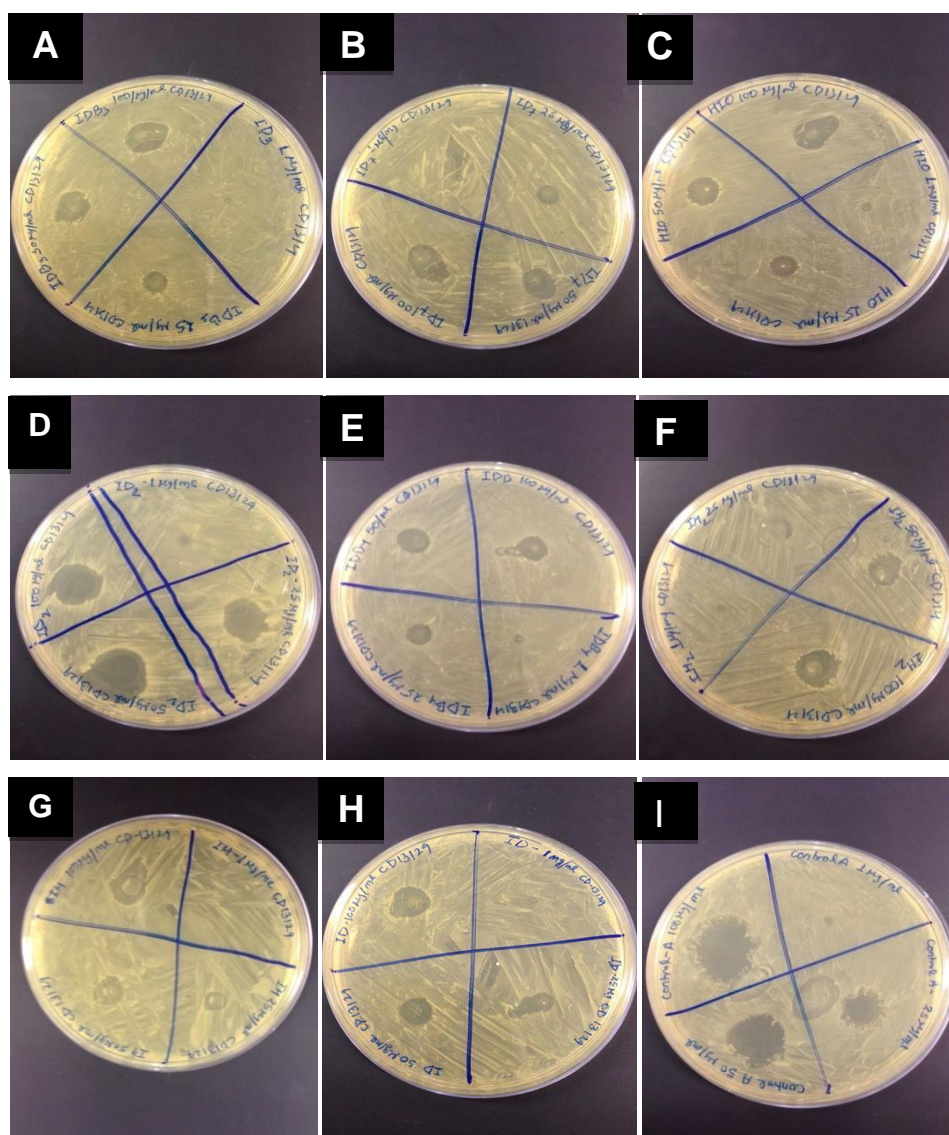


Figure 33: Evaluation of anti *Corynebacterium diphtheriae* activity of isosteviol derivatives by disk diffusion test. 1) Disk A: correspond to compound **4g**, 2) Disk B: correspond to compound **5m**, 3) Disk C: correspond to **5j**, 4) Disk D: correspond to **3g**, 5) Disk E correspond to **5g**, 6) Disk F correspond **5i**, 7) Disk G, correspond to **1e**, 8) Disk H correspond to **2g** (1e, 2g, 3g, 4g, 5g, 5m, 5i, 5j) the disk I, correspond to the antibiotic used as positive controle.

5 CONCLUSION

In this work, 37 derivatives of isosteviol and steviol having hydroxyl, oxime, hydrazone, lactone, benzyl ester and *p*-methoxyacetophenone ester fragments were synthesized in good yields and 25 of them are described here for the first time (**2a**, **2b**, **2c**, **2d**, **2f**, **3a**, **3b**, **3c**, **3f**, **3g**, **3h**, **4f**, **4g**, **5g**, **5k**, **5l**, **5m**, **5n**, **6i**, **6j**, **6k**, **6m**, **7k**, **7m**, **8m**), with the purpose of investigating the importance of substituents at C15, C16 and C19 for anti-malarial activity against *Plasmodium falciparum*, antitumor, anti-*Trypanosoma cruzi*, anti-*Leishmaniasis* and anti-*Corynebacterium diphtheriae* bioassays

The results revealed that introduction of hydrazone moiety in isosteviol or 17-hydroxy isosteviol has beneficial inhibition activity against *P. falciparum* than the parent skeleton.

Nine derivatives, seven containing hydrazone and two with oxime moiety, were selected for bioassays against tumor cells. All nine derivatives showed cytotoxicity against three cancer cell lines, and the most active were **2g** and **5m**. The results specify that the introduction of hydrazone and oxime fragments in isosteviol increases the cytotoxicity potency of the parent molecule.

Semi synthetic steviol/isosteviol derivatives showed weak activity against *T. cruzi* epimastigotes forms. Only compound **1c** was moderately active, but was highly cytotoxic against Vero cells.

Isosteviol, 17-hydroxyisosteviol and their hydrazone derivatives were inactive *in vitro* against *L. braziliensis* and *L. amazonensis*.

All the tested 8 derivatives of isosteviol showed weak inhibition in *C. diphtheriae* while only compound **3g** with hydrazone moiety show good inhibition. All these evidence make these compounds promising molecules to be considered in the search of new strategies and structure modification for the development of new drugs as an antiplasmodial, antitumor, anti-*Trypanosoma cruzi* and anti-*C. Diphtheriae*.

6 REFERENCES

AACHOUI, Y.; GHOSH, S.K. Immune enhancement by novel vaccine adjuvants in autoimmune-prone NZB/W F1 mice: relative efficacy and safety. **BMC Immunology**, v. 12, p.1-12, 2011.

AGUIAR, L.A.; PORTO, R.S.; LAHLOU, S.; CECCATTO, V.M.; BARBOSA, R.; LEMOS, T.L.G.; DOS SANTOS, H.S.; COELHO-DE-SOUZA, A.N.; MAGALHAES, P.J.C.; ZIN, W.A.; LEAL-CARDOSO, J.H. Antispasmodic effects of a new kaurene diterpene isolated from *Croton argyrophyloides* on rat airway smooth muscle. **Journal of Pharmacy and Pharmacology**, v. 64, p.1155-1164, 2012.

ARNOLD K, BORDOLI L, KOPP J, SCHWEDE T: The SWISS-MODEL workspace: a web-based environment for protein structure homology modelling. **Bioinformatics**, v. 22, p. 195-201, 2006

ASADA, Y.; SUKEMORI, A.; WATANABE, T.; MALLA, K.J.; YOSHIKAWA, T.; LI, W.; KUANG, X.; KOIKE, K.; CHEN, C.H.; AKIYAMA, T.; QIAN, K.; NAKAGAWA-GOTO, K.; MORRIS-NATSCHKE, S.L.; LU, Y.; LEE, K.H. Isolation, structure determination, and anti-HIV evaluation of tiglane-type diterpenes and biflavonoid from *Stellera chamaejasme*. **Journal of Natural Products**, v. 76, p.852-857, 2013.

AVENT, A.G.; HANSON, J.R.; OLIVEIRA, B.H.D. Hydrolysis of the diterpenoide Glycoside, Stevioside. **Journal of Phytochemistry**, v. 29, p.2712-2715, 1989.

AYATOLLAHI, A.M.; GHANADIAN, M.; MESAİK, M.A.; ABDELLA, O.M.; AFSHARYPUOR, S.; KOBARFARD, F.; MIRZA-TAHERI, M. New myrsinane-type diterpenoids from *Euphorbia aellenii* Rech. f. with their immunomodulatory activity. **Journal of Asian Natural Products Research**, v. 12, p.1020-1025, 2010.

BELLISLE, F.; PEREZ, C. low-energy substitutes for sugars and fats in the human diet - impact on nutritional regulation. **Neuroscience and Biobehavioral Reviews**, v. 18, p.197-205, 1994.

BOAMPONG, J.N.; AMEYAW, E.O.; ABOAGYE, B.; ASARE, K.; KYEI, S.; DONFACK, J.H.; WOODE, E. The Curative and Prophylactic Effects of Xylopic Acid on *Plasmodium berghei* Infection in Mice. **Journal of Parasitology Research**, v. 2013, p.356107, 2013.

- BODIWALA, H.S.; SABDE, S.; MITRA, D.; BHUTANI, K.K.; SINGH, I.P. Anti-HIV diterpenes from *Coleus forskohlii*. **Natural Product Communications**, v. 4, p.1173-1175, 2009.
- BONDÌ, M.L.; BRUNO, M.; PIOZZI, F.; HUSNU CAN BASER, K.; SIMMONDS, M.S.J. Diversity and antifeedant activity of diterpenes from Turkish species of *Sideritis*. **Biochemical Systematics and Ecology**, v. 28, p.299-303, 2000.
- BOONKAEWWAN, C.; AO, M.; TOSKULKAO, C.; RAO, M.C. Specific immunomodulatory and secretory activities of stevioside and steviol in intestinal cells. **Journal of Agricultural and Food Chemistry**, v. 56, p.3777-3784, 2008.
- BOONKAEWWAN, C.; BURODOM, A. Anti-inflammatory and immunomodulatory activities of stevioside and steviol on colonic epithelial cells. **Journal of Agricultural and Food Chemistry**, v. 93, p.3820-3825, 2013.
- BOONKAEWWAN, C.; TOSKULKAO, C.; VONGSAKUL, M. Anti-inflammatory and immunomodulatory activities of stevioside and its metabolite steviol on THP-1 cells. **Journal of Agricultural and Food Chemistry**, v. 54, p.785-789, 2006.
- BRACA, A.; ABDEL-RAZIK, A.F.; MENDEZ, J.; MORELLI, I. A new kaurane diterpene dimer from *Parinari campestris*. **Fitoterapia**, v. 76, p.614-619, 2005.
- CEKIC, V.; VASOVIC, V.; JAKOVLJEVIC, V.; MIKOV, M.; SABO, A. Hypoglycaemic action of stevioside and a barley and brewer's yeast based preparation in the experimental model on mice. **Bosnian Journal of Basic Medical Sciences**, v. 11, p.11-16, 2011.
- CHANG, F.R.; YANG, P.Y.; LIN, J.Y.; LEE, K.H.; WU, Y.C. Bioactive kaurane diterpenoids from *Annona glabra*. **Journal of Natural Products**, v. 61, p.437-439, 1998.
- CHATSUDTHIPONG, V.; MUANPRASAT, C. Stevioside and related compounds: Therapeutic benefits beyond sweetness. **Pharmacology & Therapeutics**, v. 121, p.41-54, 2009.
- CHATTER, R.R.; BEN-OTHMAN, R.; RABHI, S.; KLADI, M.; TARHOUNI, S.; VAGIAS, C.; ROUSSIS, V.; GUIZANI, L.T.; KHARRAT, R. Anti-Inflammatory Activity of Neorogioltriol a New Brominated Diterpenoid Isolated from the Red Algae *Laurencia Glandulifera*. **Journal of Inflammation Research**, v. 60, p.177-177, 2011.
- CHEENPRACHA, S.; YODSAOUE, O.; KARALAI, C.; PONGLIMANONT, C.; SUBHADHIRASAKUL, S.; TEWTRAKUL, S.; KANJANA-OPAS, A. Potential anti-

allergic ent-kaurene diterpenes from the bark of *Suregada multiflora*. **Phytochemistry**, v. 67, p.2630-2634, 2006.

CHEN, B.W.; CHAO, C.H.; SU, J.H.; WEN, Z.H.; SUNG, P.J.; SHEU, J.H. Anti-inflammatory eunicellin-based diterpenoids from the cultured soft coral *Klyxum simplex*. **Organic and Biomolecular Chemistry**, v. 8, p.2363-2366, 2010.

CHEN, H.L.; LIN, K.W.; GAN, K.H.; WANG, J.P.; WON, S.J.; LIN, C.N. New diterpenoids and cytotoxic and anti-inflammatory diterpenoids from *Amentotaxus formosana*. **Fitoterapia**, v. 82, p.219-224, 2011.

CHEN, J.; ZHA, X.; SUNA, M.; CAIA, J.; JI, W.Z.A.M. Synthesis and In Vivo Acute Antihyperglycemic Evaluation of Novel. **Letters in Drug Design & Discovery**, v. 7, p.686-693, 2010.

CHEN, X.; HERMANSEN, K.; XIAO, J.; BYSTRUP, S.K.; O'DRISCOLL, L.; JEPPESEN, P.B. Isosteviol has beneficial effects on palmitate-induced alpha-cell dysfunction and gene expression. **PLoS One**, v. 7, p.e34361, 2012.

COTORAS, M.; GARCIA, C.; LAGOS, C.; FOLCH, C.; MENDOZA, L. Antifungal activity on *Botrytis cinerea* of flavonoids and diterpenoids isolated from the surface of *Pseudognaphalium* spp. **Boletin De La Sociedad Chilena De Quimica**, v. 46, p.433-440, 2001.

CRAGG, G.M.; NEWMAN, D.J.; SNADER, K.M. Natural products in drug discovery and development. **Journal of Natural Products**, v. 60, p.52-60, 1997.

CUNHA, K.M.D.; PAIVA, L.A.F.; SANTOS, F.A.; GRAMOSA, N.V.; SILVEIRA, E.R.; RAO, V.S.N. Smooth muscle relaxant effect of kaurenoic acid, a diterpene from *Copaifera langsdorffii* on rat uterus in vitro. **Phytotherapy Research**, v. 17, p.320-324, 2003.

DE ANDRADE, B.B.; MOREIRA, M.R.; AMBROSIO, S.R.; FURTADO, N.A.J.C.; CUNHA, W.R.; HELENO, V.C.G.; SILVA, A.N.; SIMAO, M.R.; DA ROCHA, E.M.P.; MARTINS, C.H.G.; VENEZIANI, R.C.S. Evaluation of ent-Kaurenoic Acid Derivatives for their Anticariogenic Activity. **Natural Product Communications**, v. 6, p.777-780, 2011.

DE SOUZA PEREIRA, H.; LEAO-FERREIRA, L.R.; MOUSSATCHE, N.; TEIXEIRA, V.L.; CAVALCANTI, D.N.; DA COSTA, L.J.; DIAZ, R.; FRUGULHETTI, I.C. Effects of diterpenes isolated from the Brazilian marine alga *Dictyota menstrualis* on HIV-1 reverse transcriptase. **Planta Medica**, v. 71, p.1019-1024, 2005.

DING, L.; HOU, Q.A.; ZHOU, Q.Y.; ZHANG, Q.O.; HOU, T.D.; LIU, G.A. Structure-activity relationships of eight ent-kaurene diterpenoids from three *Isodon* plants. **Research on Chemical Intermediates**, v. 36, p.443-452, 2010.

DING, L.; ZHOU, Q.Y.; WANG, L.; WANG, W.; ZHANG, S.D.; LIU, B. Comparison of cytotoxicity and DNA damage potential induced by ent-kaurene diterpenoids from *Isodon* plant. **Natural Product Research**, v. 25, p.1402-1411, 2011.

DUAN, H.Q.; TAKAISHI, Y.; MOMOTA, H.; OHMOTO, Y.; TAKI, T.; JIA, Y.F.; LI, D. Immunosuppressive diterpenoids from *Tripterygium wilfordii*. **Journal of Natural Products**, v. 62, p.1522-1525, 1999.

FATOPE, M.O.; AUDU, O.T.; TAKEDA, Y.; ZENG, L.; SHI, G.; SHIMADA, H.; MCLAUGHLIN, J.L. Bioactive ent-kaurene diterpenoids from *Annona senegalensis*. **Journal of Natural Products**, v. 59, p.301-303, 1996.

FILHO, V.C. PRINCIPAIS AVANÇOS E Perspectivas na área de produtos naturais ativos: estudos desenvolvidos no niqfar/univali. **QUÍMICA NOVA**, v. 23, 2000.

FORMARIZ, T.P.; URBAN, M.C.C.; JÚNIOR, A.A.D.S.; GREMIÃO, M.P.D.; OLIVEIRA, A.G.D. Microemulsões e fases líquidas cristalinas como sistemas de liberação de fármacos. **Brazilian Journal of Pharmaceutical Sciences**, v. 41, 2005.

GARCÍA, P.A.; OLIVEIRA, A.B.D.; BATISTA, R. Occurrence, Biological Activities and Synthesis of Kaurane Diterpenes and their Glycosides. **Molecules**, v. 12, p. 455-483, 2007.

GARIFULLIN, B.F.; CHESTNOVA, R.V.; MIRONOV, V.F.; KATAEV, V.E. Synthesis and antituberculosis activity of conjugates of the diterpenoid isosteviol and the drug dimephosphon. **Chemistry of Natural Compounds**, v. 48, p.794-798, 2012.

GHOUMARI, H.; BENAJIBA, M.-H.; AZMANI, A.; GARCÍA-GRANADOS, A.; MARTÍNEZ, A.; PARRA, A.; RIVAS, F.; SOCORRO, O. ent-Kauranoid derivatives from *Sideritis moorei*. **Phytochemistry**, v. 66, p.1492-1498, 2005.

GOYAL, S.K.; SAMSHER; GOYAL, R.K. Stevia (*Stevia rebaudiana*) a bio-sweetener: a review. **International Journal of Food Sciences and Nutrition**, v. 61, p.1-10, 2010.

GREGERSEN, S.; JEPPESEN, P.B.; HOLST, J.J.; HERMANSEN, K. Antihyperglycemic effects of stevioside in type 2 diabetic subjects. **Metabolism-Clinical and Experimental**, v. 53, p.73-76, 2004.

GUI, M.Y.; AOYAGI, Y.; JIN, Y.R.; LI, X.W.; HASUDA, T.; TAKEYA, K. Excisanin h, a novel cytotoxic 14, 20-epoxy-ent-kaurene diterpenoid, and three new ent-kaurene diterpenoids from *Rabdosia excisa*. **Journal of Natural Products**, v. 67, p.373-376, 2004.

GUSTAFSON, K.R.; MUNRO, M.H.G.; BLUNT, J.W.; CARDELLINA, J.H.; MCMAHON, J.B.; GULAKOWSKI, R.J.; CRAGG, G.M.; COX, P.A.; BRINEN, L.S.; CLARDY, J.; BOYD, M.R. Hiv Inhibitory Natural-Products .3. Diterpenes from *Homalanthus-Acuminatus* and *Chrysobalanus-Icaco*. **Tetrahedron**, v. 47, p.4547-4554, 1991.

HAN, L.; HUANG, X.S.; SATTLER, I.; DAHSE, H.M.; FU, H.Z.; GRABLEY, S.; LIN, W.H. Three new pimaren diterpenoids from marine mangrove plant, *Bruguiera gymnorhiza*. **Pharmazie**, v. 60, p.705-707, 2005.

HAN, L.; HUANG, X.S.; SATTLER, I.; DAHSE, H.M.; FU, H.Z.; LIN, W.H.; GRABLEY, S. New diterpenoids from the marine mangrove *Bruguiera gymnorhiza*. **Journal of Natural Products**, v. 67, p.1620-1623, 2004.

HANSON, J.R.; DEOLIVEIRA, B.H. STEVIOSIDE AND RELATED SWEET DITERPENOID GLYCOSIDES. **Natural Product Reports**, v. 10, p.301-309, 1993.

HARAGUCHI, S.K.; SILVA, A.A.; VIDOTTI, G.J.; DOS SANTOS, P.V.; GARCIA, F.P.; PEDROSO, R.B.; NAKAMURA, C.V.; DE OLIVEIRA, C.M.; DA SILVA, C.C. Antitrypanosomal activity of novel benzaldehyde-thiosemicarbazone derivatives from kaurenoic acid. **Molecules**, v. 16, p.1166-1180, 2011.

HERNANDEZPEREZ, M.; RABANAL, R.M.; DELATORRE, M.C.; RODRIGUEZ, B. Analgesic, anti-inflammatory, antipyretic and haematological effects of aethiopinone, an omicron-naphthoquinone diterpenoid from *Salvia aethiopsis* roots and two hemisynthetic derivatives. **Planta Medica**, v. 61, p.505-509, 1995.

SHIBATA. H., SONOK. S., OCHIAI, H., , NISHIHASHI, H., YAMAD .M., Glucosylation of stevioside and steviol glucosides in extract from *stevia rebaudiana* Bertoni. **Journal Of Plant Of Physiology**. v. 95, p.152-156, 1991

HSU, Y.H.; LIU, J.C.; KAO, P.F.; LEE, C.N.; CHEN, Y.J.; HSIEH, M.H.; CHAN, P. Antihypertensive effect of stevioside in different strains of hypertensive rats. **Zhonghua Yi Xue Za Zhi (Taipei)**, v. 65, p.1-6, 2002.

HUANG, T.J.; CHOU, B.H.; LIN, C.W.; WENG, J.H.; CHOU, C.H.; YANG, L.M.; LIN, S.J. Synthesis and antiviral effects of isosteviol-derived analogs against the hepatitis B virus. **Phytochemistry**, v. 99, p.107-114, 2014.

JAHAN, I.A.; NAHAR, N.; MOSIHUZZAMAN, M.; SHAHEEN, F.; ATTA-UR-RAHMANN; CHOUDHARY, M.I. Six new diterpenoids from *Suregada multiflora*. **Journal of Natural Products**, v. 67, p.1789-1795, 2004.

JAIN, D.C.; GUPTA, M.M.; SAXENA, S.; KUMAR, S. LC analysis of hepatoprotective diterpenoids from *Andrographis paniculata*. **Journal of Pharmaceutical and Biomedical Analysis**, v. 22, p.705-709, 2000.

JIA, Z.J.; SHI, J.G.; YANG, L. Ent-Kaurane Diterpenoids from *Euphorbia-Wangii*. **Journal of Natural Products**, v. 57, p.811-816, 1994.

KEDIK, S.A.; YARTSEV, E.I.; STANISHEVSKAYA, I.E. Antiviral activity of dried extract of *Stevia*. **Pharmaceutical Chemistry Journal**, v. 43, p.198-199, 2009.

KHAYBULLIN, R.N.; STROBYKINA, I.Y.; DOBRYNIN, A.B.; GUBAYDULLIN, A.T.; CHESTNOVA, R.V.; BABAIEV, V.M.; KATAEV, V.E. Synthesis and antituberculosis activity of novel unfolded and macrocyclic derivatives of ent-kaurane steviol. **Bioorganic and Medicinal Chemistry Letters**, v. 22, p.6909-6913, 2012.

KIM, T.H.; LI, H.; WU, Q.; LEE, H.J.; RYU, J.H. A new labdane diterpenoid with anti-inflammatory activity from *Thuja orientalis*. **Journal of Ethnopharmacology**, v. 146, p.760-767, 2013.

KINGHORN, A.D.; KANEDA, N.; BAEK, N.I.; KENNELLY, E.J.; SOEJARTO, D.D. Noncariogenic intense natural sweeteners. **Medicinal Research Reviews**, v. 18, p.347-360, 1998.

KONDOH, M.; NAGASHIMA, F.; SUZUKI, I.; HARADA, M.; FUJII, M.; ASAKAWA, Y.; WATANABE, Y. Induction of apoptosis by new ent-kaurene-type diterpenoids isolated from the New Zealand liverwort *Jungermannia* species. **Planta Medica**, v. 71, p.1005-1009, 2005.

KONOSHIMA, T.; TAKASAKI, M.; TAKAYASU, J.; TOKUDA, H. Chemopreventive effects of stevioside against naturally occurring tumor promoter, Teleocidin. **Planta Medica**, v. 74, p.1007-1007, 2008.

KOROCHKINA, M.G.; BABAIEV, V.M.; STROBYKINA, I.Y.; VOLOSHINA, A.D.; KULIK, N.V.; KATAEV, V.E. synthesis and antimicrobial activity of several bis-quaternized ammonium derivatives of the diterpenoid isosteviol. **Chemistry of Natural Compounds**, v. 47, p.914--917, 2012.

KOS, O.; CASTRO, V.; MURILLO, R.; POVEDA, L.; MERFORT, I. Ent-kaurane glycosides and sesquiterpene lactones of the hirsutinolide type from *Vernonia triflosculosa*. **Phytochemistry**, v. 67, p.62-69, 2006.

KUBANEK, J.; PRUSAK, A.C.; SNELL, T.W.; GIESE, R.A.; HARDCASTLE, K.I.; FAIRCHILD, C.R.; AALBERSBERG, W.; RAVENTOS-SUAREZ, C.; HAY, M.E. Antineoplastic diterpene-benzoate macrolides from the Fijian red alga *Callophycus serratus*. **Organic Letters**, v. 7, p.5261-5264, 2005.

KUBO, I.; XU, Y.L.; SHIMIZU, K. Antibacterial activity of ent-kaurane diterpenoids from *Rabdosia rosthornii*. **Phytotherapy Research**, v. 18, p.180-183, 2004.

LANE, A.L.; STOUT, E.P.; LIN, A.S.; PRUDHOMME, J.; LE ROCH, K.; FAIRCHILD, C.R.; FRANZBLAU, S.G.; HAY, M.E.; AALBERSBERG, W.; KUBANEK, J. Antimalarial bromophycolides J-Q from the Fijian red alga *Callophycus serratus*. **Journal of Organic Chemistry**, v. 74, p.2736-2742, 2009.

LE QUESNE, P.W.; HONKAN, V.; ONAN, K.D.; MORROW, P.A.; TONKYN, D. Oxidized kaurane derivatives from leaves of *Solidago missouriensis* and *S. Rigida*. **Phytochemistry**, v. 24, p.1785-1787, 1985.

LI, J.; ZHANG, D.Y.; WU, X.M. Synthesis and biological evaluation of novel exo-methylene cyclopentanone tetracyclic diterpenoids as antitumor agents. **Bioorganic Medicinal Chemistry Letters**, v. 21, p.130-132, 2011.

LI, X.; XIAO, W.L.; PU, J.X.; BAN, L.L.; SHEN, Y.H.; WENG, Z.Y.; LI, S.H.; SUN, H.D. Cytotoxic ent-kaurane diterpenoids from *Isodon phyllostachys*. **Phytochemistry**, v. 67, p.1336-1340, 2006.

LILILI; LI, G.-Y.; HUANG, S.-X.; LI, S.-H.; ZHOU, Y.; XIAO, W.-L.; LILOU; LIDING; SUN, H.-D. 7 α ,20-Epoxy-ent-kauranoids from *Isodon parvifolius*. **Journal of Natural Products**, v. 69, p.645-649, 2006.

LIMA, L.M. Modern medicinal chemistry: Challenges and brazilian contribution. **QUÍMICA NOVA**, v. 30, p.1456-1468, 2007.

LIN, C.Y.; LU, M.C.; SU, J.H.; CHU, C.L.; SHIUAN, D.; WENG, C.F.; SUNG, P.J.; HUANG, K.J. Immunomodulatory Effect of Marine Cembrane-Type Diterpenoids on Dendritic Cells. **Marine Drugs**, v. 11, p.1336-1350, 2013.

LIN, L.H.; LEE, L.W.; SHEU, S.Y.; LIN, P.Y. Study on the stevioside analogs of steviolbioside, steviol, and isosteviol 19-alkyl amide dimers: Synthesis and cytotoxic and antibacterial activity. **Chemical & Pharmaceutical Bulletin**, v. 52, p.1117-1122, 2004.

LIU, Z.G.; LI, Z.L.; BAI, J.; MENG, D.L.; LI, N.; PEI, Y.H.; ZHAO, F.; HUA, H.M. Anti-inflammatory diterpenoids from the roots of *Euphorbia ebracteolata*. **Journal of Natural Products**, v. 77, p.792-799, 2014.

LIZARTE NETO, F.S.; TIRAPELLI, D.P.C.; AMBROSIO, S.R.; TIRAPELLI, C.R.; OLIVEIRA, F.M.; NOVAIS, P.C.; PERIA, F.M.; OLIVEIRA, H.F.; CARLOTTI JUNIOR, C.G.; TIRAPELLI, L.F. Kaurene diterpene induces apoptosis in U87 human malignant glioblastoma cells by suppression of anti-apoptotic signals and activation of cysteine proteases. **Brazilian Journal of Medical and Biological Research**, v. 46, p.71-78, 2013.

MA, J.; MA, Z.; WANG, J.; MILNE, R.W.; XU, D.; DAVEY, A.K.; EVANS, A.M. Isosteviol reduces plasma glucose levels in the intravenous glucose tolerance test in Zucker diabetic fatty rats. **Diabetes Obesity Metabolism**, v. 9, p.597-599, 2007.

MENDOZA, L.; WILKENS, M.; URZUA, A. Antimicrobial study of the resinous exudates and of diterpenoids and flavonoids isolated from some Chilean *Pseudognaphalium* (Asteraceae). **Journal of Ethnopharmacology**, v. 58, p.85-88, 1997.

MIZUSHINA, Y.; AKIHISA, T.; UKIYA, M.; HAMASAKI, Y.; MURAKAMI-NAKAI, C.; KURIYAMA, I.; TAKEUCHI, T.; SUGAWARA, F.; YOSHIDA, H. Structural analysis of isosteviol and related compounds as DNA polymerase and DNA topoisomerase inhibitors. **Life Sciences**, v. 77, p.2127-2140, 2005.

MOTHANA, R.A.; AL-SAID, M.S.; AL-MUSAYEIB, N.M.; EL GAMAL, A.A.; AL-MASSARANI, S.M.; AL-REHAILY, A.J.; ABDULKADER, M.; MAES, L. In Vitro Antiprotozoal Activity of Abietane Diterpenoids Isolated from *Plectranthus barbatus* Andr. **International journal of molecular sciences**, v. 15, p.8360-8371, 2014.

MOTHANA, R.A.A.; JANSEN, R.; GRUENERT, R.; BEDNARSKI, P.J.; LINDEQUIST, U. Antimicrobial and cytotoxic abietane diterpenoids from the roots of *Meriandra benghalensis* (Roxb.) Benth. **Pharmazie**, v. 64, p.613-615, 2009.

MÜLLER, W.; HASTEDT, H.; THIES, C.; WERZ, N., **Politik der Erinnerung : Beiträge**. Universität Rostock, Rostock, 2000.

MURTHY, M.M.; SUBRAMANYAM, M.; BINDU, M.H.; ANNAPURNA, J. Antimicrobial activity of clerodane diterpenoids from *Polyalthia longifolia* seeds. **Fitoterapia**, v. 76, p.336-339, 2005.

NAKAMURA, Y.; SAKIYAMA, S.; TAKENAGA, K. Suppression of syntheses of high molecular weight nonmuscle tropomyosins in macrophages. **Cell Motil Cytoskeleton**, v. 31, p.273-282, 1995.

NEWMAN, D.J.; CRAGG, G.M. Natural products as sources of new drugs over the last 25 years. **Journal of Natural Products**, v. 70, p.461-477, 2007.

NEWMAN, D.J.; CRAGG, G.M.; SNADER, K.M. Natural products as sources of new drugs over the period 1981-2002. **Journal of Natural Products**, v. 66, p.1022-1037, 2003.

NIELSEN, J. Combinatorial synthesis of natural products. **Current Opinion in Chemical Biology**, v. 6, p.297-305, 2002.

NORDENTOFT, I.; JEPPESEN, P.B.; HONG, J.; ABUDULA, R.; HERMANSEN, K. Isosteviol increases insulin sensitivity and changes gene expression of key insulin regulatory genes and transcription factors in islets of the diabetic KKAY mouse. **Diabetes Obesity Metabolism**, v. 10, p.939-949, 2008.

OKOYE, T.C.; AKAH, P.A.; OMEJE, E.O.; OKOYE, F.B.; NWORU, C.S. Anticonvulsant effect of kaurenoic acid isolated from the root bark of *Annona senegalensis*. **Pharmacology Biochemistry and Behavior**, v. 109, p.38-43, 2013.

OZDEMIR, M.; SADIKOGLU, H. Characterization of rheological properties of systems containing sugar substitutes and carrageenan. **International Journal of Food Science and Technology**, v. 33, p.439-444, 1998.

PAIVA, L.A.; GURGEL, L.A.; SILVA, R.M.; TOME, A.R.; GRAMOSA, N.V.; SILVEIRA, E.R.; SANTOS, F.A.; RAO, V.S. Anti-inflammatory effect of kaurenoic acid, a diterpene from *Copaifera langsdorffii* on acetic acid-induced colitis in rats. **Vascular Pharmacology**, v. 39, p.303-307, 2002.

PAUL, S.; SENGUPTA, S.; BANDYOPADHYAY, T.K.; BHATTACHARYYA, A. Stevioside Induced ROS-Mediated Apoptosis Through Mitochondrial Pathway in Human Breast Cancer Cell Line MCF-7. **Nutrition and Cancer-an International Journal**, v. 64, p.1087-1094, 2012.

PINHEIRO, M.V.S.; OLIVEIRA, M.N.; PENNA, A.L.B.; TAMIME, A.Y. The effect of different sweeteners in low-calorie yogurts - a review. **International Journal of Dairy Technology**, v. 58, p.193-199, 2005.

PROKSCH, P.; EDRADA, R.A.; EBEL, R. Drugs from the seas - current status and microbiological implications. **Applied Microbiology and Biotechnology**, v. 59, p.125-134, 2002.

QUIJANO, L.; CALDERÓN, J.S.; GÓMEZ, F.; VEGA, J.L.; RÍOS, T. Diterpenes from *Stevia monardaefolia*. **Phytochemistry**, v. 21, p.1369-1371, 1982.

R. C. CAMBIE; G. R. CLARK; A. R. LAL; C. E. F. RM~RD; RUTLEDGE, P.S.; WOODGATE, P.D. Structure and Absolute Configuration of Two ent-Atisane Diterpenes from *Euphorbia fidjiana*. **Acta Crystallographica**, v. 46, p.2387-2389, 1990.

REZENDE, M.C.; URZUA, A.; BORTOLUZZI, A.J.; VÁSQUEZ, L. Variation of the antimicrobial activity of *Pseudognaphalium vira vira* (Asteraceae): isolation and X-ray structure of ent-3 β -hydroxy-16-kauren-19-oic acid. **Journal of Ethnopharmacology**, v. 72, p.459-464, 2000.

RODRIGUEZLINDE, M.E.; DIAZ, R.M.; GARCIAGRANADOS, A.; QUEVEDOSARMIENTO, J.; MORENO, E.; ONORATO, M.R.; PARRA, A.; RAMOSCORMENZANA, A. Antimicrobial Activity of Natural and Semisynthetic Diterpenoids from *Sideritis* Spp. **Microbios**, v. 77, p.7-13, 1994.

SCOTT, J.R., AND ZAHNER, D. Pili with strong attachments: Gram-positive bacteria do it differently. **Molecular Microbiology** v. 62, p.320–330, 2006

SHARIPOVA, R.R.; LODOCHNIKOVA, O.A.; STROBYKINA, I.Y.; R. Z. MUSIN, A.V.M.B., A; MOROZOV, V.I.; POD"YACHEV, S.N.; CHESTNOVA, R.V.; KATAEVA, V.E. Synthesis, structures, and properties of 15 oxoisosteviol thiosemicarbazone and oxime **Russian Chemical Bulletin, International Edition**, v. 62, p.175-182, 213.

SHARIPOVA, R.R.; STROBYKINA, I.Y.; MORDOVSKOI, G.G.; CHESTNOVA, R.V.; MIRONOV, V.F.; KATAEV, V.E. antituberculosis activity of glycosides from *stevia rebaudiana* and hybrid compounds of steviolbioside and pyridine carboxylic acid hydrazides. **Chemistry of Natural Compounds**, v. 46, p.902-905, 2011.

SHARMA, D.; PURI, M.; TIWARY, A.K.; SINGH, N.; JAGGI, A.S. Antiamnesic effect of stevioside in scopolamine-treated rats. **Indian Journal of Pharmacology**, v. 42, p.164-167, 2010.

SOMOVA, L.I.; SHODE, F.O.; MOODLEY, K.; GOVENDER, Y. Cardiovascular and diuretic activity of kaurene derivatives of *Xylopiya aethiopica* and *Alepidea amatymbica*. **Journal of Ethnopharmacology**, v. 77, p.165-174, 2001.

SPIRIG T1, WEINER EM, CLUBB RT. Sortase enzymes in Gram-positive bacteria. **Molecular Microbiology** v. 82, p.1044–1059, 2011

STEFANIA, R.; TEI, L.; BARGE, A.; GENINATTI CRICH, S.; SZABO, I.; CABELLA, C.; CRAVOTTO, G.; AIME, S. Tuning glutamine binding modes in Gd-DOTA-based probes for an improved MRI visualization of tumor cells. **Chemistry**, v. 15, p.76-85, 2009.

STOUT, E.P.; PRUDHOMME, J.; ROCH, K.L.; FAIRCHILD, C.R.; FRANZBLAU, S.G.; AALBERSBERG, W.; HAY, M.E.; KUBANEK, J. Unusual antimalarial meroditerpenes from tropical red macroalgae. **Bioorganic Medicinal Chemistry Letters**, v. 20, p.5662-5665, 2010.

SUN, H.-D.; HUANG, S.-X.; HAN, Q.-B. Diterpenoids from *Isodon* species and their biological activities. **Natural Product Reports**, v. 23, p.673-698, 2006.

TAI, C.J.; SU, J.H.; HUANG, C.Y.; HUANG, M.S.; WEN, Z.H.; DAI, C.F.; SHEU, J.H. Cytotoxic and anti-inflammatory eunicellin-based diterpenoids from the soft coral *Cladiella krempfi*. **Marine Drugs**, v. 11, p.788-799, 2013.

TAKAHASHI, K.; MATSUDA, M.; OHASHI, K.; TANIGUCHI, K.; NAKAGOMI, O.; ABE, Y.; MORI, S.; SATO, N.; OKUTANI, K.; SHIGETA, S. Analysis of anti-rotavirus activity of extract from *Stevia rebaudiana*. **Antiviral Research**, v. 49, p.15-24, 2001).

TAKAHASHI, K.; SUN, Y.; YANAGIUCHI, I.; HOSOKAWA, T.; SAITO, T.; KOMORI, M.; OKINO, T.; KURASAKI, M. Stevioside enhances apoptosis induced by serum deprivation in PC12 cells. **Toxicology Mechanisms and Methods**, v. 22, p.243-249, 2012.

TAKASAKI, M.; KONOSHIMA, T.; KOZUKA, M.; TOKUDA, H.; TAKAYASU, J.; NISHINO, H.; MIYAKOSHI, M.; MIZUTANI, K.; LEE, K.-H. Cancer preventive agents. Part 8: Chemopreventive effects of stevioside and related compounds. **Bioorganic & Medicinal Chemistry**, v. 17, p.600-605, 2009.

TATSIMO, S.J.N.; TANE, P.; SRINIVAS, P.V.; SONDEGAM, B.L.; MELISSA, J.; OKUNJI, C.O.; SCHUSTER, B.M.; IWU, M.M.; KHAN, I.A. Novel antimicrobial diterpenoids from *Turraeanthus africanus*. **Planta Medica**, v. 71, p.1145-1151, 2005.

THIRUGNANASAMPANDAN, R.; JAYAKUMAR, R.; BAI, V.N.; MARTIN, E.; PRASAD, K.J.R. Antiacetylcholinesterase and antioxidant ent-kaurene diterpenoid, melissoidesin from *Isodon wightii* (Bentham) H. Hara. **Natural Product Research**, v. 22, p.681-688, 2008.

TIRAPELLI, C.R.; AMBROSIO, S.R.; DA COSTA, F.B.; DE OLIVEIRA, A.M. Diterpenes: a therapeutic promise for cardiovascular diseases. **Recent Patents Cardiovascular Drug Discovery**, v. 3, p.1-8, 2008.

THOMSEN R, CHRISTENSEN MH: MolDock: a new technique for high-accuracy molecular docking. **Journal of medicinal chemistry** v.49. p 3315-3321, 2006

TOMITA, T.; SATO, N.; ARAI, T.; SHIRAISHI, H.; SATO, M.; TAKEUCHI, M.; KAMIO, Y. Bactericidal activity of a fermented hot-water extract from *Stevia rebaudiana* Bertoni towards enterohemorrhagic *Escherichia coli* O157:H7 and other food-borne pathogenic bacteria. **Microbiology and Immunology**, v. 41, p.1005-1009, 1997.

TRINGALI, C.; PIATTELLI, M.; NICOLOSI, G.; HOSTETTMANN, K. Molluscicidal and Antifungal Activity of Diterpenoids from Brown-Algae of the Family Dictyotaceae. **Planta Medica**, v., p.404-406, 1986.

UKIYA, M.; SAWADA, S.; KIKUCHI, T.; KUSHI, Y.; FUKATSU, M.; AKIHISA, T. Cytotoxic and apoptosis-inducing activities of steviol and isosteviol derivatives against human cancer cell lines. **Chemistry and Biodiversity**, v. 10, p.177-188, 2013.

VELIKOVA, M.; BANKOVA, V.; TSVETKOVA, I.; KUJUMGIEV, A.; MARCUCCI, M.C. Antibacterial ent-kaurene from Brazilian propolis of native stingless bees. **Fitoterapia**, v. 71, p.693-696, 2000.

VIDAL, V.; POTTERAT, O.; LOUVEL, S.; HAMY, F.; MOJARRAB, M.; SANGLIER, J.J.; KLIMKAIT, T.; HAMBURGER, M. Library-based discovery and characterization of daphnane diterpenes as potent and selective HIV inhibitors in *Daphne gnidium*. **Journal of Natural Products**, v. 75, p.414-419, 2012.

VIEIRA, H.S.; TAKAHASHI, J.A.; DE OLIVEIRA, A.B.; CHIARI, E.; BOAVENTURA, M.A.D. Novel derivatives of kaurenoic acid: Preparation and evaluation of their trypanocidal activity. **Journal of the Brazilian Chemical Society**, v. 13, p.151-157, 2002.

WANG, J.L.; SHEN, X.L.; CHEN, Q.H.; QI, G.; WANG, W.; WANG, F.P. Structure-Analgesic Activity Relationship Studies on the C-18- and C-19-Diterpenoid Alkaloids. **Chemical & Pharmaceutical Bulletin**, v. 57, p.801-807, 2009.

WU, Y.; DAI, G.F.; YANG, J.H.; ZHANG, Y.X.; ZHU, Y.; TAO, J.C. Stereoselective synthesis of 15- and 16-substituted isosteviol derivatives and their cytotoxic activities. **Bioorganic Medicinal Chemistry Letters**, v. 19, p.1818-1821, 2009.

WU, Y.; LIU, C.-J.; LIU, X.; DAI, G.-F.; DU, J.-Y.; TAO, J.-C. Stereoselective Synthesis, Characterization, and Antibacterial Activities of Novel Isosteviol

Derivatives with D-Ring Modification. **Helvetica Chimica Acta**, v. 93, p.2052-2069, 2010.

WU, Y.; YANG, J.H.; DAI, G.F.; LIU, C.J.; TIAN, G.Q.; MA, W.Y.; TAO, J.C. Stereoselective synthesis of bioactive isosteviol derivatives as alpha-glucosidase inhibitors. **Bioorganic Medicinal Chemistry**, v. 17, p.1464-1473, 2009.

YANG, L.B.; LI, L.; HUANG, S.X.; PU, J.X.; ZHAO, Y.; MA, Y.B.; CHEN, J.J.; LENG, C.H.; TAO, Z.M.; SUN, H.D. Anti-hepatitis B virus and cytotoxic diterpenoids from *Isodon lophanthoides* var. *gerardianus*. **Chemical and Pharmaceutical Bulletin (Tokyo)**, v. 59, p.1102-1105, 2011.

YANG, S.P.; DONG, L.; WANG, Y.; WU, Y.; YUE, J.M. Antifungal diterpenoids of *Pseudolarix kaempferi*, and their structure-activity relationship study. **Bioorganic Medicinal Chemistry**, v. 11, p.4577-4584, 2003.

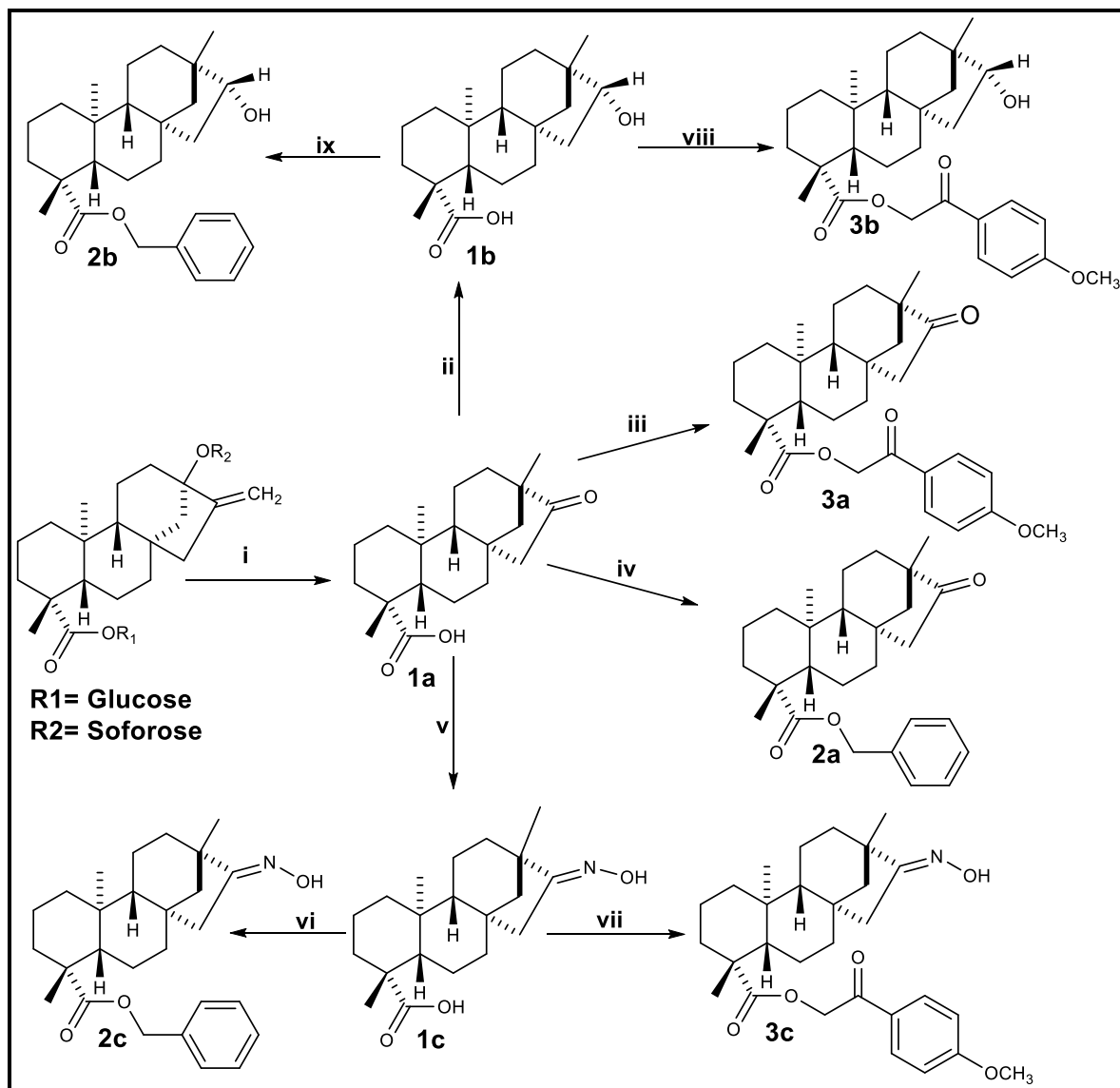
ZHANG, T.; LU, L.-H.; LIU, H.; WANG, J.-W.; WANG, R.-X.; ZHANG, Y.-X.; TAO, J.-C. D-ring modified novel isosteviol derivatives: Design, synthesis and cytotoxic activity evaluation. **Bioorganic Medicinal Chemistry Letters**, v. 22, p.5827-5832, 2012.

ZHAO, A.H.; ZHANG, Y.; XU, Z.H.; LIU, J.W.; JIA, W. Immunosuppressive entkaurene diterpenoids from *Isodon serra*. **Helvetica Chimica Acta**, v. 87, p.3160-3166, 2004.

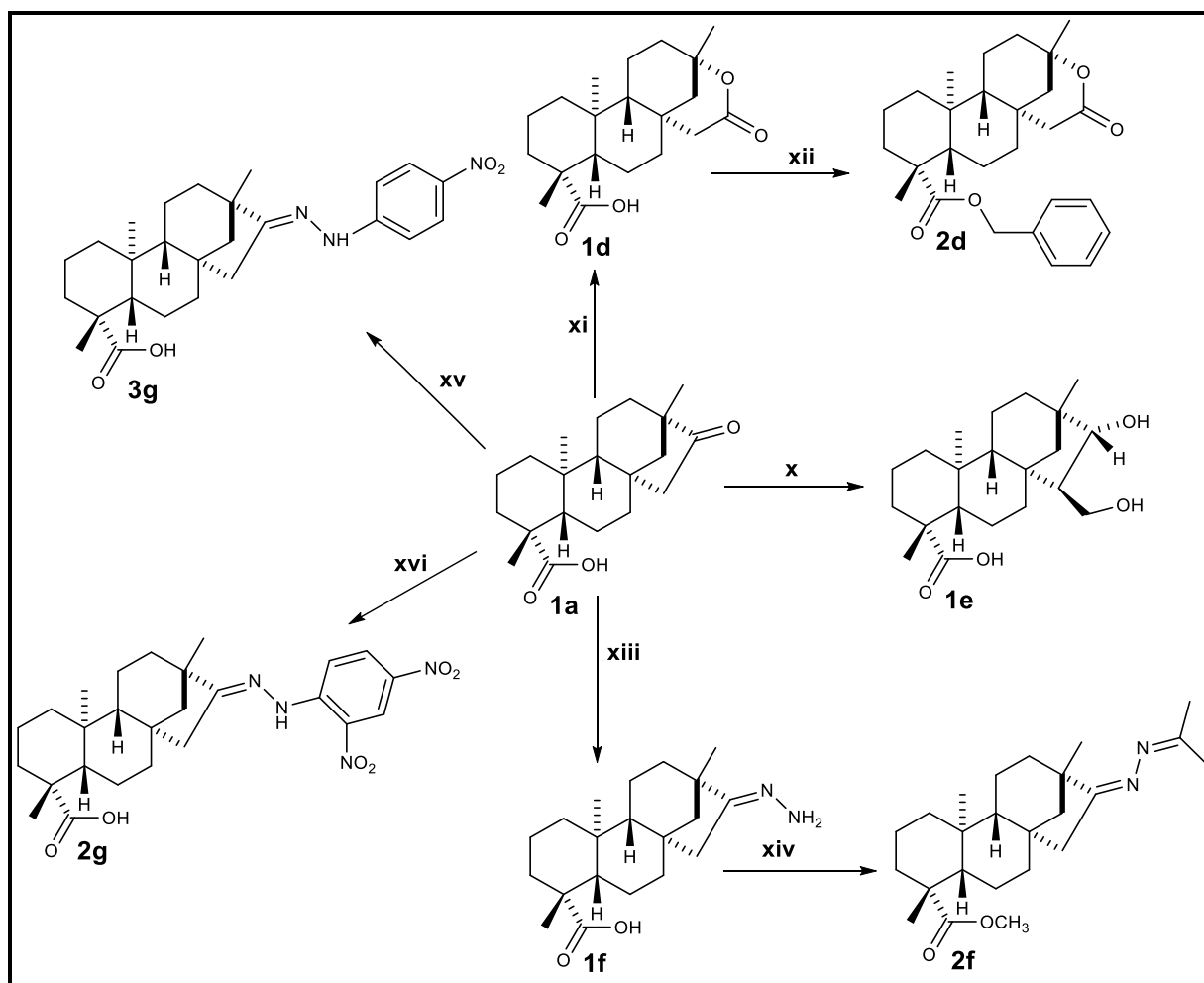
ZHU, S.L.; WU, Y.; LIU, C.J.; WEI, C.Y.; TAO, J.C.; LIU, H.M. Design and stereoselective synthesis of novel isosteviol-fused pyrazolines and pyrazoles as potential anticancer agents. **European Journal Medicinal Chemistry**, v. 65, p.70-82, 2013.

7 ANNEXES

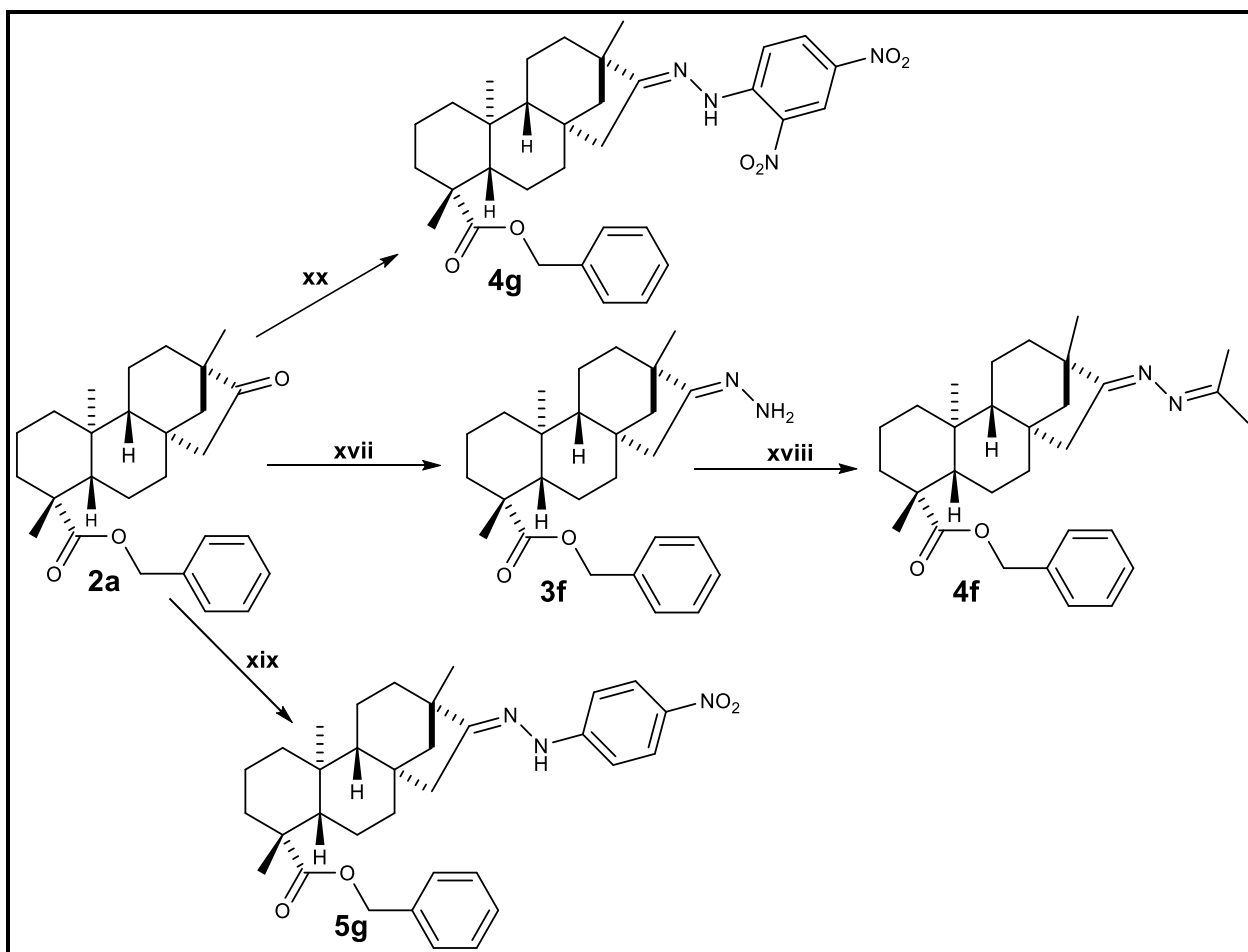
7.1 SCHEMES



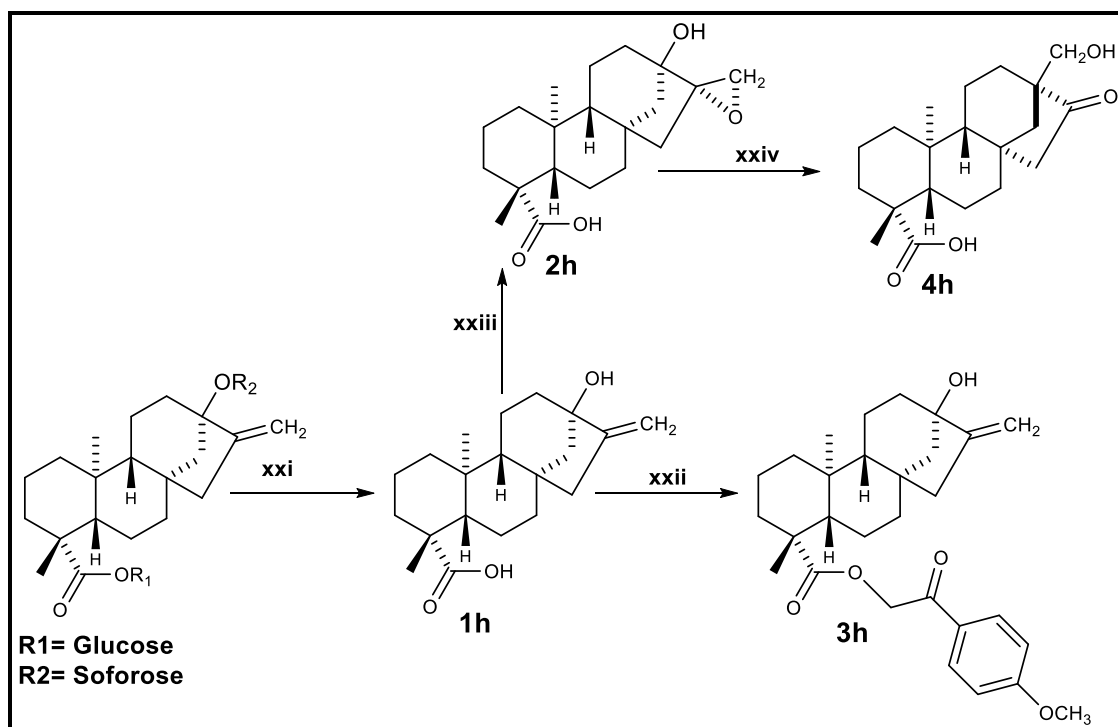
Scheme 1 i) 5% HCl, 1h reflux, 33%; ii) $NaBH_4$, C_2H_5OH , $0^\circ C$, 1h, 88%; iii), vii), viii) 2-bromo-4'-methoxyacetophenone, $(CH_3CH_2)_3N$, CH_3COCH_3 , microwave, 4 min, 81%; iv), vi), ix) $PhCH_2Cl$, K_2CO_3 , CH_3COCH_3 , 2h reflux, 82%; v) $HONH_2Cl$, CH_3COONa , C_2H_5OH 12h, 78%.



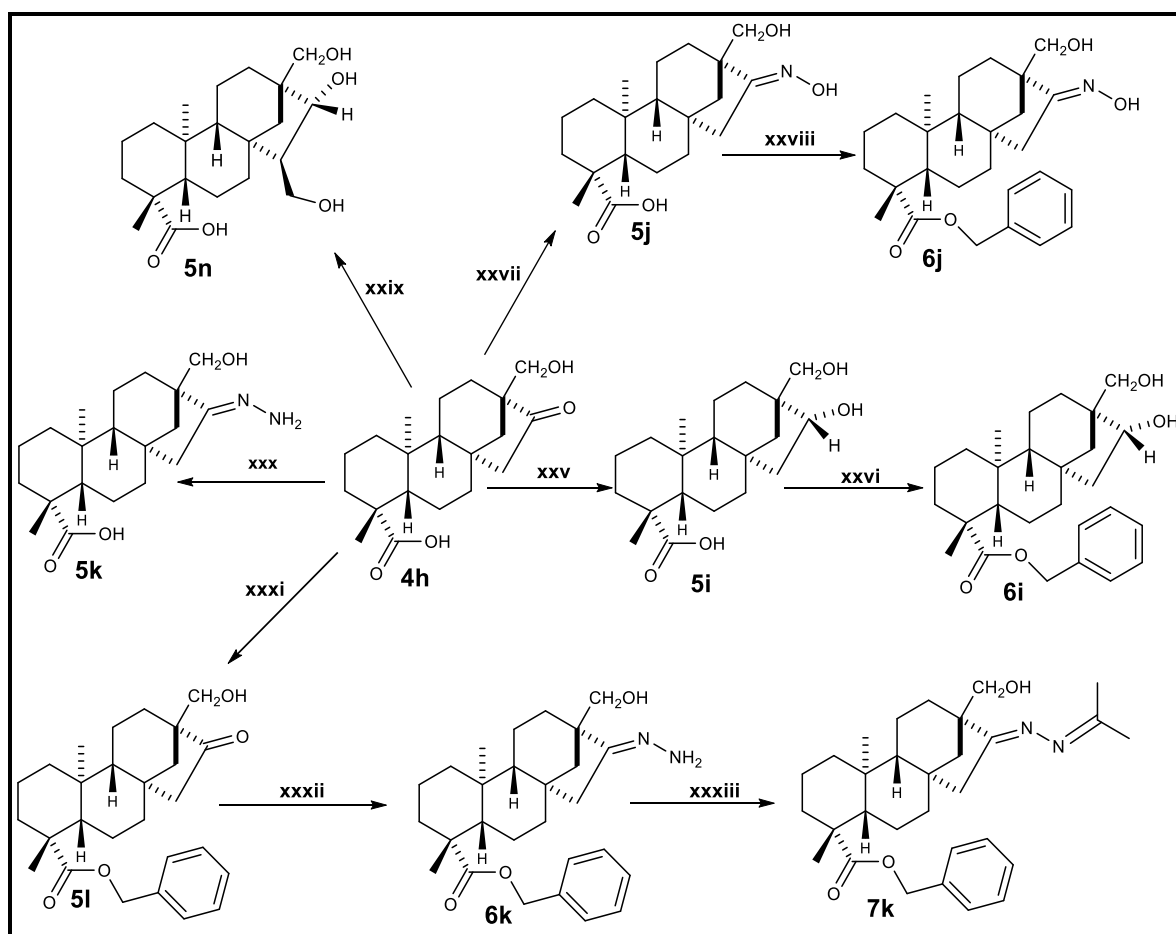
Scheme 2: x) H_2CO 37%, $\text{C}_2\text{H}_5\text{OH}$, NaOH ; xi) H_2O_2 (30%), CH_3COOH , 72h, 25 $^\circ\text{C}$ 39%; xii) PhCH_2Cl , K_2CO_3 , CH_3COCH_3 , 2h reflux, 76%; xiii) $\text{NH}_2\text{NH}_2 \cdot \text{H}_2\text{O}$, CH_3OH , reflux, 6h, 83%; xiv) CH_2N_2 , CH_3OH , and CH_3COCH_3 , reflux, 1h, 84%; xv) 4-NPH, H_2SO_4 , H_2O , $\text{C}_2\text{H}_5\text{OH}$ 12h, 51%; xvi) 2, 4 DNPH, H_2SO_4 , H_2O , $\text{C}_2\text{H}_5\text{OH}$, 12h, 70%.



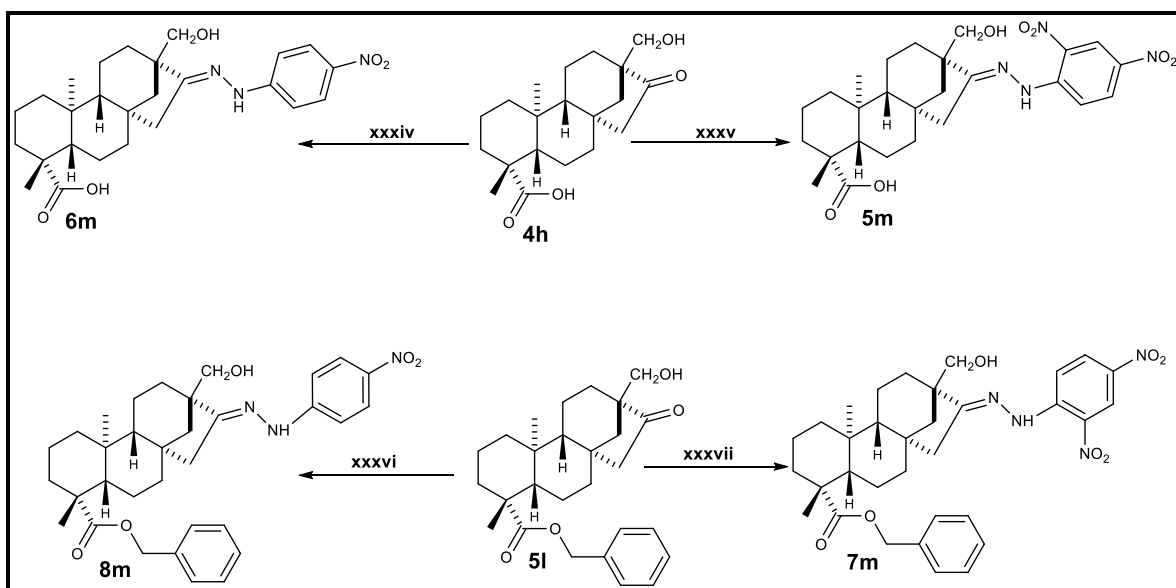
Scheme 3: xvii) $\text{NH}_2\text{NH}_2 \cdot \text{H}_2\text{O}$, CH_3OH , reflux, 6h, 84%; xviii) CH_3COCH_3 , reflux, 1h, 75%; xix) 2, 4 DNPH, H_2SO_4 , H_2O , $\text{C}_2\text{H}_5\text{OH}$ 12h, 45%; xx) 4-NPH, H_2SO_4 , H_2O , $\text{C}_2\text{H}_5\text{OH}$ 12h, 46%;



Scheme 4: xxi) NaIO_4 , NaOH , reflux 1h, 13%; xxii) 2-bromo-4'-methoxyacetophenone, $(\text{CH}_3\text{CH}_2)_3\text{N}$, CH_3COCH_3 , microwave, 4 min, 78%; xxiii) *m*-chloro per-benzoic acid, DCM; 24h stirring 25 °C, 60%; xxiv) 0.5% HCl, CH_3COCH_3 , 58 °C, 30 min, 64%.



Scheme 5: xxv) NaBH_4 , $\text{C}_2\text{H}_5\text{OH}$, 0°C , 1h, 73%; xxvi), xxviii), xxxi) PhCH_2Cl , K_2CO_3 , CH_3COCH_3 , 2h reflux, 77%, 66%, 69%; xxx), xxxii), $\text{NH}_2\text{NH}_2 \cdot \text{H}_2\text{O}$, CH_3OH , 6h reflux 86%, 73%; xxvii) HONH_2Cl , CH_3COONa , $\text{C}_2\text{H}_5\text{OH}$, 68%; xxix) H_2CO 37%, $\text{C}_2\text{H}_5\text{OH}$, NaOH , 71%; xxxiii) CH_3COCH_3 , reflux, 1h, 65%/



Scheme 6: xxxv), xxxvii) 2, 4 DNPH, H_2SO_4 , H_2O , $\text{C}_2\text{H}_5\text{OH}$, 12 h, 57%, 40%

xxxiv) xxxvi) 4-NPH, H_2SO_4 , H_2O , $\text{C}_2\text{H}_5\text{OH}$, 12 h, 49%, 51%.

7.2 ¹H NMR TableTable 20: ¹H NMR chemical shifts (δ , ppm), for compounds **1a-1d**: multiplicity and coupling constants (Hz)

¹ H	1a	1b	1c	1d
12	2.17 (1H, br, d, $J = 12.50$ Hz)	2.17 (1H, br, d, $J = 12.40$ Hz)	2.19 (1H, br, d, $J = 12.67$ Hz)	2.18 (1H, br, d, $J = 12.90$ Hz)
13				
14	1.55 (1H, dd, J $= 11.30, 2.2$ Hz)		1.34 (1H, dd, J $= 17.5, 3.9$ Hz)	
15	2.63 (1H, dd, J $= 18.6, 3.6$ Hz)		2.98 (1H, dd, J $= 18.3, 2.9$ Hz), 2.19 (1H, d, J $= 13.14$ Hz)	3.89 (1H, dd, J $= 18.7, 2.6$ Hz)
16		3.85 (1H, dd, J $= 10.2, 5.4$ Hz)		
17	0.98 (3H, s)	1.16 (3H, s)	1.11 (3H, s)	1.17 (3H, s)
18	1.19 (3H, s)	0.90 (3H, s)	1.2 (3H, s)	1.34 (3H, s)
19				
20	0.68 (3H, s)	0.71 (3H, s)	0.76 (3H, s)	0.75 (3H, s)
OMe	3.64 (3H, s)	3.62 (3H, s)	3.62 (3H, s)	3.62 (3H, s)

Table 21: ^1H NMR chemical shifts (δ , ppm), for compounds **1e–2h**: multiplicity and coupling constants (Hz).

^1H	1e	1f	1h	2h
12		2.17 (1H, d, J = 12.9 Hz)		2.20 (1H, d, J = 10.9 Hz)
13				
14			1.87 (1H, dd, J = 10.8, 2.5 Hz)	
15	3.99 (1H, dd, J = 9.9, 4.9 Hz)	2.6 (2H, dd, J = 17.5, 2.0 Hz)		
16				
17	1.15 (3H,s)	1.26 (3H ,s)	4.9 (1H, br, s) 4.8 (1H, br, s)	2.9 (1H, d, J = 4.4 Hz), 2.8 (1H, d, J = 4.4 Hz)
18	0.93 (3H,s)	1.08 (3H ,s)	1.19 (3H,s)	1.19 (3H,s)
19				
20	0.74 (3H,s)	0.87 (3H ,s)	0.84 (3H,s)	0.86 (3H,s)
OMe	3.62 (3H,s)		3.66 (3H,s)	3.64 (3H,s)
1'	3.46 (2H, t, J = 10.3 Hz)			

Table 22: ^1H NMR chemical shifts (δ , ppm), for compounds **4h–5j**: multiplicity and coupling constants (Hz)

^1H	4h	5i	5n	5j
12	2.20 (1H, d, J = 12.9 Hz)	2.12 (2H, br, s)		2.13 (2H, br, s)
13				
14				
15	2.68 (1H, dd, J = 18.9, 3.7Hz)		2.9 (2H, s)	2.99 (1H, dd, J = 18.4, 3.0 Hz)
16		4.2 (1H, dd, J = 10.5, 5.1 Hz)		
17	3.5 (1H, d, J = 10.9 Hz)	3.45 (1H, d, J = 10.15 Hz), 3.56 (1H, d, J = 10.15 Hz)	3.62 (2H, s)	3.54 (1H, dd, J = 16.7, 10.9 Hz)
18	1.21 (3H,s)	1.20 (3H,s)	1.16 (3H, s)	1.22 (3H,s)
19				
20	0.71 (3H,s)	0.77 (3H,s)	0.79 (3H, s)	0.90 (3H,s)
OMe	3.65 (3H, s)	3.66 (3H, s)		
1'			3.34 (1H, br, d, J = 5.6 Hz)	

Table 23: ^1H NMR chemical shifts (δ , ppm), for compounds **5k–2b**: multiplicity and coupling constants (Hz).

^1H	5k	2f	2a	2b
15	2.88 (1H, br, d, $J = 17.9$ Hz)	2.7 (1H, dd, $J = 18.5, 3.2$ Hz)	2.55 (1H, dd, $J = 18.7, 3.6$ Hz)	
16				3.86 (1H, dd, $J = 9.6, 5.6$ Hz)
17	3.57 (2H, br, s)	1.84 (3H, s)	1.21 (3H, s)	1.21 (3H, s)
18	1.18 (3H, s)	1.13 (3H, s)	0.97 (3H, s)	0.93 (3H, s)
19				
20	0.94 (3H, s)	0.69 (3H, s)	0.60 (3H, s)	0.70 (3H, s)
1'		1.83 (3H, s)		
2'				
3'		2.01 (3H, s)		
OMe		3.64 (3H, s)		
Aromatic			7.3 (5H, s)	7.3 (5H, s)
H2''-H6''				
-CH2- (H7'')			5.1 (1H, dd, $J = 17.6, 12.5$ Hz)	5.1 (1H, d, $J = 12.4$ Hz), 5.0 (1H, d, $J = 12.4$ Hz)

*

Table 24: ^1H NMR chemical shifts (δ , ppm), for compounds **2c-3f**: multiplicity and coupling constants (Hz).

^1H	2c	2d	3f
12	2.24 (1H, d, J = 11.6 Hz)	2.22 (1H, d, J = 13.7 Hz)	
14			
15	2.94 (1H, dd, J = 18.6, 3.0 Hz)	3.01 (1H, dd, J = 18.8, 2.4 Hz)	2.55 (1H, dd, J = 17.5, 2.8 Hz)
16			
17	1.24 (3H,s)	1.35 (3H,s)	1.22 (3H ,s)
18	1.13 (3H,s)	1.22 (3H.s)	1.06 (3H ,s)
19			
20	0.73 (3H, s)	0.70 (3H.s)	0.66 (3H ,s,)
Aromatic-	7.4 (5H, s)	7.3 (5H, s)	7.4 (5H, s)
H2''-H6''			
-CH2- (H7'')	5.0 (1H, d, J = 12.5 Hz), 5.2 (1H, d, J = 12.5 Hz)	5.0 (1H, d, J = 12.3 Hz), 5.2 (1H, d, J = 12.3 Hz)	5.1 (1H, d, J = 12.4 Hz), 5.2 (1H, d, J = 12.4 Hz)

Table 25: ^1H NMR chemical shifts (δ , ppm), for compounds **6j-6i**: multiplicity and coupling constants (Hz).

^1H	6j	5l	6i
12	2.20 (1H, br, d, J = 13.6 Hz)	2.24 (1H, br, d, J = 13.5 Hz)	2.16 (1H, br, J = 12.7 Hz)
13			
14			
15	2.92 (1H, br, d, J = 18.4 Hz)	2.61 (1H, dd, J = 18.9, 3.8 Hz)	
16			4.11 (1H, dd, J = 11.3, 4.1 Hz)
17	3.6 (2H, s)	3.5 (1H, d, J = 11.4 Hz), 3.6 (1H, d, J = 11.4 Hz)	3.33 (1H, dd, J = 16.9, 10.6 Hz)
18	1.20 (3H, s)	1.24 (3H,s)	1.18 (3H, s)
19			
20	0.69 (3H, s)	0.63 (3H,s)	0.72 (3H, s)
Aromatic	7.3 (5H, s)	7.4 (5H, s)	7.4 (5H, s)
H2''-H6''			
-CH2-	5.0 (1H, d, J = 12.4	5.0 (1H, d, J = 12.3	5.0 (1H, d, J = 12.4
H7''	Hz), 5.2 (1H, d, J = 12.4 Hz)	Hz), 5.1 (1H, d, J = 12.3 Hz)	Hz), 5.1 (1H, d, J = 12.4 Hz)

Table 26: ¹H NMR chemical shifts (δ , ppm), for compounds **2g-6m**: multiplicity and coupling constants (Hz).

¹ H	2g	3g	5m	6m
12	2.18 (1H, br, d, $J = 12.9$ Hz)	2.22 (1H, br, d, $J = 12.16$)	2.20 (2H, br, s)	
15	2.6 (1H, dd, $J = 18.7, 3.6$ Hz)	2.8 (1H, d, $J = 16.9$ Hz)	2.98 (1H, dd, $J = 18.3, 2.5$ Hz)	2.97 (1H, dd, $J = 18.2, 2.8$ Hz)
16				
17	1.28 (3H,s)	1.3 (3H,s)	3.8 (1H, d, $J = 11.4$ Hz), 3.7 (1H, d, $J = 11.3$ Hz)	3.7 (1H, d, $J = 10.9$ Hz), 3.6 (1H, d, $J = 10.9$ Hz)
18	1.19 (3H, s)	1.2 (3H, s)	1.30 (3H, s)	1.21 (3H, s)
19				
20	0.92 (3H, s)	0.90 (3H, s)	0.94 (3H, s)	0.87 (3H, s)
1'				
2'		7.07 (1H, d, $J = 9.1$ Hz)		7.18 (1H, d, $J = 9.3$ Hz)
3'	8.9 (1H, d, $J = 2.5$ Hz)	8.15 (1H, d, $J = 9.1$ Hz)	9.00 (1H, d, $J = 2.5$ Hz)	8.11 (1H, d, $J = 9.3$ Hz)
4'				
5'	8.1 (1H, dd, $J = 9.6, 2.5$ Hz)	8.15 (1H, d, $J = 9.1$ Hz)	8.2 (1H, dd, $J = 9.6, 2.5$ Hz)	8.11 (1H, d, $J = 9.3$ Hz)
6'	7.80 (1H, d, $J = 9.6$ Hz)	7.07 (1H, d, $J = 9.1$ Hz)	7.7 (1H, d, $J = 9.6$ Hz)	7.18 (1H, d, $J = 9.3$ Hz)
NH	10.6 (1H,s)		10.7 (1H, s)	9.13 (1H, s)

Table 27: ^1H NMR chemical shifts (δ , ppm), for compounds **7k-6k**: multiplicity and coupling constants (Hz).

^1H	7k	4f	6K
12	2.19 (2H, s)	2.20 (1H, d, J = 14.8 Hz)	2.20 (1H, br, d, J = 12.9 Hz)
13			
14			
15	2.8 (1H, dd, J = 18.8, 3.0 Hz)	2.63 (1H, dd, J = 18.5, 3.1 Hz)	2.56 (1H, dd, J = 17.3, 2.4 Hz)
16			
17	3.76 (1H, d, J = 10.9 Hz), 3.55 (1H, d, J = 10.7, Hz)	1.2 (3H, s)	3.5 (1H, d, J = 11.0 Hz), 3.6 (1H, d, J = 11.0 Hz)
18	1.22 (3H, s)	1.12 (3H, s)	1.20 (3H, s)
19			
20	0.66 (3H, s)	0.63 (3H, s)	0.65 (3H, s)
Aromatic H2''-H6''	7.4 (5H, s)	7.3 (5H, s)	7.3 (5H, s)
-CH2- (H7'')	5.2 (1H, d, J = 12.4 Hz), 5.1 (1H, d, J = 12.42 Hz)	5.1 (1H, dd, J = 18.3, 12.4 Hz)	5.0 (1H, d, J = 12.3 Hz), 5.1 (1H, d, J = 12.30 Hz)
1'	1.9 (3H, s)	1.8 (3H, s)	
2'			
3'	2.1 (3H, s)	2.0 (3H, s)	

Table 28: ^1H NMR chemical shifts (δ , ppm), for compounds **3a-3h**: multiplicity and coupling constants (Hz).

^1H	3a	3b	3c	3h
12	2.29 (1H, d, J = 13.2 Hz)	2.17 (2H, s)	2.20 (2H,s)	2.28 (1H, d, J = 12.1 Hz)
14				2.13 (1H, d, J = 10.6 Hz)
15	2.65 (1H, dd, J = 18.7, 3.6 Hz)		3.9 (1H, dd, J = 18.5, 2.6 Hz)	
16				
17	1.33 (3H, s)	1.31 (3H, s)	1.36 (3H, s)	4.8 (1H, br, s), 4.9 (1H, br, s)
18	0.97 (3H, s)	0.91 (3H. s)	1.13 (3H, s)	1.32 (3H,s)
19				
20	0.77 (3H ,s)	0.80 (3H.s)	0.86 (3H, s)	0.90 (3H,s)
1'				
H2', H6'	7.89 (2H, d, J = 8.9 Hz)	7.90 (2H, d, J = 8.9 Hz)	7.93 (2H, d, J = 8.9 Hz)	7.90 (2H, d, J = 8.9 Hz)
H3', H5'	6.94 (2H, d, J = 9.0 Hz)	6.95 (2H, d, J = 8.9 Hz)	6.99 (2H, d, J = 8.8 Hz)	6.95 (2H, d, J = 8.9 Hz)
8'	5.2 (1H, d, J = 16.1 Hz), 5.3 (1H, d, J = 16.1 Hz)	5.2 (1H, d, J = 16.0 Hz), 5.3 (1H, d, J = 16.0 Hz)	5.1 (1H, d, J = 16.0 Hz), 5.4 (1H, d, J = 16.0 Hz)	5.2 (1H, d, J = 16.1 Hz), 5.4 (1H, d, J = 16.1 Hz)
9' (OMe)	3.87 (3H, s)	3.87 (3H, s)	3.87 (3H, s)	3.87 (3H, s,)

Table 29: ^1H NMR chemical shifts (δ , ppm), for compounds **4g-8m**: multiplicity and coupling constants (Hz).

^1H	4g	5g	7m	8m
12	2.2 (1H, br, d, $J = 13.2$ Hz)	2.3 (1H, br, d, $J = 13.2$ Hz)	2.2 (1H, br, d, $J = 13.3$ Hz)	2.2 (1H, br, d, $J = 12.8$ Hz)
15	2.88 (1H, d, $J = 16.9$ Hz)	2.66 (1H, dd, $J = 17.4, 2.5$ Hz)	2.86 (1H, dd, $J = 17.9, 2.6$ Hz)	2.73 (1H, dd, $J = 17.5, 2.4$ Hz)
16				
17	1.22 (3H, s)	1.23 (3H, s)	3.73 (1H, dd, $J = 17.9, 11.4$ Hz)	3.69 (2H, s)
18	1.19 (3H, s)	1.1 (3H, s)	1.23 (3H, s)	1.23 (3H, s)
19				
Aromatic	7.4 (5H, s)	7.4 (5H, s)	7.4 (5H, s)	7.4 (5H, s)
-CH₂-(7'')	5.1 (2H, s)	5.0 (1H, d, $J = 12.6$ Hz), 5.2 (1H, d, $J = 12.6$ Hz)	5.1 (2H, s)	5.0 (1H, d, $J = 12.5$ Hz), 5.2 (1H, d, $J = 12.6$ Hz)
2'		7.03 (1H, d, $J = 9.2$ Hz)		6.95 (1H, d, $J = 9.2$ Hz)
3'	9.13 (1H, d, $J = 2.5$ Hz)	8.14 (1H, d, $J = 9.3$ Hz)	9.1 (1H, d, $J = 2.5$ Hz)	8.1 (1H, d, $J = 9.2$ Hz)
4'				
5'	8.29 (1H, dd, $J = 9.7, 2.5$ Hz)	8.1 (1H, d, $J = 9.3$ Hz)	8.3 (1H, dd, $J = 9.6, 2.5$ Hz)	8.1 (1H, d, $J = 9.2$ Hz)
6'	7.96 (1H, d, $J = 9.6$ Hz)	7.03 (1H, d, $J = 9.2$ Hz)	7.8 (1H, d, $J = 9.6$ Hz)	6.9 (1H, d, $J = 9.2$ Hz)
NH	10.7 (1H, s)		10.79 (1H, s)	

7.3 ^{13}C NMR TableTable 30: ^{13}C NMR chemical shifts (δ , ppm) for compounds **1a**–**5n**.

^{13}C	1a	1b	1c	1d	1e	1f	1h	2h	4h	5i	5n
1	39.8	39.9	40.8	39.9	39.6	39.9	40.6	40.7	39.8	39.9	39.6
2	18.8	18.9	18.8	18.8	18.9	18.9	19.1	19.0	18.9	18.9	18.8
3	37.2	37.9	38.0	38.4	37.9	37.9	38.1	37.9	37.9	38.0	37.8
4	43.7	43.7	43.7	43.7	43.7	43.6	43.7	43.7	43.7	43.7	43.4
5	57.0	57.1	57.1	57.2	57.7	57.1	56.9	56.8	56.9	57.1	58.5
6	21.6	21.7	21.7	19.5	22.1	21.7	21.8	21.8	21.7	21.7	22.1
7	41.4	41.7	39.9	37.8	34.7	39.3	41.3	41.2	41.3	41.6	37.8
8	39.3	41.9	40.6	34.8	40.8	40.8	41.6	41.5	39.6	42.5	42.6
9	54.7	55.8	54.8	55.7	57.1	54.9	53.7	53.8	55.4	56.5	57.0
10	37.9	37.9	37.9	37.5	38.1	38.2	39.2	39.2	38.0	38.0	38.1
11	20.3	20.4	20.4	18.5	19.5	20.5	20.4	19.5	19.8	19.9	19.0
12	37.8	33.7	36.7	38.6	33.1	36.3	39.2	34.7	32.1	29.3	34.9
13	48.6	42.0	43.7	80.2	42.5	44.1	80.2	74.7	54.1	46.5	45.6
14	54.2	55.2	56.2	47.7	54.2	56.3	47.4	45.7	48.9	50.0	49.1
15	48.4	42.8	39.4	43.6	50.3	41.2	46.9	46.5	48.9	42.1	50.2
16	---	80.5	170.2	172.5	86.7	165.5	156.1	65.2	----	78.5	80.7
17	19.8	24.8	22.1	28.2	24.9	22.1	102.9	48.6	65.1	71.2	68.3
18	28.8	28.8	28.7	28.5	28.8	29.1	28.7	28.6	28.8	28.8	28.1
19	177.7	178.1	178.0	177.5	177.9	182.4	177.9	177.8	177.7	178.0	177.1
20	13.1	13.1	13.1	13.3	13.0	13.5	15.3	15.5	13.1	13.1	12.6
OMe	51.2	51.1	51.1	51.2	51.2		51.1	51.1			
1'	----	---	---	---	64.9						63.1

Table 31: ^{13}C NMR chemical shifts (δ , ppm) for compounds **5j**–**6j**.

^{13}C	5j	5k	2f	2a	2b	2c	2d	3f	6i	6j
1	39.8	40.2	39.9	39.8	39.9	39.8	39.8	39.8	39.8	39.8
2	18.9	19.2	18.9	18.9	18.9	18.9	18.8	18.9	18.8	18.9
3	37.8	38.6	37.9	37.3	38.0	38.0	37.8	37.9	37.9	37.9
4	43.2	44.1	43.8	43.8	43.8	43.7	43.8	43.8	43.6	43.9
5	56.7	57.4	57.2	57.2	57.3	57.2	57.3	57.3	57.1	57.2
6	21.7	21.9	21.7	21.7	21.7	21.7	19.5	21.7	21.8	21.6
7	36.9	36.8	39.4	41.5	41.7	40.8	38.4	39.3	41.8	37.0
8	40.7	40.8	40.6	39.4	42.0	40.6	34.8	40.7	42.0	40.9
9	55.4	55.6	55.0	54.6	55.7	54.8	55.7	54.9	56.5	55.6
10	38.1	38.0	37.9	37.9	38.0	38.0	37.8	38.0	37.9	38.1
11	19.8	19.6	20.5	20.3	20.4	20.4	18.5	20.5	19.8	19.9
12	34.9	34.2	39.0	37.9	33.7	36.7	38.5	35.8	29.3	34.1
13	48.9	49.1	44.2	48.6	42.0	43.8	80.2	43.9	46.9	49.4
14	51.3	51.0	56.0	54.2	55.2	56.3	47.7	56.3	50.1	51.0
15	40.7	41.2	41.1	48.3	42.7	39.4	43.6	41.2	42.4	40.8
16	167.5	165.4	174.3	---	80.5	170.2	172.5	164.4	75.5	169.2
17	66.4	66.1	24.9	19.8	24.9	22.1	28.2	22.2	68.2	66.67
18	28.5	28.8	28.8	28.9	28.9	28.9	28.7	28.9	28.2	28.9
19	178.7	182.9	177.9	176.9	177.3	177.1	176.7	177.0	176.5	177.1
20	13.0	12.9	13.2	13.3	13.3	13.2	13.5	13.4	13.1	13.3
1''			22.2	135.9	136.1	136.1	135.8	136.1	136.5	136.1
2''			159.1	128.3	128.2	128.1	128.3	128.2	128.2	128.2
3''			17.6	128.4	128.4	128.5	128.5	128.4	128.4	128.5
4'				128.1	128.0	128.0	128.2	128.0	127.9	128.1
5''				128.4	128.4	128.5	128.5	128.4	128.4	128.5
6''				128.3	128.2	128.1	128.3	128.2	128.2	128.2
7''				65.1	65.9	65.9	66.1	65.9	65.5	65.9

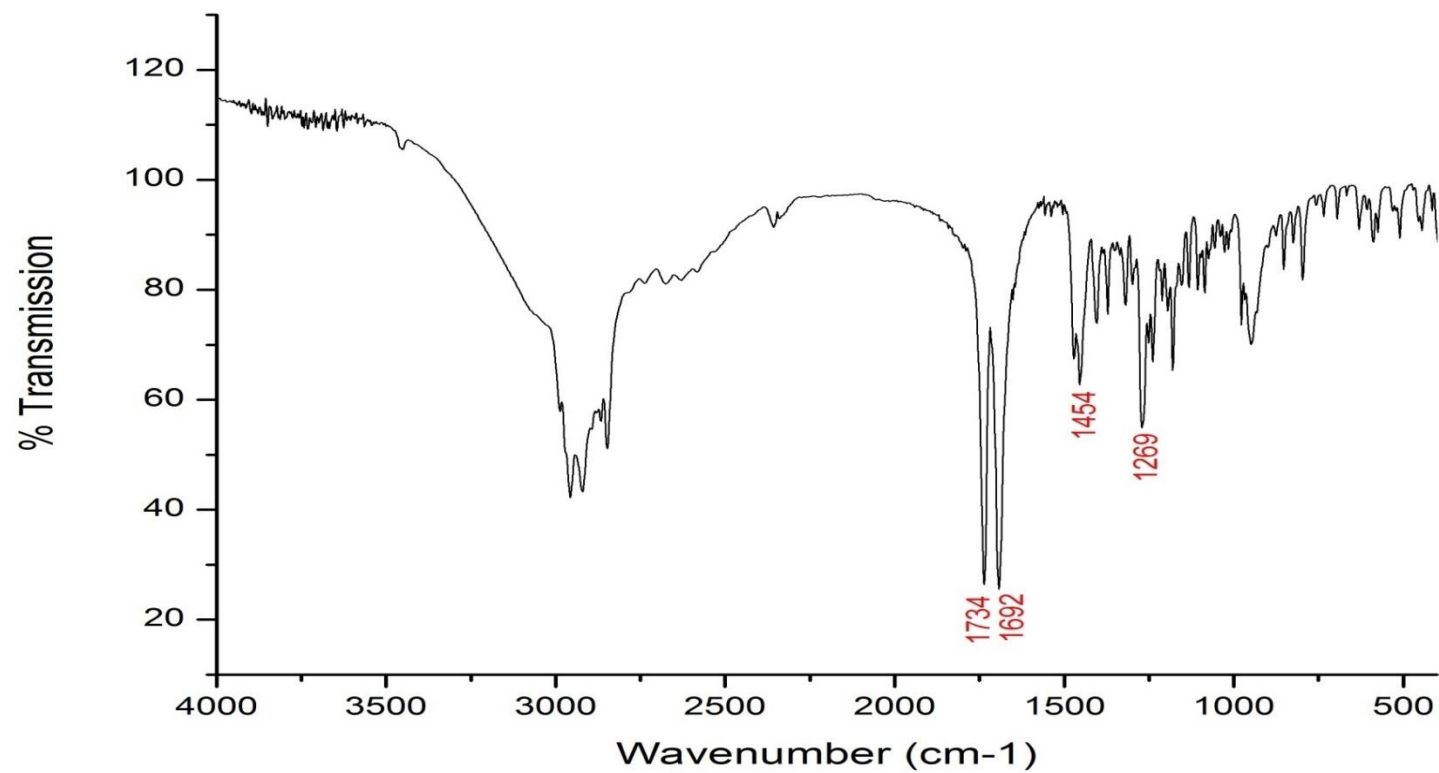
Table 32: ^{13}C NMR chemical shifts (δ , ppm) for compounds **5l—4f**.

^{13}C	5l	6k	2g	3g	5m	6m	7k	4f
1	39.7	39.8	39.5	39.8	39.6	39.8	39.8	39.8
2	18.9	18.9	18.7	18.8	18.7	18.9	18.9	18.9
3	37.9	37.8	37.6	37.6	37.9	37.9	37.9	37.9
4	43.9	43.9	43.6	43.7	43.6	43.2	43.8	43.9
5	57.1	57.2	56.8	56.9	56.8	56.7	57.2	57.3
6	21.7	21.7	21.5	21.6	21.5	21.7	21.7	21.7
7	41.3	36.2	40.7	39.4	37.6	37.8	39.5	39.3
8	39.6	41.4	41.4	41.4	41.5	41.1	41.3	40.6
9	55.3	55.6	54.8	54.8	55.4	55.3	55.7	54.9
10	38.1	38.1	38.3	38.3	38.3	38.0	38.1	38.0
11	19.8	20.0	20.3	20.6	19.7	19.8	20.0	20.5
12	32.1	33.9	37.4	36.6	34.3	34.5	33.9	38.9
13	54.1	48.7	45.2	44.7	50.6	50.0	48.9	44.2
14	48.9	51.1	55.8	55.9	50.5	50.8	50.9	55.9
15	48.9	41.1	39.5	41.1	40.6	40.9	40.9	41.1
16		164.7	171.7	163.5	170.9	162.7	162.2	174.1
17	65.0	67.9	22.1	22.2	66.4	65.9	68.0	24.9
18	28.9	28.9	28.9	29.0	28.9	28.5	28.9	28.9
19	176.9	177.0	184.4	184.0	183.7	178.1	177.9	177.1
20	13.2	13.5	12.8	13.6	12.9	13.1	13.4	13.4
1'	135.9	136.1	128.8	139.6	128.8	138.8	136.1	136.1
2'	128.3	128.2	137.2	111.4	137.7	111.1	128.2	128.2
3'	128.5	128.4	129.5	126.1	129.9	125.6	128.4	128.4
4'	128.1	128.0	144.9	150.6	144.5	151.5	128.0	127.9
5'	128.5	128.4	123.4	126.1	123.4	125.6	128.4	128.4
6'	128.3	128.2	116.2	111.4	115.8	111.1	128.2	128.2
7''	66.1	65.9					65.9	65.9
1							25.2	22.2
2							177.0	158.7
3							18.0	17.6

Table 33: ^{13}C NMR chemical shifts (δ , ppm) for compounds **3a–8m**.

^{13}C	3a	3b	3c	3h	^{13}C	4g	5g	7m	8m
1	39.8	39.9	39.9	40.6	1	39.8	39.7	39.8	39.7
2	18.9	18.9	18.9	19.1	2	18.9	18.9	18.8	18.9
3	37.3	38.1	38.1	38.1	3	37.9	37.8	37.9	37.8
4	44.1	44.0	43.7	44.1	4	43.8	43.9	43.8	43.9
5	57.1	57.2	57.1	56.9	5	57.1	57.2	57.0	57.1
6	21.6	21.7	21.7	21.9	6	21.6	21.7	21.6	21.7
7	41.5	41.7	39.5	41.3	7	40.9	39.4	37.9	37.0
8	39.5	41.9	40.6	41.6	8	41.4	41.4	41.5	41.7
9	54.7	55.8	54.9	53.7	9	54.8	54.7	55.4	55.4
10	38.1	38.1	38.1	39.4	10	38.1	38.1	38.1	38.2
11	20.3	20.4	20.4	20.4	11	20.4	20.5	19.9	20.0
12	38.0	33.7	36.7	39.2	12	37.4	36.4	34.2	34.1
13	48.7	42.1	44.0	80.3	13	45.2	44.7	50.6	49.8
14	54.3	55.3	56.3	47.4	14	55.9	55.9	50.6	50.7
15	48.5	42.8	40.9	46.9	15	39.4	41.1	40.8	40.9
16		80.5	170.4	156.2	16	171.1	163.5	170.6	163.6
17	19.8	24.9	22.1	102.9	17	22.1	22.2	66.5	65.9
18	29.1	29.1	29.0	28.9	18	28.9	28.9	28.9	28.9
19	176.8	177.0	176.9	176.9	19	176.9	177.0	176.8	176.9
20	13.5	13.5	13.5	15.7	20	13.3	13.6	13.3	13.6
1'	127.4	127.5	127.0	127.5	1'	145.2	139.6	144.7	140.1
2'	130.0	130.0	130.1	130.1	2'	137.5	111.4	137.9	111.5
3'	114.0	113.9	113.9	113.9	3'	129.8	126.2	130.1	126.2
4'	163.9	163.9	163.9	163.9	4'	128.9	150.5	129.2	149.8
5'	114.0	113.9	113.9	113.9	5'	123.5	126.2	123.5	126.2
6'	130.0	130.0	130.1	130.1	6'	116.4	111.4	115.9	111.5
7'	190.9	191.1	191.0	191.0	1''	135.9	136.2	135.9	136.2
8'	65.2	65.2	65.2	65.2	2''	128.5	128.0	128.5	128.5
9'	55.5	55.5	55.5	55.5	3''	128.5	128.5	128.6	128.0
					4''	128.2	128.0	128.2	128.0
					5''	128.5	128.5	128.6	128.0
					6''	128.5	128.0	128.5	128.5
					7''	66.2	65.9	66.5	67.2

7.4 SPECTRA

Figure 34: IR spectrum of compound **1a**.

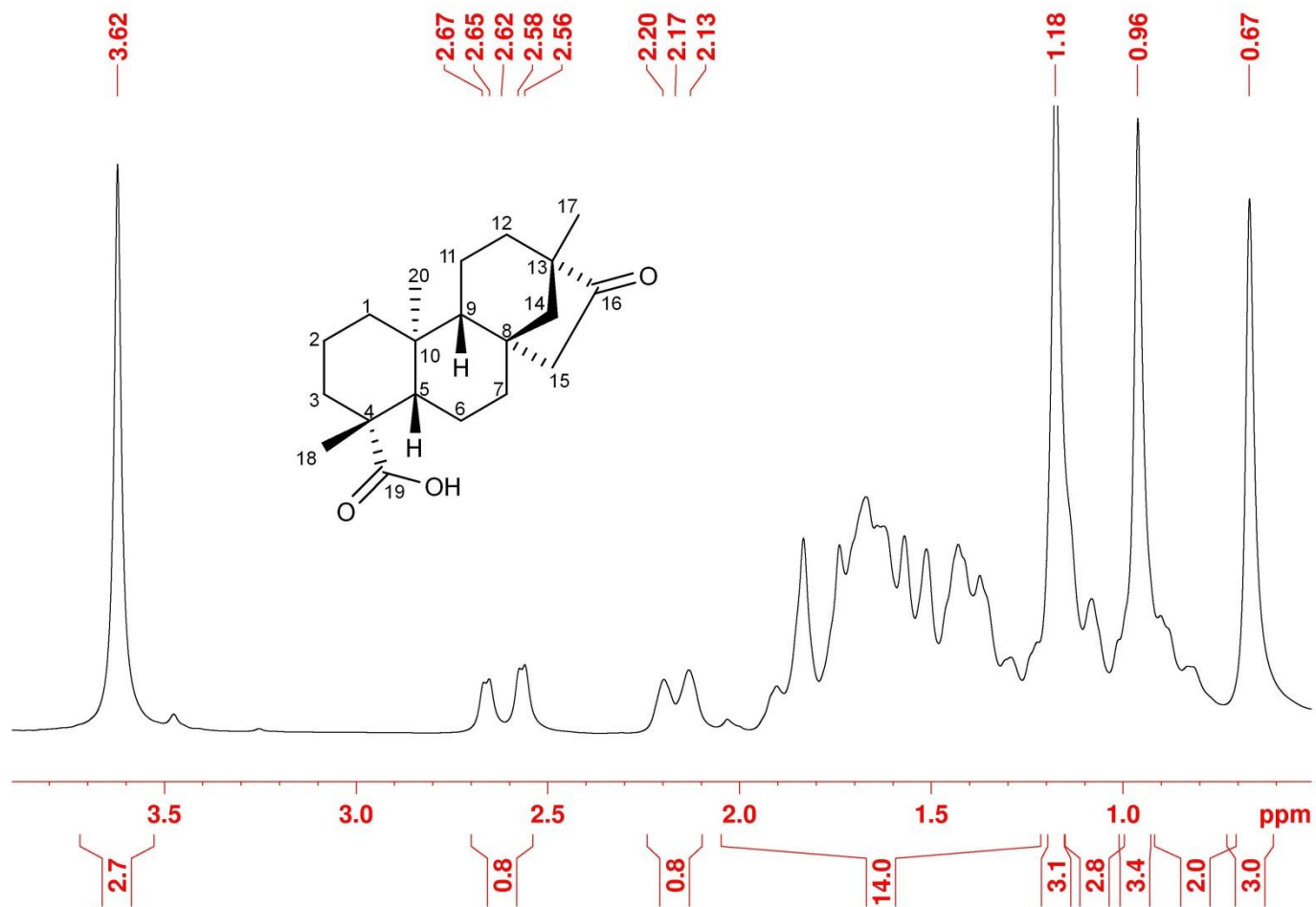


Figure 35: $^1\text{H-NMR}$ (200 MHz, CDCl_3) spectrum of compound **1a**.

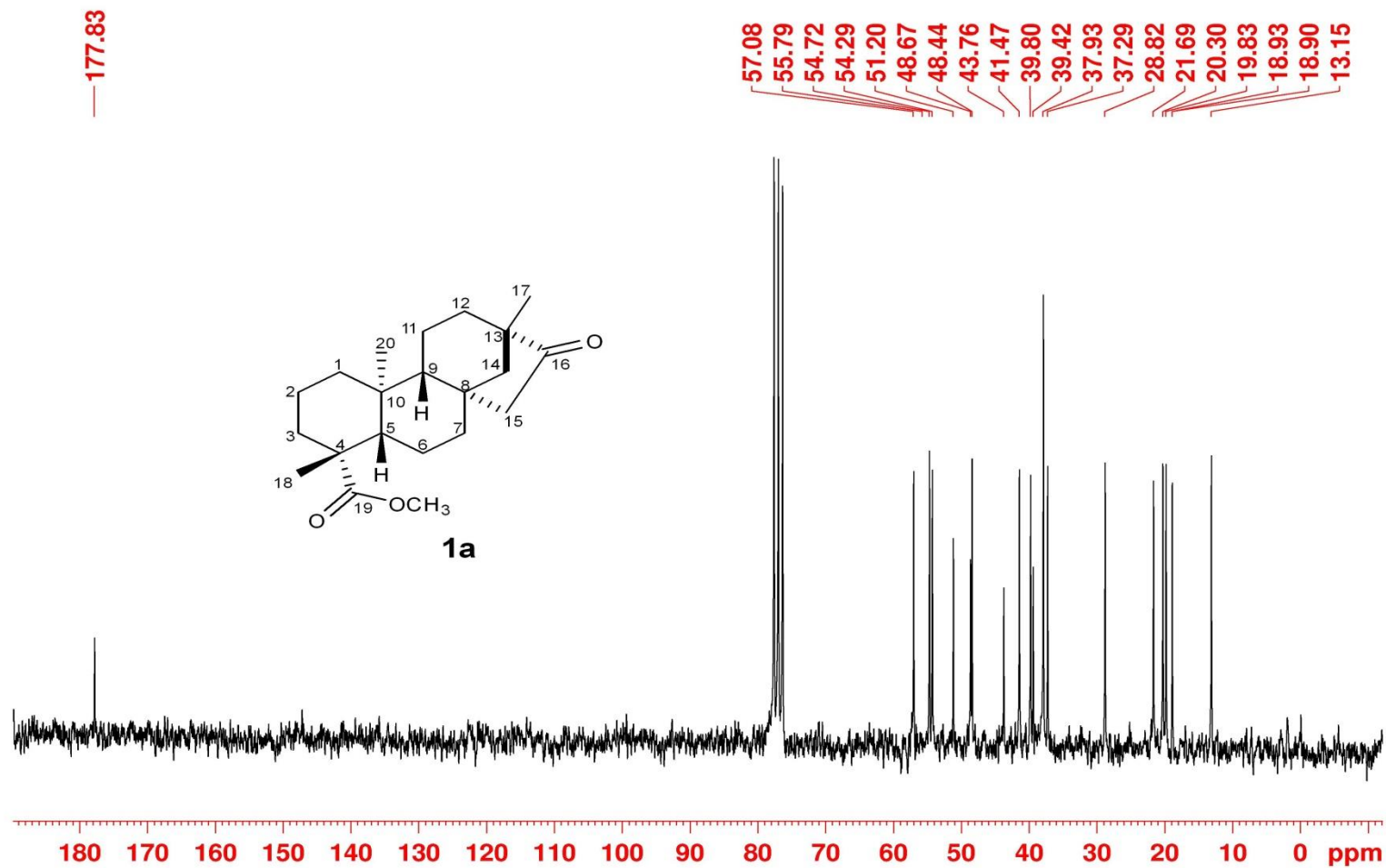


Figure 36: $^{13}\text{C} \{^1\text{H}\}$ NMR (50 MHz, CDCl_3) spectrum of compound **1a**.

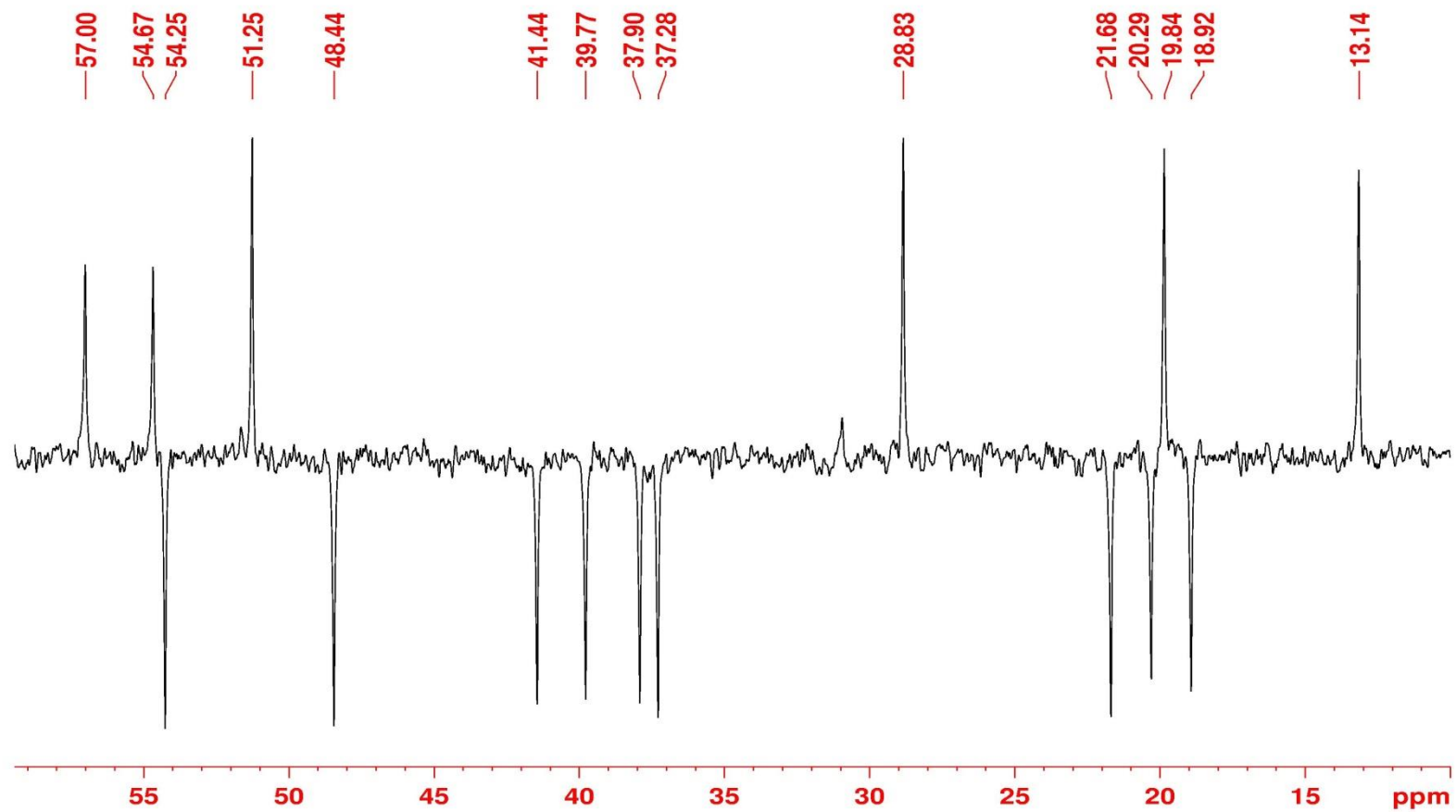


Figure 37: ^{13}C { ^1H } DEPT NMR (50 MHz, CDCl_3) spectrum of compound **1a**.

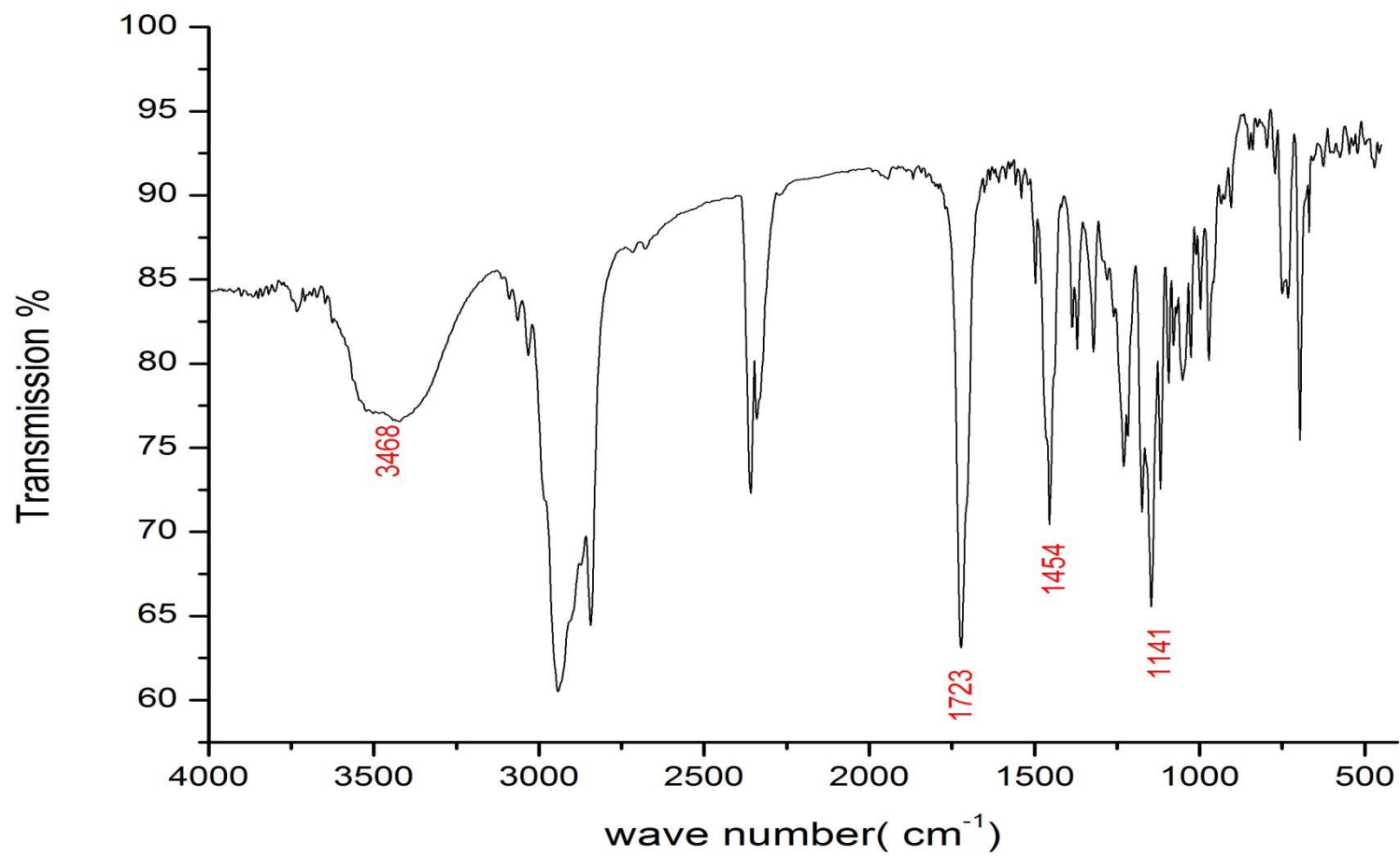


Figure 38: IR spectrum of compound **1b**.

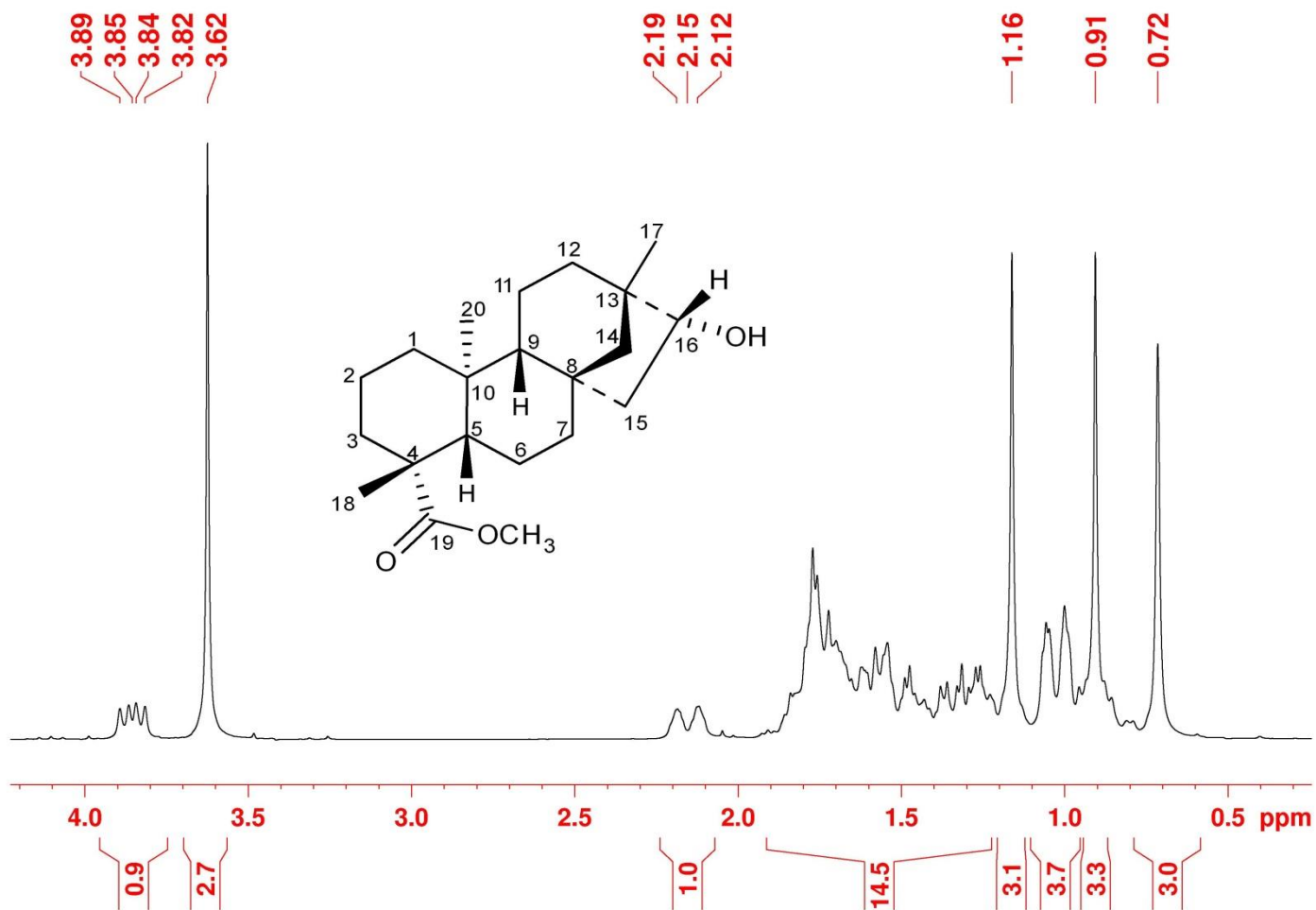


Figure 39: ¹H-NMR (200 MHz, CDCl₃) spectrum of compound **1b**.

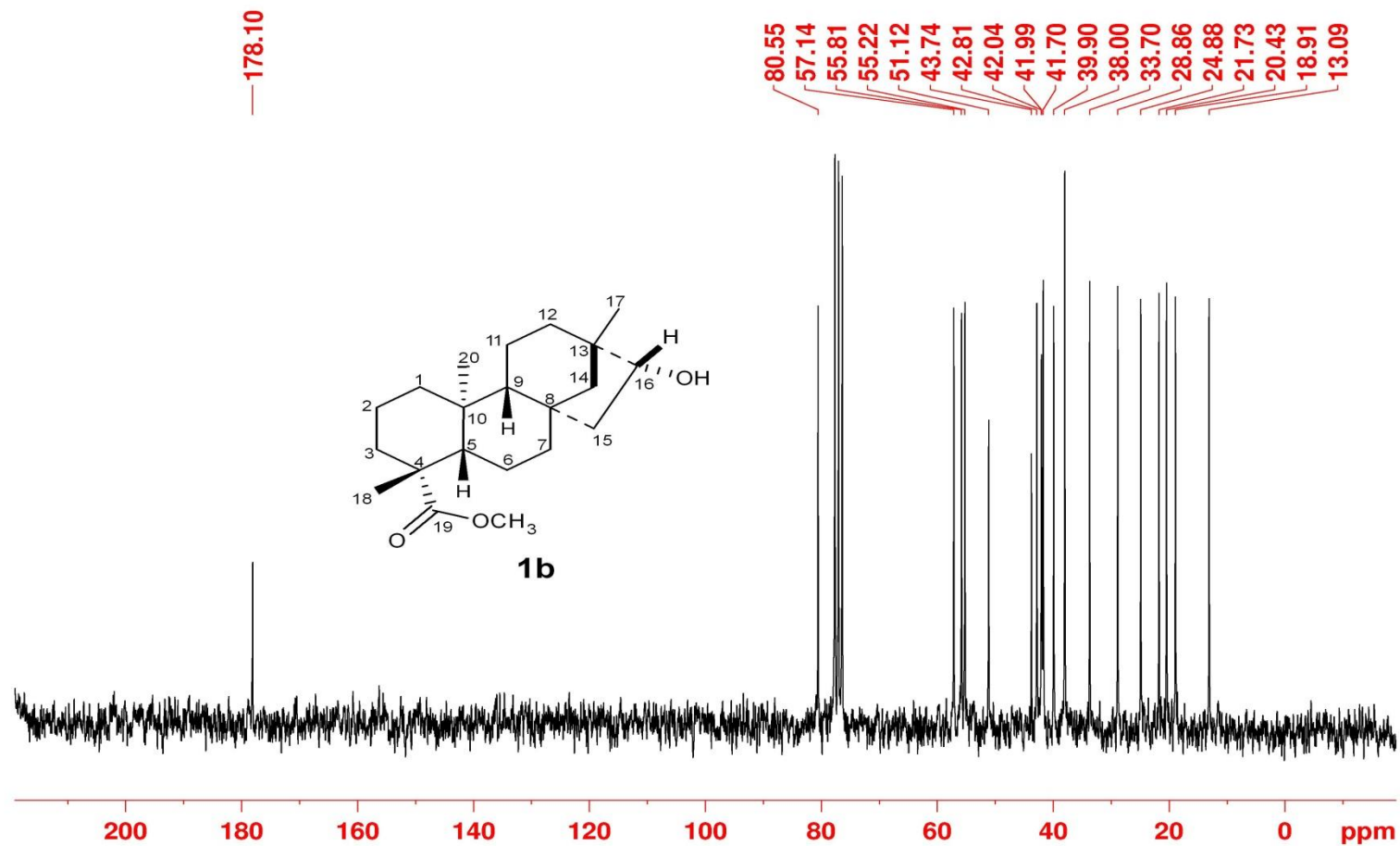


Figure 40 ^{13}C $\{^1\text{H}\}$ NMR (50 MHz, CDCl_3) spectrum of compound **1b**.

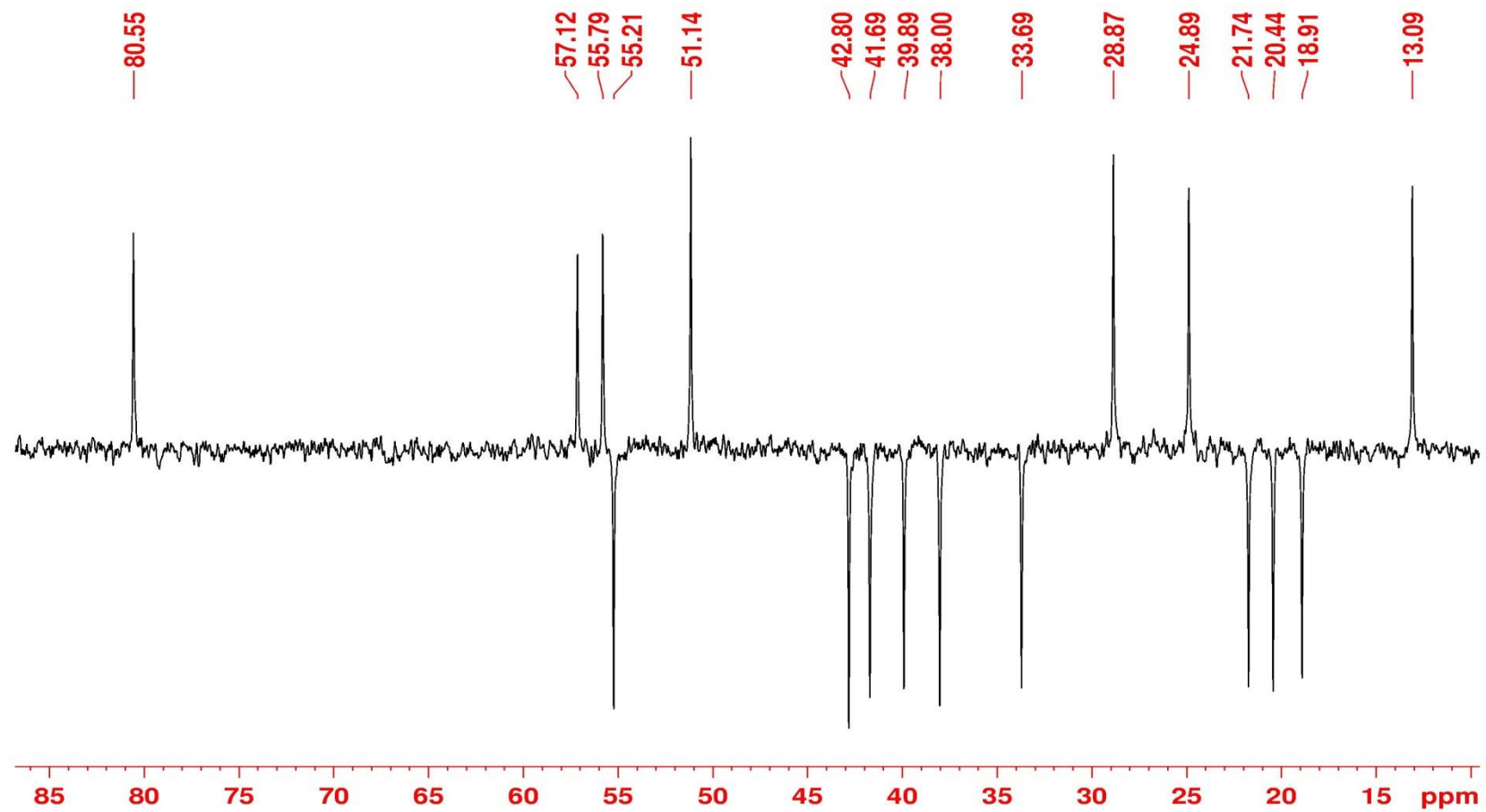
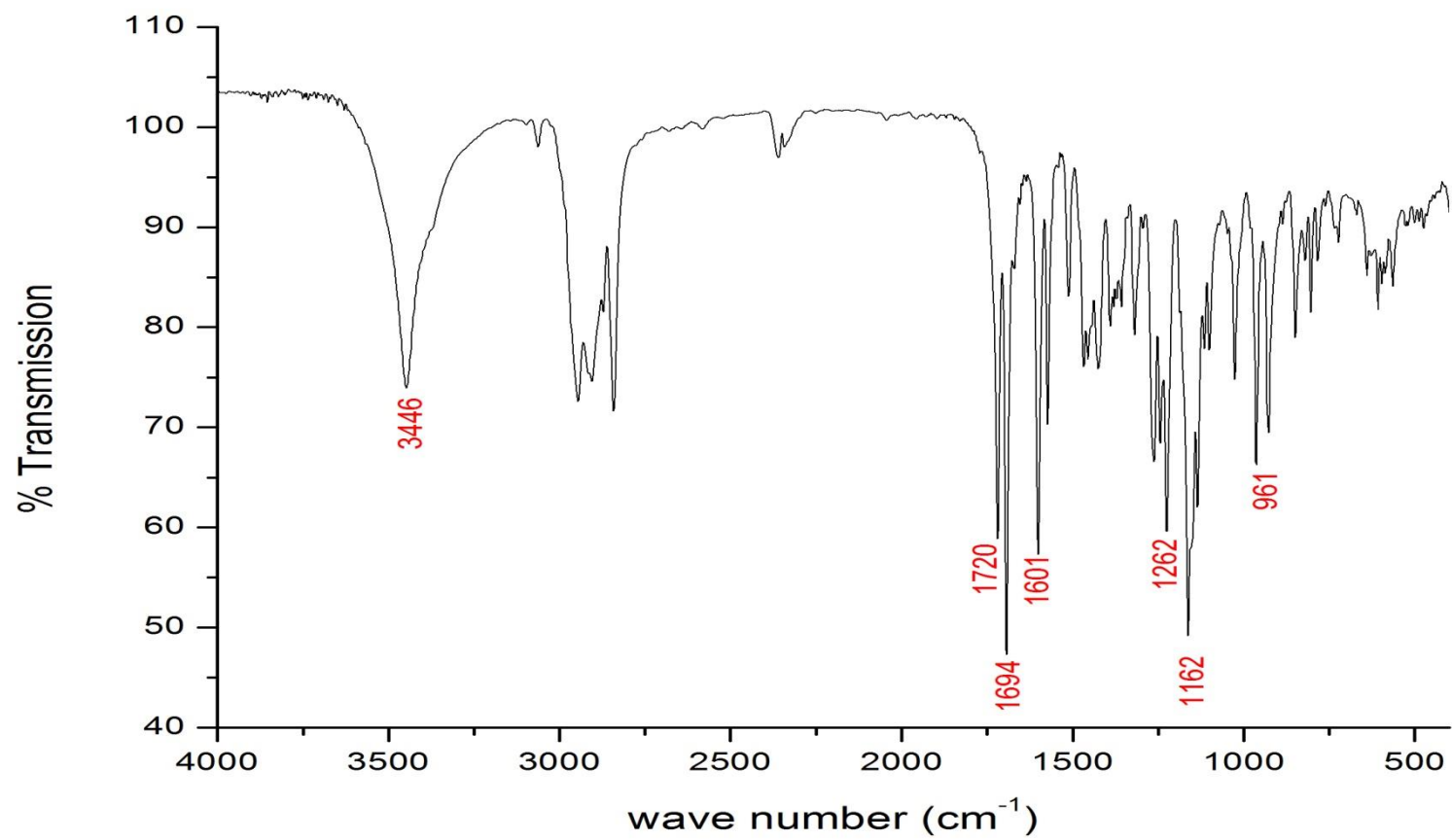


Figure 41: ^{13}C { ^1H } DEPT NMR (50 MHz, CDCl_3) spectrum of compound **1b**.

Figure 42: IR spectrum of compound **1c**.

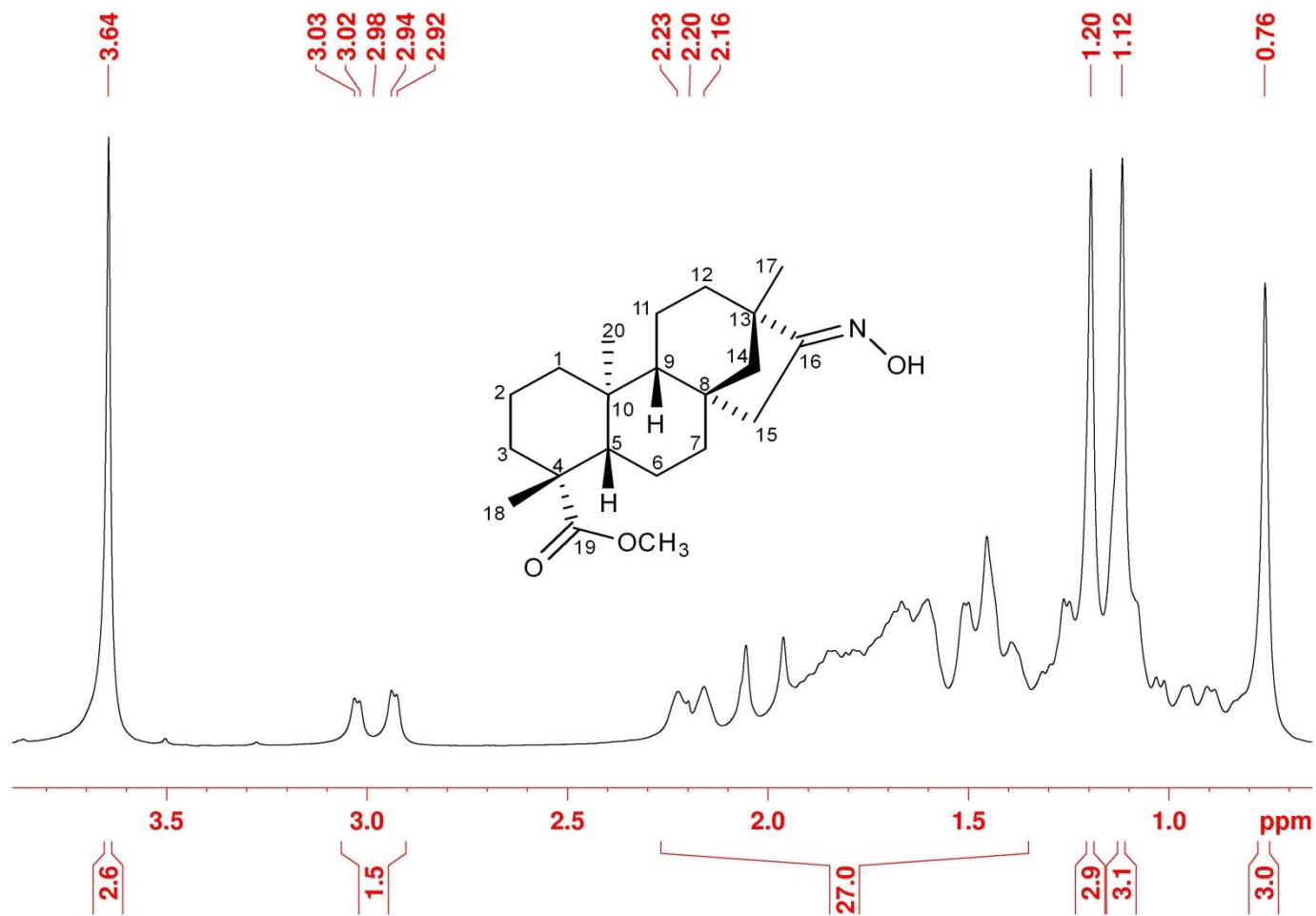


Figure 43: $^1\text{H-NMR}$ (200 MHz, CDCl_3) spectrum of compound **1c**.

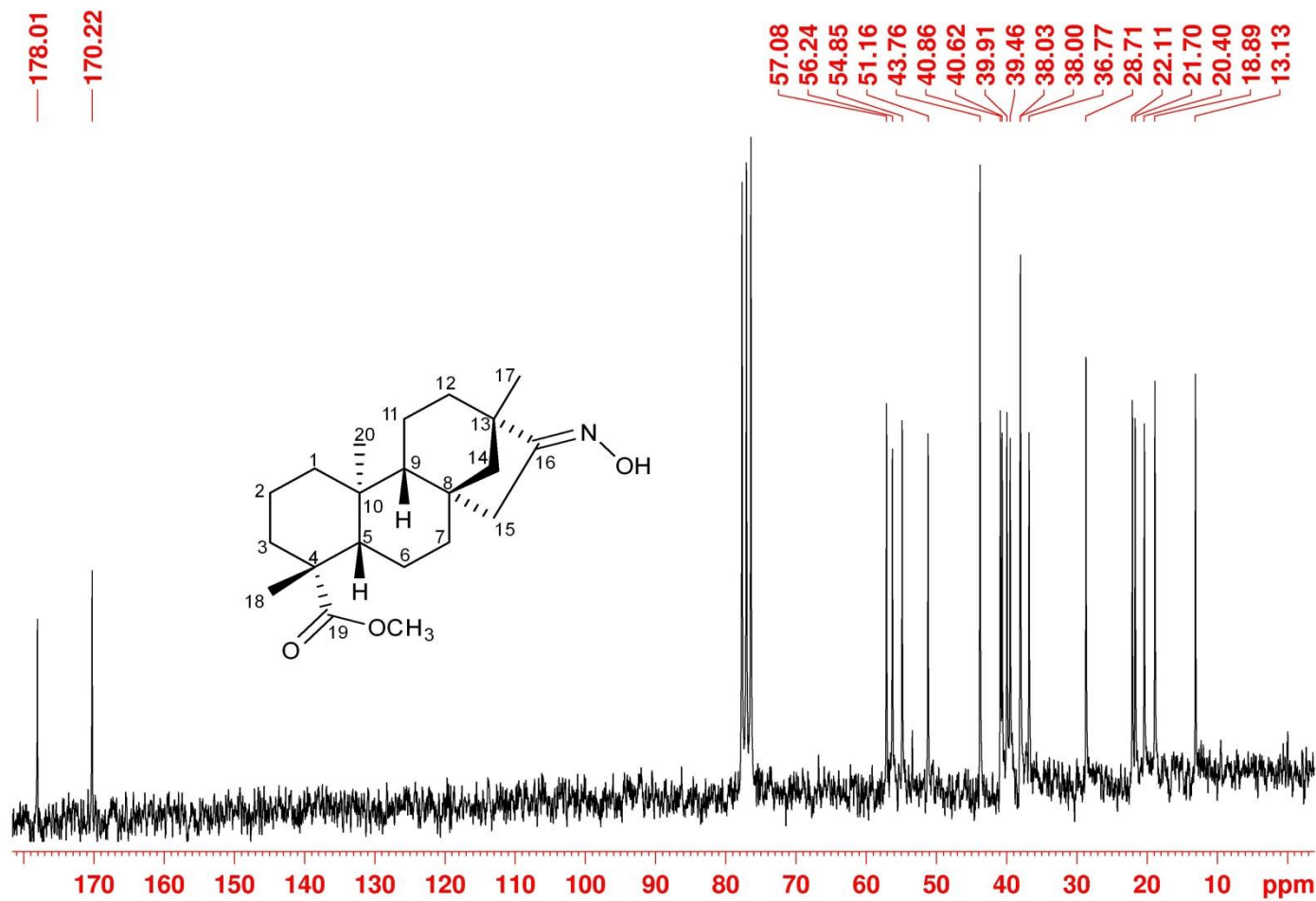


Figure 44: ^{13}C $\{^1\text{H}\}$ NMR (50 MHz, CDCl_3) spectrum of compound **1c**.

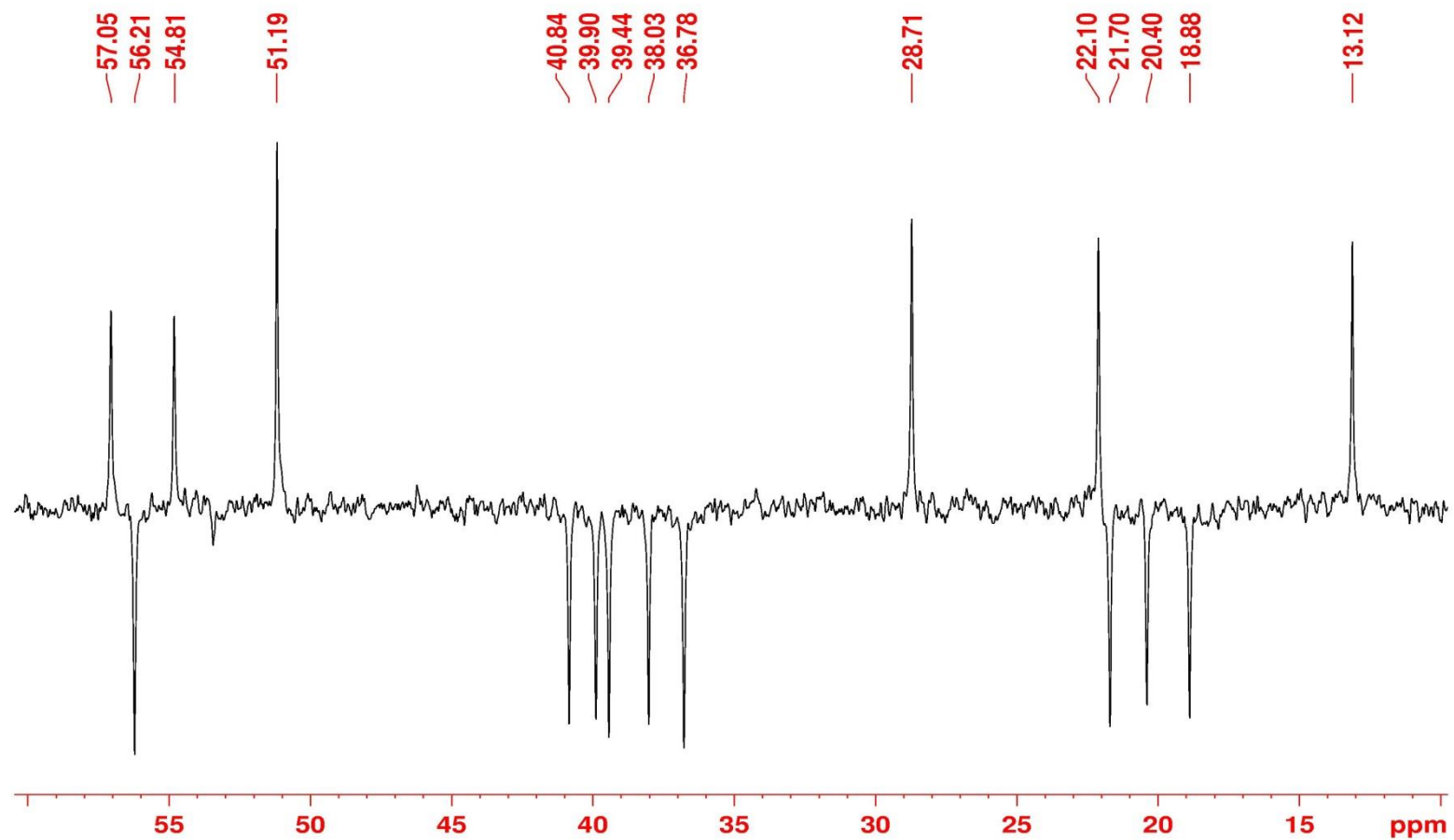


Figure 45: ^{13}C $\{^1\text{H}\}$ DEPT NMR (50 MHz, CDCl_3) spectrum of compound **1c**.

IL_130806114724 #1832 RT: 4.35 AV: 1 NL: 2.39E2
T: ITMS + c ESI Full ms2 334.45@cid0.00 [90.00-500.00]

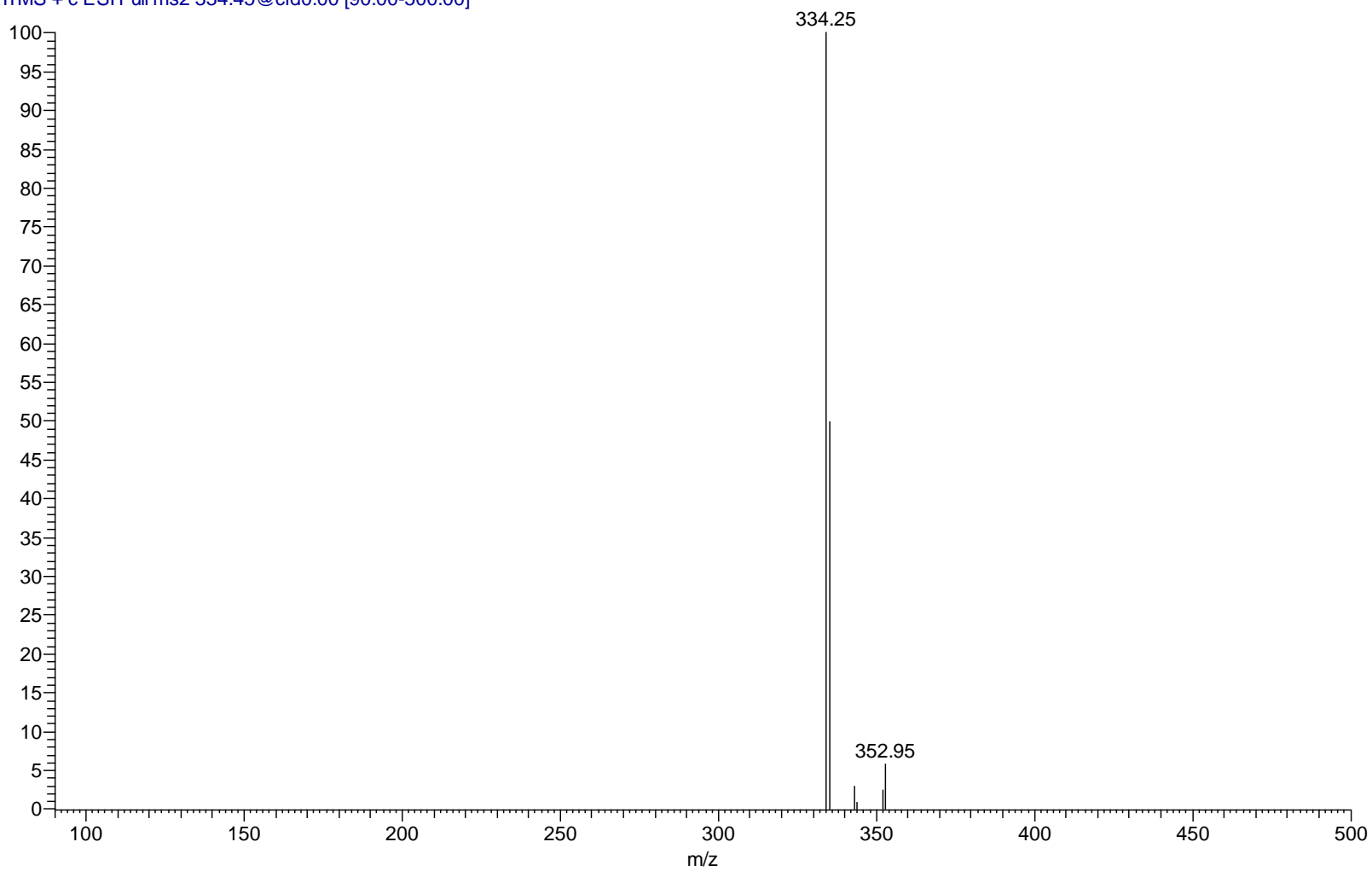
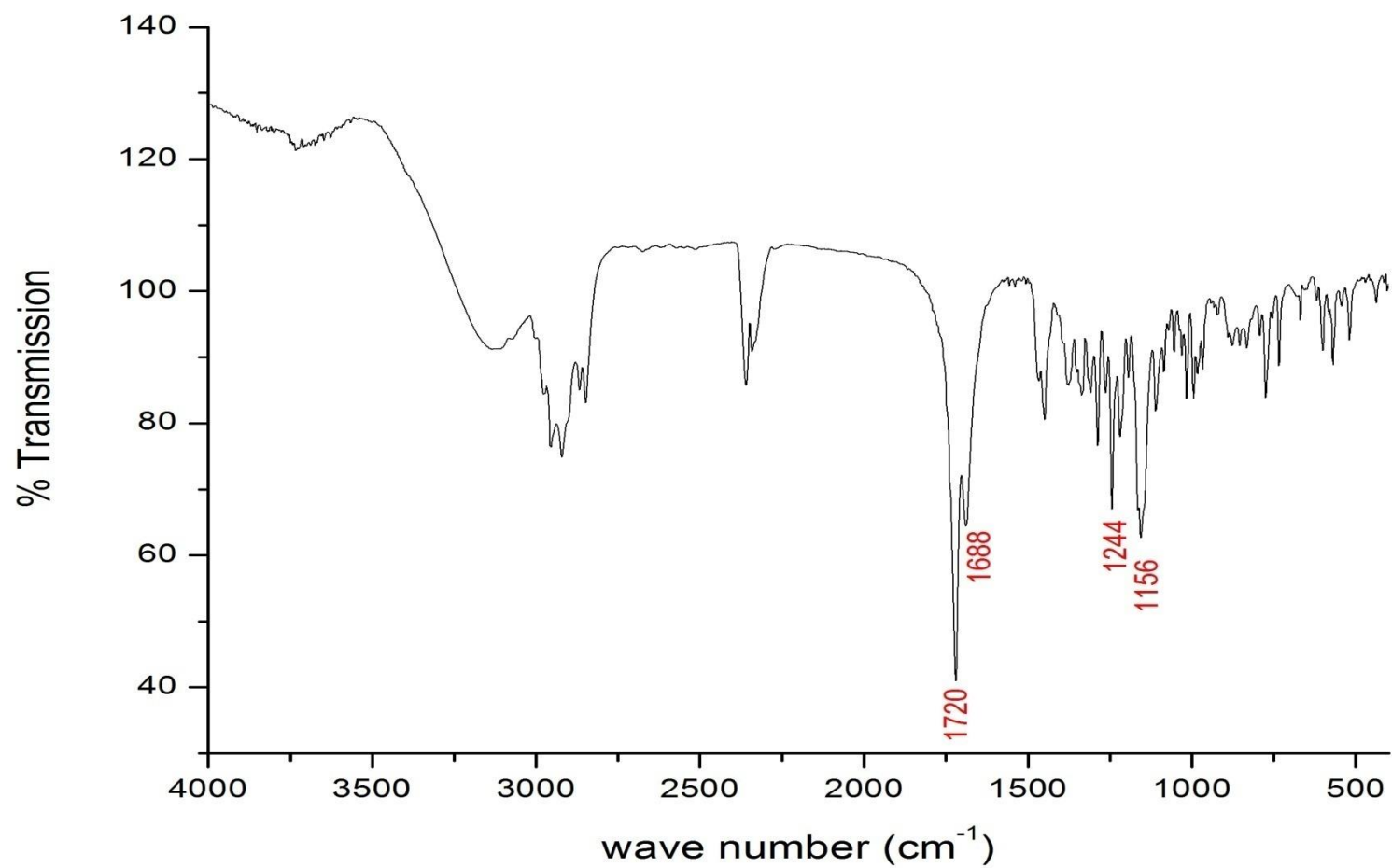


Figure 46: ESI-MS spectrum of compound **1d**.

Figure 47: IR spectrum of compound **1d**.

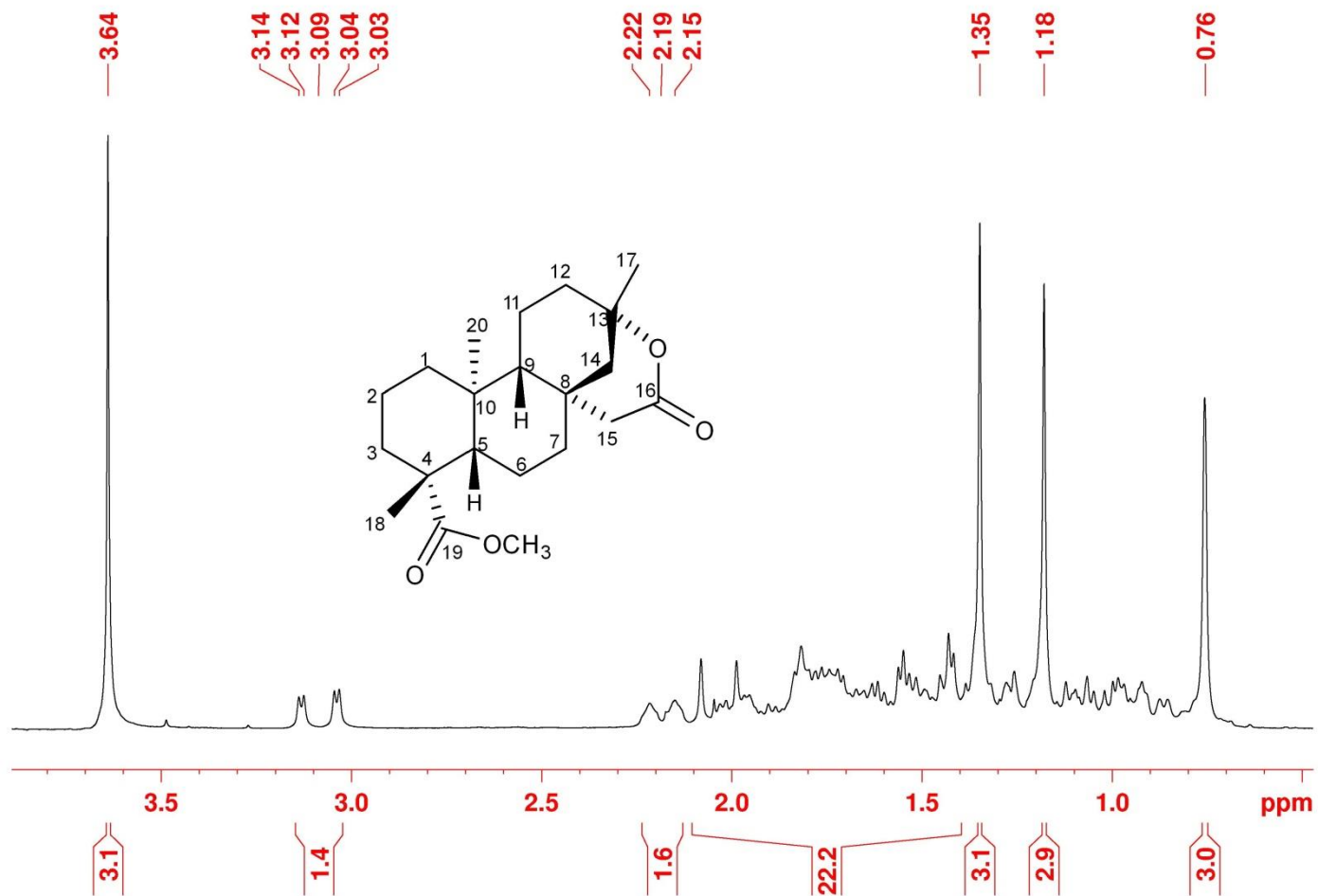


Figure 48: ¹H-NMR (200 MHz, CDCl₃) spectrum of compound **1d**.

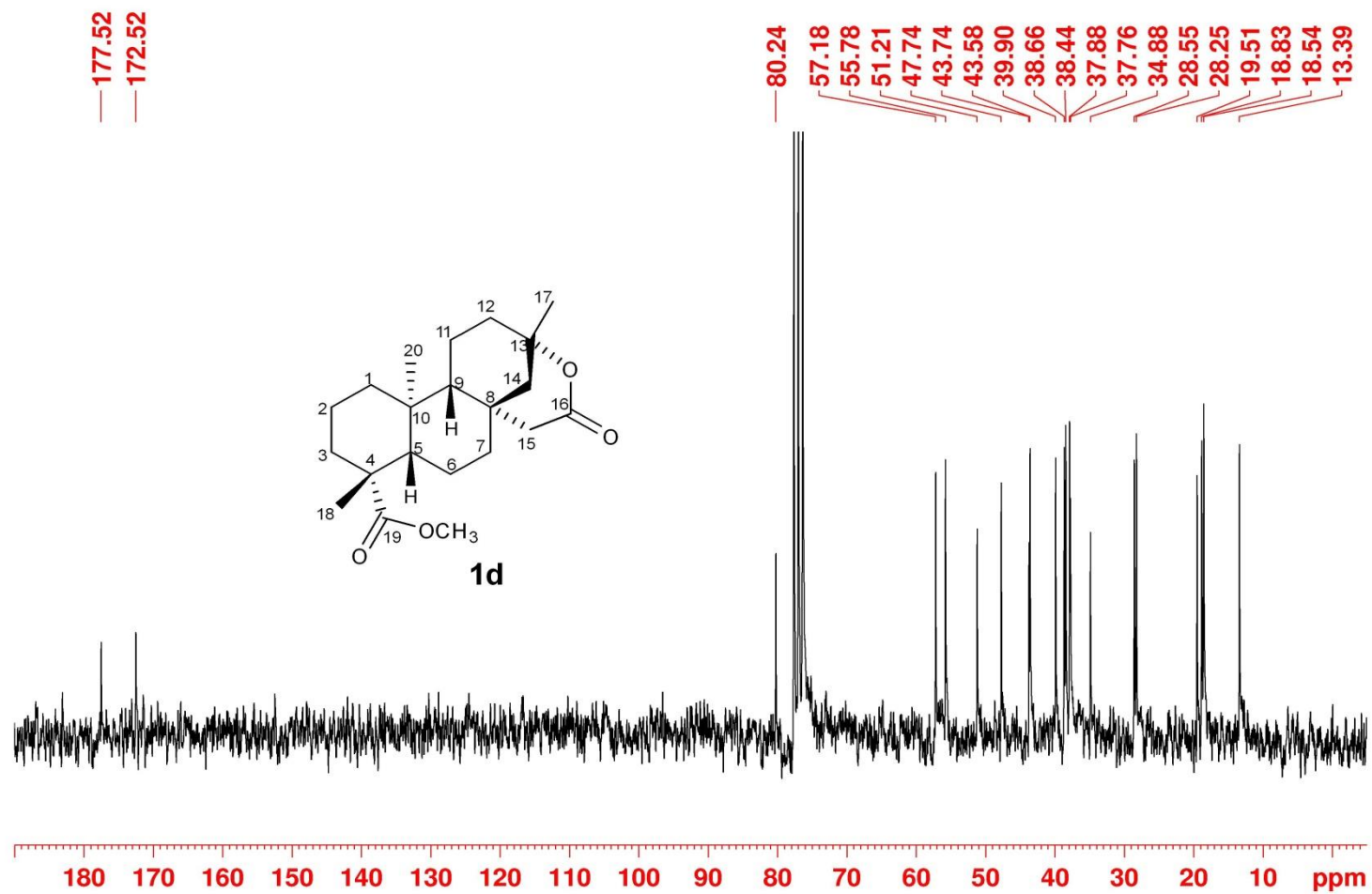


Figure 49: ^{13}C $\{^1\text{H}\}$ NMR (50 MHz, CDCl_3) spectrum of compound **1d**.

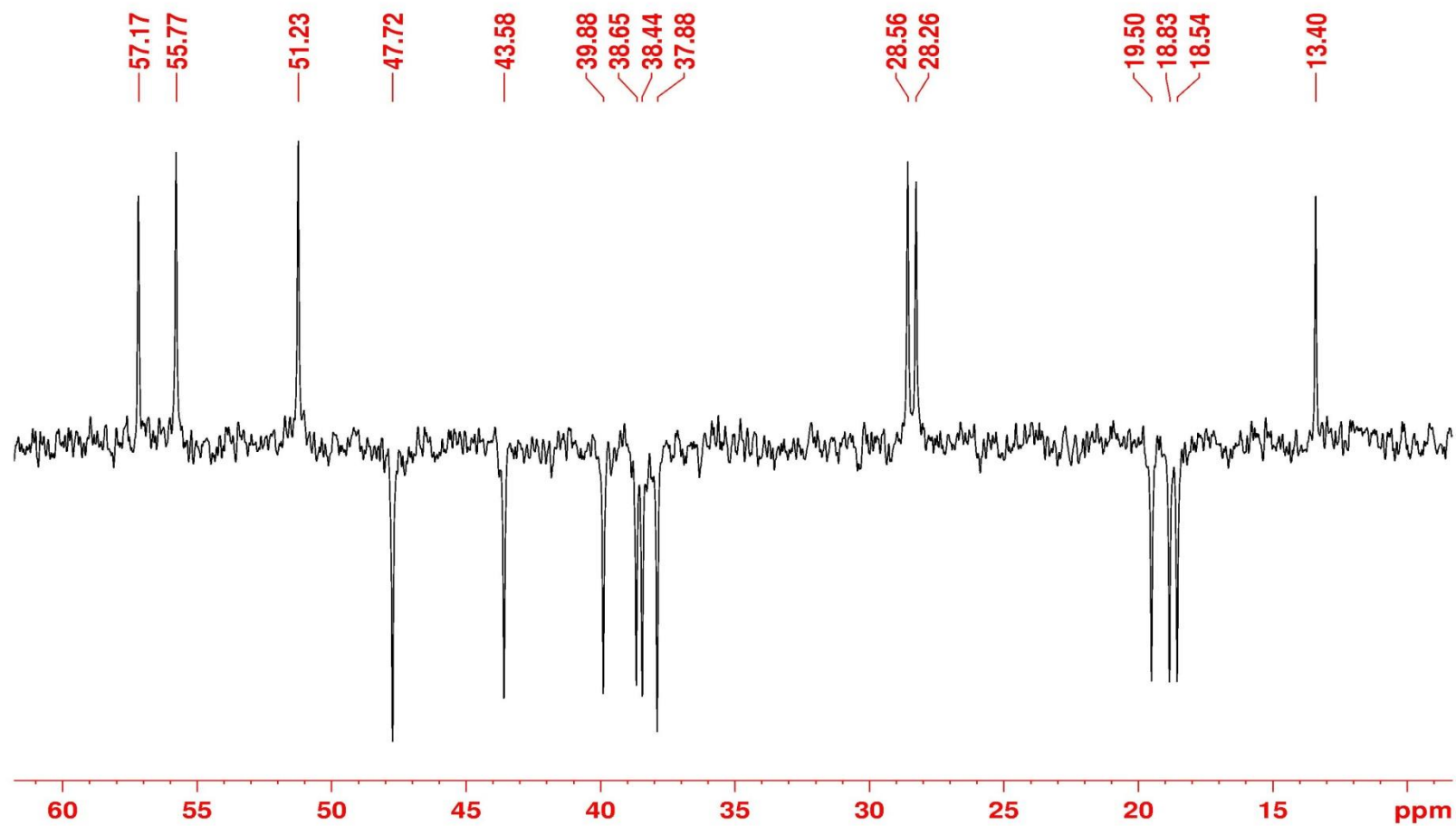


Figure 50: ^{13}C $\{^1\text{H}\}$ DEPT NMR (50 MHz, CDCl_3) spectrum of compound **1d**.

2OH_130805164801 #681 RT: 4.77 AV: 1 NL: 3.53E4
T: ITMS + c ESI Full ms2 723.40@cid30.00 [195.00-750.00]

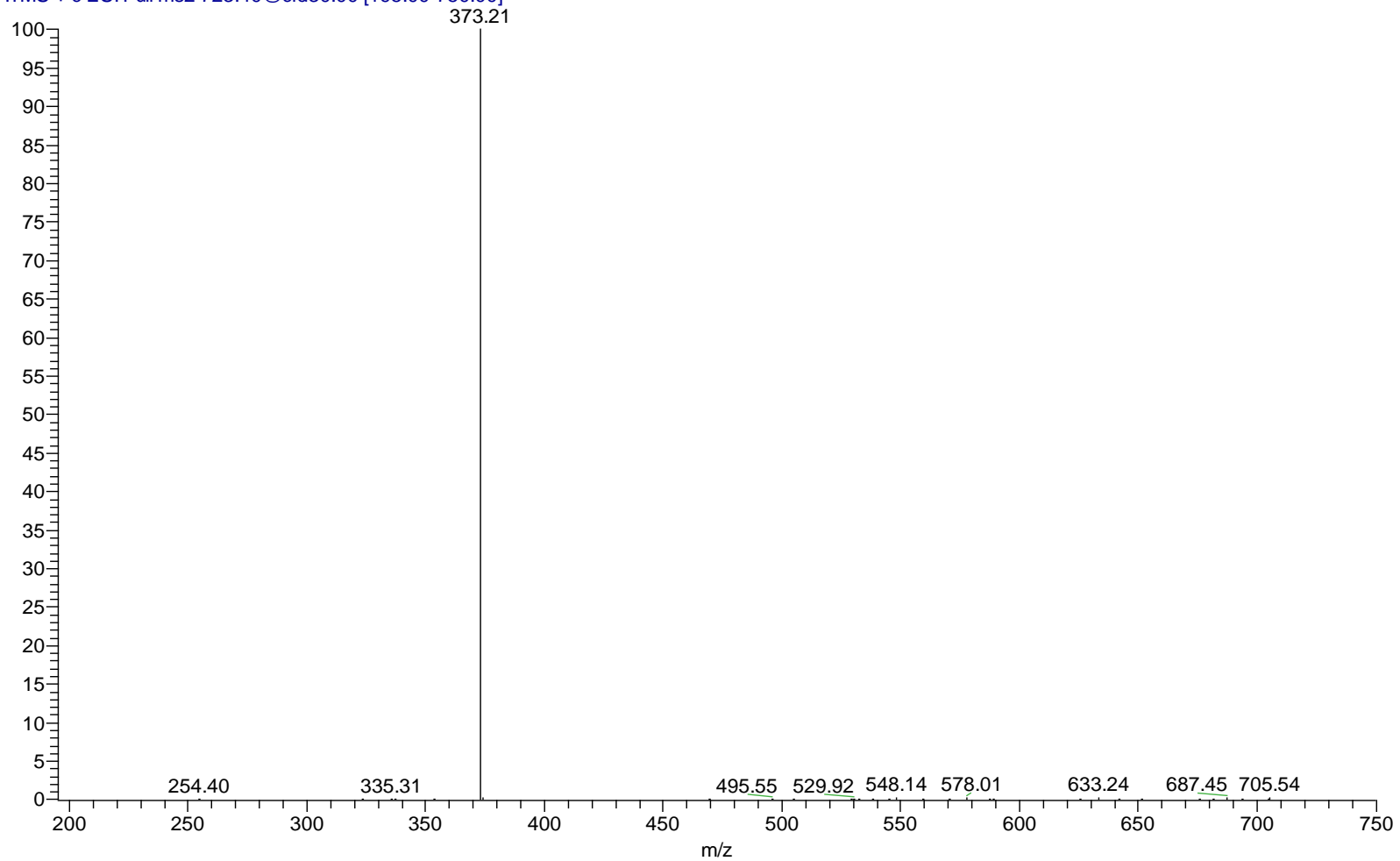
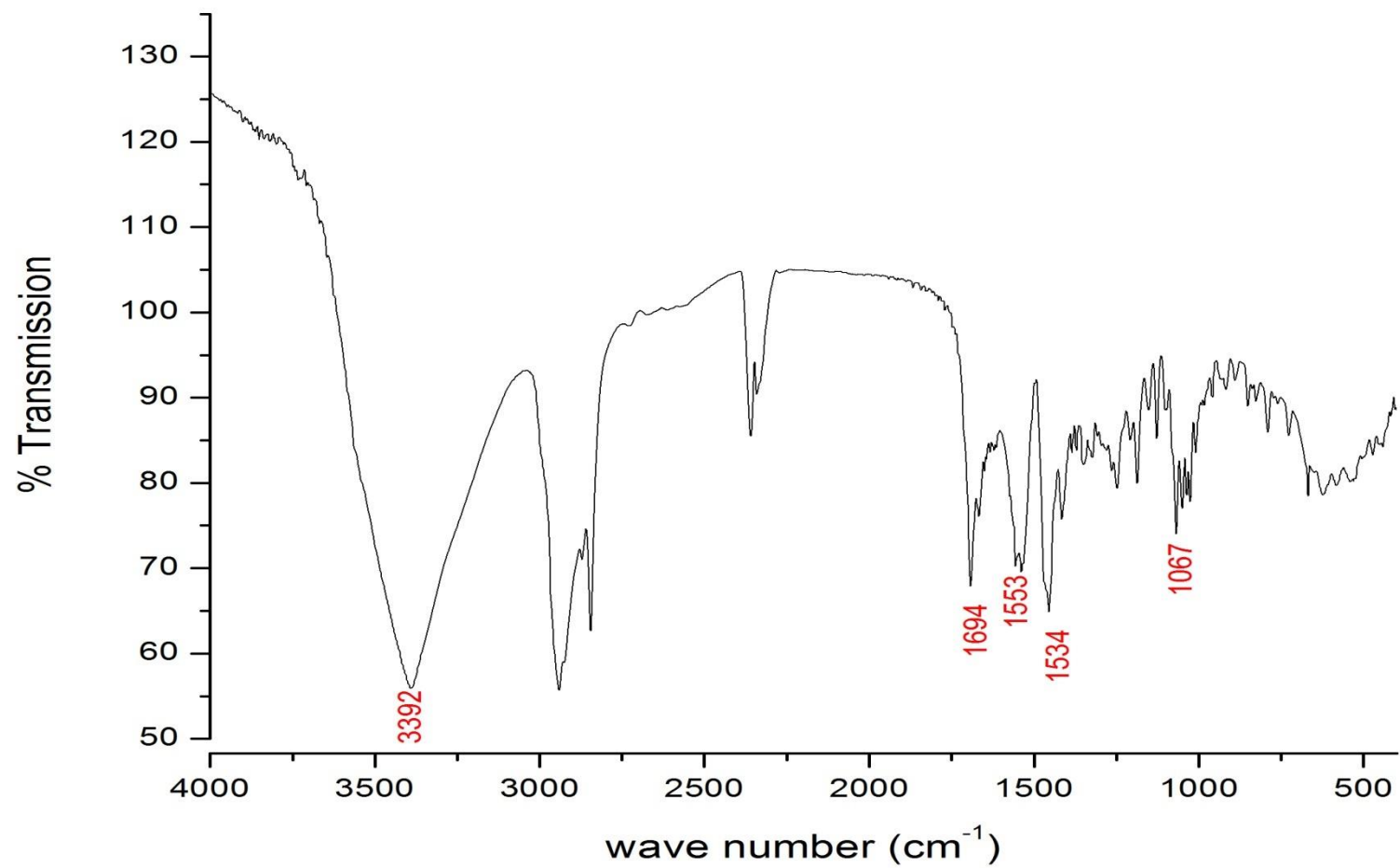


Figure 51: ESI-MS spectrum of compound **1e**.

Figure 52: IR spectrum of compound **1e**.

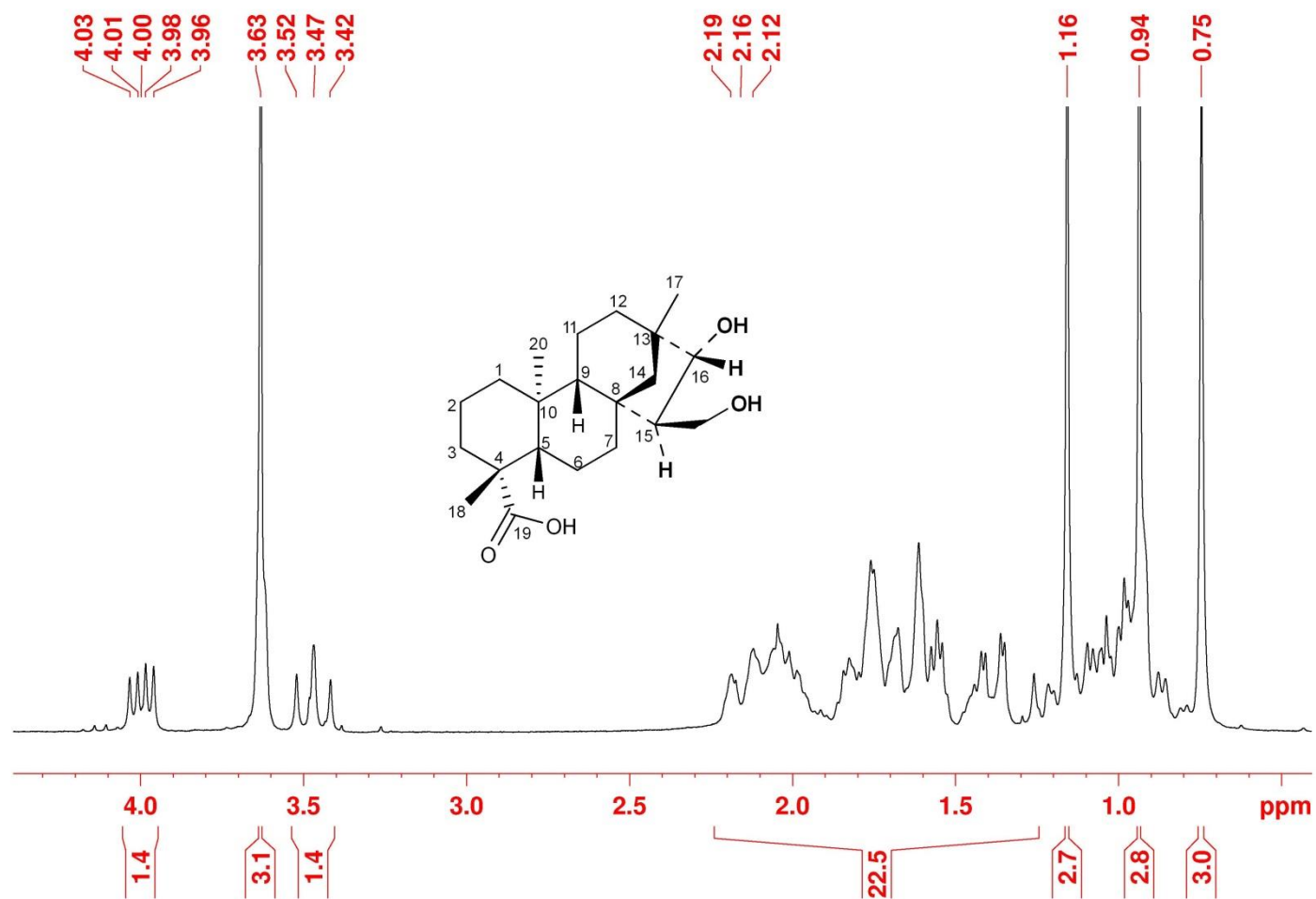


Figure 53: $^1\text{H-NMR}$ (200 MHz, CDCl_3) spectrum of compound **1e**.

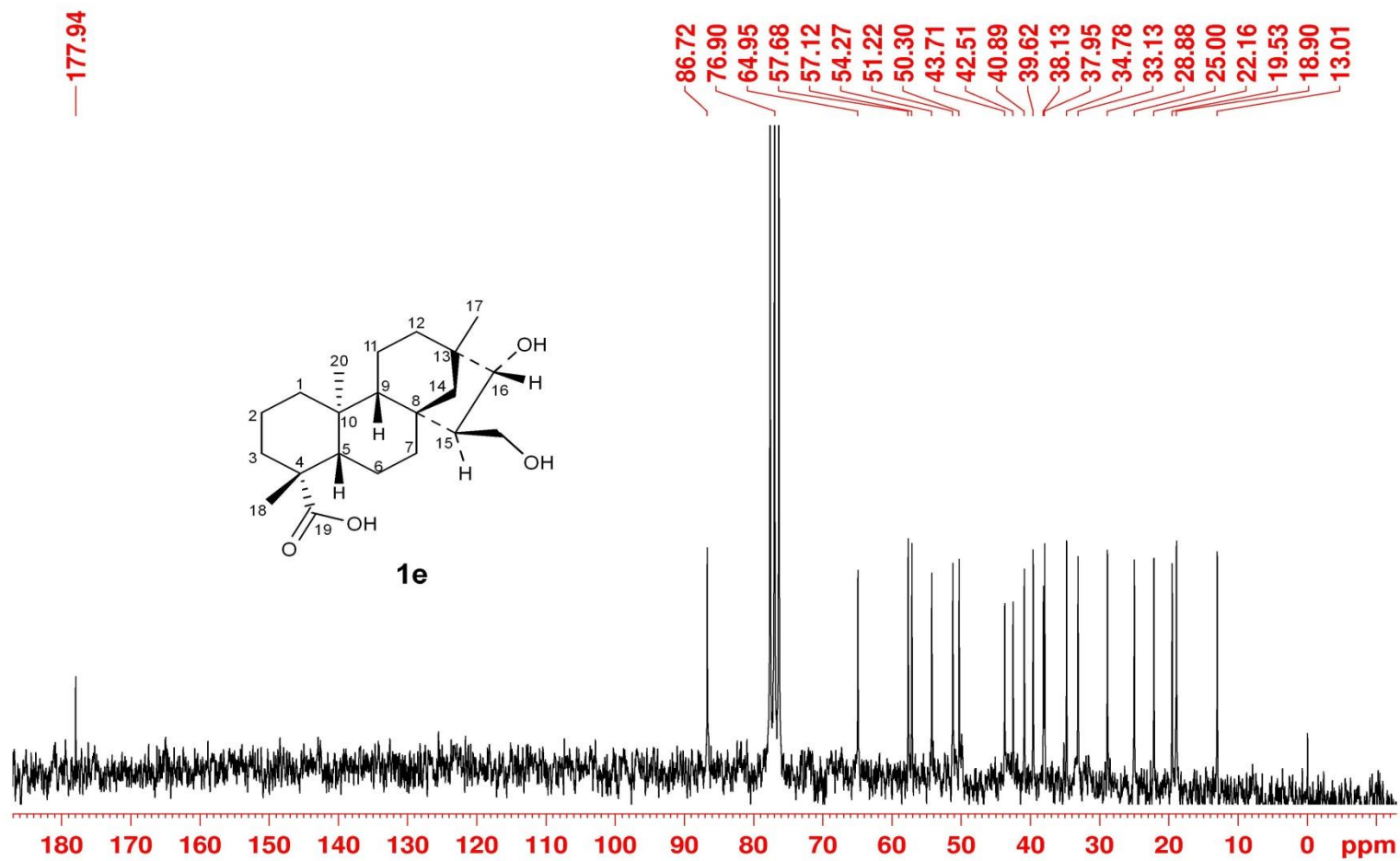


Figure 54: ^{13}C $\{^1\text{H}\}$ NMR (50 MHz, CDCl_3) spectrum of compound **1e**.

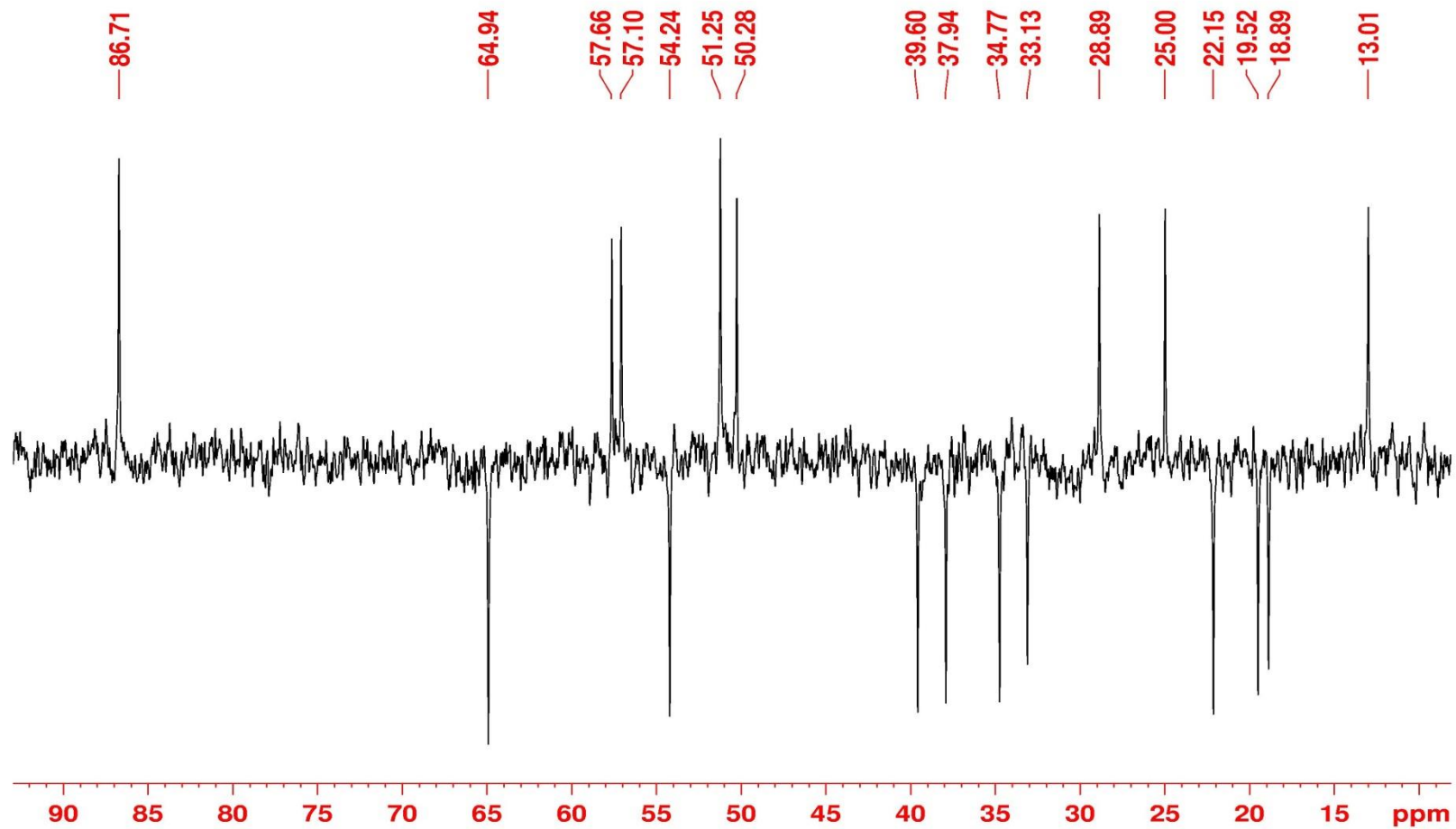


Figure 55: ^{13}C $\{^1\text{H}\}$ DEPT NMR (50 MHz, CDCl_3) spectrum of compound **1e**.

190-ASAD-ID4_131107172421 #548 RT: 1.64 AV: 1 NL: 1.81E6
T: ITMS + c ESI Full ms [90.00-1000.00]

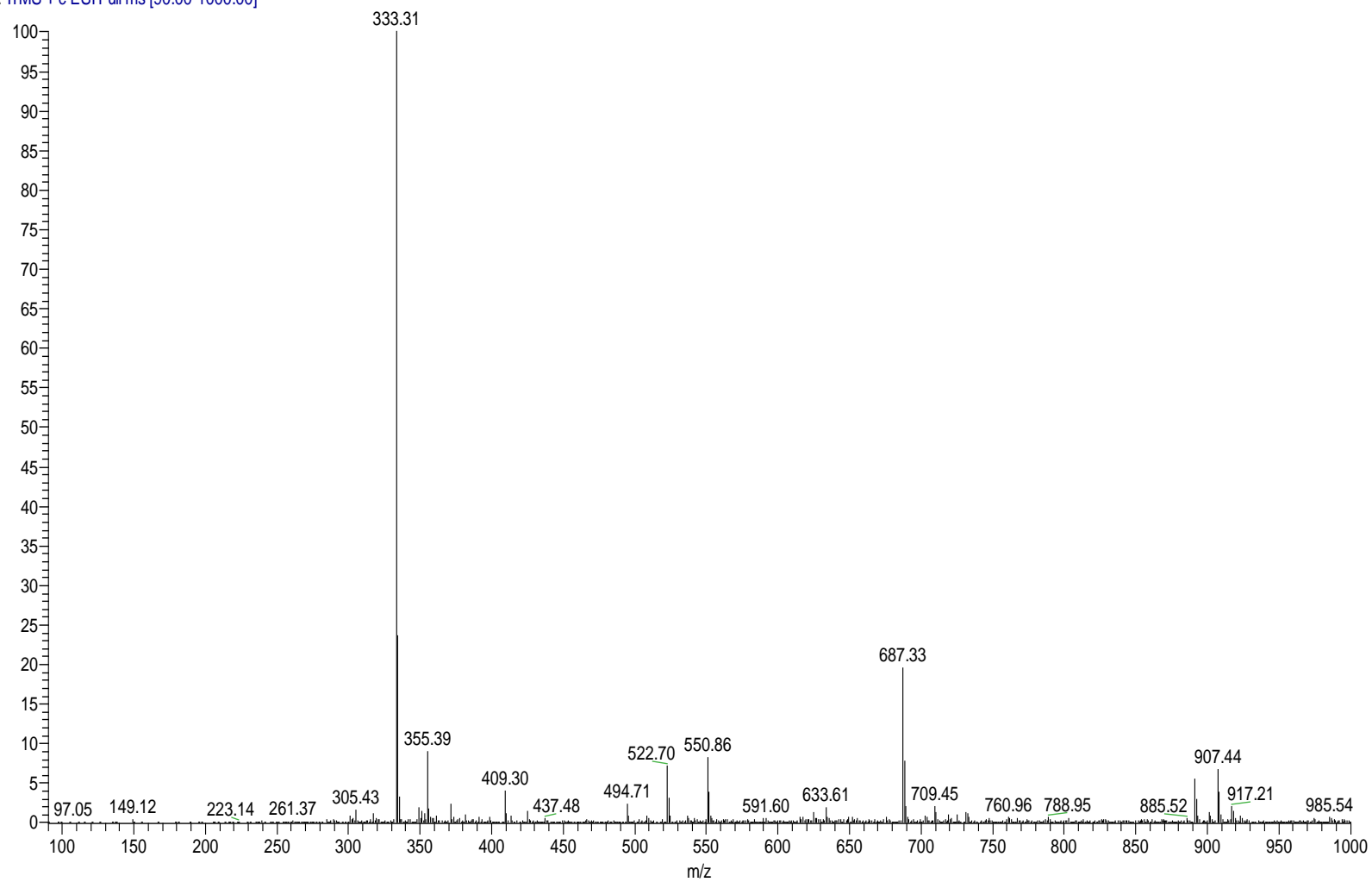


Figure 56: ESI-MS spectrum of compound **1f**.

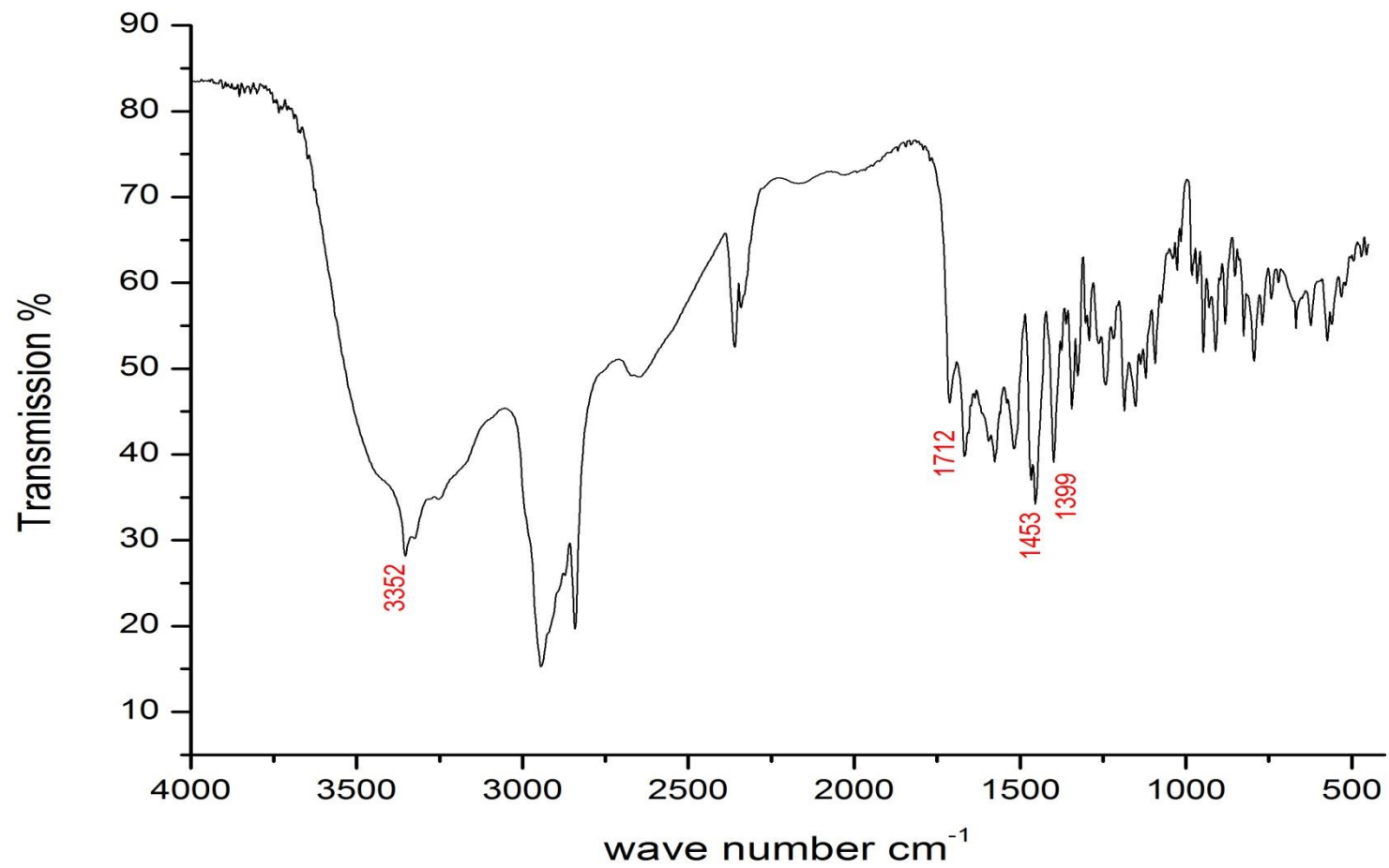


Figure 57: IR spectrum of compound **1f**.

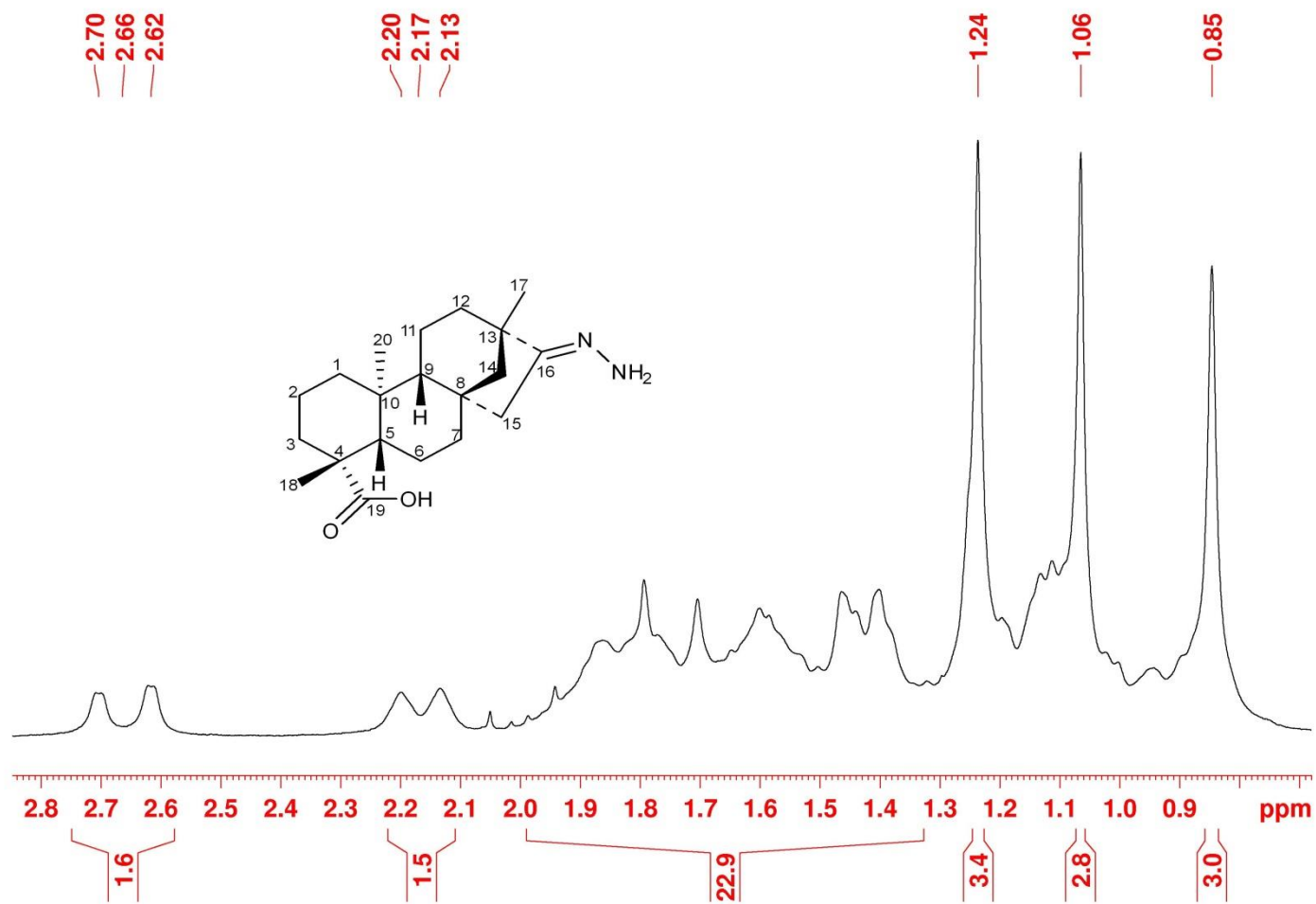


Figure 58: ¹H-NMR (200 MHz, CDCl₃) spectrum of compound **1f**.

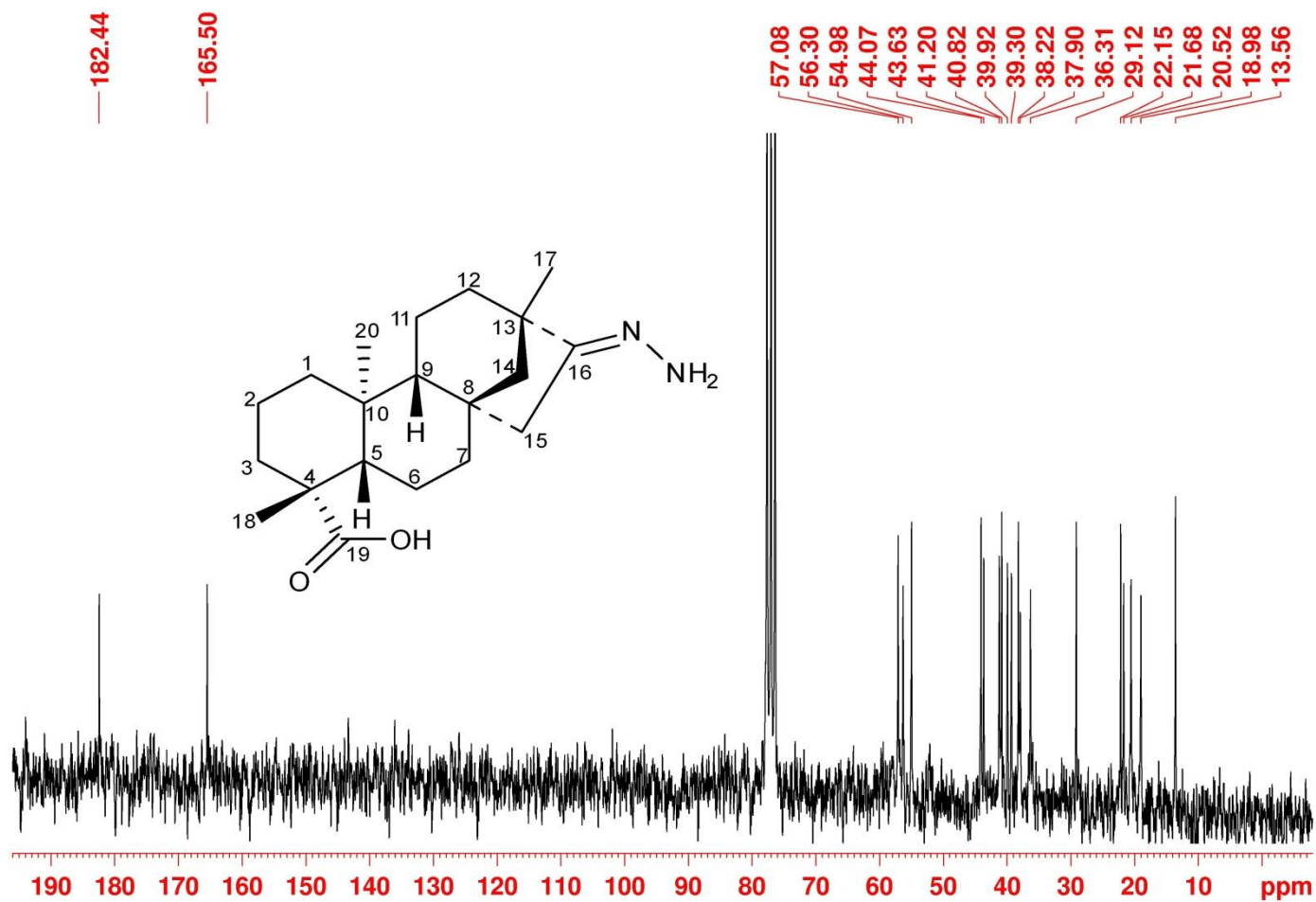


Figure 59: ^{13}C $\{^1\text{H}\}$ NMR (50 MHz, CDCl_3) spectrum of compound **1f**.

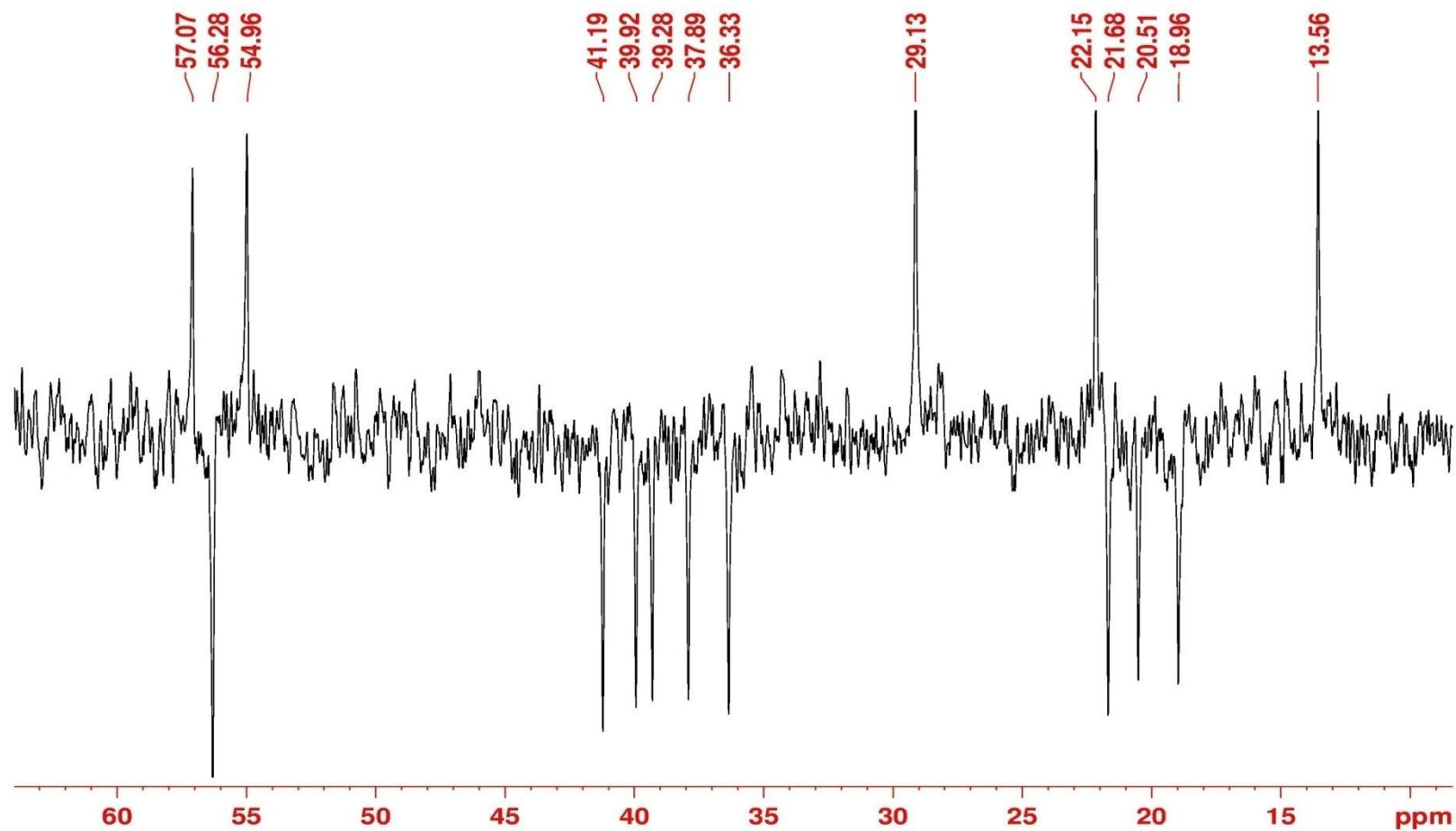


Figure 60: ^{13}C { ^1H } DEPT NMR (50 MHz, CDCl_3) spectrum of compound **1f**.

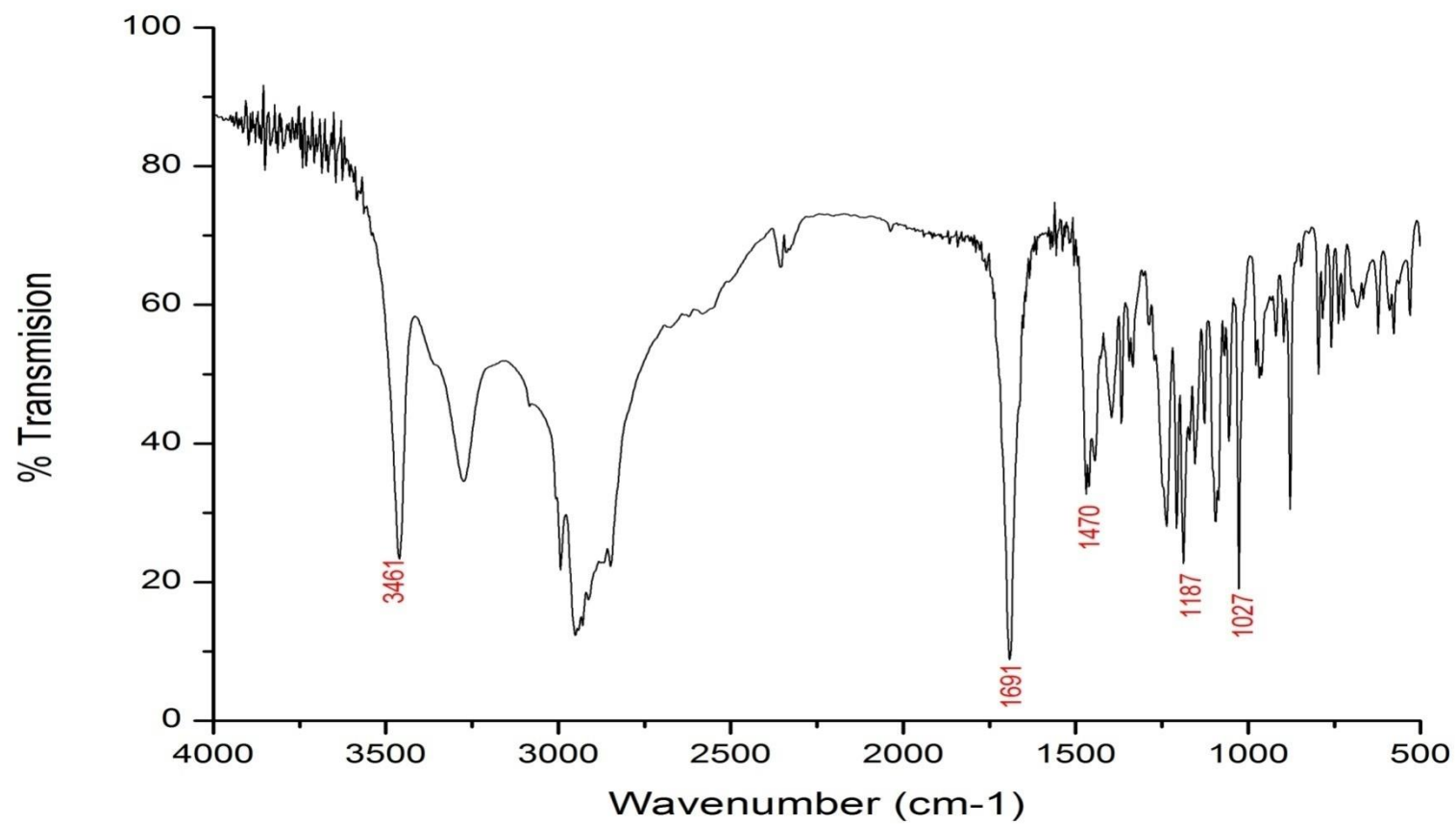


Figure 61: IR spectrum of compound **1h**.

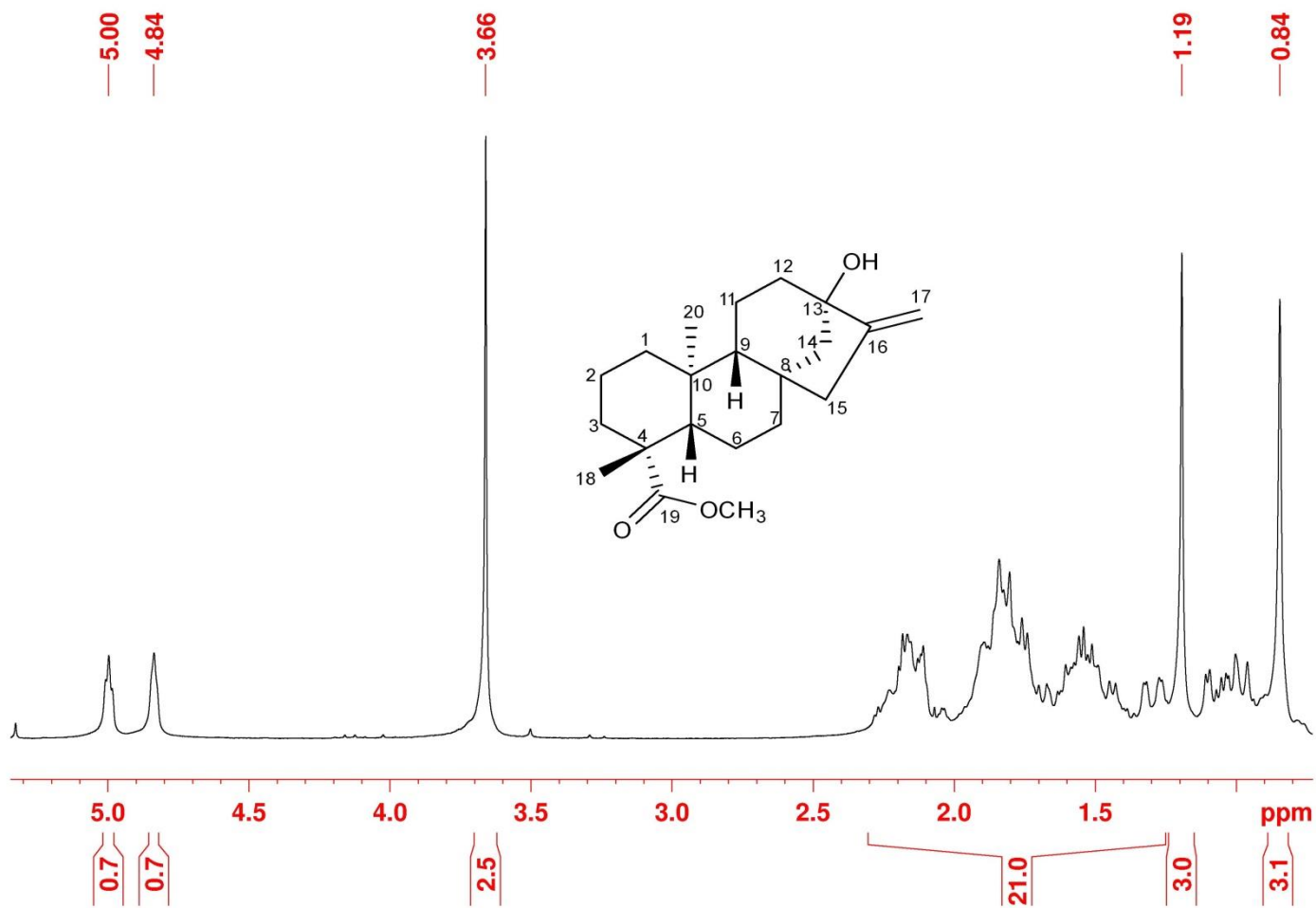


Figure 62: $^1\text{H-NMR}$ (200 MHz, CDCl_3) spectrum of compound **1h**.

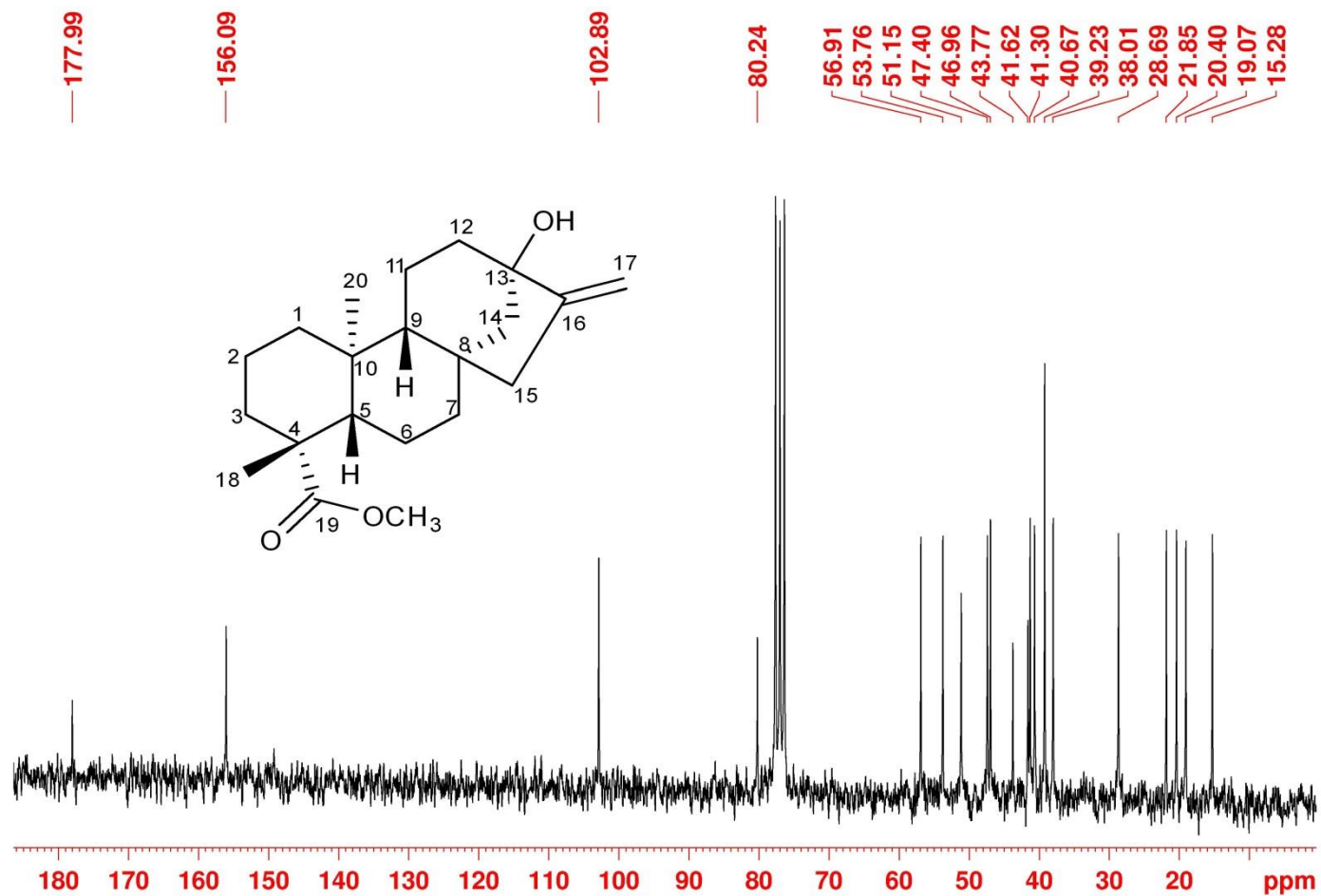


Figure 63: ^{13}C $\{^1\text{H}\}$ NMR (50 MHz, CDCl_3) spectrum of compound **1h**.

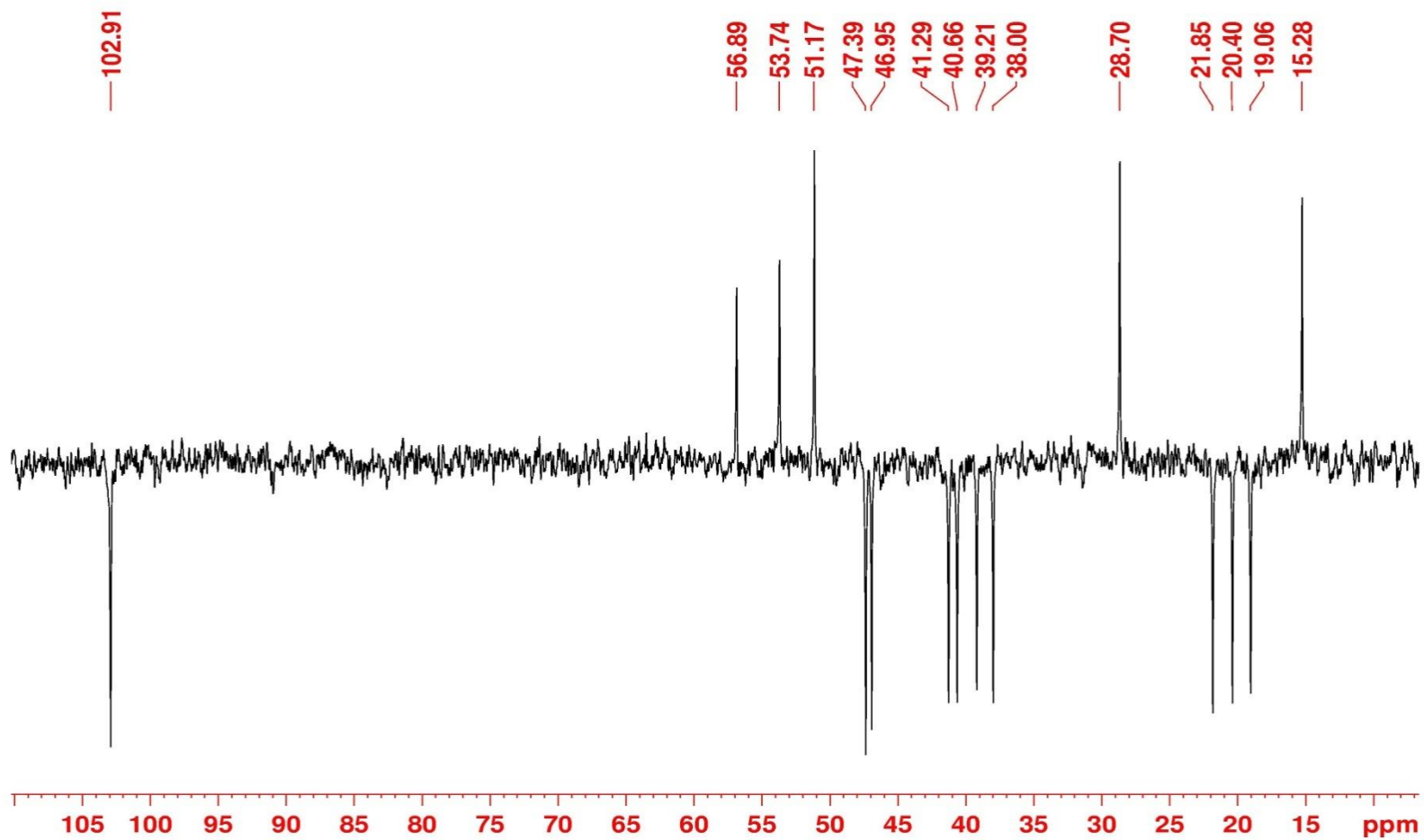


Figure 64: ^{13}C $\{^1\text{H}\}$ DEPT NMR (50 MHz, CDCl_3) spectrum of compound **1h**.

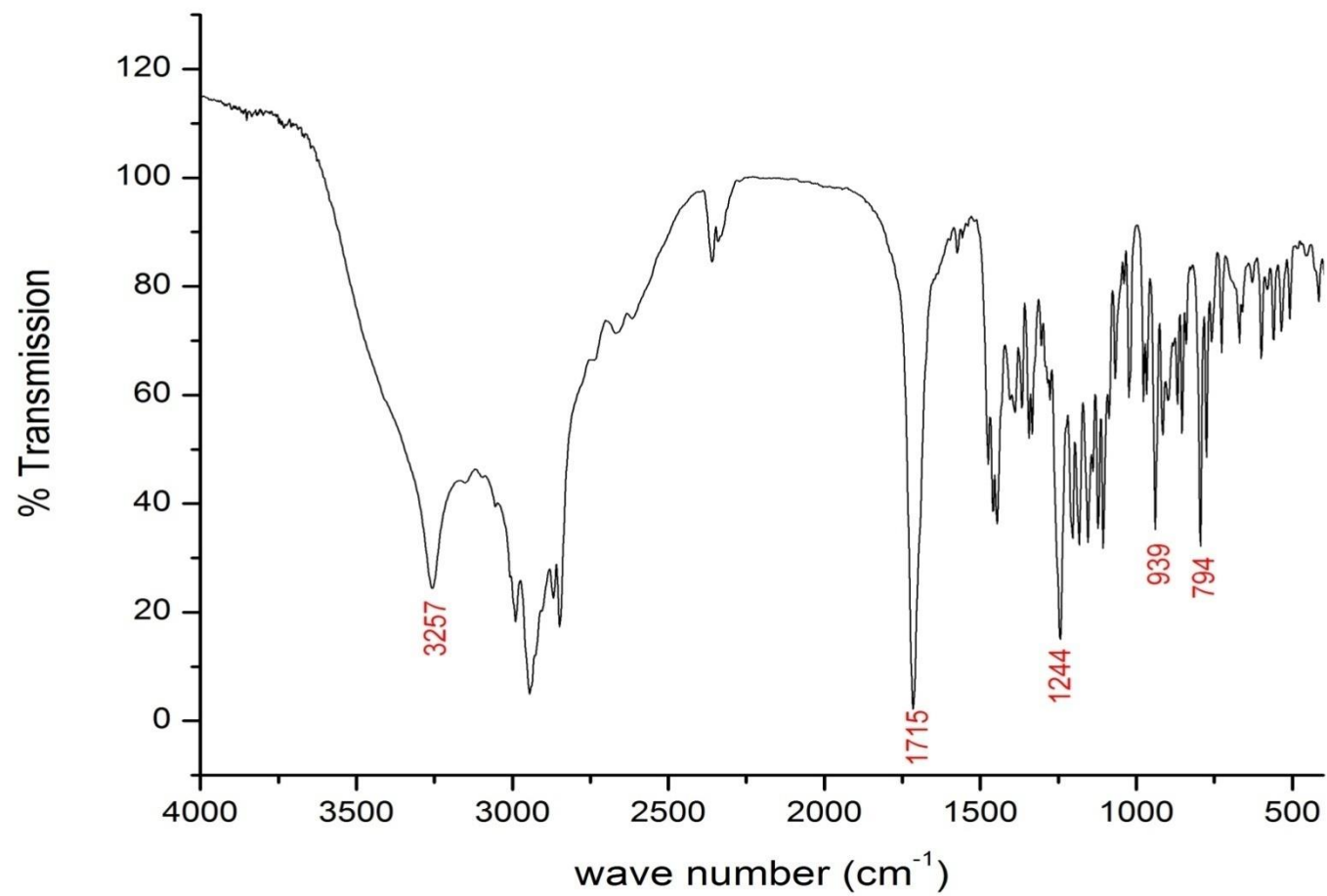


Figure 65: IR spectrum of compound **2h**.

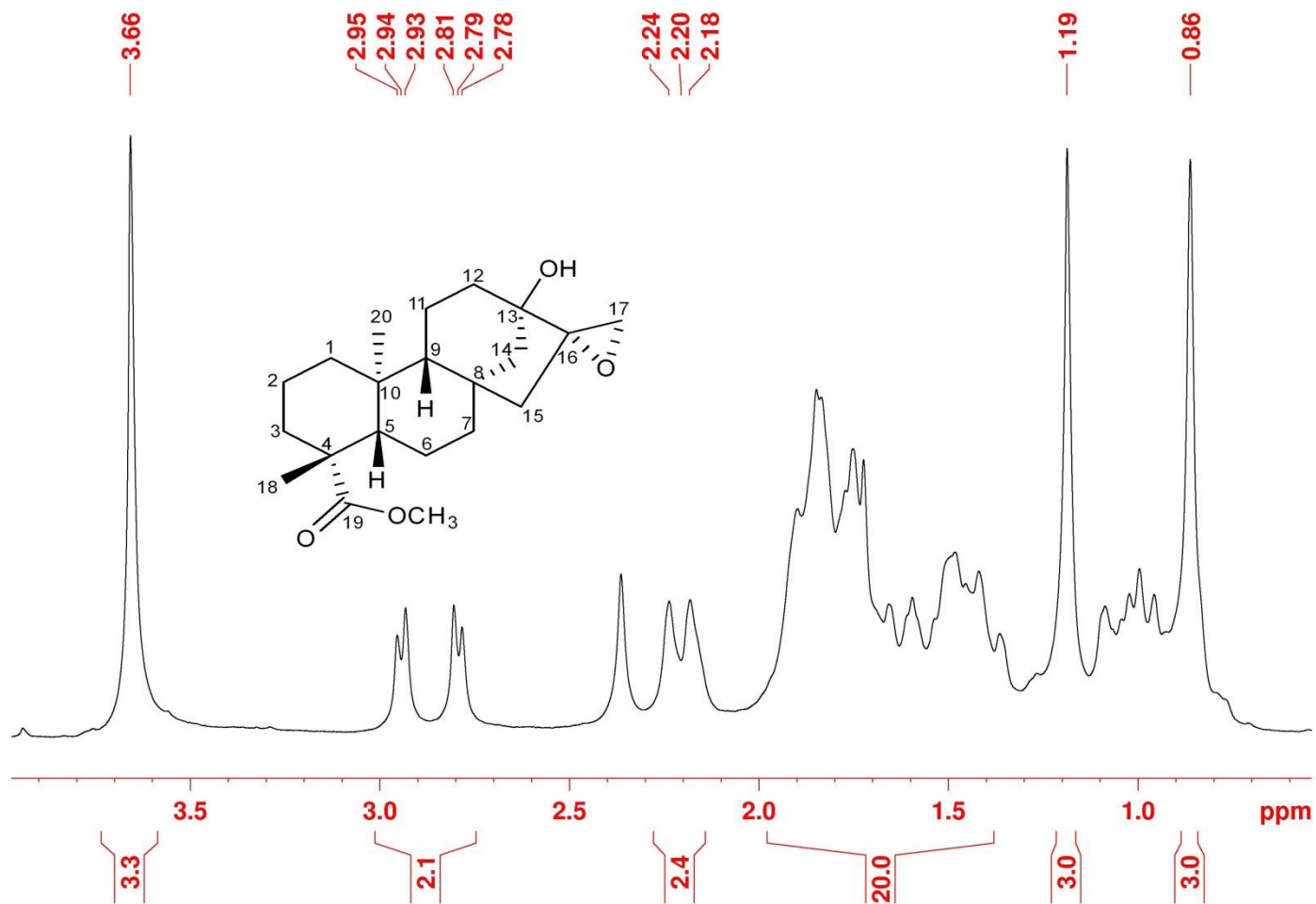


Figure 66: ¹H-NMR (200 MHz, CDCl₃) spectrum of compound **2h**.

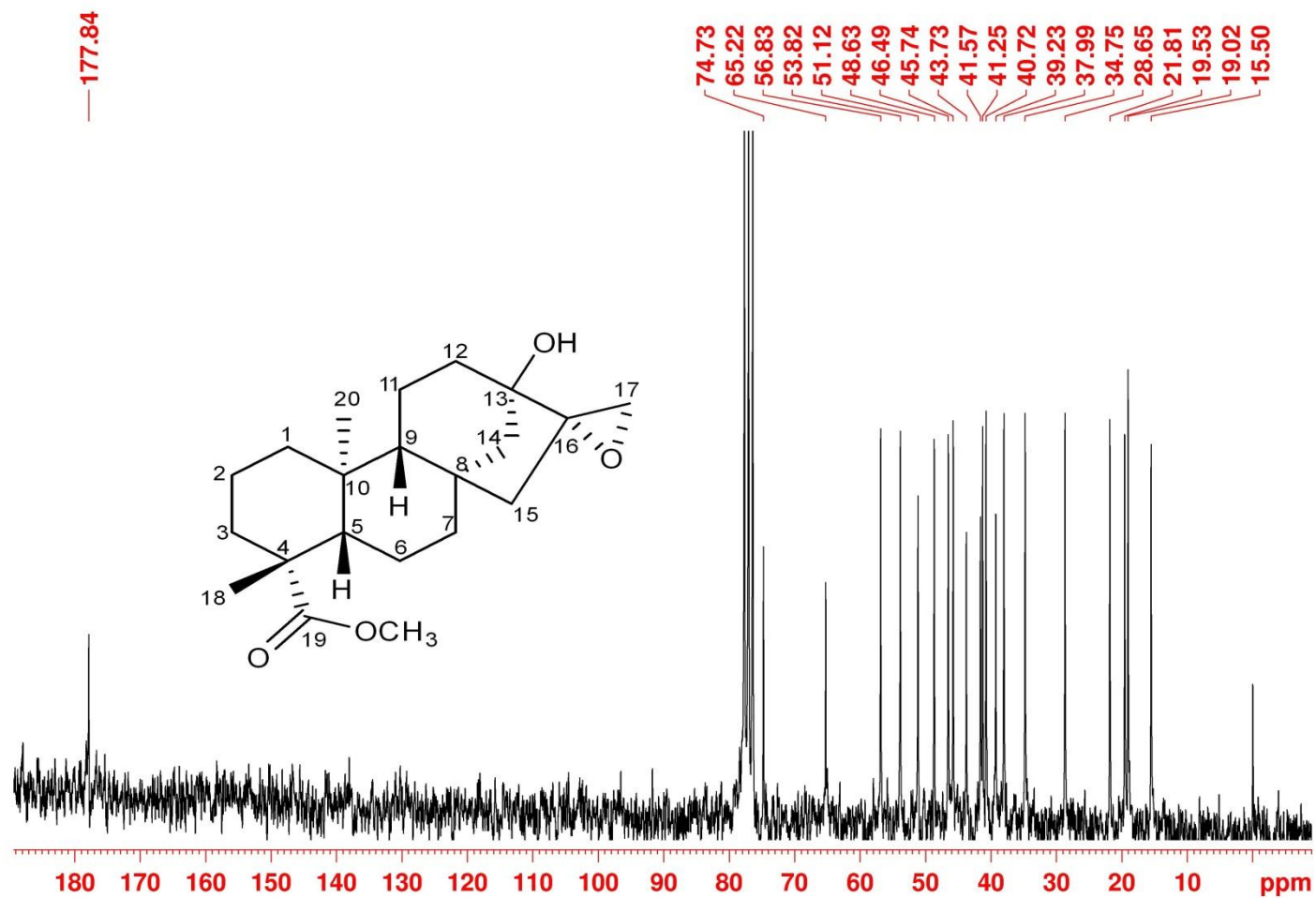


Figure 67: ^{13}C $\{^1\text{H}\}$ NMR (50 MHz, CDCl_3) spectrum of compound **2h**.

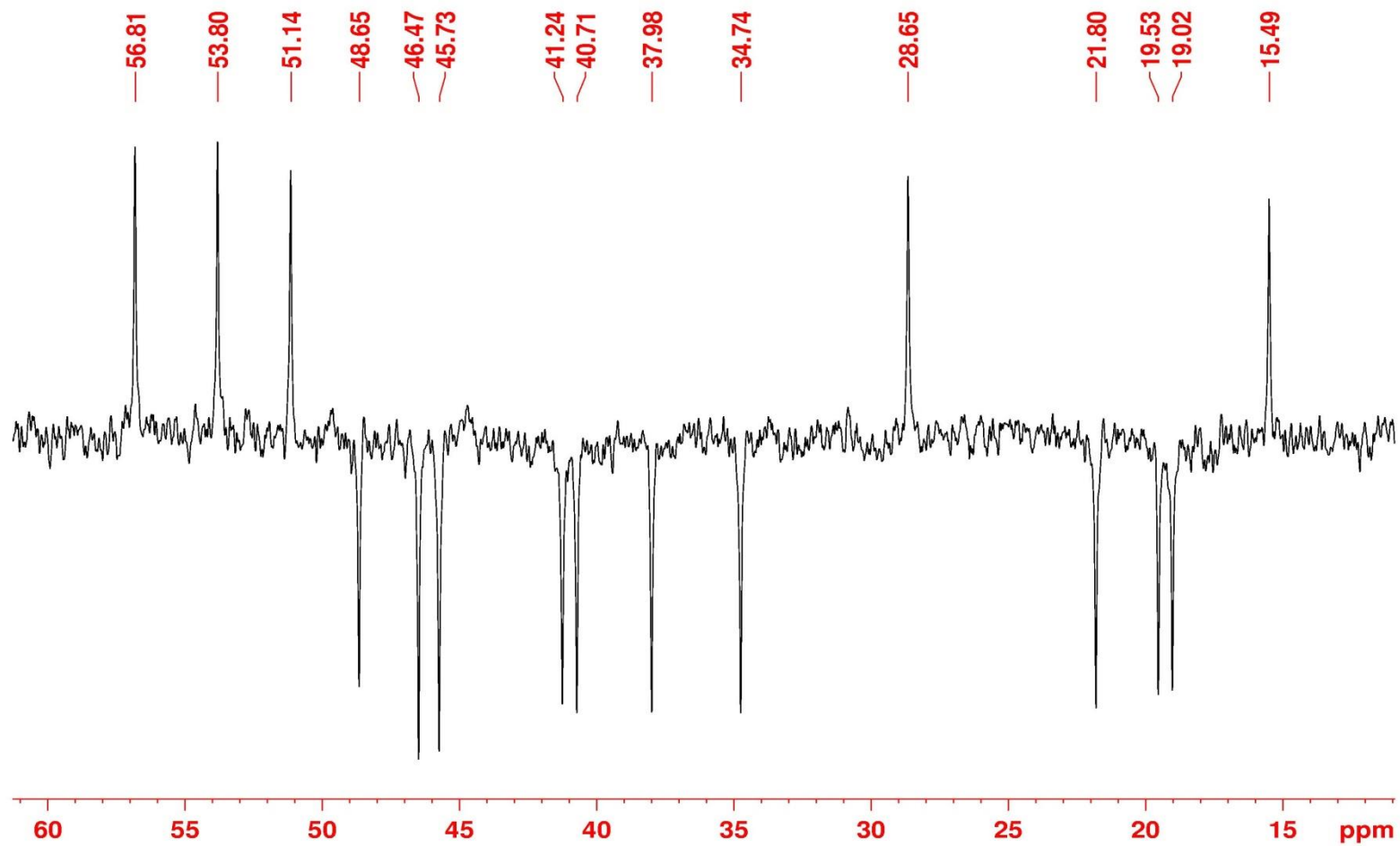


Figure 68: ^{13}C $\{^1\text{H}\}$ DEPT NMR (50 MHz, CDCl_3) spectrum of compound **2h**.

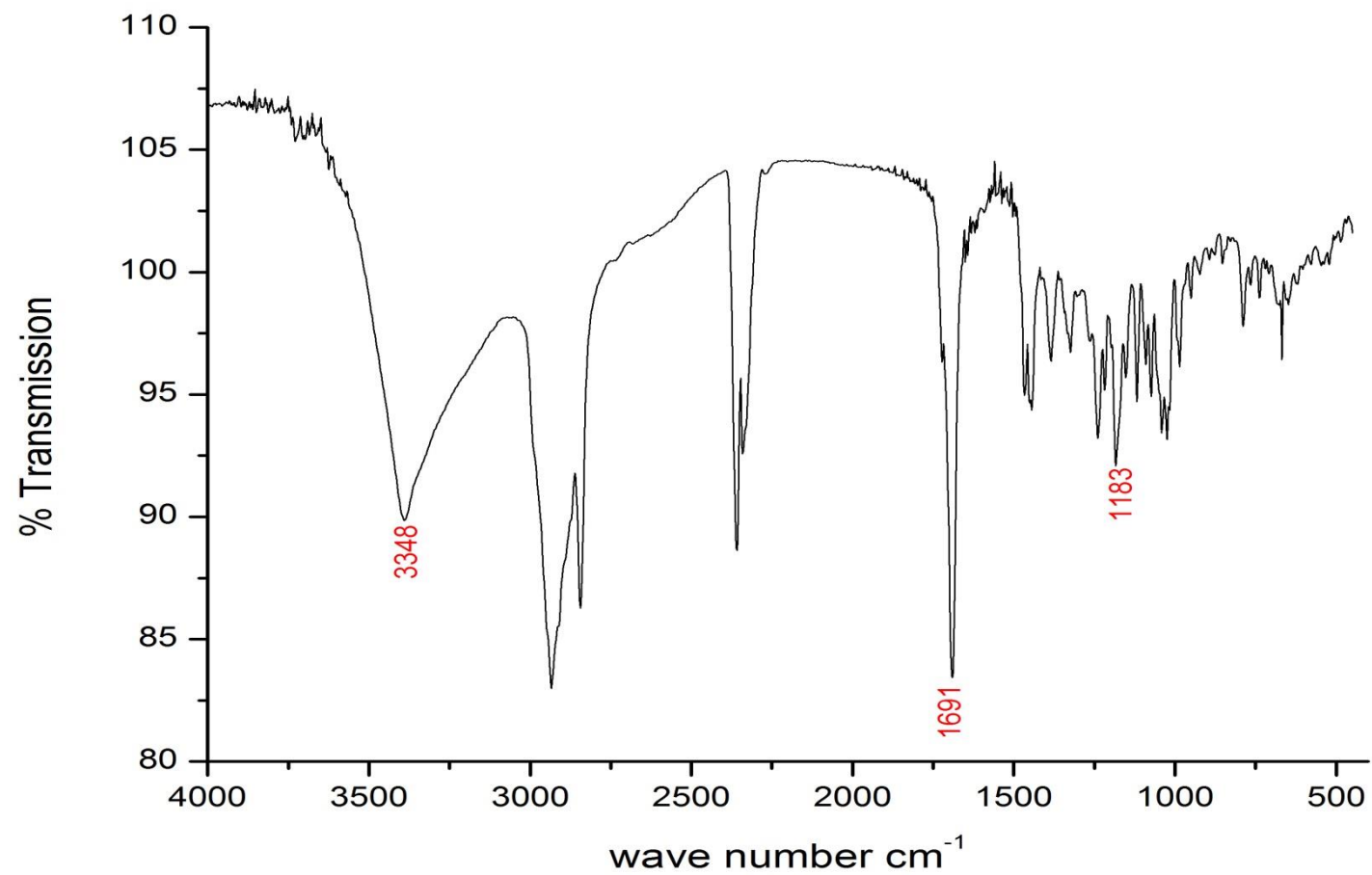


Figure 69: IR spectrum of compound **4h**.

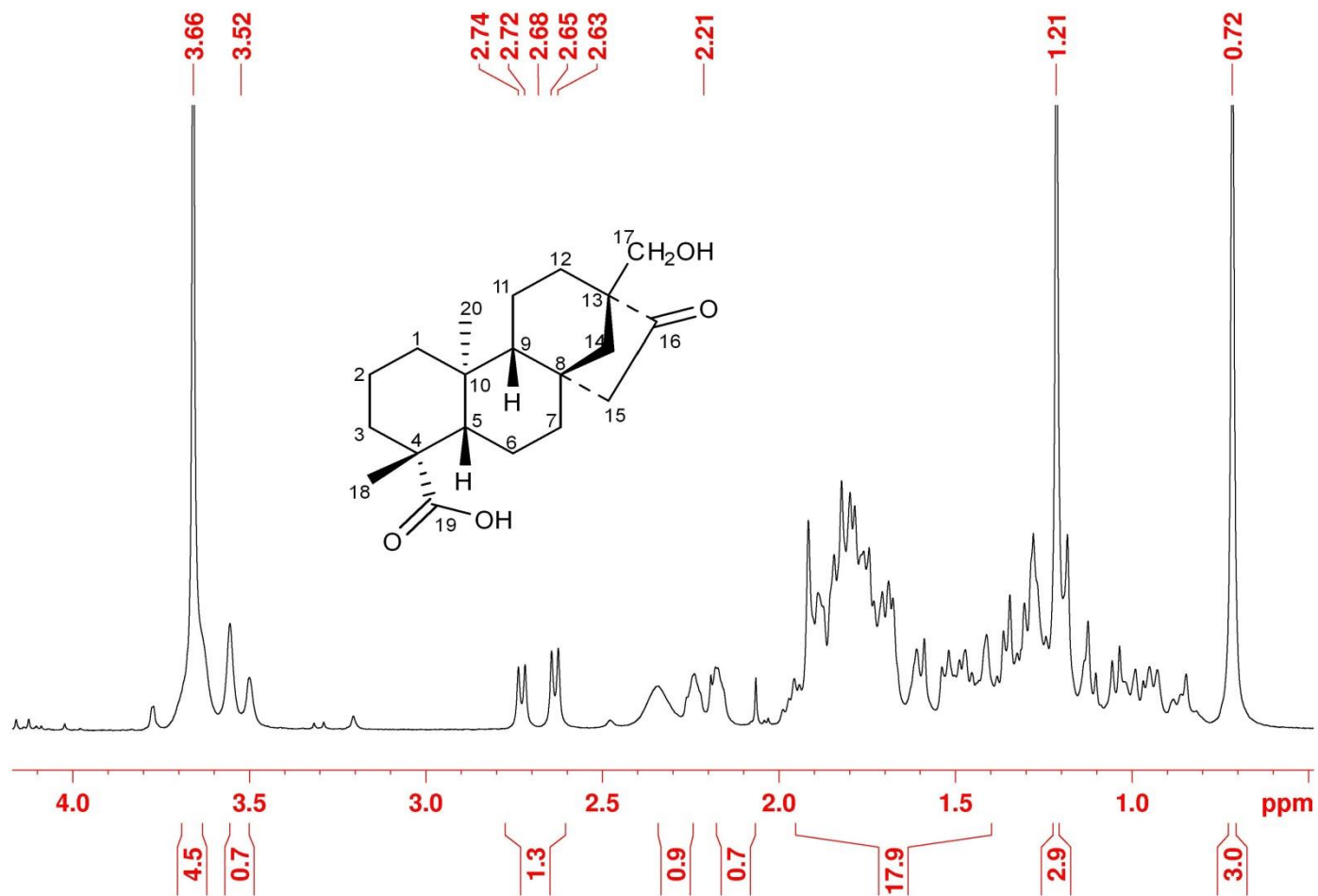


Figure 70: ¹H-NMR (200 MHz, CDCl₃) spectrum of compound **4h**.

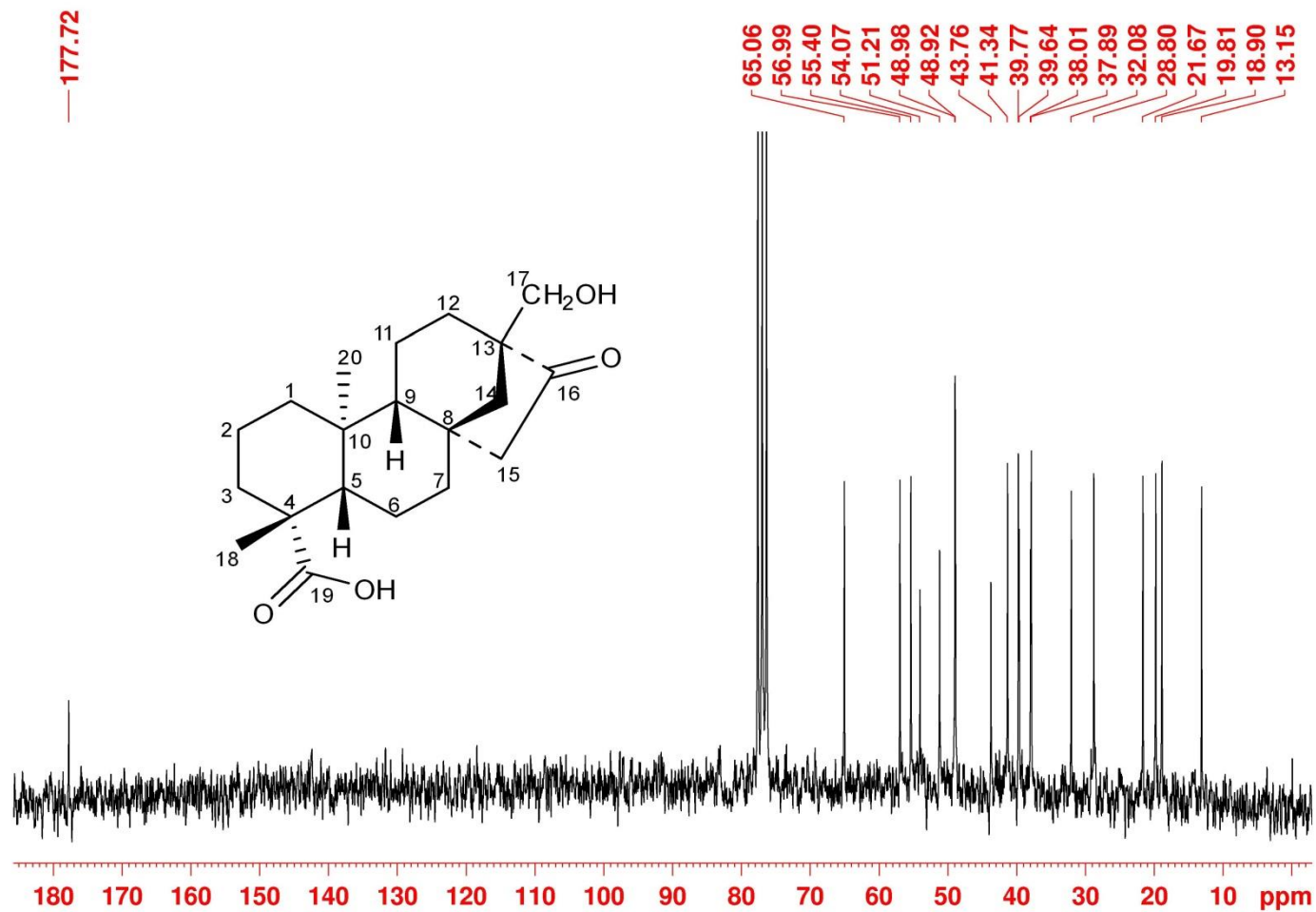


Figure 71: ^{13}C $\{^1\text{H}\}$ NMR (50 MHz, CDCl_3) spectrum of compound **4h**.

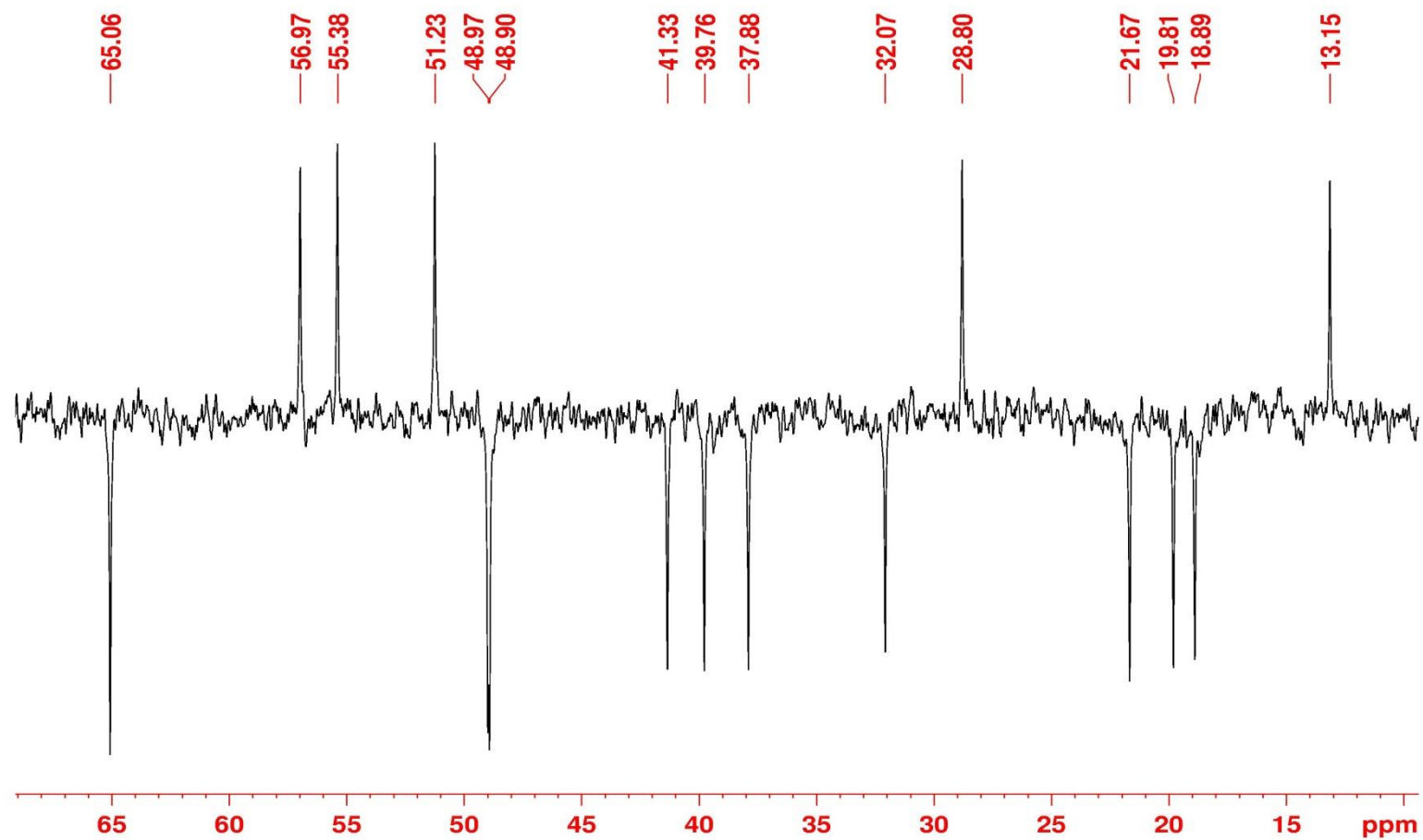


Figure 72: ^{13}C $\{^1\text{H}\}$ DEPT NMR (50 MHz, CDCl_3) spectrum of compound **4h**.

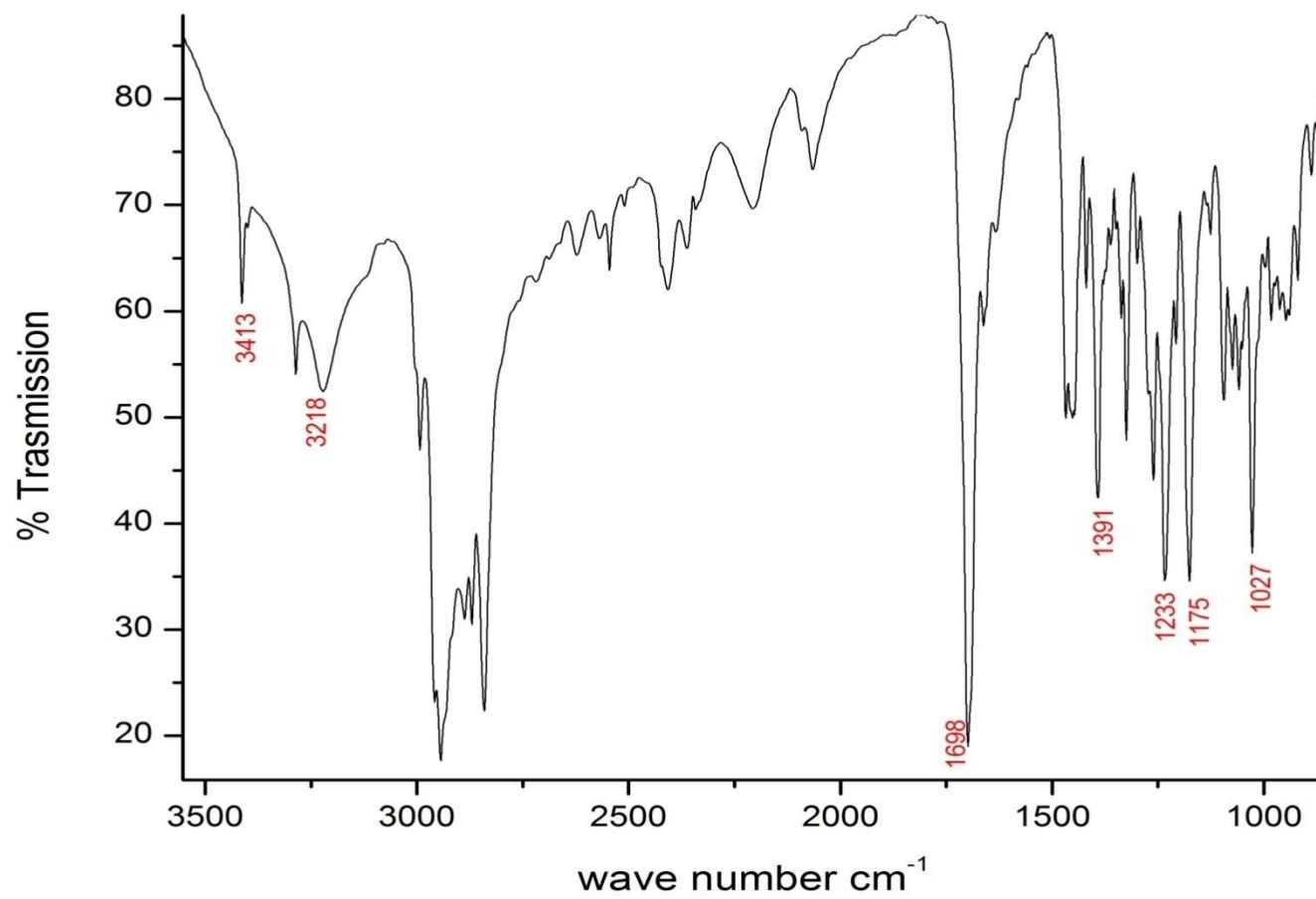


Figure 73: IR spectrum of compound **5i**.

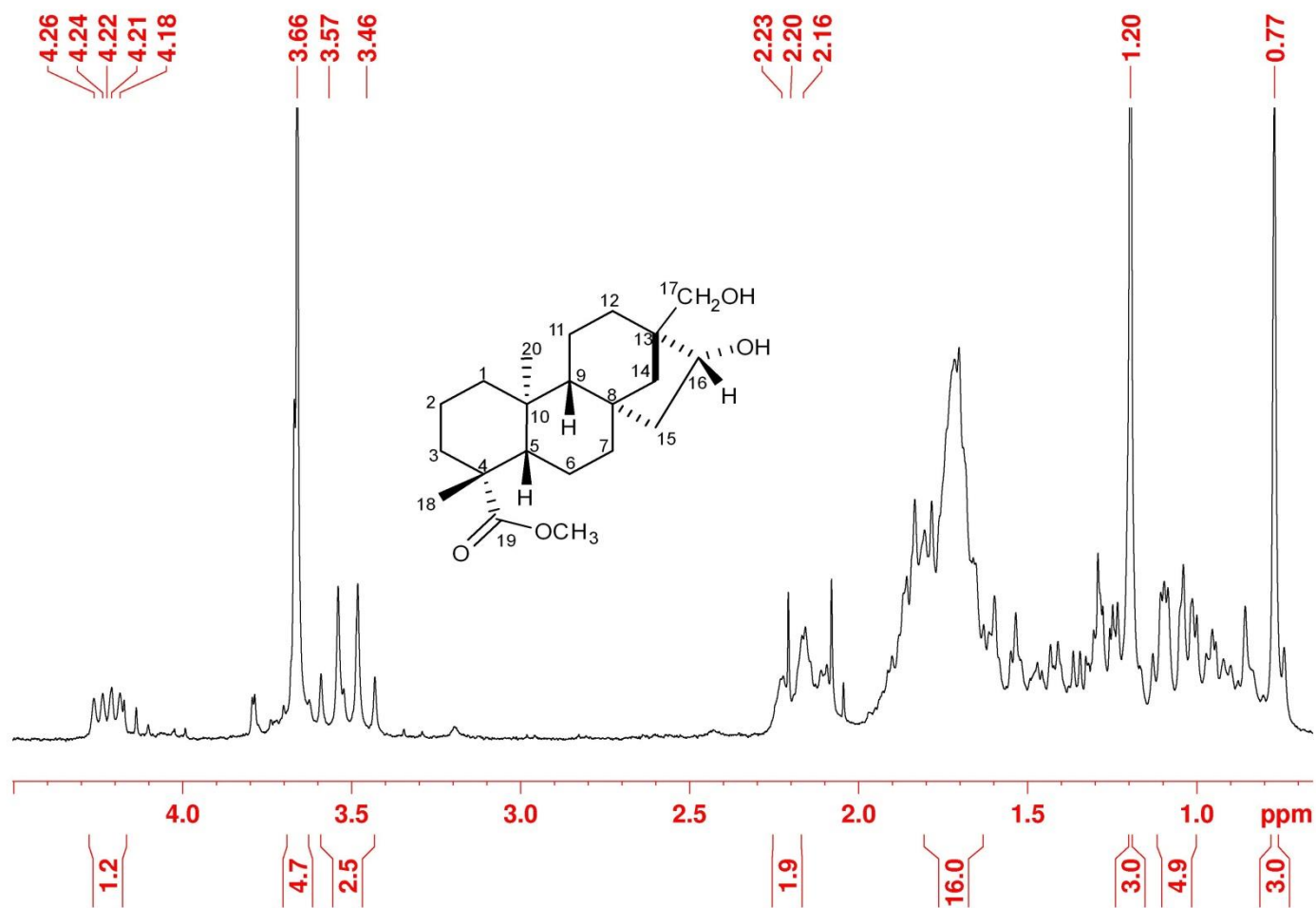


Figure 74: ¹H-NMR (200 MHz, CDCl₃) spectrum of compound **5i**.

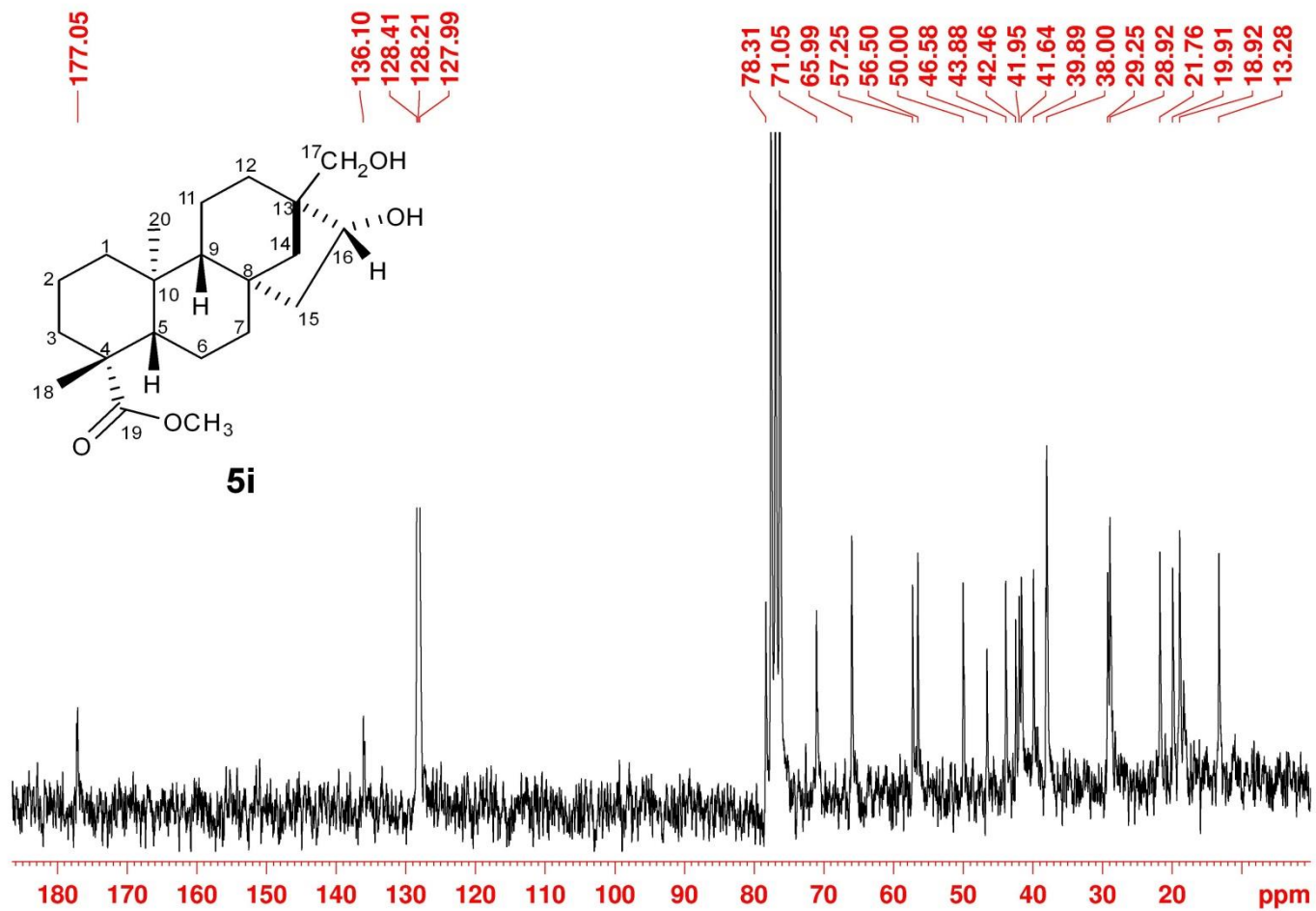


Figure 75: ^{13}C $\{^1\text{H}\}$ NMR (50 MHz, CDCl_3) spectrum of compound **5i**.

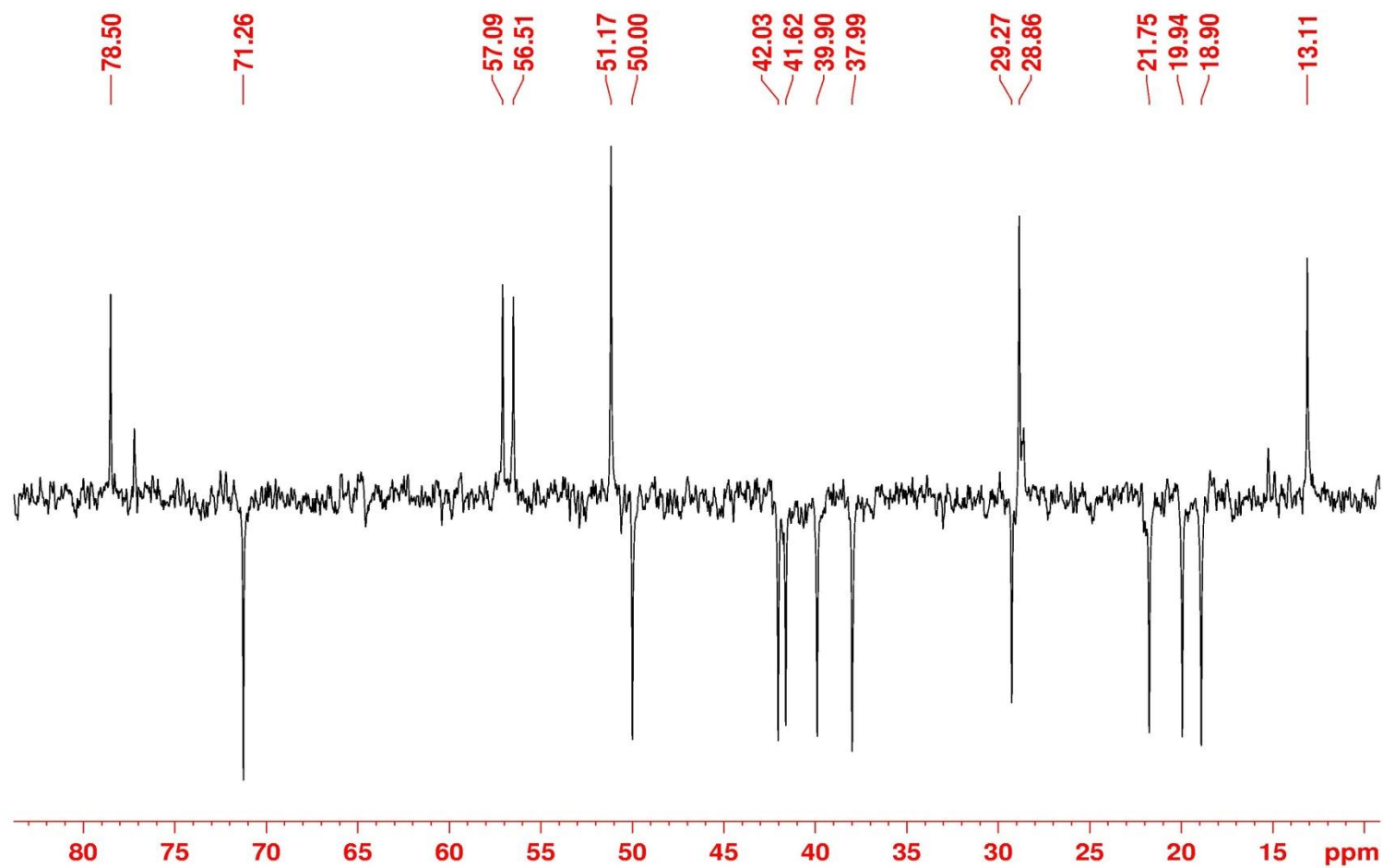


Figure 76: ^{13}C { ^1H } DEPT NMR (50 MHz, CDCl_3) spectrum of compound 5i.

tri_140227190523 #2095 RT: 5.36 AV: 1 NL: 5.33E6
T: TMS - c ESI Full ms [280.00-450.00]

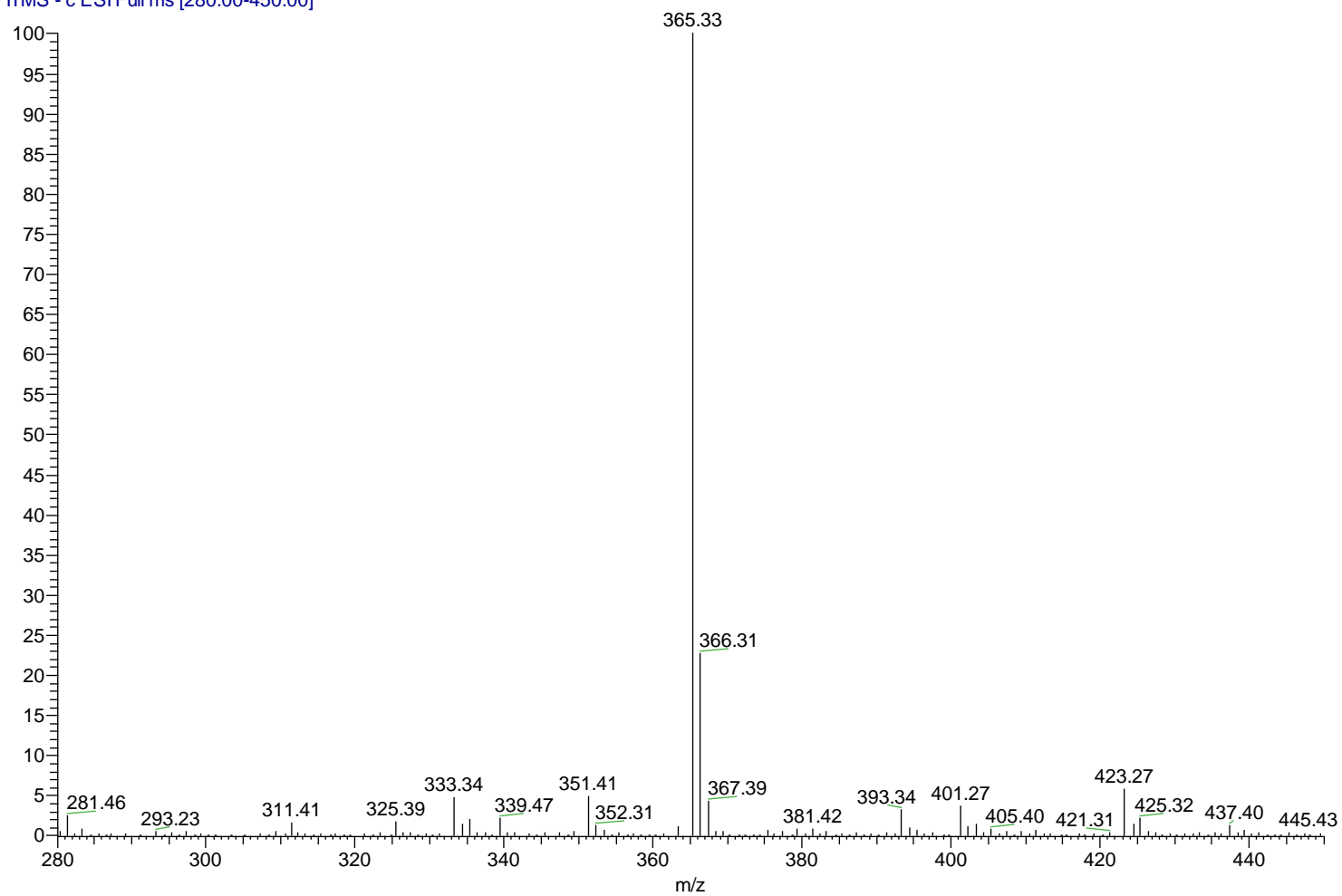


Figure 77: ESI-MS spectrum of compound **5n**.

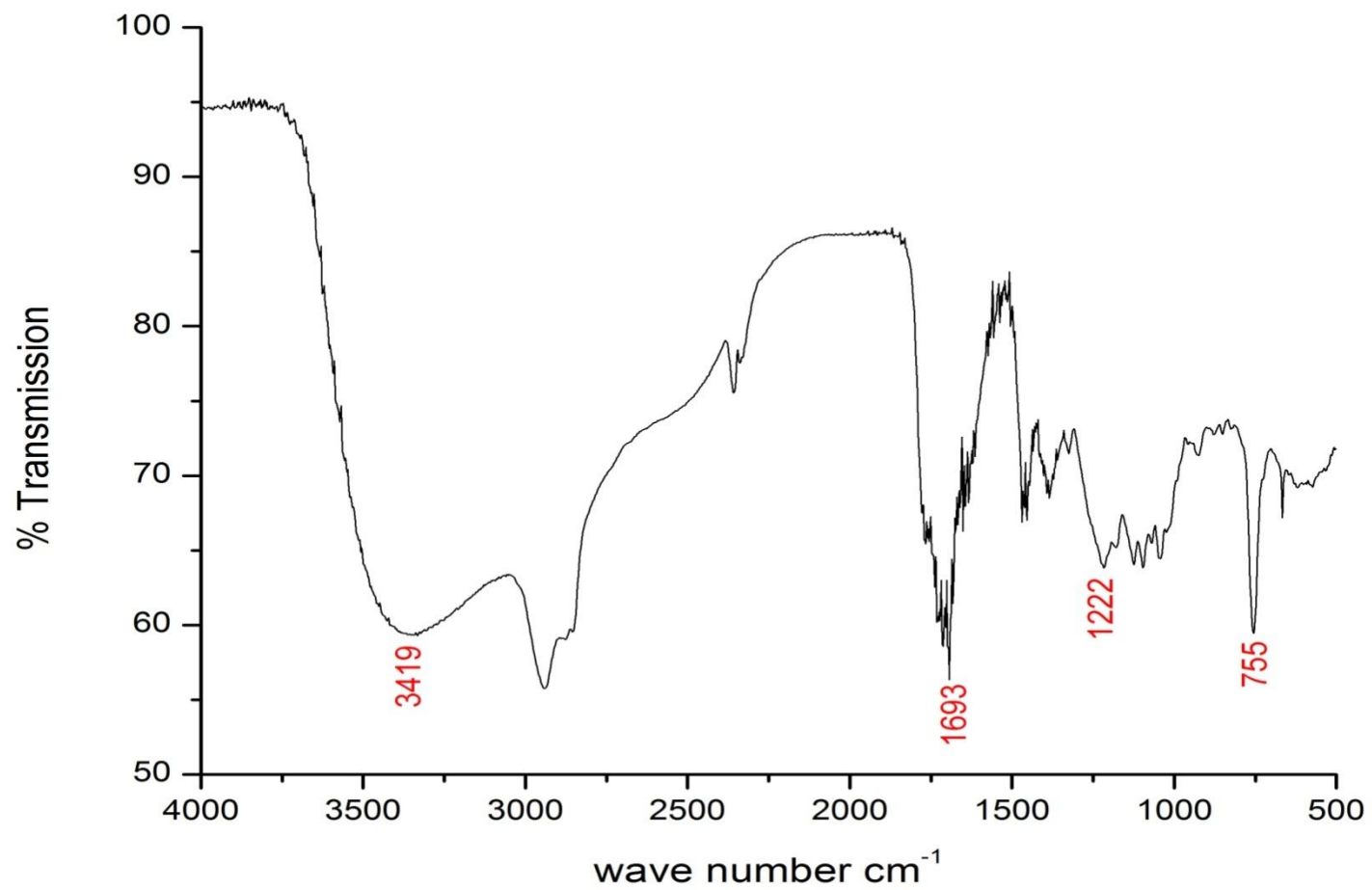


Figure 78: IR spectrum of compound 5n.

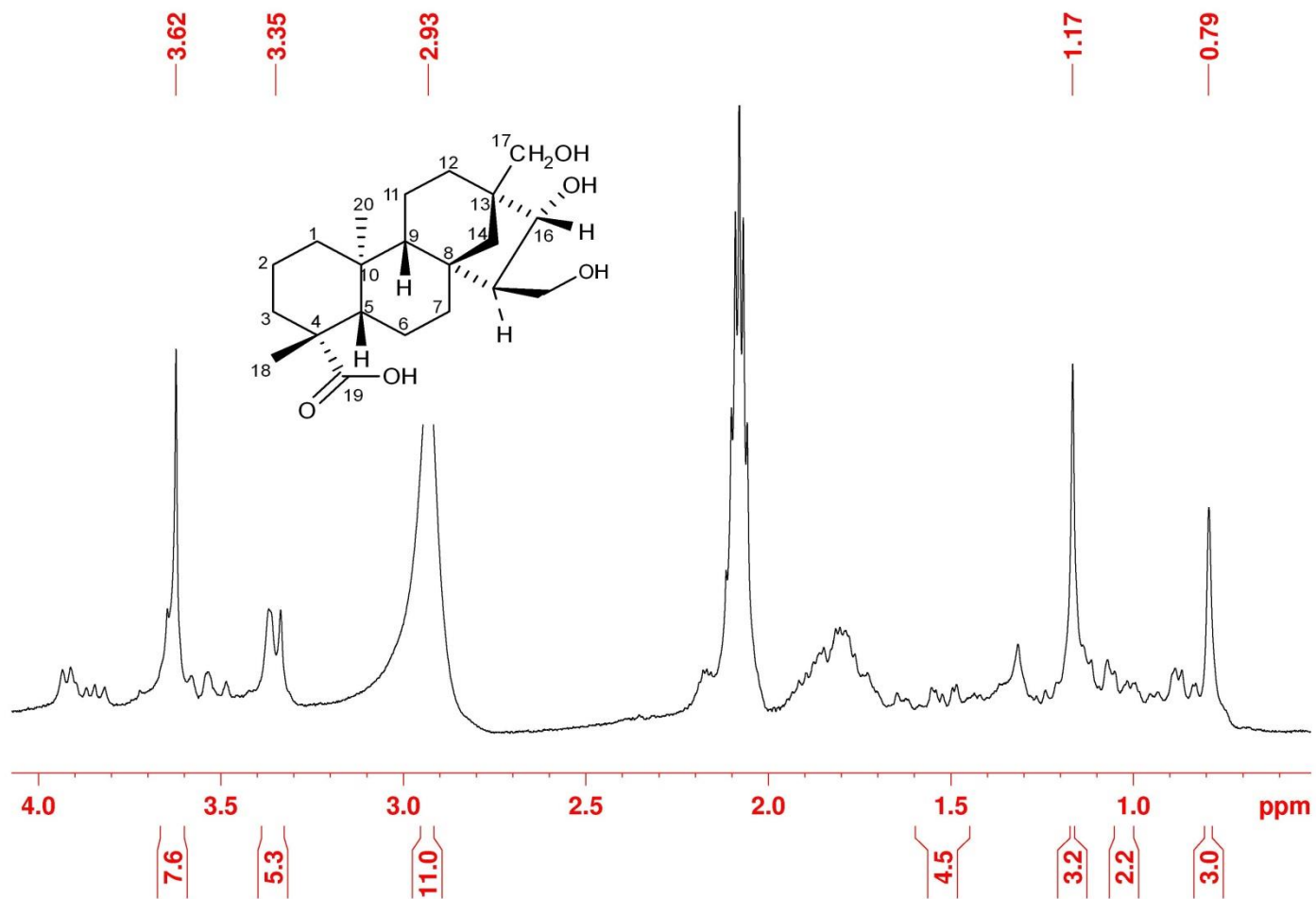


Figure 79: $^1\text{H-NMR}$ (200 MHz, CD_3OD) spectrum of compound **5n**.

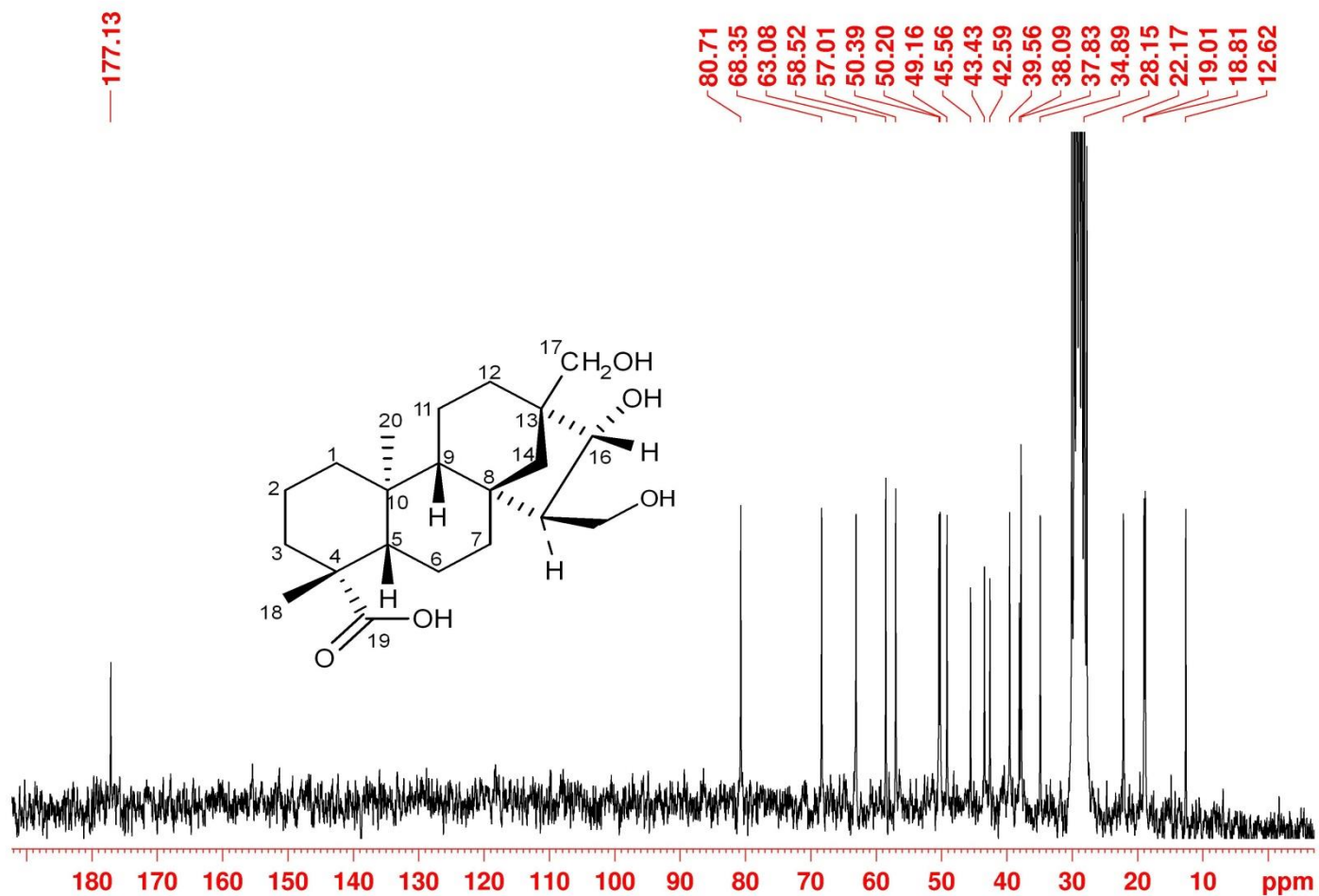


Figure 80: ^{13}C $\{^1\text{H}\}$ NMR (50 MHz, CD_3OD) spectrum of compound **5n**.

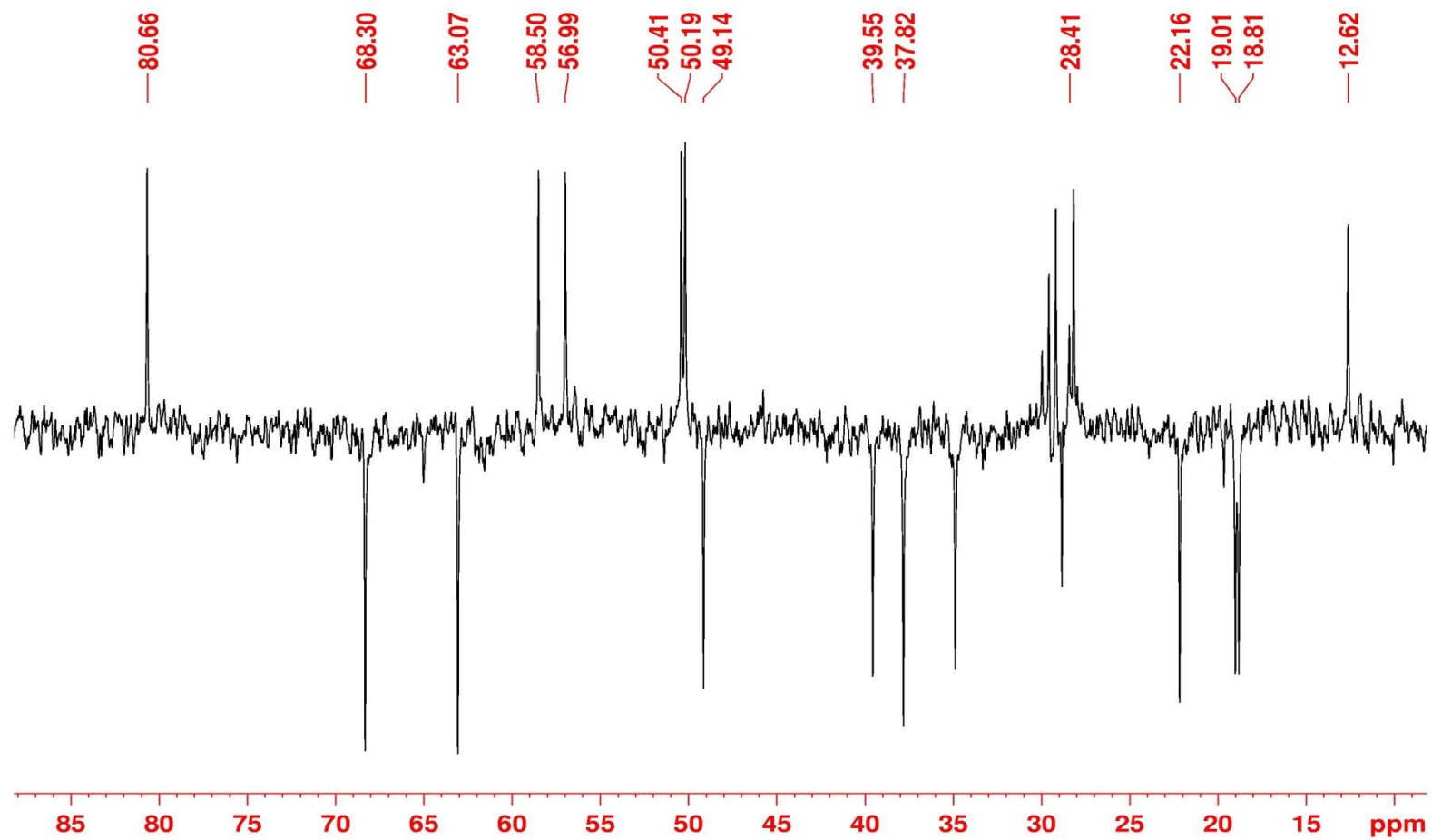
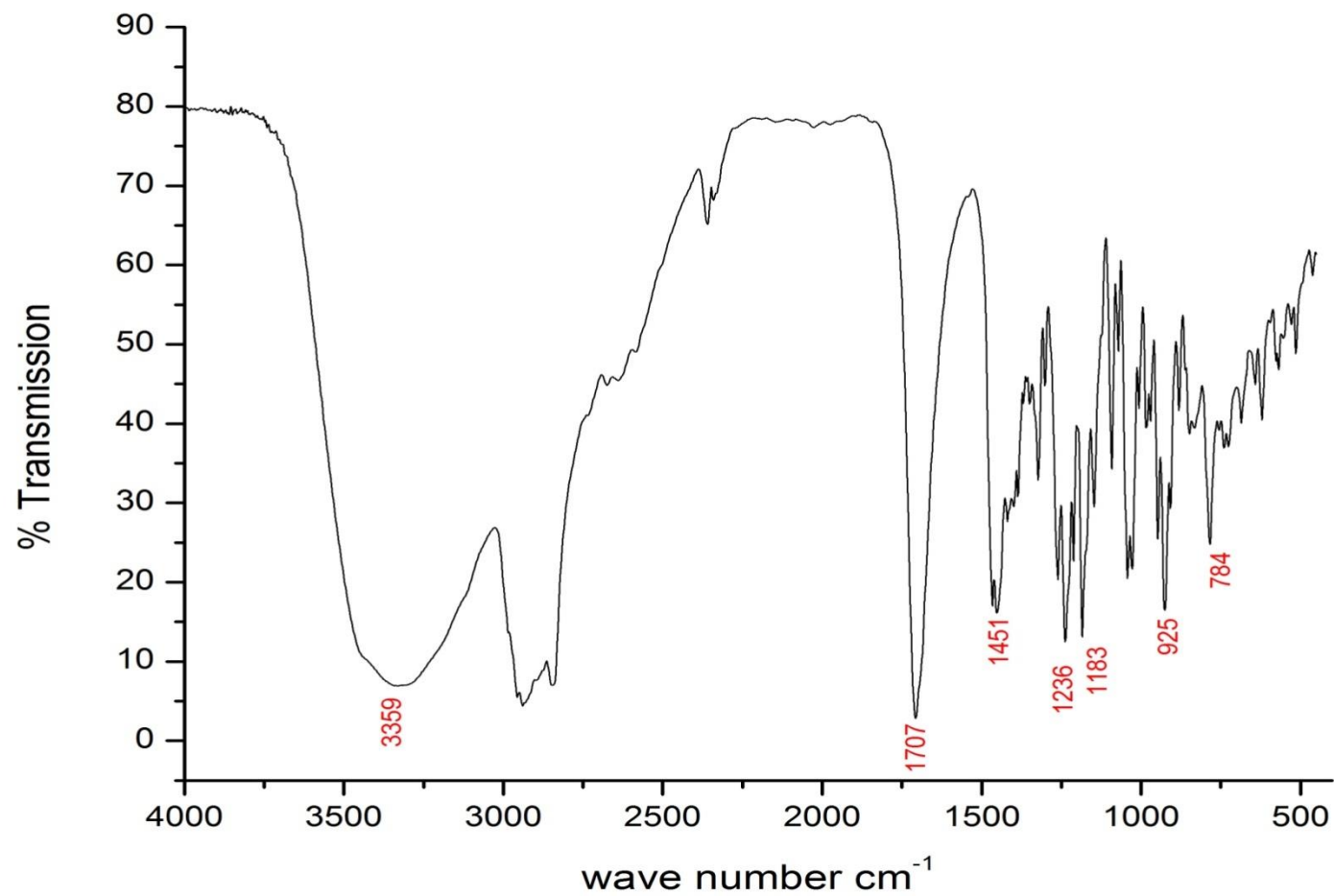


Figure 81: $^{13}\text{C} \{^1\text{H}\}$ DEPT-NMR (50 MHz, CD_3OD) spectrum of compound **5n**.

Figure 82: IR spectrum of compound **5j**.

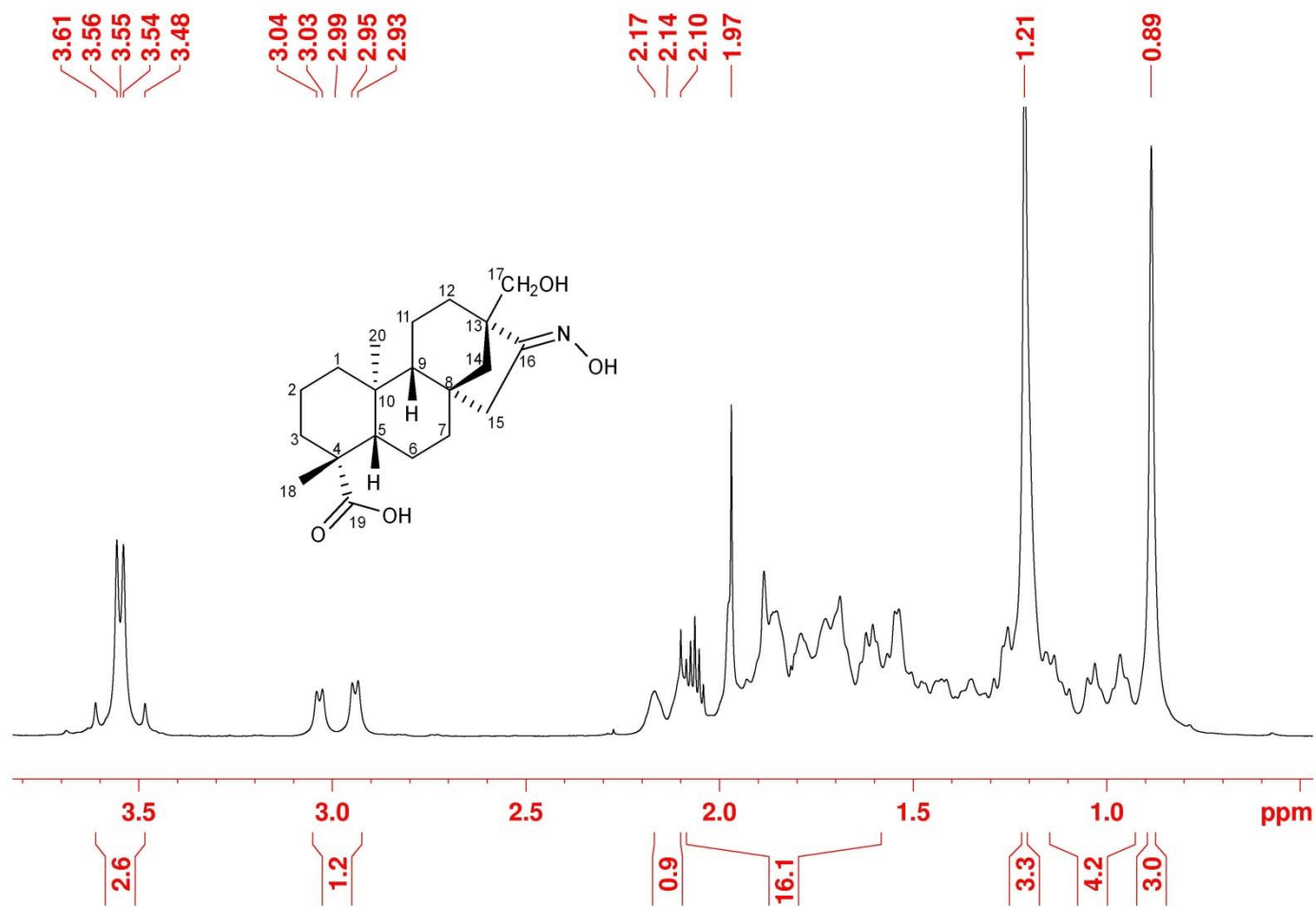


Figure 83: ¹H-NMR (200 MHz, Acetone-d₆) spectrum of compound **5j**.

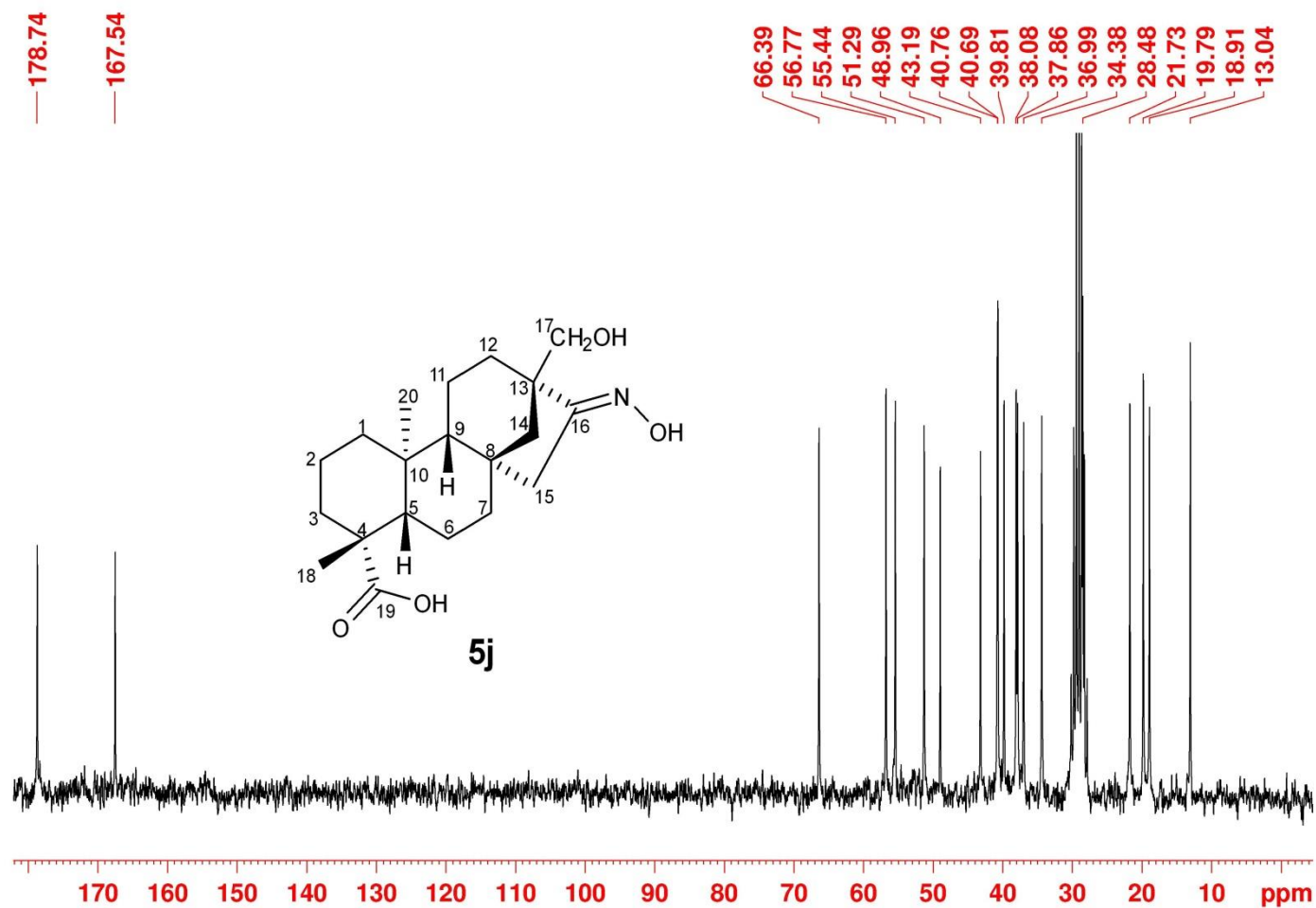


Figure 84: ^{13}C $\{^1\text{H}\}$ NMR (50 MHz, Acetone- d_6) spectrum of compound **5j**.

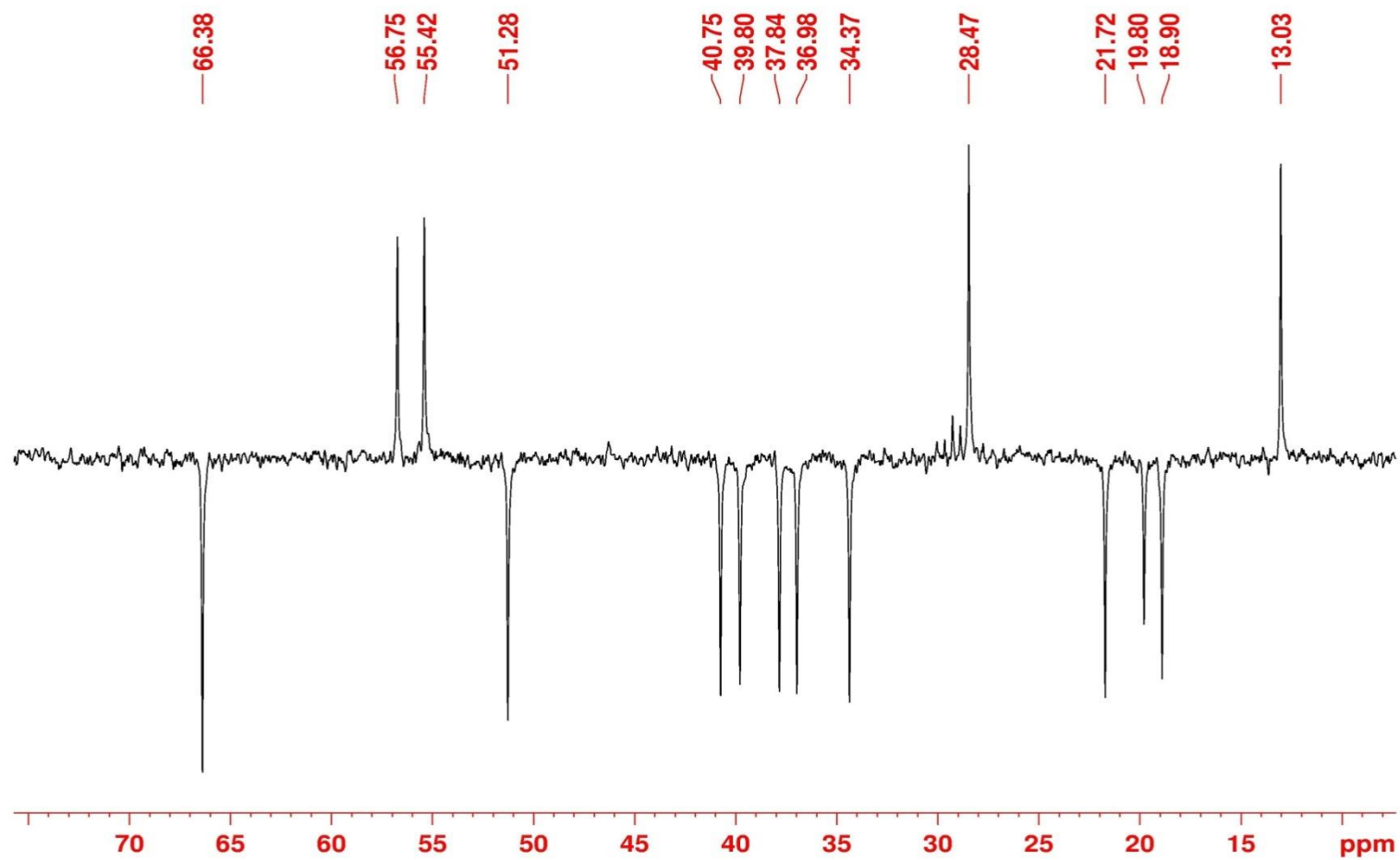


Figure 85: ^{13}C { ^1H } DEPT-NMR (50 MHz, Acetone- d_6) spectrum of compound **5j**.

201-ASADHD9_131125163213 #745 RT: 1.67 AV: 1 NL: 9.47E4
T: ITMS - c ESI Full ms2 347.30@cid0.00 [95.00-600.00]

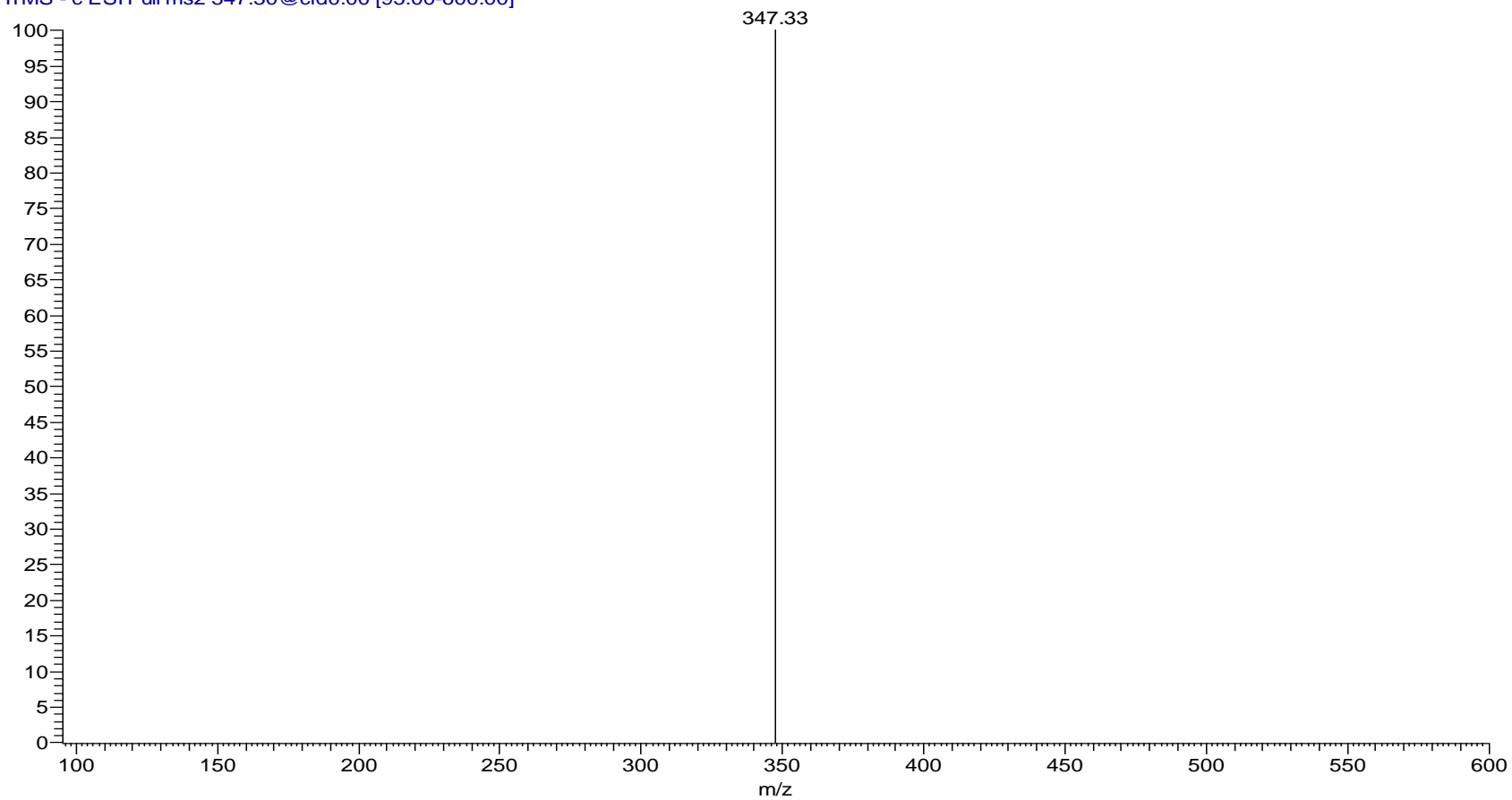


Figure 86: ESI-MS spectrum of compound **5k**.

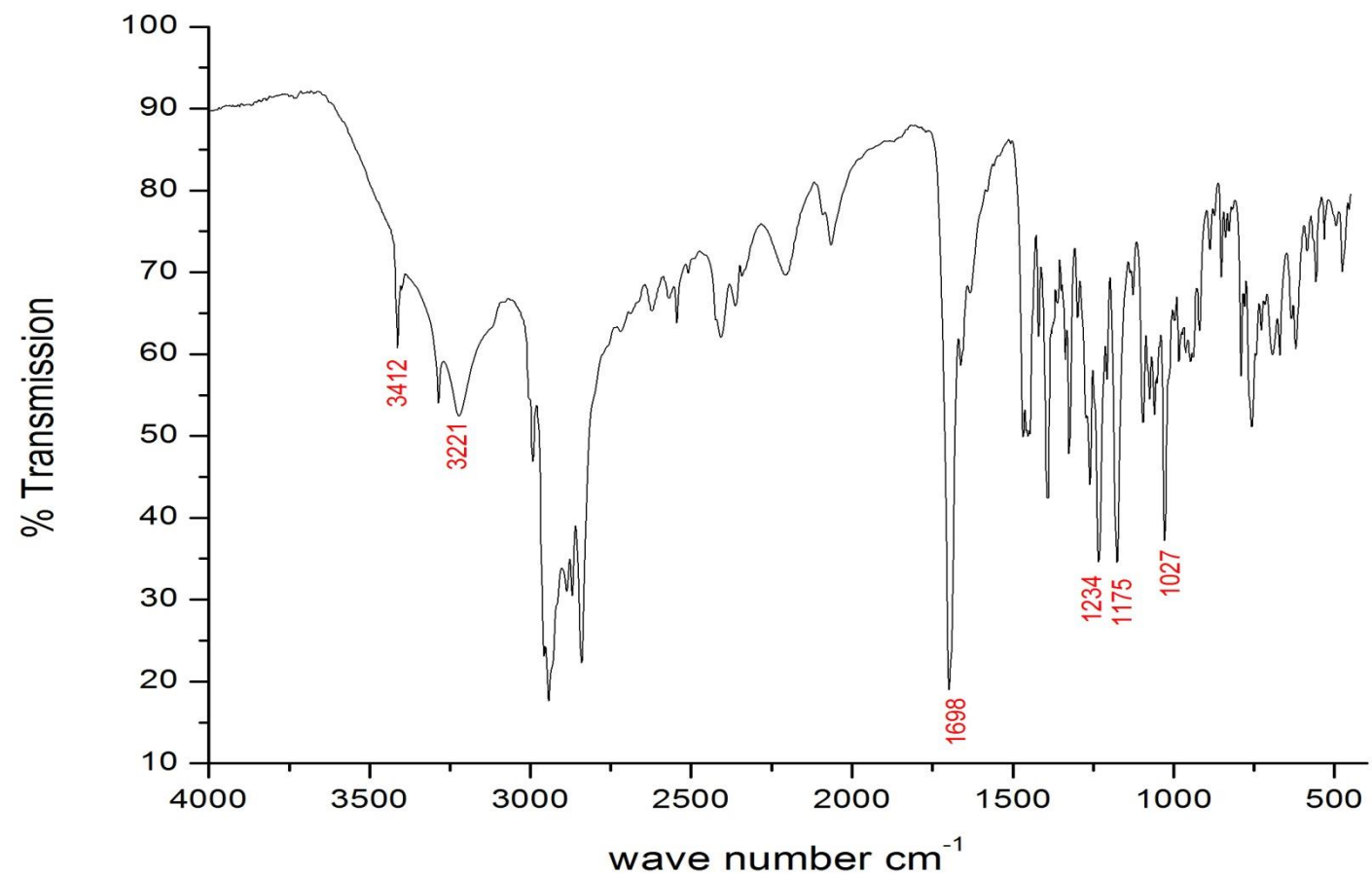


Figure 87: IR spectrum of compound **5k**.

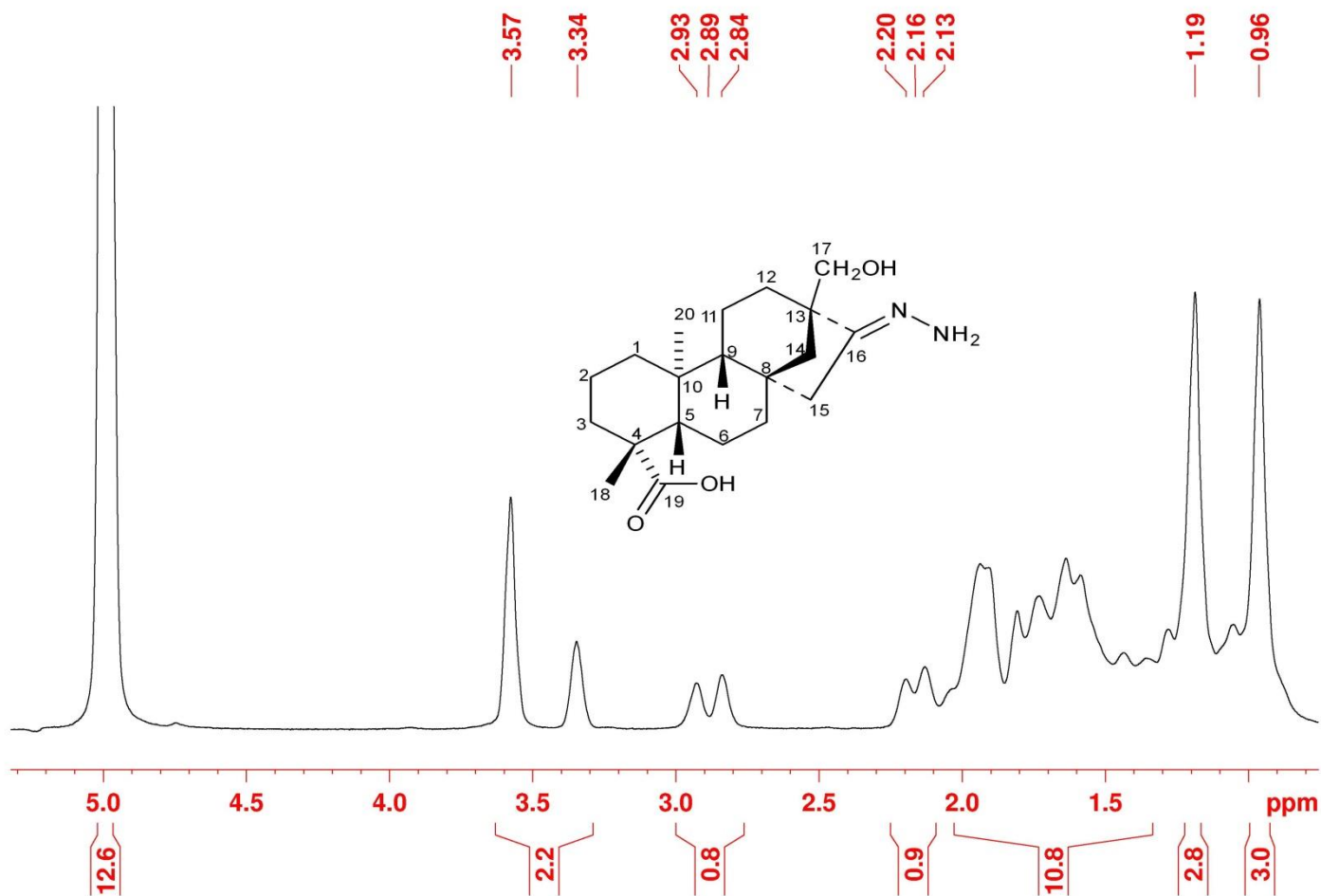


Figure 88: ¹H-NMR (200 MHz, Methanol-d₄) spectrum of compound **5k**.

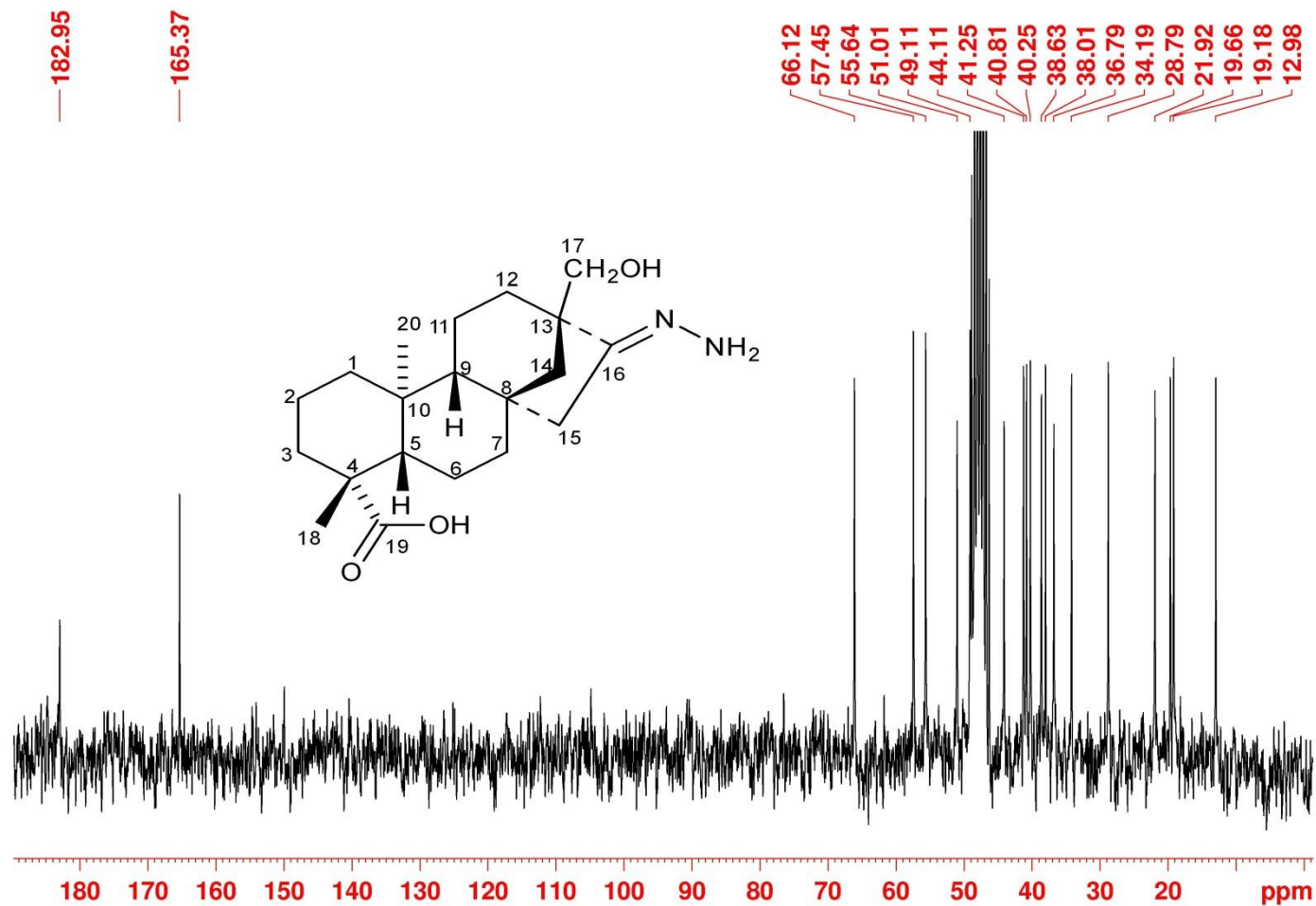


Figure 89: ^{13}C $\{^1\text{H}\}$ NMR (50 MHz, Methanol- d_4) spectrum of compound **5k**.

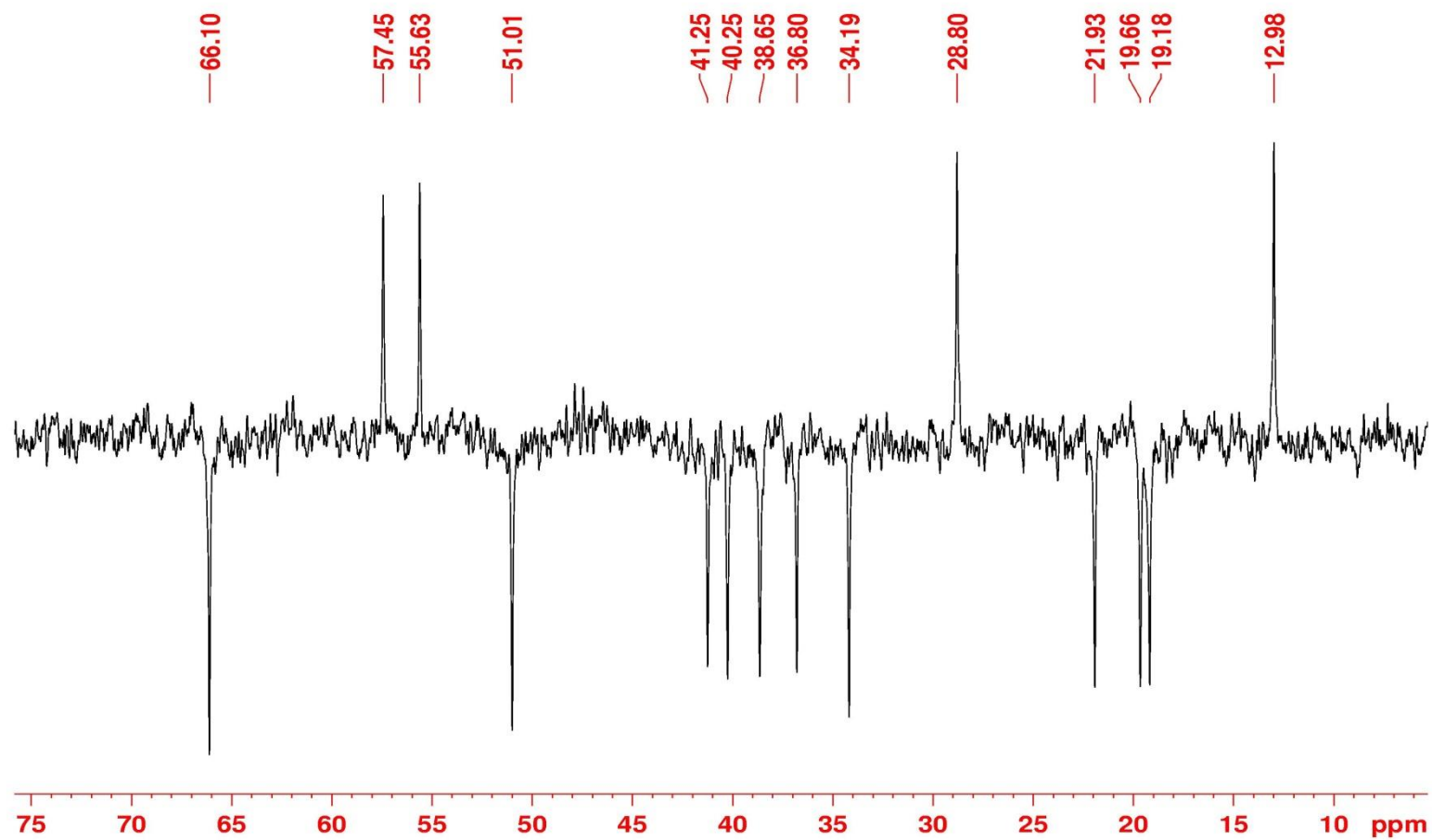


Figure 90: ^{13}C $\{^1\text{H}\}$ DEPT-NMR (50 MHz, Methanol-d₄) spectrum of compound **5k**.

169-ASADHSONH_131011180217 #3638 RT: 12.83 AV: 1 NL: 3.73E2
T: ITMS + c ESI Full ms2 386.00@cid0.00 [105.00-500.00]

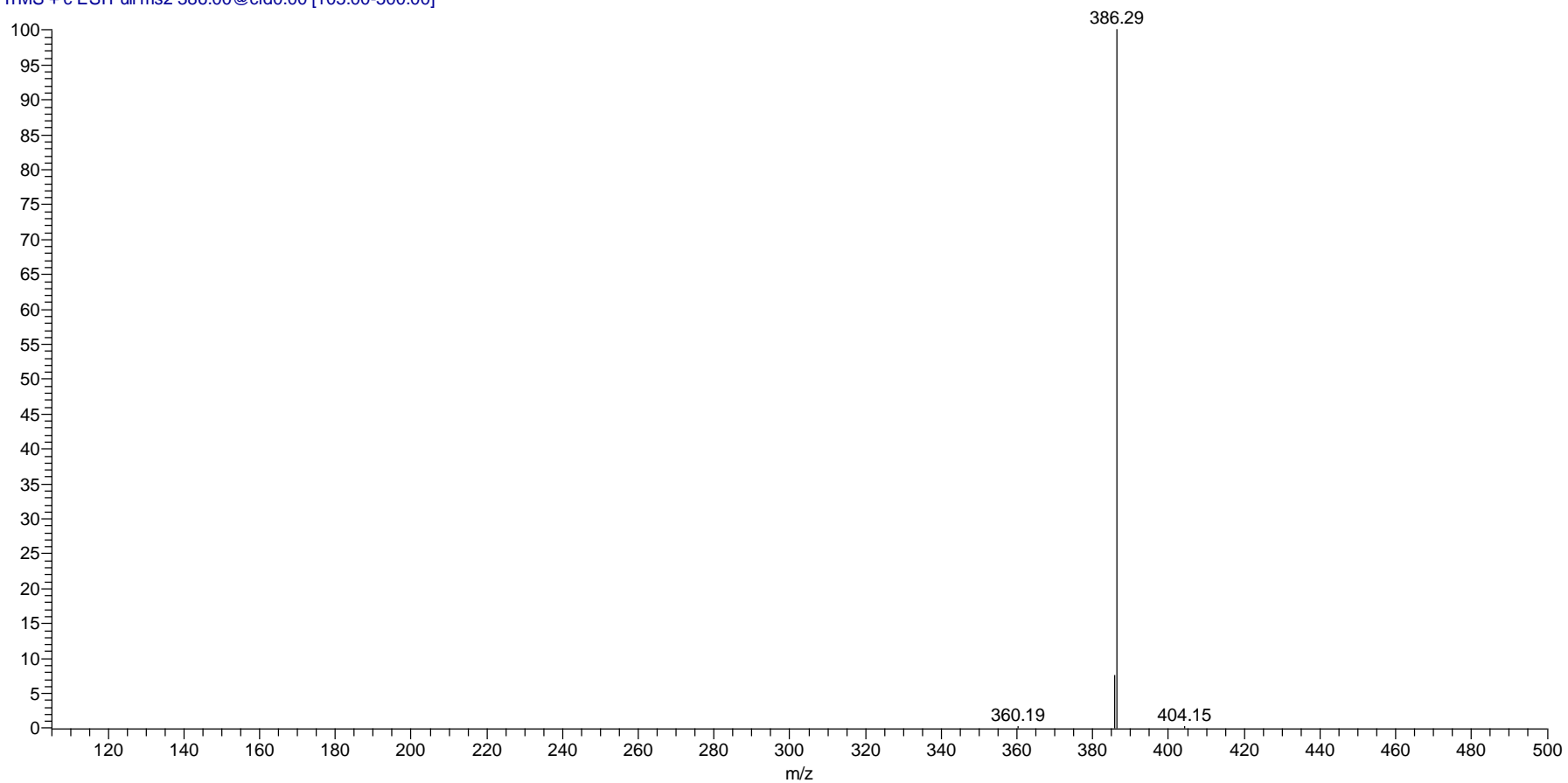


Figure 91: ESI-MS spectrum of compound **2f**.

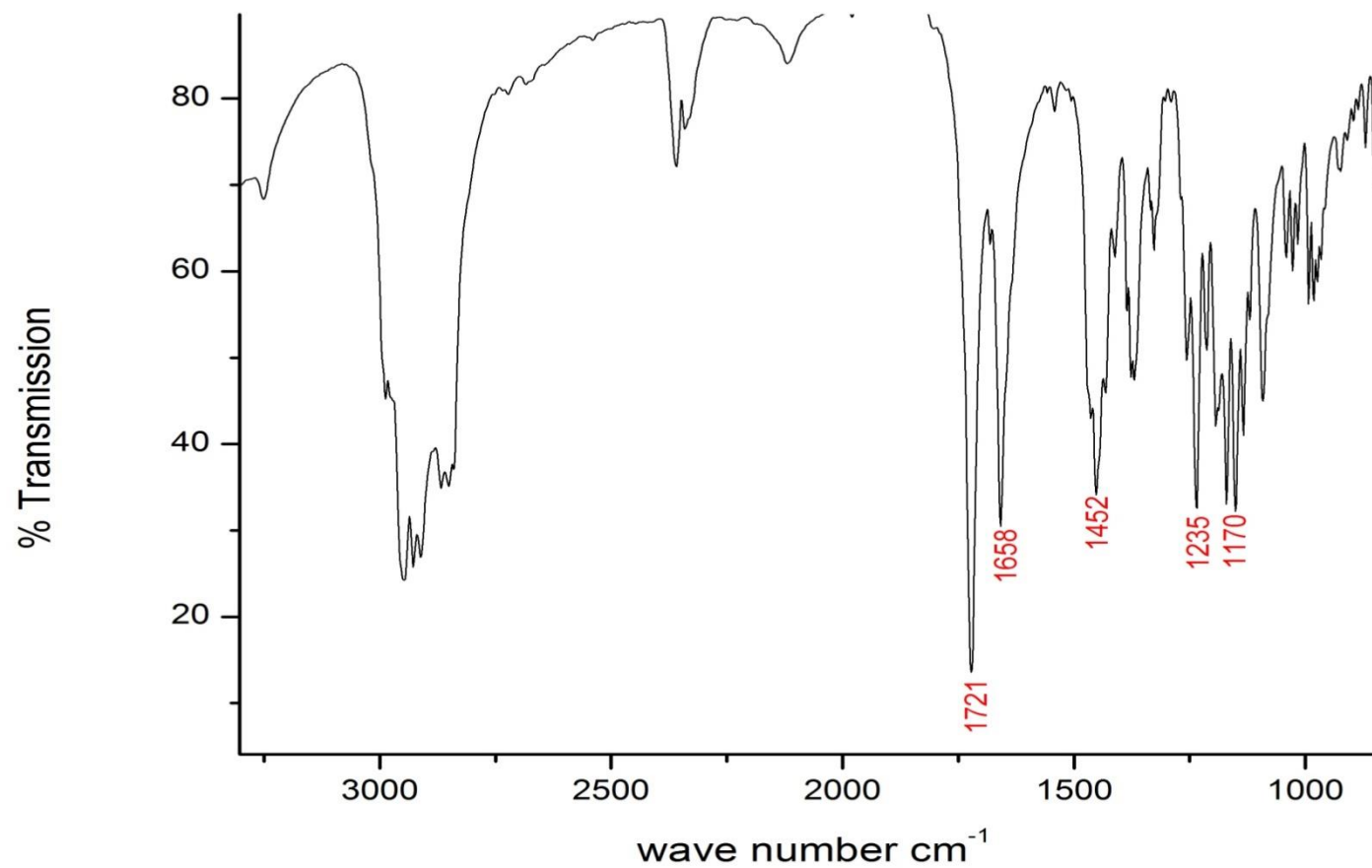


Figure 92: IR spectrum of compound **2f**.

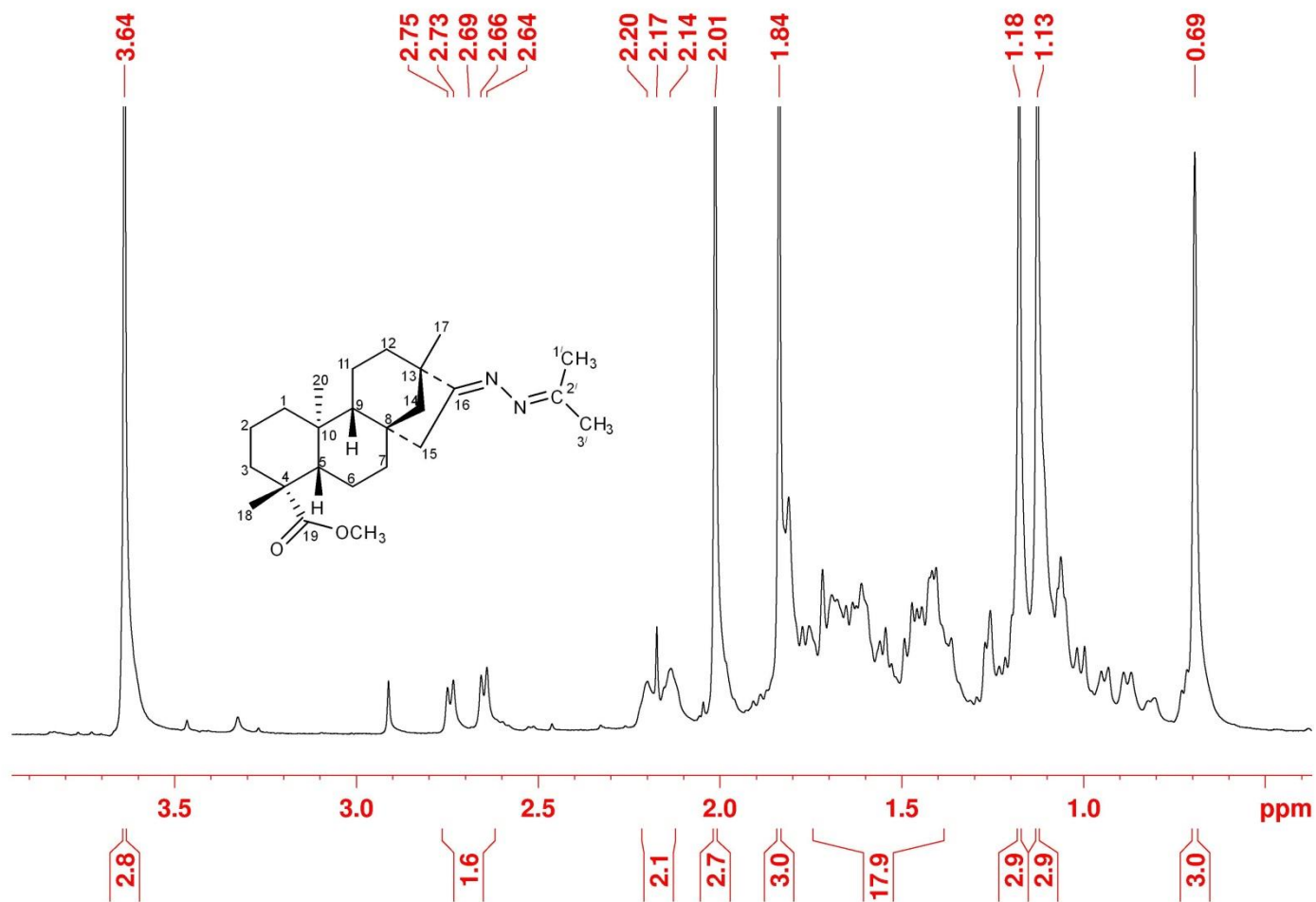


Figure 93: ¹H-NMR (200 MHz, CDCl₃) spectrum of compound **2f**.

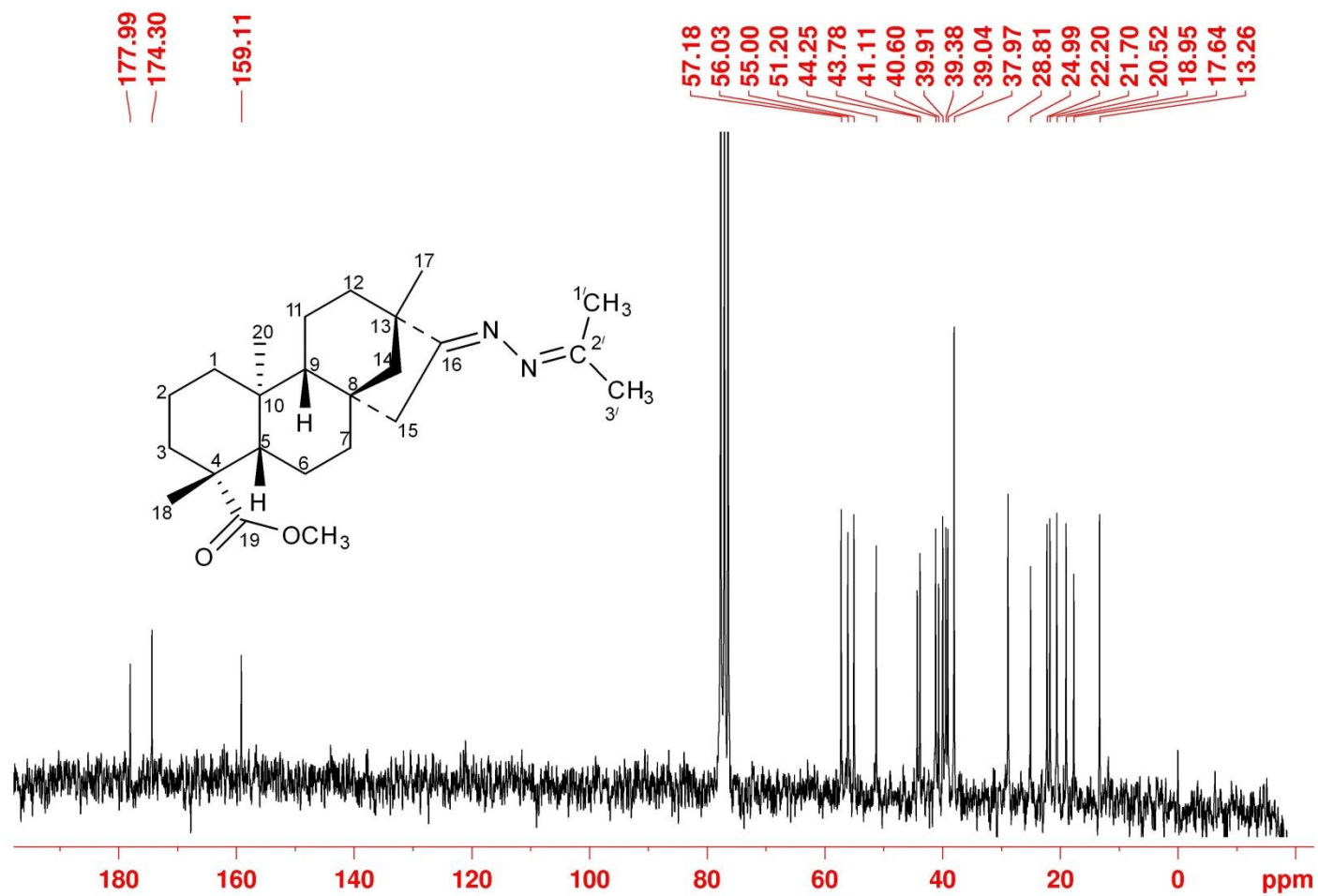


Figure 94: ^{13}C $\{^1\text{H}\}$ NMR (50 MHz, CDCl₃) spectrum of compound **2f**

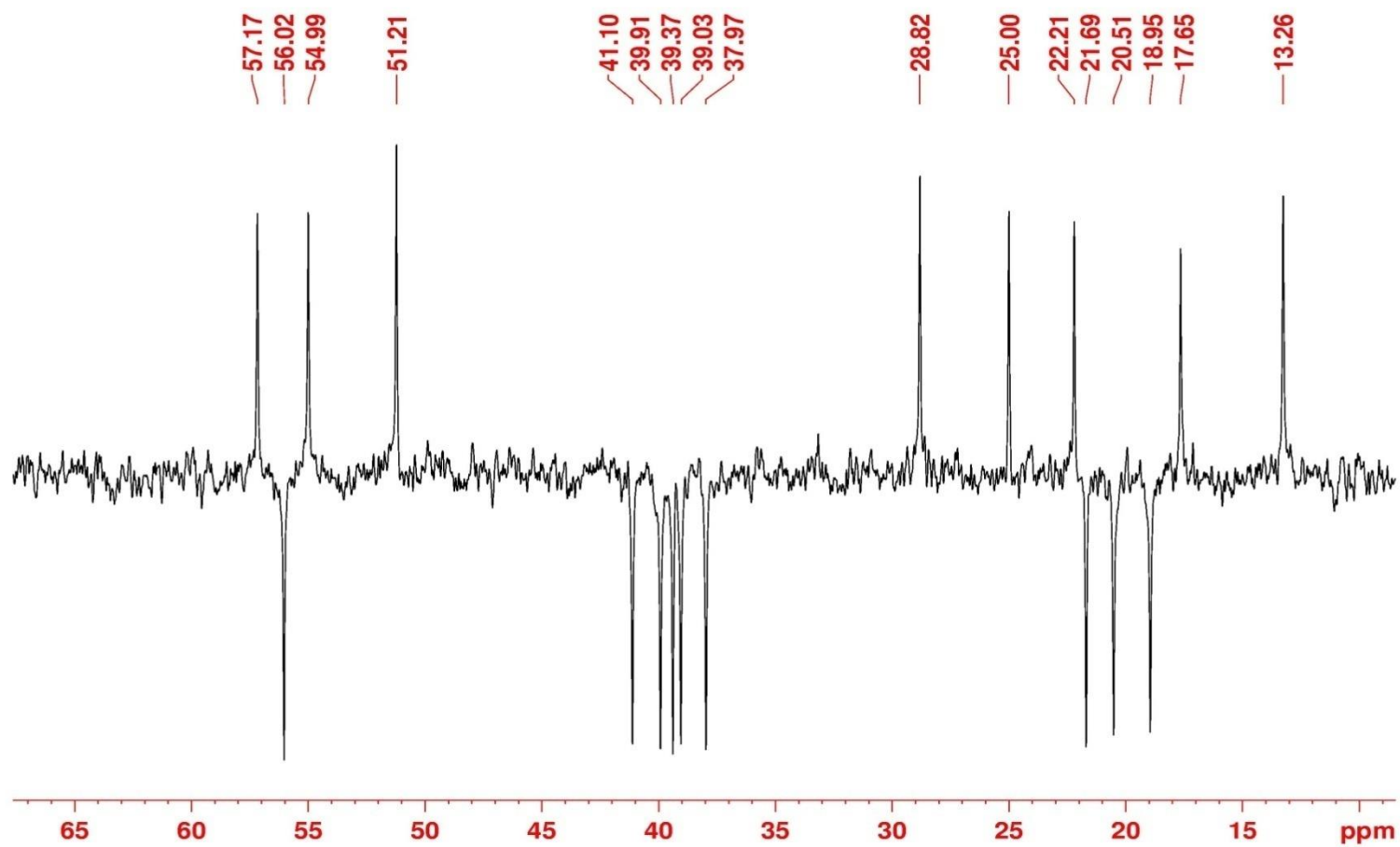


Figure 95: ^{13}C { ^1H } DEPT NMR (50 MHz, CDCl_3) spectrum of compound **2f**.

195-ASADHBE_131125163213 #2230 RT: 5.74 AV: 1 NL: 1.38E2
T: ITMS - c ESI Full ms2 407.00@cid22.00 [110.00-500.00]

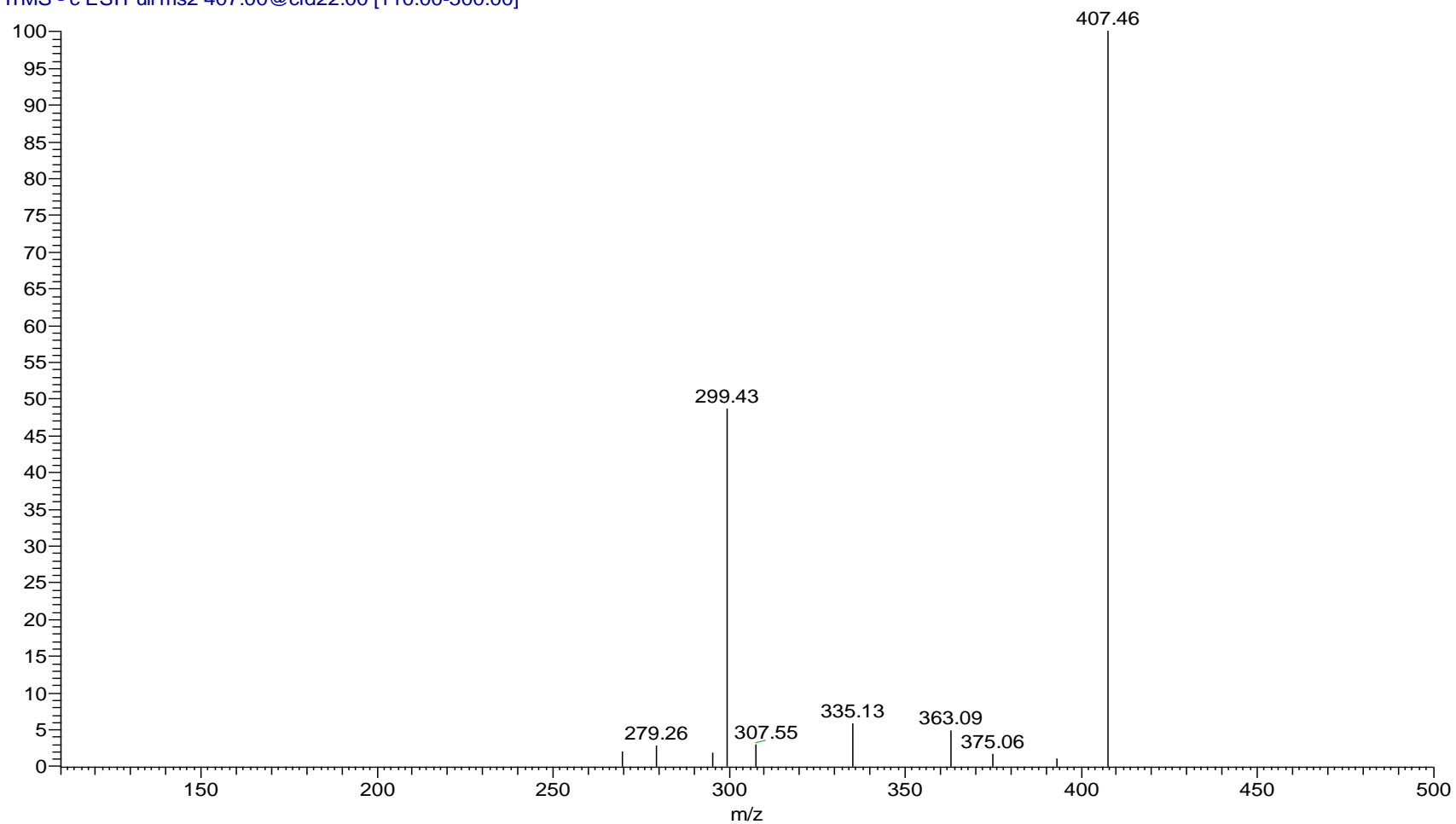


Figure 96: ESI-MS spectrum of compound **2a**.

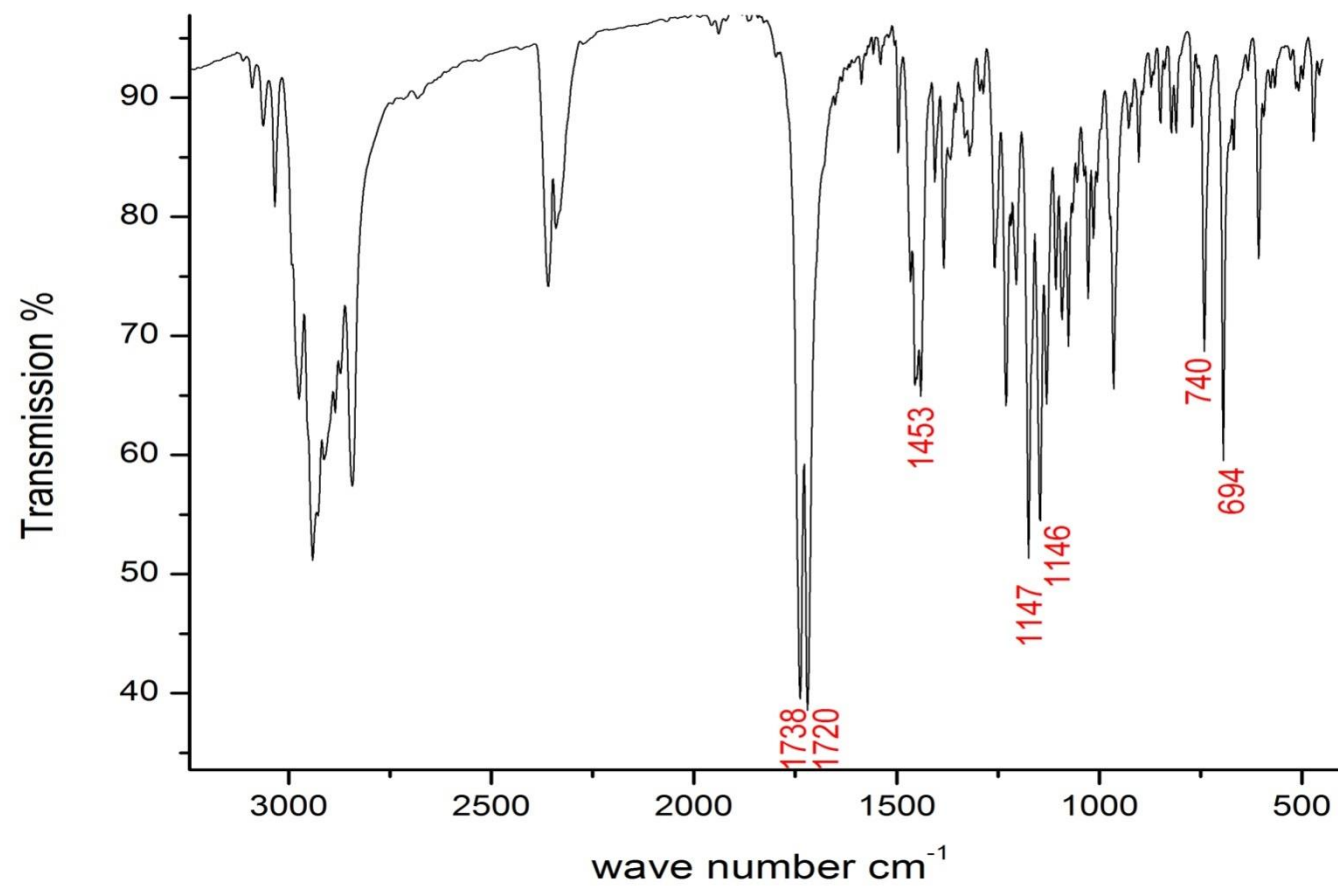


Figure 97: IR spectrum of compound **2a**.

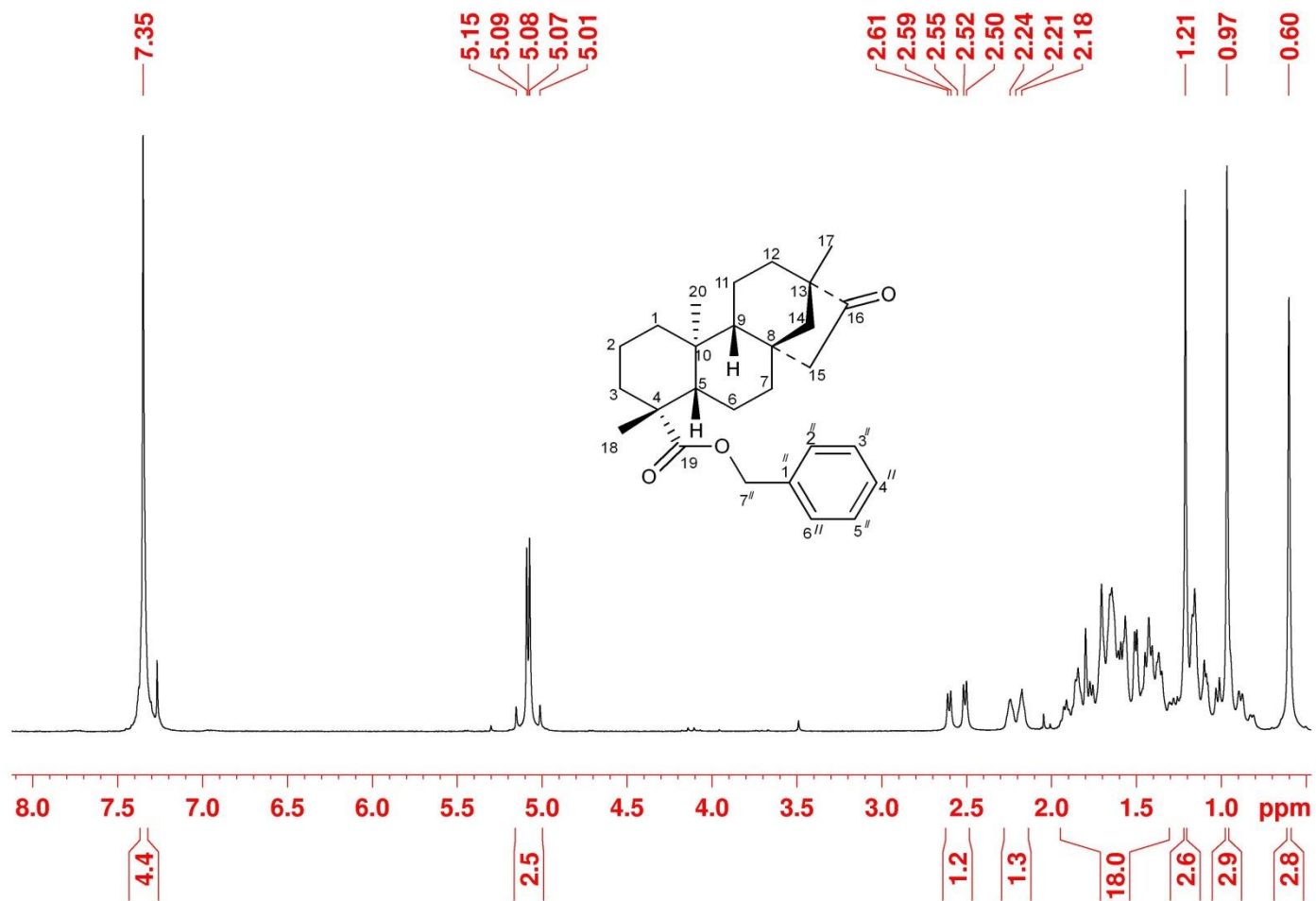


Figure 98: ^1H NMR (200 MHz, CDCl_3) spectrum of compound **2a**.

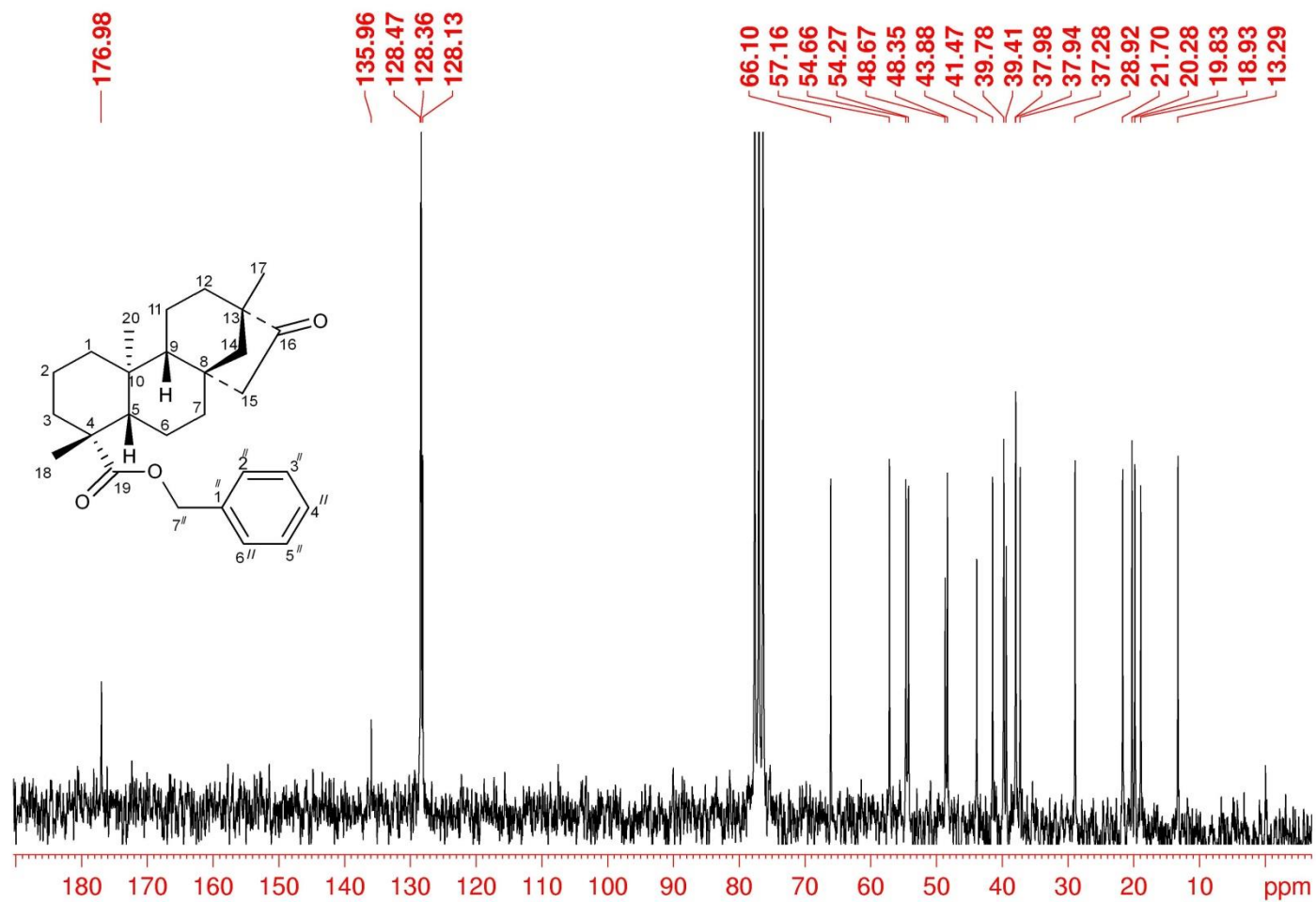


Figure 99: ^{13}C $\{^1\text{H}\}$ NMR (50 MHz, CDCl_3) spectrum of compound **2a**.

194-ASADI-HBE_131125163213 #909 RT: 2.51 AV: 1 NL: 3.00E3
T: ITMS - c ESI Full ms2 409.40@cid0.00 [110.00-500.00]

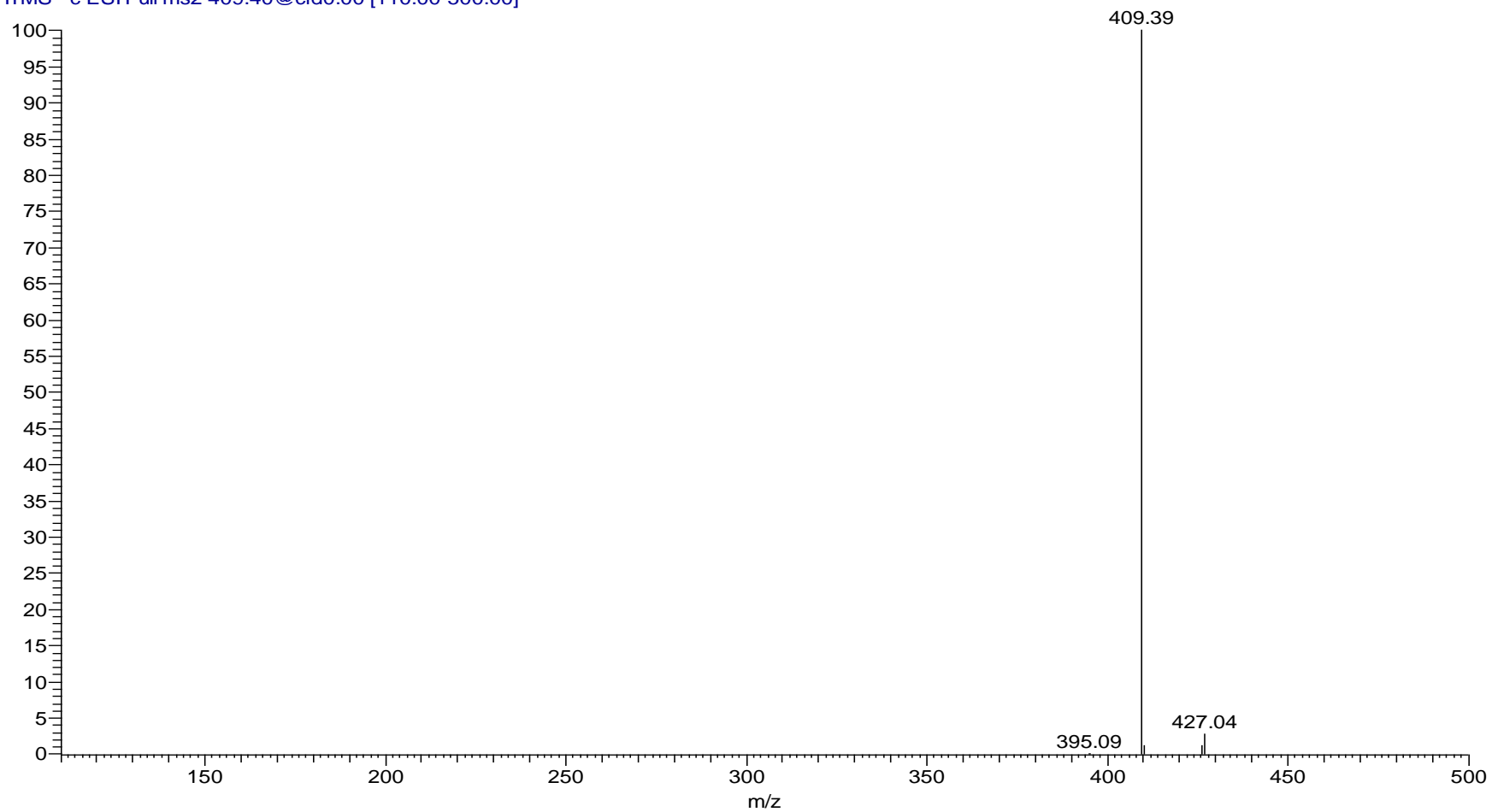


Figure 100: ESI-MS spectrum of compound **2b**.

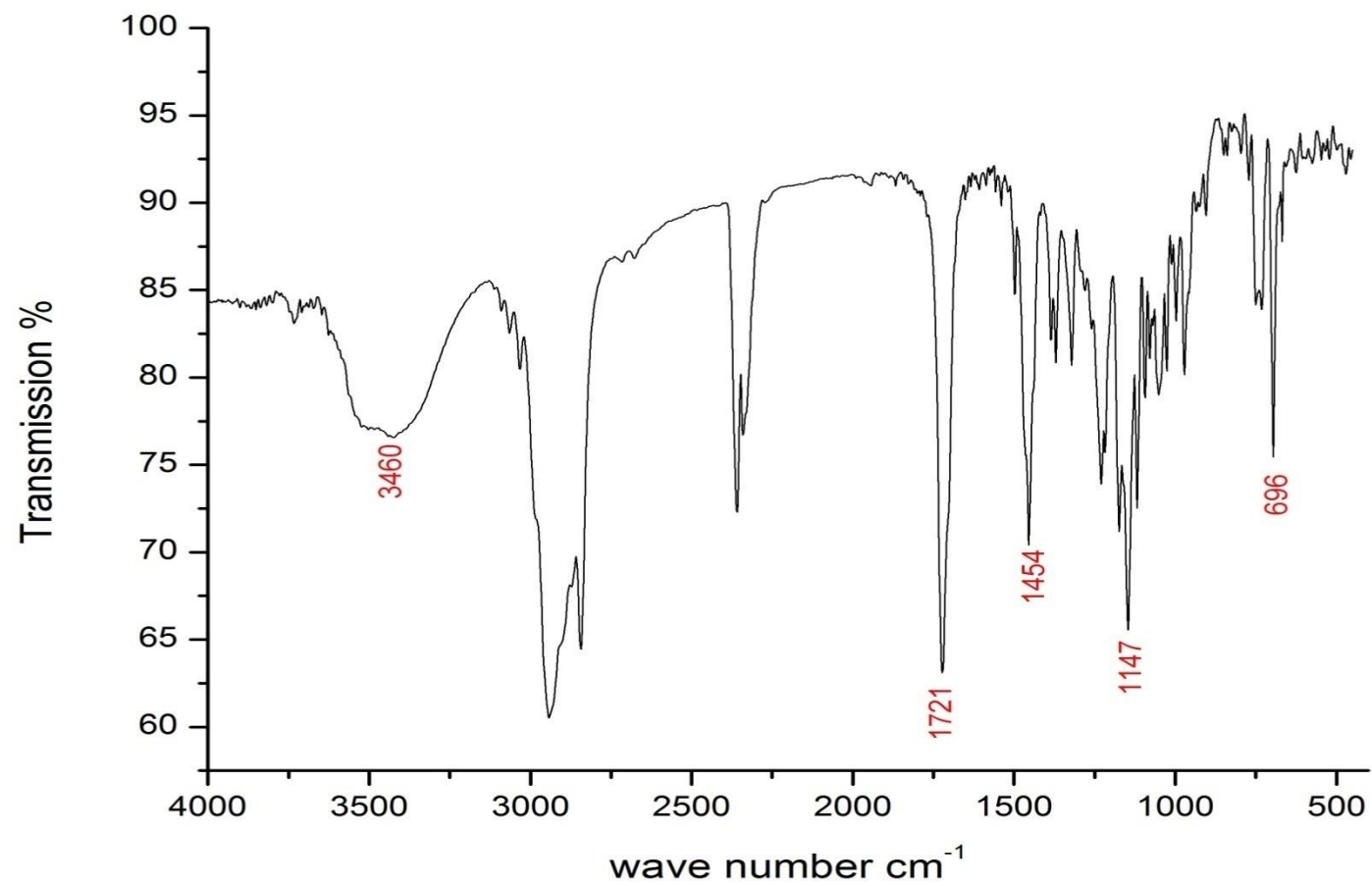


Figure 101: IR spectrum of compound **2b**.

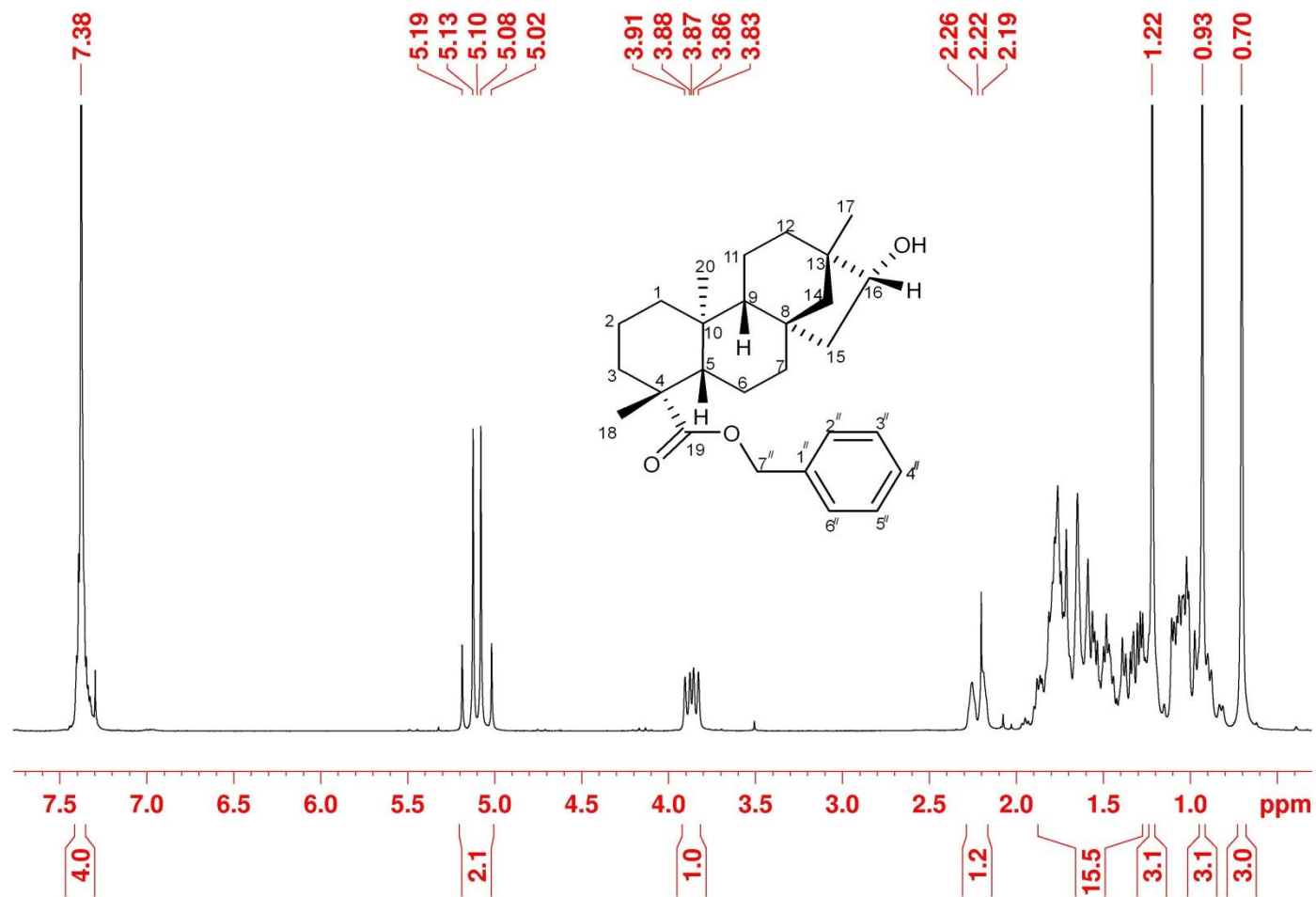


Figure 102: $^1\text{H-NMR}$ (200 MHz, CDCl_3) spectrum of compound **2b**.

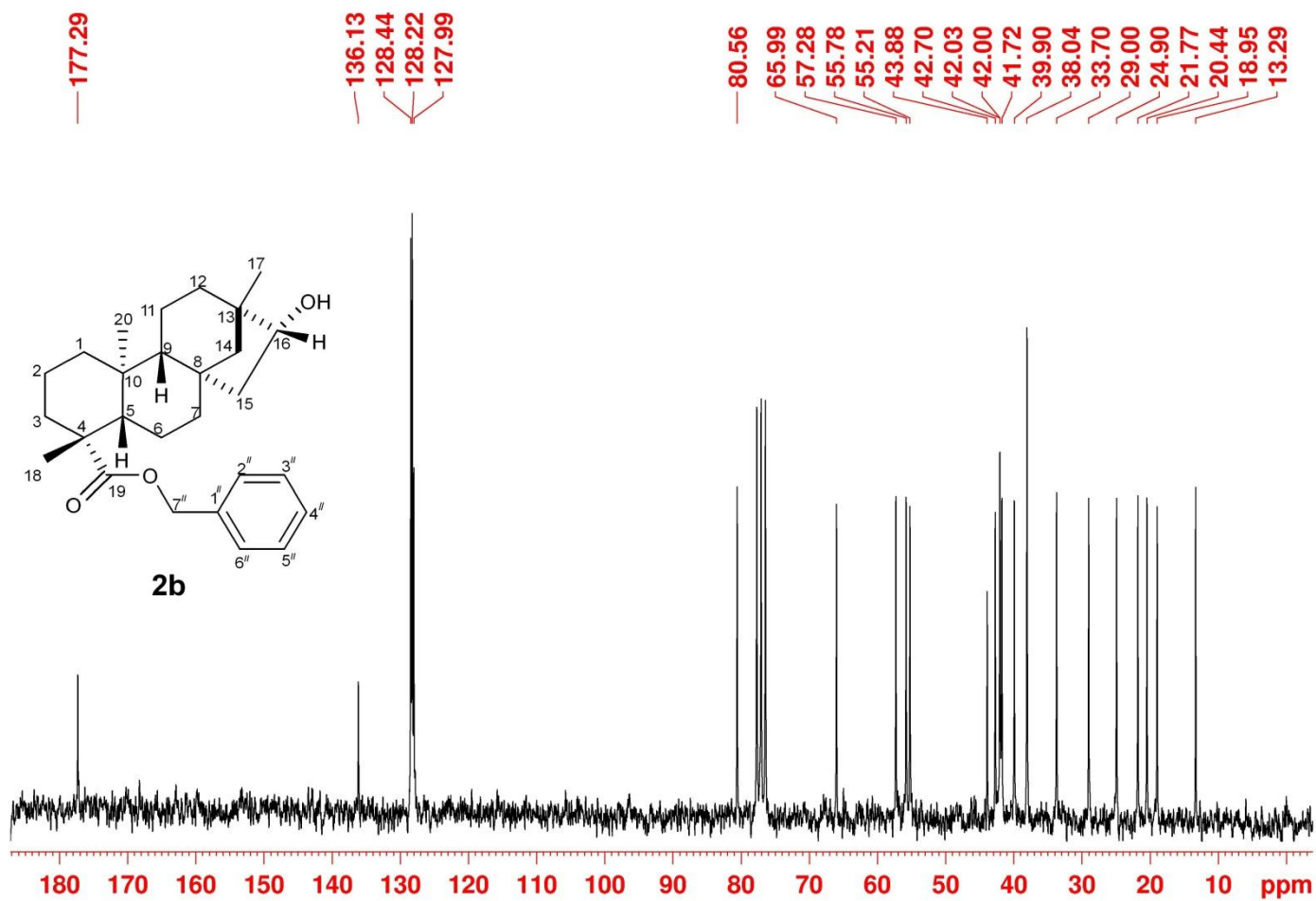


Figure 103: ^{13}C $\{^1\text{H}\}$ NMR (50 MHz, CDCl_3) spectrum of compound **2b**.

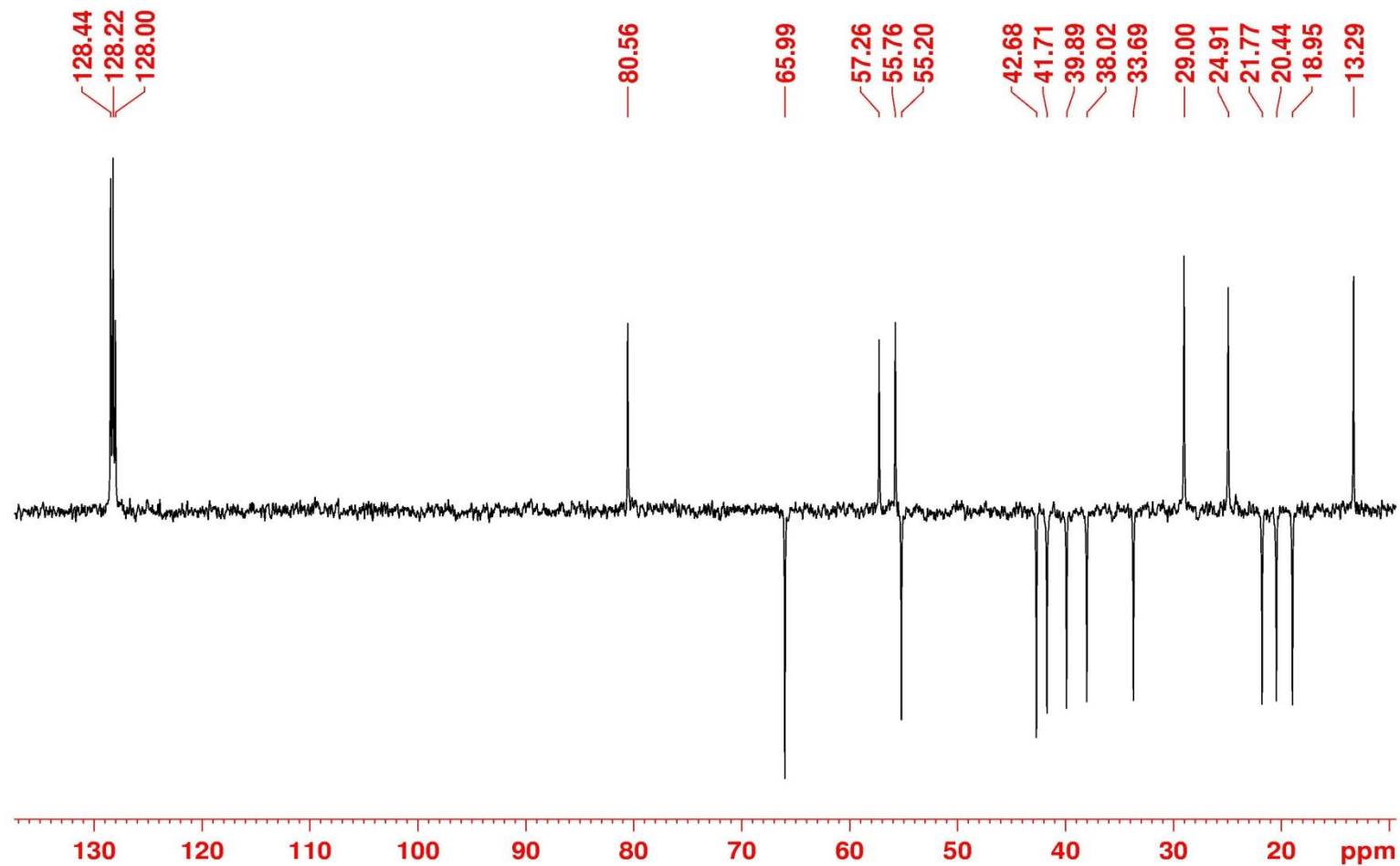


Figure 104: ^{13}C $\{^1\text{H}\}$ DEPT-NMR (50 MHz, CDCl_3) spectrum of compound **2b**.

193-ASADI-OBE_131125163213 #403 RT: 0.97 AV: 1 NL: 3.78E3
T: ITMS - c ESI Full ms2 422.00@cid0.00 [115.00-800.00]

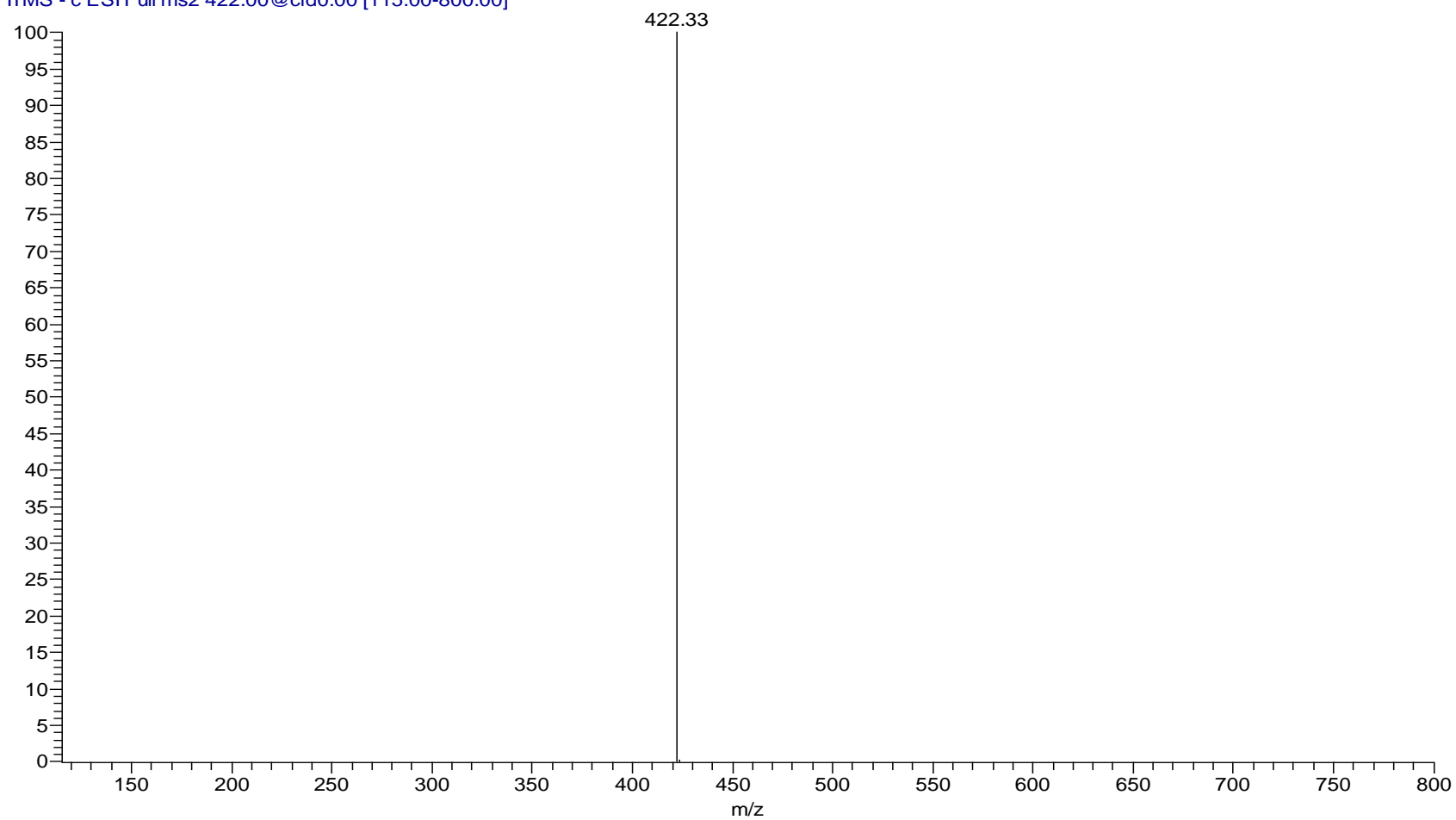


Figure 105: ESI-MS spectrum of compound **2c**.

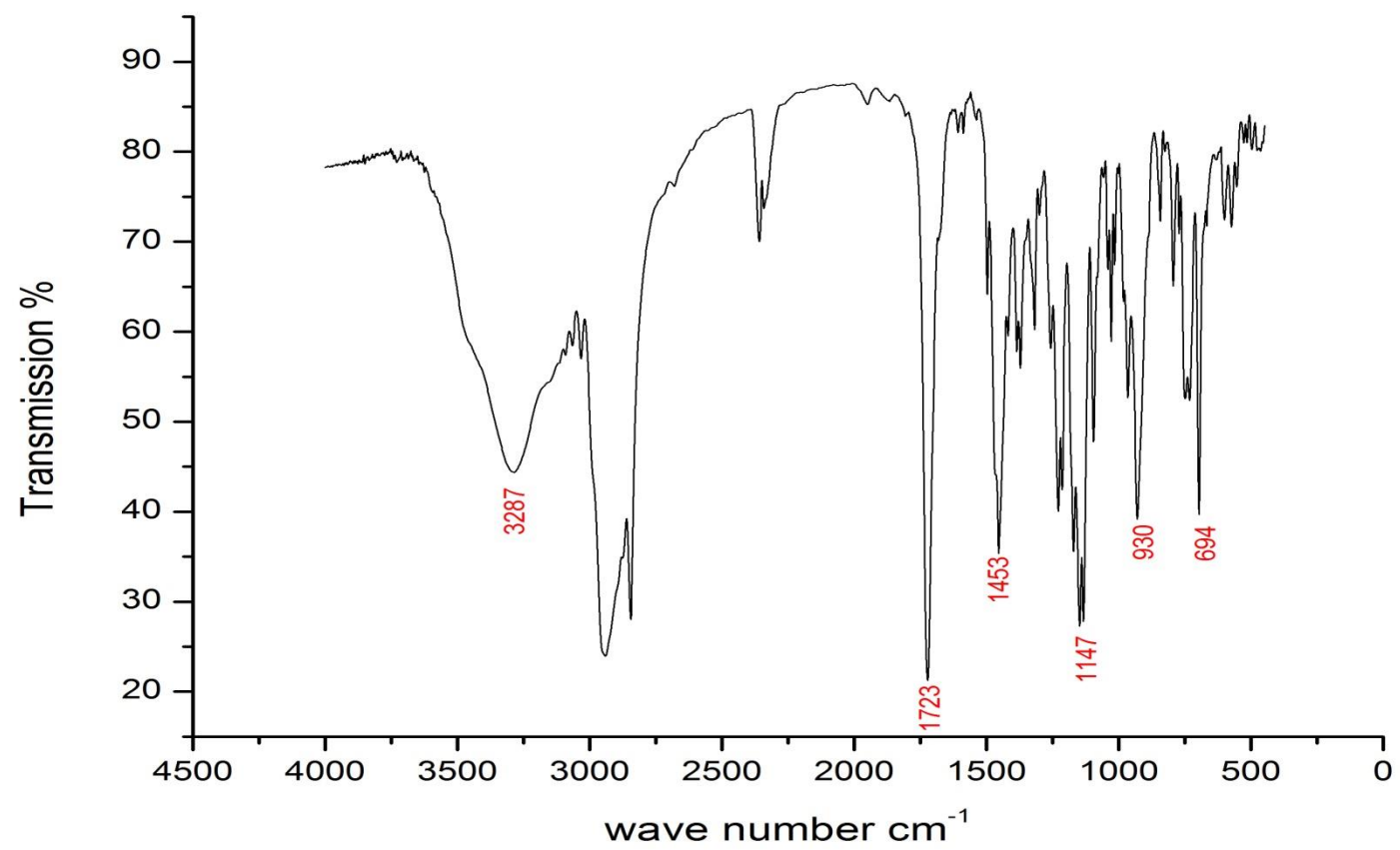


Figure 106: IR spectrum of compound **2c**.

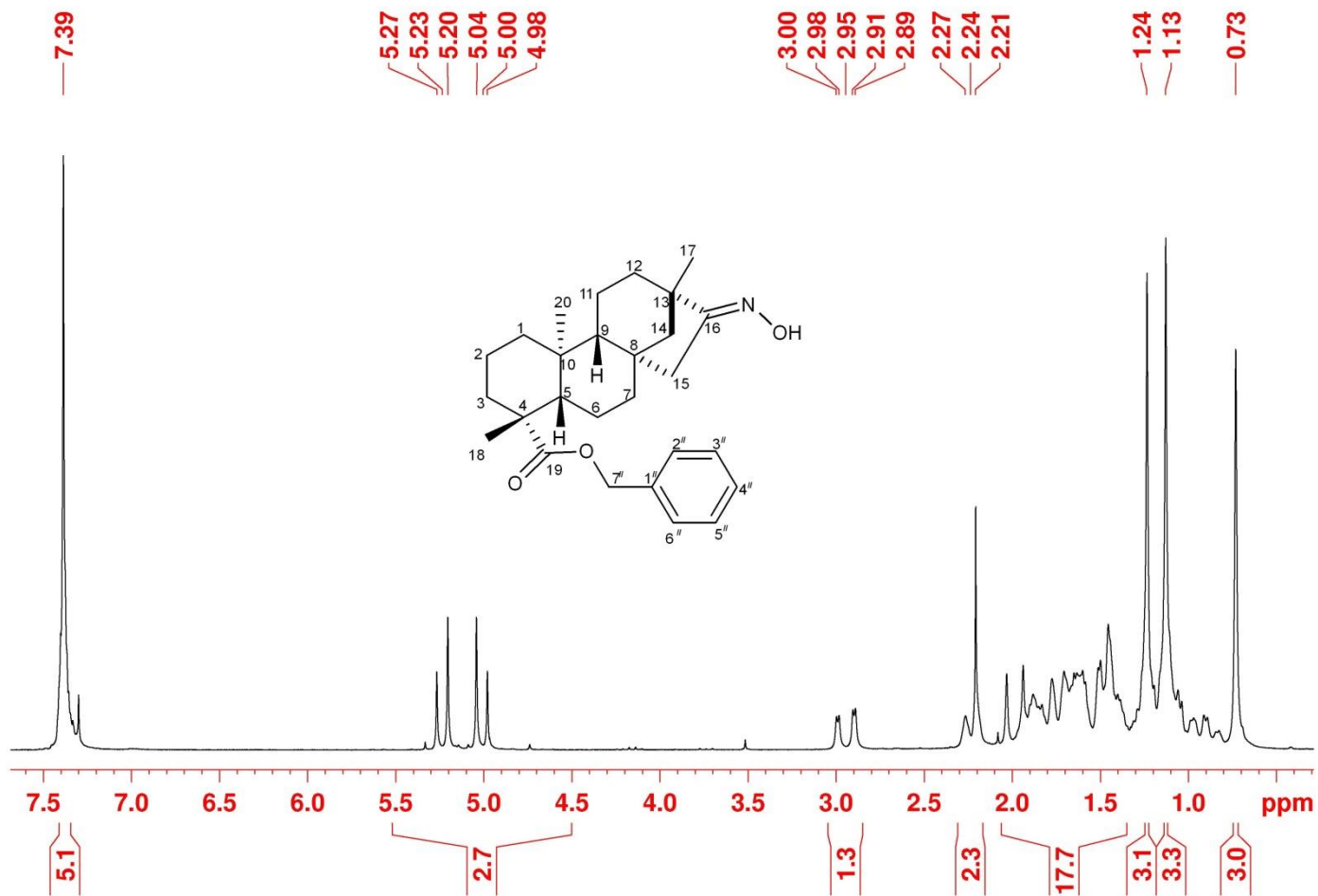


Figure 107: ¹H-NMR (200 MHz, CDCl₃) spectrum of compound **2c**.

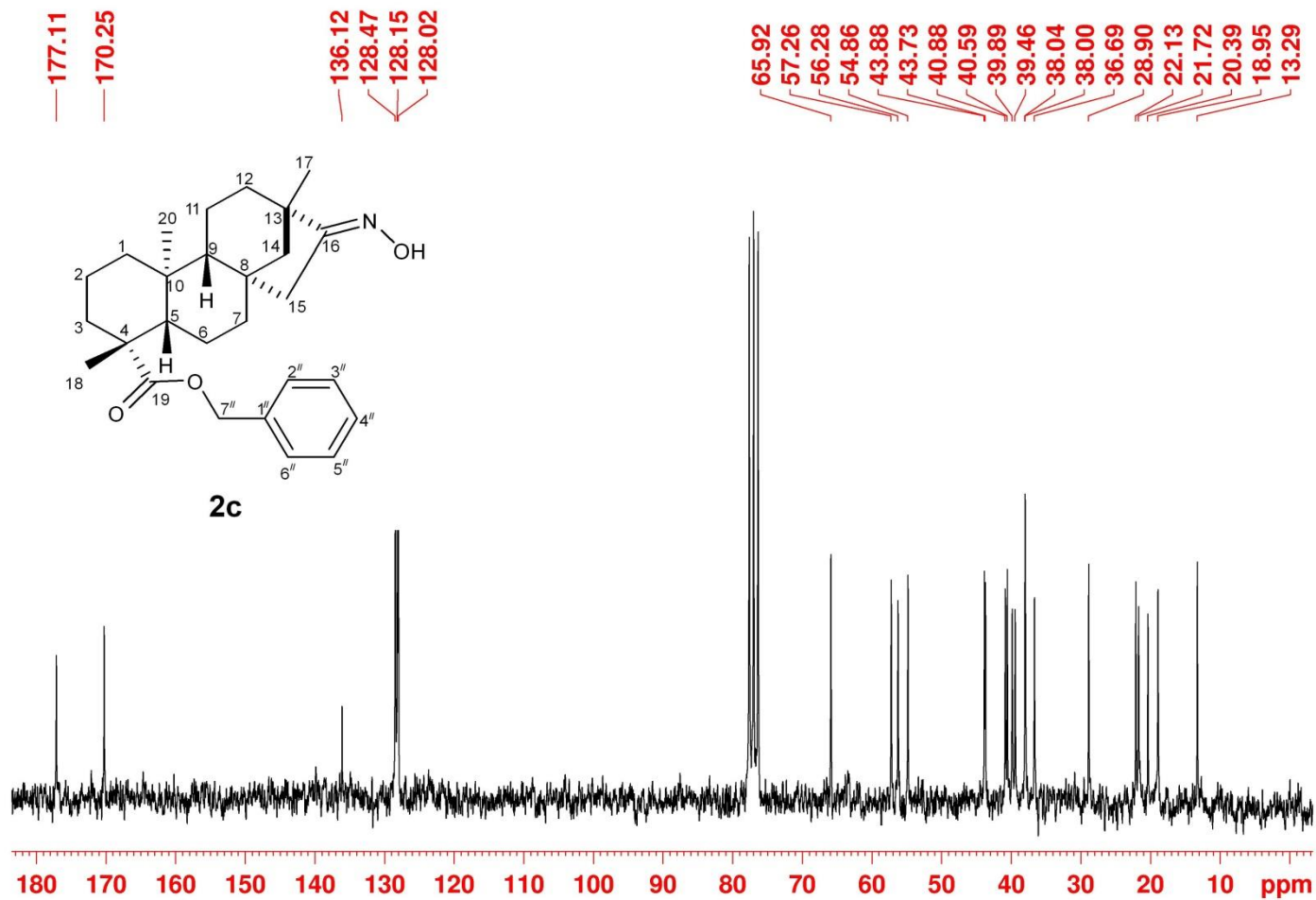


Figure 108: ^{13}C $\{^1\text{H}\}$ NMR (50 MHz, CDCl_3) spectrum of compound **2c**.

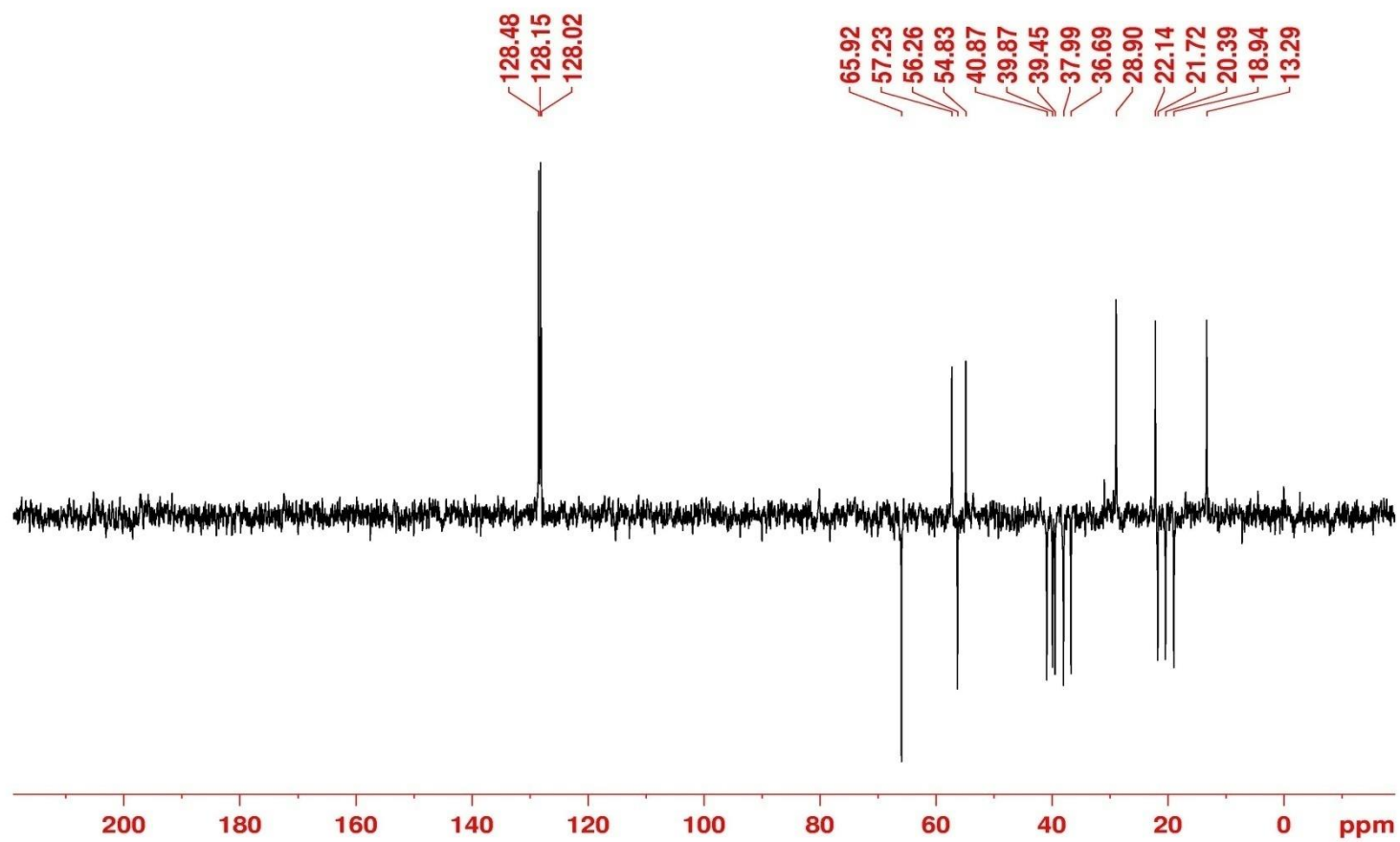


Figure 109: ^{13}C $\{^1\text{H}\}$ DEPT-NMR (50 MHz, CDCl_3) spectrum of compound **2c**.

ILB_140724164207 #1967 RT: 4.69 AV: 1 NL: 1.61E6
T: ITMS + c ESI Full ms [355.00-470.00]

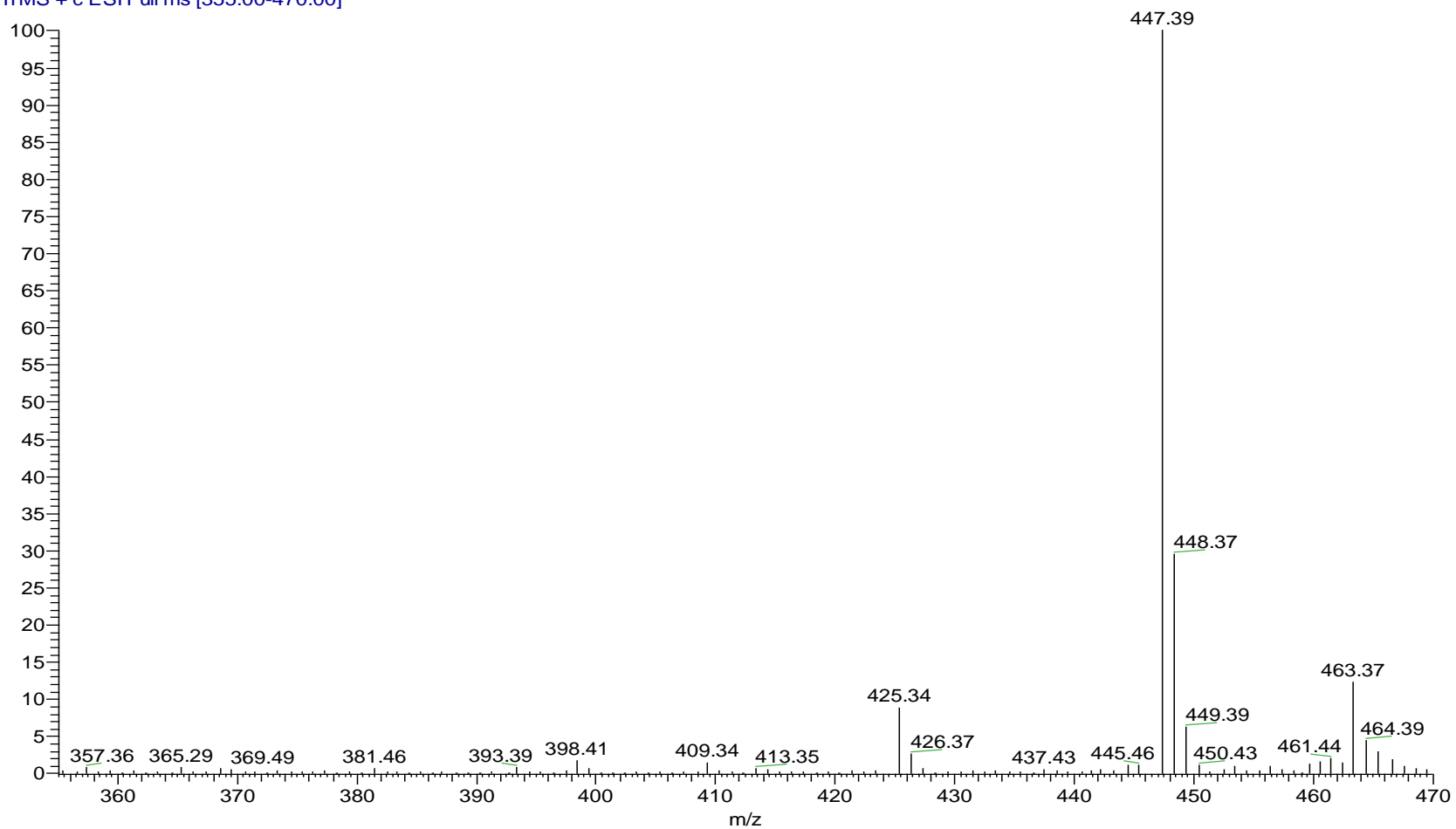


Figure 110: ESI-MS spectrum of compound **2d**.

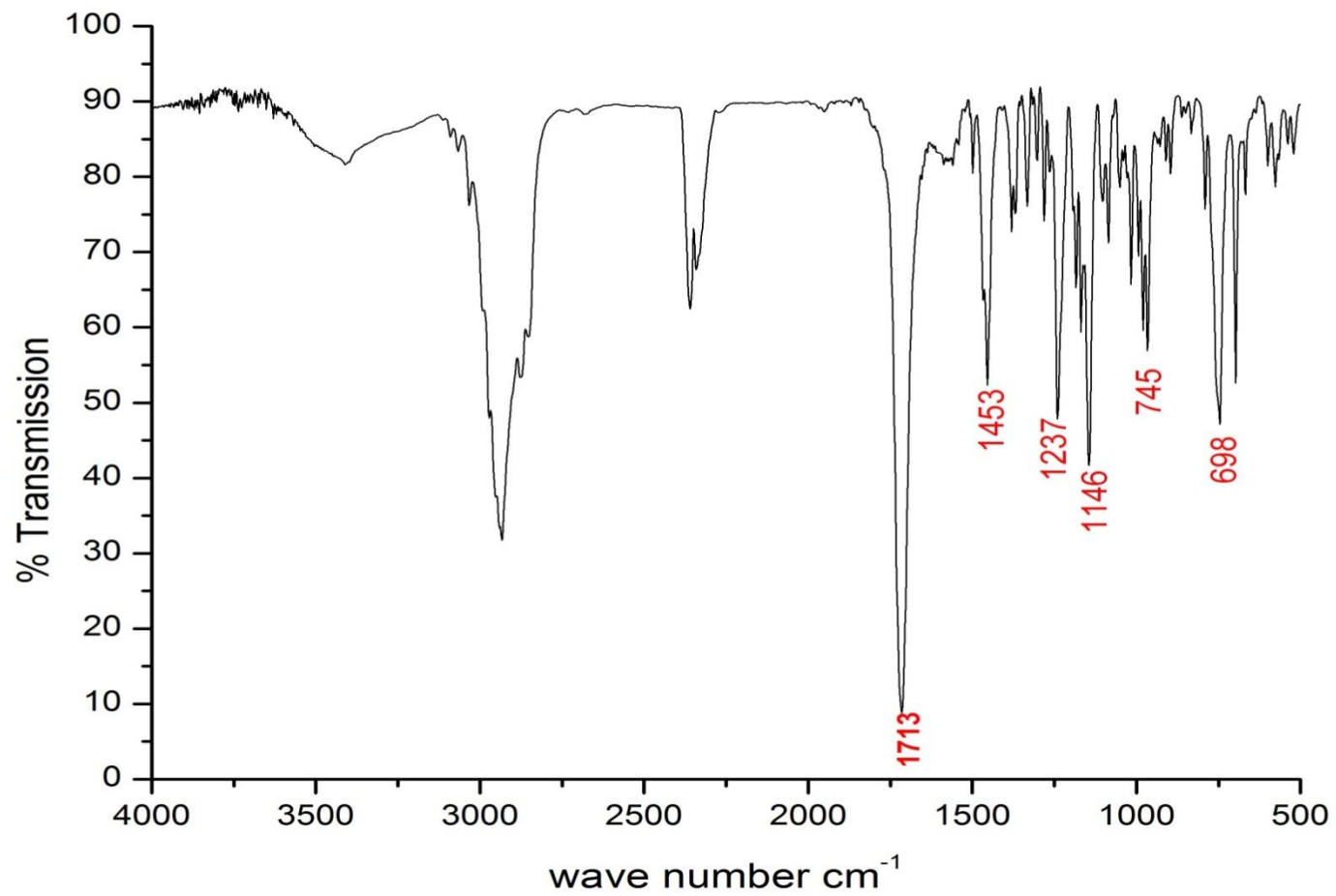


Figure 111: IR spectrum of compound **2d**.

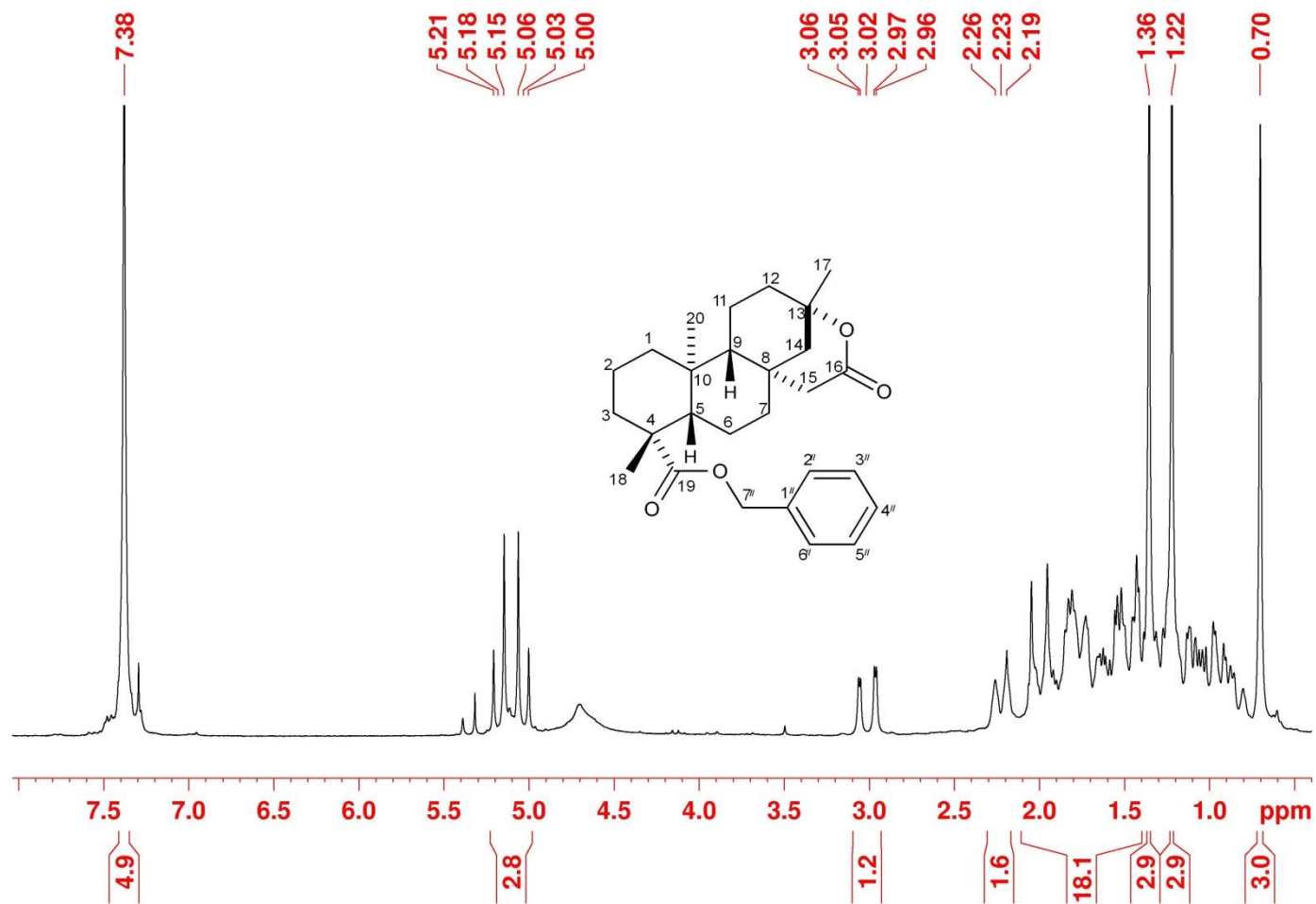


Figure 112: ¹H-NMR (200 MHz, CDCl₃) spectrum of compound **2d**.

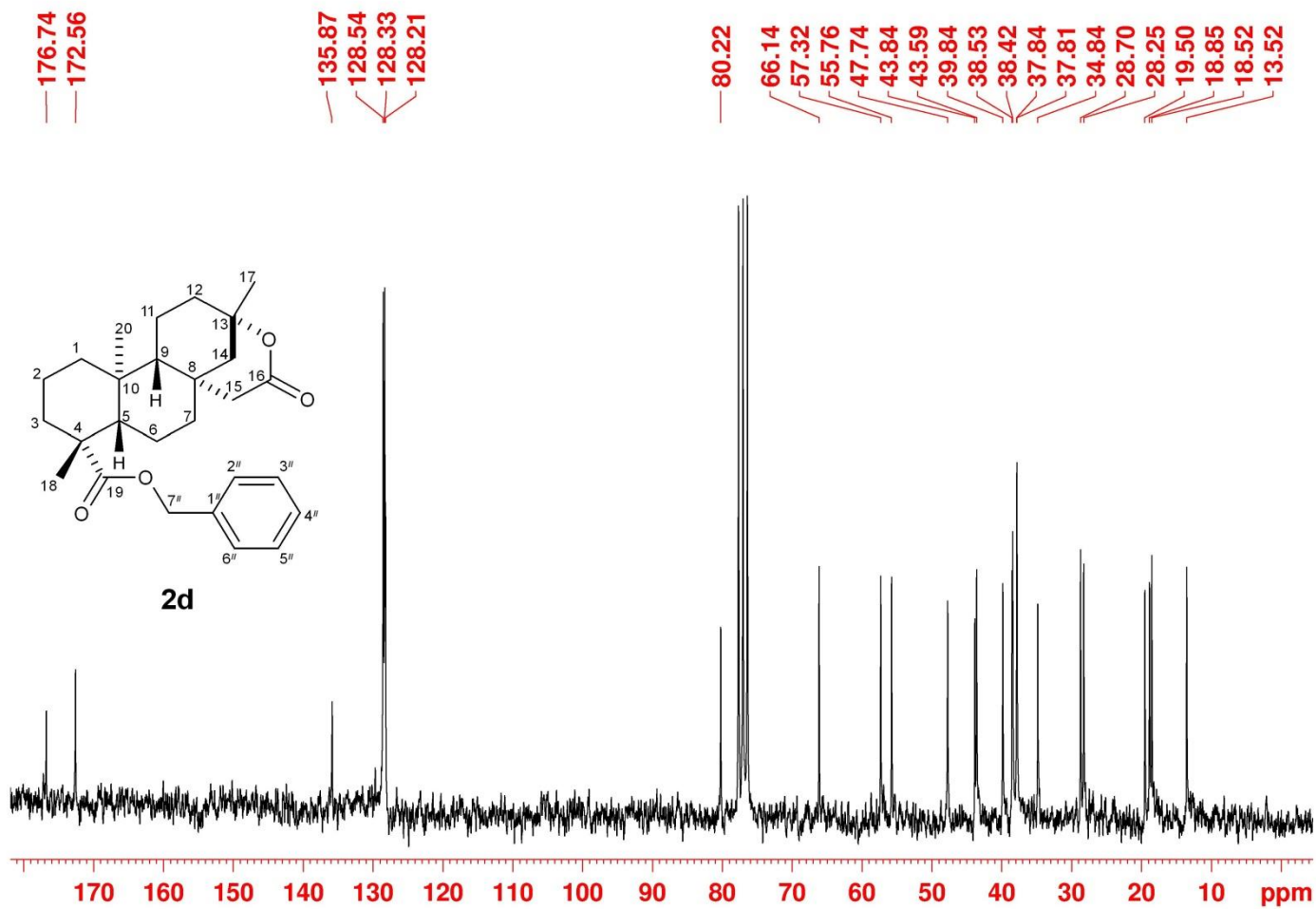


Figure 113: ^{13}C $\{^1\text{H}\}$ NMR (50 MHz, CDCl_3) spectrum of compound **2d**.

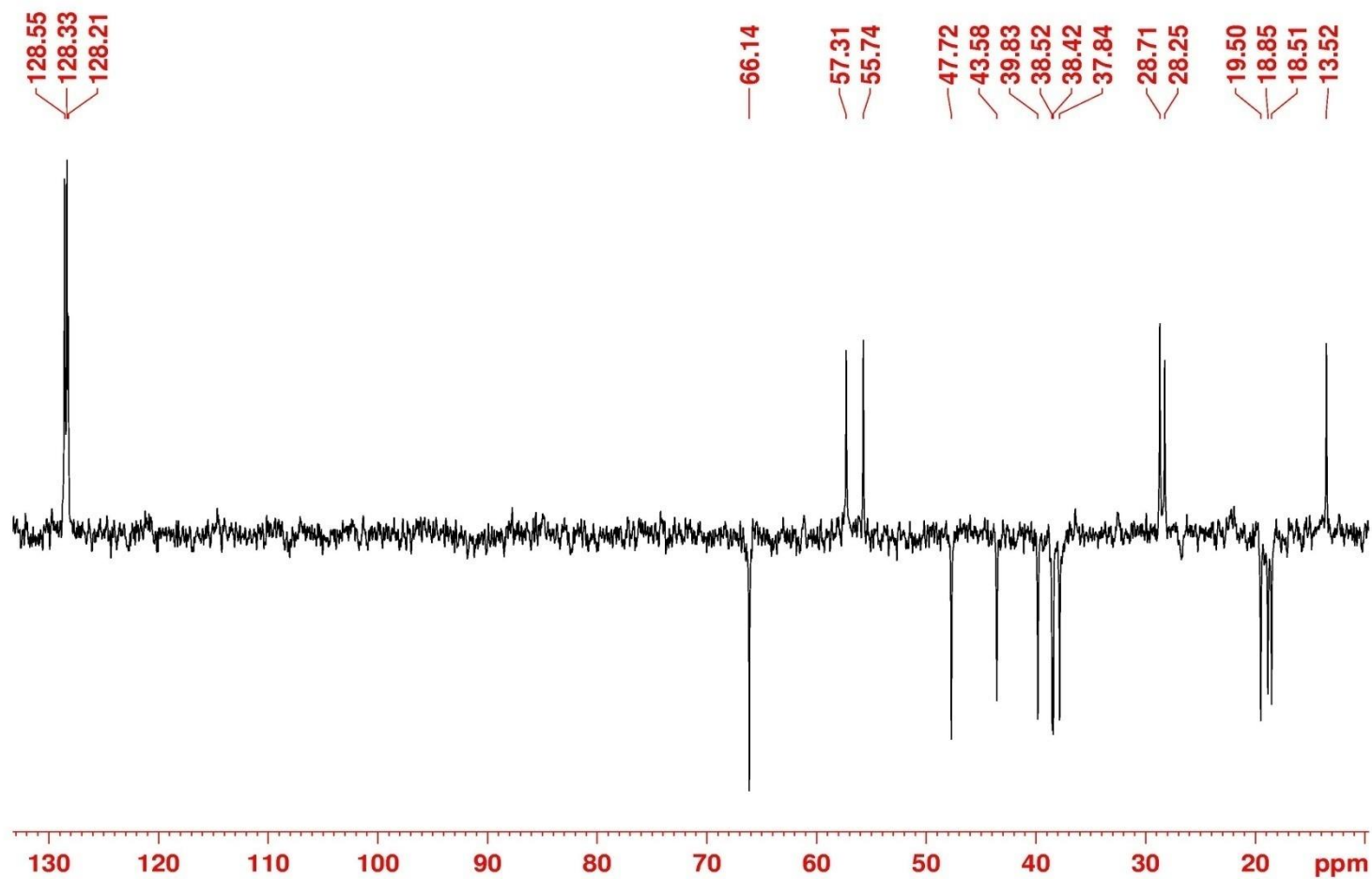


Figure 114: ^{13}C { ^1H } DEPT-NMR (50 MHz, CDCl_3) spectrum of compound **2d**.

IDB1_140724173744 #860 RT: 2.26 AV: 1 NL: 7.77E4
T: ITMS + c ESI Full ms2 423.00@cid0.00 [115.00-600.00]

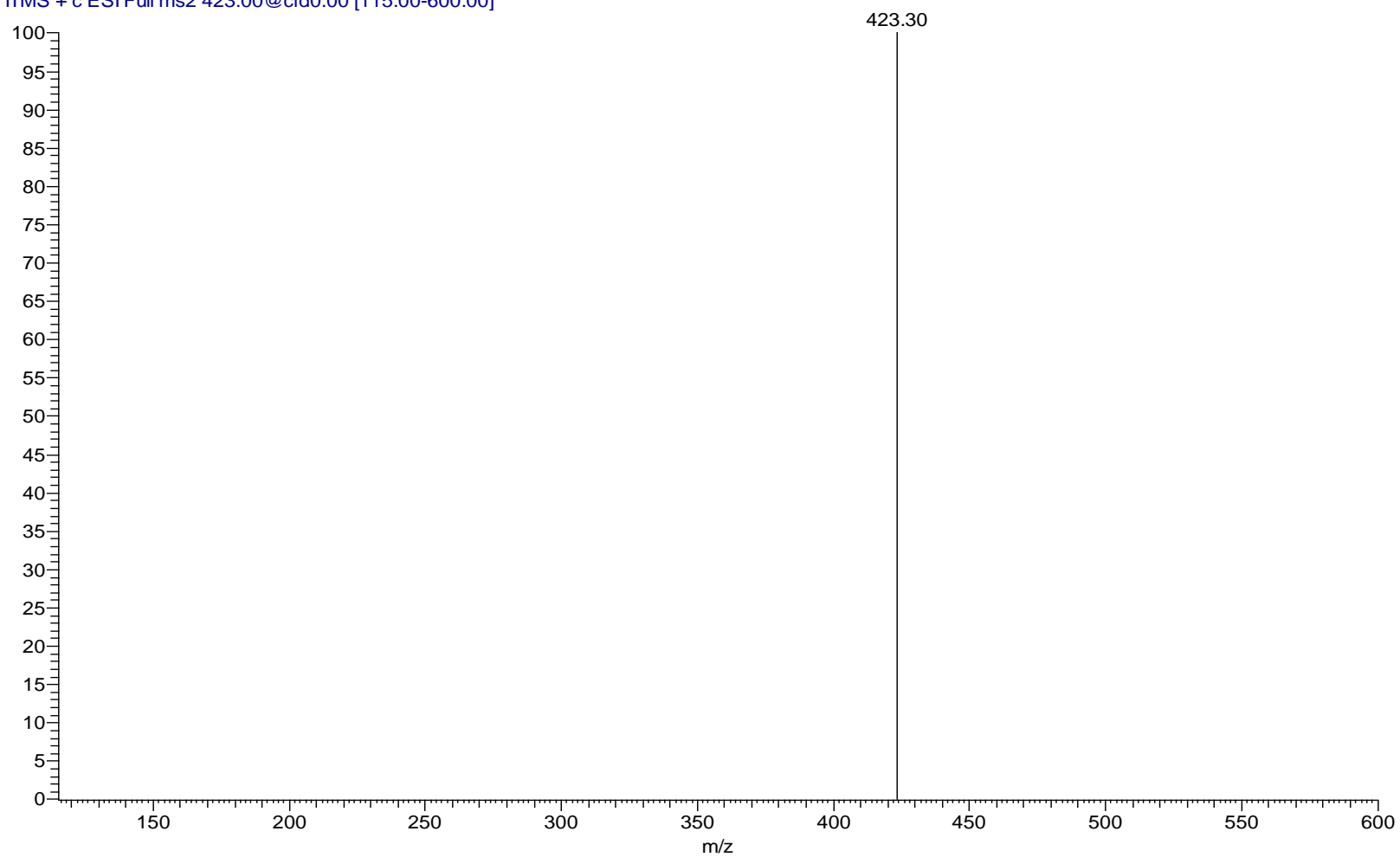


Figure 115: ESI-MS spectrum of compound **3f**.

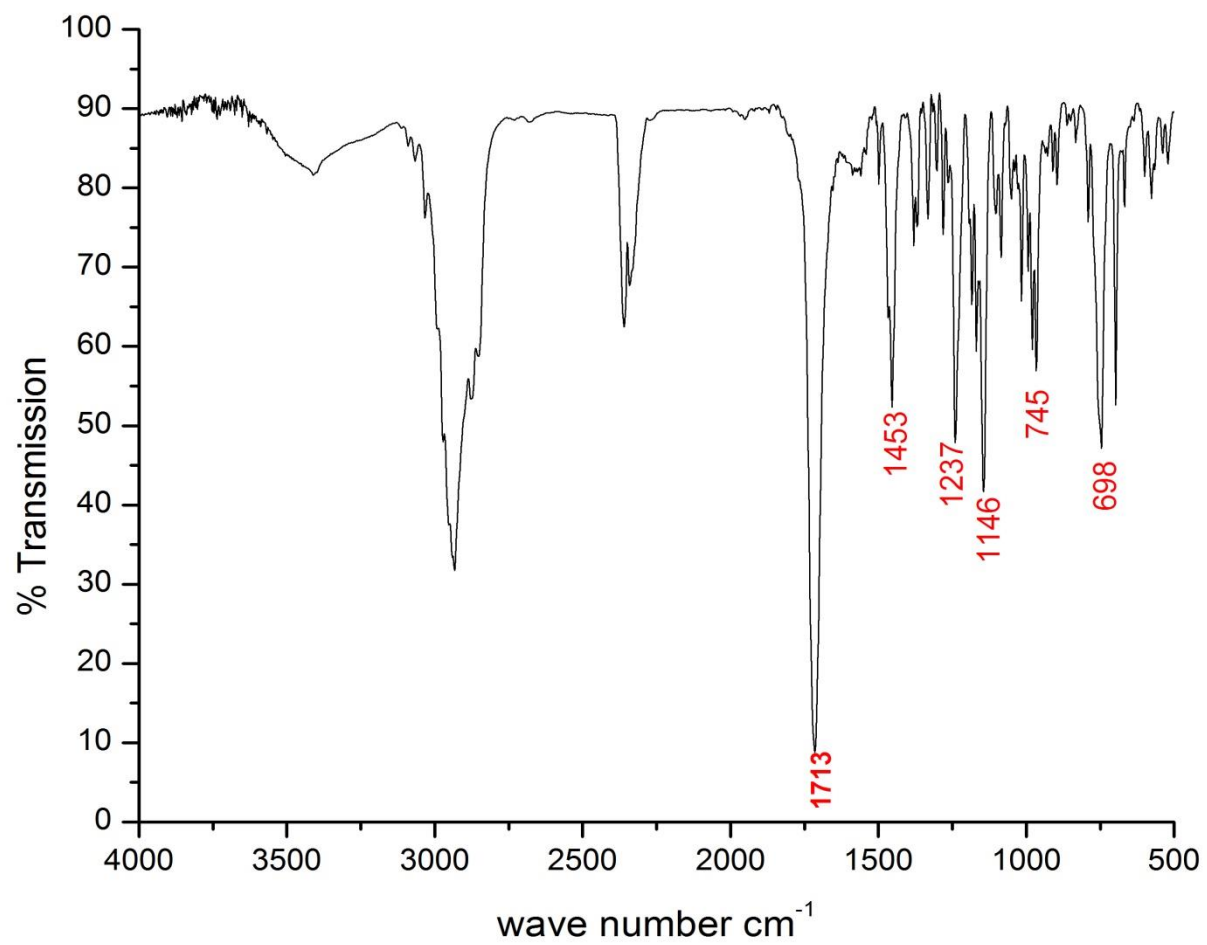


Figure 116: IR spectrum of compound **3f**.

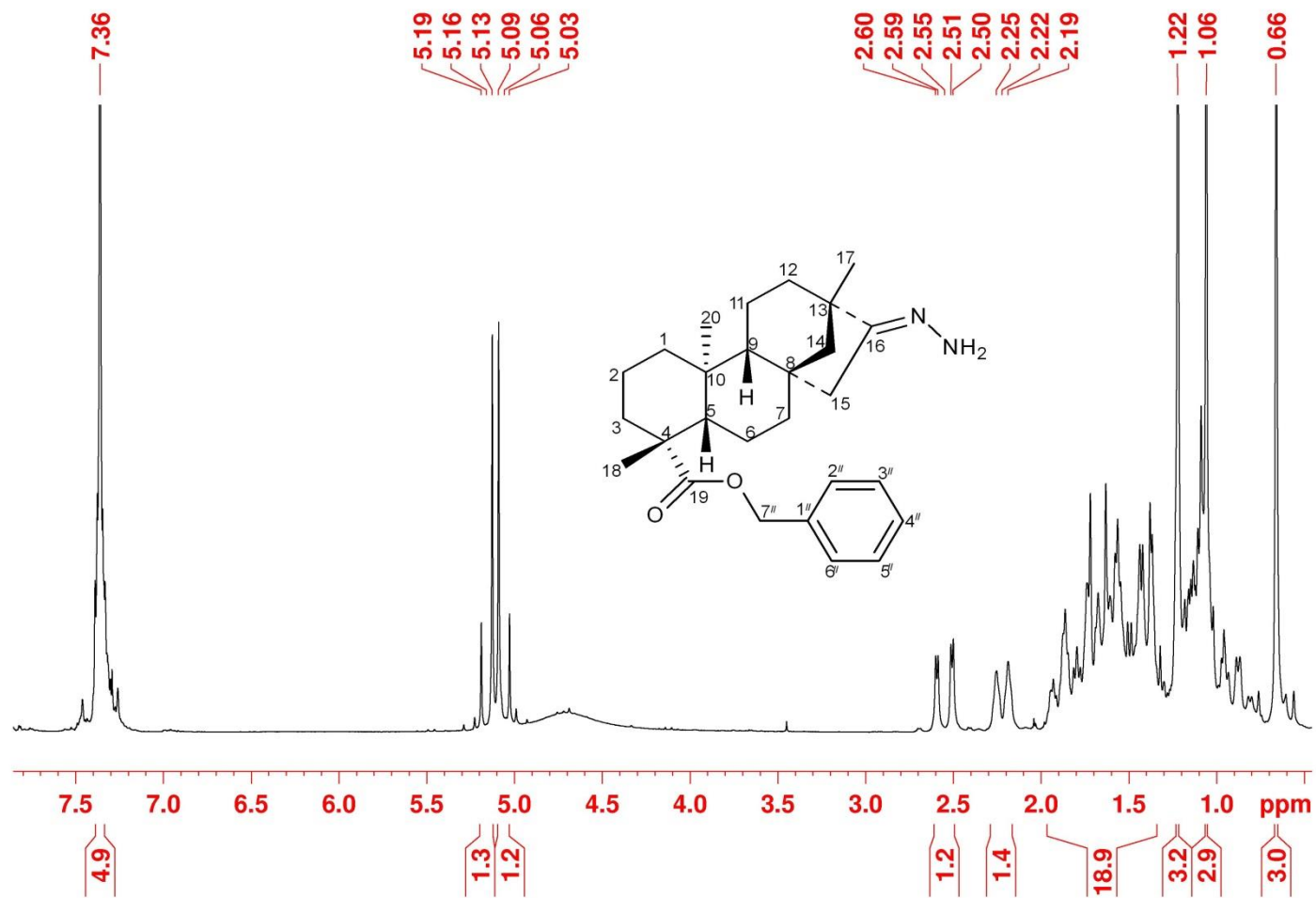


Figure 117: $^1\text{H-NMR}$ (200 MHz, CDCl_3) spectrum of compound **3f**.

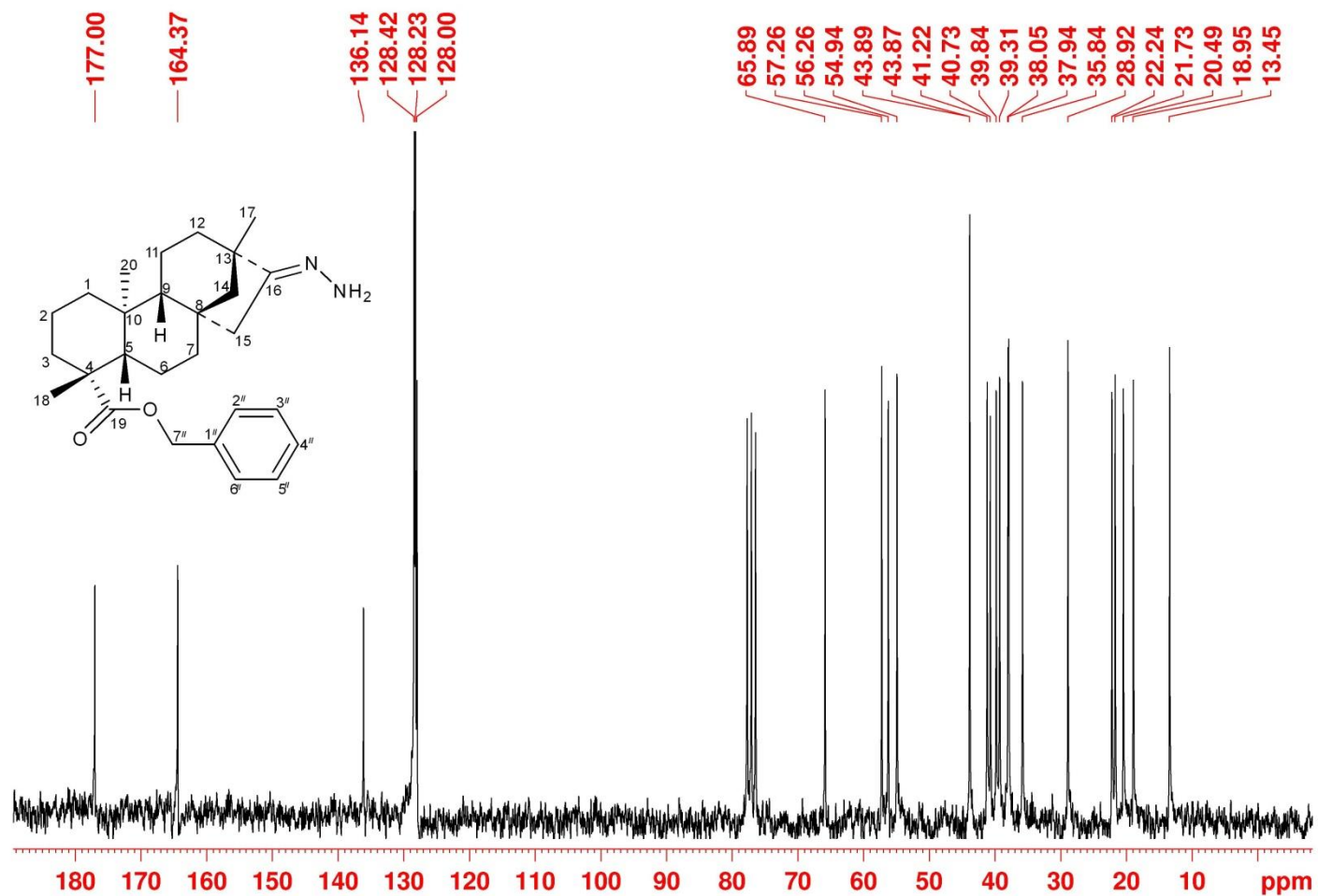


Figure 118: ^{13}C $\{^1\text{H}\}$ NMR (50 MHz, CDCl_3) spectrum of compound **3f**.

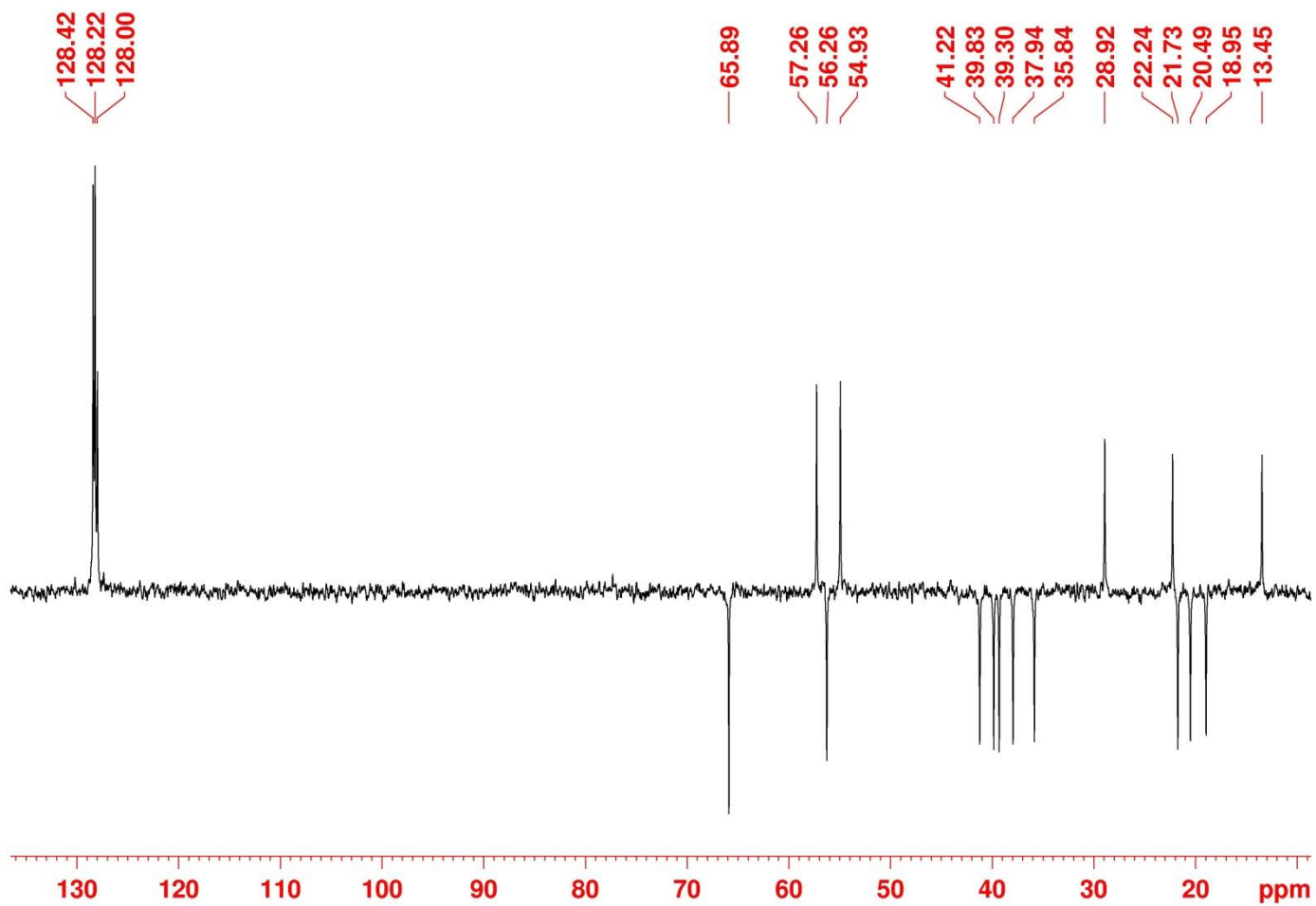


Figure 119: $^{13}\text{C} \{^1\text{H}\}$ DEPT-NMR (50 MHz, CDCl_3) spectrum of compound **3f**.

264-ASAD-HOBE_140821145748 #1377 RT: 4.02 AV: 1 NL: 8.03E4
T: ITMS + p ESI Full ms2 425.40@cid0.00 [115.00-600]

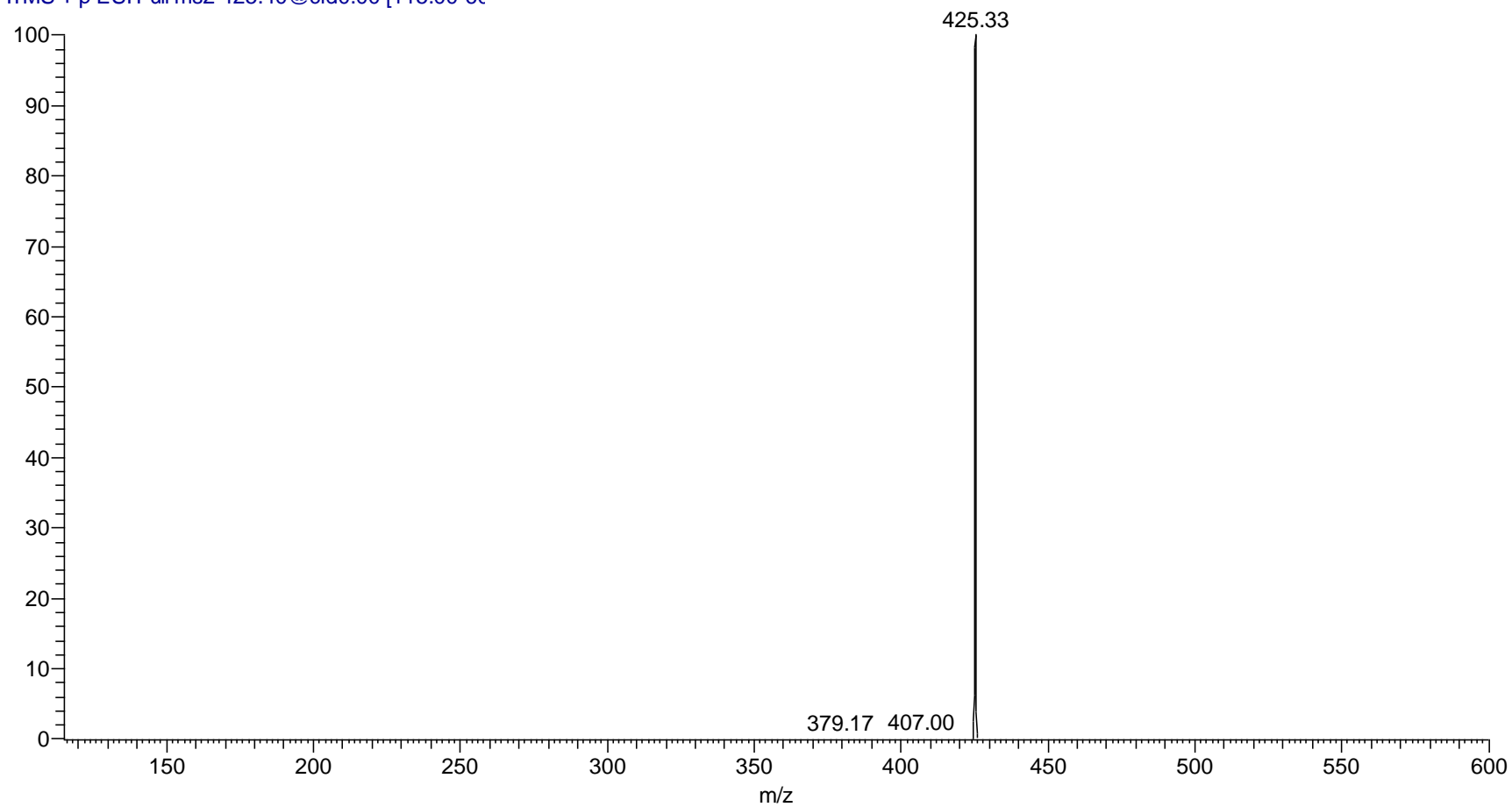


Figure 120: ESI-MS spectrum of compound **5I**.

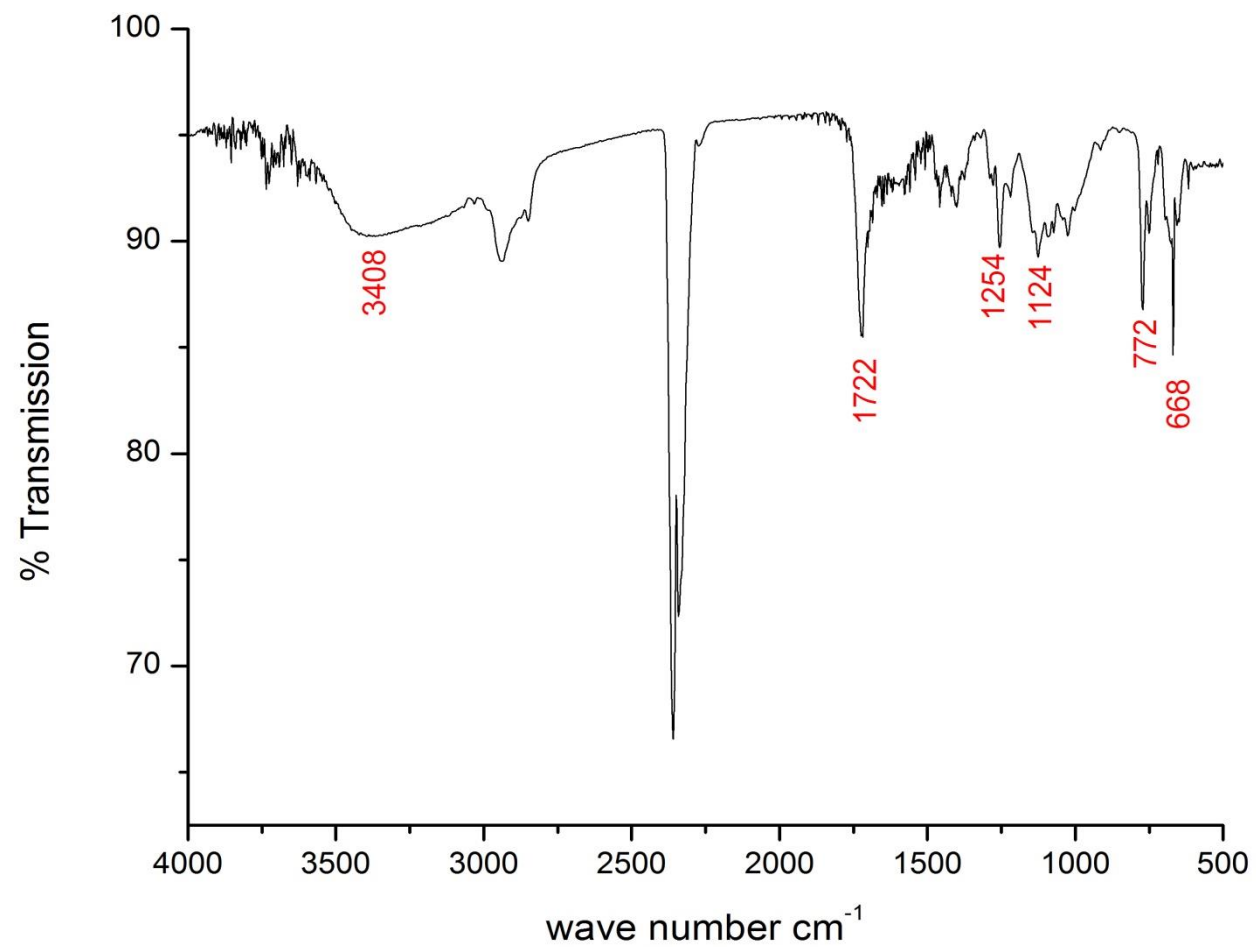


Figure 121: IR spectrum of compound 5I.

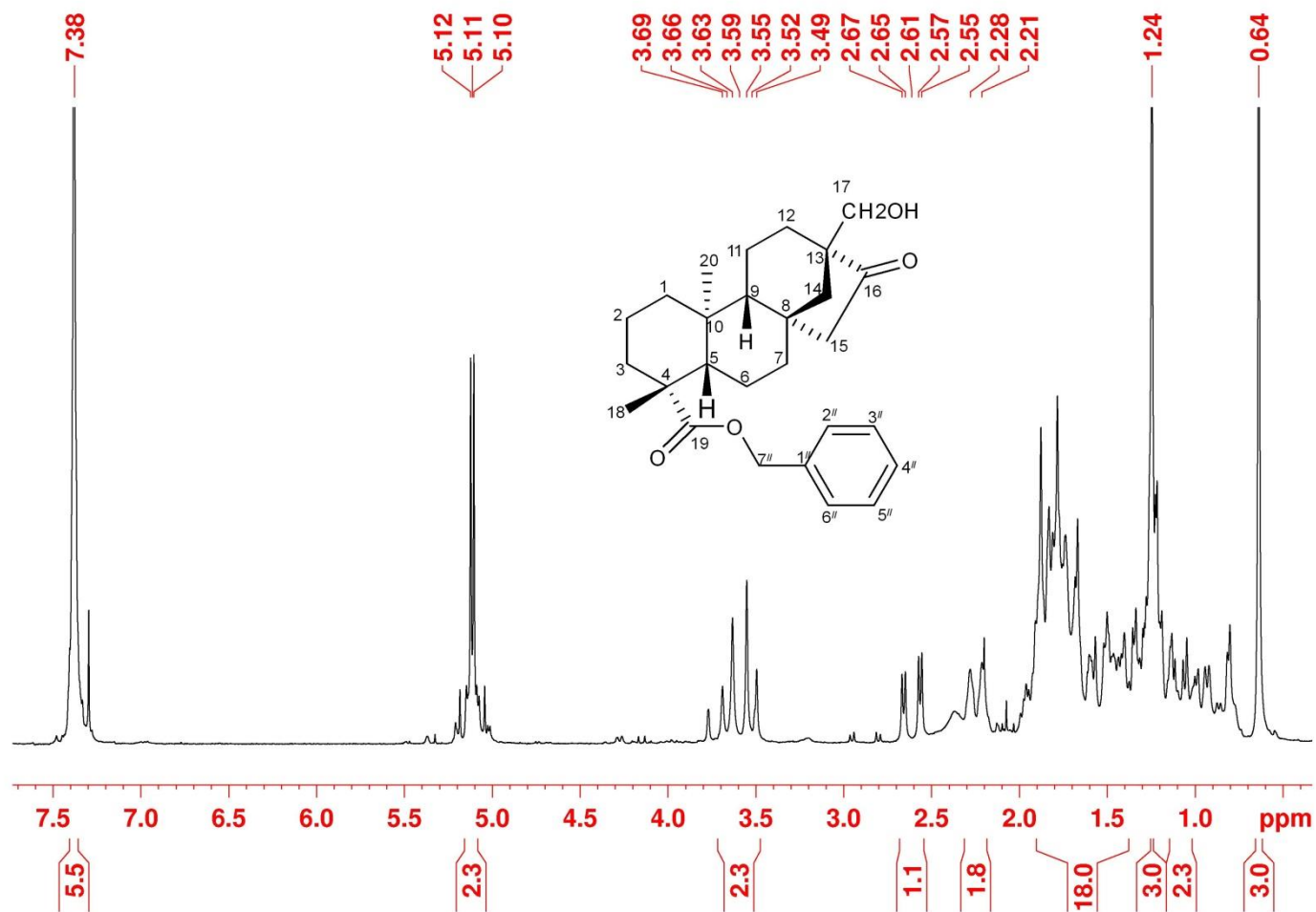


Figure 122: $^1\text{H-NMR}$ (200 MHz, CDCl_3) spectrum of compound **5l**.

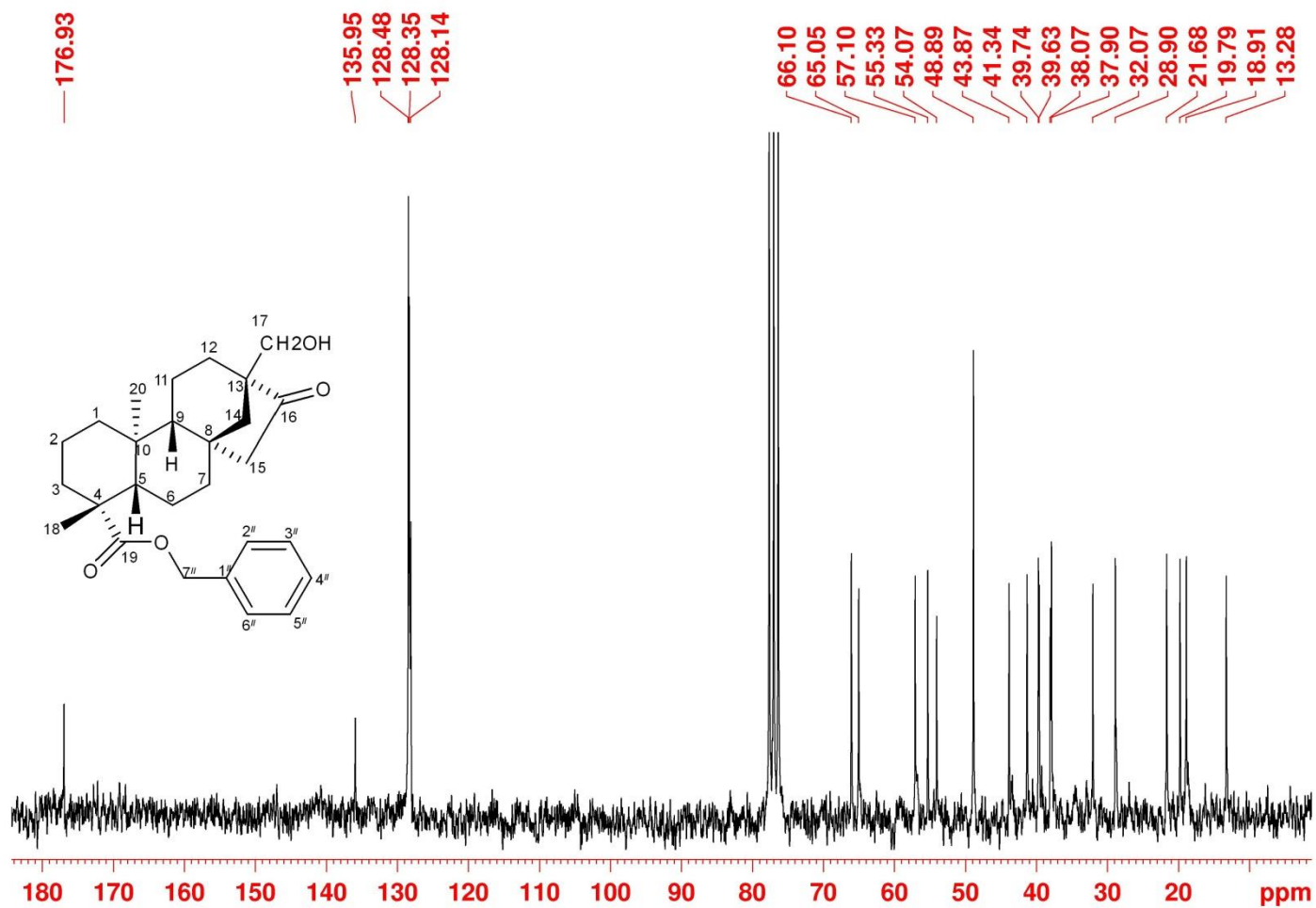


Figure 123: $^{13}\text{C}\{^1\text{H}\}$ NMR (50 MHz, CDCl_3) spectrum of compound **5I**.

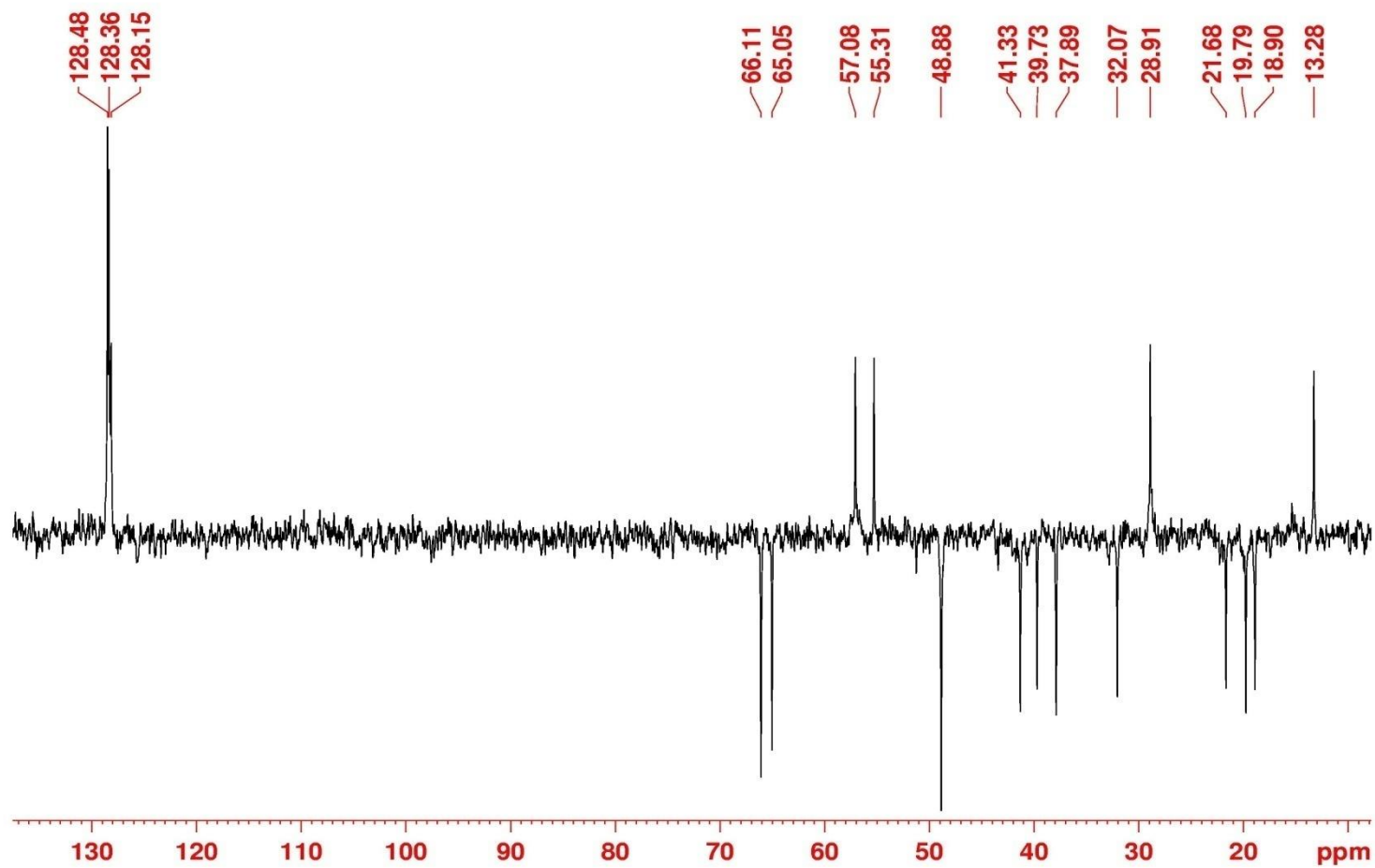


Figure 124: ^{13}C { ^1H } DEPT-NMR (50 MHz, CDCl_3) spectrum of compound 5I.

325-ASAD-IHBE_141120161924 #640 RT: 1.28 AV: 1 NL: 1.24E6
T: ITMS - c ESI Full ms [300.00-600.00]

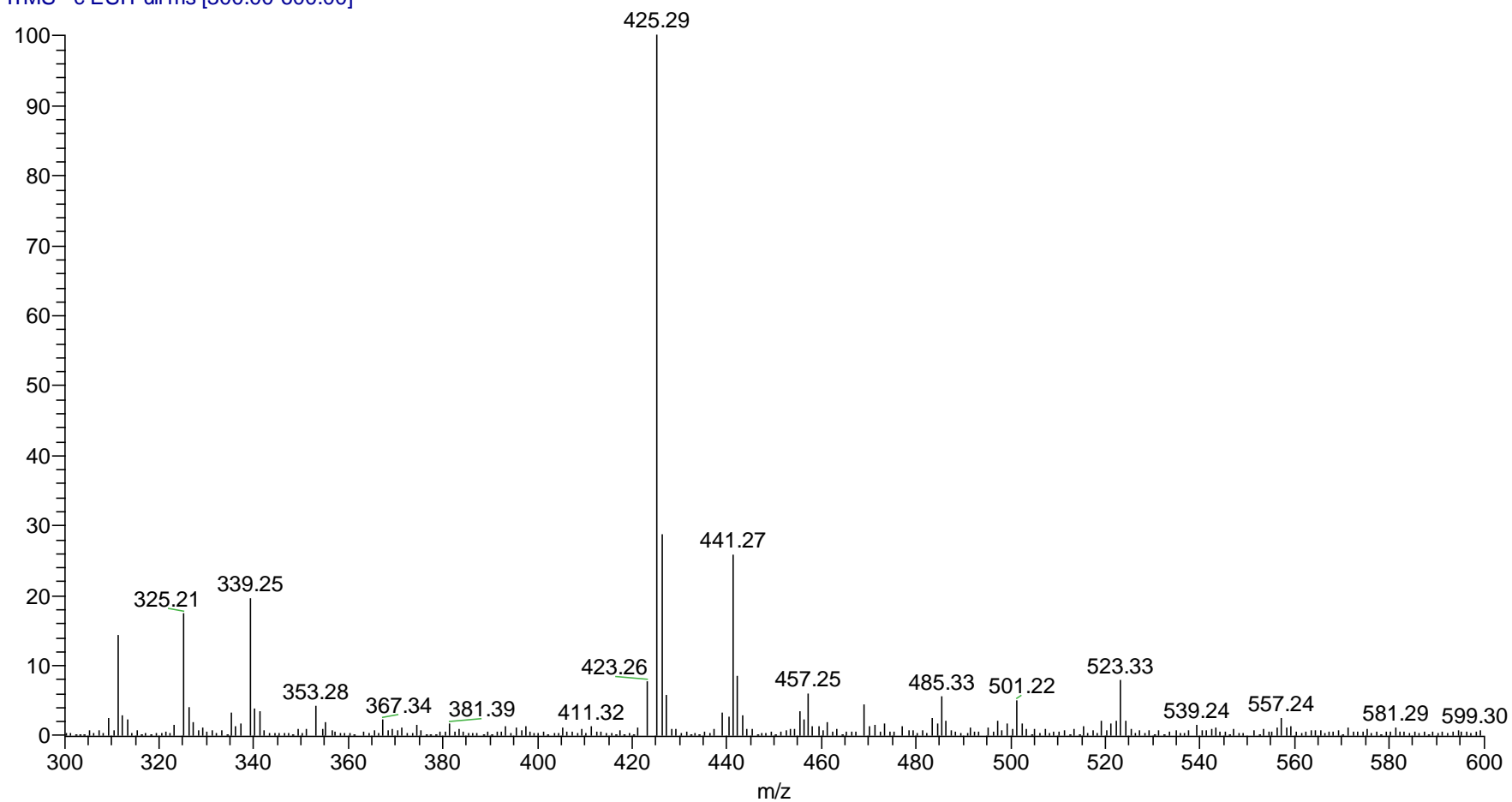


Figure 125: ESI MS spectrum of compound **6i**.

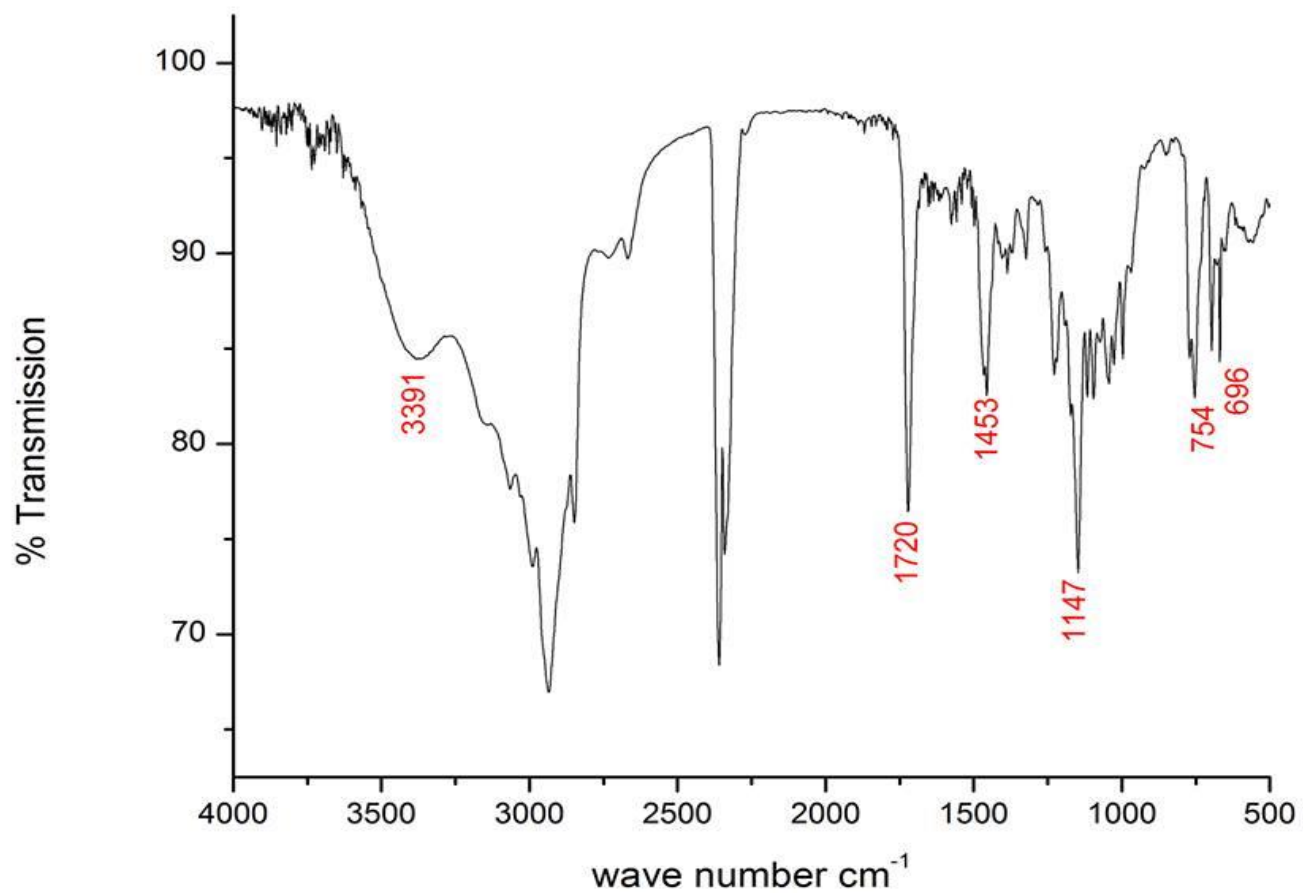


Figure 126: IR spectrum of compound 6i.

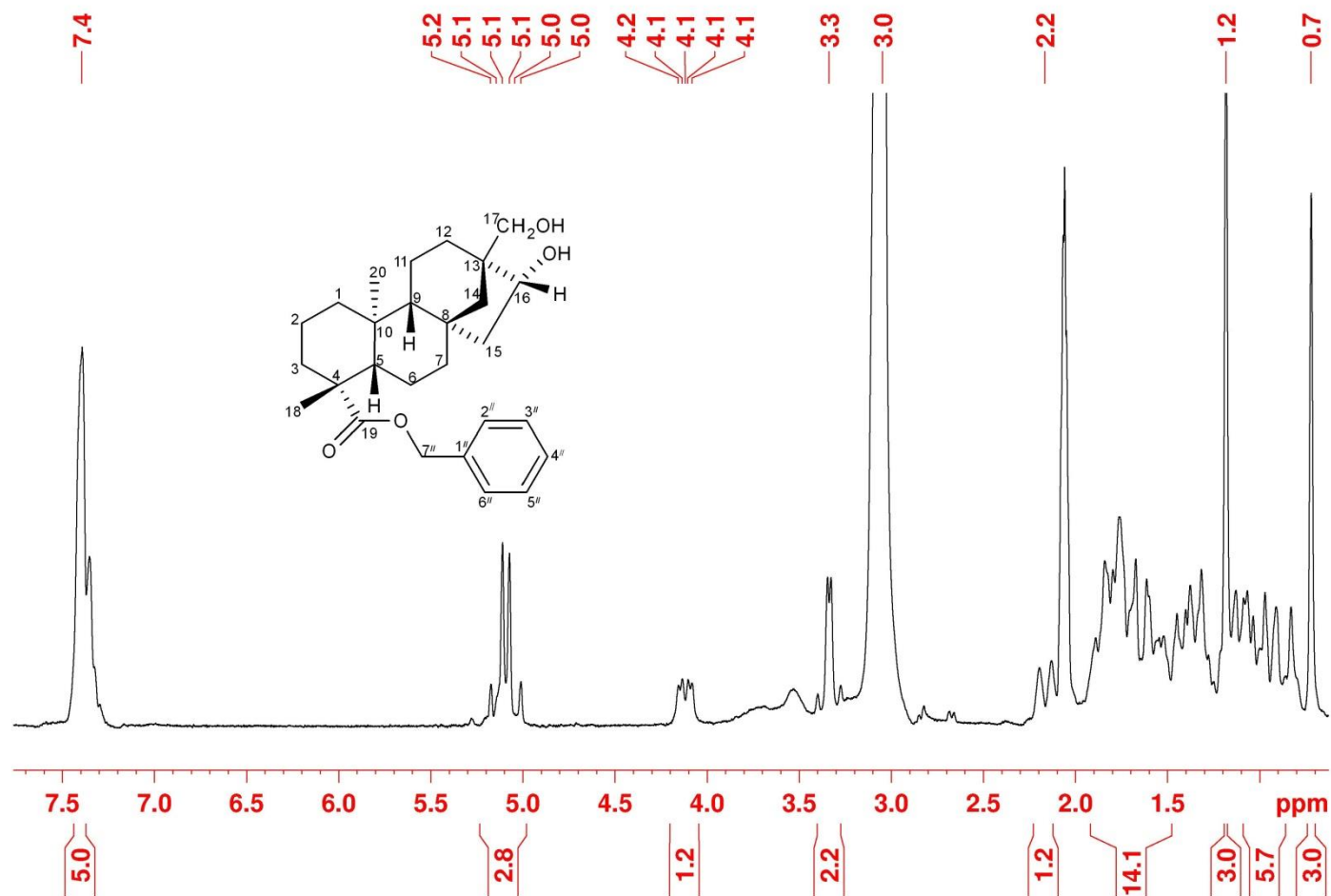


Figure 127: $^1\text{H-NMR}$ (200 MHz, CDCl_3) spectrum of compound **6i**.

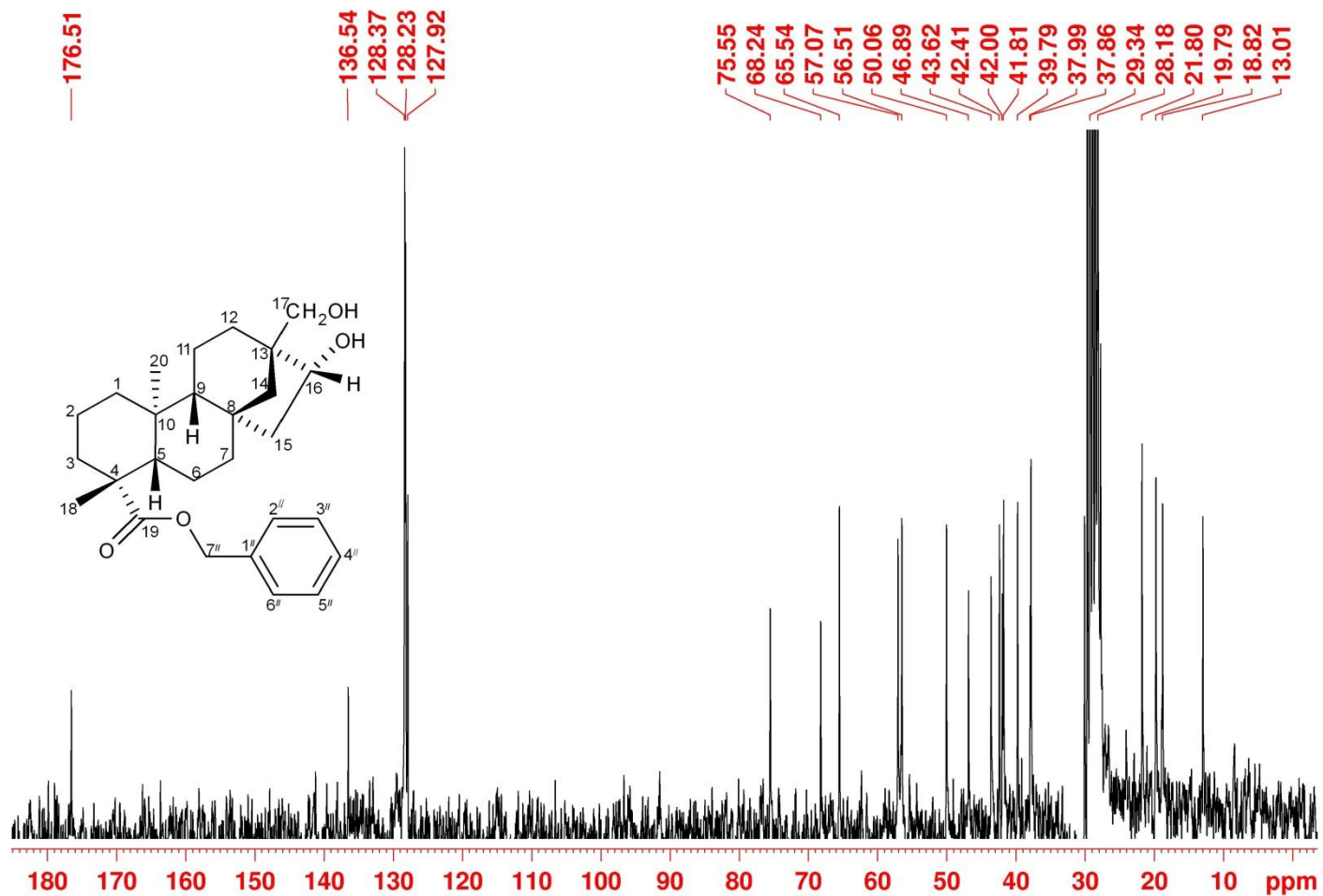


Figure 128: ^{13}C $\{^1\text{H}\}$ -NMR (50 MHz, CDCl_3) spectrum of compound **6i**.

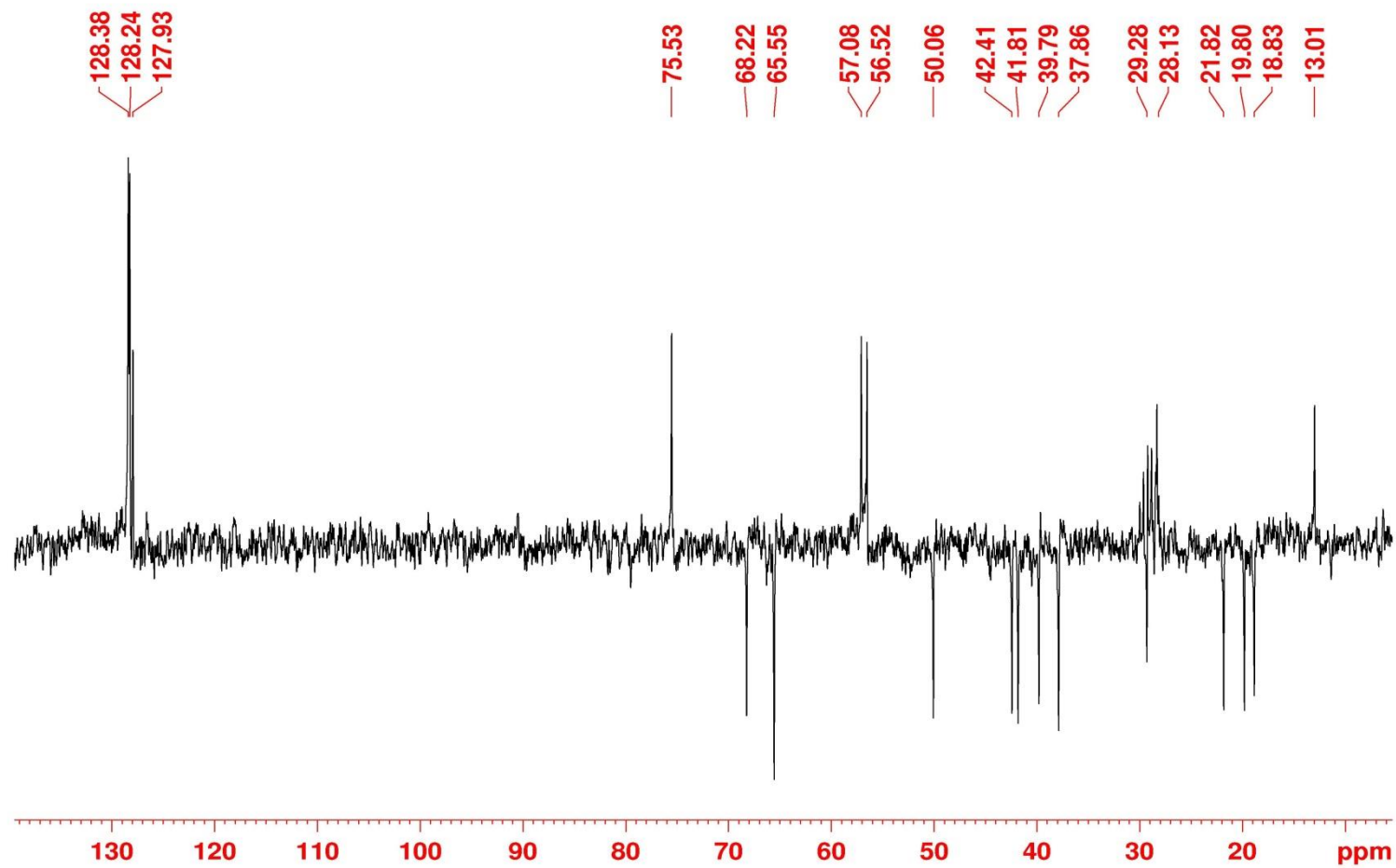


Figure 129: ^{13}C $\{^1\text{H}\}$ DEPT-NMR (50 MHz, CDCl_3) spectrum of compound **6i**.

267-ASADI-HIOB_140821145748 #431 RT: 1.77 AV: 1 NL: 1.57E5
T: ITMS + c ESI Full ms2 440.00@cid0.00 [120.00-50

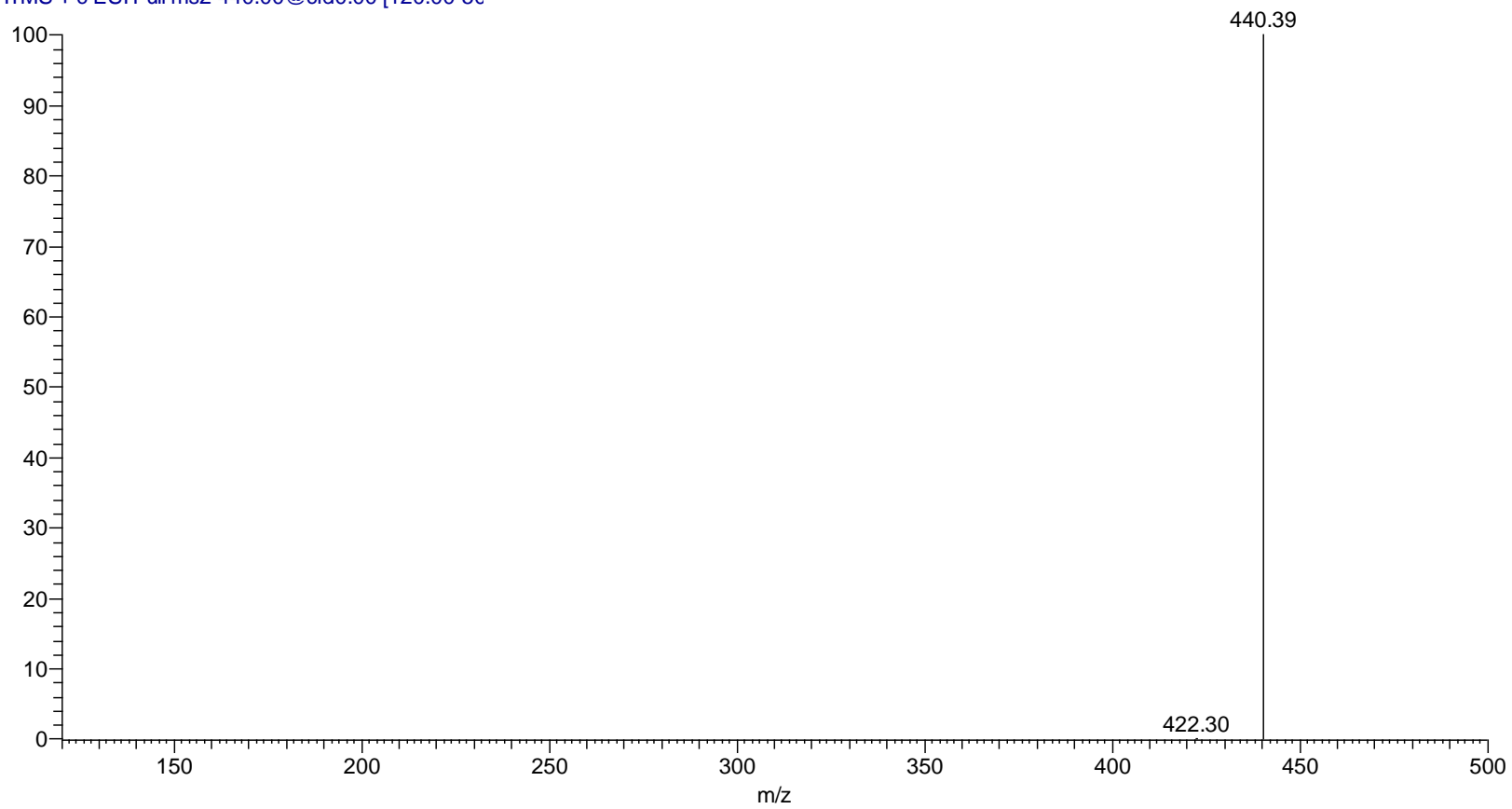


Figure 130: ESI-MS spectrum of compound **6j**.

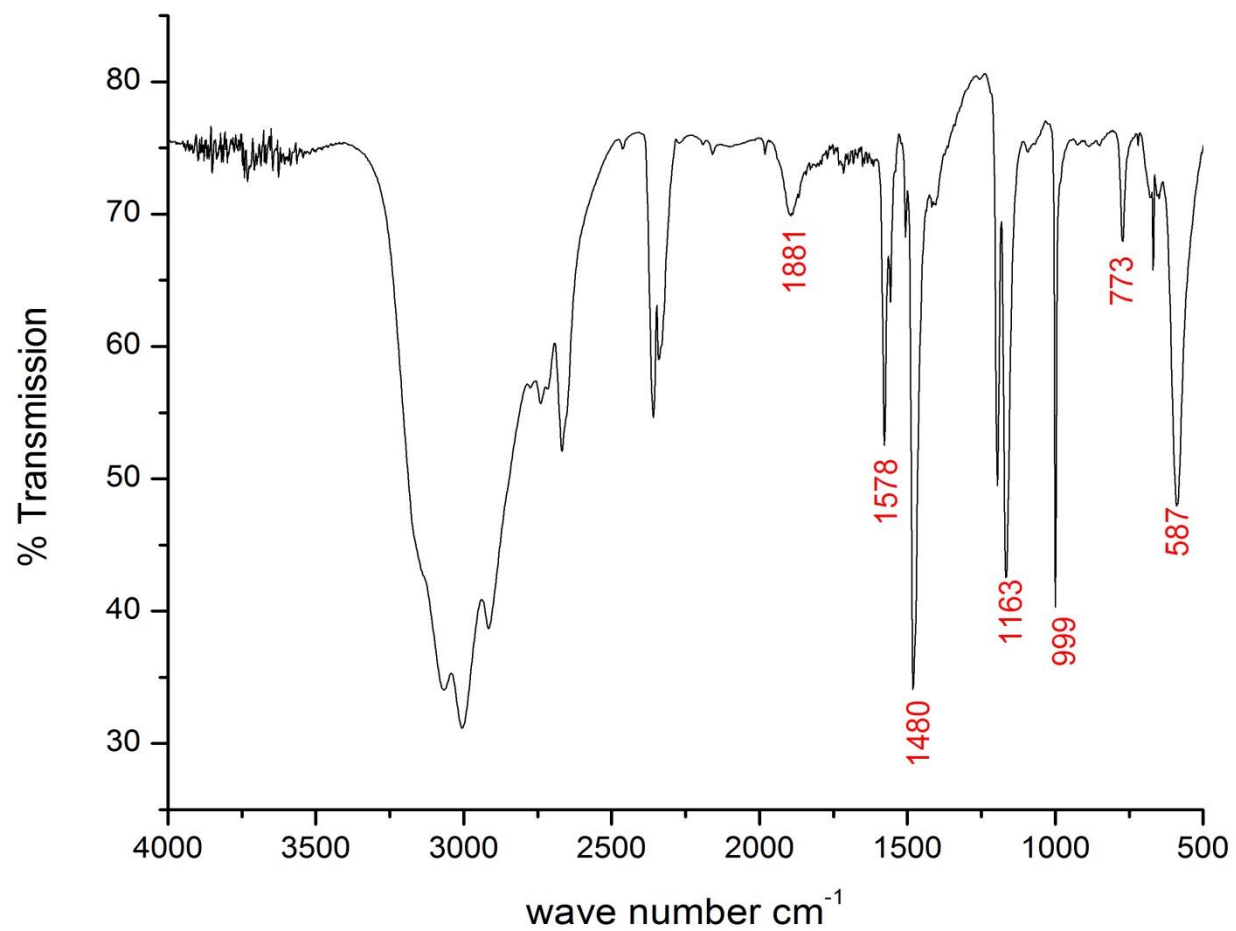


Figure 131: IR spectrum of compound **6j**.

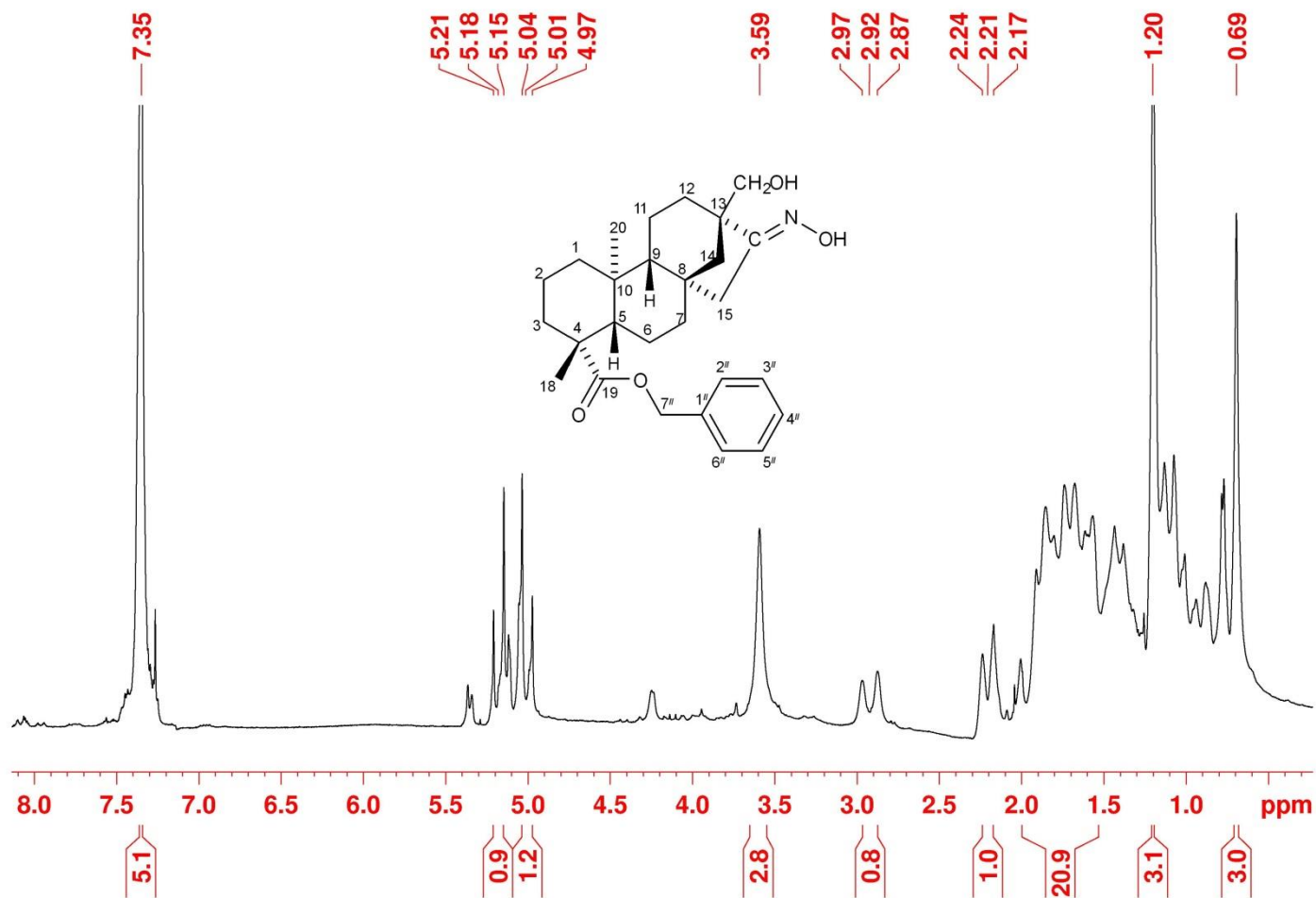


Figure 132: ¹H-NMR (200 MHz, CDCl₃) spectrum of compound **6j**.

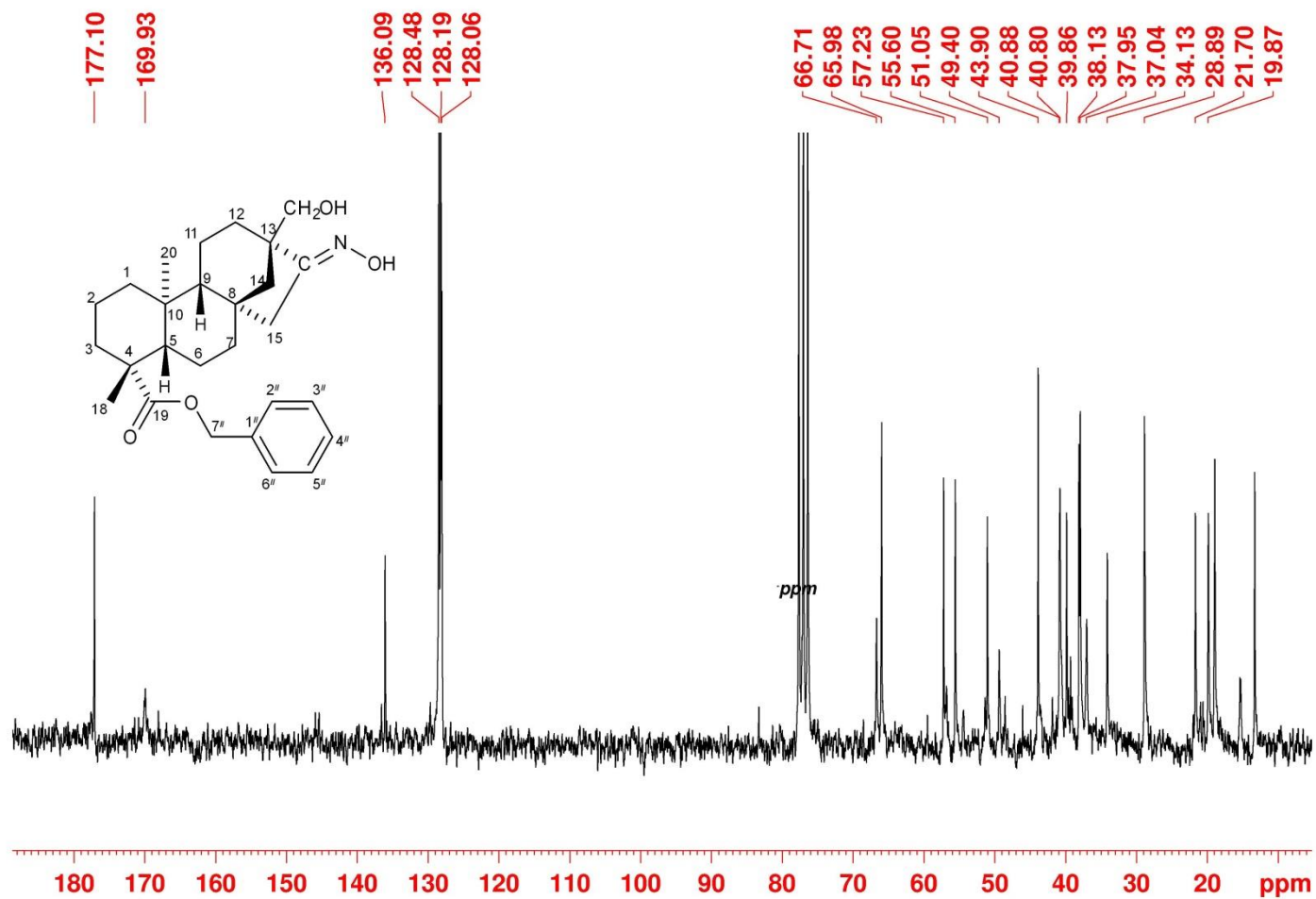


Figure 133: ^{13}C $\{^1\text{H}\}$ NMR (50 MHz, CDCl_3) spectrum of compound **6j**.

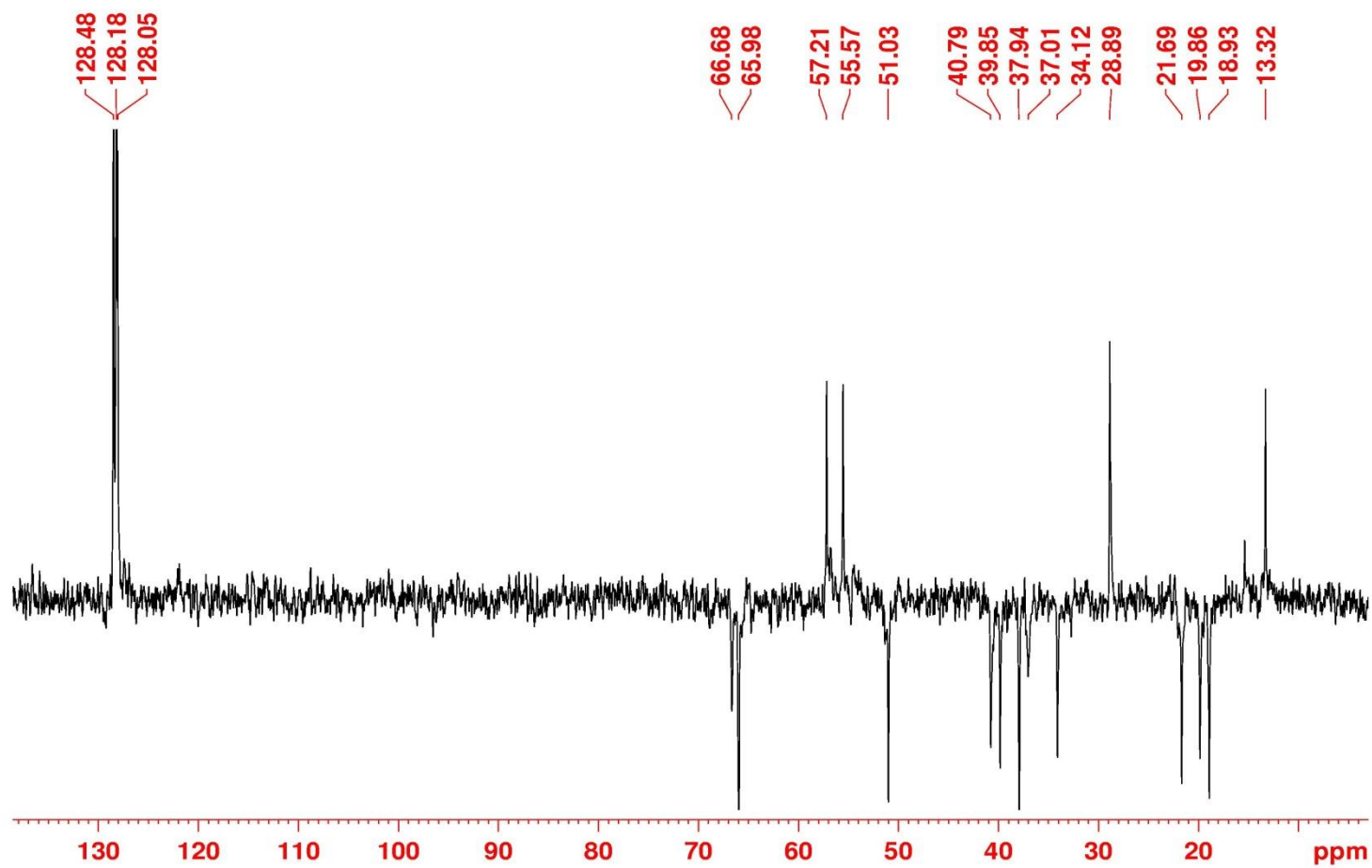


Figure 134: ^{13}C { ^1H } DEPT-NMR (50 MHz, CDCl_3) spectrum of compound **6j**.

161-ASADHB_131001131000 #196 RT: 0.68 AV: 1 NL: 2.44E3
T: ITMS + c ESI Full ms2 466.00@cid0.00 [125.00-500.00]

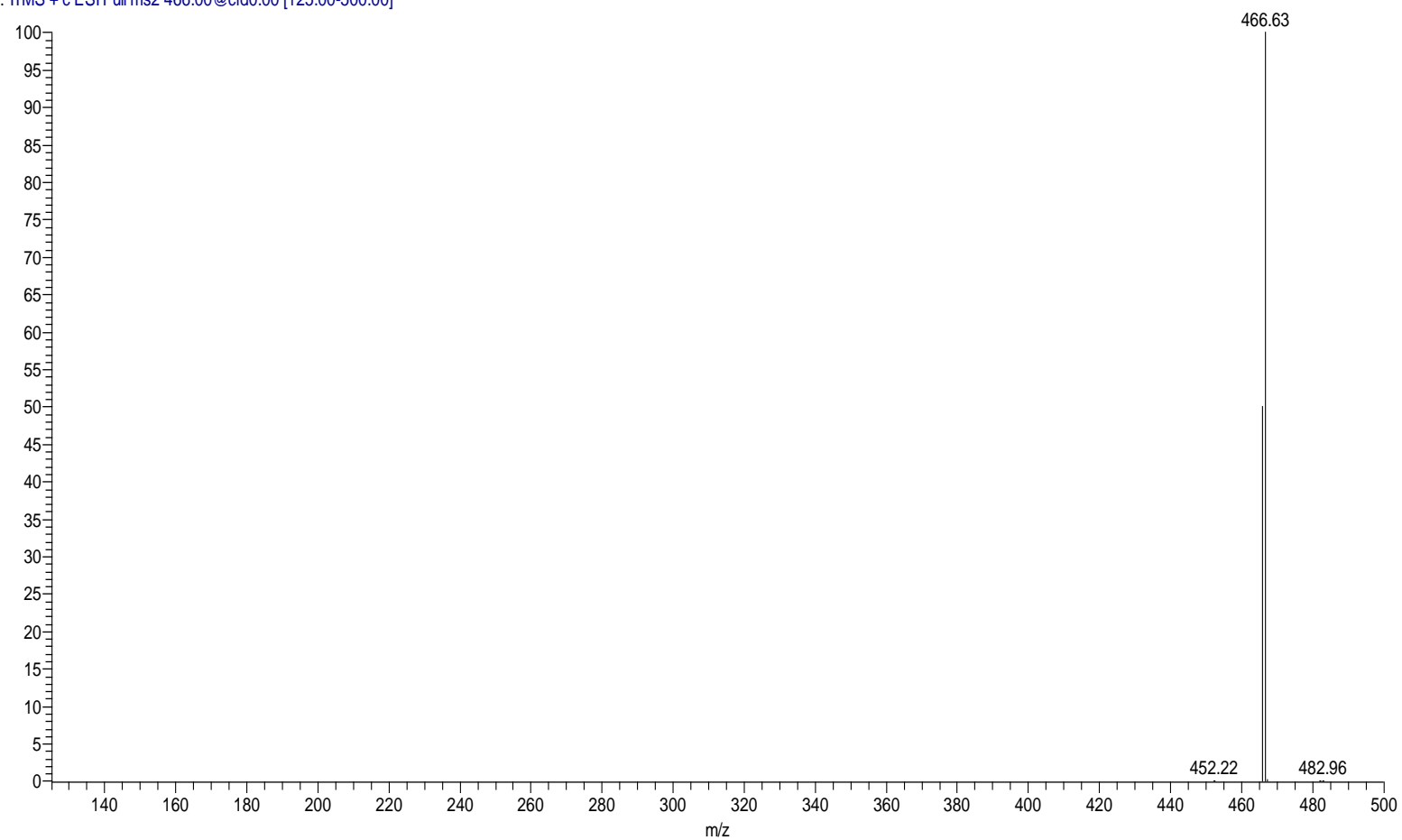


Figure 135: ESI-MS spectrum of compound **3a**.

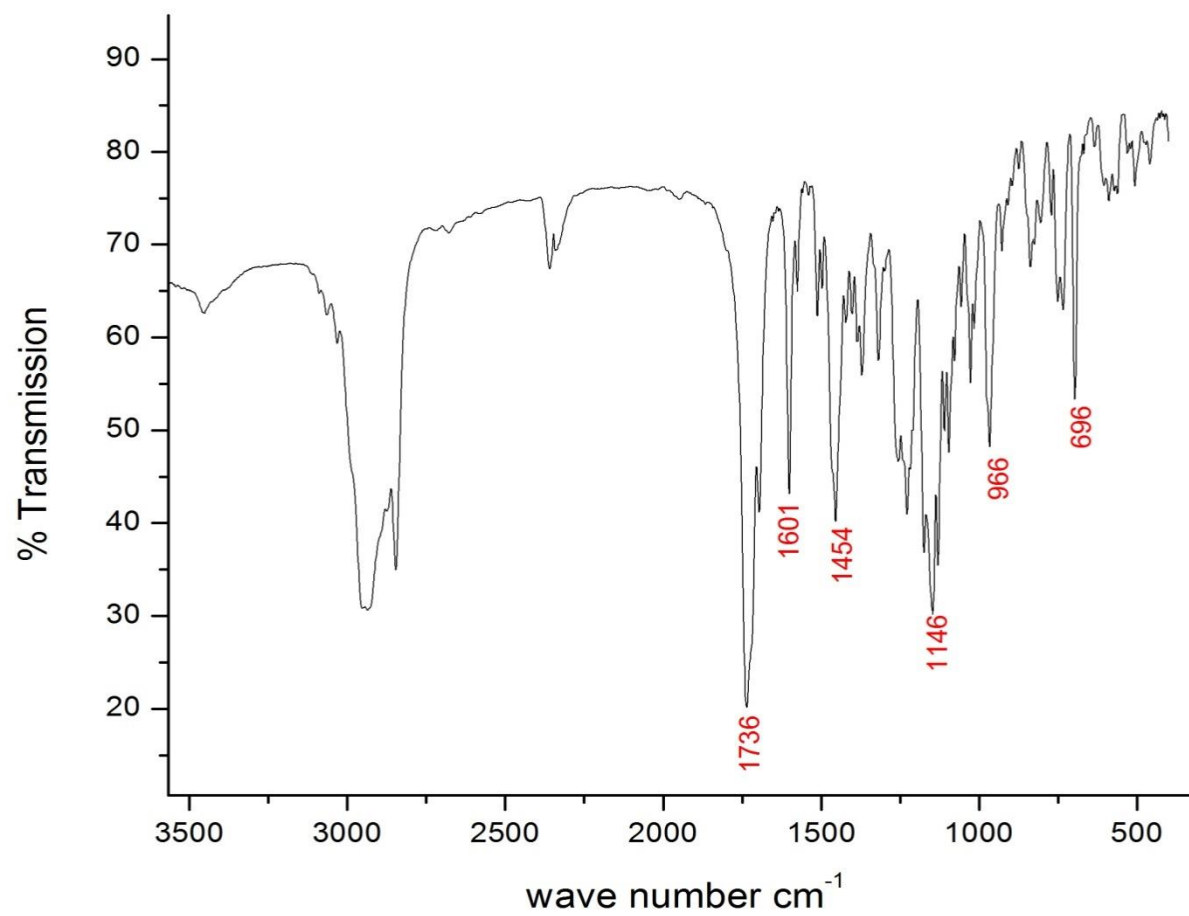


Figure 136: IR spectrum of compound **3a**.

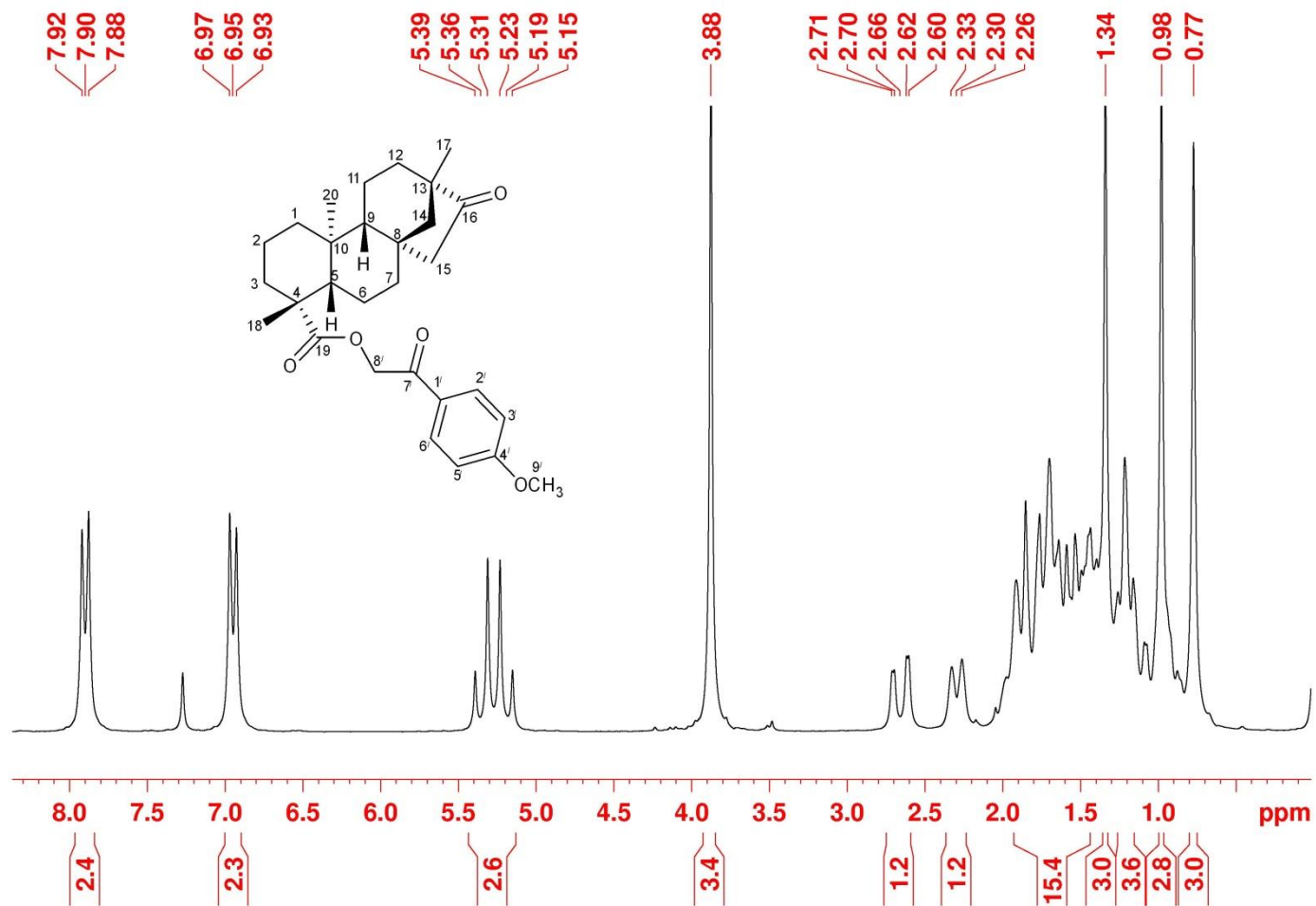


Figure 137: ¹H-NMR (200 MHz, CDCl₃) spectrum of compound 3a.

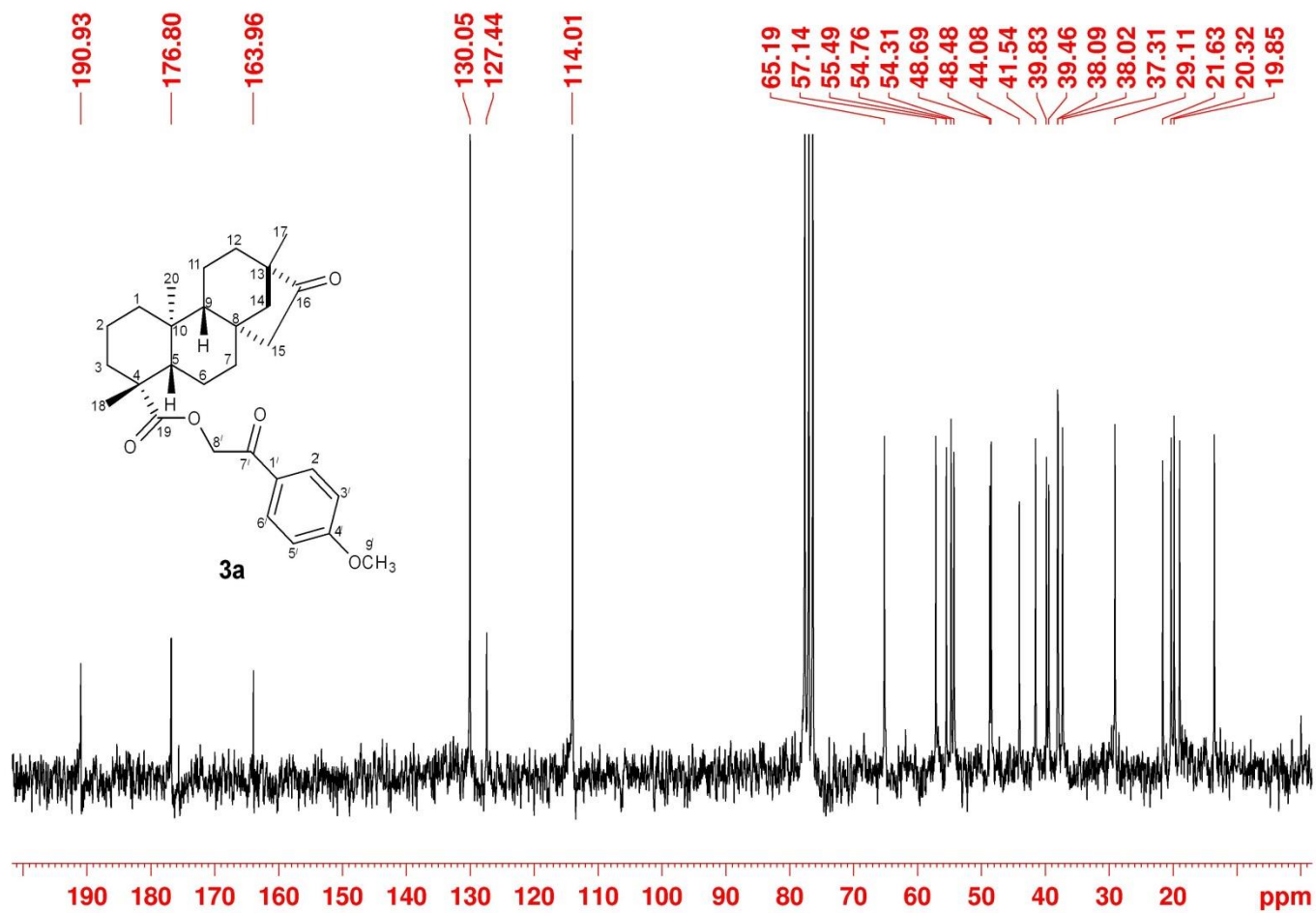


Figure 138: ^{13}C $\{^1\text{H}\}$ NMR (50 MHz, CDCl_3) spectrum of compound **3a**.

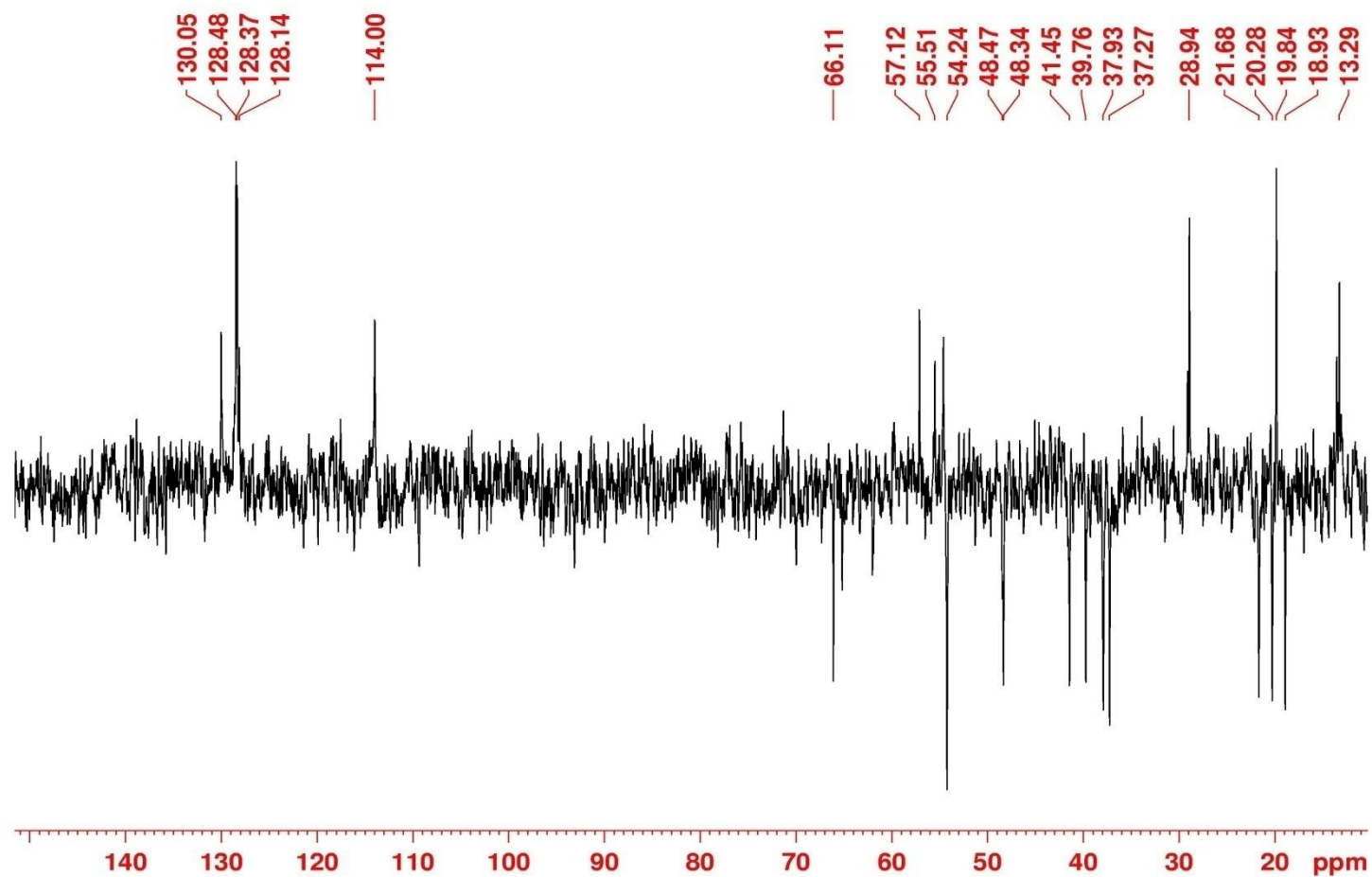


Figure 139: ^{13}C { ^1H } DEPT-NMR (50 MHz, CDCl_3) spectrum of compound **3a**.

165-ASADI-OLB_131001140603 #859 RT: 2.78 AV: 1 NL: 9.21E4
T: ITMS + c ESI Full ms [150.00-500.00]

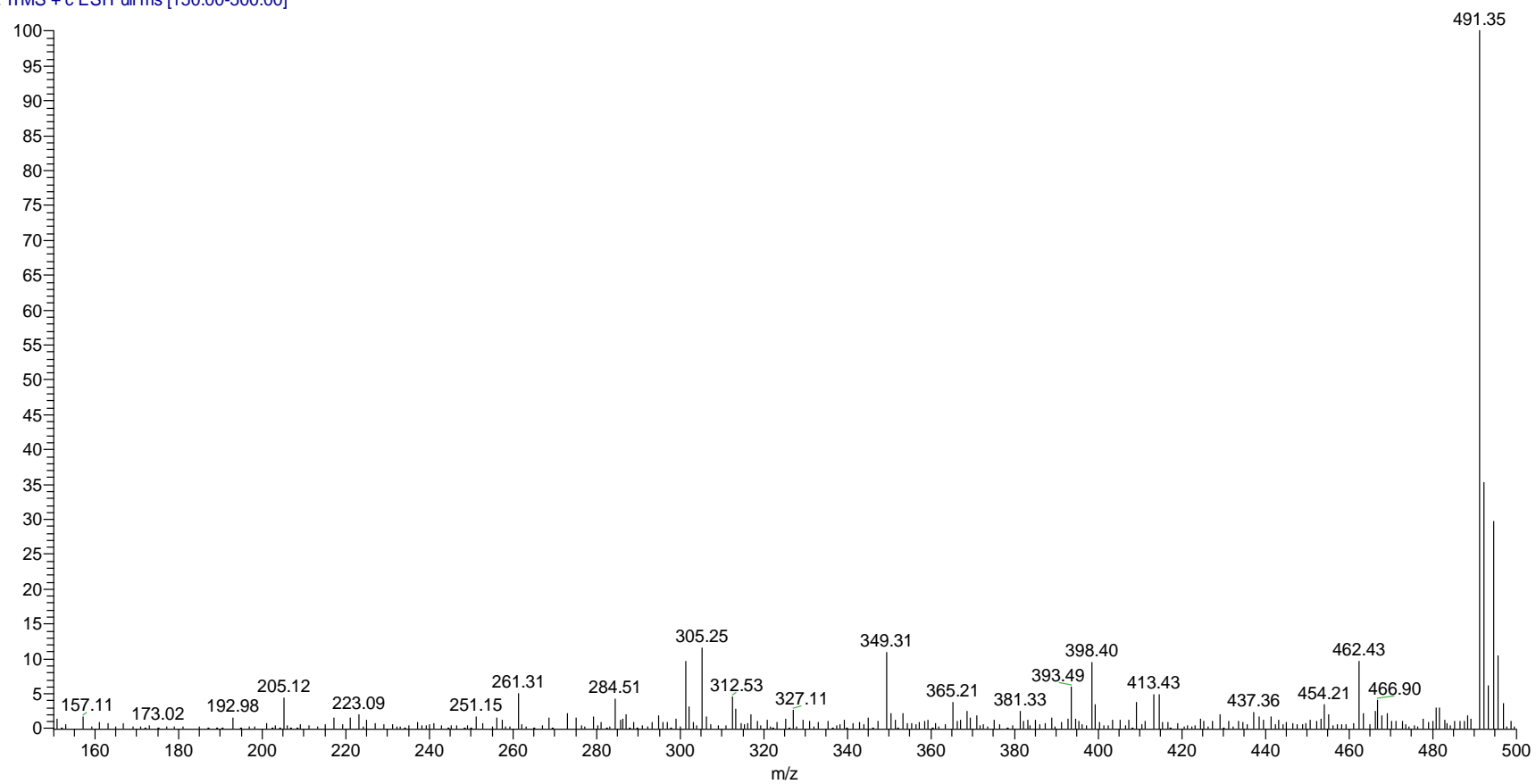
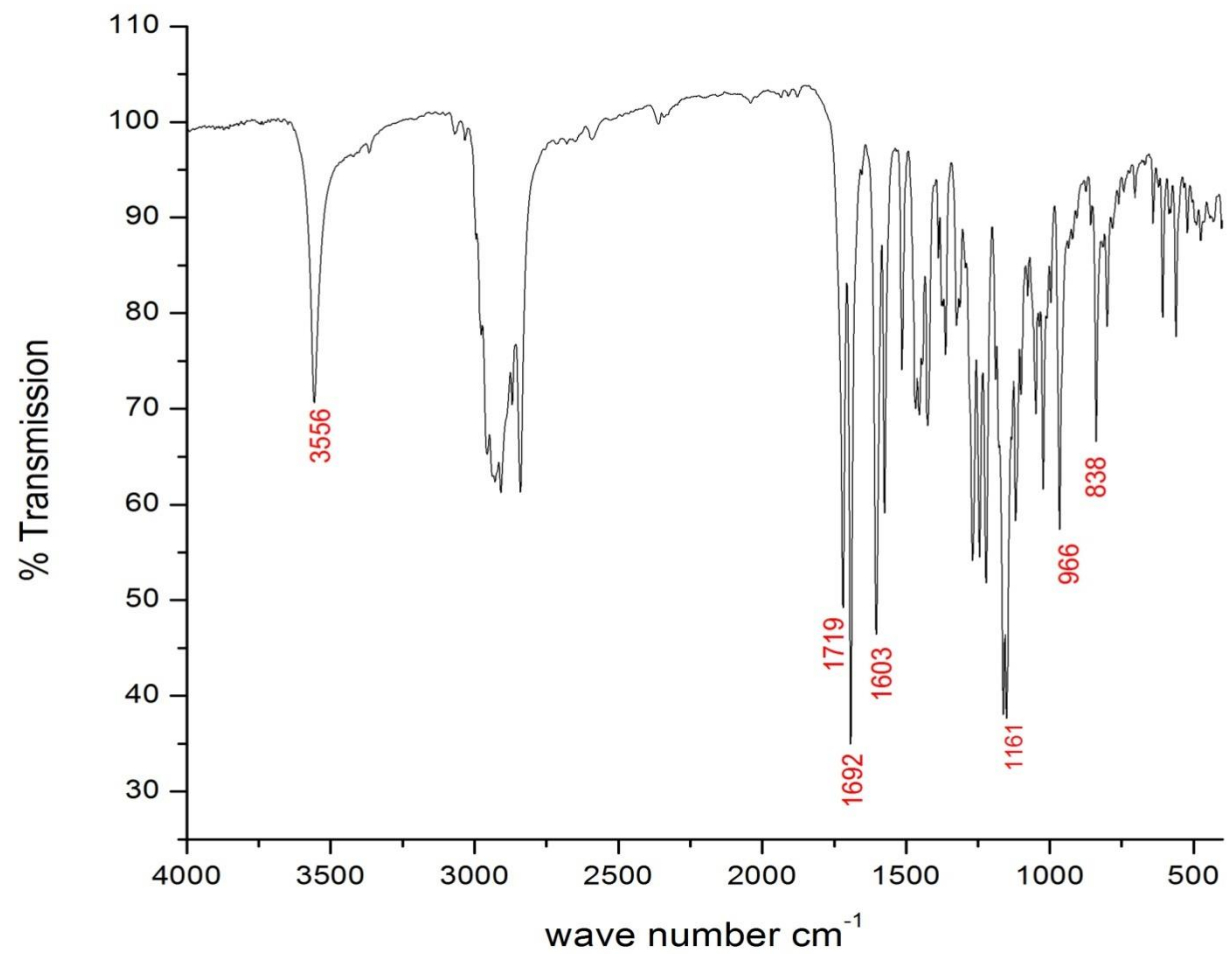


Figure 140: ESI-MS spectrum of compound **3b**.

Figure 141: IR spectrum of compound **3b**.

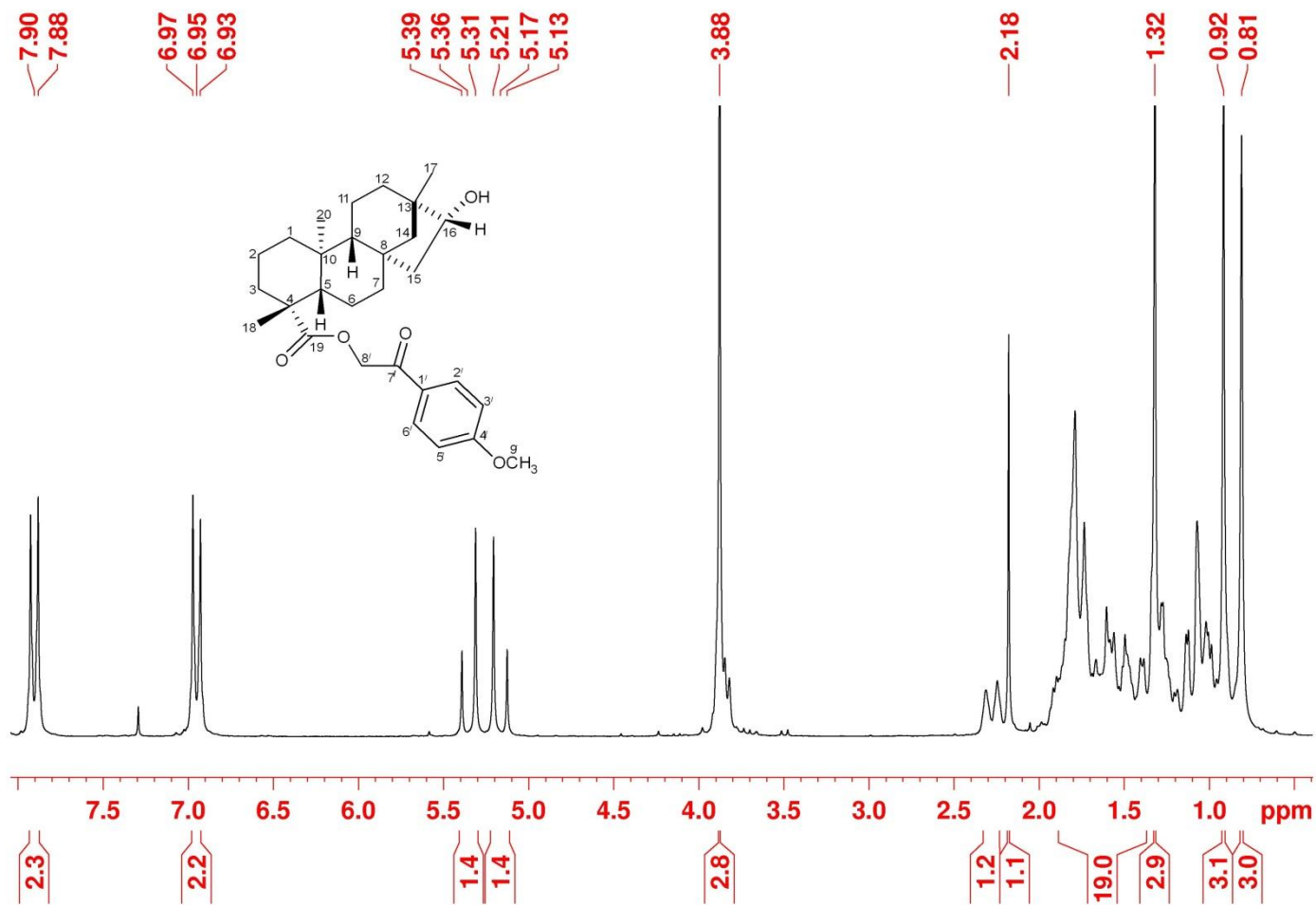


Figure 142: ¹H-NMR (200 MHz, CDCl₃) spectrum of compound **3b**.

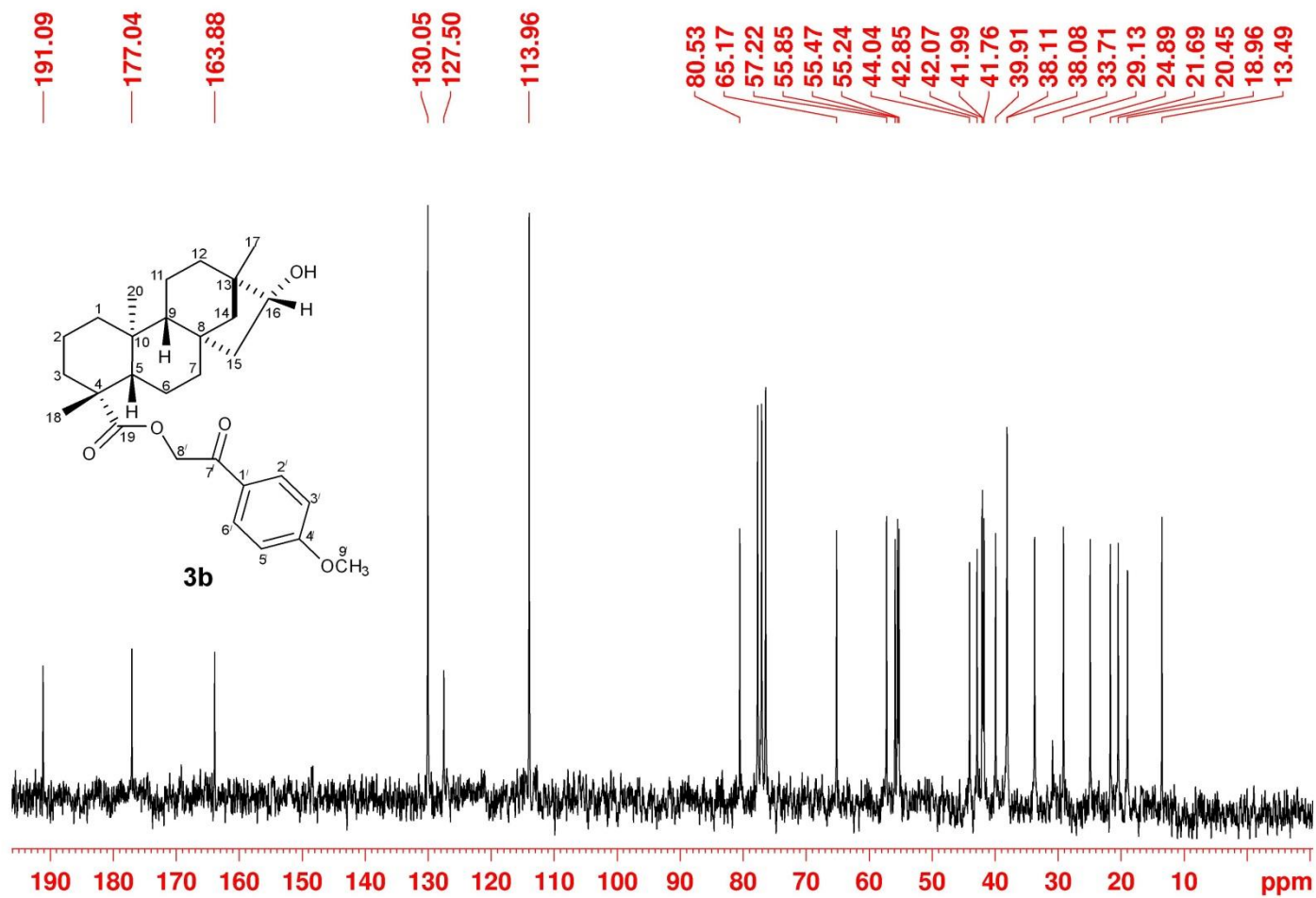


Figure 143: ^{13}C $\{^1\text{H}\}$ NMR (50 MHz, CDCl_3) spectrum of compound **3b**.

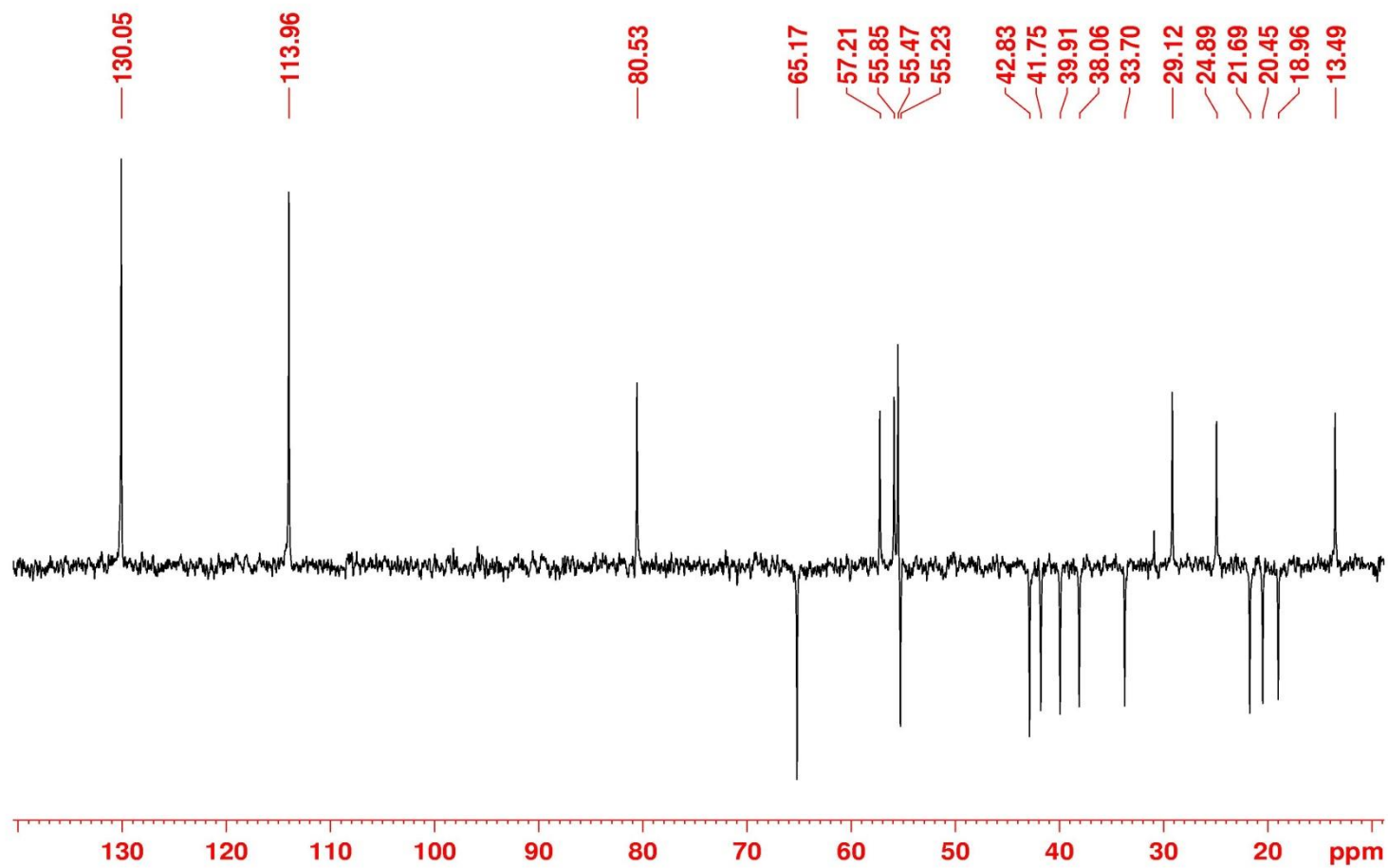


Figure 144: $^{13}\text{C} \{^1\text{H}\}$ DEPT-NMR (50 MHz, CDCl_3) spectrum of compound **3b**.

168-ASADHOB_131011180217 #2665 RT: 8.53 AV: 1 NL: 2.21E4
T: ITMS - c ESI Full ms2 481.40@cid0.00 [130.00-500.00]

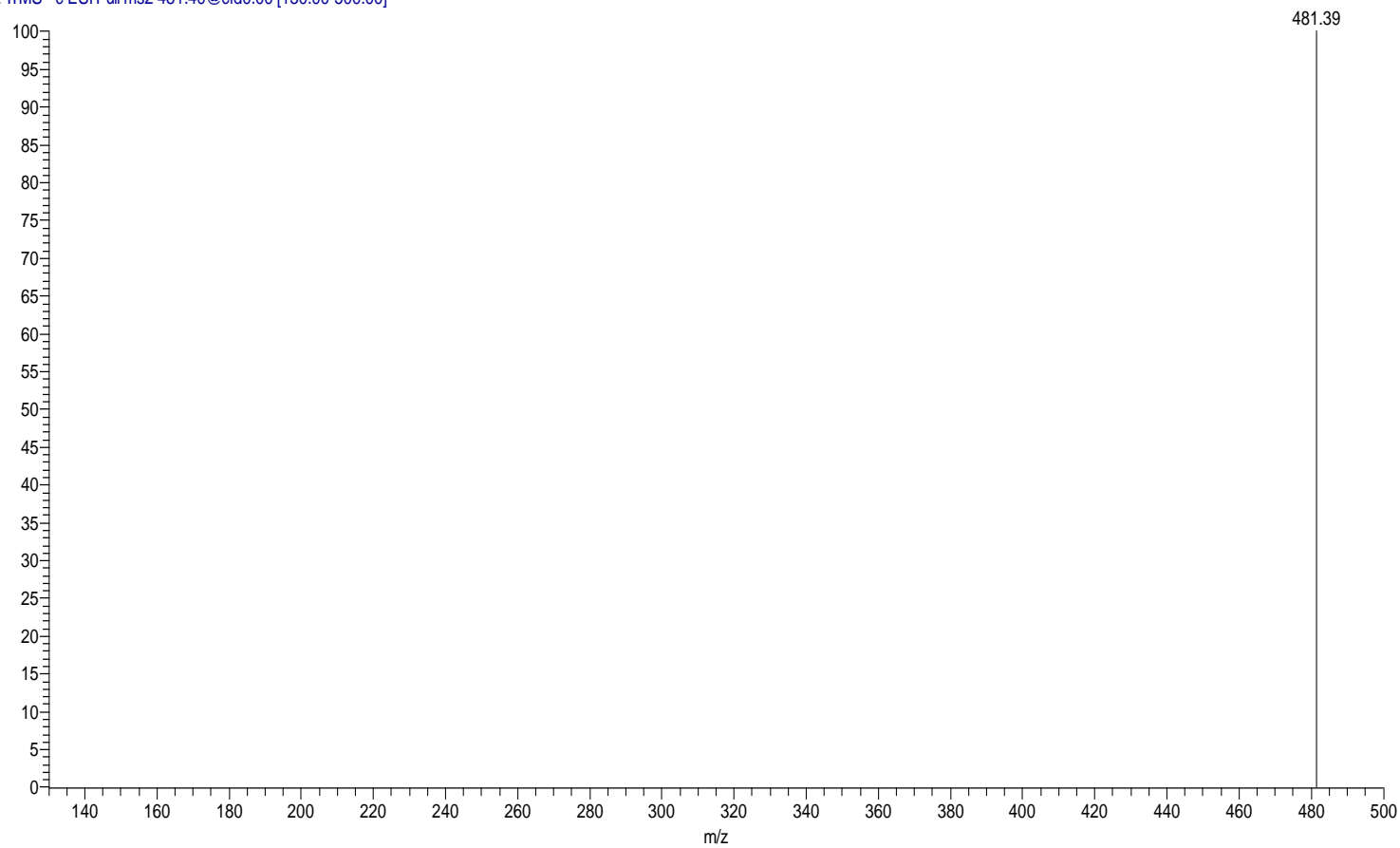


Figure 145: ESI-MS spectrum of compound **3c**.

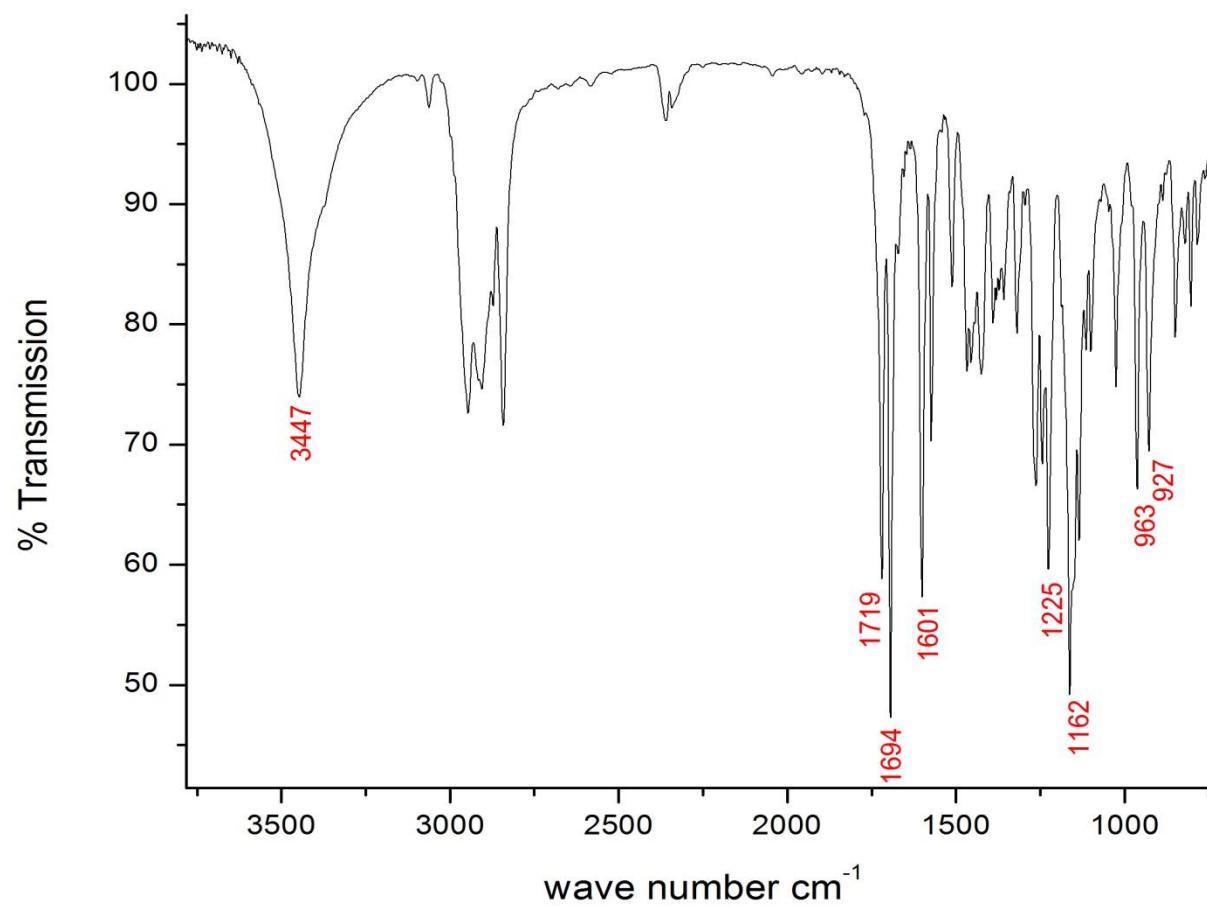


Figure 146: IR spectrum of compound **3c**.

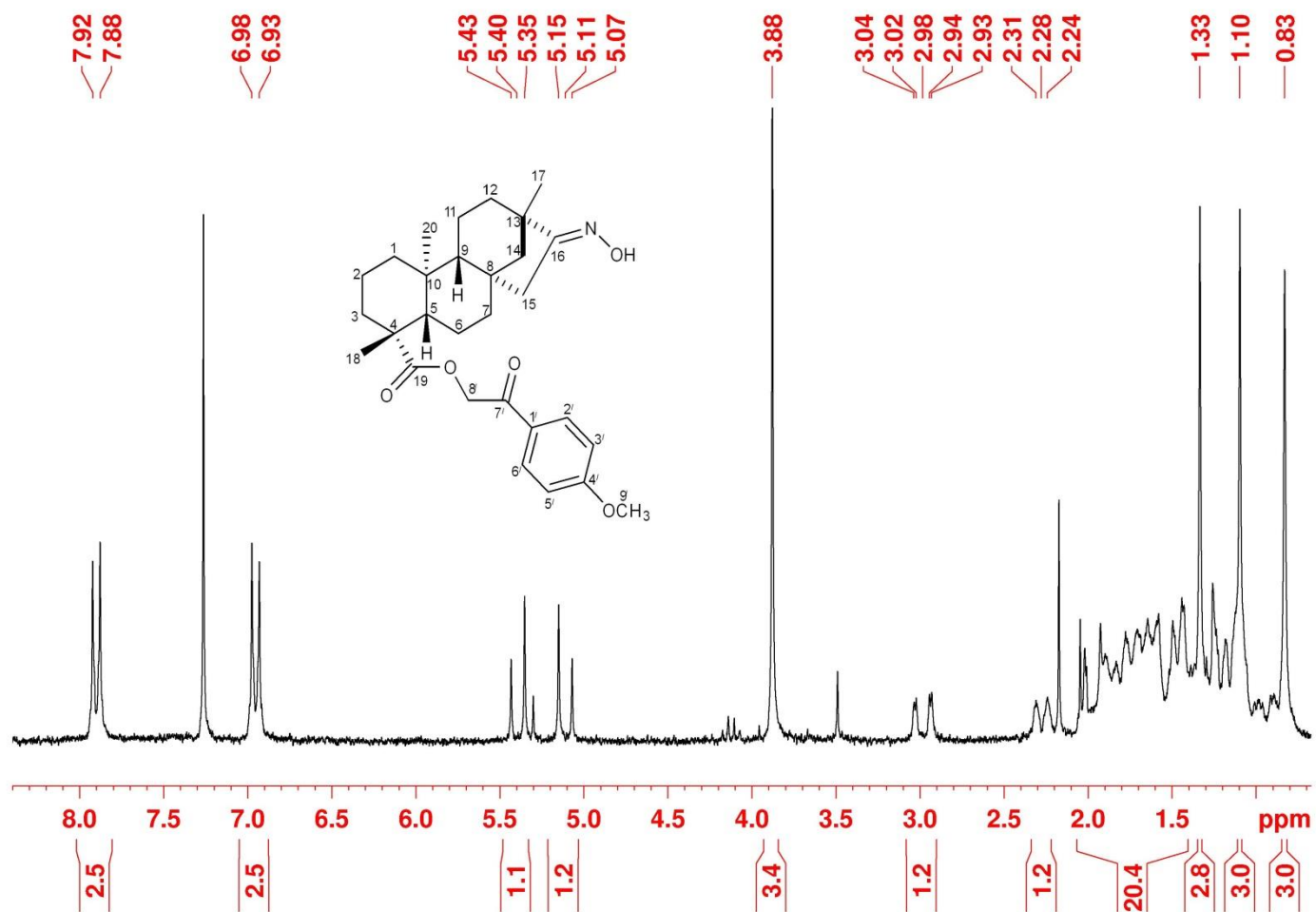


Figure 147: ¹H-NMR (200 MHz, CDCl₃) spectrum of compound **3c**.

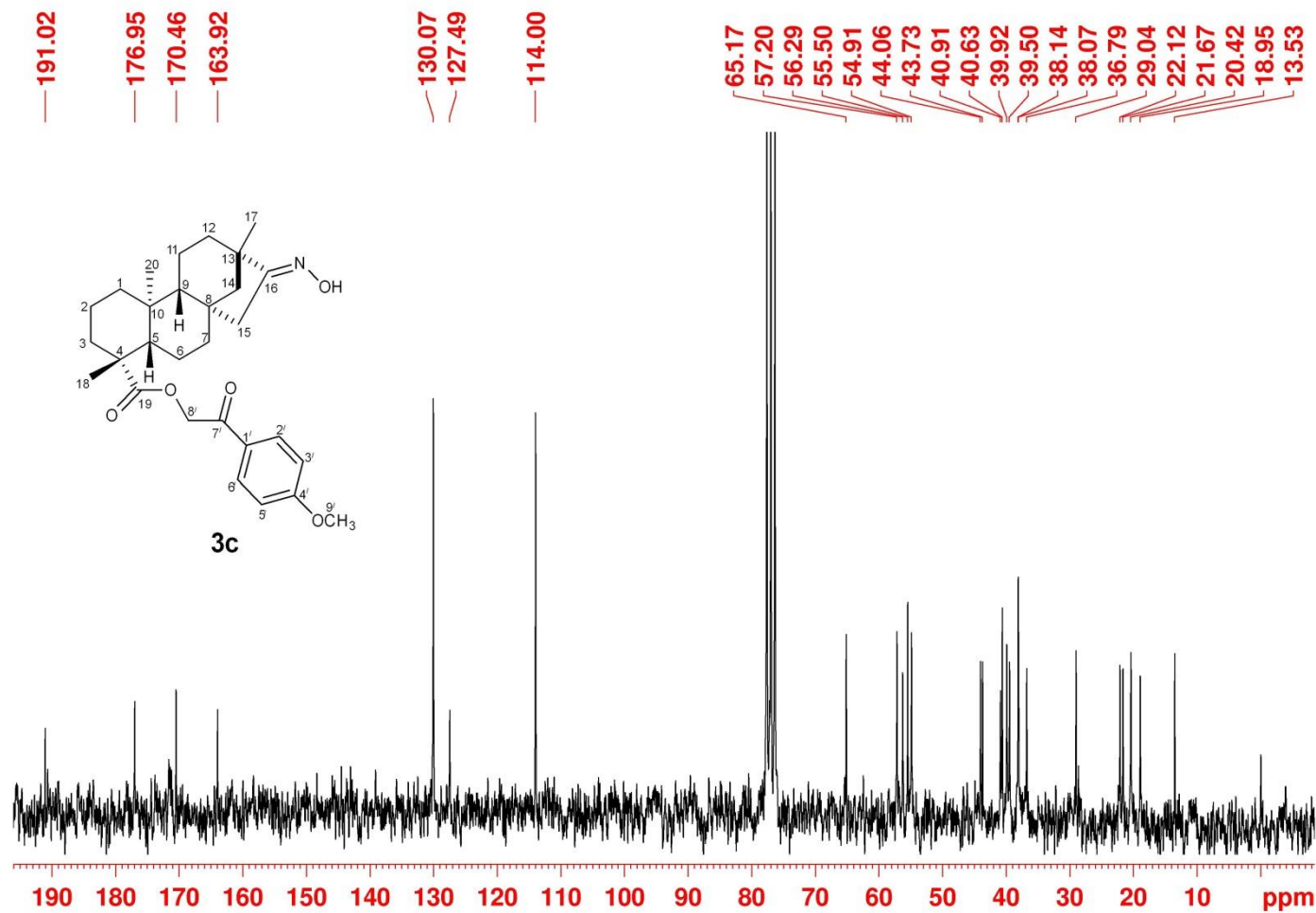


Figure 148: ^{13}C $\{^1\text{H}\}$ NMR (50 MHz, CDCl_3) spectrum of compound **3c**.

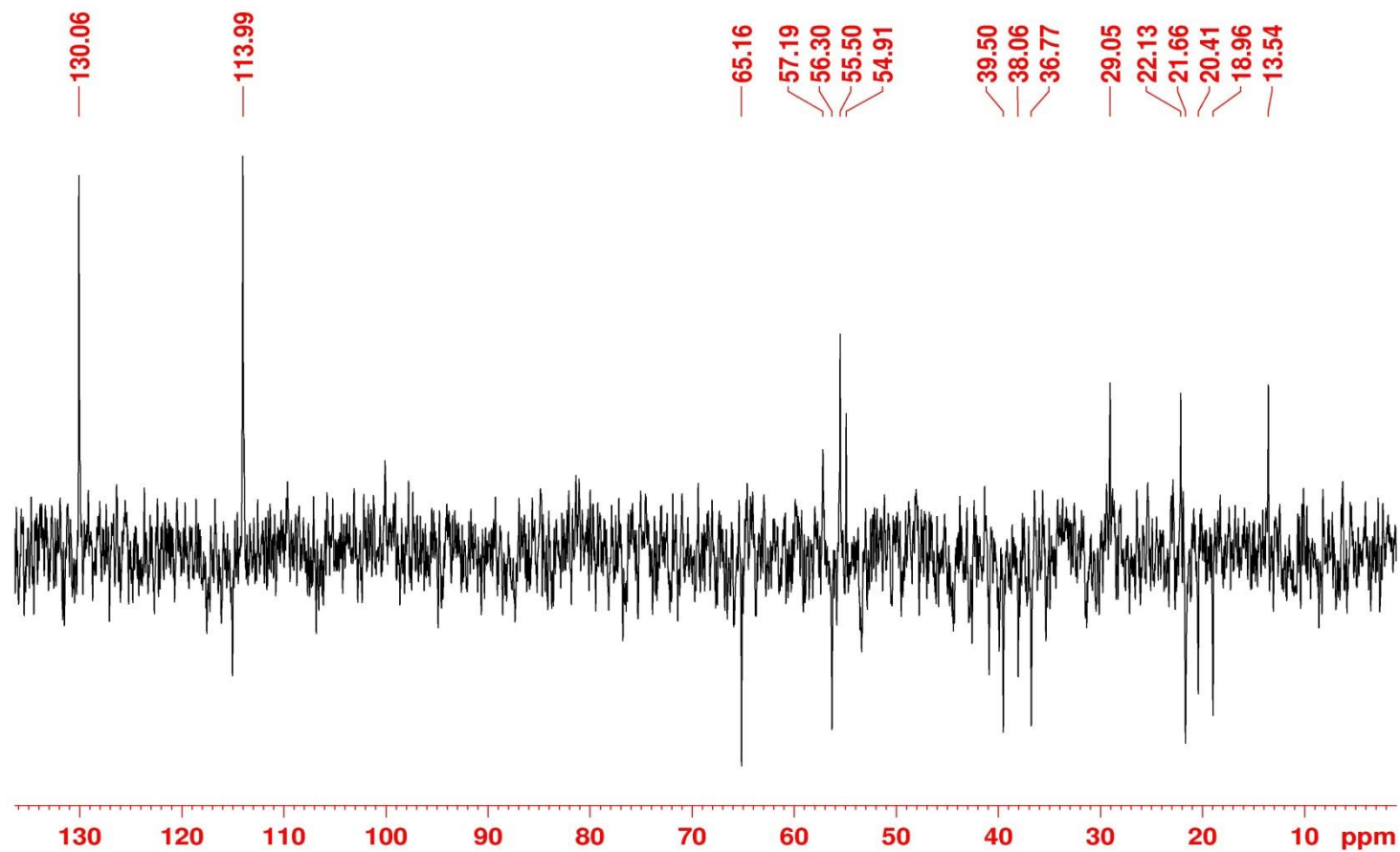


Figure 149: ^{13}C { ^1H } DEPT-NMR (50 MHz, CDCl_3) spectrum of compound **3c**.

166-ASADHEB_131112175848 #1142 RT: 5.31 AV: 1 NL: 2.47E6
T: ITMS + c ESI Full ms [120.00-2000.00]

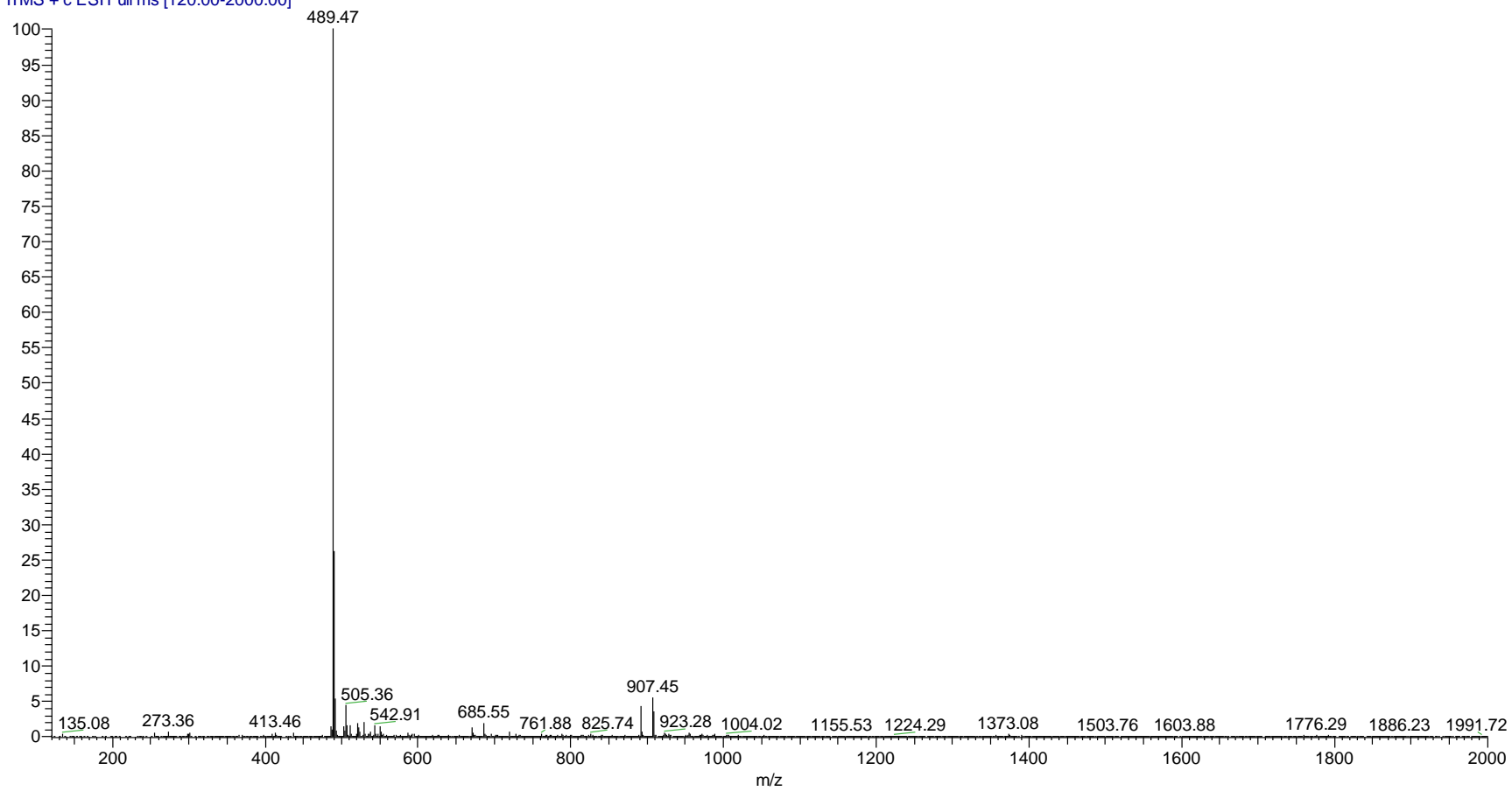
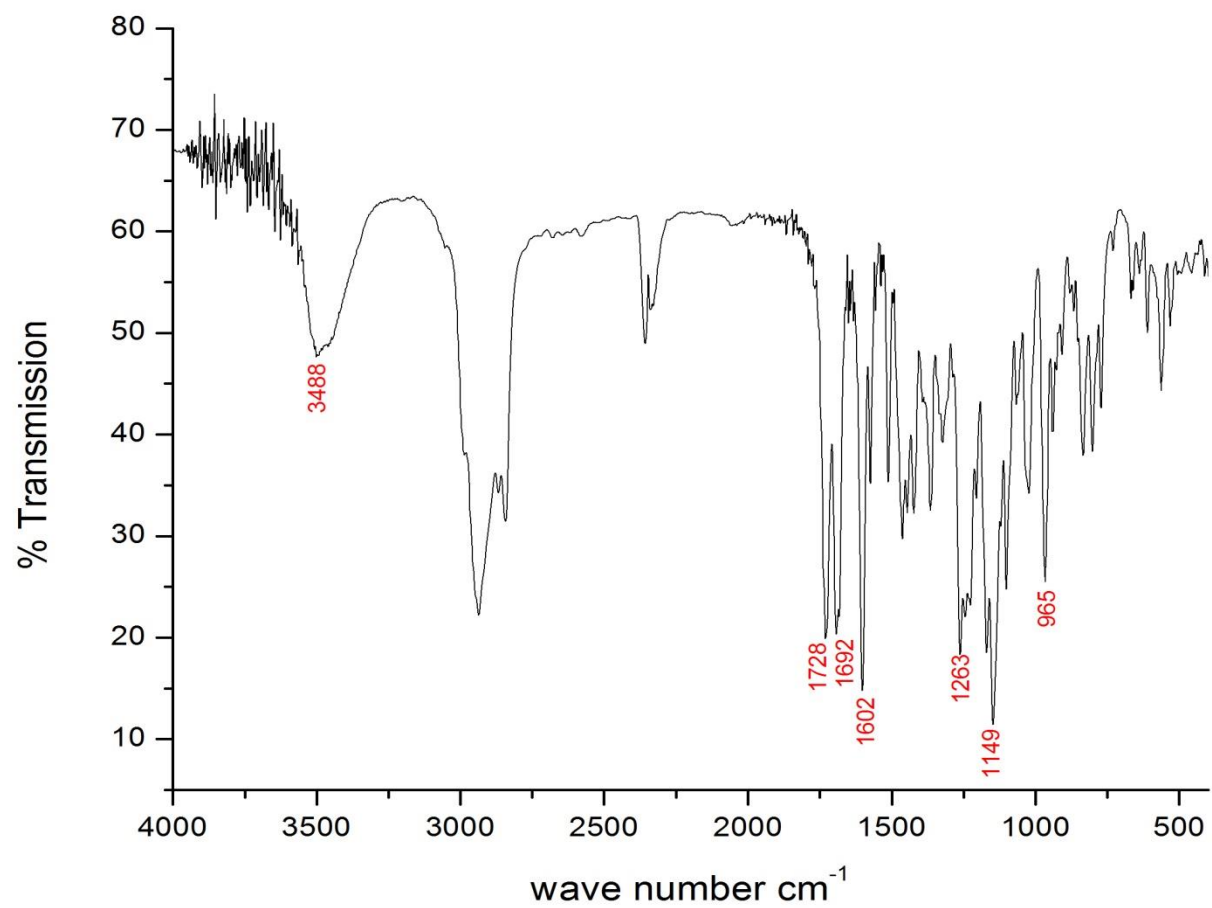


Figure 150: ESI-MS spectrum of compound **3h**.

Figure 151: IR spectrum of compound **3h**.

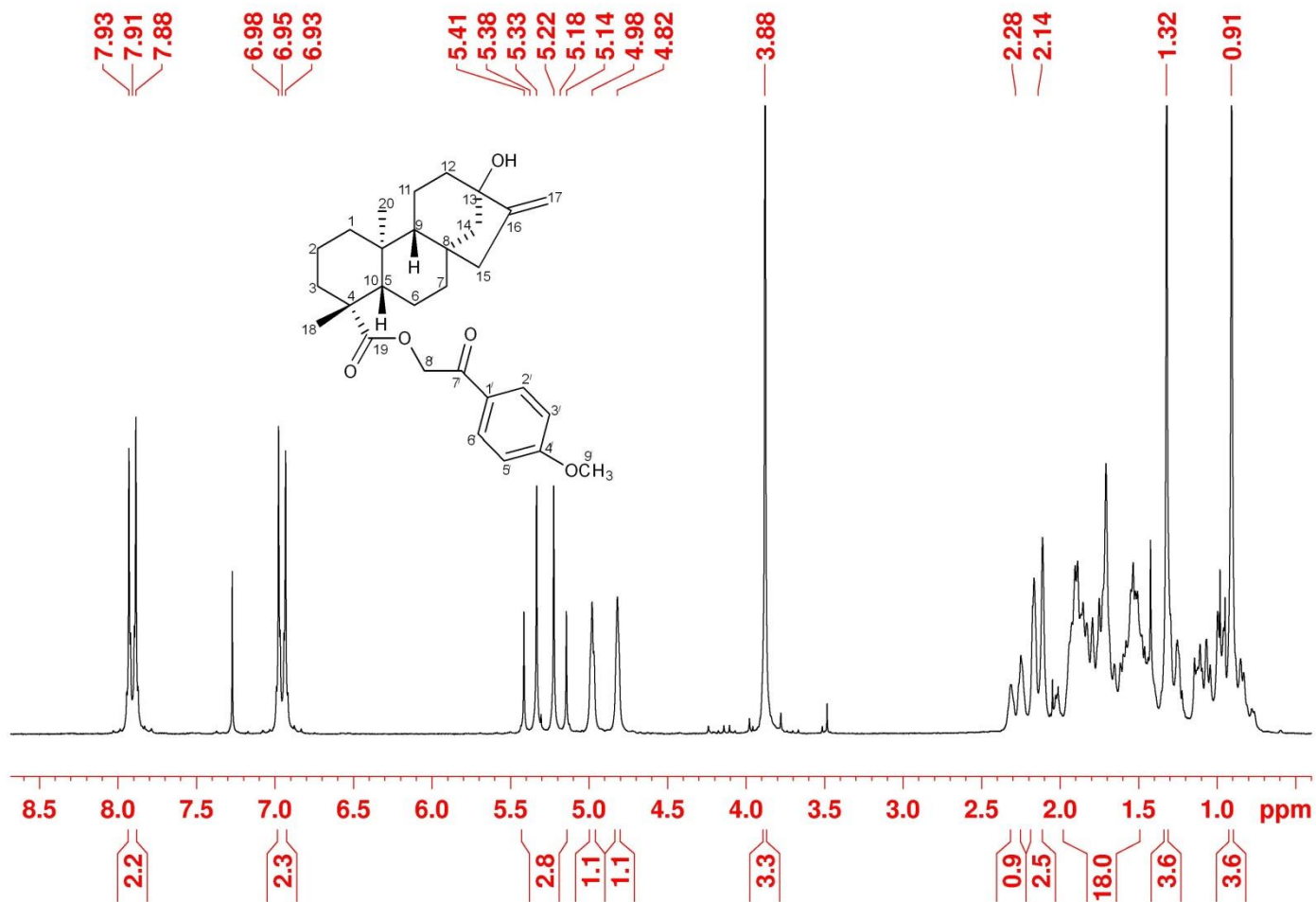


Figure 152: ¹H-NMR (200 MHz, CDCl₃) spectrum of compound **3h**.

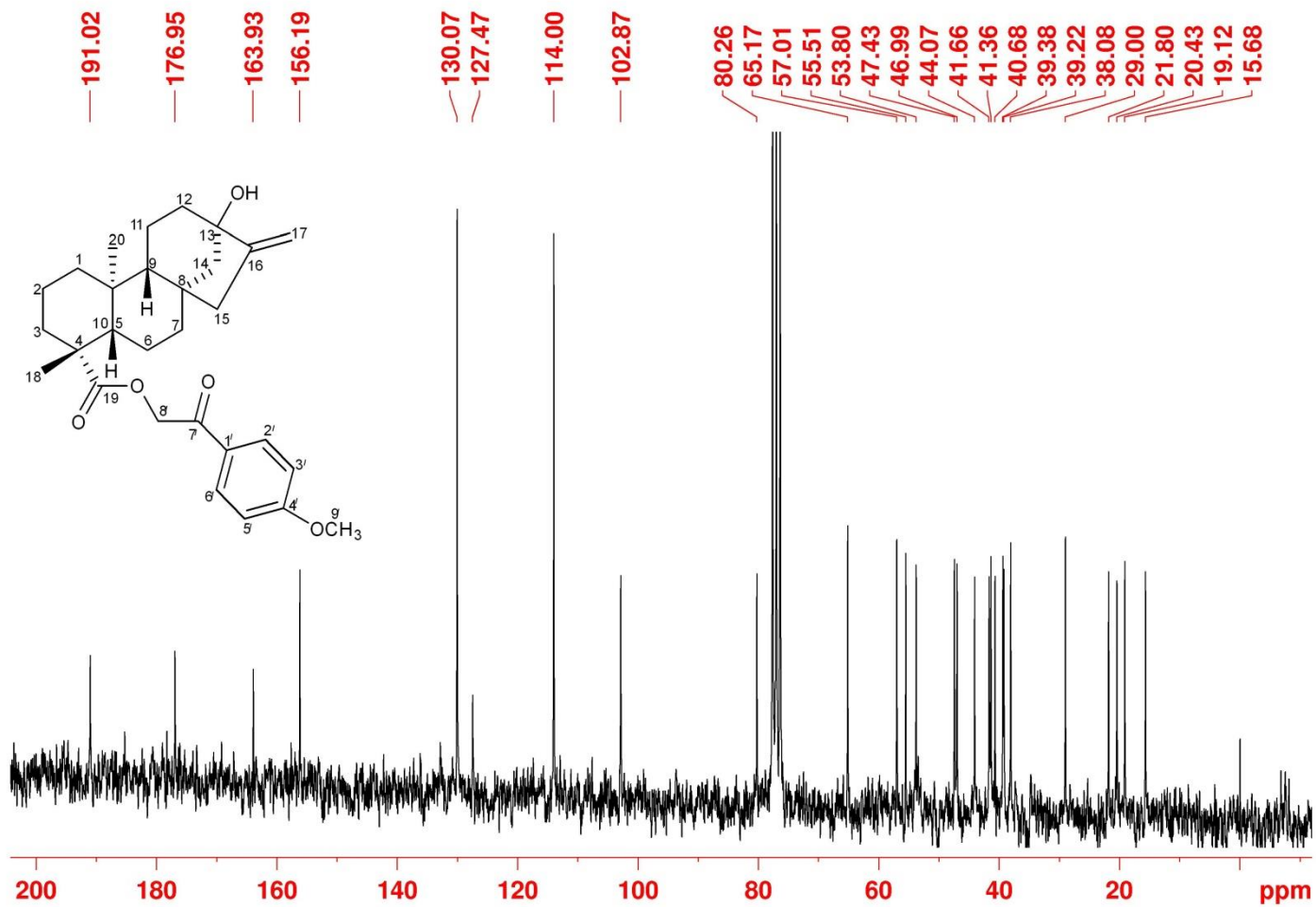


Figure 153: ^{13}C $\{^1\text{H}\}$ NMR (50 MHz, CDCl_3) spectrum of compound **3h**.

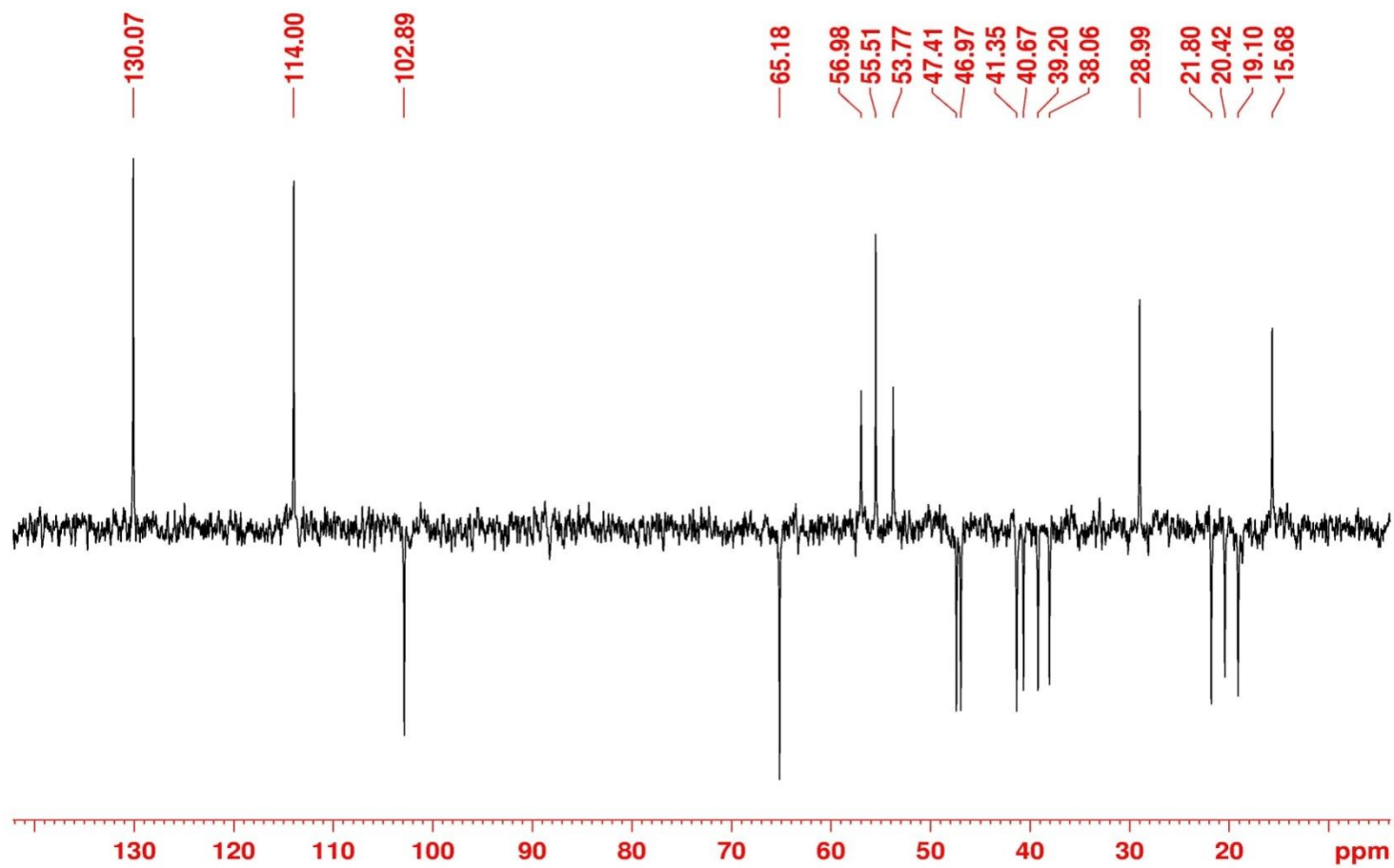


Figure 154: ^{13}C $\{^1\text{H}\}$ DEPT-NMR (50 MHz, CDCl_3) spectrum of compound **3h**.

id9b_140821145748 #1313 RT: 2.94 AV: 1 NL: 7.90E5
T: ITMS + p ESI Full ms2 439.00@cid0.00 [120.00-6C

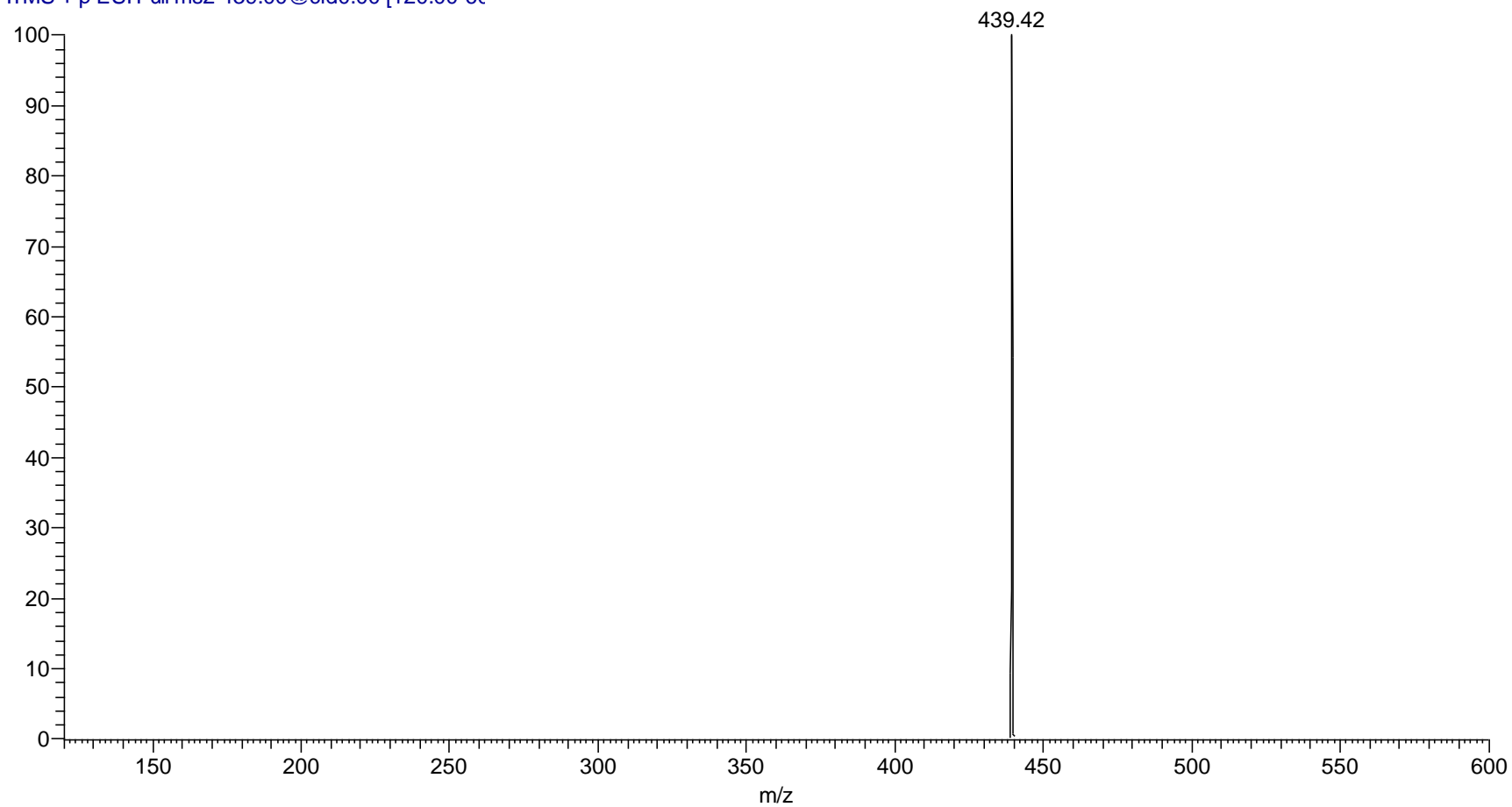
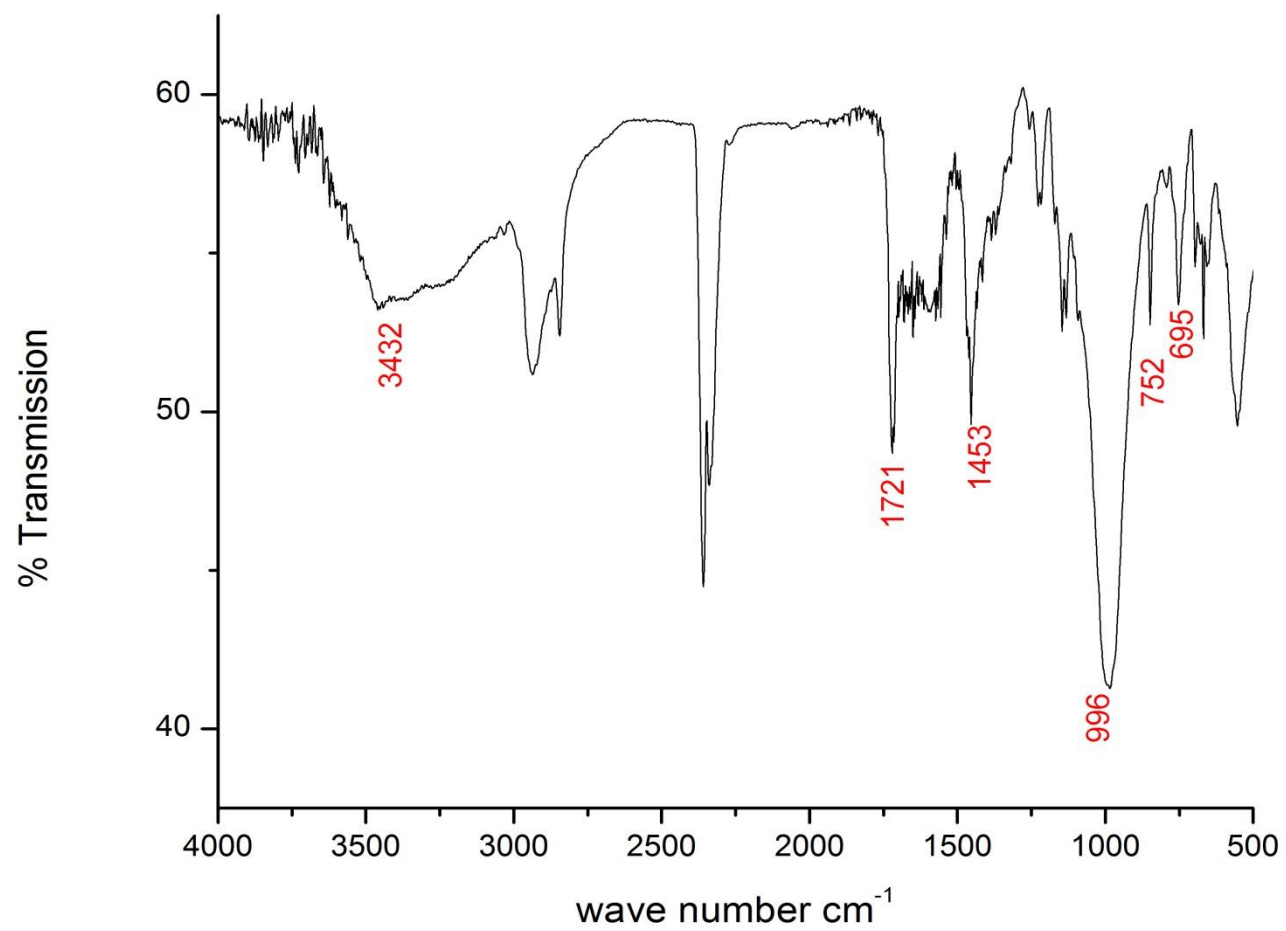


Figure 155: ESI-MS spectrum of compound **6k**.

Figure 156: IR spectrum of compound **6k**.

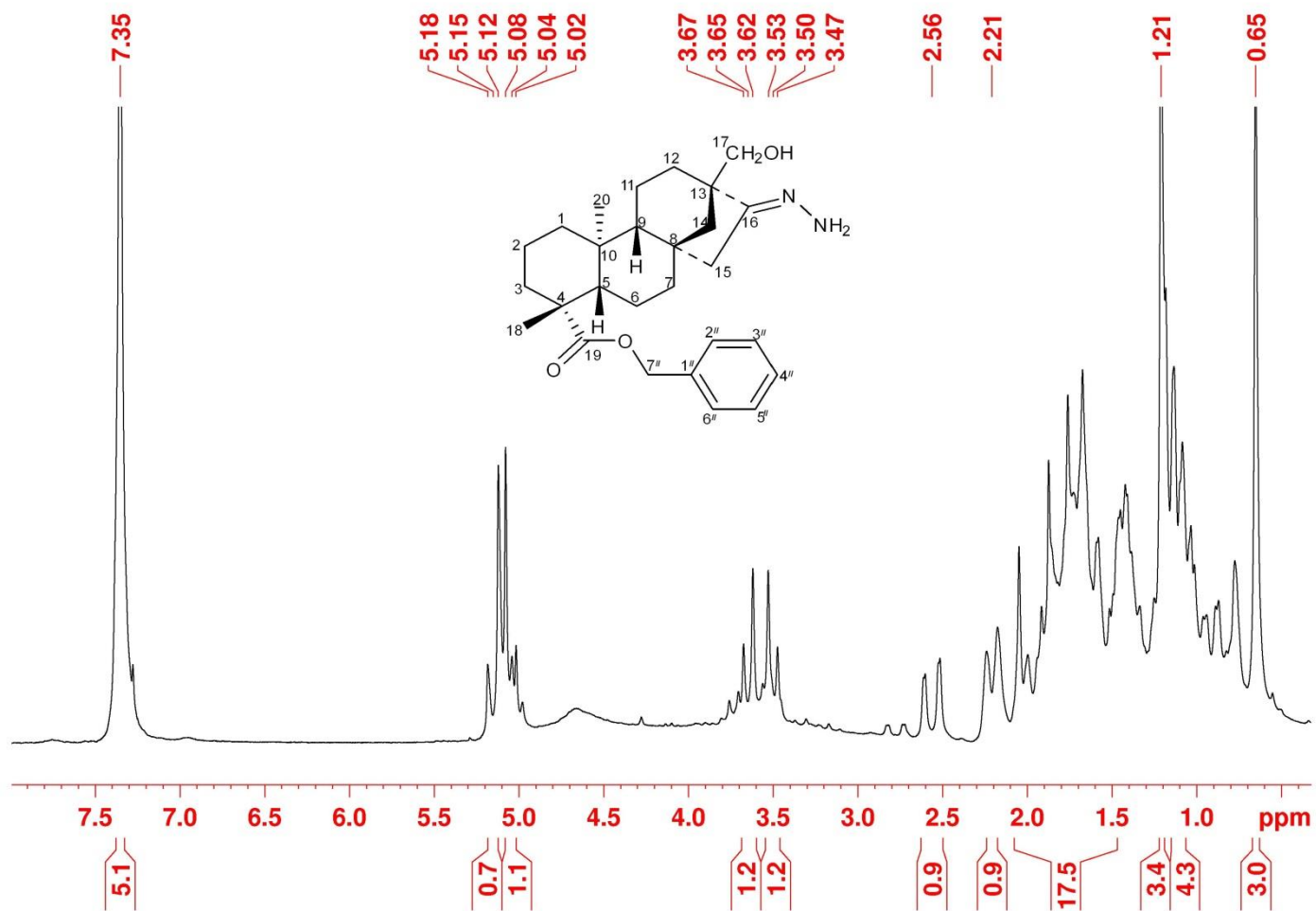


Figure 157: ¹H-NMR (200 MHz, CDCl₃) spectrum of compound **6k**.

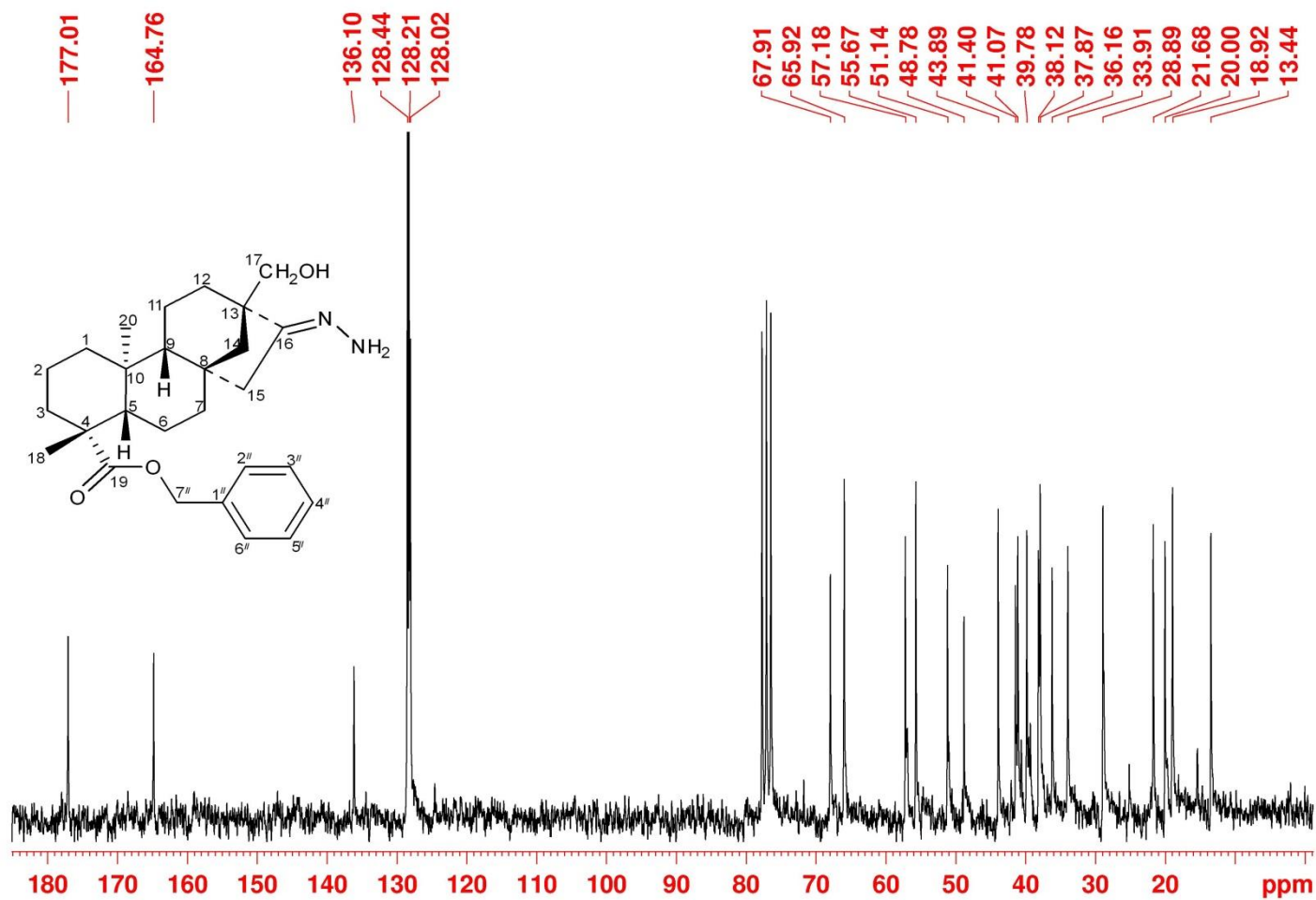


Figure 158: ^{13}C $\{^1\text{H}\}$ NMR (50 MHz, CDCl_3) spectrum of compound **6k**.

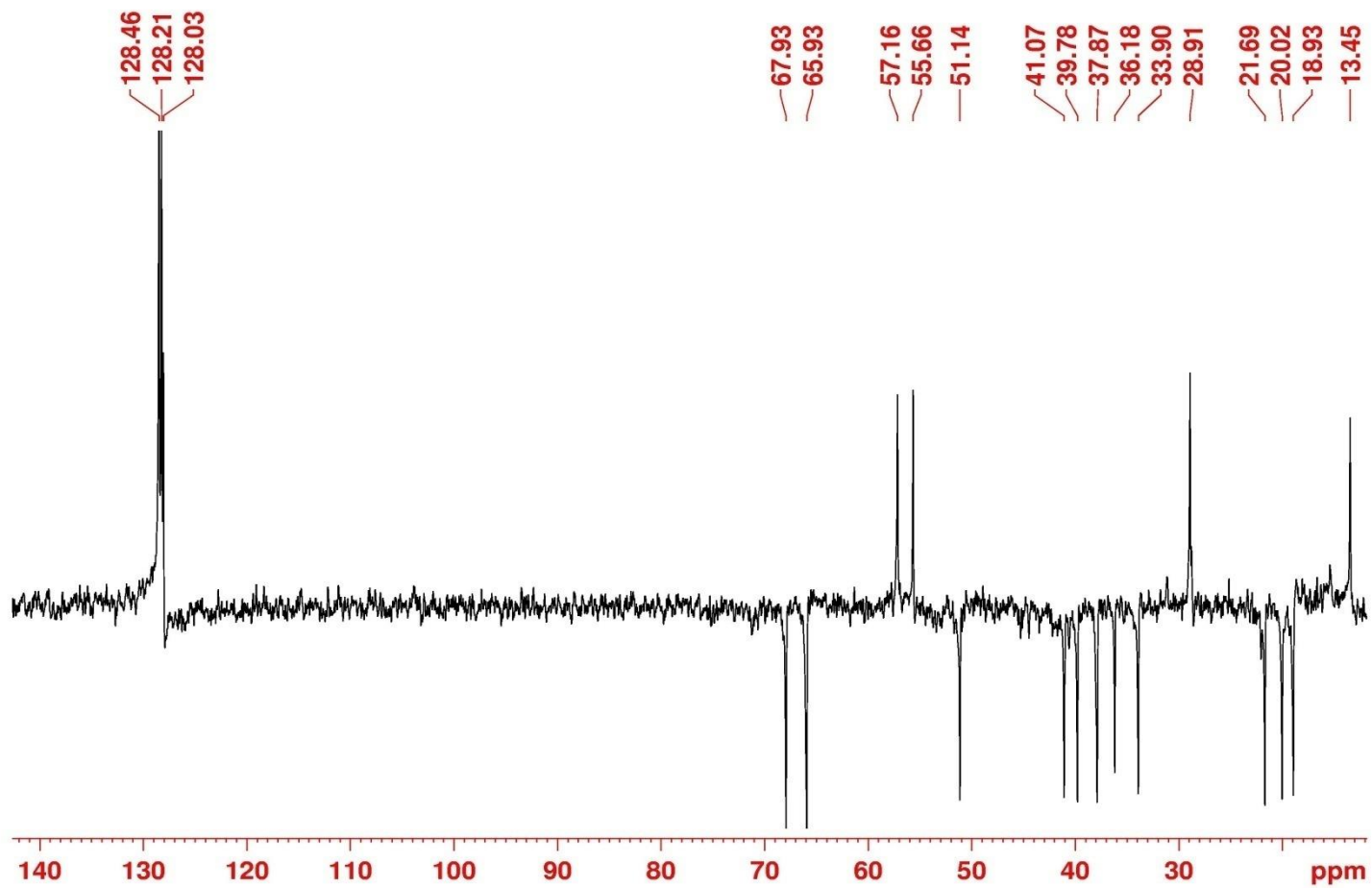


Figure 159: ^{13}C { ^1H } DEPT-NMR (50 MHz, CDCl_3) spectrum of compound **6k**.

IDB2_140724173744 #755 RT: 1.56 AV: 1 NL: 4.89E6
T: ITMS + c ESI Full ms [150.00-600.00]

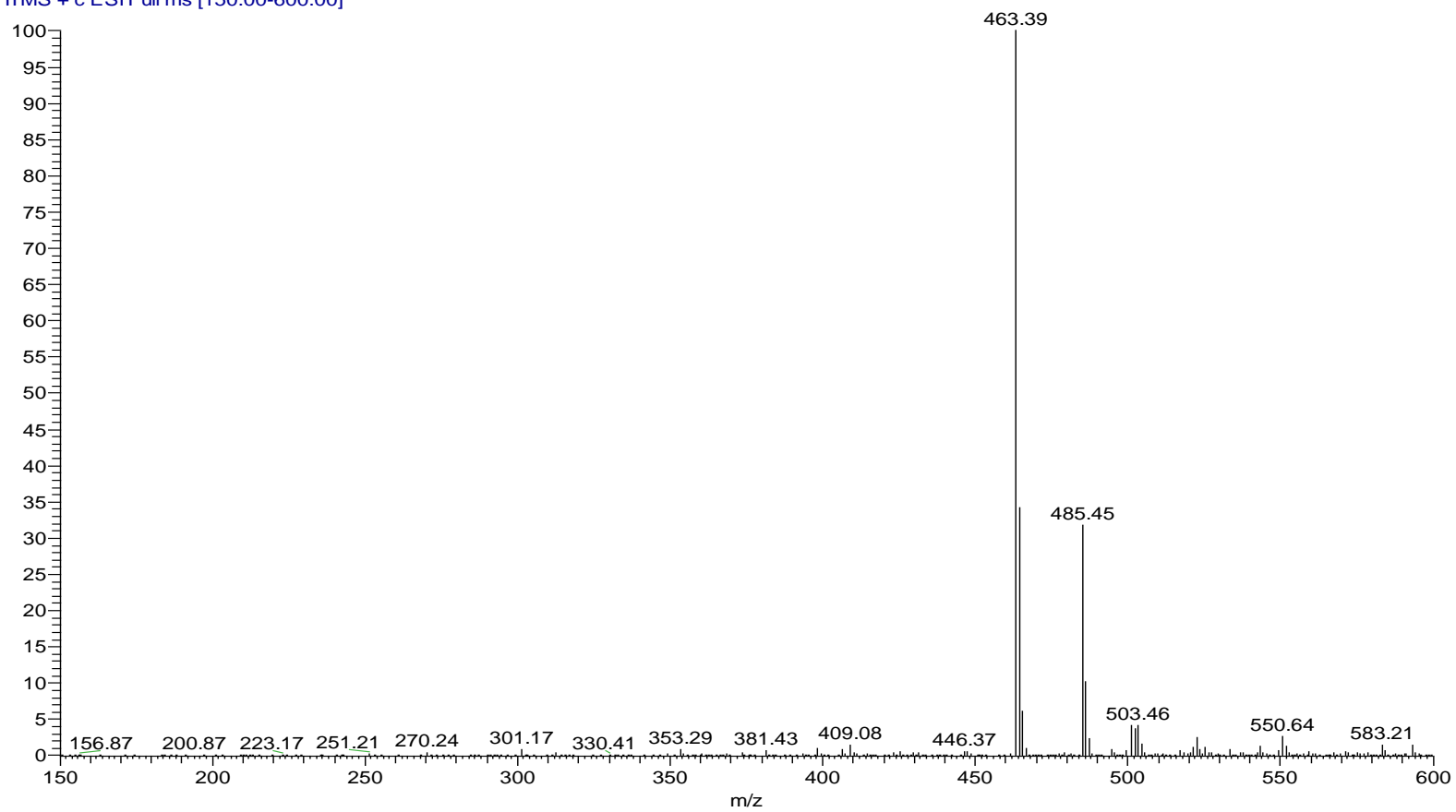


Figure 160: ESI-MS spectrum of compound 4f.

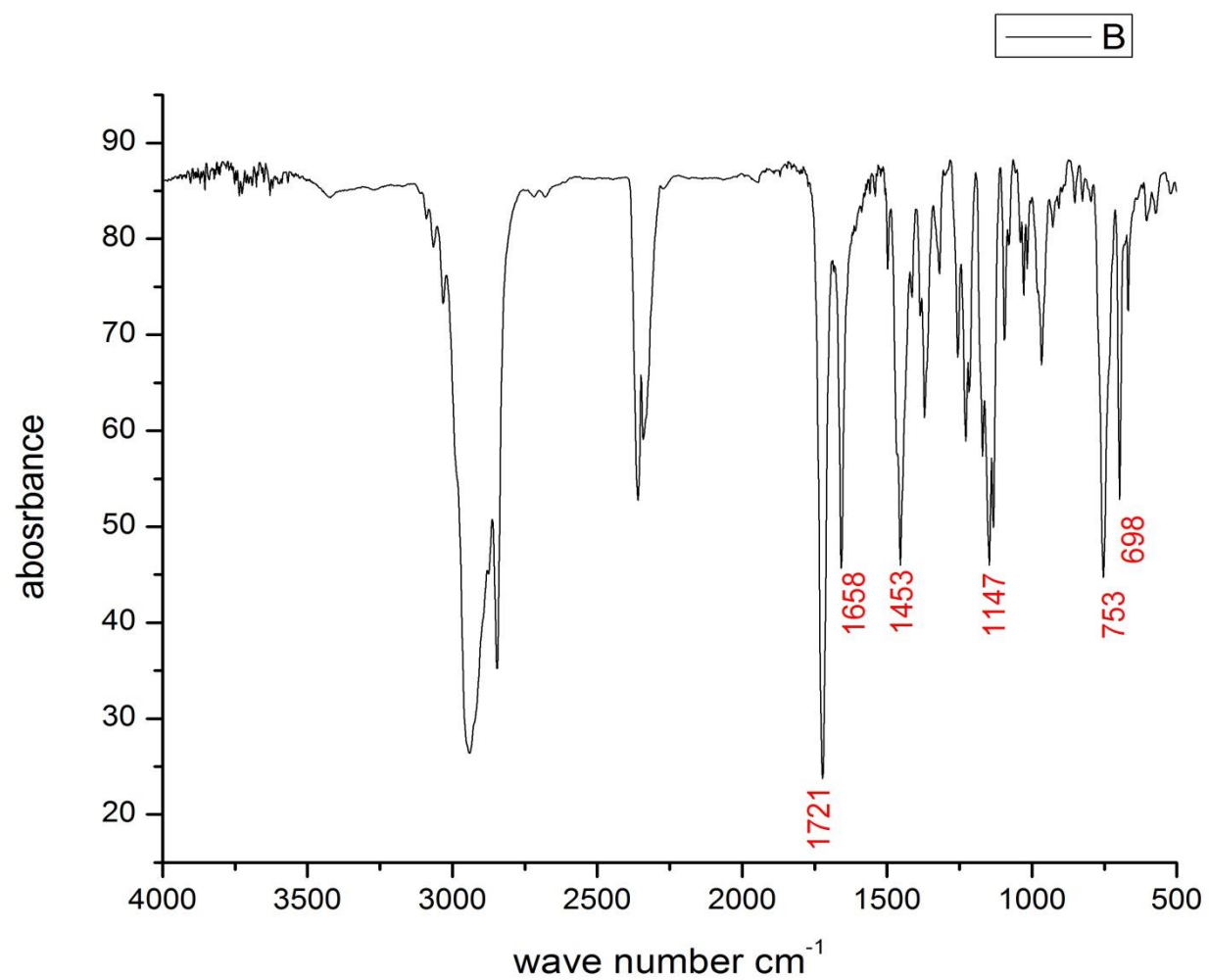


Figure 161: IR spectrum of compound 4f.

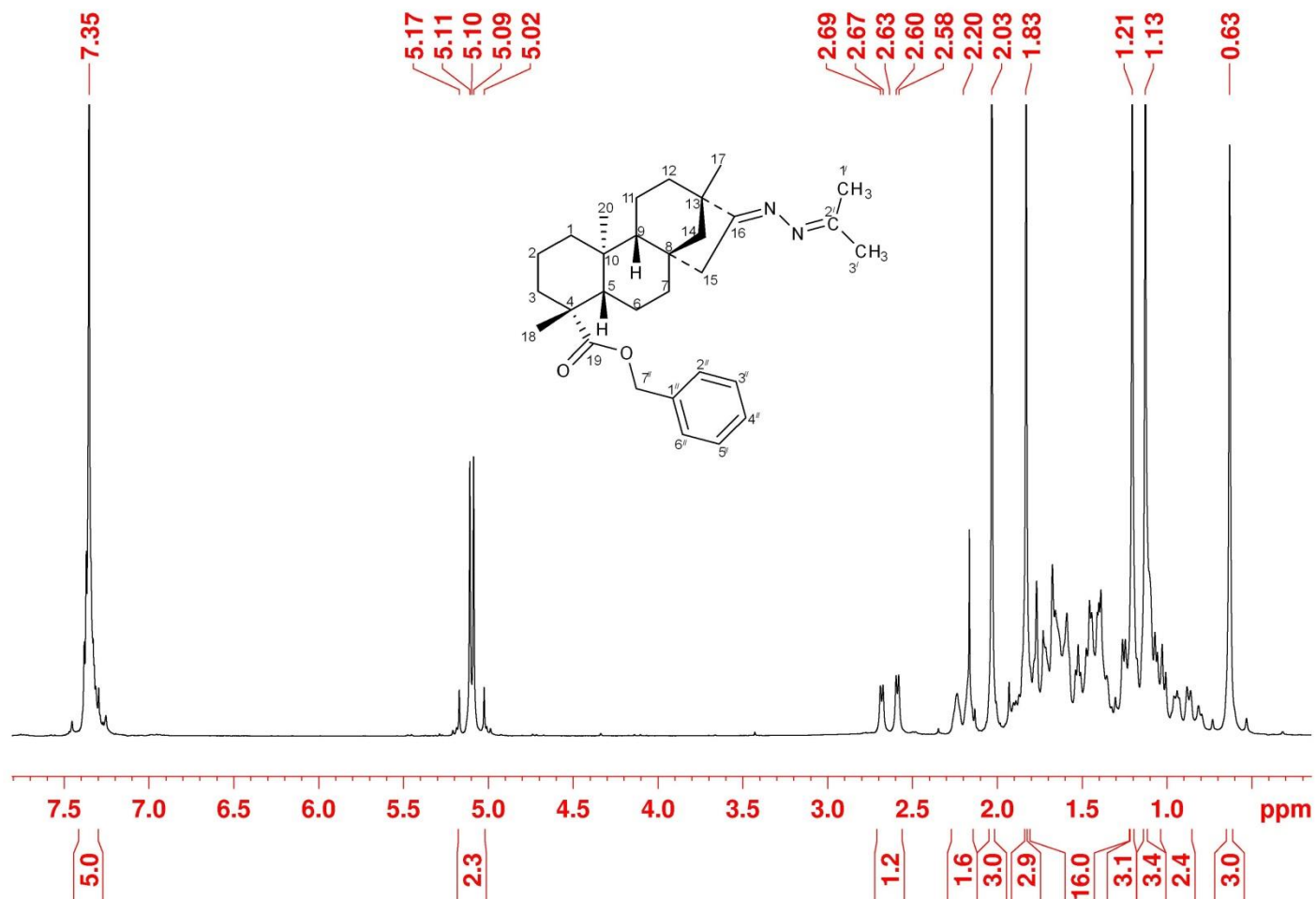


Figure 162: ¹H-NMR (200 MHz, CDCl₃) spectrum of compound 4f.

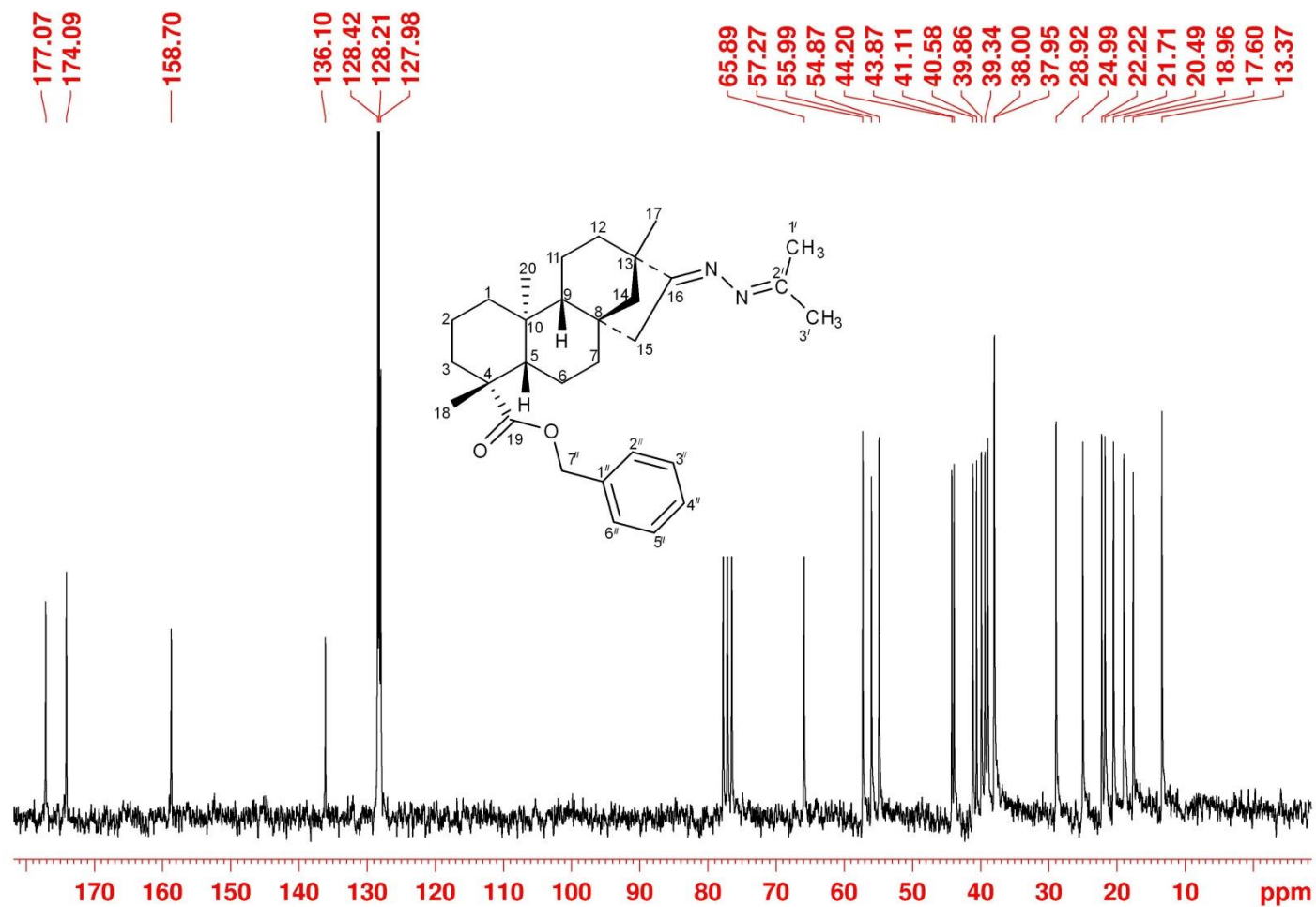


Figure 163: ^{13}C $\{^1\text{H}\}$ NMR (50 MHz, CDCl_3) spectrum of compound **4f**.

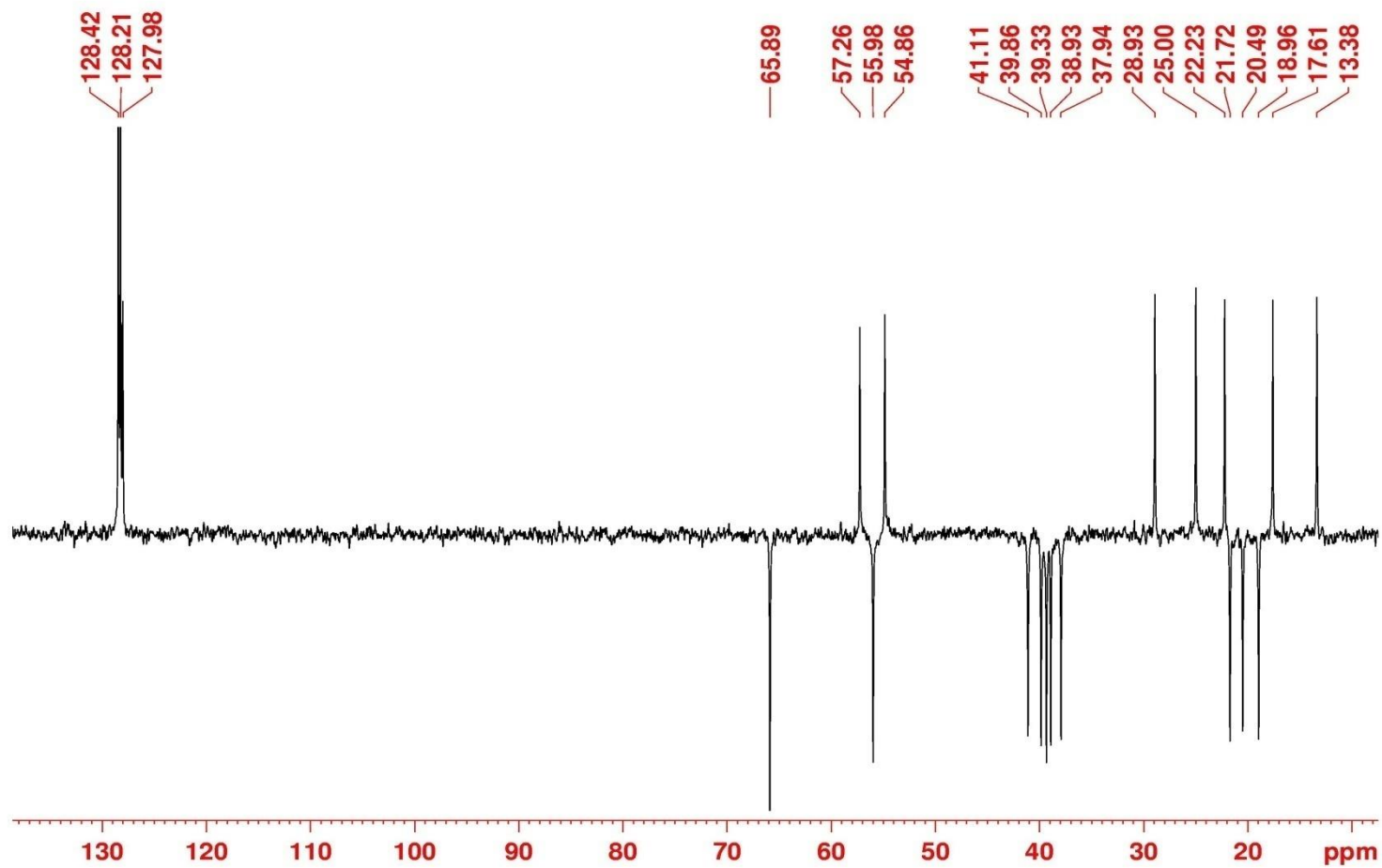


Figure 164: $^{13}\text{C} \{^1\text{H}\}$ DEPT-NMR (50 MHz, CDCl_3) spectrum of compound **4f**.

id9b_140821145748 #1657 RT: 5.32 AV: 1 NL: 6.10E5
T: ITMS + p ESI Full ms [245.00-2000.00]

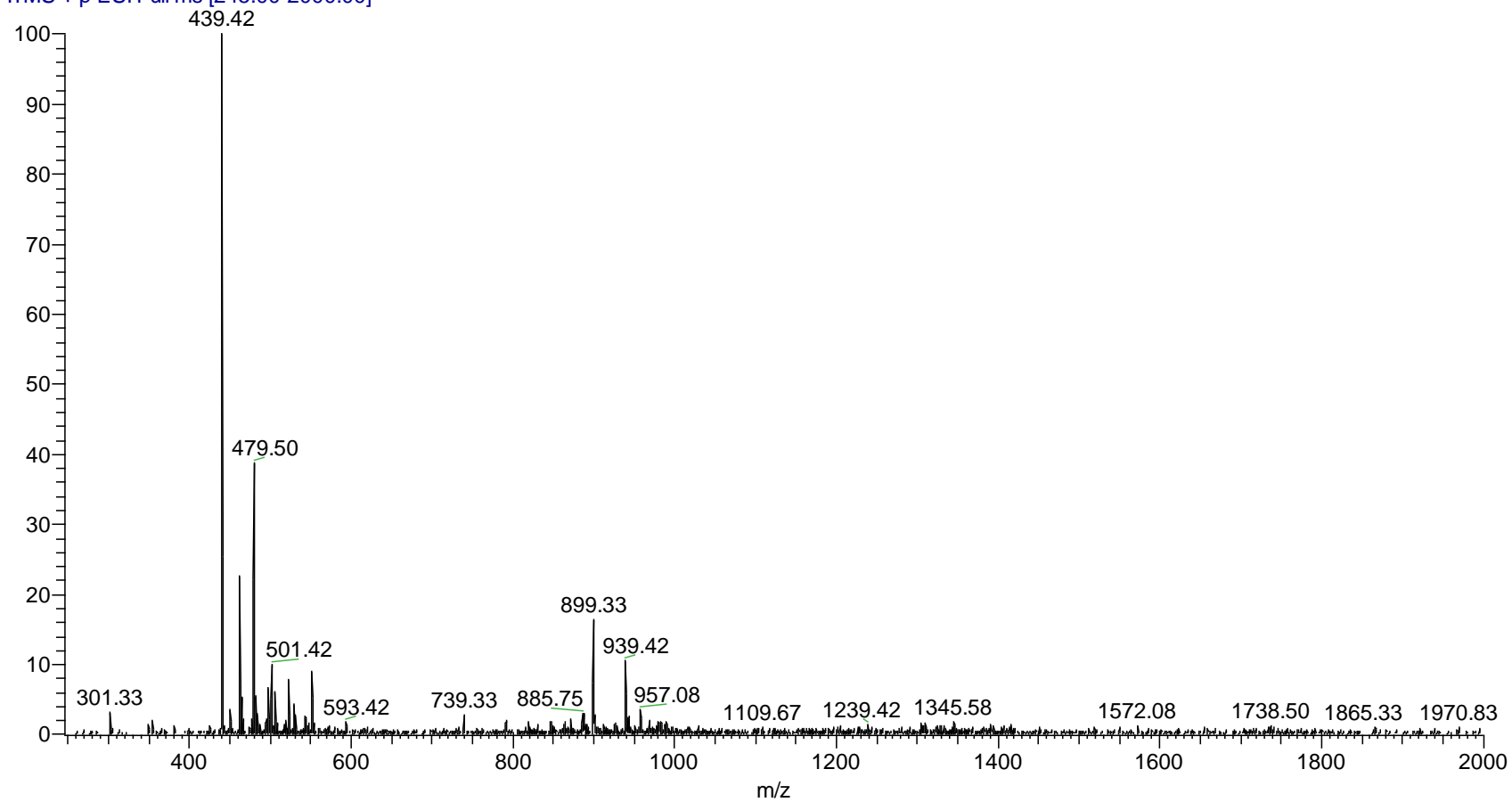
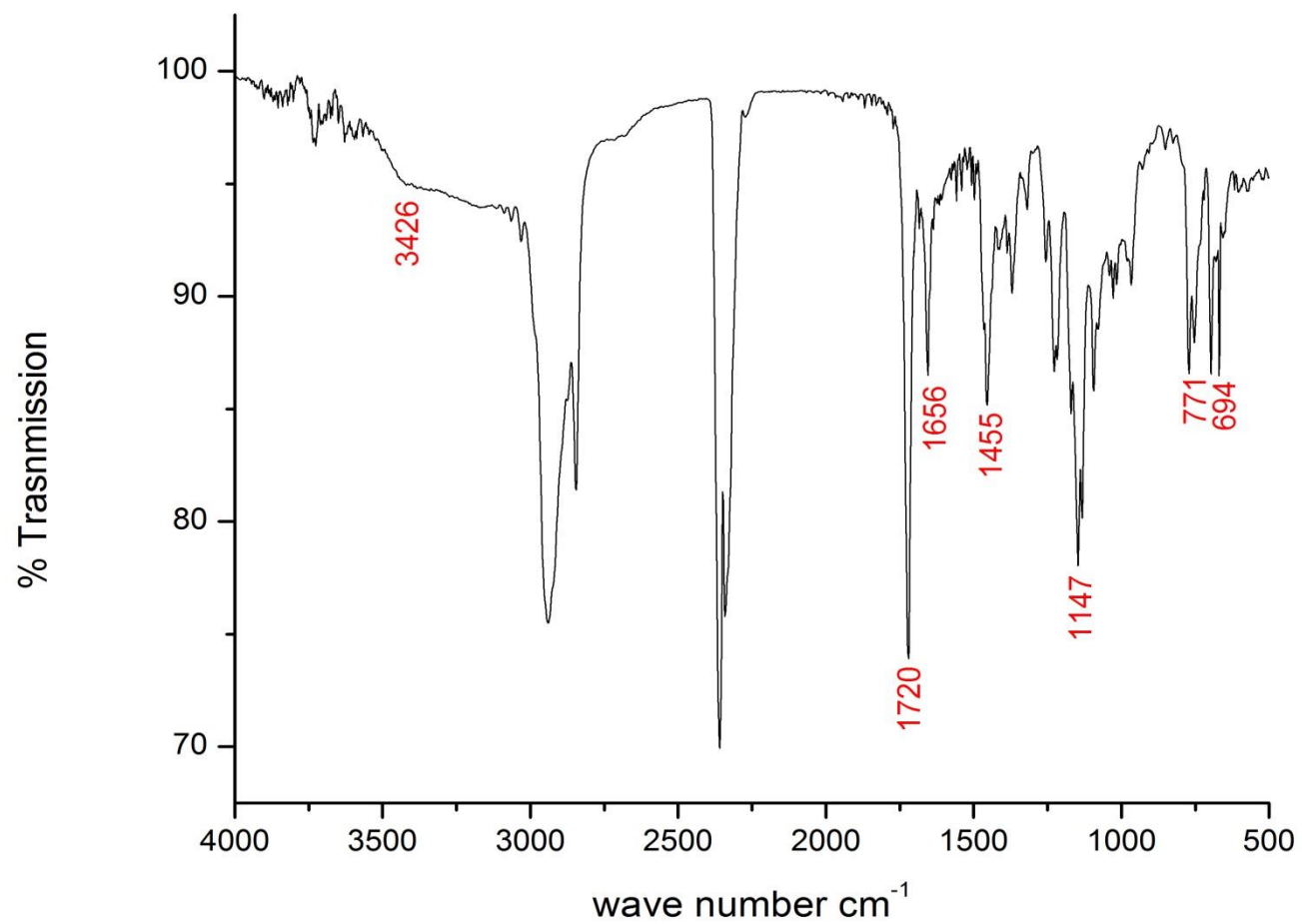


Figure 165: ESI-MS spectrum of compound **7k**.

Figure 166: IR spectrum of compound **7k**.

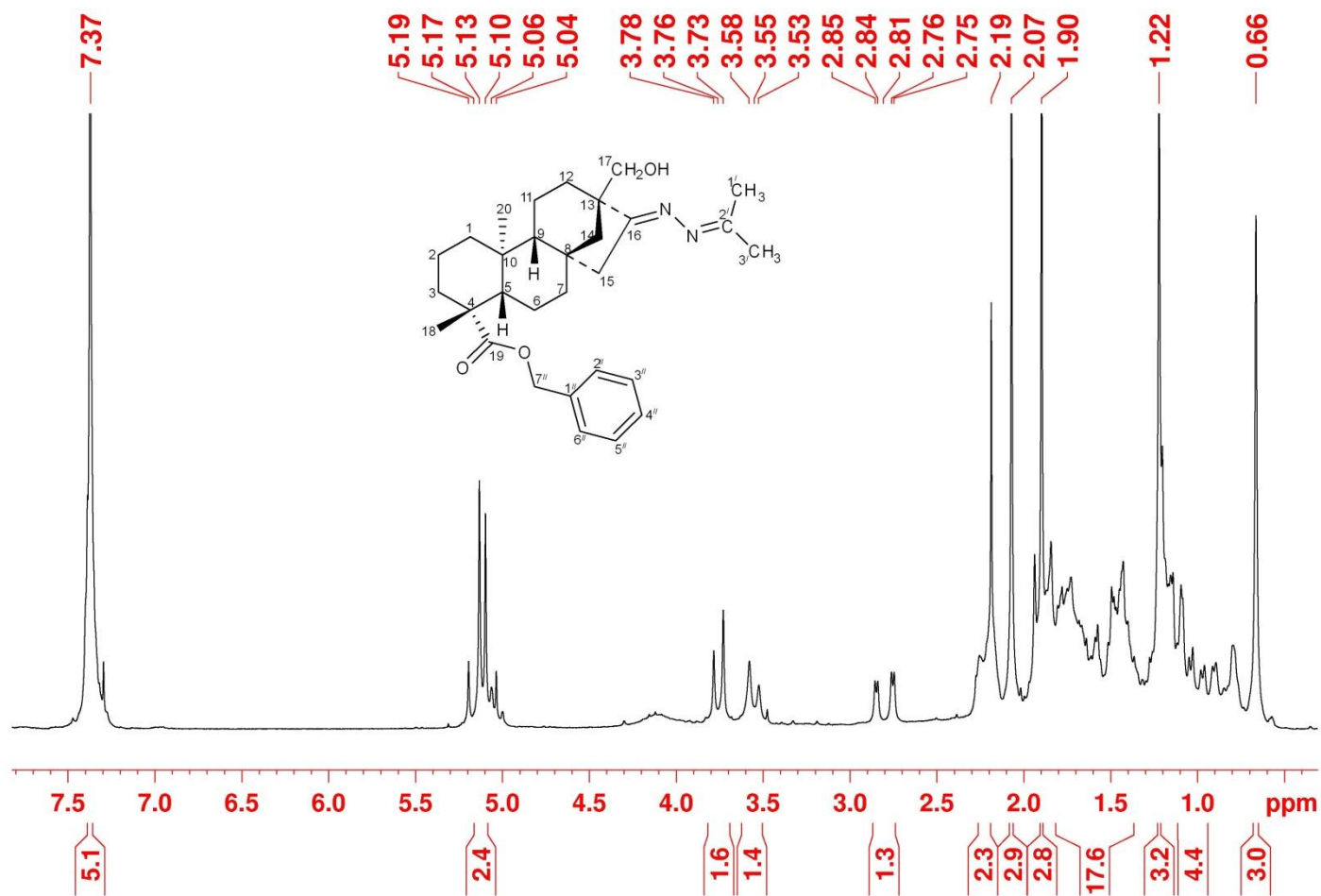


Figure 167: ¹H-NMR (200 MHz, CDCl₃) spectrum of compound **7k**.

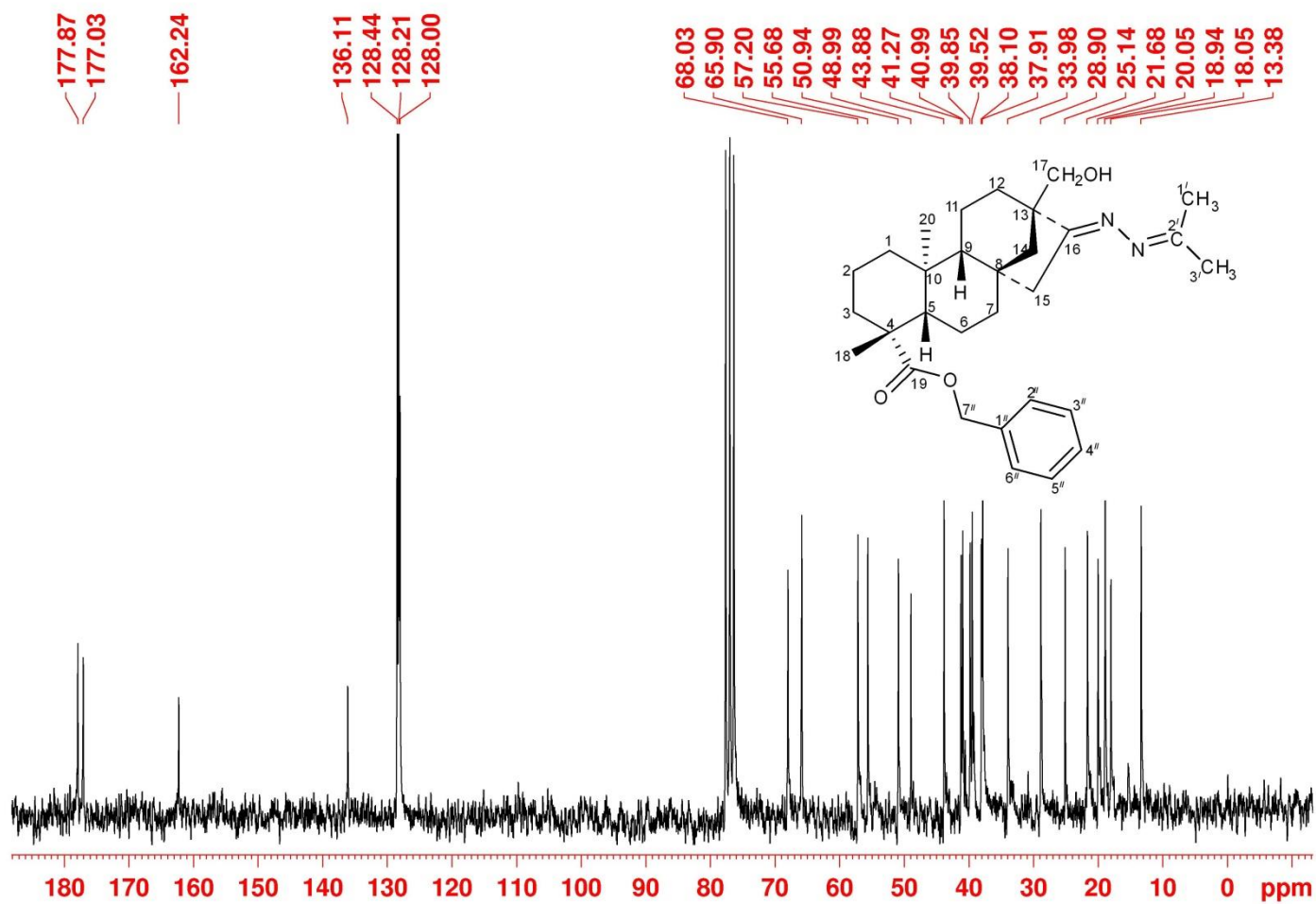


Figure 168: ^{13}C $\{^1\text{H}\}$ NMR (50 MHz, CDCl_3) spectrum of compound **7k**.

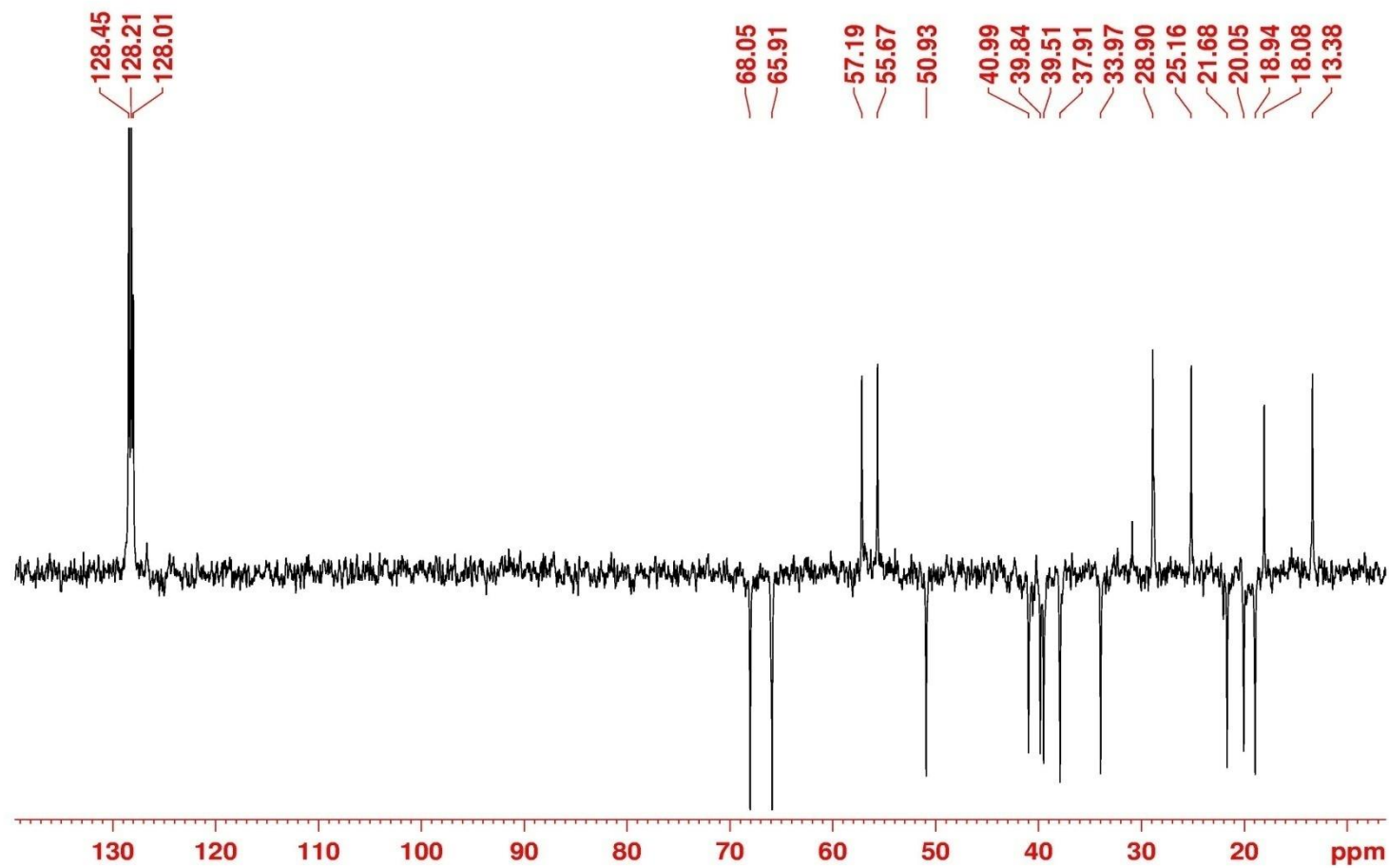


Figure 169: ^{13}C $\{^1\text{H}\}$ DEPT-NMR (50 MHz, CDCl_3) spectrum of compound **7k**.

164-ASADH-DNPH_131001140603 #2245 RT: 6.89 AV: 1 NL: 1.46E5
T: ITMS - c ESI Full ms [115.00-600.00]

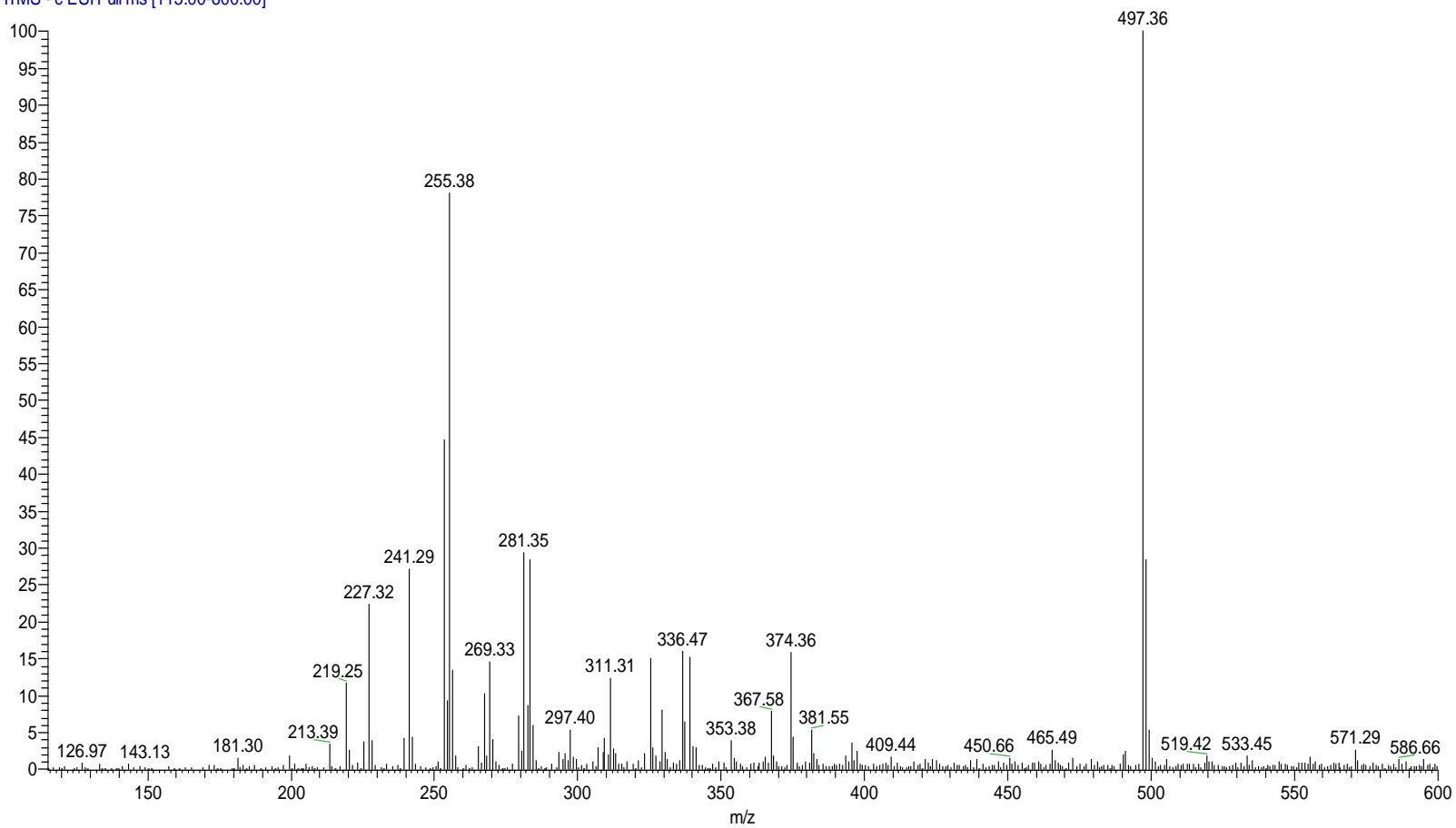


Figure 170: ESI-MS spectrum of compound **2g**.

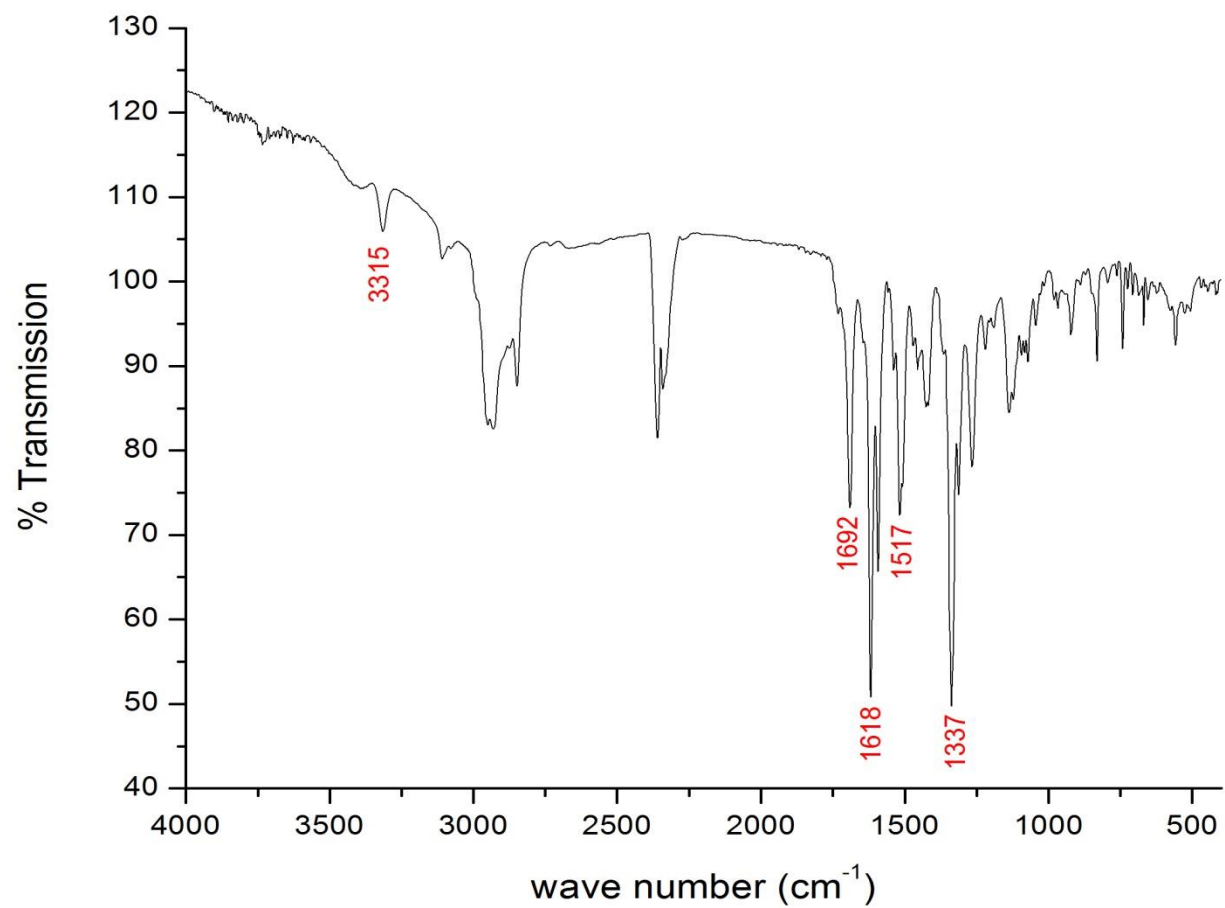


Figure 171: IR spectrum of compound **2g**.

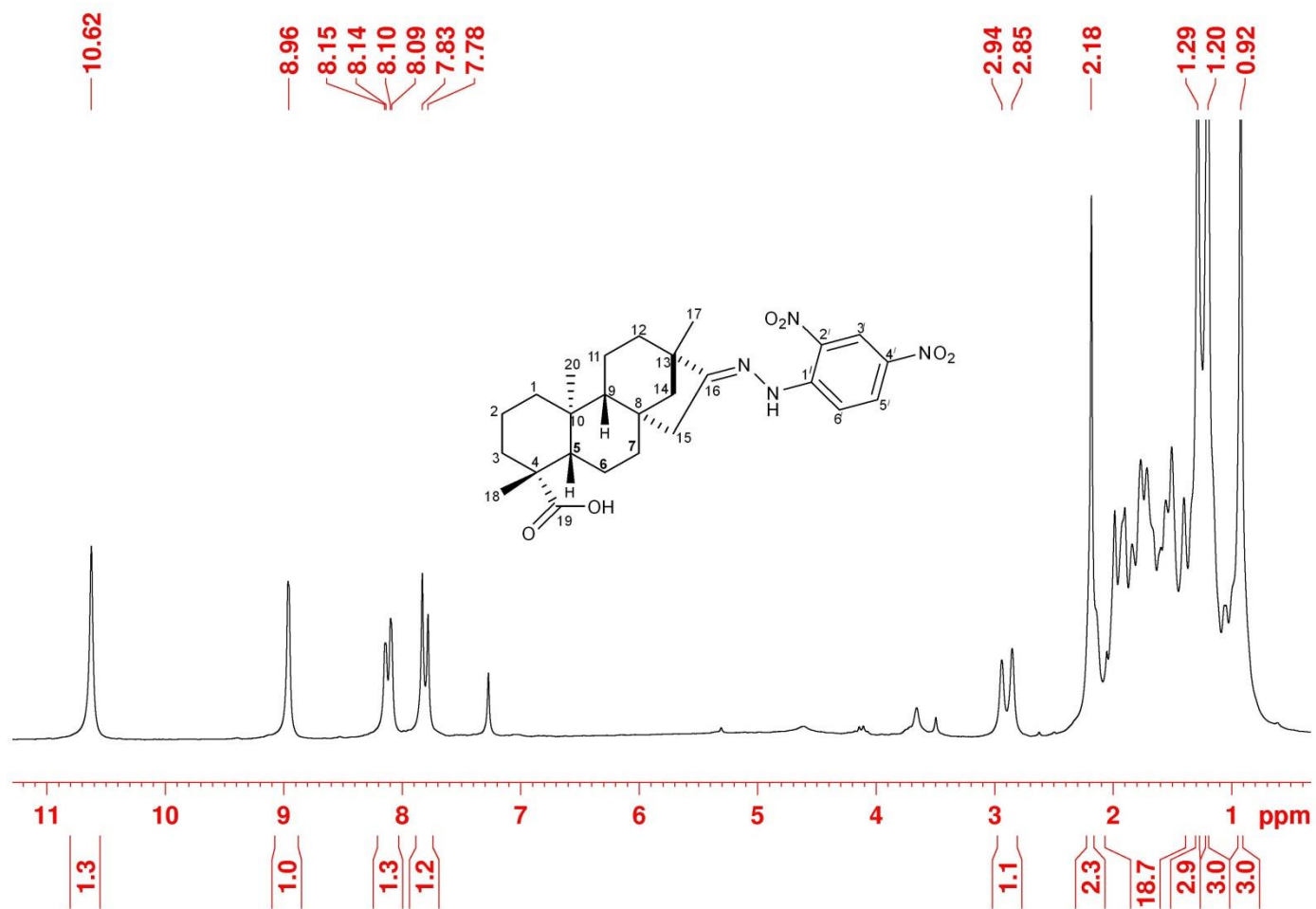


Figure 172: $^1\text{H-NMR}$ (200 MHz, CDCl_3) spectrum of compound **2g**.

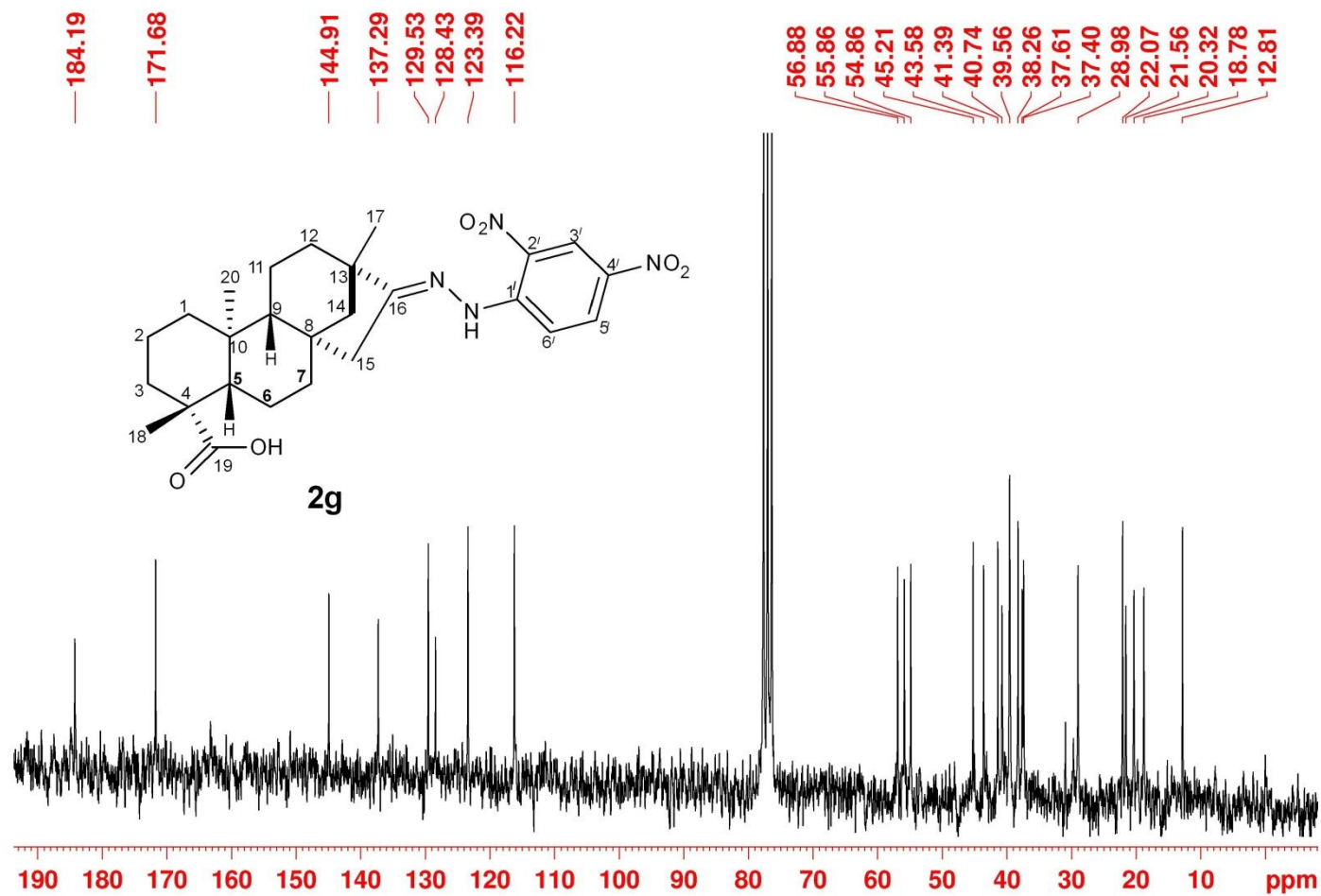


Figure 173: ^{13}C $\{^1\text{H}\}$ NMR (50 MHz, CDCl_3) spectrum of compound **2g**.

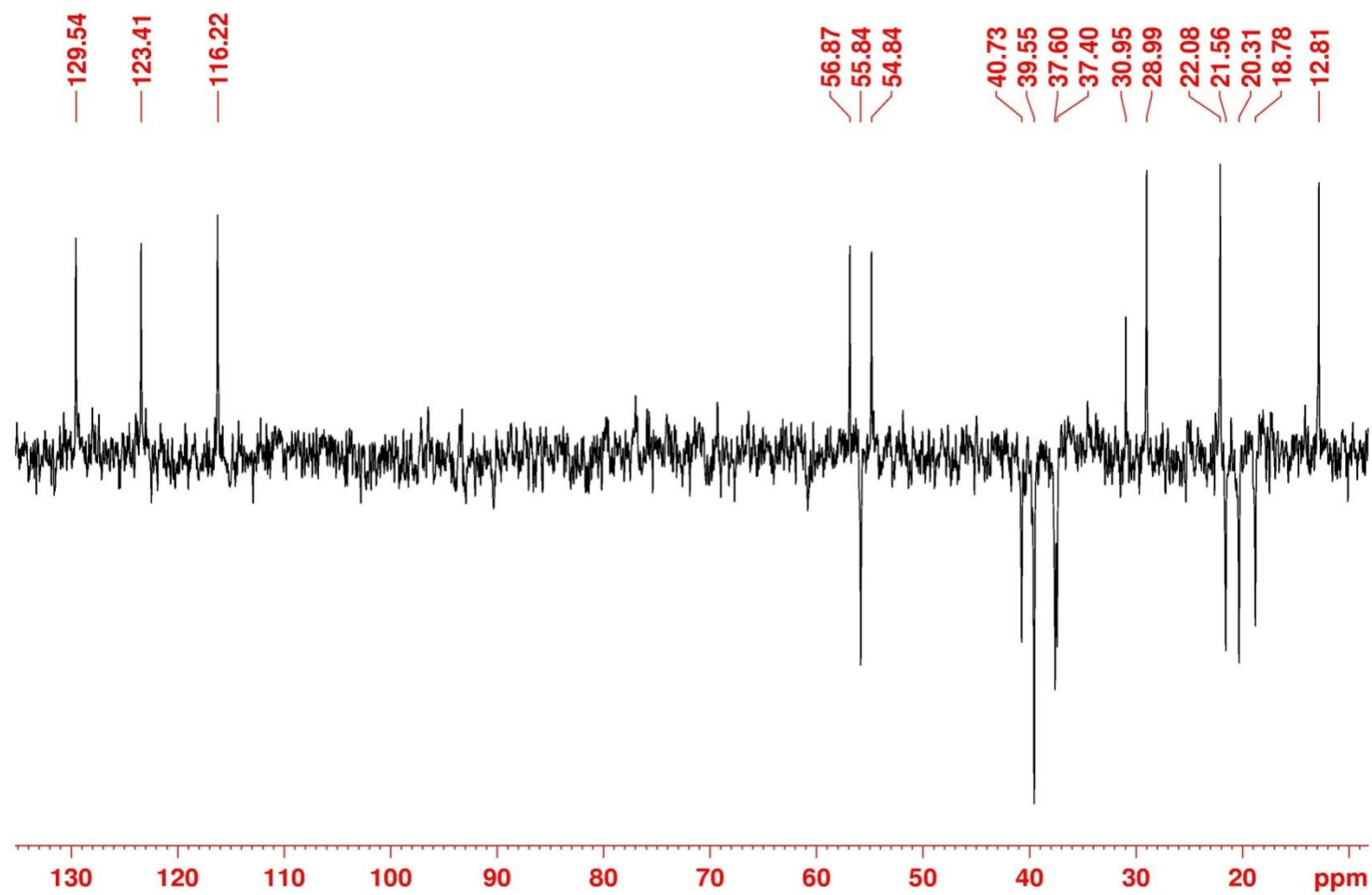


Figure 174: $^{13}\text{C} \{^1\text{H}\}$ DEPT-NMR (50 MHz, CDCl_3) spectrum of compound **2g**.

170-ASADI-ISO4DNPH_131031141705 #1740 RT: 3.92 AV: 1 NL: 4.33E5
T: ITMS - c ESI Full ms [120.00-600.00]

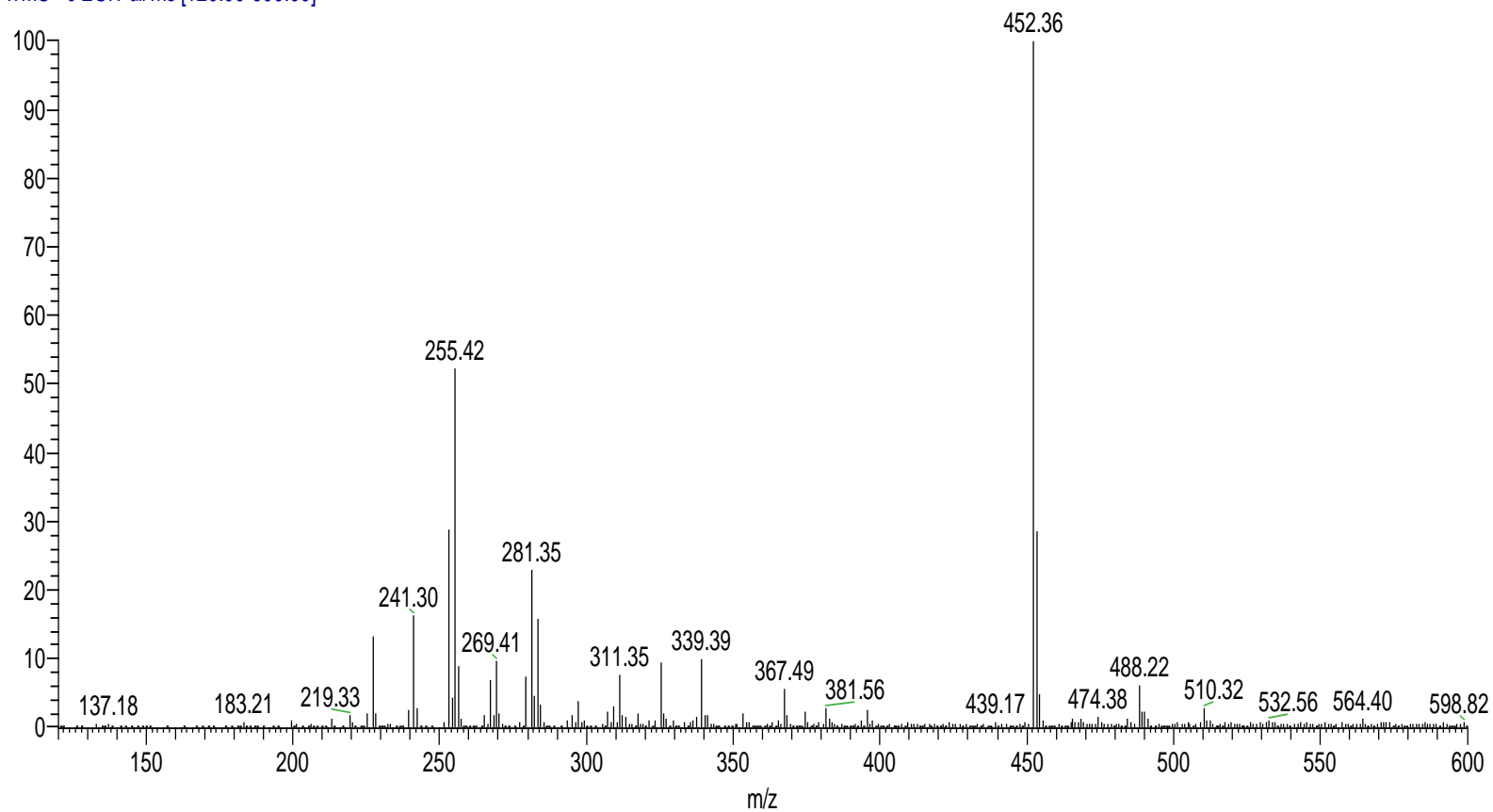


Figure 175: ESI-MS spectrum of compound **3g**.

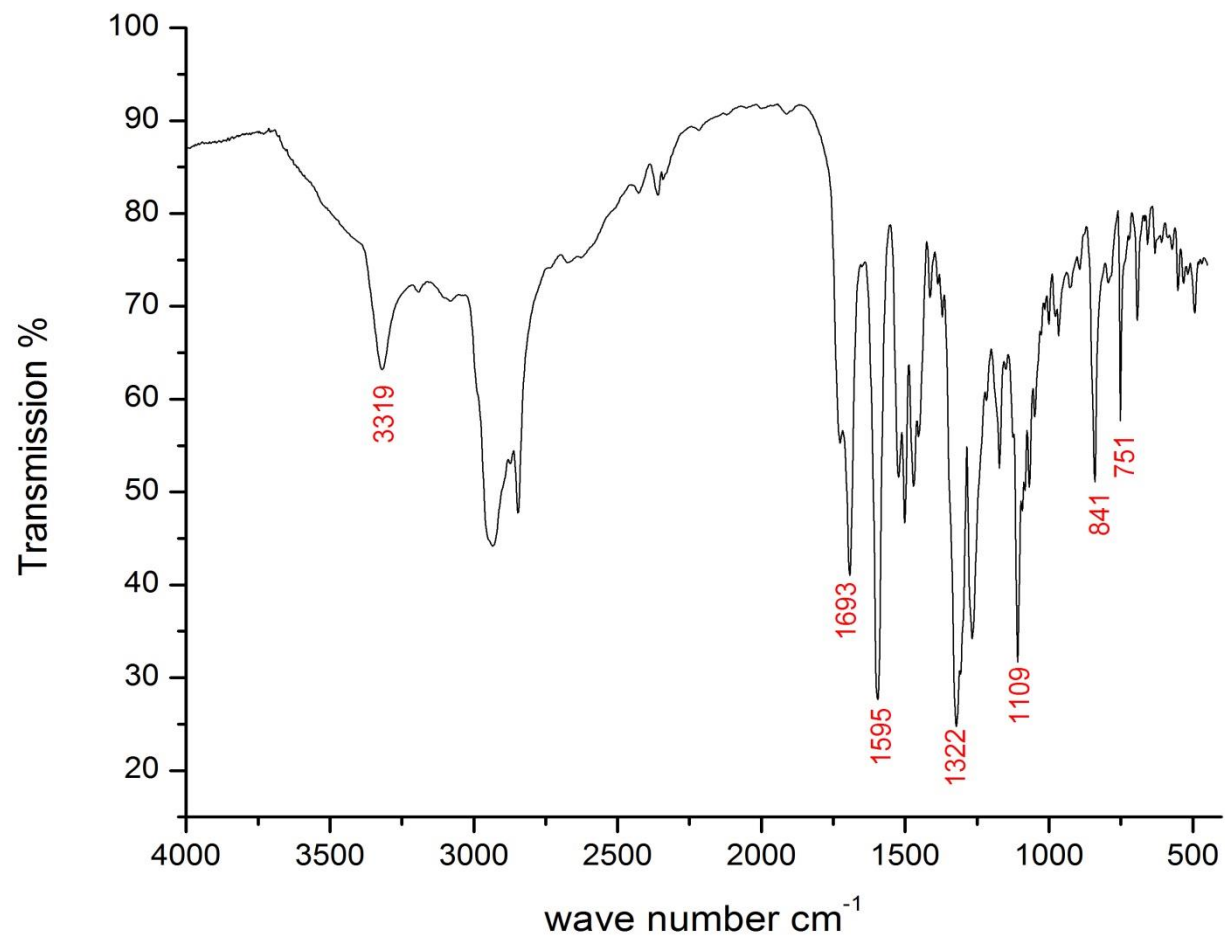


Figure 176: IR spectrum of compound **3g**.

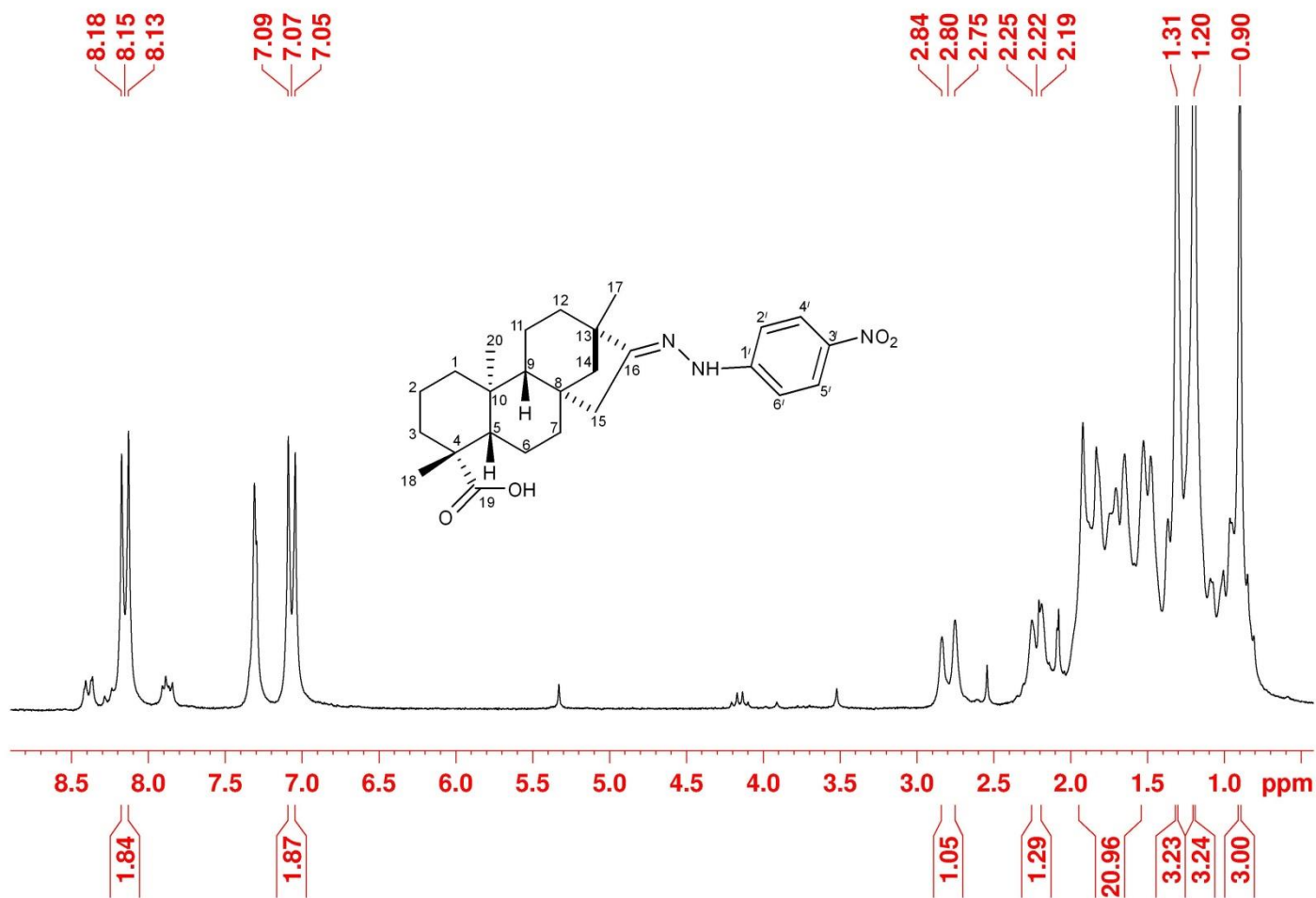


Figure 177: ¹H-NMR (200 MHz, CDCl₃) spectrum of compound **3g**.

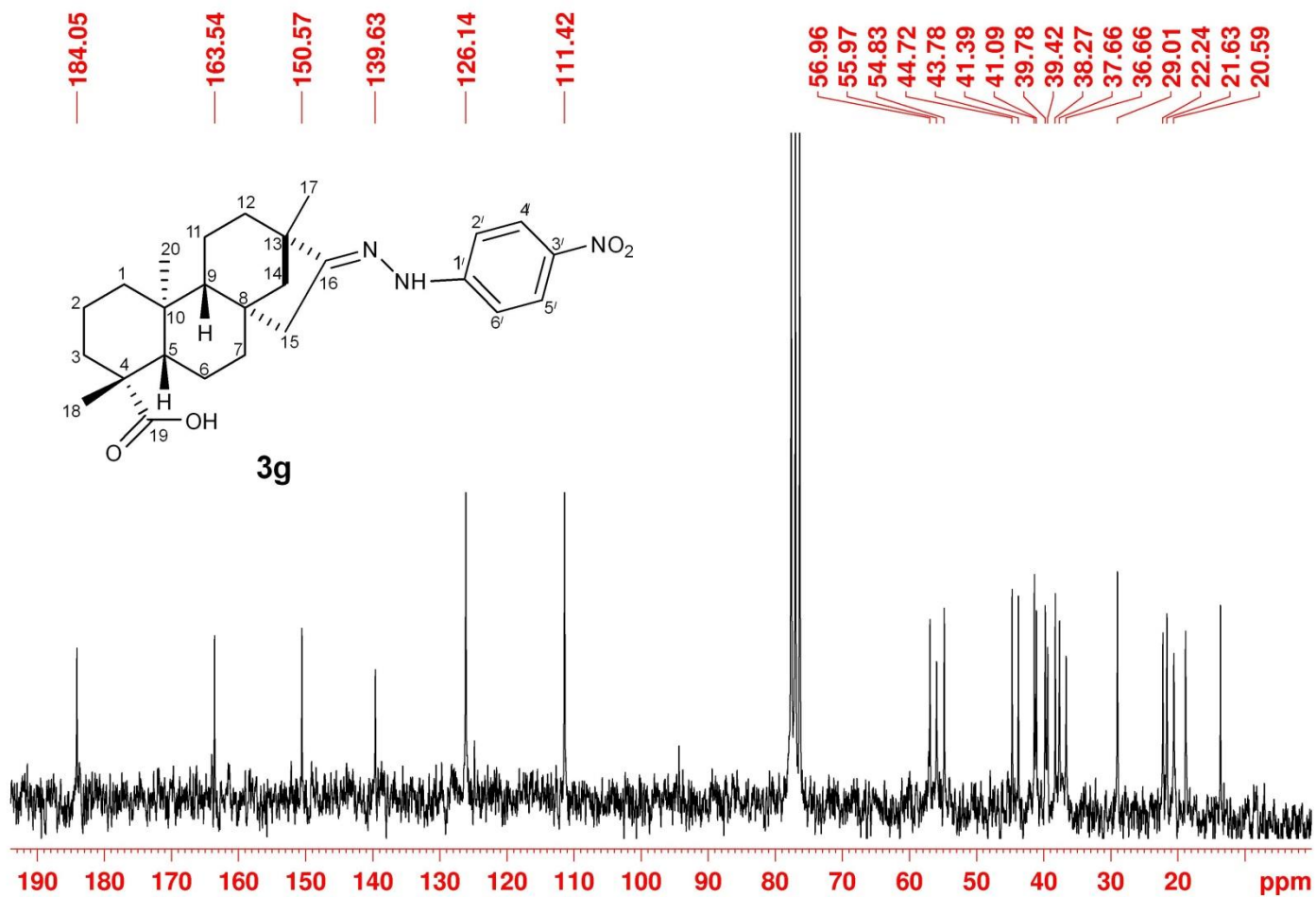


Figure 178: ^{13}C $\{^1\text{H}\}$ NMR (50 MHz, CDCl_3) spectrum of compound **3g**.

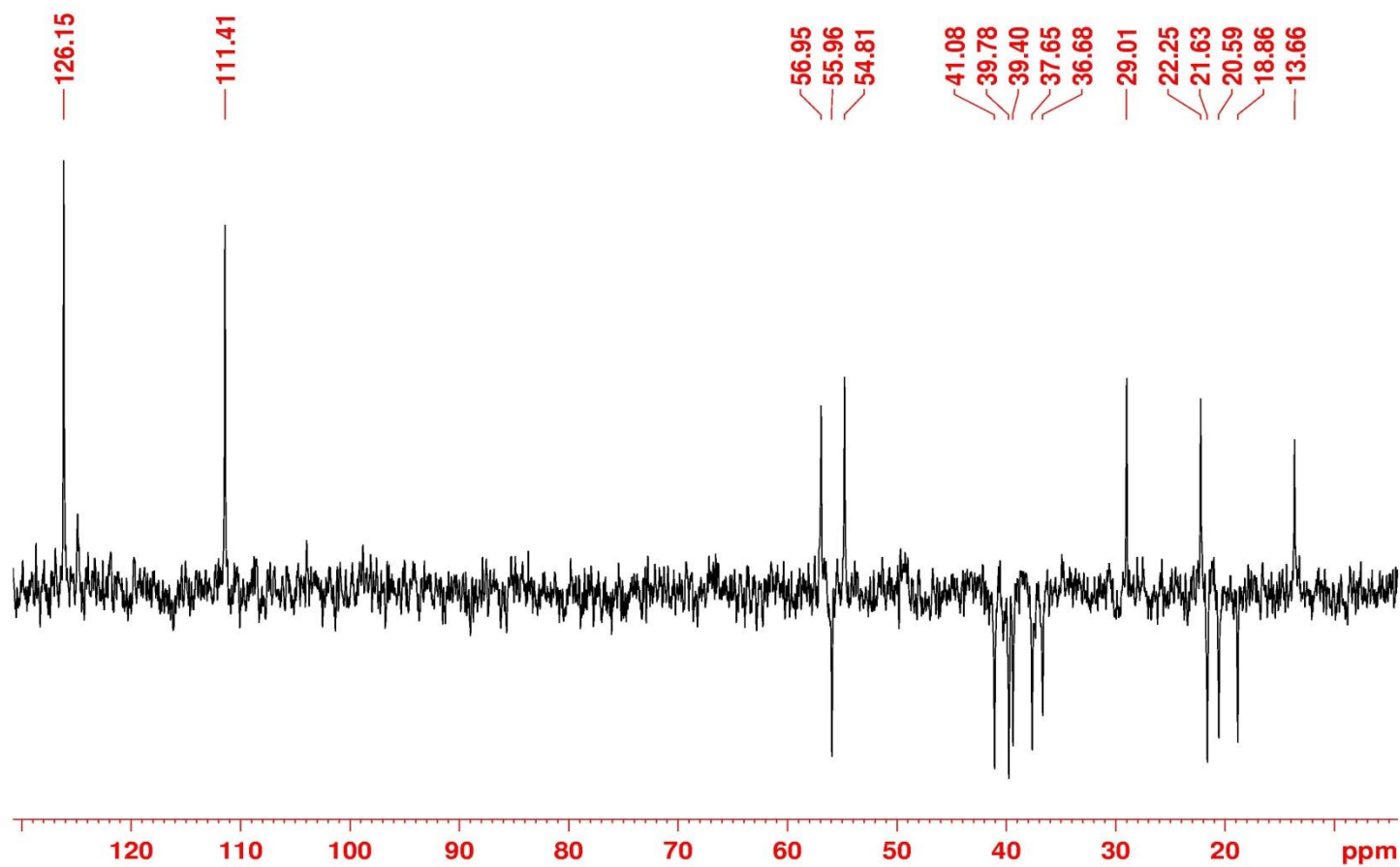


Figure 179: ^{13}C { ^1H } DEPT-NMR (50 MHz, CDCl_3) spectrum of compound **3g**.

IDB3_140724164207 #786 RT: 1.65 AV: 1 NL: 1.05E6
T: ITMS - c ESI Full ms [400.00-800.00]

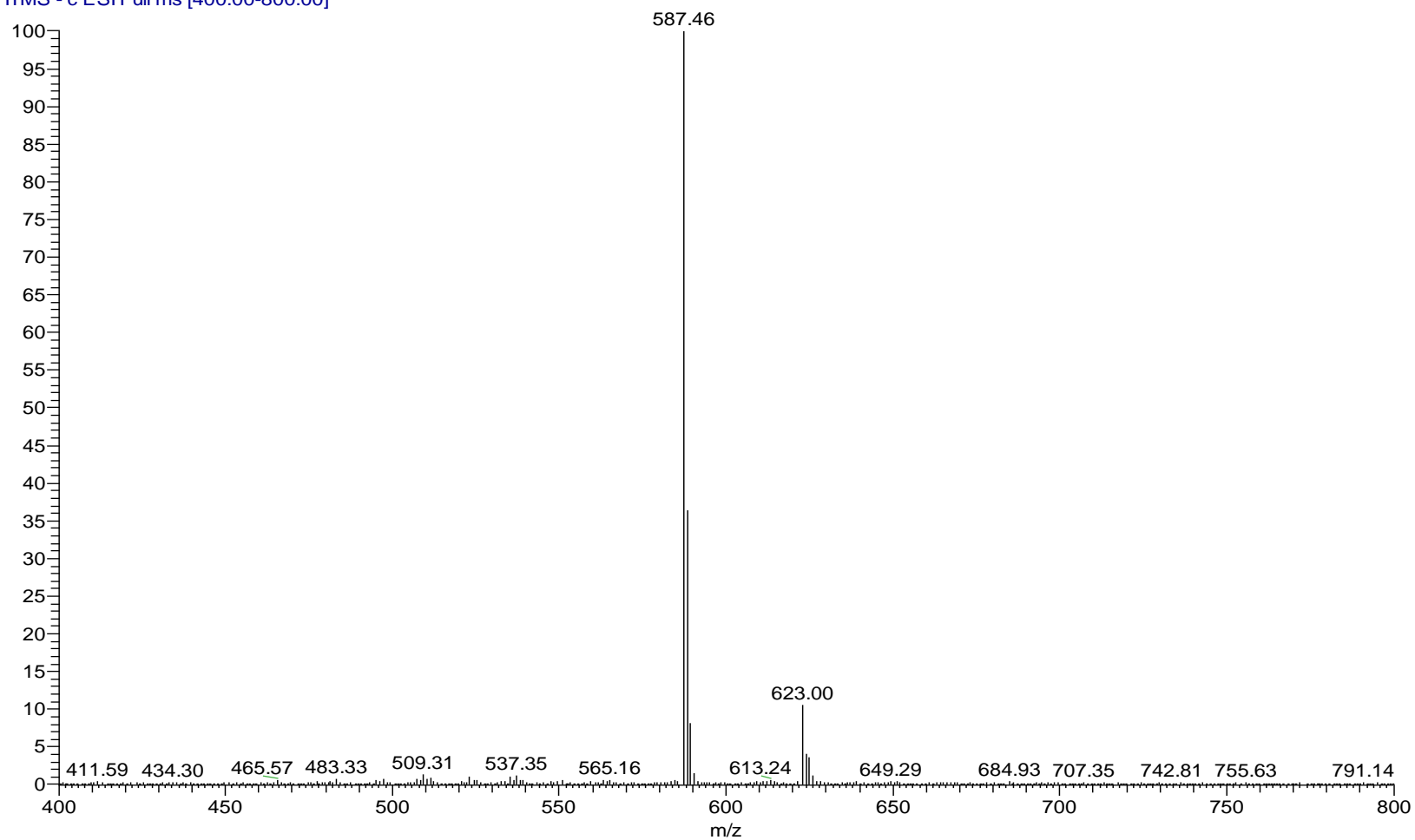


Figure 180: ESI-MS spectrum of compound 4g.

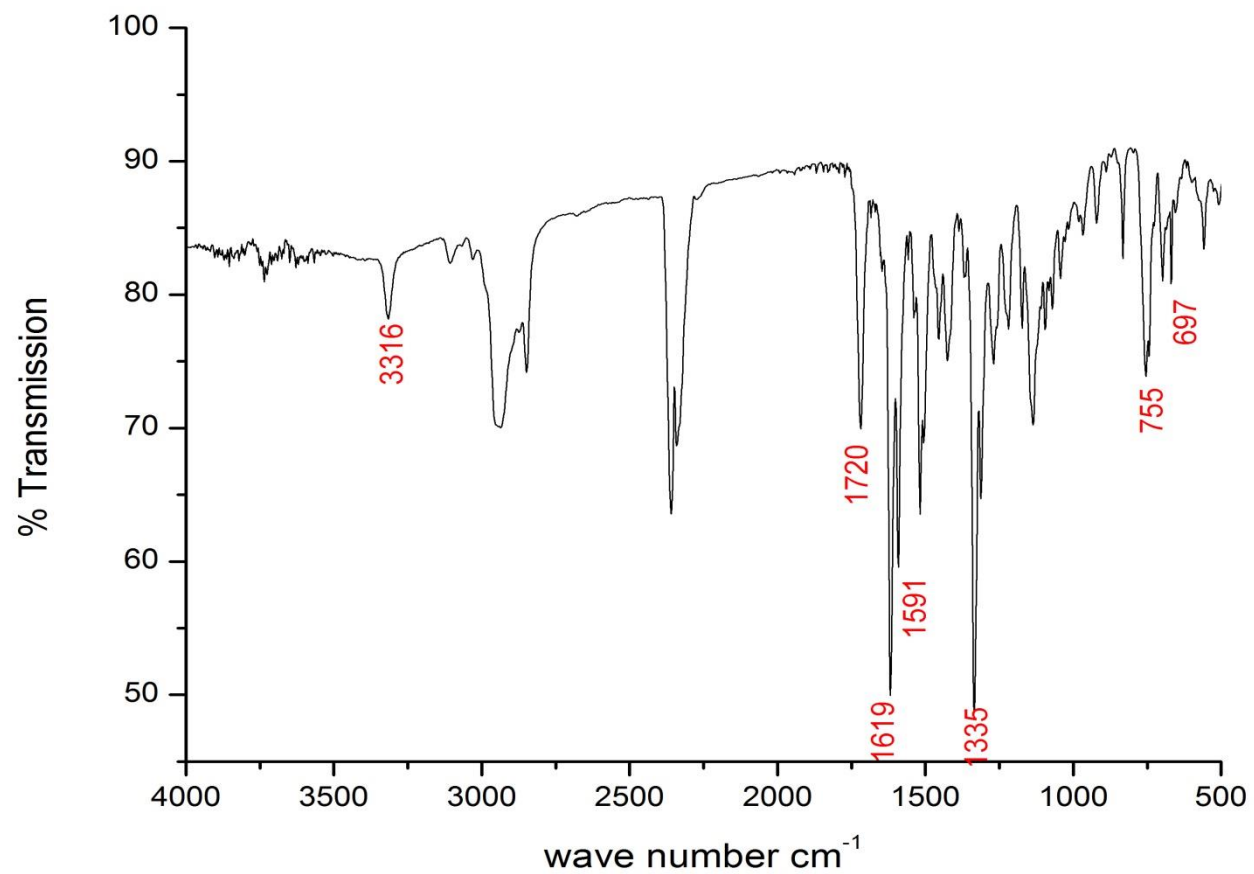


Figure 181: IR spectrum of compound **4g**.

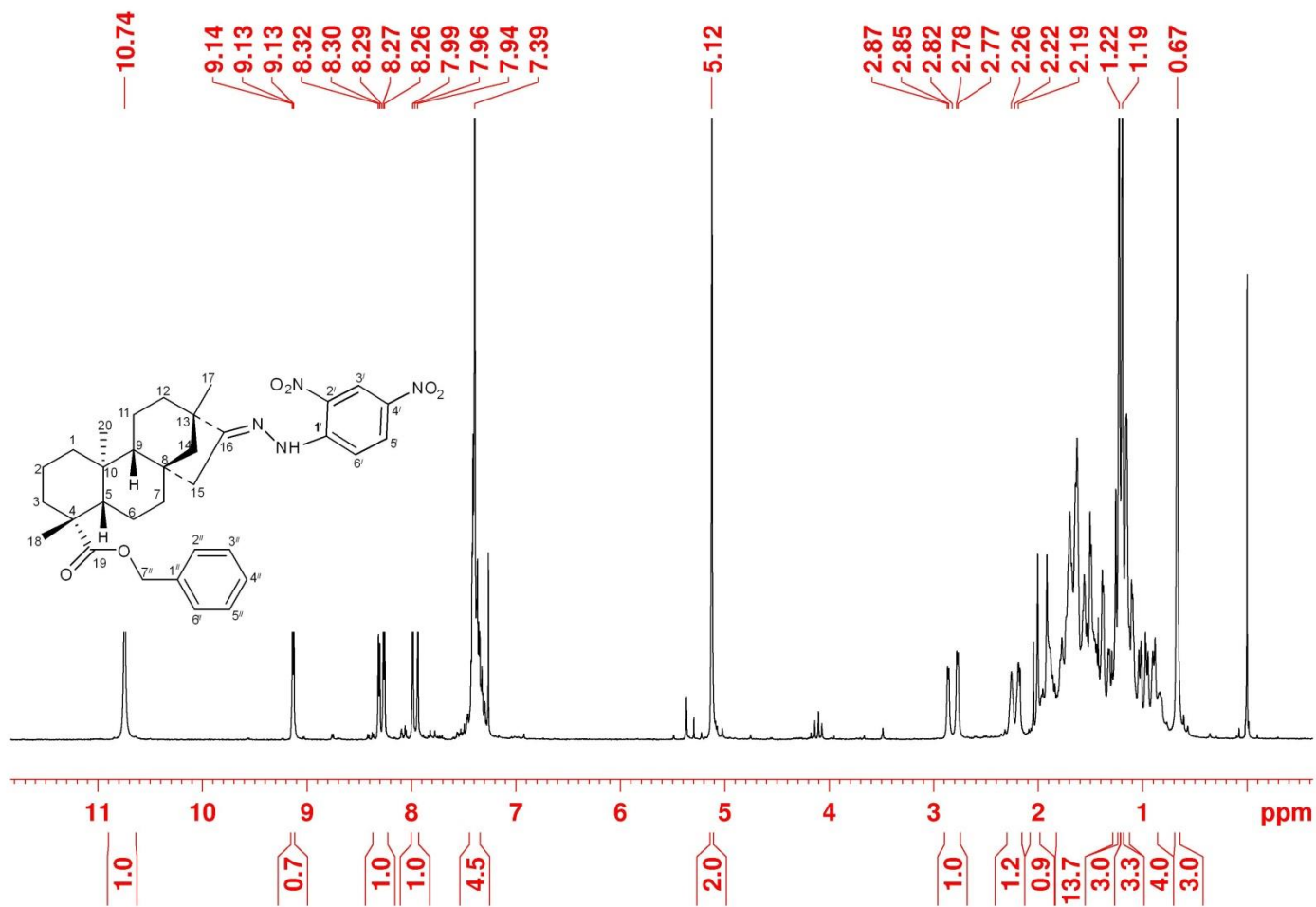


Figure 182: $^{13}\text{C} \{^1\text{H}\}$ DEPT-NMR (200 MHz, CDCl_3) spectrum of compound **4g**.

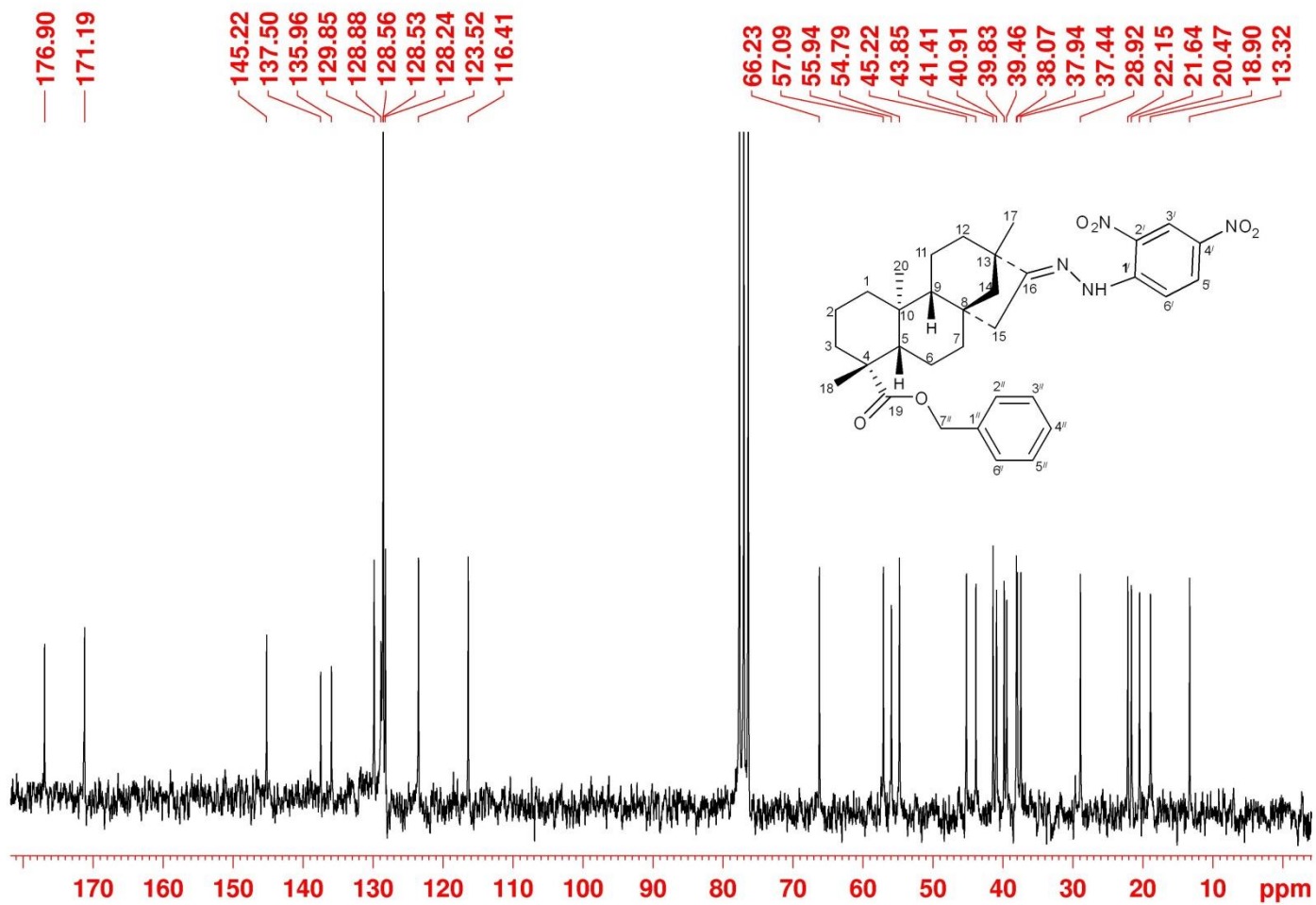


Figure 183: ^{13}C $\{^1\text{H}\}$ NMR (50 MHz, CDCl_3) spectrum of compound **4g**.

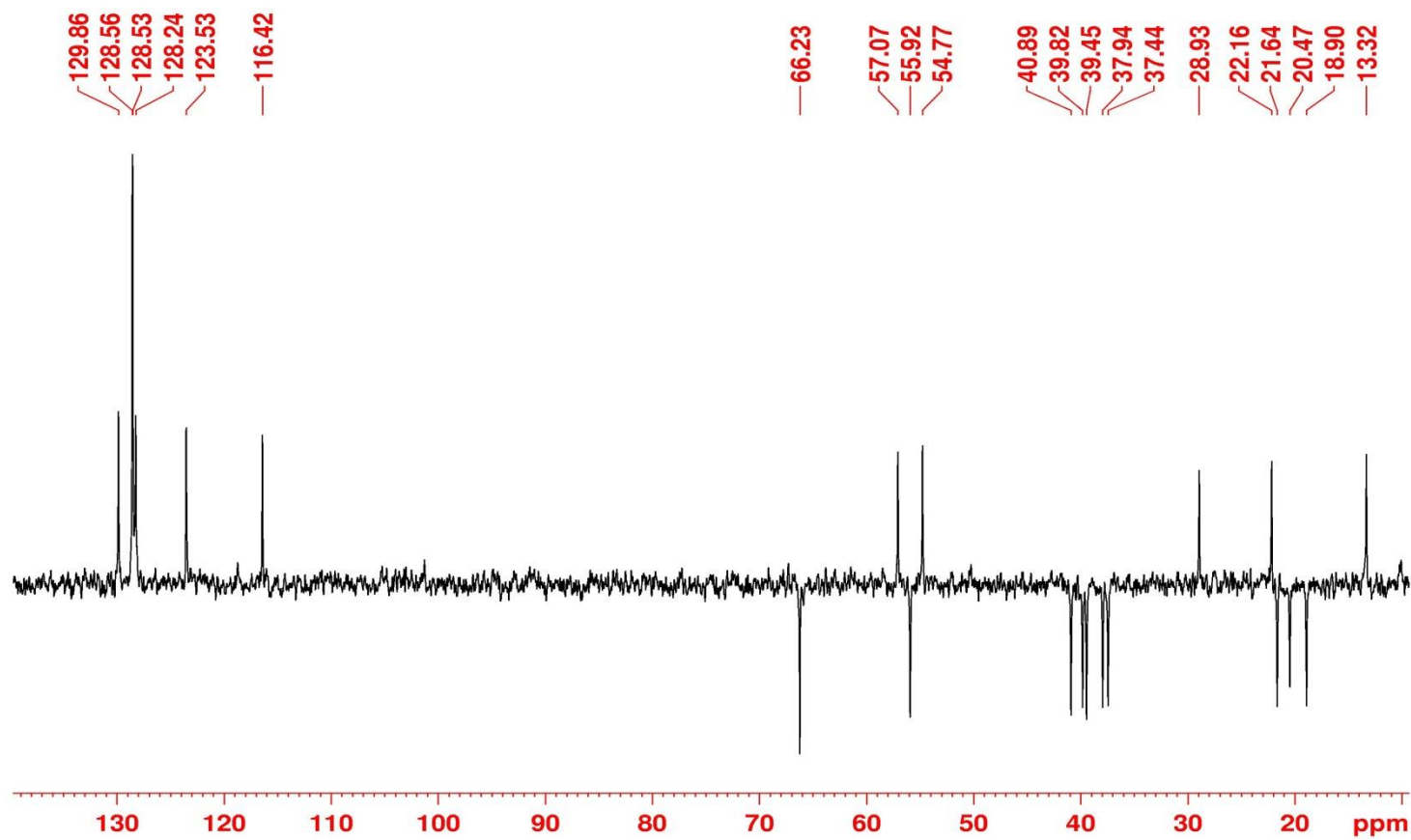


Figure 184: ^{13}C { ^1H } DEPT-NMR (50 MHz, CDCl_3) spectrum of compound **4g**.

IDB4_140724164207 #2298 RT: 5.41 AV: 1 NL: 2.48E6
T: ITMS - c ESI Full ms2 542.50@cid0.00 [145.00-650.00]

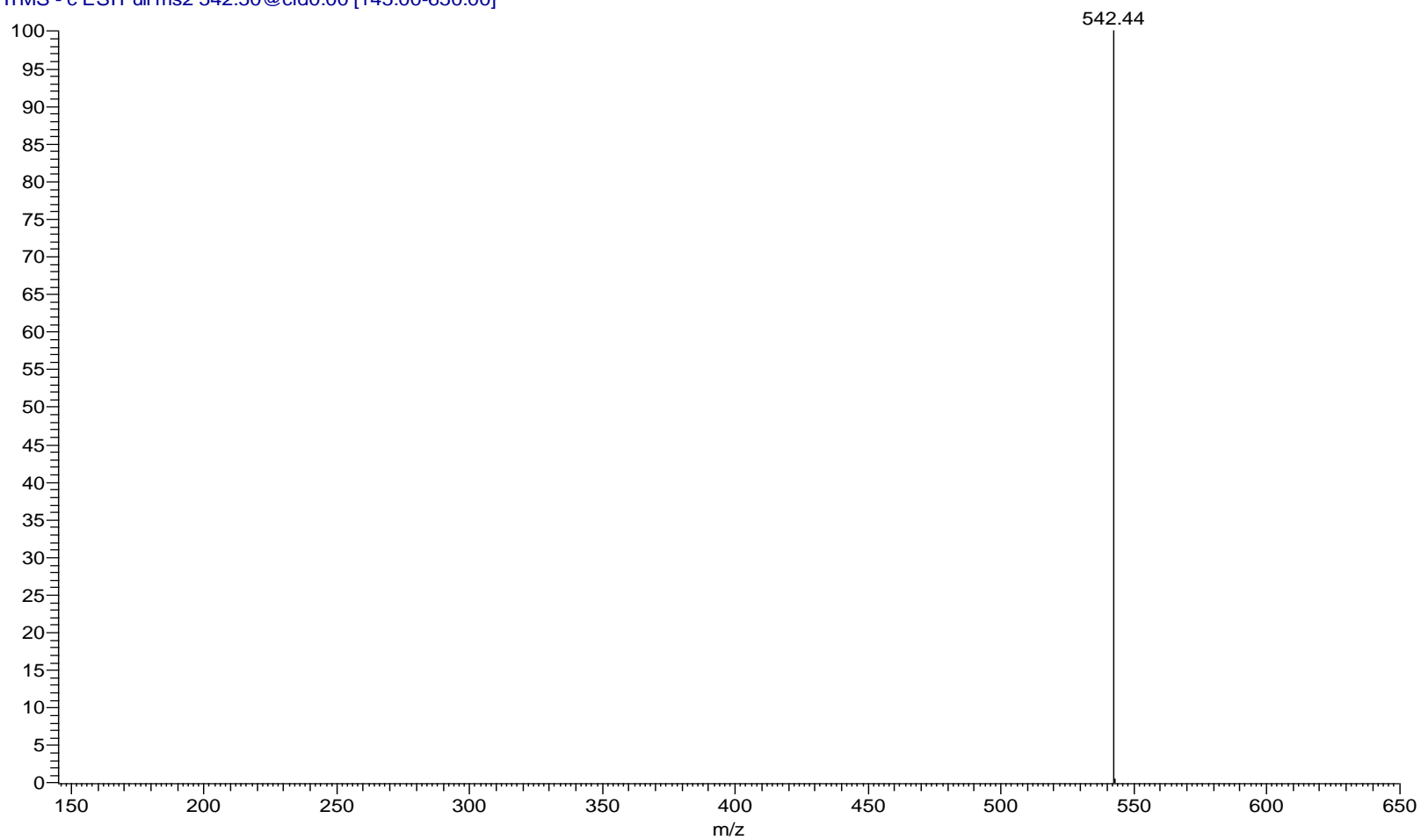
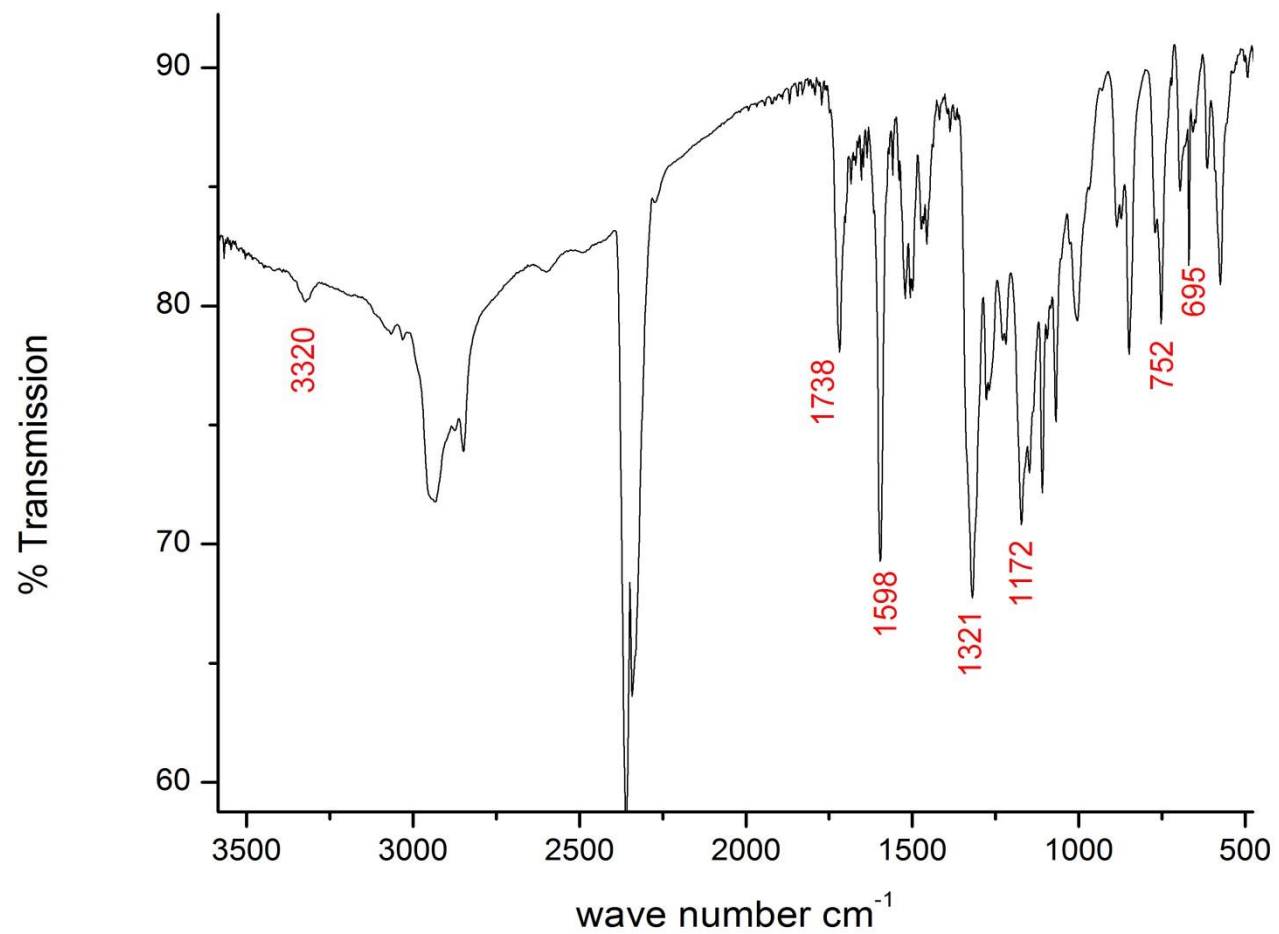


Figure 185: ESI-MS spectrum of compound **5g**.

Figure 186: IR spectrum of compound **5g**.

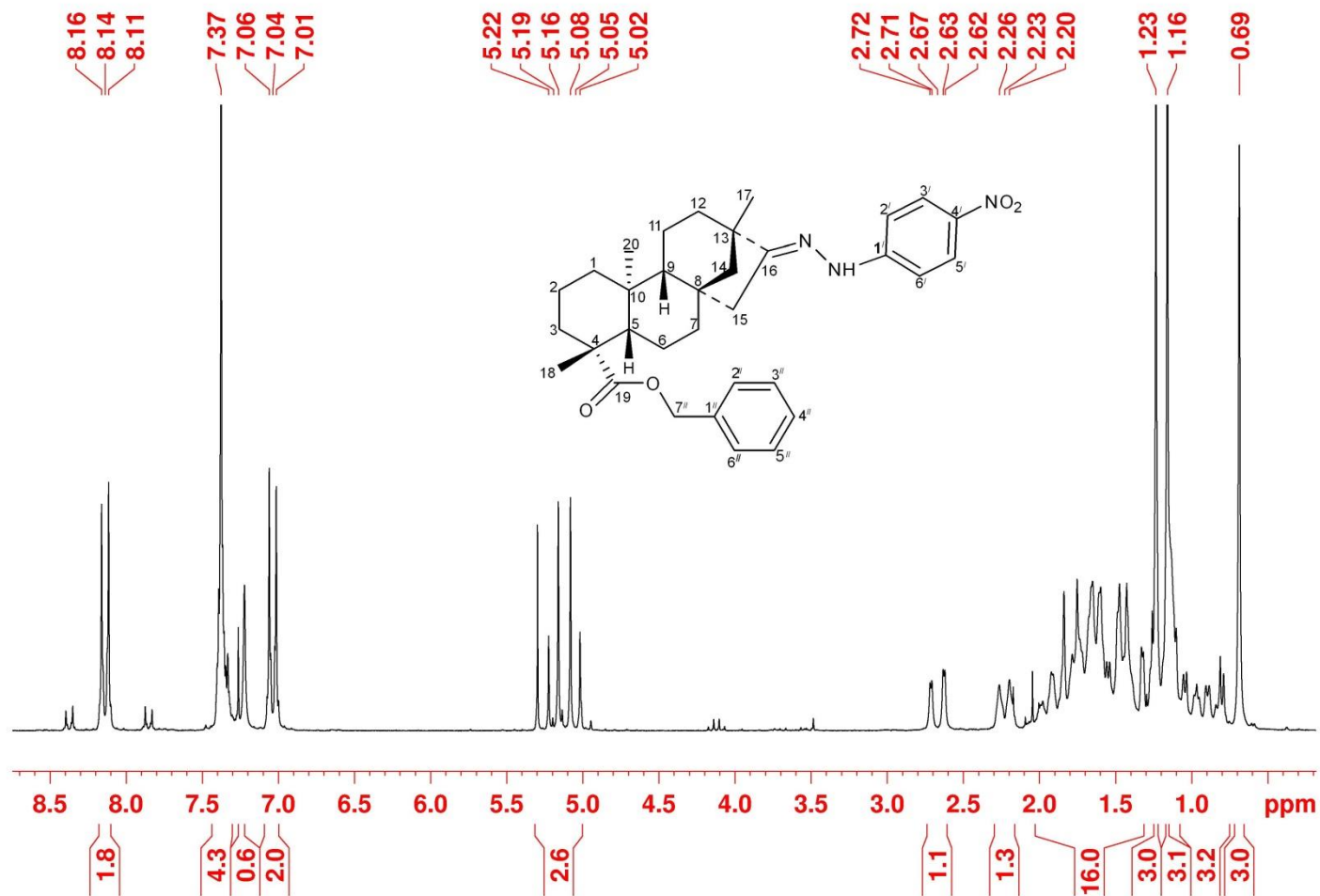


Figure 187: ¹H-NMR (200 MHz, CDCl₃) spectrum of compound **5g**.

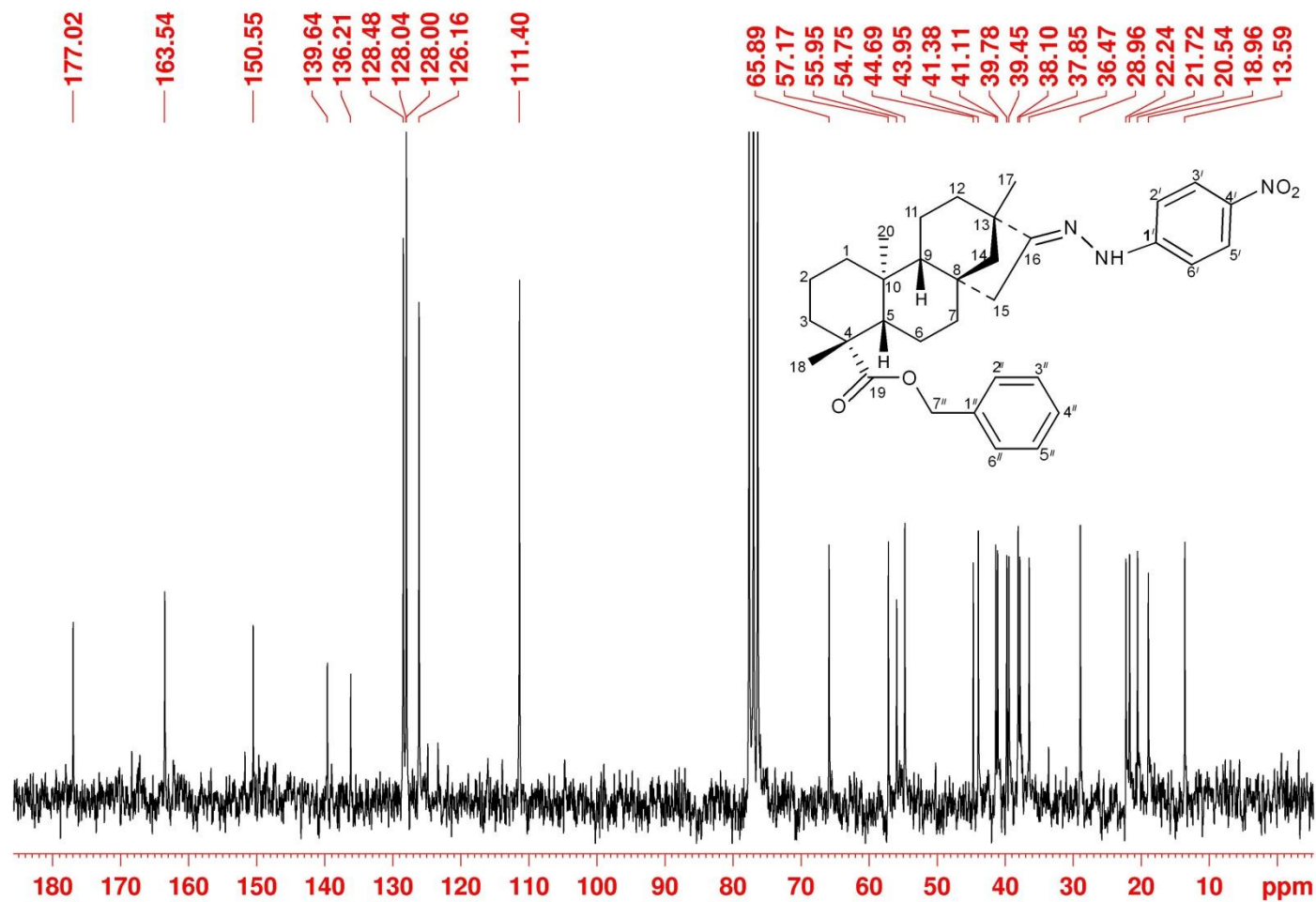


Figure 188: ^{13}C $\{^1\text{H}\}$ NMR (50 MHz, CDCl_3) spectrum of compound **5g**.

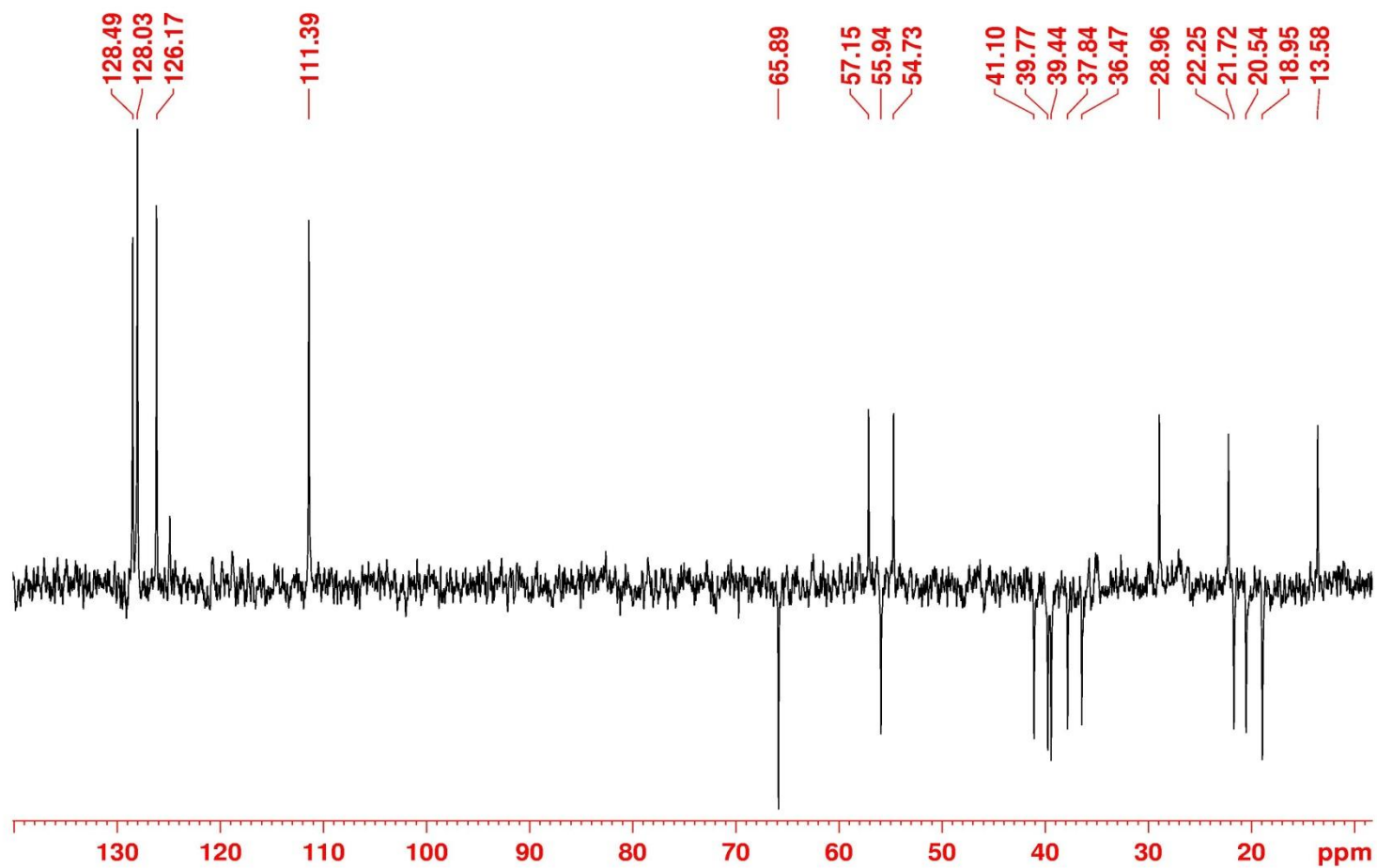


Figure 189: ^{13}C { ^1H } DEPT-NMR (50 MHz, CDCl_3) spectrum of compound **5g**.

191-ASADHD7_131111150209 #53 RT: 0.12 AV: 1 NL: 1.70E5
T: ITMS - c ESI Full ms [90.00-1000.00]

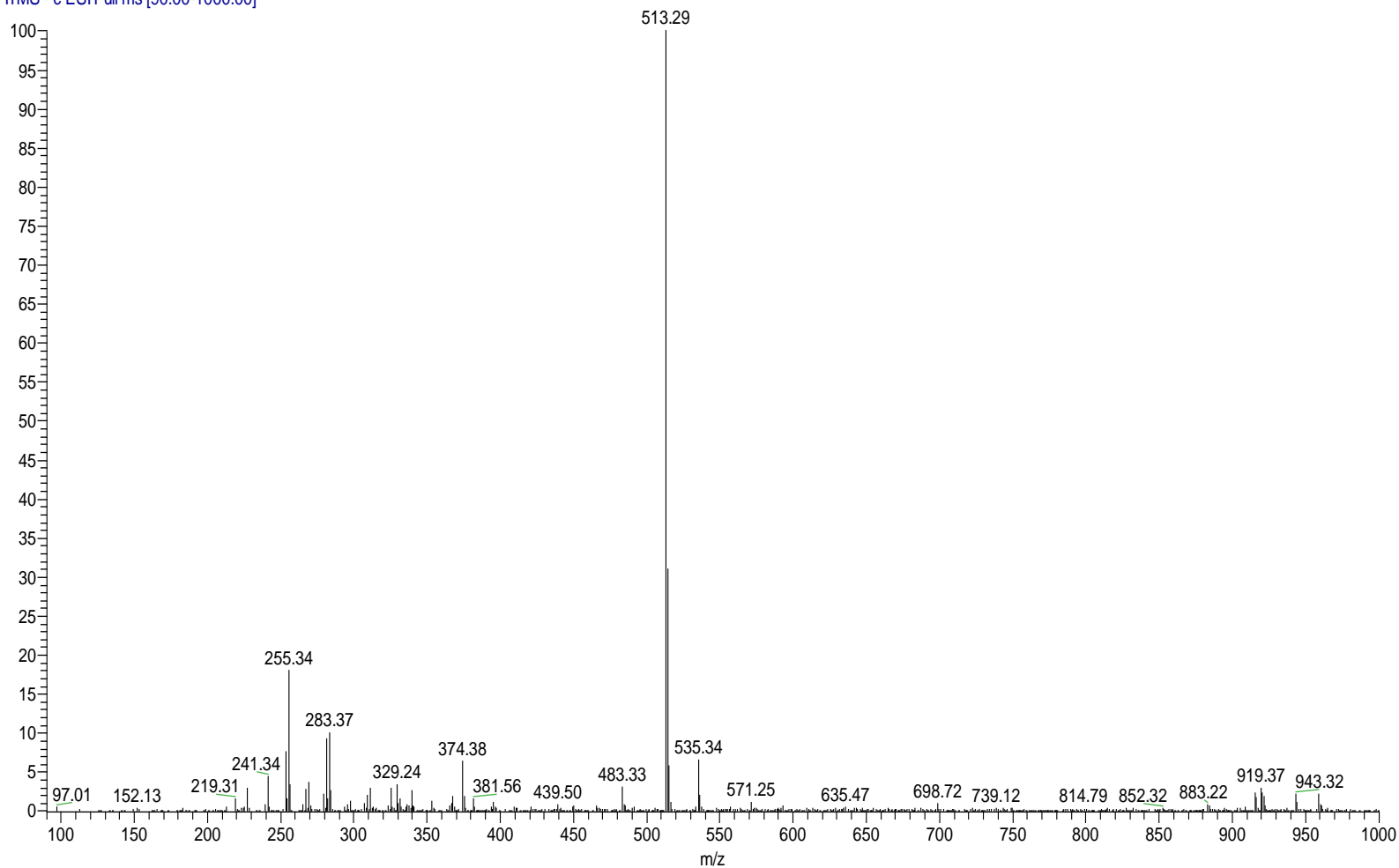


Figure 190: ESI-MS spectrum of compound **5m**.

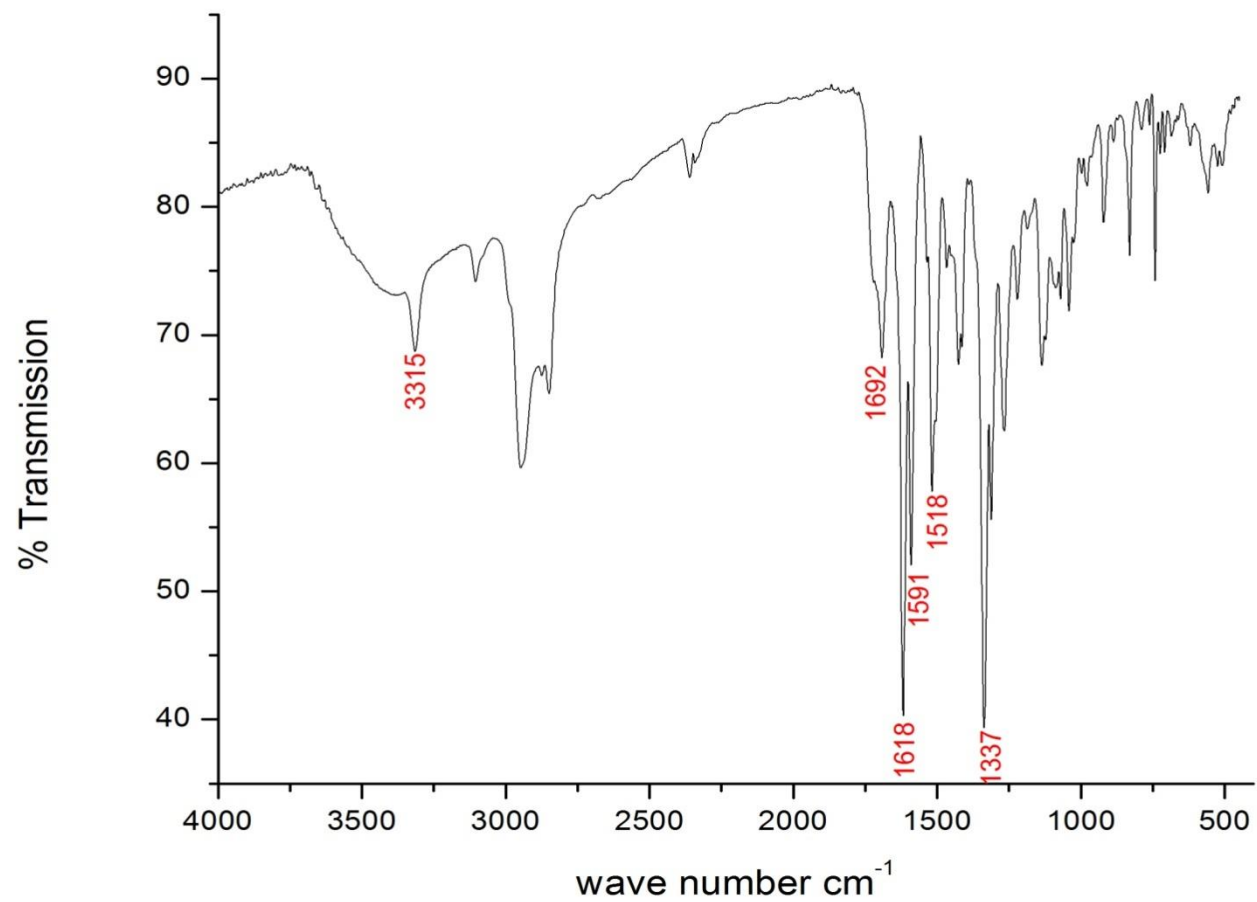


Figure 191: IR spectrum of compound **5m**.

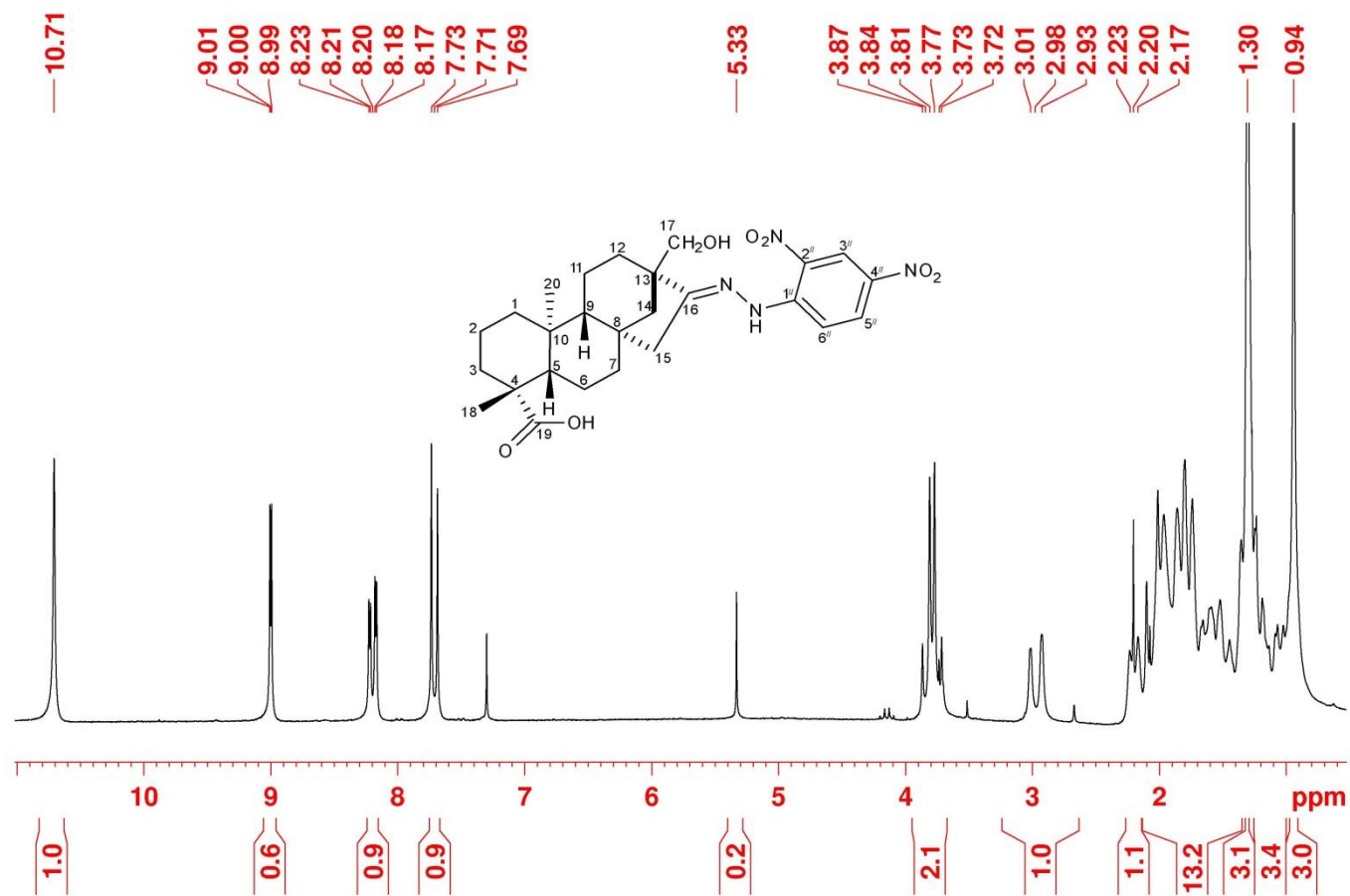


Figure 192: ¹H-NMR (200 MHz, CDCl₃) spectrum of compound **5m**.

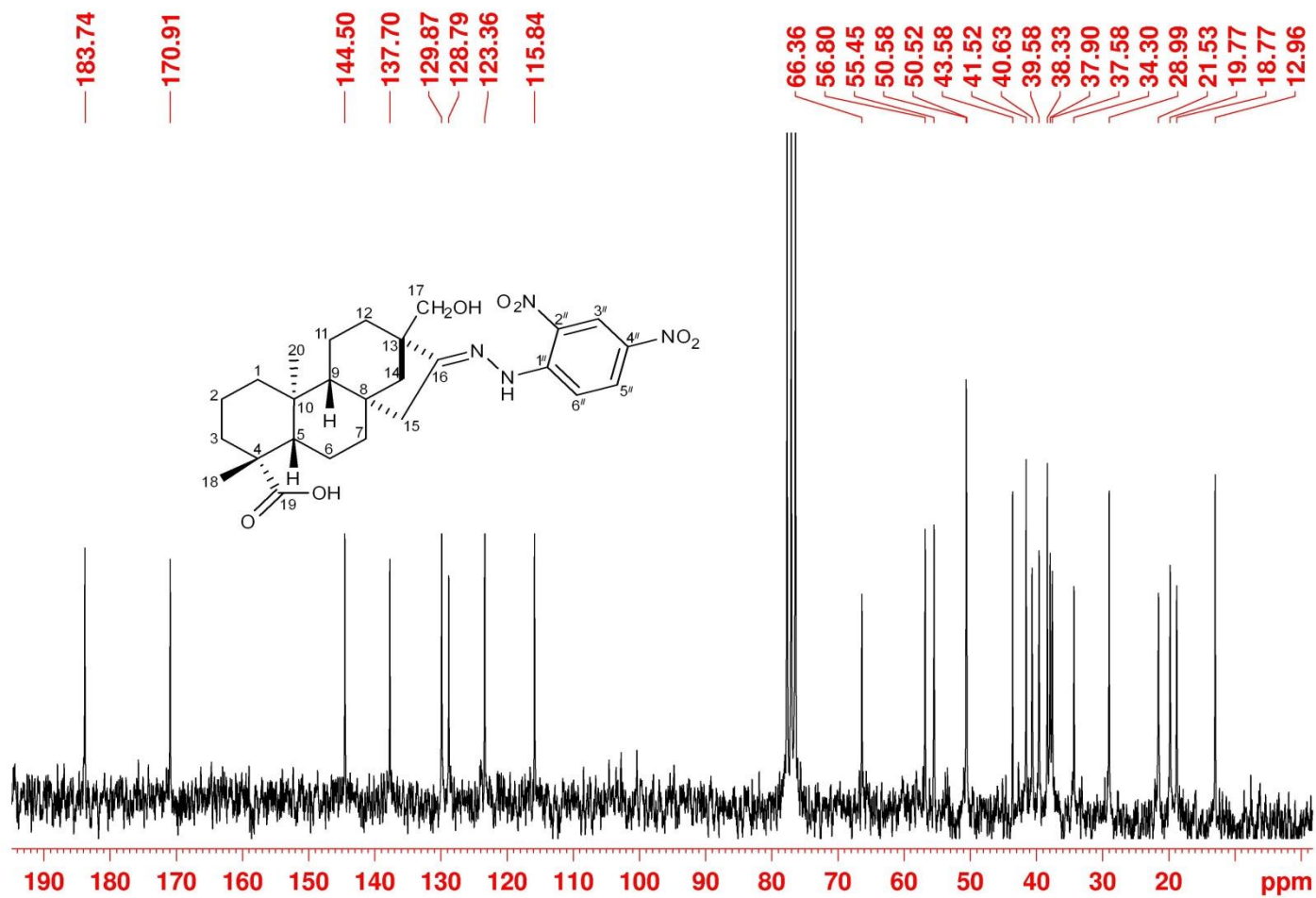


Figure 193: ^{13}C $\{^1\text{H}\}$ NMR (50 MHz, CDCl_3) spectrum of compound **5m**.

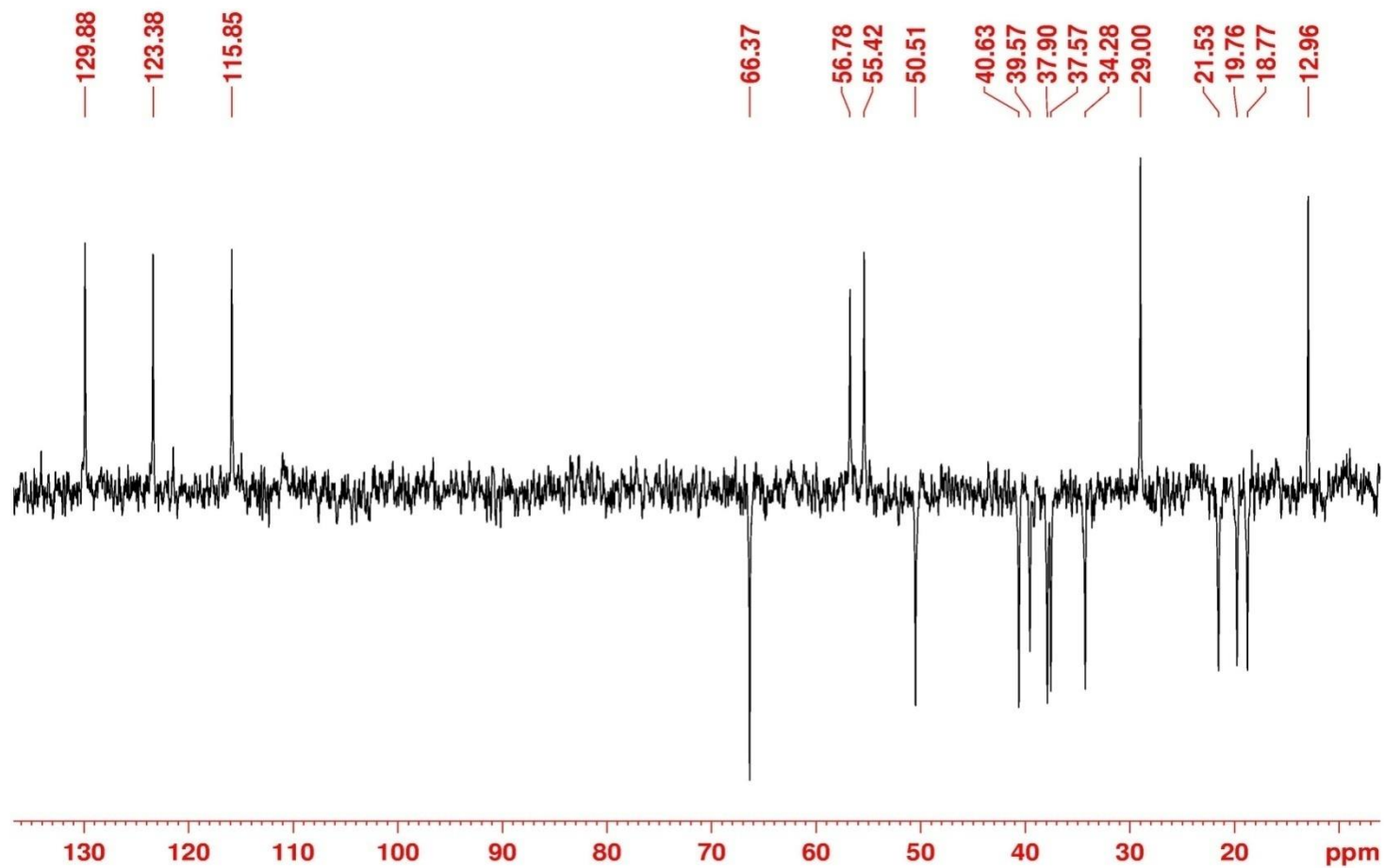


Figure 194: ^{13}C { ^1H } DEPT-NMR (50 MHz, CDCl_3) spectrum of compound **5m**.

266-ASADHDB5_140821145748 #1460 RT: 3.02 AV: 1 NL: 8.87E5
T: ITMS - c ESI Full ms2 603.40@cid20.00 [165.00-6:

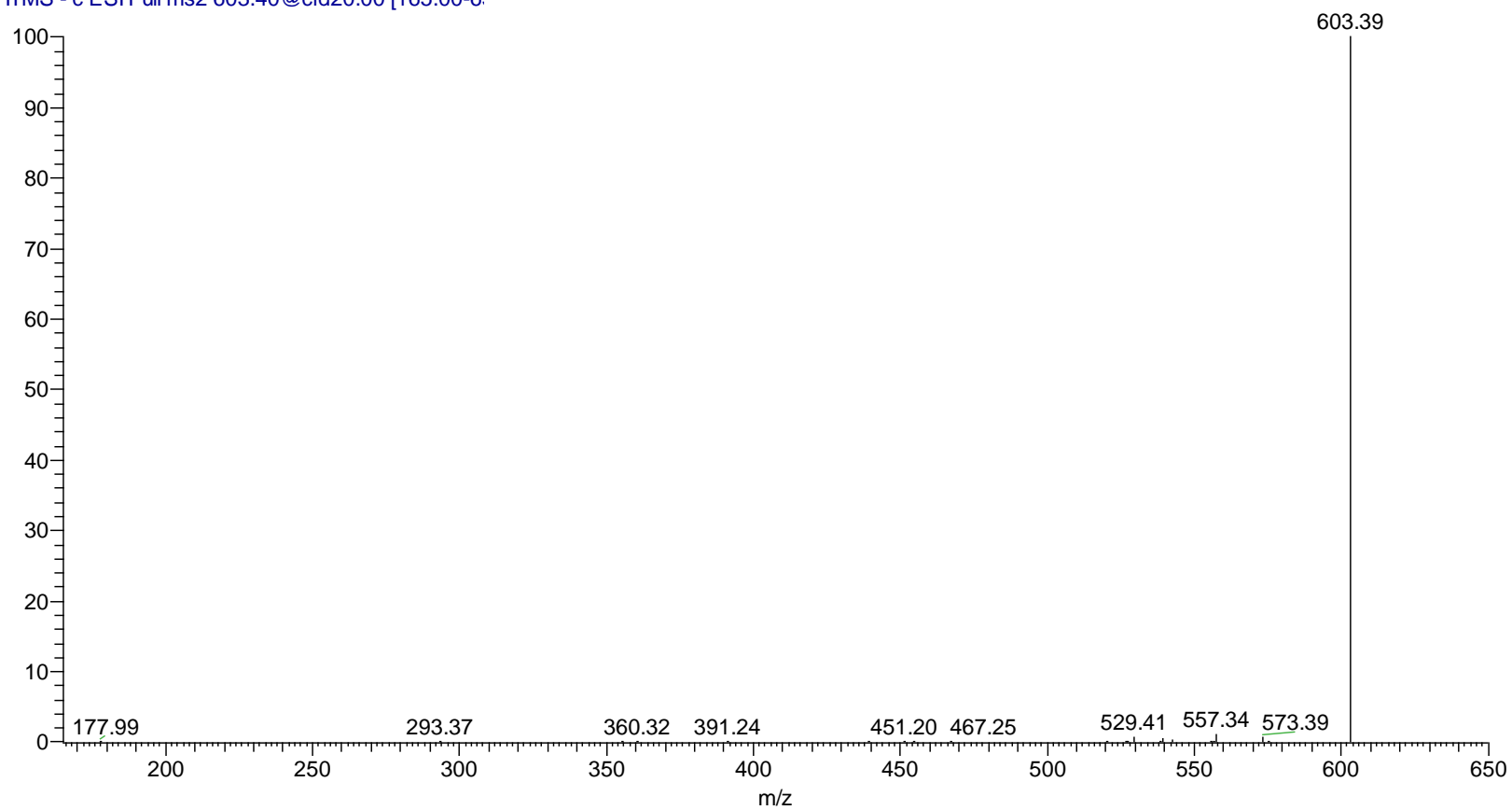


Figure 195: ESI-MS spectrum of compound **7m**.

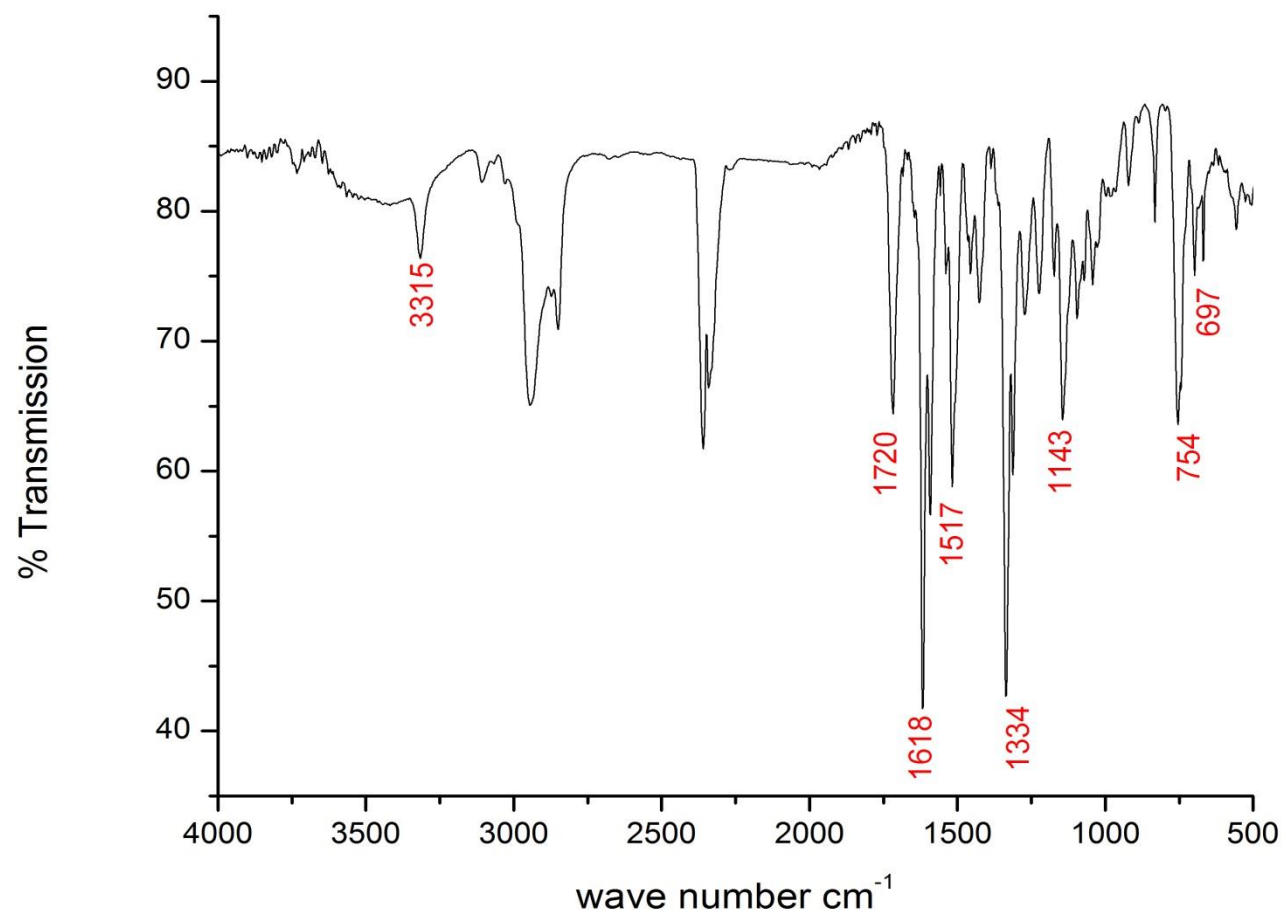


Figure 196: IR spectrum of compound **7m**.

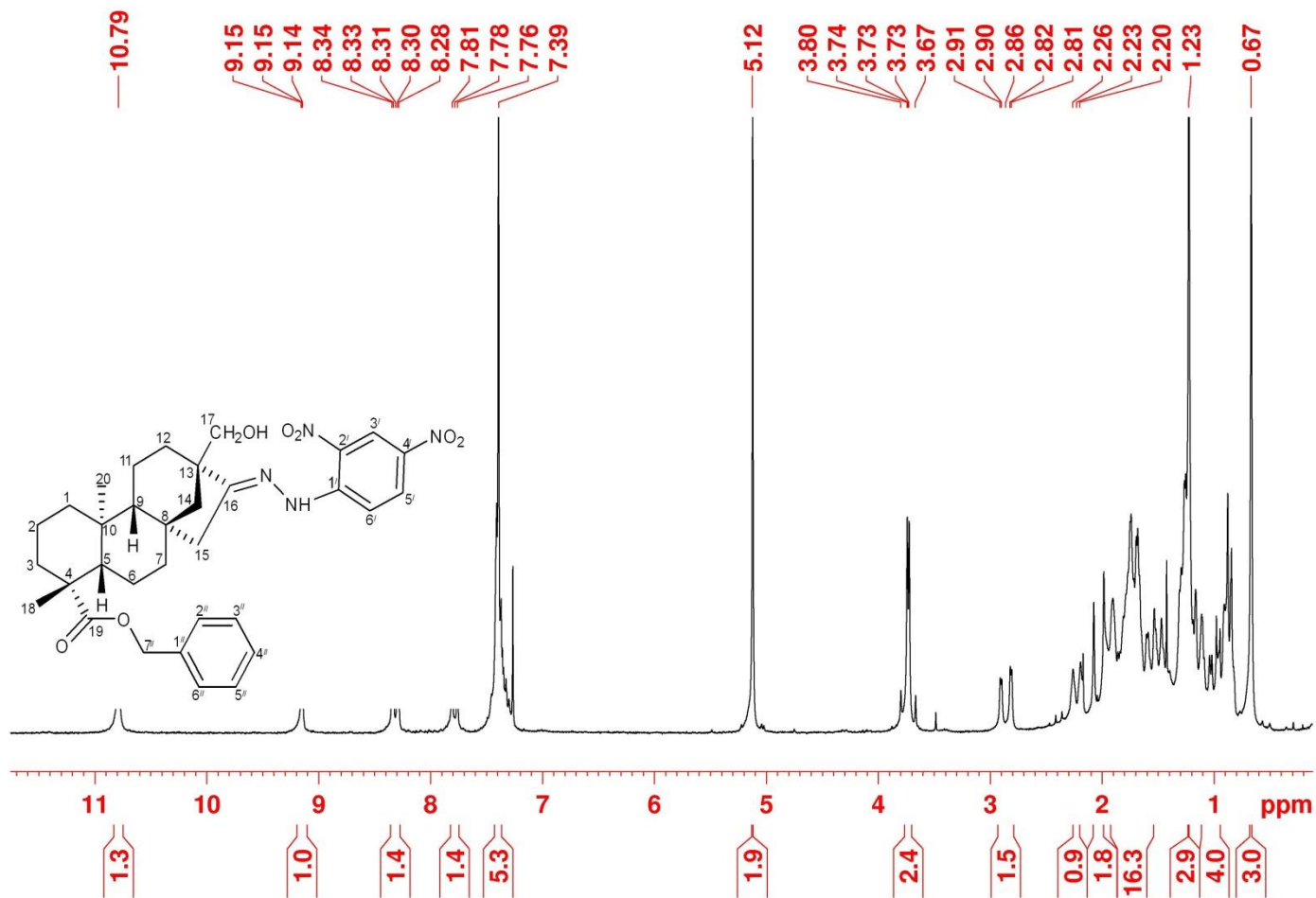


Figure 197: $^1\text{H-NMR}$ (200 MHz, CDCl_3) spectrum of compound **7m**.

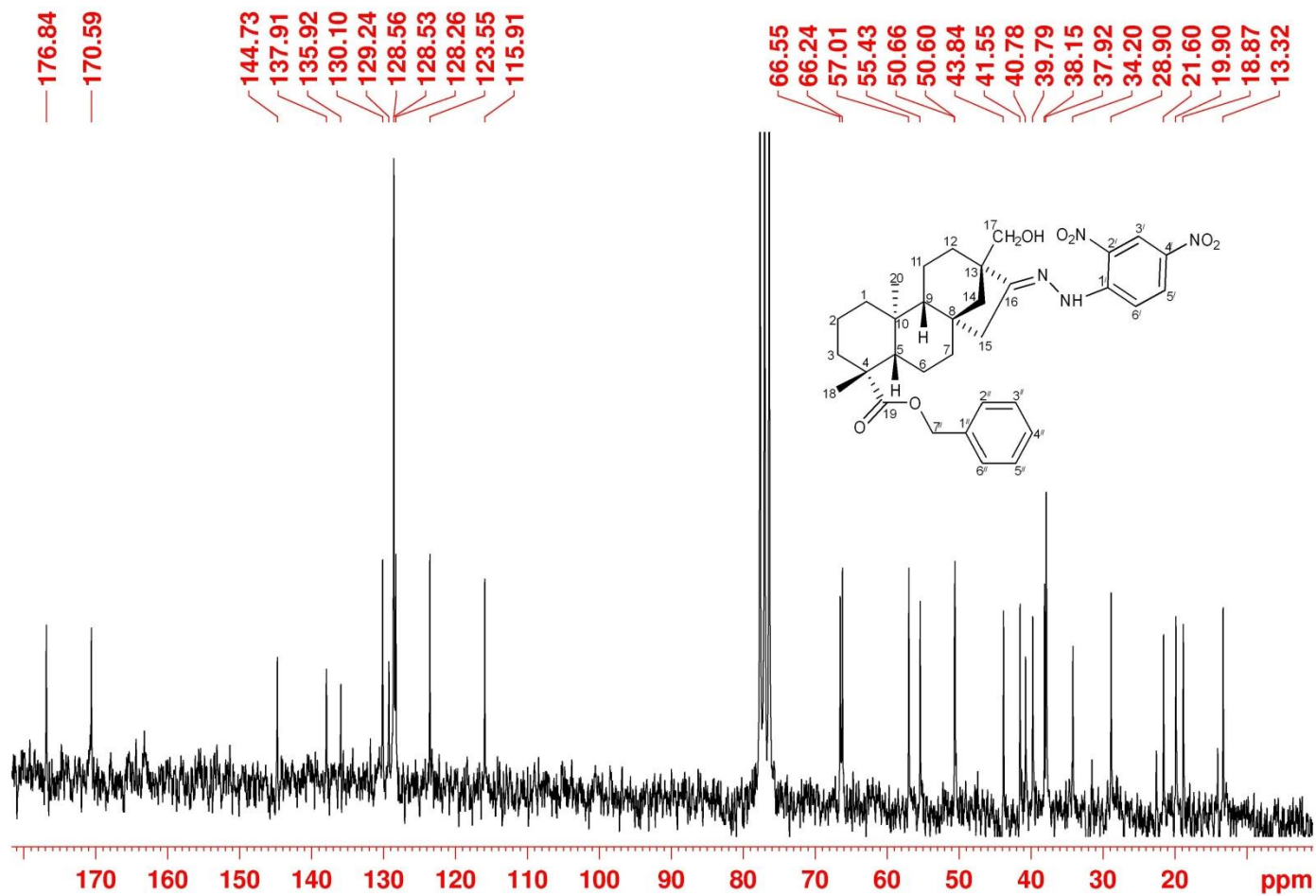


Figure 198: ^{13}C $\{^1\text{H}\}$ NMR (50 MHz, CDCl_3) spectrum of compound **7m**.

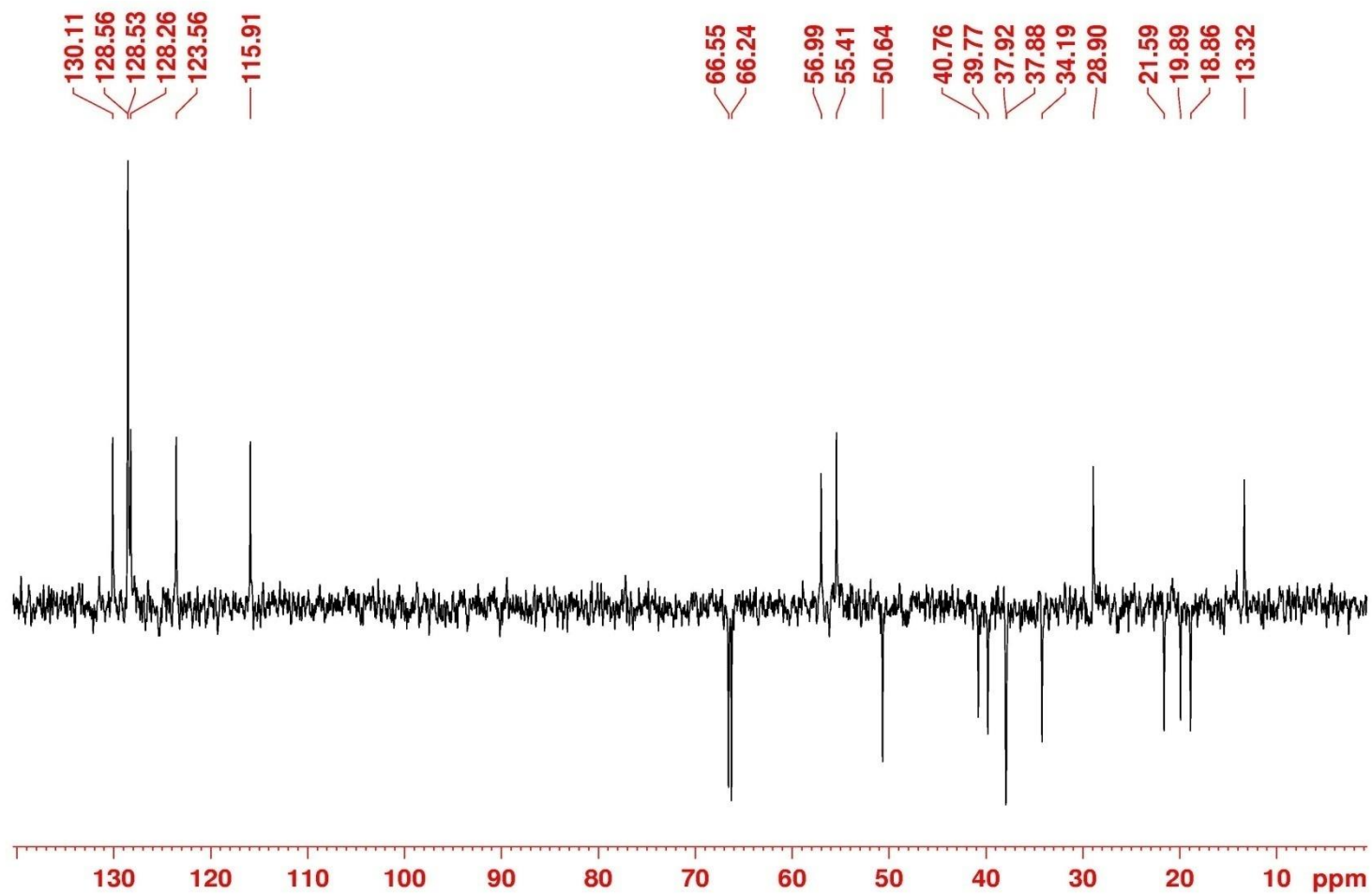


Figure 199: ^{13}C { ^1H } DEPT-NMR (50 MHz, CDCl_3) spectrum of compound **7m**.

220-ASADHD8_131205154739 #1628 RT: 4.33 AV: 1 NL: 8.04E4
T: ITMS - c ESI Full ms2 468.00@cid23.00 [125.00-600.00]

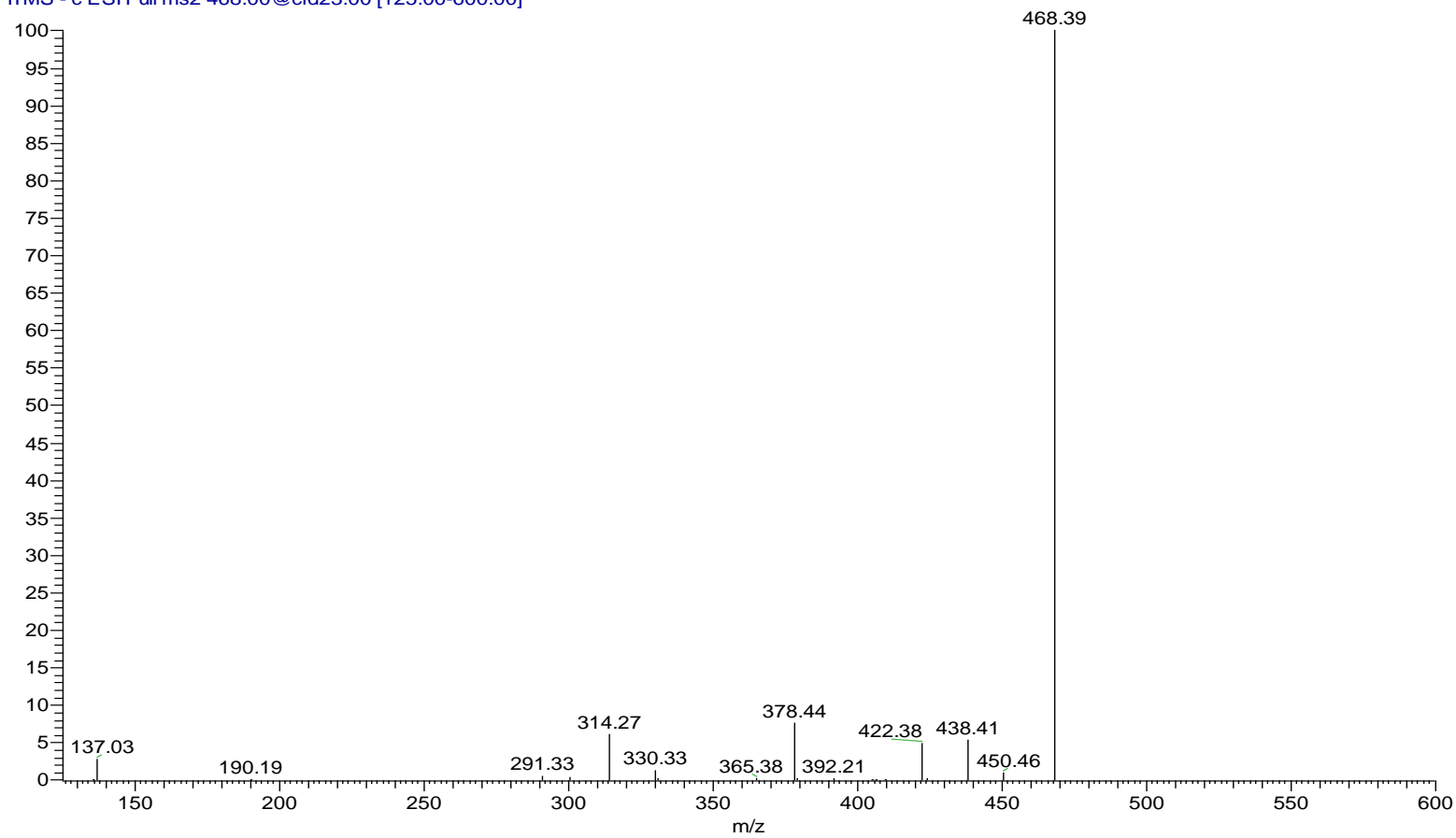


Figure 200: ESI-MS spectrum of compound **6m**.

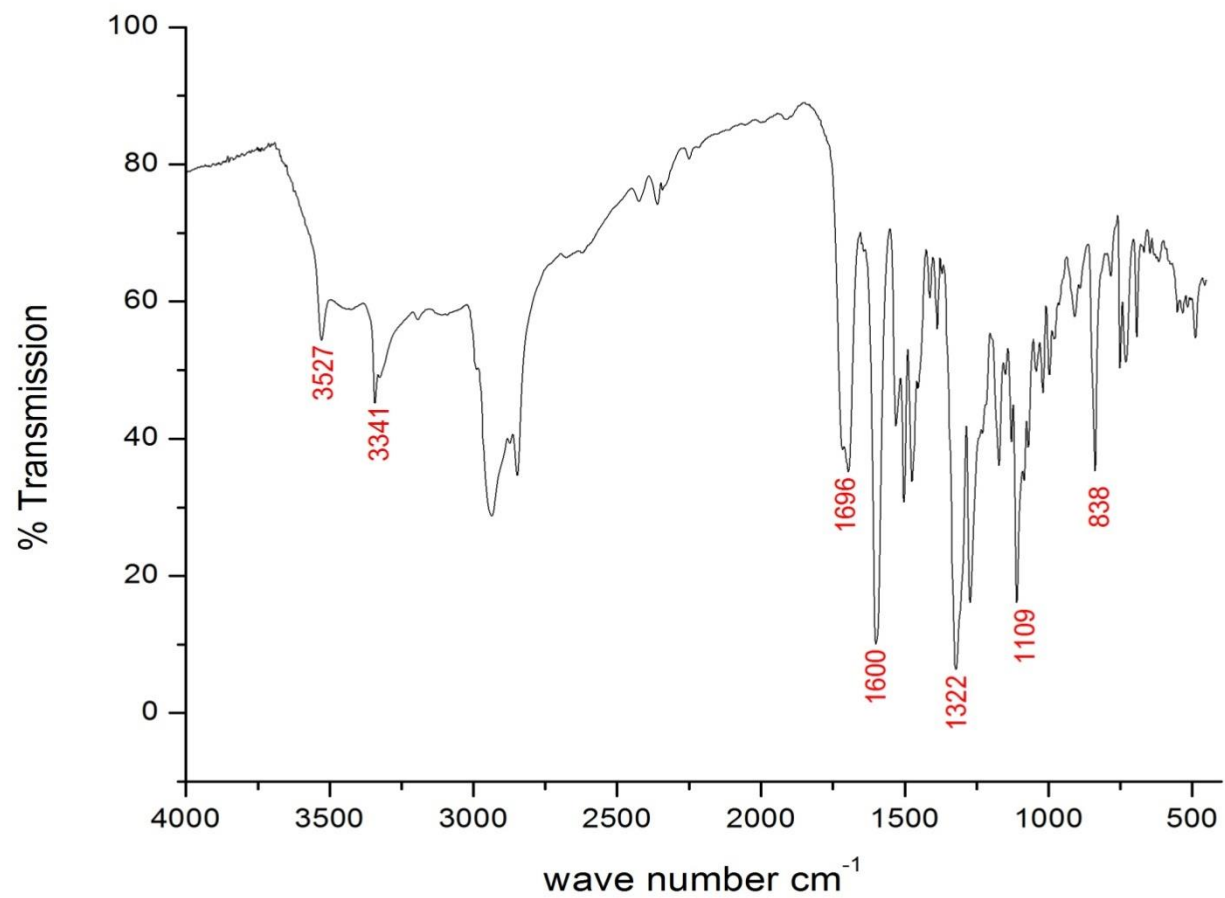


Figure 201: IR spectrum of compound **6m**.

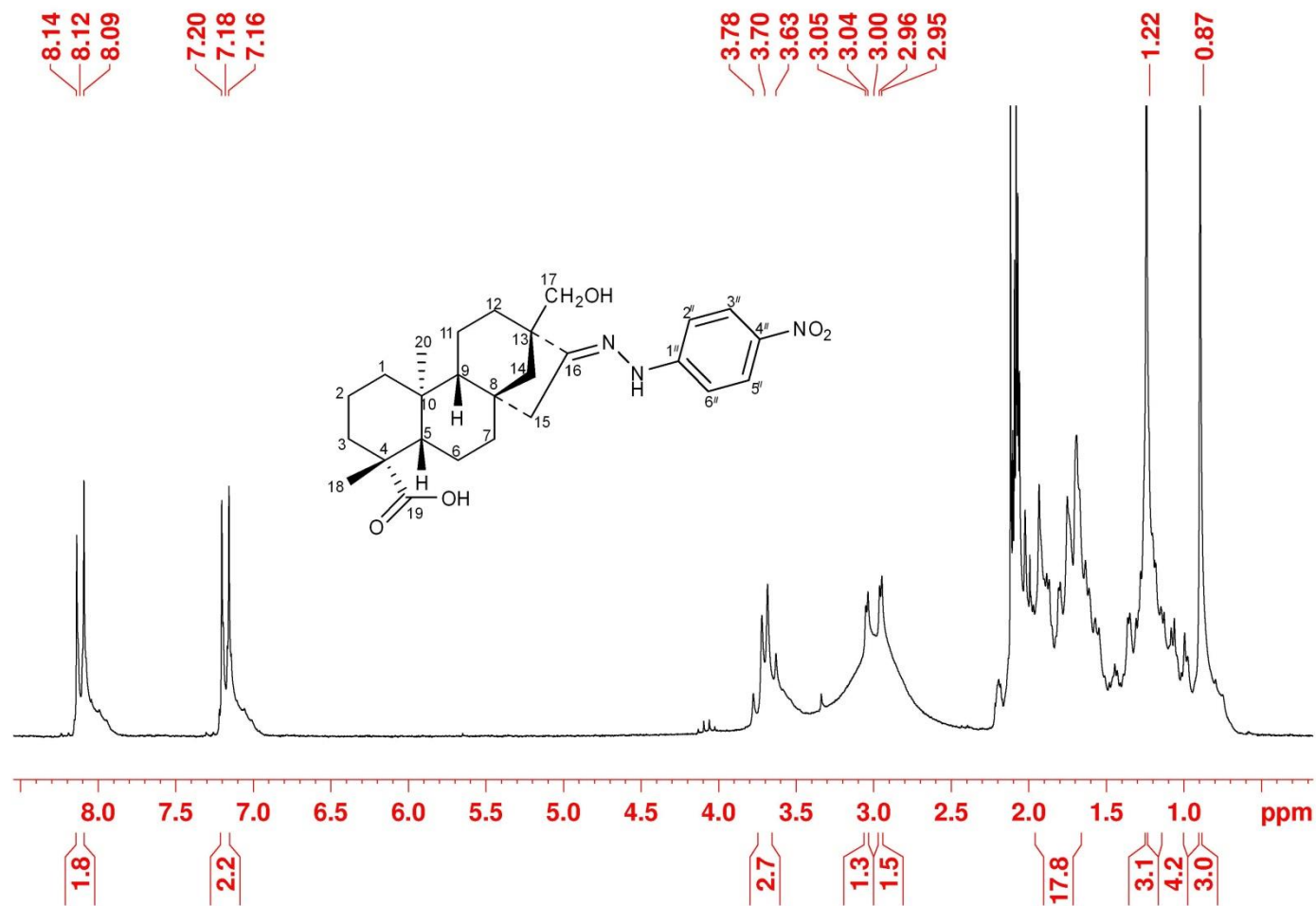


Figure 202: ¹H-NMR (200 MHz, Acetone-d₆) spectrum of compound **6m**.

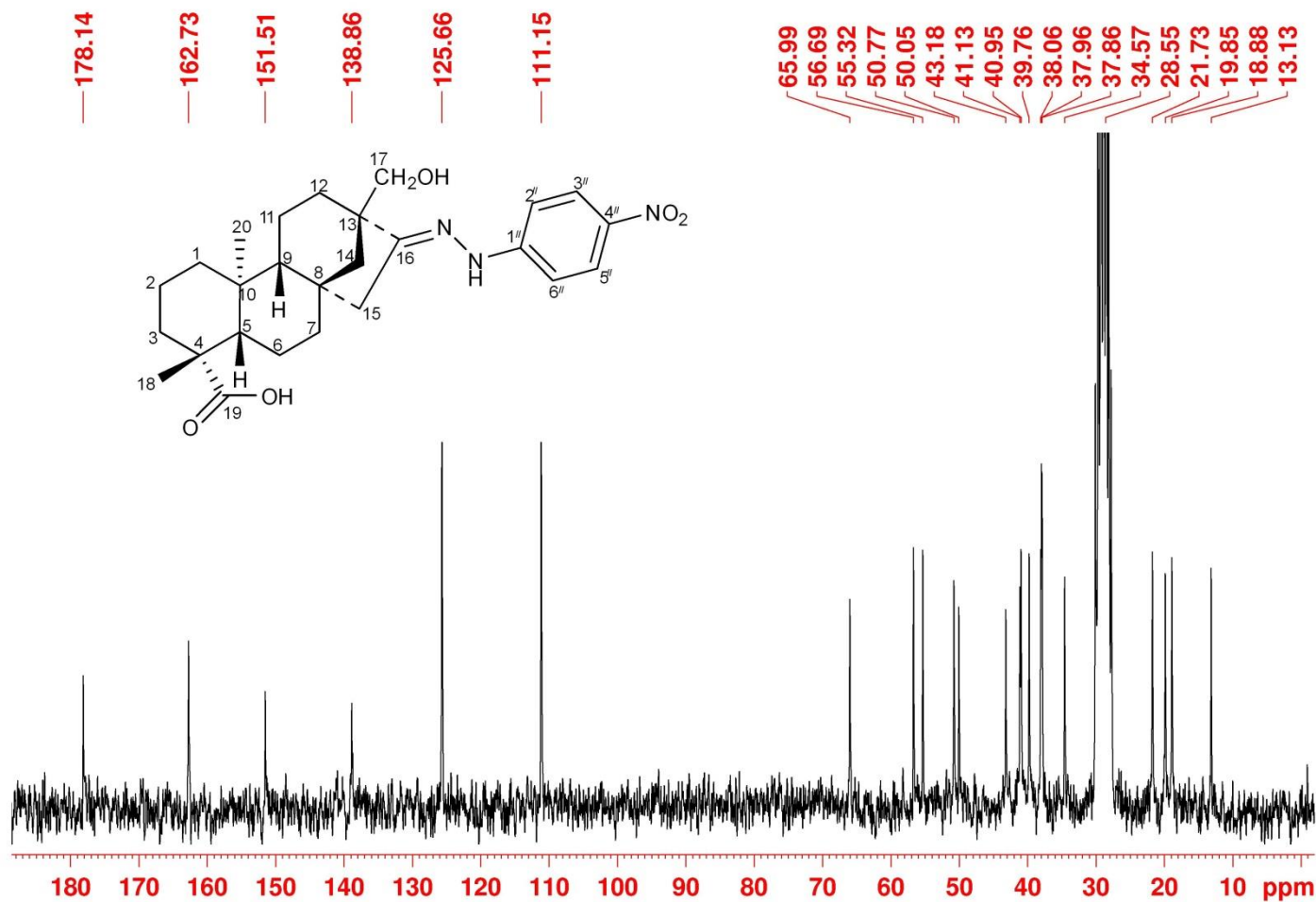


Figure 203: ^{13}C $\{^1\text{H}\}$ NMR (50 MHz, Acetone- d_6) spectrum of compound **6m**.

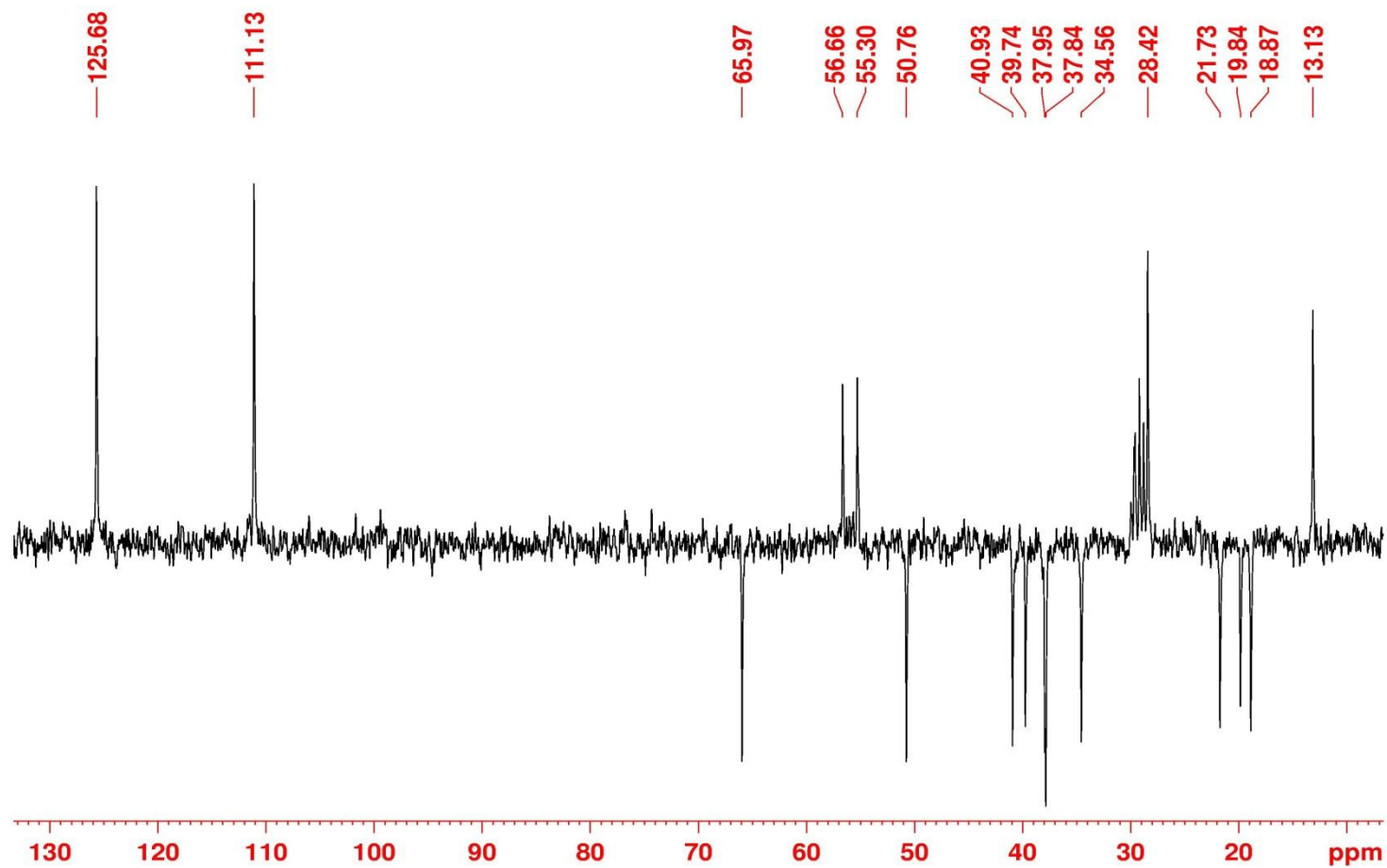


Figure 204: ^{13}C { ^1H } DEPT-NMR (50 MHz, Acetone- d_6) spectrum of compound **6m**.

323-ASADHD8B_141120114247 #399 RT: 0.94 AV: 1 NL: 1.53E6
T: ITMS - c ESI Full ms [500.00-620.00]

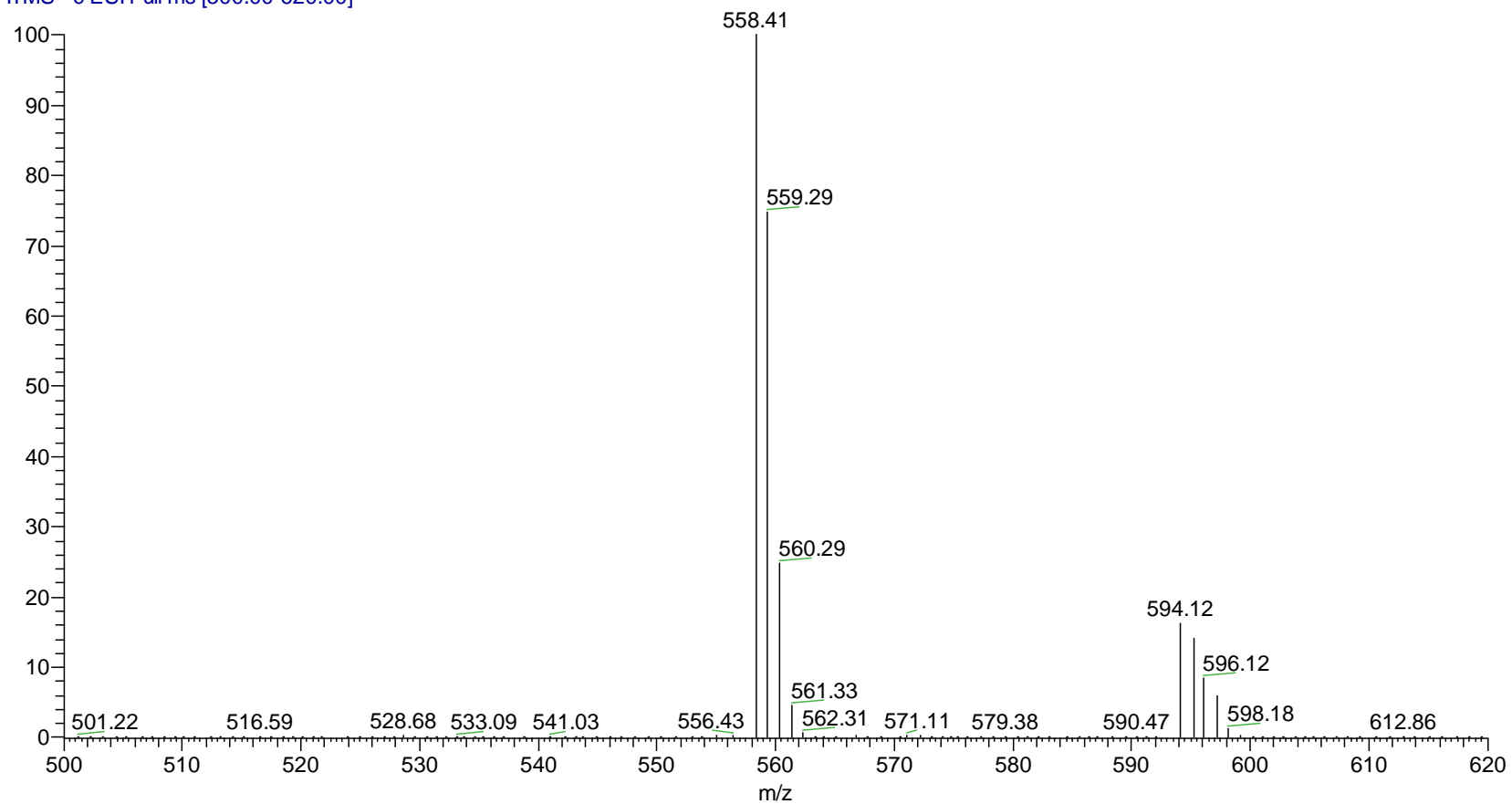


Figure 205: ESI-MS spectrum of compound **8m**.

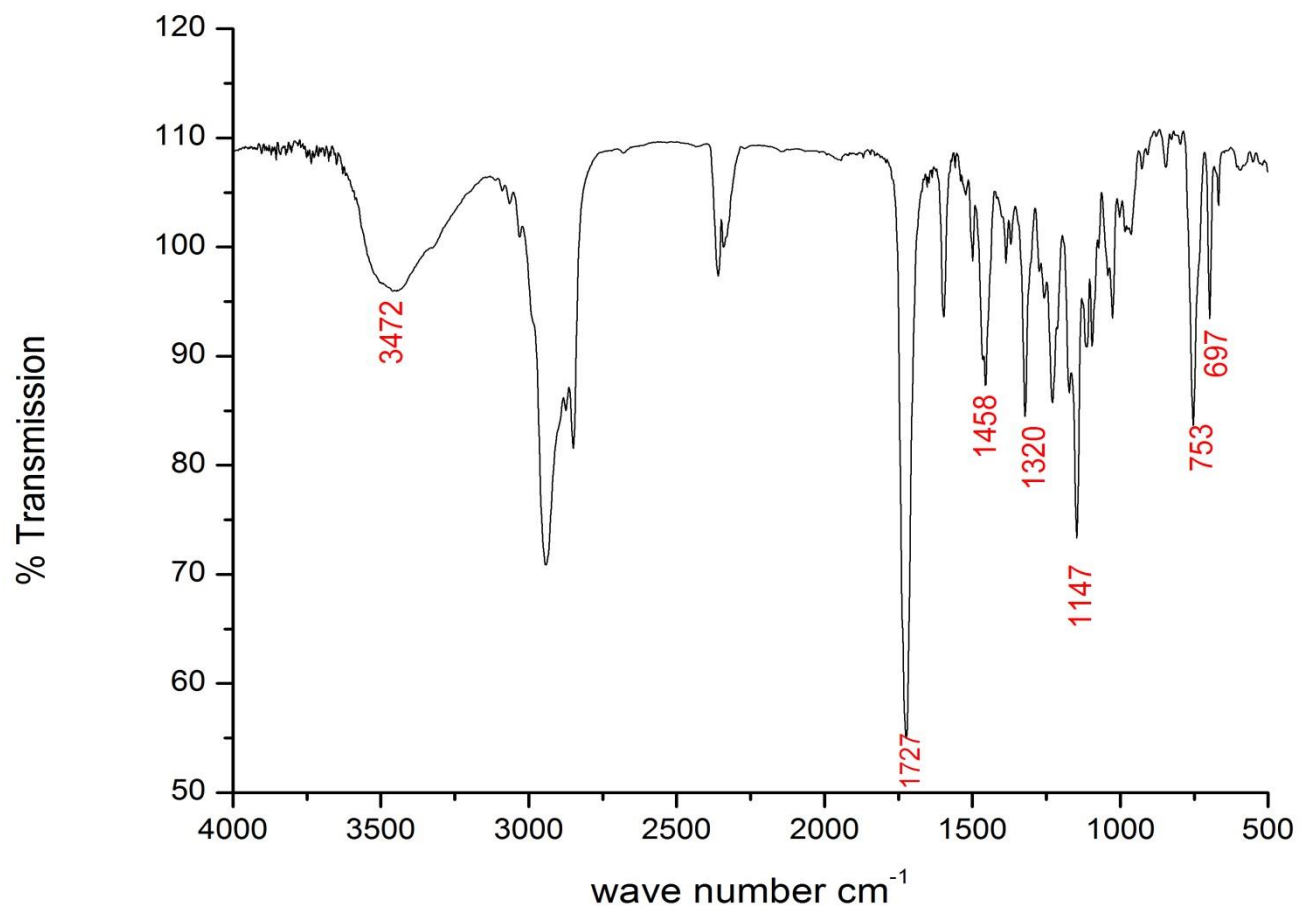


Figure 206: IR spectrum of compound **8m**.

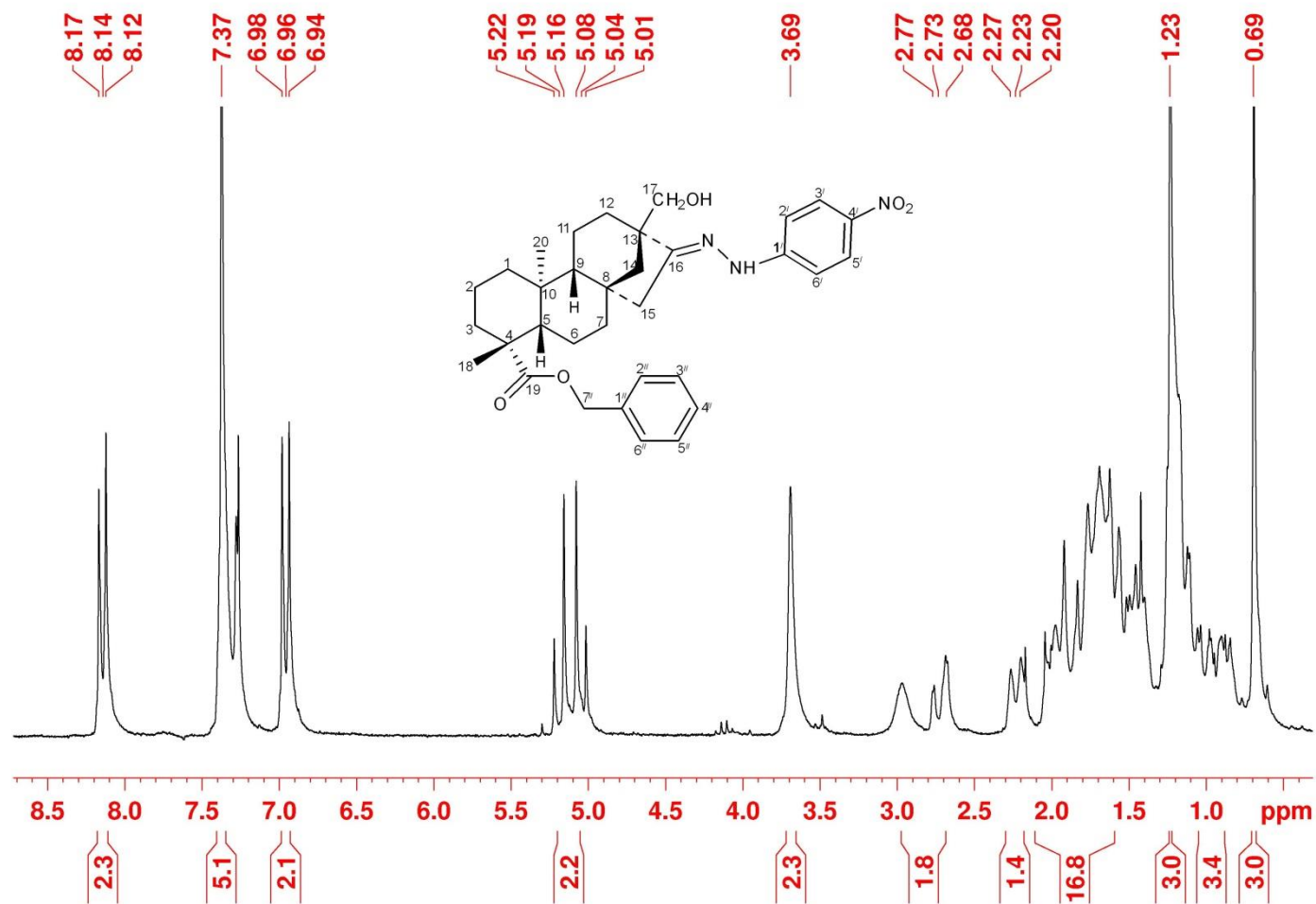


Figure 207: ¹H-NMR (200 MHz, CDCl₃) spectrum of compound **8m**.

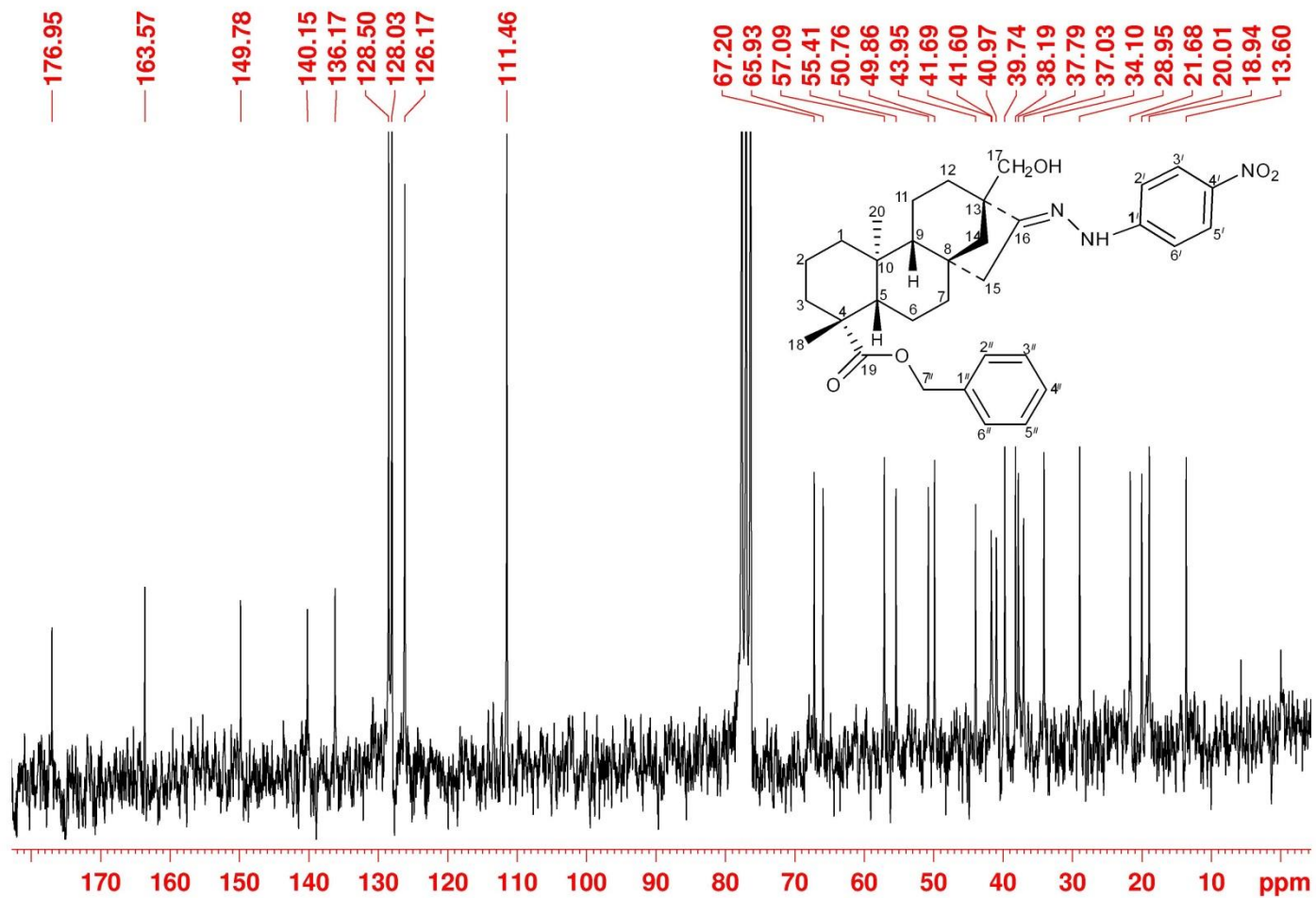


Figure 208: ^{13}C $\{^1\text{H}\}$ NMR (50 MHz, CDCl_3) spectrum of compound 8m.

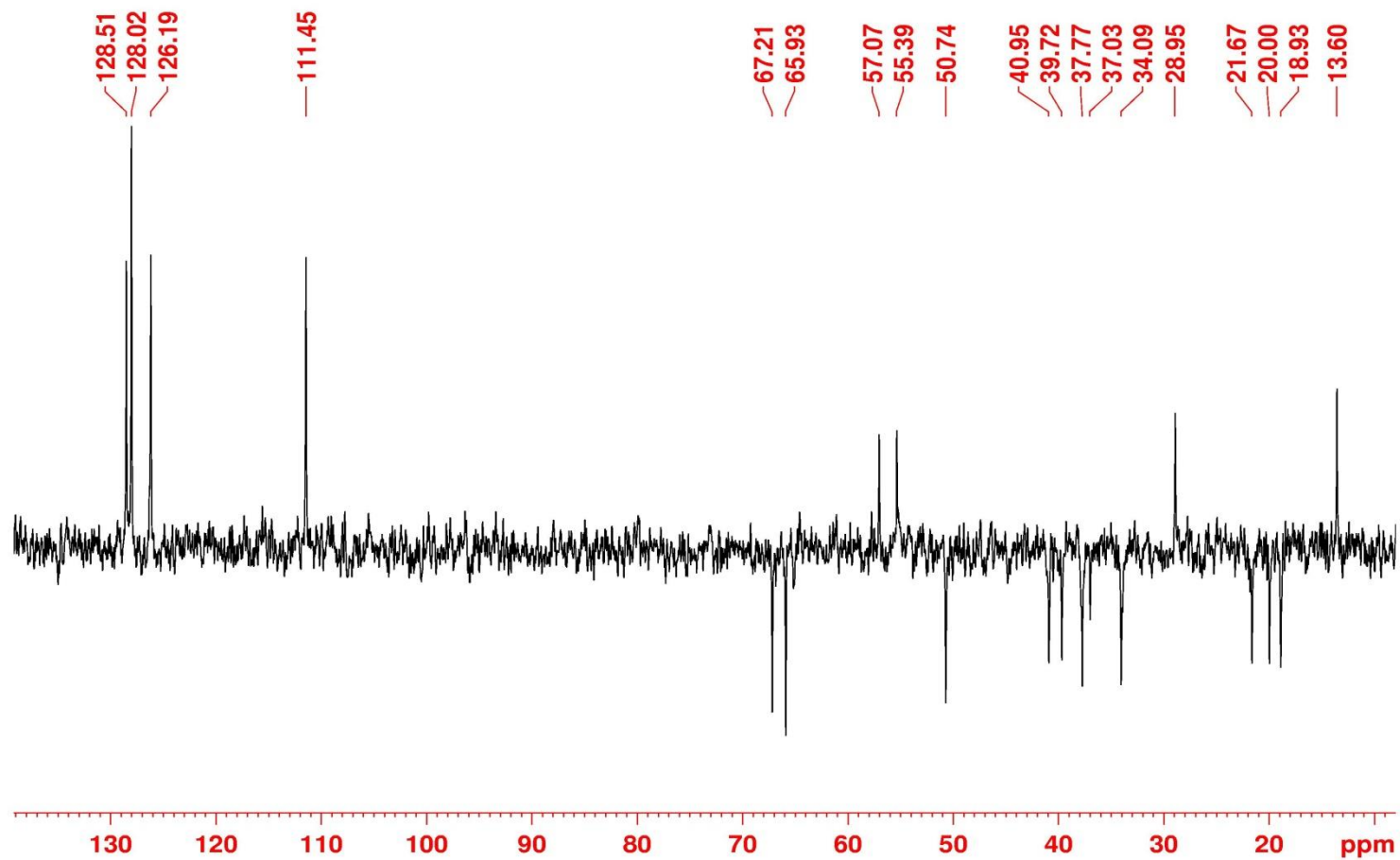


Figure 209: ^{13}C { ^1H } DEPT-NMR (50 MHz, CDCl_3) spectrum of compound **8m**.